

Advancements in Organocatalytic Site Selective Oxidations

Robert Michael Bruce Dyer

New Orleans, Louisiana

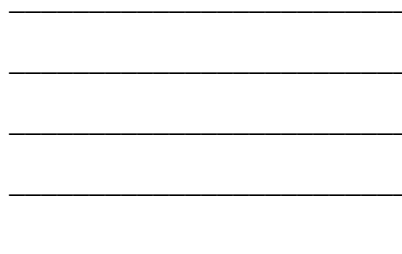
B.S. in Chemistry with a specialization in Biochemistry, University of Virginia 2016

A Dissertation presented to the Graduate Faculty of the University of Virginia in Candidacy for
the Degree of Doctor of Philosophy

Department of Chemistry

University of Virginia

October 2022



Copyright Information

The following chapters contain data and experiments from previously published works.

Chapter 2: Dyer, R. M. B.; Hahn, P. L.; Hilinski, M. K. Selective Heteroaryl N-Oxidation of Amine Containing Molecules. *Organic Letters*. **2018**, *20* (7), 2011–2014.

Chapter 4: Rotella, M. E.; Dyer, R. M.B.; Hilinski, M. K., Gutierrez, O.; Mechanism of Iminium Salt-Catalyzed C (sp³)–H Amination: Factors Controlling Hydride Transfer versus H-Atom Abstraction *ACS Catal.*, **2020**, *10*(1) 897-906.

Abstract

Billions of years of evolution have led to the biosynthesis of complex molecules that dictate and control life from simple precursors. Synthetic chemists have continued to pursue discoveries that mimic the capability of enzymatic biosynthesis. In following this pursuit, we have focused on developing new methods that enable site selective oxidations and improve upon current methodology of iminium organocatalysis.

Heteroaromatic N-oxides are an important class of molecules as bioactive compounds, drug metabolites, and synthetic precursors. The oxidation of nitrogen heterocycles in the presence of aliphatic amines is a transformation that typically requires exhaustive oxidation followed by selective reduction to achieve. We have developed a method using a strong Brønsted acid that protonates and deactivates the more electron rich aliphatic amine, enabling selective oxidation of less electron-rich heterocyclic nitrogen by an iminium catalyst. The N-oxide products can be subjected to a large selection of known transformations. This method can be used as a platform to synthesize enzymatic metabolites or as means for late-stage functionalization of nitrogen heterocycles.

Direct oxidation of unactivated C–H bonds is a field of increasing importance in modern synthetic chemistry. A longstanding problem in the is the lack of a general method to achieve chemoselective C–H oxidations when in the presence of other oxidizable groups. Our lab has previously developed two methods utilizing the same iminium catalyst for selective C–H hydroxylation and amination. We have streamlined and improved the synthesis of this iminium catalyst and have developed a library of new iminium salts to pursue a second-generation catalyst improving on our hydroxylation and amination methodology. Additionally, we have introduced new conditions and iminoiodinane reagents to improve our iminium catalyst's amination capabilities. These new iminoiodinane reagents can be used in intramolecular and intermolecular aminations and provide enhanced reactivity over traditional iminoiodinane reagents.

Acknowledgements

Chapter 2 contains contributions made by Dr. Philip L. Hahn. The amine scope substrates reported and the reversion experiments were performed by him.

Chapter 3 contains contributions made by Dr. William G. Shuler and Carrick Clark-Cearley. Dr. William G. Shuler made and tested several previous catalysts and is referred to for comparison. Carrick Clark-Cearley made and tested the aryl fluorinated catalysts whose data is referred to for comparison.

Chapter 4 contains contributions from Dr. Jared M. Lowe and Jonathan Rodriguez. Dr. Jared M. Lowe synthesized several of the iodinated and iminoiodinated screened including TMI-NBs and TMI-NTs, and proposed the TMI-NBs iodinated. Jonathan Rodriguez originally made the TMI-NBs and TMI-NTs iodinated under Dr. Jared M. Lowe's direction.

To Prof. Hilinski for allowing me to pursue my Ph.D. and work in his lab and for all the guidance and feedback I have received throughout these years as an undergraduate and graduate student. All of this would not be possible without you

To my committee members, Prof. Dean Harman, Prof. Kevin Lynch, Prof. Charlie Machan, Prof. Marcos Pires, Prof. Lin Pu and Prof. Tim Macdonald. Thank you for the courses you have taught, the conversations and insight you have provided, and the help over the years and especially your time and patience.

To my family and friends who have helped me along the way. I would not be here without you.

Forsan et haec olim meminisse juvabit

List of Abbreviations

Ar	Aryl
AO	Aldehyde Oxidase
Bn	Benzyl
br	Broad
Boc	tert-Butoxycarbonyl
CAN	Ceric Ammonium Nitrate
Cat.	Catalyst
Cond.	Conditions
Conv.	Conversion
Cy	Cyclohexyl
CYP	Cytochrome P450
d	Doublet
DCE	Dichloroethane
DCM	Dichloromethane
DFT	Density Functional Theory
DMDO	Dimethyldioxirane
DMF	N,N-Dimethylformamide
DMSO	Dimethylsulfoxide
dr	Diastereomeric Ratio
ee	Enantiomeric Excess
eq	equivalent
Et	Ethyl
EtOAc	Ethyl Acetate
EtOH	Ethanol
ESI-MS	Electrospray Ionization Mass Spectroscopy
FMO	Flavin-containing monooxygenase
GC	Gas Chromatography

HAT	H-atom transfer
HFIP	1,1,1,3,3,3-Hexafluoroisopropanol
HOTf	Trifluoromethanesulfonic Acid
HPLC	High-Performance Liquid Chromatography
iPr	Isopropyl
LAH	Lithium Aluminum Hydride
m	Multiplet
<i>m</i> -CPBA	<i>meta</i> -Chloroperoxybenzoic Acid
Me	Methyl
MeCN	Acetonitrile
MeOH	Methanol
MS	Mass Spectrometry
Ms	Mesyl
NIS	N-Iodosuccinimide
nHex	n-Hexyl
NMR	Nuclear Magnetic Resonance
nPr	n-Propyl
[O]	Oxidant
OAc	Acetate
OBz	Benzoate
OPiv	Pivalate
OTf	Trifluoromethylsulfonate
OTs	Tosylate
Ph	Phenyl
PhMe	Toluene
Piv	Pivalyl
q	Quartet
Rh ₂ (esp) ₂	Bis[rhodium($\alpha,\alpha,\alpha',\alpha'$ -tetramethyl-1,3-benzenedipropionic acid)]

rsm	Recovered Starting Material
rt	Room Temperature
rxn	reaction
s	Singlet
SAR	Structure–Activity Relationship
SOM	Site of metabolism
Smr	Starting Material Remaining
SNAr	Nucleophilic Aromatic Substitution
t	Triplet
^t Bu	<i>tert</i> -Butyl
TFA	Trifluoroacetic Acid
TFAA	Trifluoroacetic anhydride
TFDO	Methyl(trifluoromethyl)dioxirane
TFE	2,2,2-Trifluoroethanol
THF	Tetrahydrofuran
TMS	Trimethylsilyl
Ts	Tosyl
UHP	Urea Hydrogen Peroxide

Table of Contents

Copyright information	I
Abstract	II
Acknowledgements	III
List of Abbreviations	IV
Table of Contents	VII
List of Figures	XI
List of Schemes	XI
List of Tables	XIII
1: Late-stage Hydroxylation and Aminations of Unactivated C–H bonds	1
1.1 Late-stage Functionalization	1
1.2 Late-Stage Hydroxylation	2
1.2.1 Palladium C–H Hydroxylations	6
1.2.2 Ruthenium Hydroxylations	8
1.2.3 Iron Hydroxylations	10
1.2.4 Manganese Hydroxylations	13
1.2.5 Organic <i>O</i> -atom Transfer Reagents	14
1.3 Late-Stage Aminations	20
1.3.1 Rhodium Aminations	20
1.3.2 Silver Aminations	27
1.3.3 Iron Aminations	29
1.3.4 Manganese Aminations	30
1.3.5 Organocatalytic Amination	31
1.4 Conclusions	32
1.5 References	33
2: Chemoselective Oxidation of Nitrogen	39
2.1 Enzymatic Metabolism	39
2.2 Metabolism and Drug Discovery	40
2.3 Aldehyde Oxidase	41
2.4 Chemoselective Catalytic N-Oxidation	43
2.4.1 Reaction Development	47
2.4.2 Reaction Scope	48
2.4.3 Catalytic Cycle	53
2.5 Conclusions and outlook for selective N-oxidation	55
2.6 References	57
3: Synthesis and Evaluation of New Iminium Salt Catalysts	59

3.1. Parent Iminium Catalyst.....	60
3.1.2 Iminium Synthetic Route.....	61
3.1.3. Selection of Model Substrates.....	63
3.2.1 Polyfluorinated Iminiums.....	64
3.2.2. Polyfluorinated aryl iminium synthesis.....	65
3.2.3 Polyfluorinated Alky Iminium Synthesis.....	65
3.2.4 Polyfluorinated Aryl Iminiums Substrate Screening.....	65
3.2.5 Polyfluorinated Alkyl Iminiums Substrate Screening.....	67
3.3.1 Aryl Functionalized Iminium Salts.....	68
3.3.2 Aryl Functionalized Iminium Salt Synthesis.....	69
3.3.3 Aryl Functionalized Iminium Salt Substrate Screening.....	70
3.4.1 Benzylic Cycloalkyl Iminium Salts.....	71
3.4.2 Benzylic Cycloalkyl Iminium Salt Synthesis.....	72
3.4.3. Benzylic Cycloalkyl Iminium Salt Substrate Screening.....	73
3.5.1 Cyclopropyl Methoxy Iminium Salt.....	73
3.5.2 Cyclopropyl Methoxy Iminium Salt Synthesis.....	74
3.5.3 Cyclopropyl Methoxy Iminium Salt Substrate Screening.....	75
3.6.1 Phenyl <i>N</i> -Iminium Salts.....	75
3.6.2 Synthesis of <i>N</i> -phenyl Iminium Salts.....	76
3.7 Improved Synthesis of the Parent Iminium Catalyst.....	78
3.8. Conclusions.....	79
3.9 References.....	80
4: New Iminoiodinanes For C–H Amination.....	82
4.1 Organocatalytic Amination.....	82
4.2.1 Intramolecular Amination with a preformed iodine.....	84
4.2.1 Solvent Screening of preformed intramolecular iminoiodine.....	85
4.2.2 Catalyst Screening.....	86
4.3.1 Intramolecular amination via in situ iminoiodine formation.....	87
4.3.2 Solvent Screening for in-situ intramolecular amination.....	88
4.3.3 Iodobenzene iodine ligand screening.....	89
4.4.1 Iminoiodine Exchange for intramolecular amination.....	91
4.4.2 Iminoiodine Screening.....	92
4.4.3 Development of new more soluble iminoiodinanes.....	93

4.4.1 TMI-NBs Synthesis.....	97
4.4.2 Solvent Screen with TMI-NBs.....	98
4.4.3 Temperature Screening.....	99
4.4.4 Screening for Intramolecular Substrates.....	100
4.6 Conclusions.....	102
4.7 References.....	102
A1. Appendix One: Chapter Two Supporting Information.....	105
1.1 General Information.....	105
1.2 Screening of Oxidant Conditions.....	106
1.3 Substrate Synthesis.....	106
1.4 Oxidation Reactions.....	151
1.5 References.....	194
A2. Appendix Two: Chapter Three Supporting Information.....	195
2.1 General Information.....	195
2.2 Catalyst Synthesis.....	195
2.2.1 Benzylic Alkylation.....	195
2.2.2 Nitrile Reduction.....	210
2.2.3 Aniline Formation.....	210
2.2.4 Acetamide Formation.....	215
2.2.5 Bischler-Naperialski Cyclization.....	259
2.2.6 Imine Methylation.....	301
2.3 Substrate Screening.....	339
2.3 References.....	339
A3. Appendix Three: Chapter Four Supporting Information.....	341
3.1 General Information.....	341
3.2 Sulfamate Synthesis.....	341
3.3 Iodinane Synthesis.....	365
3.4 Iodoarene Synthesis.....	371
3.5 Oxidation of iodoarenes.....	375
3.6 Amination Products.....	388
3.7 References.....	396

List of Figures

Figure 1.1: Sites of Oxidation of Betulin and Betulinic Acid.....	5
Figure 1.2: Ruthenium catalyzed hydroxylations	8
Figure 1.3: (Me ₃ tacn)RuO ₂ and [(Me ₄ N ₄)RuO ₂] Complexes.....	9
Figure 1.4: Unreactive steroid derivatives under Rh ₂ (esp) ₂ amination conditions	24
Figure 2.1: Oxidized nitrogen containing drugs by metabolic enzymes CYPs, FMOs and AO .	42
Figure 3.1: Points of modulation for the Hilinski iminium catalyst	64
Figure 3.2: Hydroxylation screening substrates.....	66
Figure 3.3: Amination screening substrates	66
Figure 3.4: Polyfluorinated Iminiums.....	67
Figure 3.5: Aryl functionalized iminium salts	72
Figure 3.6: Previously synthesized aryl functionalized iminiums	73
Figure 3.7: Benzylic cycloalkyl iminium salts.....	75
Figure 3.8: Cyclopropyl methoxy iminium salt.....	77
Figure 3.9: <i>N</i> -Phenyl iminium salts	80
Figure 4.1: Proposed catalytic cycle of organocatalytic C–H amination based on DFT and molecular dynamics calculations.	88
Figure 4.2: Iminoiodinane exchange equilibrium	97
Figure 4.3: Methylated (tosyliminoiodo) toluenes.....	99
Figure 4.4: Comparison of soluble iminoiodinanes reactivity with triphenyl phosphine.....	100

List of Schemes

Scheme 1.1: Irenotecan synthesis from Camptothecin.....	2
Scheme 1.2: Biosynthesis of Taxol	4
Scheme 1.3: Late-stage diversification of Betulin and Betulinic Acid under synthetic and enzymatic oxidative conditions.....	5
Scheme 1.4: Paspaline and oridamycin B total synthesis utilizing a Pd catalyzed hydroxylation	7
Scheme 1.5: (Me ₃ tacn)RuO ₂ oxidation of complex products	9
Scheme 1.6: cis-[Ru(dtby) ₂ Cl ₂] oxidation of complex products	10
Scheme 1.7: Fe(PDP) oxidation of complex products	11
Scheme 1.8: Fe(CF ₃ -PDP) comparison and oxidation of complex products	12
Scheme 1.9: Asymmetric manganese hydroxylation	13
Scheme 1.10: Manganese ligand-controlled site selective hydroxylations	14
Scheme 1.11: Dioxiranes for <i>O</i> -atom Transfer	15
Scheme 1.12: Dioxirane oxidations of steroidal substrates.....	16
Scheme 1.13: Dioxirane oxidation of Bryostatin	17
Scheme 1.14: Catalytic ketone dioxirane mediated C–H hydroxylation	18
Scheme 1.15: Iminium-catalyzed C–H hydroxylation	19
Scheme 1.16: Amine-catalyzed hydroxylation.....	20
Scheme 1.17: Rhodium-catalyzed intramolecular amination.....	21
Scheme 1.18: Rh ₂ (esp) ₂ -catalyzed intermolecular amination of complex substrates.....	22
Scheme 1.19: Intramolecular guanidine amination	23
Scheme 1.20: Rh ₂ (esp) ₂ -catalyzed amination of brassinosteroid derivative	24
Scheme 1.21: Enantioselective rhodium-catalyzed amination.....	26
Scheme 1.22: Rhodium-catalyzed selective tertiary C–H amination.....	27
Scheme 1.23: Silver-catalyzed selective aziridination	29
Scheme 1.24: Silver-catalyzed selective intermolecular allylic amination	30
Scheme 1.25: Iron-catalyzed C–H amination.....	31
Scheme 1.26: Comparison of Mn(ClPc)SbF ₆ amination and Rh ₂ esp ₂ amination	32
Scheme 1.27: Mn(ClPc)SbF ₆ catalyzed C–H amination.....	33
Scheme 1.28: Iminium catalyzed C–H amination.....	34
Scheme 2.1: Synthetic strategy to access pyridyl N-oxides	46
Scheme 2.2: Strategy for chemoselective oxidations in the presence of free amines	48
Scheme 2.3: N-Oxidation substrate scope: Amines	51
Scheme 2.4: N-Oxidation substrate scope: Functionalized Pyridines.....	52
Scheme 2.5: N-Oxidation substrate scope: Azaheterocycles	53
Scheme 2.6: Drug-like substrates with 0% yield of heteroaryl N-oxidation.....	54
Scheme 2.7: N-oxide reversion experiment	55
Scheme 2.8: Proposed Catalytic cycle of pyridyl oxidation.....	56
Scheme 2.9: Mimicking AO through selective N-oxidation.....	57
Scheme 2.10: Peptide-based chemoselective nitrogen oxidation and desymmetrization	58
Scheme 3.1: Iminium salt catalyst for hydroxylation or amination of C–H bonds.....	63
Scheme 3.2: Iminium catalyst synthetic route.....	65

Scheme 3.3: Polyfluorinated aryl iminium synthesis	68
Scheme 3.4: Polyfluorinated alky iminium synthesis	69
Scheme 3.5: Iminium hydroxylation degradation pathway	71
Scheme 3.6: Aryl functionalized iminium salt synthesis	73
Scheme 3.7: Cycloalkyl iminium salt synthesis	76
Scheme 3.8: Cyclopropyl methoxy iminium salt synthesis	78
Scheme 3.9: N-phenyl iminium synthesis	81
Scheme 3.10: 1,3 Dimethoxy <i>N</i> -phenyl iminium synthesis	81
Scheme 3.11: Improved synthesis of the parent iminium catalyst	83
Scheme 4.1: Intramolecular amination with preformed iminoiodinane	90
Scheme 4.2: Solvent screening of preformed iminoiodinane amination.....	91
Scheme 4.3: Catalyst screening of preformed iminoiodinane amination.....	92
Scheme 4.4: Intramolecular amination with diacetoxy iodobenzene	94
Scheme 4.5: Intramolecular amination with oxidized iodobenzenes	95
Scheme 4.6: Intramolecular amination screening of functionalized diacetoxy iodobenzenes	96
Scheme 4.7: Screening of iminoiodinanes for intramolecular amination	98
Scheme 4.8: Soluble iodine screening for intramolecular amination	102
Scheme 4.9: Synthesis of <i>tert</i> -butyl methoxy iodobenzene iminoiodinanes.....	103
Scheme 4.10: TMI-NBs solvent screening.....	104
Scheme 4.11: TMI-NBs solvent screening at elevated temperatures.....	105
Scheme 4.12: Intramolecular amination substrates and respective product yields	107
Scheme 4.13 <i>m</i> -CBA iodine amination	108

List of Tables

Table 2.1: Optimization of N-oxidation conditions	49
Table 3.1: Polyfluorinated aryl iminium hydroxylation and amination performance.....	70
Table 3.2: Polyfluorinated alkyl iminium hydroxylation and amination performance.....	71
Table 3.3: Aryl functionalized iminium hydroxylation and amination performance	74
Table 3.4: Cycloalkyl iminium hydroxylation and amination performance	77
Table 3.5: Cyclopropyl methoxy iminium hydroxylation and amination performance.....	79

Chapter One

Late-stage Hydroxylation and Aminations of Unactivated C–H bonds

Introduction

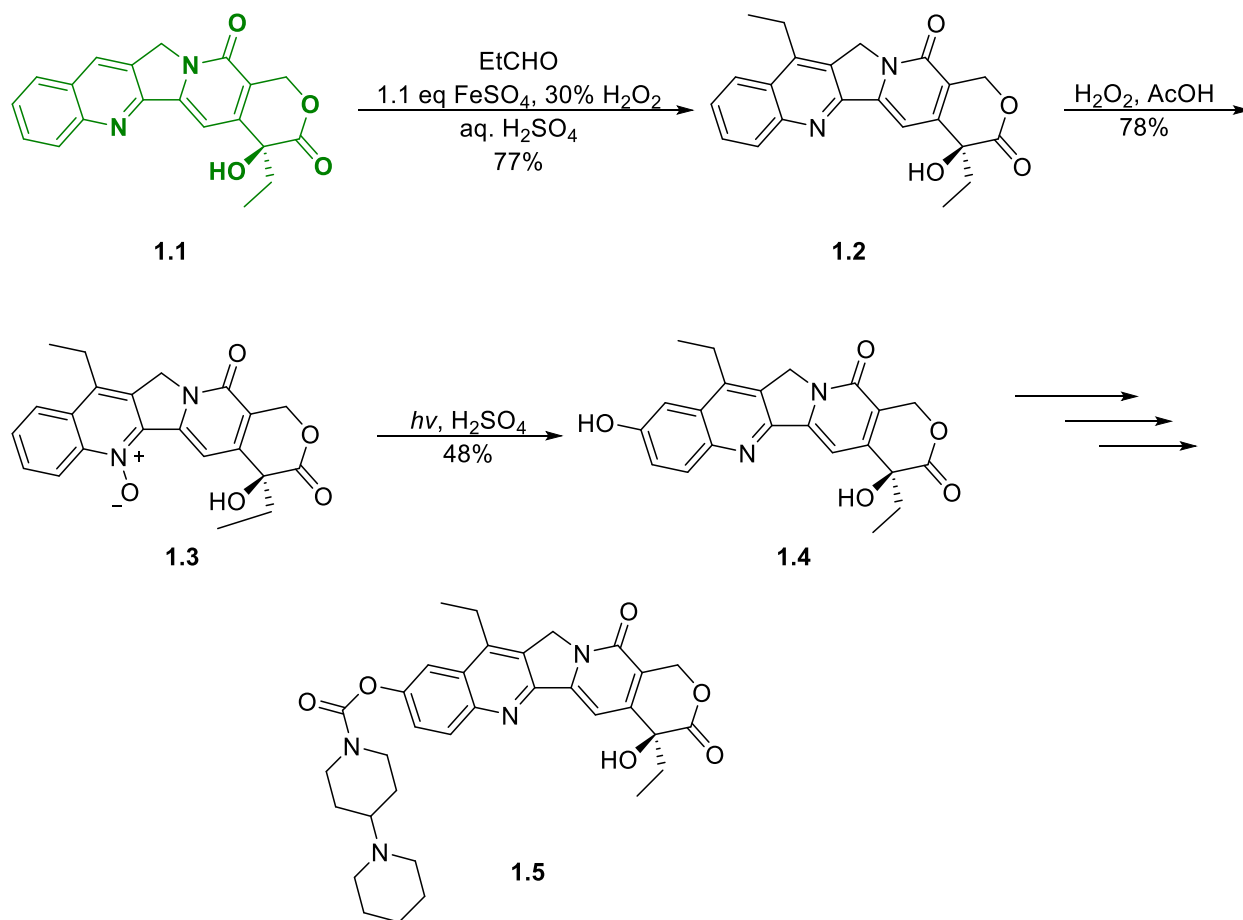
An intrinsic challenge of organic chemistry is selectivity, that is to say the ability to precisely modify one chemical bond over another. This becomes increasingly difficult as the compound to be modified becomes more structurally complex, and as the diversity of functional groups present increases. Weaker and more reactive bonds tend to be targeted to facilitate these transformations; however, the presence of numerous bonds closely related in energy makes this selectivity harder to achieve.

1.1 Late-stage Functionalization

Late-stage functionalization focuses on the introduction of functional groups towards the end of a synthesis, when a majority of the desired functionality and stereochemistry has already been incorporated into the molecule.¹ These methods must have high functional group tolerance to prevent any undesired or destructive side reactions. In particular, late-stage functionalization that selectively oxidizes C–H bonds in the carbon framework of complex molecules is one challenging type of late-stage functionalization that is highly valuable. Prior to the advent of C–H functionalization, chemists typically did not consider unactivated C–H bonds practical options for synthetic transformations given their ubiquity and high bond dissociation energy; methods that would break C–H bonds would also react with pre-installed functional groups. However, new research has developed methods to selectively target C–H bonds over other reactive bonds.^{2,3} This methodology provides a new tool to efficiently synthesize complex organic molecules.

Irenotecan (**1.5**) was synthesized following the concept of late-stage functionalization in the 1990s starting from the natural product, camptothecin (**1.1**).⁴ The initial steps show the radical alkylation to **1.2** and photochemical arene oxidation to **1.3** to yield the original drug scaffold (**1.4**) for structure activity relationship (SAR) studies leading to irenotecan (**1.5**) (**Scheme 1.1**)

Scheme 1.1: Irenotecan synthesis from Camptothecin

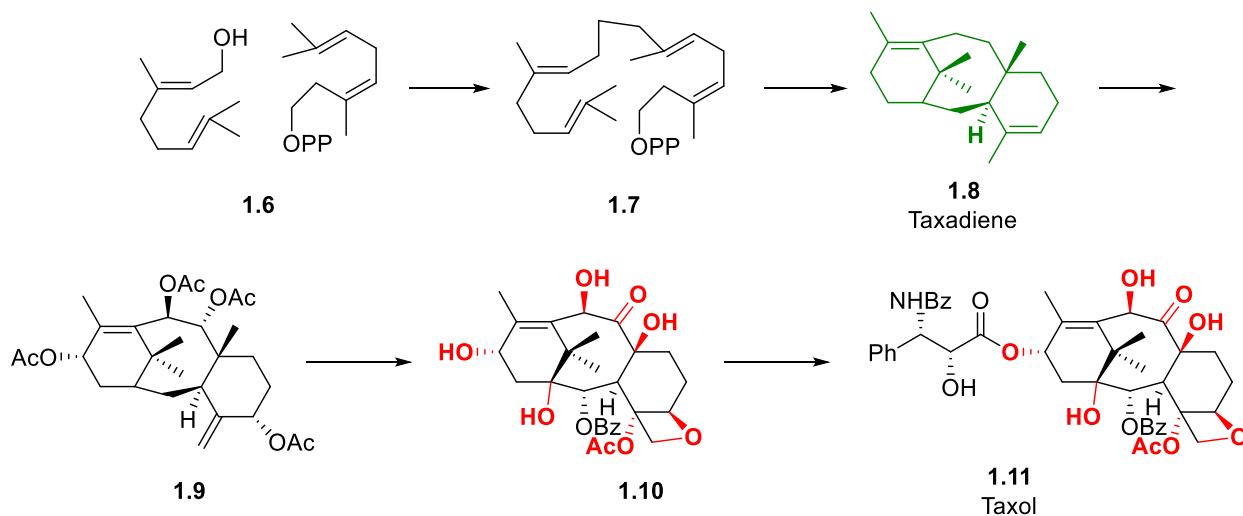


1.2 Late-Stage Hydroxylation

Late-stage functionalization has been established as a viable strategy in complex molecule synthesis through efficient modulation of complex organic compounds. The past decades have seen an explosion of new selective late-stage functionalization methods. Late-stage hydroxylation

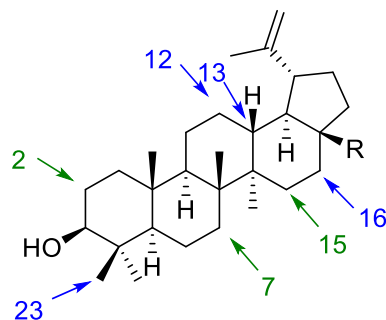
is a highly valuable tool for synthesis and drug development given the improved water solubility and the amenability for further diversification from the installation of alcohols. Hydroxylation of aliphatic alkanes is ubiquitous in biosynthesis of complex molecules.⁵ Within a biological system, the carbon framework of a molecule is produced first, followed by a series of enzymatic oxidations to produce the final molecule.

The biosynthesis of Taxol (**1.11**) illustrates this pathway.⁶ Taxol is an important drug for its anti-cancer capabilities and a challenging target for total synthesis.⁷ The initial hydrocarbon framework of taxadiene (**1.8**) is formed from the sequential coupling of terpenes **1.6** and cyclization of **1.7** before the carbon skeleton undergoes several oxidative steps to **1.10** and finally to **1.11** (**Scheme 1.2**). Although, now manufactured via semisynthesis, it remains an interest as a challenging target for total synthesis due to the potential to provide access to analogs of greater structural diversity than semisynthesis.⁸ Many synthetic labs have spent decades developing the total synthesis of this compound, using a variety of approaches. These strategies mainly involve conventional synthetic steps that utilize protecting groups, oxidation state interconversions, and atom-inefficient functional group manipulations.⁹

Scheme 1.2: Biosynthesis of Taxol

Conversely, Baran and coworkers utilized a combination of enzymatic and synthetic methods to functionalize terpenes betulin (**1.12**) and betulinic acid (**1.13**) with hydroxy groups to improve its solubility for potential oral delivery as a therapeutic. The green sites are enzymatically oxidized, whereas the blue sites are synthetically oxidized in **Figure 1.1**. The lupine core of **1.12** was first derivatized into four new scaffolds (**1.14-1.17**) that were subsequently screened under both synthetic and enzymatic oxidation conditions (**Scheme 1.3**). They demonstrated the utility of late-stage functionalization by synthesizing and identifying hydroxylated derivatives with better solubility in biological systems than the original natural product.¹⁰ Though useful, these methods were low-yielding and required several steps to get the desired selective hydroxylation through directed methods. Screening demonstrated the potential, but also showed that advancements are still needed to improve their utility, especially to become widely applicable for medicinal chemists given the low yields and lack of reactivity of some methods.

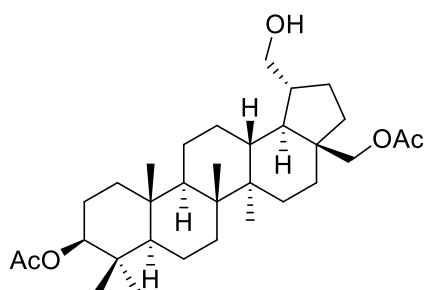
Figure 1.1: Sites of Oxidation of Betulin and Betulinic Acid



1.12 Betulin R = C₂OH

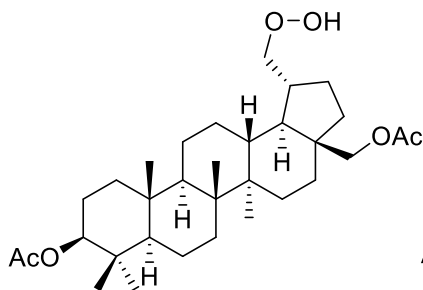
1.13 Betulinic Acid R = COOH

Scheme 1.3: Late-stage diversification of Betulin and Betulinic Acid under non-enzymatic and enzymatic oxidative conditions



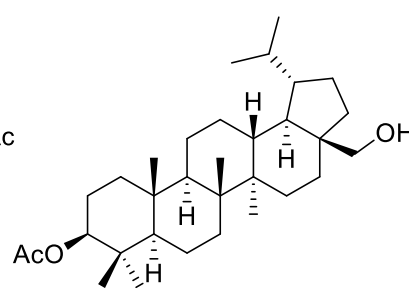
1.14

PIDA, I ₂ , hv	C12
Pb(OAc) ₄ , I ₂ , hv	C12
NOCl, Pyr	N.R.
TFDO	C16
DMDO	N.R.
KMNO ₄	N.R.
CrO ₃ , ⁿ Bu ₄ NIO ₄	decomp.
RuCl ₃ · xH ₂ O, KBrO ₃	N.R.
Crabtree's IR catalyst	N.R.



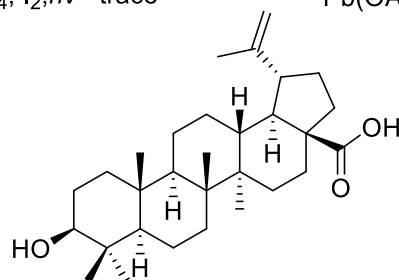
1.15

PIDA, I ₂ , hv	C12
Pb(OAc) ₄ , I ₂ , hv	trace



1.16

PIDA, I ₂ , hv	decomp.
Pb(OAc) ₄ , I ₂ , hv	C13



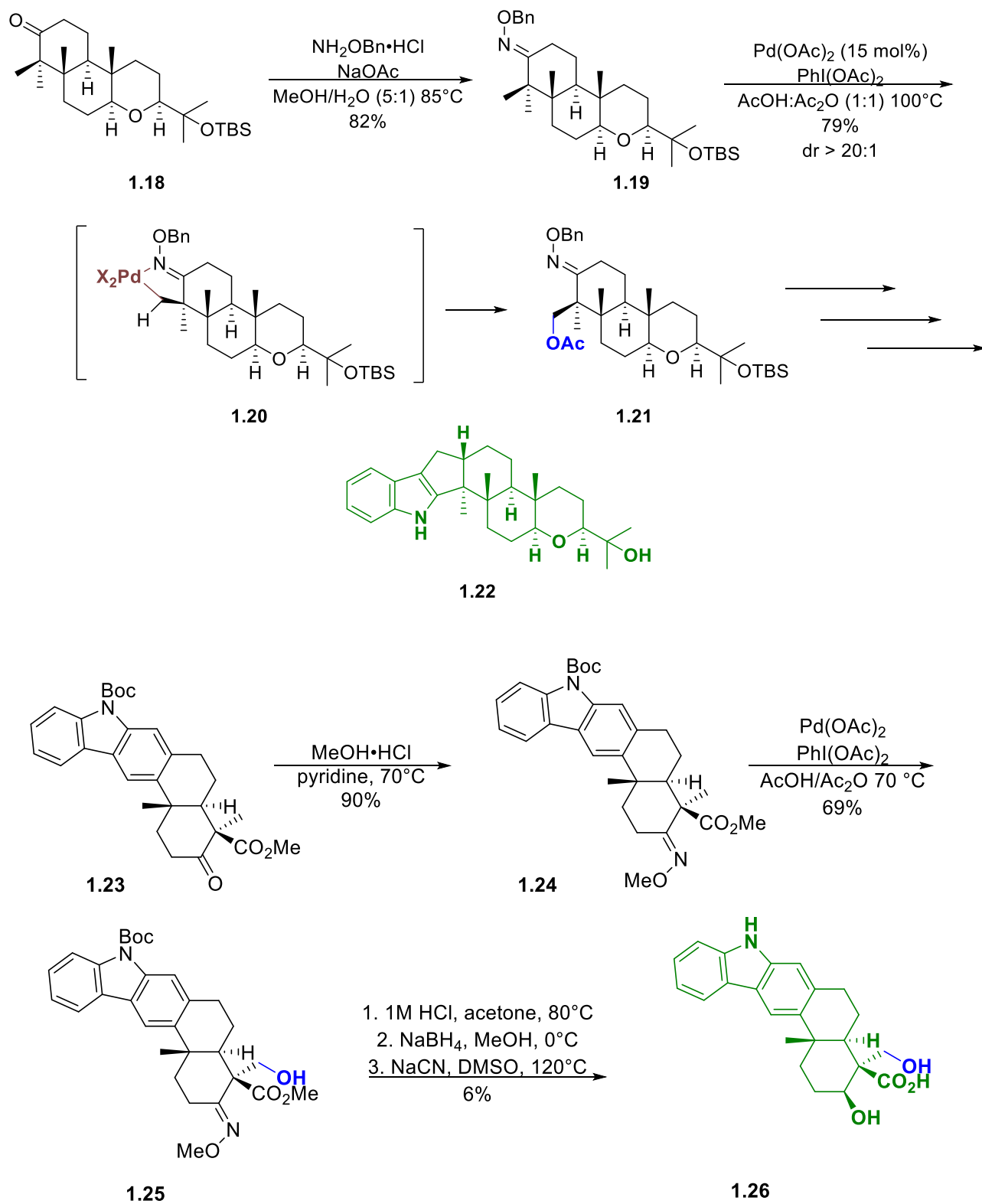
1.17

Hartwigs 1,3 diol	C23
<i>Streptomyces fragilis</i>	C2/C7
<i>Bacillus megaterium</i>	C7/C15

1.2.1 Palladium C–H Hydroxylations

Early work for these methods began with Baldwin and coworkers utilizing stoichiometric palladium for C–H activation on relatively simple hydrocarbon frameworks. Utilizing *O*-methyl oximes with Na₂PdCl₄ afforded isolable palladacycles capable of further functionalization, as demonstrated on E-Lupanone oxime to a single site-selective oxidation of the methyl group.¹¹ This work was further developed towards catalytic methods with PhI(OAc)₂ by Sanford demonstrating that quinolines and *O*-methyl oximes can be stereospecifically acetoxyated for primary and secondary C–H bond oxidation.¹² These same methods were used in the total synthesis of paspaline (**1.22**) and oridamycin B (**1.26**) by Johnson and Trotta, respectively (**Scheme 1.4**).^{13,14} Although this palladium method is catalytic and site-selective, an oxime directing group (**1.20**) is necessary for its selectivity and limits the versatility of this method.

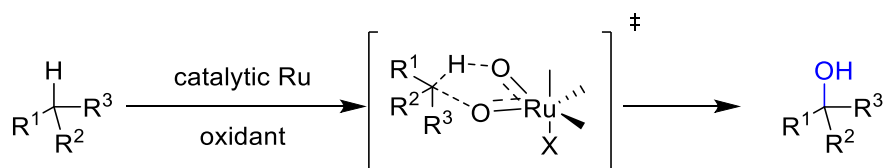
Scheme 1.4: Paspaline and oridamycin B total synthesis utilizing a Pd-catalyzed hydroxylation



1.2.2 Ruthenium Hydroxylations

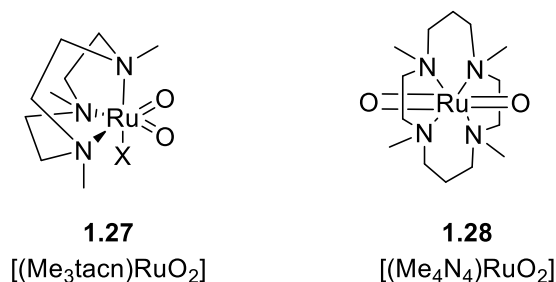
Ruthenium-catalyzed systems undergo a concerted oxidation mechanism, wherein the selectivity is based on steric accessibility and electron richness of the C–H bond. These methods utilize the innate reactivity of the molecule, as opposed to directing groups, to efficiently oxidize scaffolds with stereo- and site-specificity (**Figure 1.2**).¹⁵ Ruthenium tetroxide is a potent oxidant under stoichiometric conditions that indiscriminately oxidizes aromatic rings, pi systems, and saturated C–H bonds.¹⁶ In pursuit of better methods for oxidizing steroidal derivatives, Fuchs developed a catalytic method to make the oxidizing ruthenium tetroxide using perbromate as the terminal oxidant in a buffered solution. The hydroxylations were high-yielding and site-selective, but alkenes and free alcohols were susceptible to further oxidation. Du Bois later developed similar conditions for catalytic ruthenium-oxo hydroxylations using perbromate and a catalytic amount of pyridine, presumably acting as a ligand.¹⁷ These conditions can still easily oxidize alkenes, alkynes, ethers, and other readily oxidizable functionality.

Figure 1.2: Ruthenium-catalyzed hydroxylations.



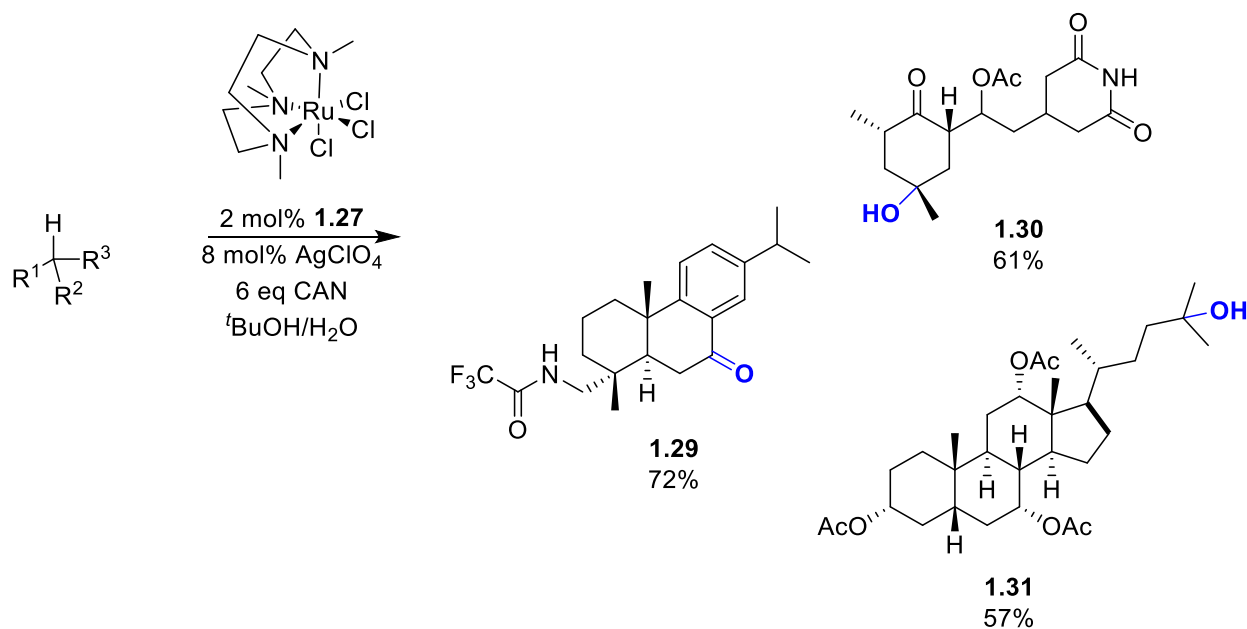
Later work employed (Me₃tacn)RuCl₃ (**1.27**) as a catalyst using ceric (IV) ammonium nitrate (CAN) as the terminal oxidant in an aqueous environment.¹⁸ This framework provides an open steric environment and a *cis*-dioxo oxidant that both shields the catalyst from deactivation through multimerization and allows for substrate access. A similar complex (**1.28**) with the *trans* orientation does not provide the same oxidative improvement (**Figure 1.3**).

Figure 1.3: $(\text{Me}_3\text{tacn})\text{RuO}_2$ and $[(\text{Me}_4\text{N}_4)\text{RuO}_2]$ Complexes



Benzylic and tertiary C–H bonds could easily be oxidized under these conditions for simple substrates and some complex products (**1.32** and **1.33**). Secondary C–H bonds, however, would be over oxidized to give ketone products (**1.31**) instead of alcohols (**Scheme 1.5**).

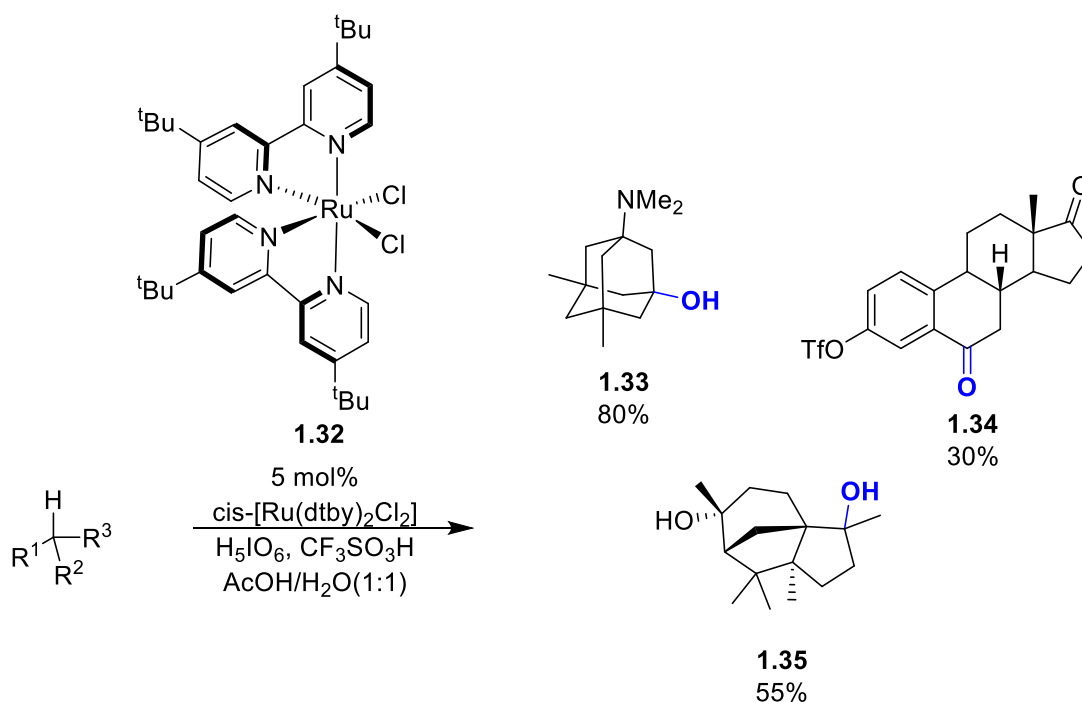
Scheme 1.5: $(\text{Me}_3\text{tacn})\text{RuO}_2$ oxidation of complex products



Several years later, the Du Bois group utilized a bis(bipyridine)Ru catalyst (**1.32**) under acidic aqueous conditions to achieve stereoretentive C–H hydroxylation of benzylic (**1.34**) and tertiary centers (**1.35**) in the presence of amines (**Scheme 1.6**).¹⁹ This new ligand set could be more

easily modulated compared to **1.27** wherein even minor changes of the structure would adversely affect performance and was incapable of enantiospecific oxidations.²⁰ Unprotected amines (**1.33**) could also compete for oxidation or complex with metals to arrest catalytic activity. Acidic conditions ensured the protonation of amine functionalities in the substrates, preventing undesired oxidation of the amines to N-oxides.

Scheme 1.6: cis-[Ru(dtby)₂Cl₂] oxidation of complex products

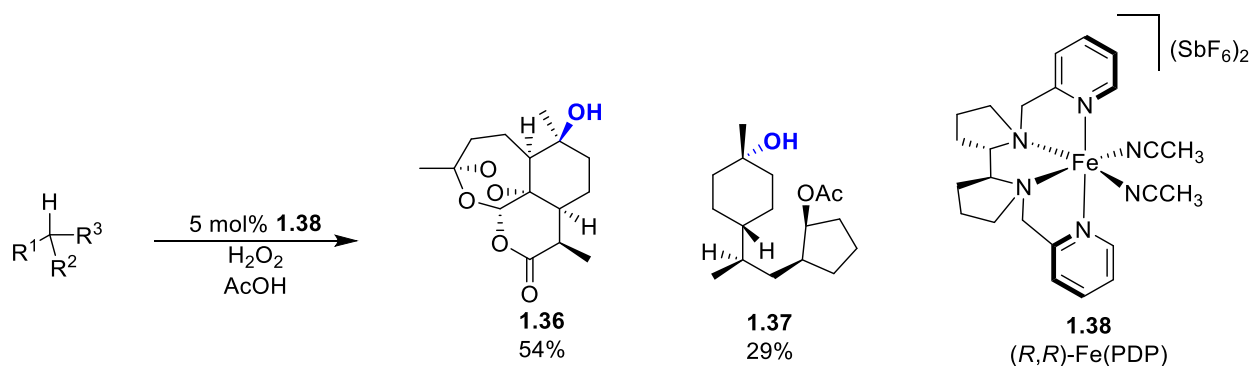


1.2.3 Iron Hydroxylations

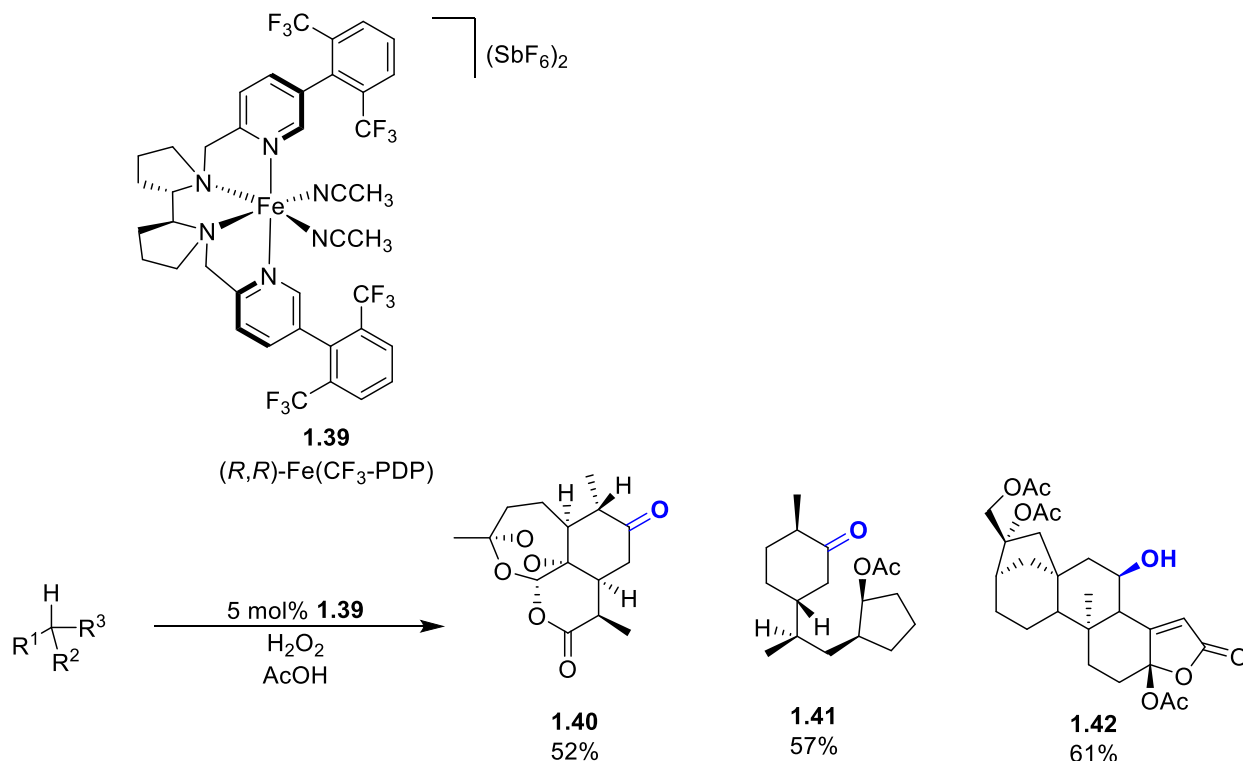
Radical rebound hydroxylations are biologically inspired from iron- and manganese-containing enzymes. The metal-oxo species abstracts a hydrogen atom to form a carbon radical and hydroxide-bound metal, and these species recombine to give the hydroxylated product and the reduced metal complex. Early examples began with iron catalysts, requiring high catalyst loading and excess substrate, eventually leading to iron-porphyrin systems.^{21,22,23} White's work using

Fe(PDP) (**1.38**) with hydrogen peroxide was an important advancement in the development of C–H functionalization, demonstrating the ability to hydroxylate artemisinin (**1.36**) at a single position with diastereocontrol (**Scheme 1.7**).²⁴ The open coordination site of the catalyst allows for directed oxidations to override the inherent selectivity. In the presence of an unprotected carboxy group, the typical selectivity is overridden because the rearrangement of the radical outcompetes the radical rebound, resulting in a different major product.²⁵

Scheme 1.7: Fe(PDP) oxidation of complex products



Changes in site selectivity can be made by adjusting the steric bulk of the PDP ligand through incorporation of a 1,3-bis(trifluoromethyl)aryl group to form the CF₃-PDP ligand. This modification changes the trajectory of the substrate and catalyst interaction, restricting the catalyst towards a more accessible C–H bond compared to the smaller PDP ligand as shown by the comparison of **1.36** and **1.37** vs **1.40** and **1.41** (**Scheme 1.8**).²⁶

Scheme 1.8: Fe(CF₃-PDP) comparison and oxidation of complex products

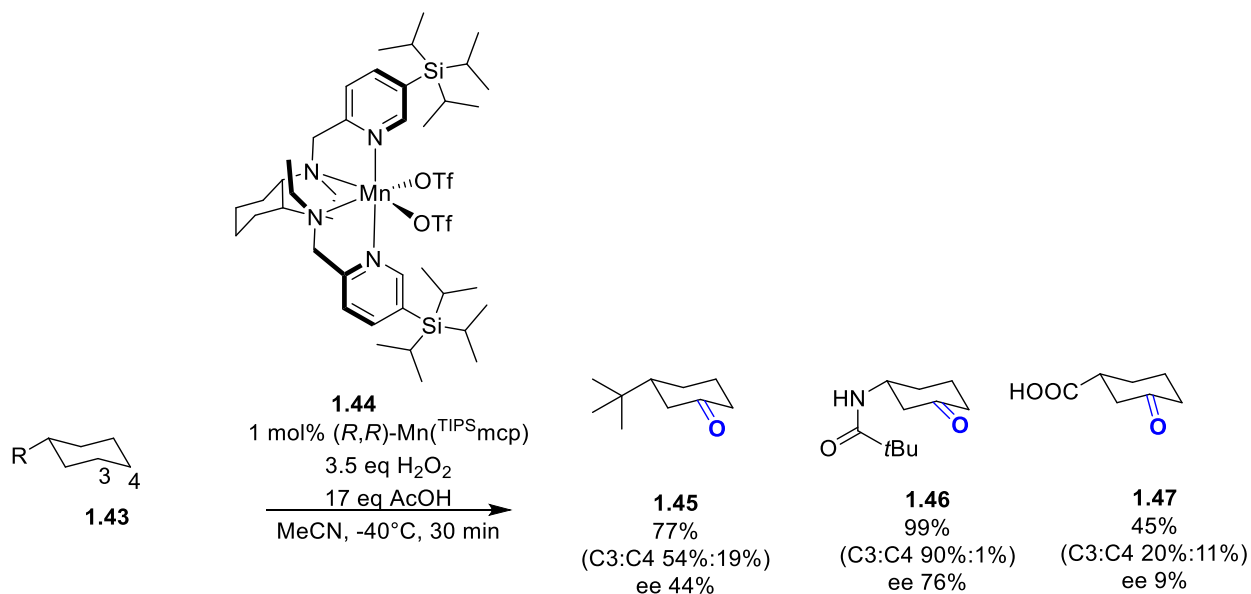
The Fe(PDP) reactions are run in an acidic environment with half an equivalent of acetic acid. Given this, there was a possibility that these catalysts could be used for C–H hydroxylation in the presence of unprotected amines. C–H functionalization in the presence of unprotected amines can be difficult given their strong nucleophilicity, ease of oxidation, and ability to coordinate with metal catalysts. The White group utilized the addition of HBF₄ or BF₃ to deactivate the nitrogen lone pair through complexation allowing for remote C–H functionalization.²⁷ Modifying the conditions of this system with the addition of methyl triflate, they were able to selectively functionalize C–H bonds in the presence of amides.²⁸ The methyl triflate forms an imidate salt with amides present in the substrates that can be easily removed with sodium iodide. These modifications to reaction conditions demonstrate the capability for late-stage

functionalization in the presence of common functional groups utilizing these Fe (PDP) complexes **1.38** and **1.39**.

1.2.4 Manganese Hydroxylations

The bulky, chiral Mn (^{TIPS}mcp) catalyst (**1.44**) developed by Costas is capable of enantioselective C–H oxidation of methylene carbons.²⁹ These oxidations utilized a tetradentate ligand framework to siteselectivity oxidize methylene units. The secondary alcohols formed, however, are rapidly oxidized to their respective achiral ketones (**1.45-1.47**). The substrates explored are desymmetrized through oxidation and enable enantioselective oxidations (**Scheme 1.9**). The electronic and steric nature of the cyclohexane substrates greatly influenced the site selectivity of the reaction.

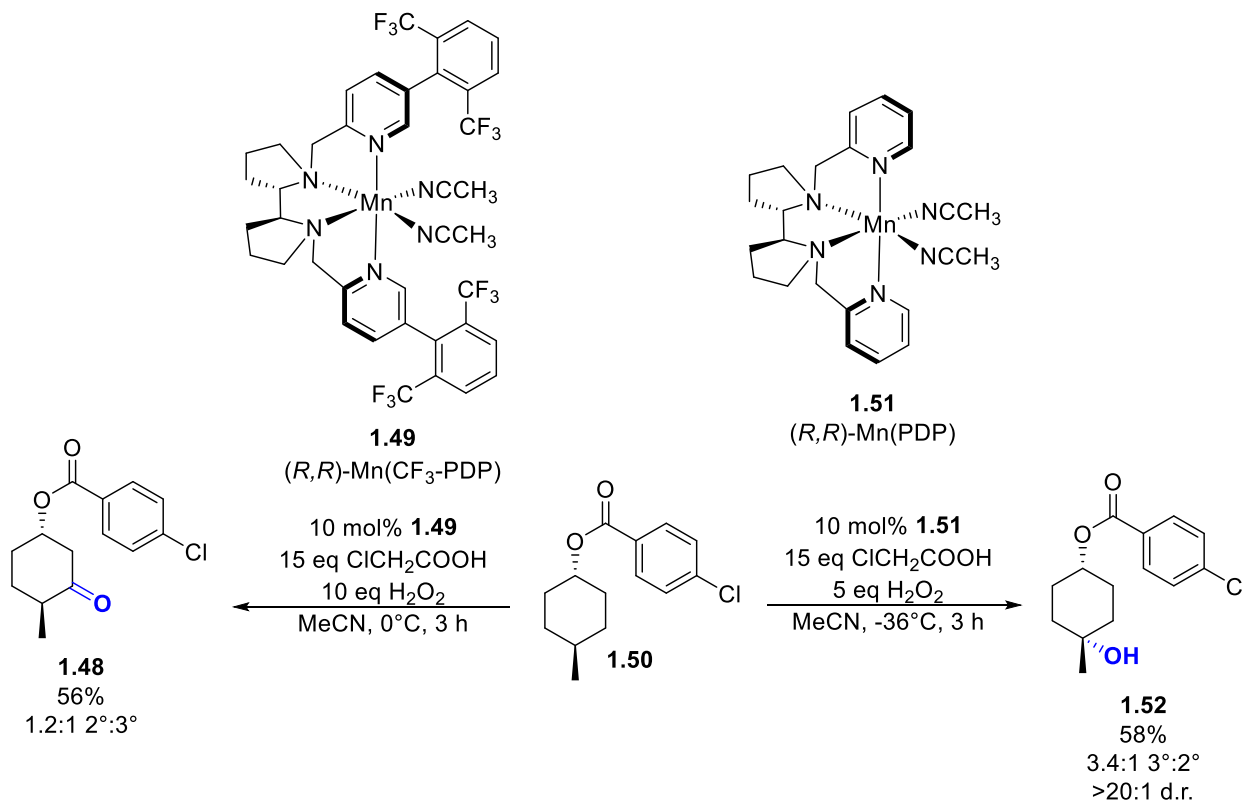
Scheme 1.9: Asymmetric manganese hydroxylation



White has also developed several manganese catalysts capable of hydroxylation in the presence of nitrogen heterocycles and methylene oxidation of drug scaffolds.^{30,31} By replacing iron

with manganese, the catalysts demonstrated improved tolerance of π -functionality that otherwise needed to be deactivated with the Fe (PDP) catalysts, due to the lower redox potential of manganese. These manganese complex catalysts were tolerant of amine functionality in the presence of a Bronsted acid like HBF_4 . The sterically larger CF_3 -PDP ligand (**1.49**) enables site-selective methylene oxidation (**1.48**) in the presence of weaker tertiary C–H bonds and helps disfavor the sterically demanding π -system oxidation, whereas the smaller PDP ligand (**1.51**) allows for access to these tertiary C–H bonds (**1.52**) (Scheme 1.10).

Scheme 1.10: Manganese ligand-controlled site-selective hydroxylations

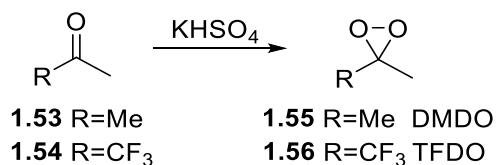


1.2.5 Organic *O*-atom Transfer Reagents

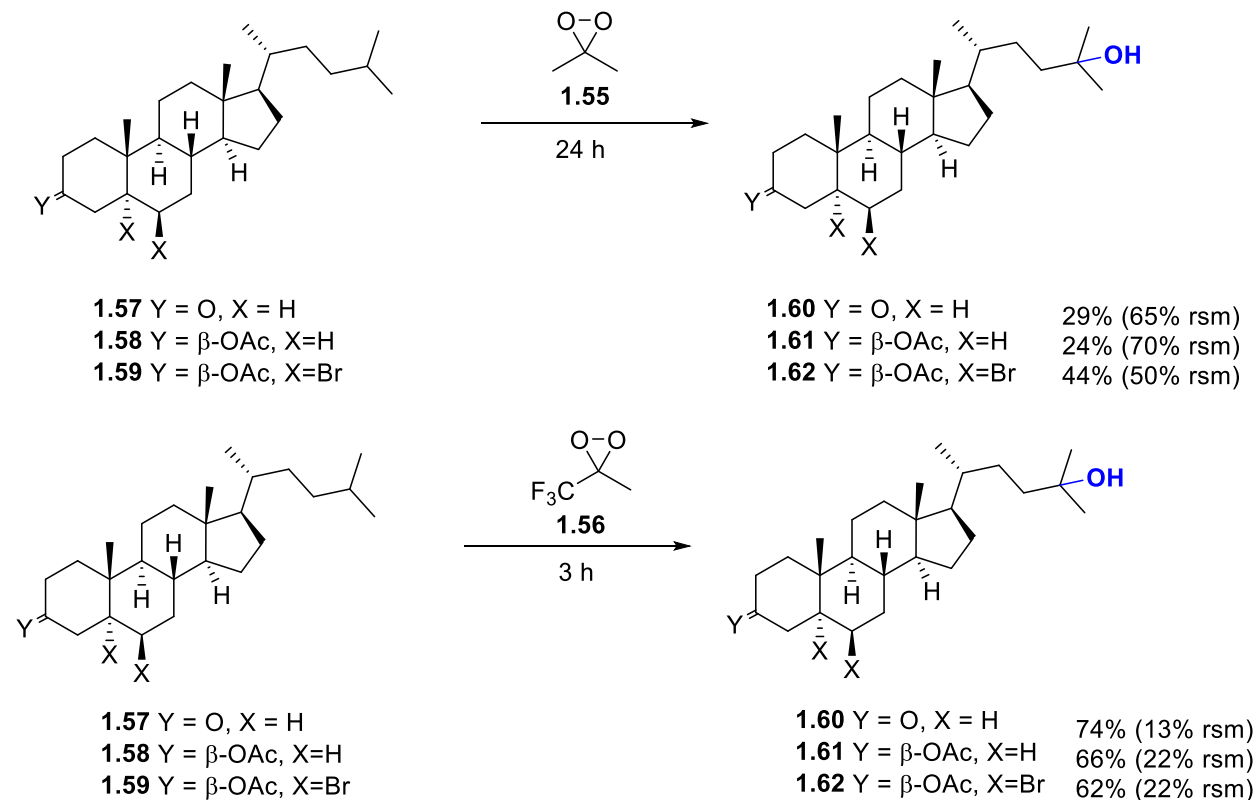
Organic C–H hydroxylation reagents have been used in synthetic chemistry since the 1980s given their relative ease of use and selectivity. These reagents tend to feature strained heteronuclear

rings that react with C–H bonds. The most common of these reagents are dimethyldioxirane (DMDO, **1.55**) and the more powerful trifluoromethyldioxirane (TFDO, **1.56**) (**Scheme 1.11**). Reactivity of **1.55** is enhanced by incorporating an electron-withdrawing trifluoromethyl group to form **1.56**. However, it is also less stable under prolonged storage. Use was further complicated by the ketone precursor, 1,1,1,-trifluoroacetone (**1.54**), possessing a high volatility with a b.p. of 23°C.³² Despite inherent difficulties in use, these strained three-membered heteronuclear rings have been used for oxidations, and also have the added benefit of less toxic byproducts and cheaper commercial availability than most metal catalysts. However, they are employed as superstoichiometric reagents amounts and are difficult-to-handle.

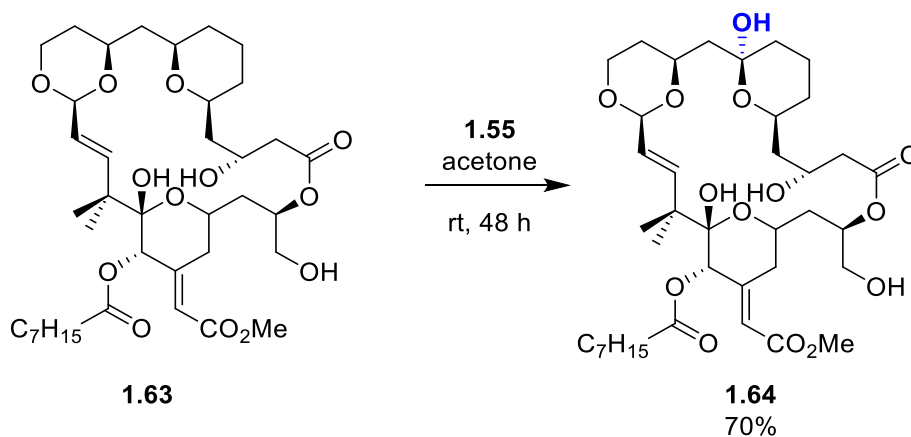
Scheme 1.11: Dioxiranes for *O*-atom Transfer



The dioxiranes exhibit moderate to high hydroxylation yields with predictable selectivity for a number of substrates. Given the highly electrophilic nature of these reagents, they can reliably react at the most electron-rich bond. The predictable and good yields led them to being synthetically useful, despite their preparative and storage inconveniences.³³ **1.56** was especially useful given its higher reactivity compared to **1.55** as shown by the yields and reaction times of the steroidal derivatives (**1.60-1.62**) (**Scheme 1.12**).

Scheme 1.12: Dioxirane oxidations of steroidal substrates

Some of the earlier uses of **1.55** in late-stage functionalization were established by the Wender group, who were able to hydroxylate several Bryostatin analogues with high site-selectivity to often sole products (**1.64**). These hydroxylated derivatives were used to probe and test their binding to protein kinase C (**Scheme 1.13**).³⁴

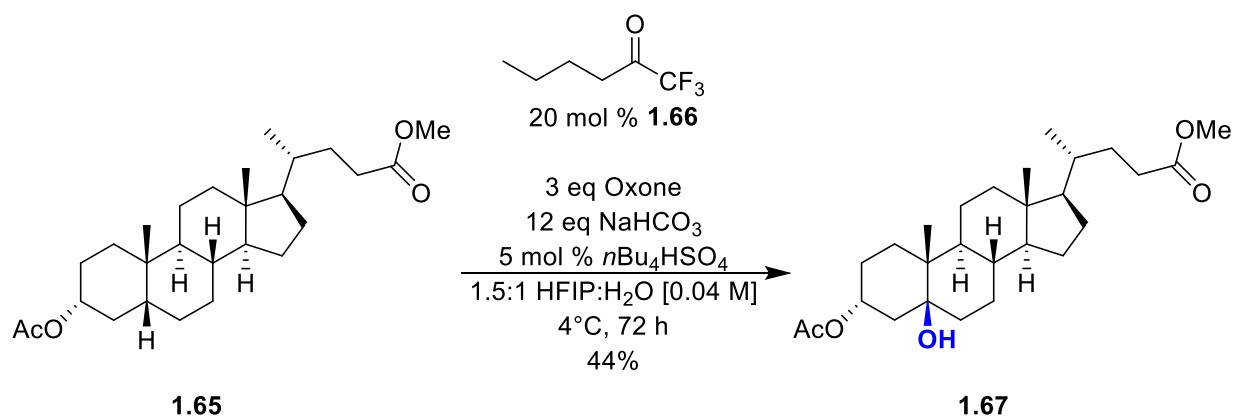
Scheme 1.13: Dioxirane oxidation of Bryostatins

To address issues related to the storage and handling of dioxiranes, conditions for the in situ generation of dioxiranes from ketones have been developed. Yang showed that **1.54**, in the presence of Oxone under neutral pH, was capable of epoxidizing a number of substrates.³⁵ This finding was expanded to chiral ketones, enabling a number of enantioselective epoxidations.³⁶ However, these early in situ methods were still incapable of C–H hydroxylations except on very limited substrates like adamantane.³⁷ More than a decade later, Baran and Houk used a sterically larger tert-butyl trifluoroacetone to form dioxiranes in situ and oxidize cyclohexane derivatives using super stoichiometric amounts.³⁸

Recent work from the Hilinski lab has shown that the hallmark substrate scope of stoichiometric dioxirane-mediated hydroxylations can be retained under catalytic conditions. We demonstrated hydroxylation of aliphatic C–H bonds on several highly reactive adamantane and decalin substrates³⁹ Further investigations into this protocol using a trifluoromethyl ketone (**1.66**) with Oxone as a terminal oxidant greatly expanded our substrate scope and functional group tolerance (**Scheme 1.14**).⁴⁰ The biphasic layer of the reaction proved to be both a benefit and a hindrance. The fluorinated solvent, 1,1,1,3,3,3-hexafluoroisopropanol (HFIP) helps promote the

reactivity of these ketones as it is known to help increase electrophilicity through hydrogen bonding.⁴¹ A phase transfer catalyst needed to be added to help transfer the Oxone into the organic layer to form the dioxirane. Substrates insoluble in HFIP like cholesterol derivatives needed a cosolvent that subsequently limited reactivity.

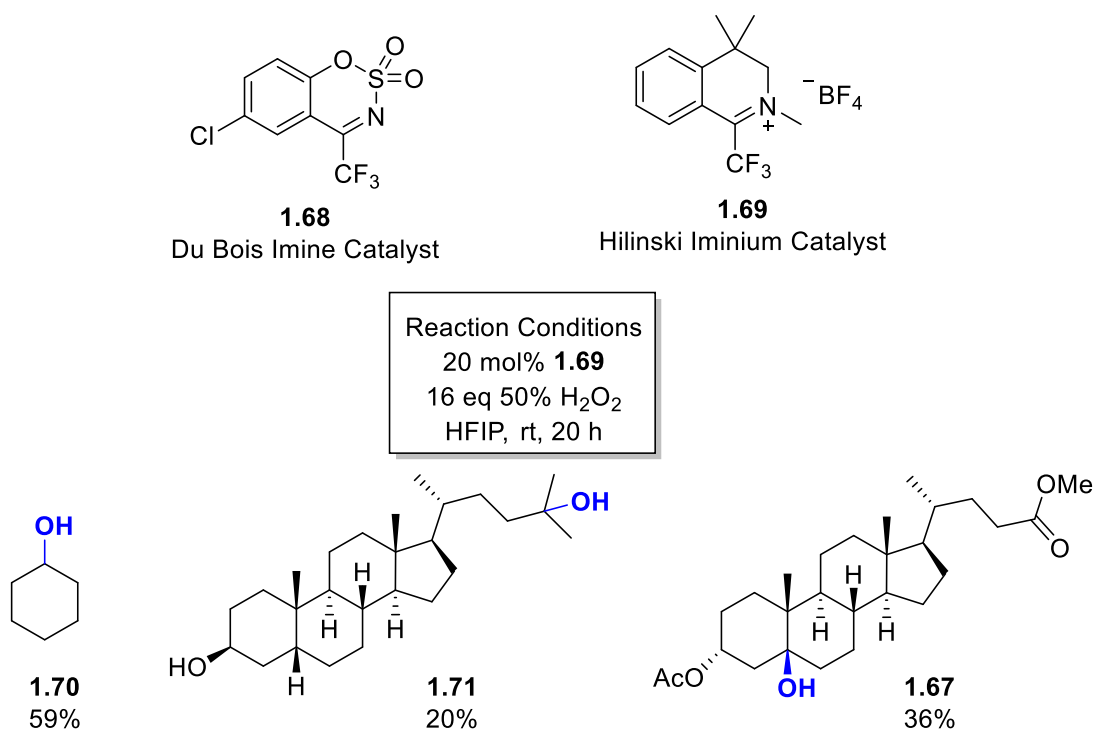
Scheme 1.14: Catalytic ketone dioxirane mediated C–H hydroxylation



Beyond dioxiranes, another series of heteronuclear rings have been developed for the expansion of the substrate scope of organocatalytic C–H hydroxylation. These rings: oxaziridines and oxaziridiniums, employ more electrophilic nitrogen atoms as members in an otherwise three-membered, oxygen-containing ring. Du Bois introduced the first benzoxathiazine catalyst (**1.68**) in 2005 that when exposed to perselenic acid, formed an oxaziridine intermediate capable of single tertiary C–H hydroxylation in modest yield.⁴² By introducing a fluorinated solvent like HFIP, there catalyst had a longer half-life and subsequently better substrate scope and yields. They also added additional functional groups to the aromatic ring of the benzoxathiazine to increase the electrophilicity of the catalyst providing higher yields.⁴³ Work by the Hilinski Lab further developed this class of catalyst with their iminium salt catalyst (**1.69**), capable of forming oxaziridiniums when exposed to hydrogen peroxide. By combining N-methyl substitution and the

addition of a trifluoromethyl group to an imine framework similar to the Du Bois catalyst, they created a highly effective catalyst capable of hydroxylation of various substrates in the presence of primary and secondary alcohols, an unprecedented accomplishment among many oxidizing catalysts at the time (**Scheme 1.15**).⁴⁴

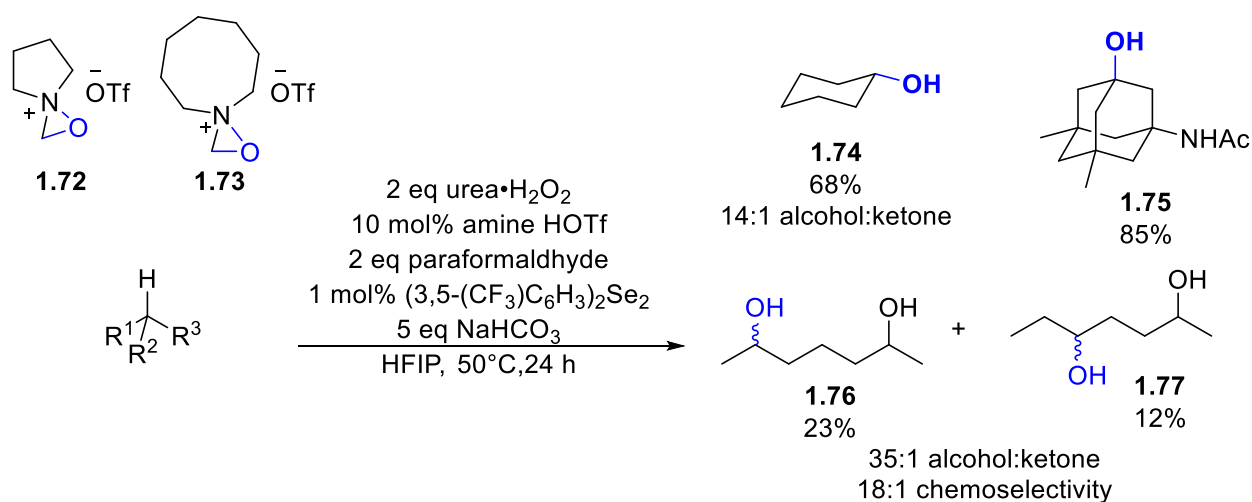
Scheme 1.15: Iminium-catalyzed C–H hydroxylation



Most recently, the Hilinski lab has shown that amines can catalyze site-selective aliphatic C–H hydroxylation via the in situ formation of oxaziridinium salts via iminium salts.⁴⁵ Yang and coworkers first demonstrated the feasibility of the general approach, using stoichiometric mixtures of amines and carbonyl compounds for asymmetric epoxidations.⁴⁶ However, this was a limited application only to epoxidation and required using high catalyst loading. The Hilinski lab were able to use a catalytic amount of secondary amine and formaldehyde with HFIP under basic conditions to allow for in situ formation of the active oxaziridinium species (**1.72**). This work

enabled tertiary and secondary C–H hydroxylation, and provided dramatic increases in chemoselectivity and yield in the presence of secondary and primary alcohols (**Scheme 1.16**). Utilization of amines opens up further exploration into amine design to address unsolved challenges in the catalyst control of selectivity and shows a promising direction for this field of organocatalytic *O*-atom transfer.

Scheme 1.16: Amine-catalyzed hydroxylation



1.3. Late-Stage Aminations

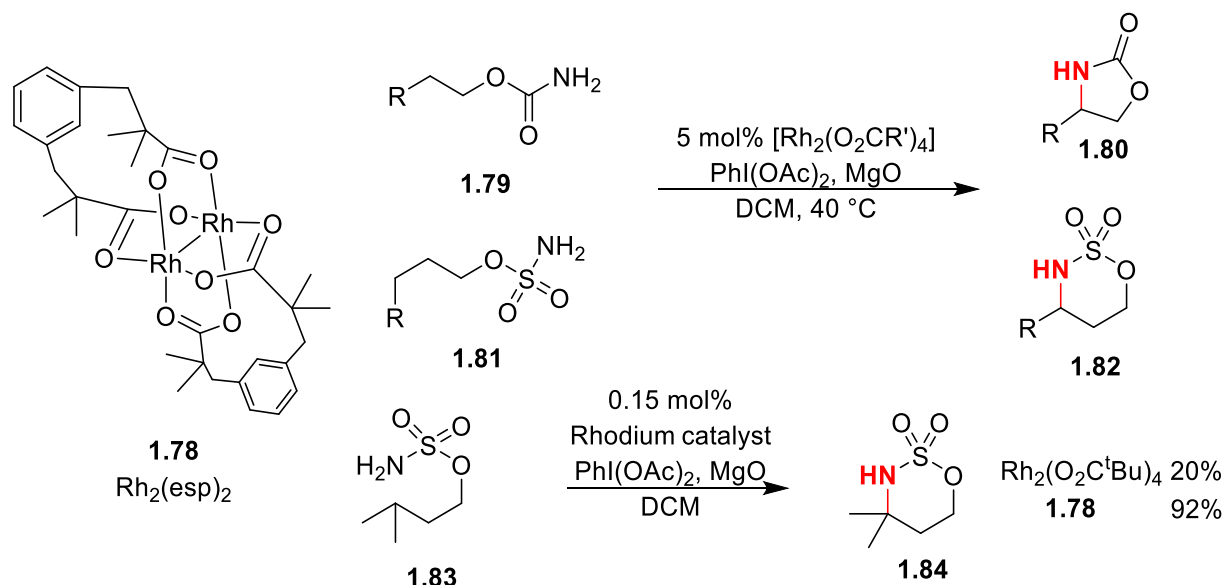
In addition to C–H hydroxylation, amination of C–H bonds is an equally enabling transformation that has received considerable attention in recent years, no doubt due to the prevalence of nitrogen functionality in both nature and therapeutics. Many of these methods involve a metal-nitrenoid C–H insertion, but only demonstrate moderate functional group tolerance. The first examples of these methods were introduced in the 1980s with Breslow's amination of cyclohexane using an iron or manganese porphyrin complex and N-sulfonyl iminoiodinane.⁴⁷ Metallonitrene intermediates allow for the insertion and functionalization to

occur close to the metal center, wherein the ligand has directed control over reactivity. Since this original work, the field has greatly expanded into utilizing metal- and organocatalyzed methods.

1.3.1 Rhodium Aminations

The first examples of rhodium-catalyzed C–H amination suffered from several factors that limited their use in late-stage functionalization: substrate used in excess, poor shelf-life of nitrogen source, and limited substrate scope.^{48,49} Du Bois' initial work with intramolecular C–H amination methods provided improvements in these areas, and eventually led to more efficient catalysts for intermolecular C–H functionalization.⁵⁰ This initial work utilized a catalytic amount of a rhodium carboxylate complex and the oxidant $\text{PhI}(\text{OAc})_2$ to oxidize and form the iminoiodinane in situ. Further investigations led to the development of the Espino ligand (abbreviated [esp]) for rhodium-catalyzed amination reactions (**Scheme 1.17**).⁵¹

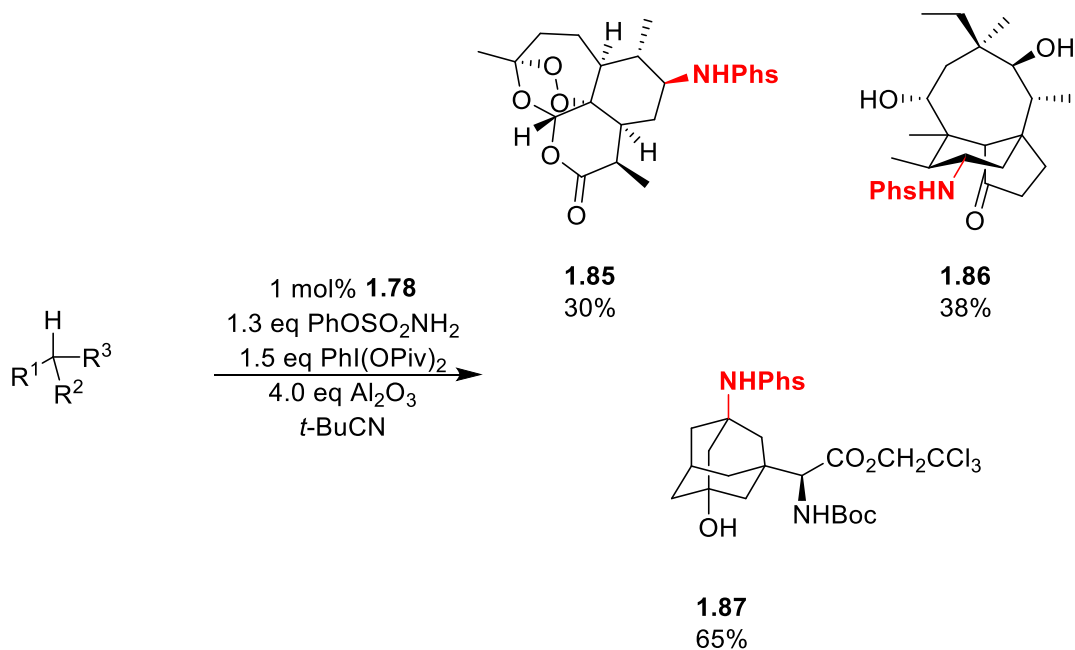
Scheme 1.17: Rhodium-catalyzed intramolecular amination



The Espino ligand is a tethered dicarboxylate, which limits carboxylate ligand detachment from the dinuclear Rh center. This careful design greatly enhanced the efficiency of the rhodium catalyst allowing for inter- and intra-molecular amination, as well as lower catalyst loading. This rhodium complex provides a more stable intermediary Rh (II)/(III) dimer that would normally decompose in solution.⁵²

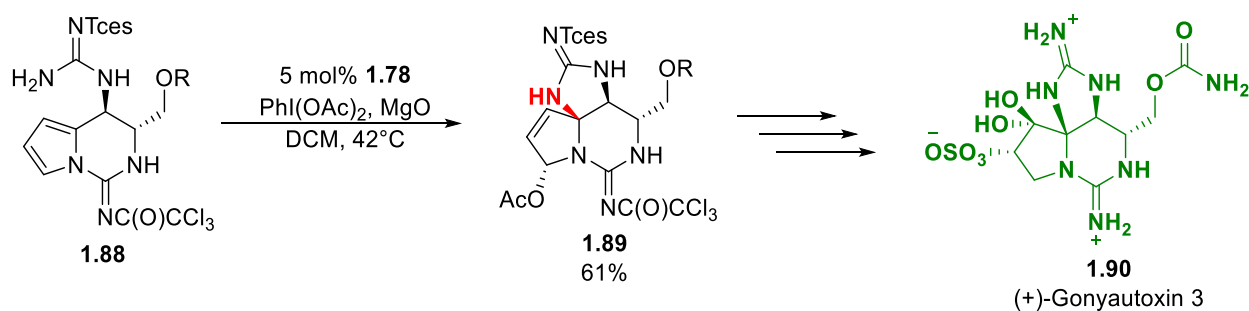
With improved half-life, there is subsequently more time for the catalyst to be reduced by carboxylic acids present in the mixture. Du Bois's latest work with this catalytic system improved scope and yield by further optimization of solvent and oxidant to prevent solvent oxidation and catalyst degradation (**Scheme 1.18**).⁵³ This new method allows for amination at benzylic and tertiary sites with a substrate scope that includes natural product drug targets and functional group tolerance of free alcohols, protected amines, amides, and esters with moderate yields, along with a more labile Phs protecting group on the inserted nitrogen.

Scheme 1.18: Rh₂(esp)₂ catalyzed intermolecular amination of complex substrates



Rhodium-catalyzed intramolecular and intermolecular amination has been utilized in the synthesis of a number of natural products. The synthesis of (+)-Gonyautoxin 3 (**1.90**) utilizes an early intramolecular guanidine amination. This step is regioselective for the pyrrole carbon and no amination was observed at the other proximal site (**Scheme 1.19**). Acetic acid, formed as a byproduct from the oxidant used in the reactions, also adds regio- and stereoselectively at the C12 carbon.⁵⁴

Scheme 1.19: Intramolecular guanidine amination



The functionalization of several steroid derivatives (**1.91,1.93,1.95-1.97**) was explored through this Rh-amination method after trying other late-stage functionalization options, including DMDO and ruthenium hydroxylations, that resulted in a mixture of products (**Scheme 1.20**). Functionalization was only successful for two (**1.91,1.93**) of the five steroids but did in fact produce a sole product, albeit in low yields (**Figure 1.4**). Previous work to functionalize at this site had required up to 21 steps. The functionalized amines were subsequently modified to include the attachment of biochemical dyes for further biological screening.⁵⁵

Scheme 1.20: Rh₂(esp)₂ catalyzed amination of brassinosteroid derivatives

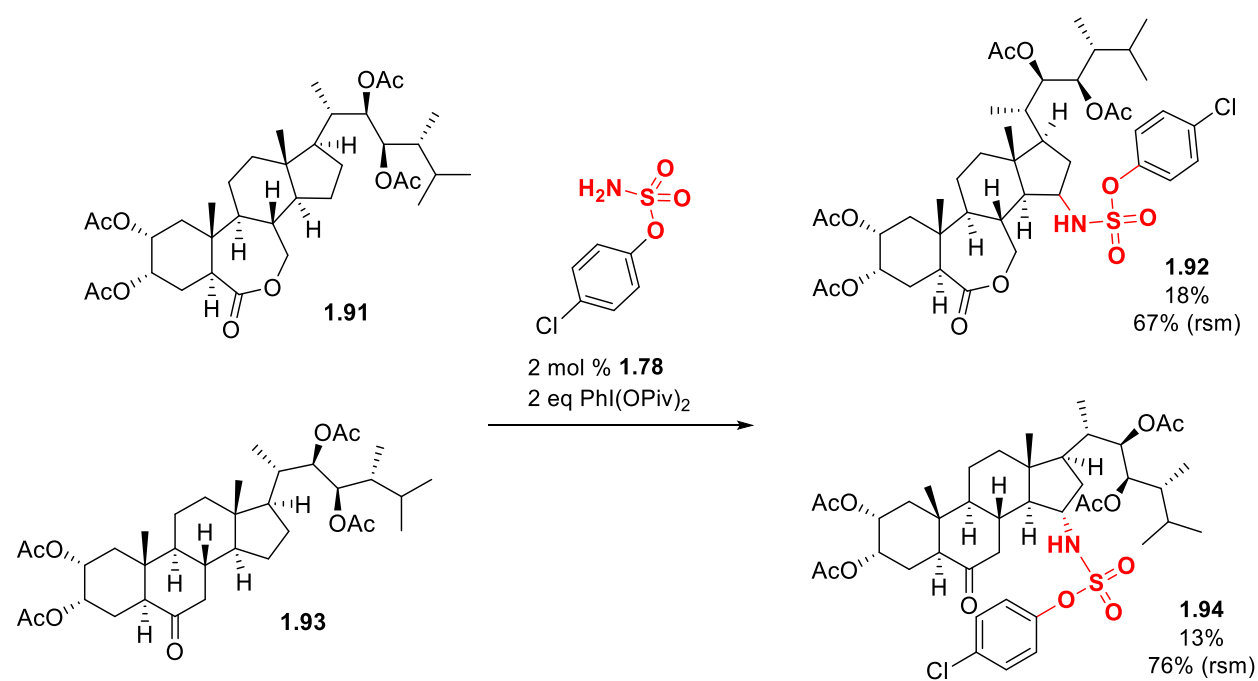
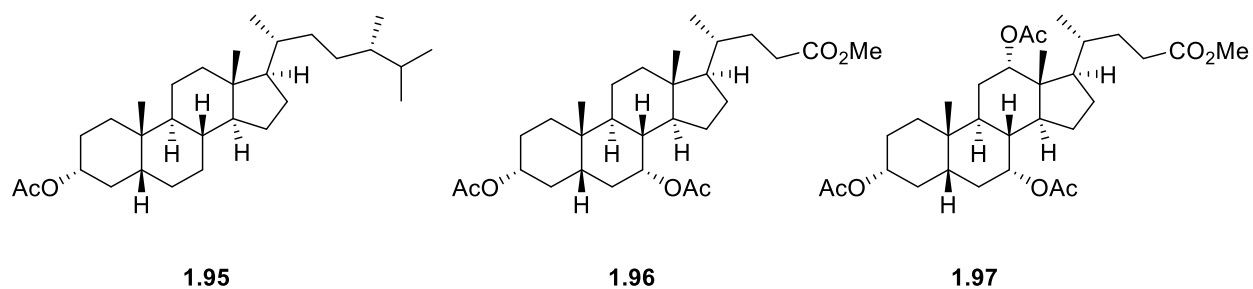
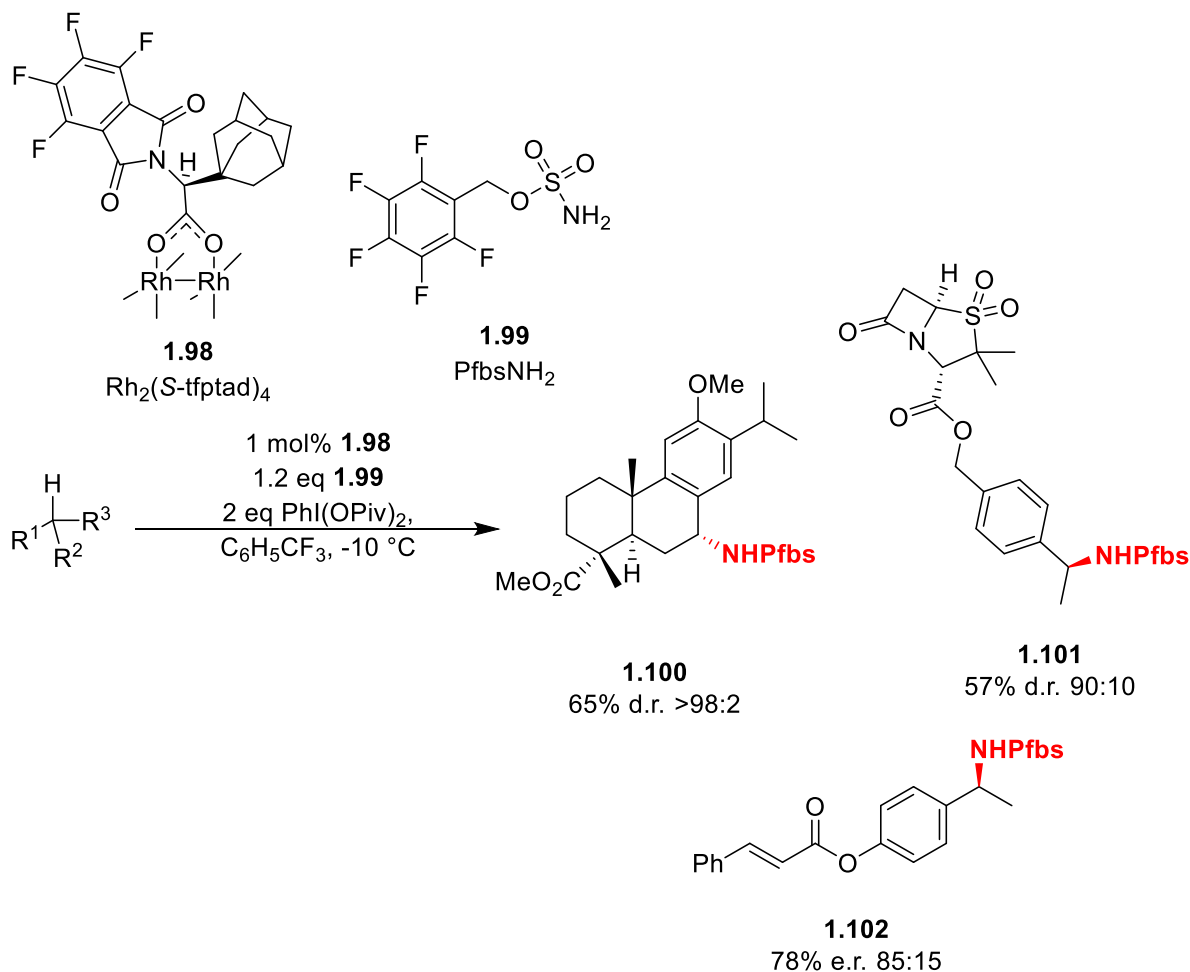


Figure 1.4: Unreactive steroid derivatives under Rh₂(esp)₂ amination conditions



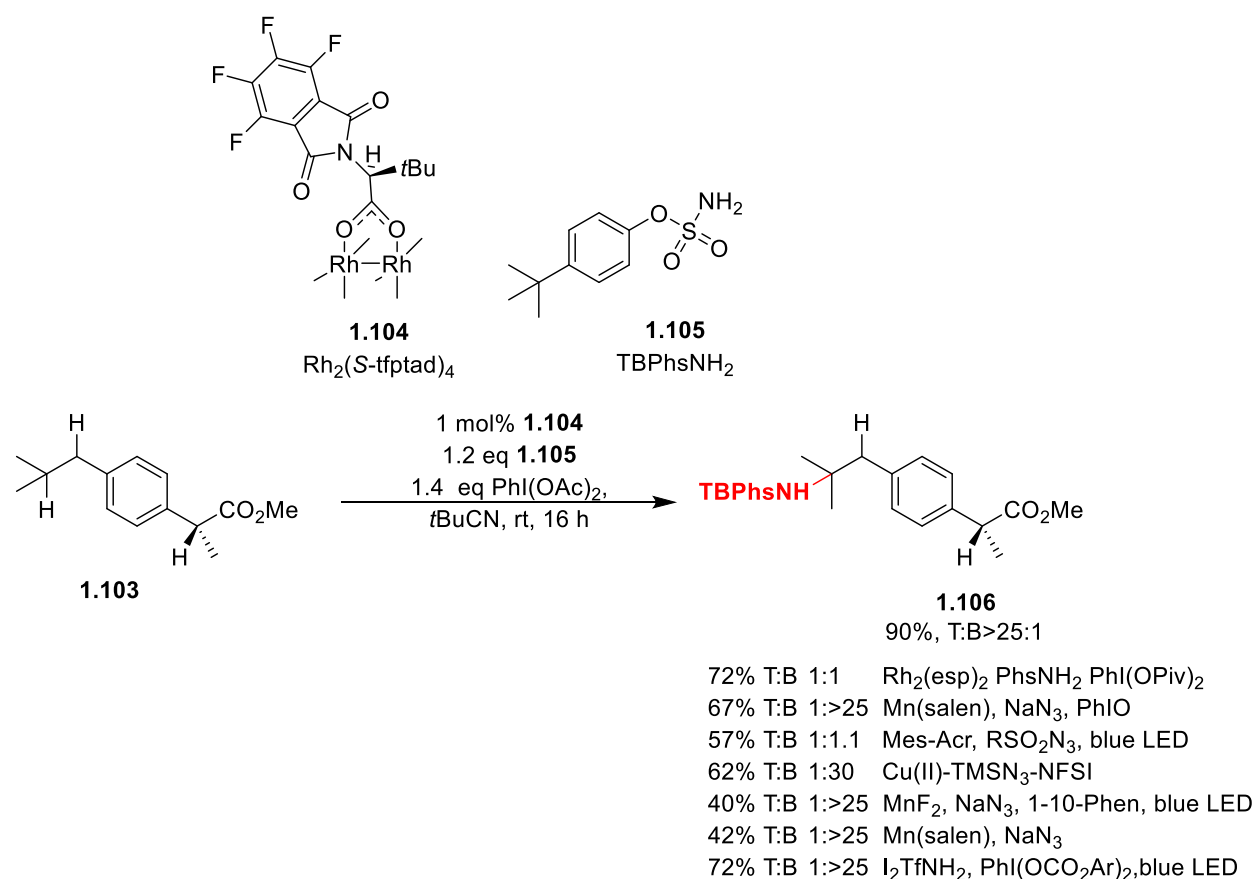
Inspired by the Rh₂esp₂ amination capabilities, the Dauban group investigated methods to provide asymmetric C(sp³)-H aminations. They explored new benzylic sulfamates as nitrene precursors and chiral rhodium (II) complexes, in combination, to develop this new method (**Scheme 1.21**).⁵⁶ Screening sulfamates, pentafluorobenzyl sulfamate (PfbsNH₂, **1.99**) provided their best yields and enantioselectivity that was further improved by a chiral rhodium complex with a sterically demanding adamantyl side chain (Rh₂(S-tfptad)₄, **1.98**). The combination of the halogenated sulfamate and halogenated rhodium ligand complex suggest halogen-bonding interactions contribute to a rigid chiral complex that helps enable the enantioselective amination of several complex analogs like dehydroabietate (**1.100**), sulbactam (**1.101**), and cinnamic acid (**1.102**).⁵⁷

Scheme 1.21: Enantioselective rhodium-catalyzed amination

This work was furthered to address regioselective amination between more reactive benzylic C–H bonds (BDE 85 kcal mol⁻¹) from tertiary C–H bonds (BDE 96 kcal mol⁻¹). The more activated benzylic site is always preferentially functionalized irrespective of the sulfamate or metal catalyst with substrates containing both C–H bonds in regards to Rh₂esp₂ aminations or manganese aminations. The Dauban group screened both the rhodium catalyst and sulfamate to provide the ideal set of conditions that enables intermolecular C–H amination of tertiary centers in the presence of benzylic positions with T/B ratio of >25:1 utilizing the synergistic combination of Rh₂(S-tfpttl)₄

(**1.104**) and *tert*-butylphenol sulfamate (TBPhsNH₂, **1.105**).⁵⁸ The phthalimido groups induce the formation of a tunable C₄-symmetrical hydrophobic pocket, not present in the Rh₂(esp)₂ complex. The bulky **1.105** was a sufficiently sterically demanding nitrene precursor that enables the high selectivity that aliphatic (TcesNH₂) or aryl sulfamates (**1.99**) cannot. The selectivity is demonstrated well on ibuprofen methyl ester (**1.103**) that would normally result in either mixtures of aminated products or benzylic amination under other conditions (**Scheme 1.22**).

Scheme 1.22: Rhodium-catalyzed selective tertiary C–H amination

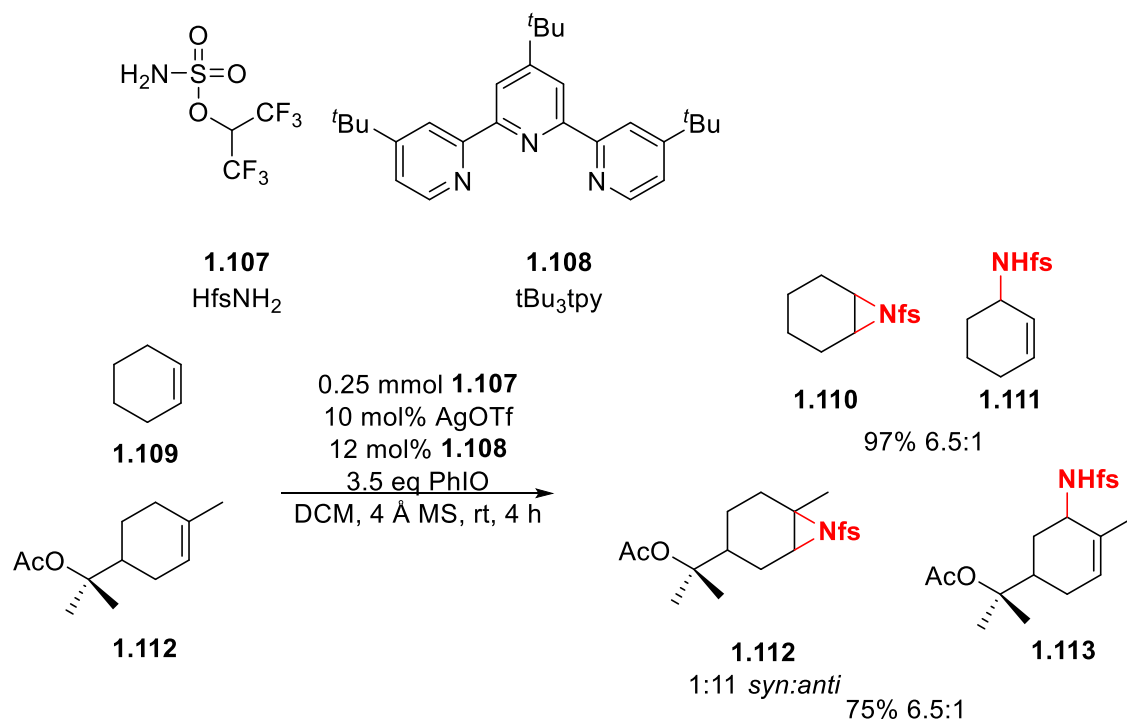


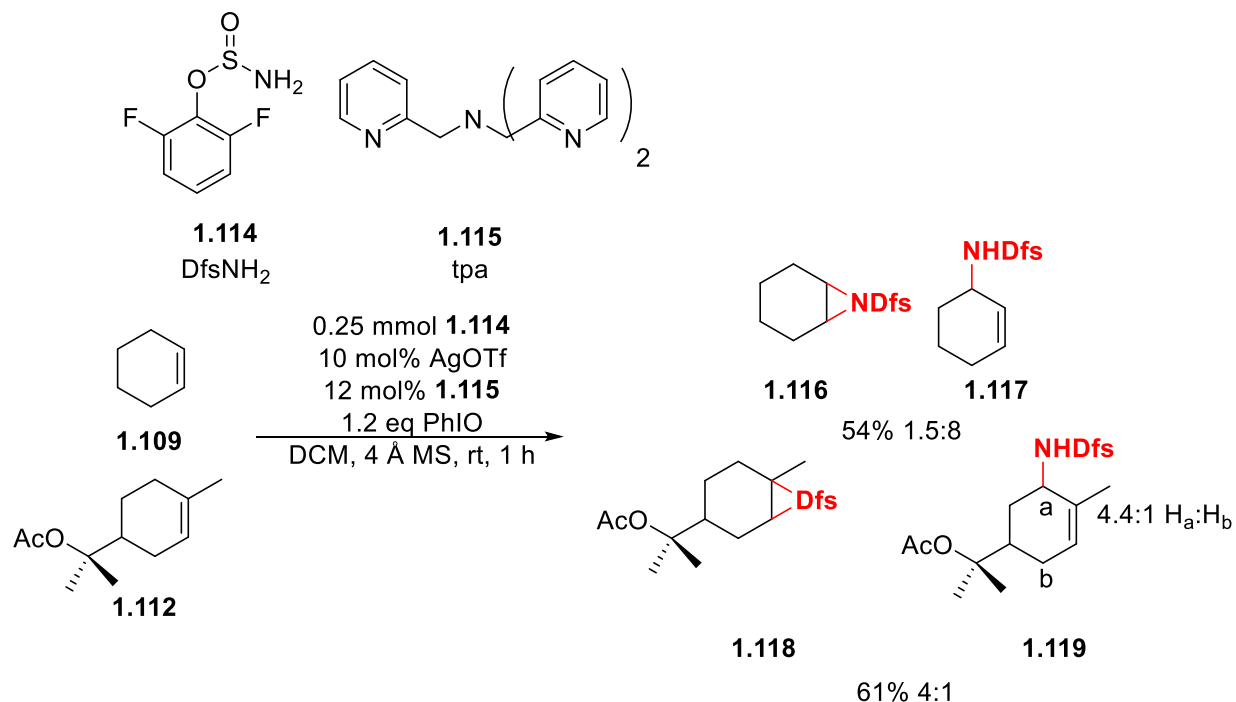
1.3.2 Silver Aminations

The Schomaker group has done extensive work to develop silver (I) catalysis for chemo- and site-selectivity of intramolecular nitrene transfer.⁵⁹ Expanding on this work towards

intermolecular amination has been more challenging but productive. Initial work began utilizing TcesNH₂ and cyclohexene to probe appropriate N-donor ligands for Ag catalysts. The *tert*-butylterpyridine (*t*bu₃tpy) ligand (**1.108**) was found to be effective for aziridination while Tris(2-pyridylmethyl)amine (tpa) ligand (**1.115**) was preferential towards allylic amination.⁶⁰ This chemoselectivity seems to originate from the difference in steric profiles of the Ag-nitrene intermediates and the two transformations occur through two distinct mechanisms. The selectivity of aziridination versus allylic amination was mostly independent of the nitrene precursor used, further demonstrating the dependence of the selectivity on the catalyst used. The hexafluoroisopropyl sulfamate (HfsNH₂, **1.107**) provided the best aziridination yields while 2,4-difluorobenzene sulfonamide (DfsNH₂, **1.114**) provided the best allylic amination yields. This reactivity was shown on several simple substrates with limited complexity in **Scheme 1.23** and **Scheme 1.24**. They later showed that Ag-catalyzed C–H intermolecular aminations are effective while using water as a solvent on several substrates.⁶¹

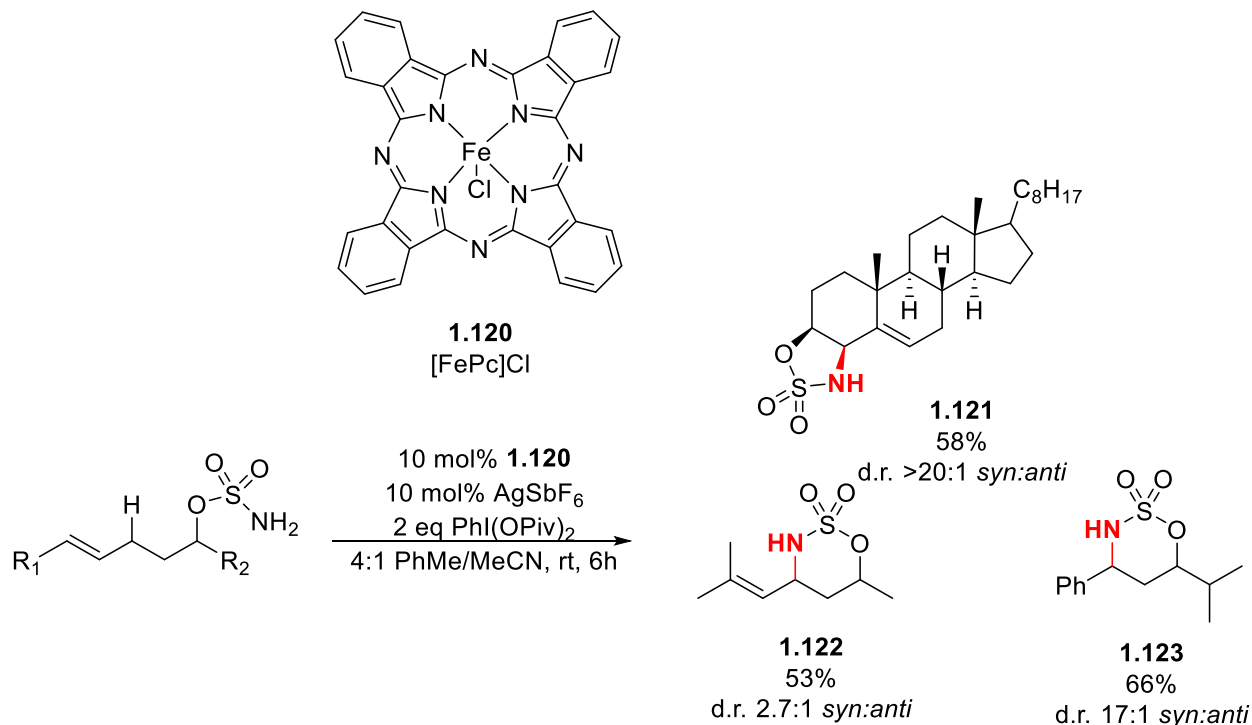
Scheme 1.23: Silver-catalyzed selective aziridination



Scheme 1.24: Silver-catalyzed selective intermolecular allylic amination

1.3.3 Iron Aminations

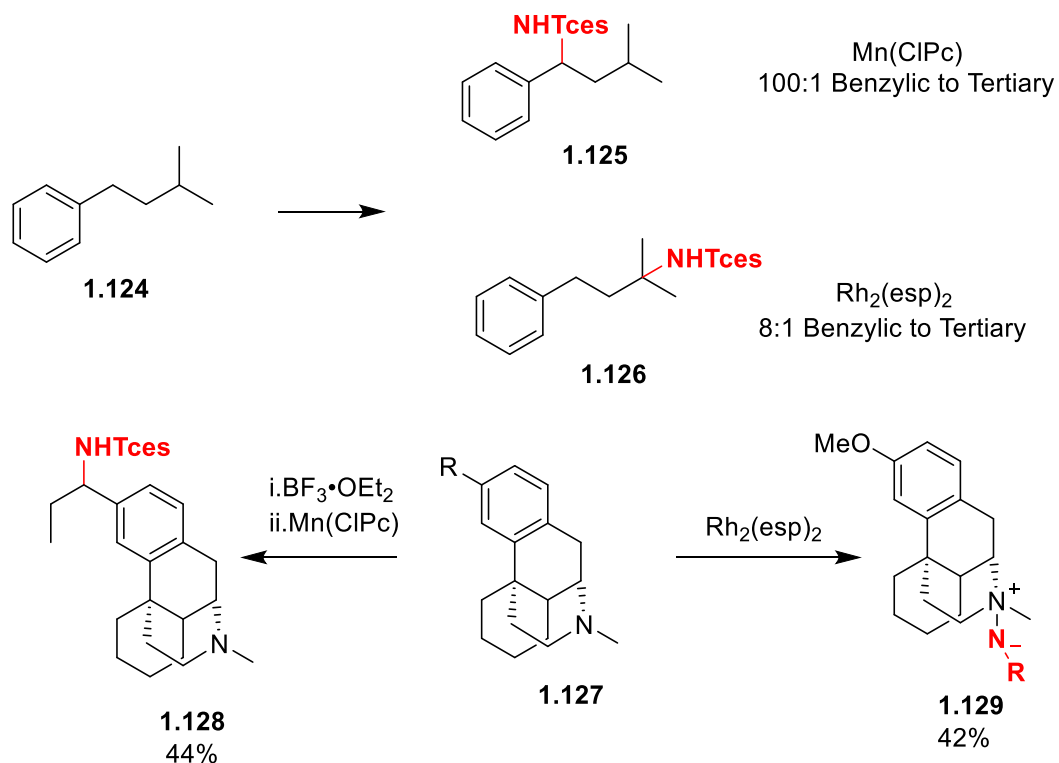
In addition to rhodium- and silver-catalyzed aminations, the White group has expanded upon work from Breslow's original porphyrin iron catalysis that had been relatively unexplored since then. They developed an Iron (III) phthalocyaninato ($[\text{Fe}^{\text{III}}\text{Pc}]$) (**1.120**) catalyzed intramolecular allylic C–H amination reaction with high chemo- and site-selectivities with strong preference to allylic amination over aziridination (**Scheme 1.25**).⁶² They initially screened their previously disclosed Fe(PDP) hydroxylation catalysts finding some low conversion before improvement with a porphyrin ligand. The phthalocyanine ligand provided the best results by providing a more electrophilic metal center due to the increased electron-withdrawing nature of the ligand. Mechanistic studies suggest a stepwise process for functionalization that occurs via initial homolytic C–H bond abstraction followed by a rapid radical rebound.

Scheme 1.25: Iron-catalyzed C–H amination

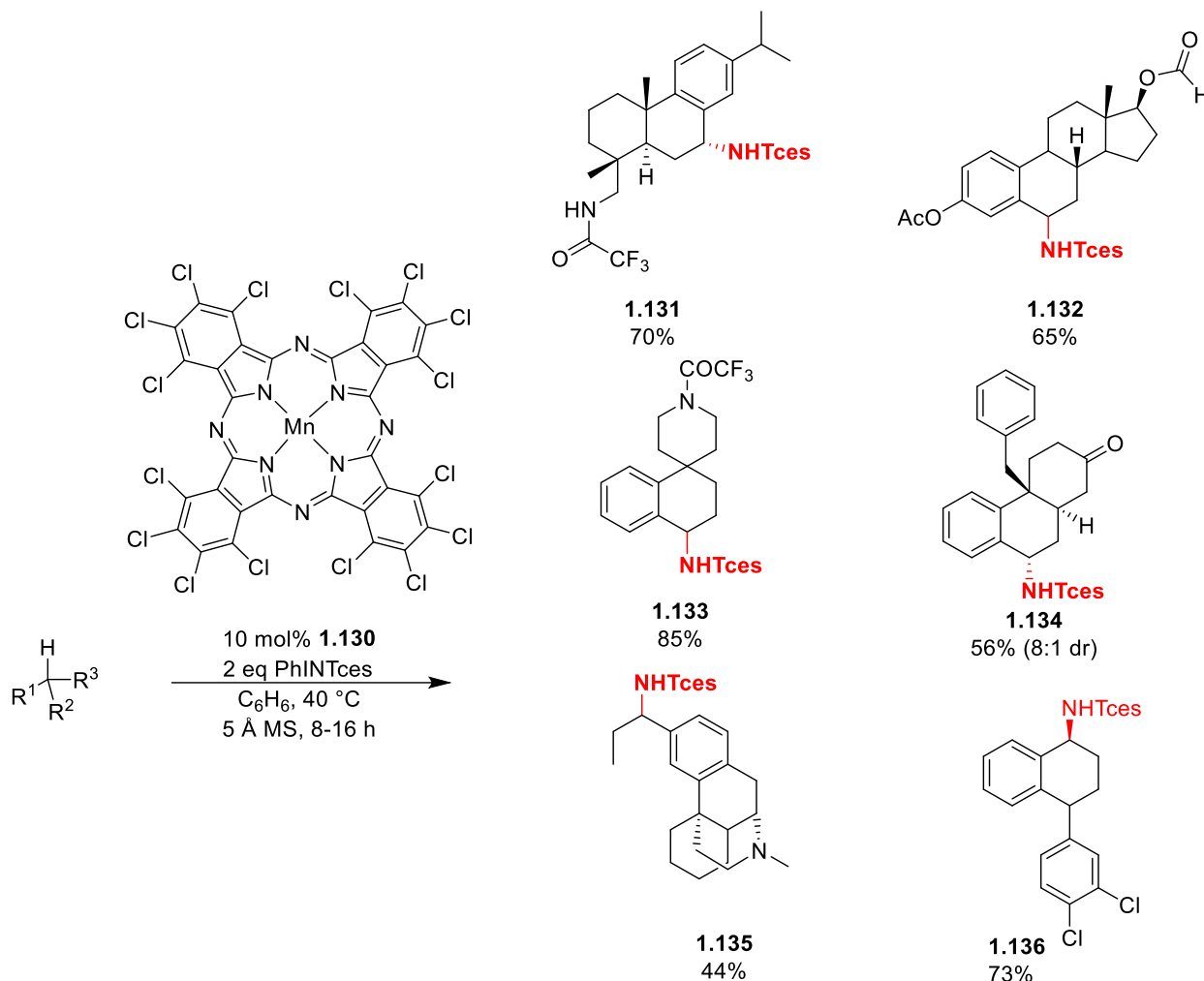
1.3.4 Manganese Aminations

Other metal centers have also been investigated for activity as amination catalysts. Manganese porphyrin-based catalysts have made a lot of progress for C–H hydroxylation and are reasonably effective as C–H amination catalysts, proceeding by a stepwise metallonitrene mechanism. The White group has worked to develop a novel ligand framework that could overcome some of the chemo-selectivity challenges of rhodium amination catalysis. They discovered a perchlorophthalocyanine ligand framework with a hexafluoroantimonate counterion that provides enhanced electrophilicity to the metal complex. This system demonstrates a strong preference for amination at more electron-rich sites having a lower BDE and capable of aminating amine-containing substrates (**1.127**) after complexation with $\text{BF}_3 \cdot \text{OEt}_2$ (**Scheme 1.26**).

Scheme 1.26: Comparison of Mn(CIPc)SbF₆ amination and Rh₂(esp)₂ amination



With optimized reaction conditions, they are able to functionalize natural products with reasonable tolerance of amines, as well as some of the highest observed site-selectivities for comparable C–H amination methods (Scheme 1.27).⁶³

Scheme 1.27: Mn(ClPc)SbF₆ catalyzed C–H amination

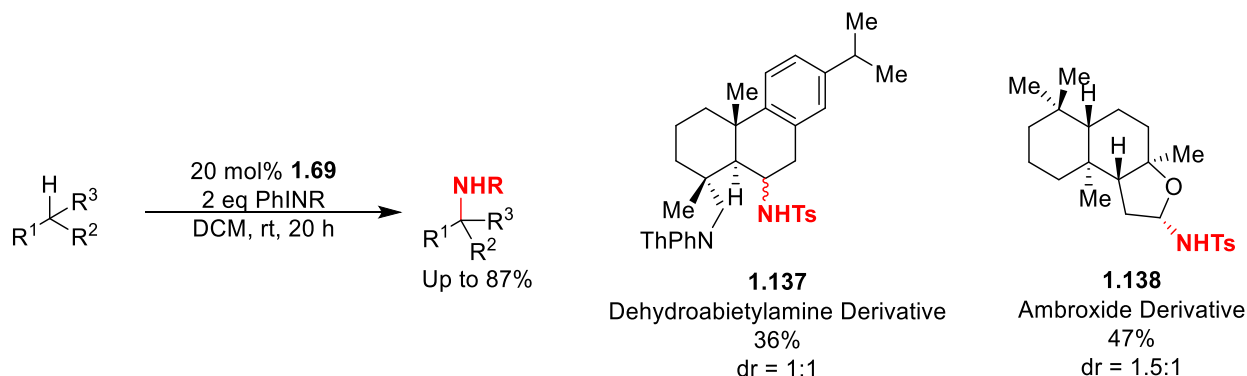
1.3.5 Organocatalytic Amination

While there are several examples of metal-catalyzed C–H amination, there are very few examples of organocatalytic C–H amination. Initial ideas postulated the use of diaziridiniums for nitrogen transfer, analogous to similar oxygen transfer methods using oxaziridiniums. Computation work by Houk initially supported that diaziridiniums might be capable reagents for aziridination of olefins.⁶⁴ Lambert and co-workers attempted to use preformed diaziridiniums for

nitrogen-transfer aziridination, but only observed ring-expansion products of their diaziridium reagent.⁶⁵

Ultimately, the Hilinski lab was first to successfully demonstrate a method for organocatalytic C–H functionalization utilizing their same hydroxylation iminium salt catalyst (**1.69**) and preformed iminoiodinane reagents for benzylic C–H amination (**Scheme 1.28**).⁶⁶ They were able to demonstrate this reactivity on several natural product analogues in moderate yields. Further work will be needed to expand this methodology's capability beyond highly activated C–H bonds and the installation of amines with more labile protecting groups, but still provides an initial step towards practical organocatalytic methods for late-stage C–H amination.

Scheme 1.28: Iminium-catalyzed C–H amination



1.4 Conclusions

In the past few decades, considerable effort has been given to the development of late-stage functionalization and have changed synthetic chemists' outlook on molecular construction. These methods have allowed for new synthetic pathways to diverse analogs of inherently complex natural products. Synthetic chemists are continuing to expand the toolbox of useful methods, and further investigation will help us to confront new and unforeseen synthetic problems, providing efficient

methods for drug development and diversification. Although numerous methods for C–H oxidations have been described, there are still areas of improvement including broader functional group tolerance and overriding inherent selectivity of substrates. Enantioselective catalysis continues to be a major goal, as well.

Further efforts towards the development organocatalytic methods of C–H oxidations are particularly fruitful, especially given the relatively lack of exploration in the area of C–H aminations. Organocatalytic methods might provide unique mechanisms of reactivity enabling site selectivity or enantioselectivity and functional group tolerance otherwise unavailable to transition metal systems. Organocatalytic C–H oxidations are a potentially untapped gold mine of applicable methods for synthesis and are ripe for exploration.

1.5 References

¹ Kelly, E. K.; Kim, N. A.; McCormick, J. C.; Stoltz, B.M. Late-Stage Diversification: A Motivating Force in Organic Synthesis. *J. Am. Chem. Soc.*, **2021**, *143* (41), 16890-16901.

² Newhouse, T.; Baran, P. S. If C–H Bonds Could Talk: Selective C–H Bond Oxidation. *Angew. Chem., Int. Ed.*, **2011**, *50*, 3362.

³ White M.C.; Zhao, J. Aliphatic C–H Oxidations for Late-Stage Functionalization. *J. Am. Chem. Soc.*, **2018**, *140* (43), 13988-14009.

⁴ Sawada, S.; Okijima, S.; Aiyama, R.; Nokata, K.; Furuta, L.T.; Yokokura, T.; Sugino, E.; Yamaguchi, K.; Miyasaka, T. Synthesis and Antitumor Activity of 20(S)-Camptothecin Derivatives: Carbamate-Linked, Water-Soluble Derivatives of 7-Ethyl-10-hydroxycamptothecin. *Chem. Pharm. Bull.*, **1991**, *39*, 1446.

⁵ Omura, T. Forty years of cytochrome P450. *Biochemical and biophysical research communications.*, **1999**, *266* (3), 690-698.

⁶ Croteau, R.; Ketchum, R.E.; Long, R.M.; Kaspera, R.; Wildung, M.R. Taxol biosynthesis and molecular genetics. *Phytochem. Rev.*, **2006**, *5* (1), 75-97.

⁷ Nicolaou, K. C.; Montagnon, T. *Molecules That Changed the World: A Brief History of the Art and Science of Synthesis and Its Impact on Society*, 1st ed.; Wiley-VCH: Weinheim, **2008**.

-
- ⁸ Denis, J. N.; Greene, A. E.; Guenard, D.; Gueritte-Voegelein, F.; Mangatal, L. Potier, P. Highly efficient, practical approach to natural taxol. *J. Am. Chem. Soc.*, **1988**, *110* (17), 5917-5919.
- ⁹ Li, Z.; Zheng, J.; Li, W.D.Z. Diverse strategic approaches en route to Taxol total synthesis. *Chin. Chem. Lett.*, **2022**, *33* (12), 4957-4968.
- ¹⁰ Michaudel, Q.; Journot, G.; Regueiro-ren, A.; Goswami, A.; Guo, Z.; Tully, T. P.; Baran, P.S. Improving Physical Properties via C–H Oxidation: Chemical and Enzymatic Approaches. *Angew. Chem. Int. Ed.*, **2014**, *53* (45), 12091-12096.
- ¹¹ Baldwin, J. E.; Jones, R. H.; Najera, C.; Yus, M. Functionalization of unactivated methyl groups through cyclopalladation reactions. *Tetrahedron.*, **1985**, *41* (4), 699-711.
- ¹² Desai, L.V.; Hull, K.L.; Sanford, M.S.; Palladium-Catalyzed Oxygenation of Unactivated sp³ C–H Bonds. *J. Am. Chem. Soc.*, **2004**, *126* (31), 9542–9543.
- ¹³ Sharpe, R.J.; Johnson, J.S.; Asymmetric Total Synthesis of the Indole Diterpene Alkaloid Paspaline. *J. Org. Chem.*, **2015**, *80* (19), 9750-9766.
- ¹⁴ Trotta, A.H. Total Synthesis of Oridamycins A and B. *Org. Lett.*, **2015**, *17* (13), 3358-3361.
- ¹⁵ Tenaglia, A.; Terranova, E.; Waegell, B. Ruthenium-catalyzed C–H bond activation oxidation of bridged bicyclic and tricyclic alkanes. *Tet. Lett.*, **1989**, *30* (39), 5271-5274.
- ¹⁶ Martín, V. S.; Palazón, J. M.; Rodríguez, C. M.; Nevill, C. R. Ruthenium (VIII) Oxide. In *e-EROS: Encyclopedia of Reagents for Organic Synthesis*; New York: John Wiley and Sons, **2006**
- ¹⁷ McNeill, E.; Du Bois, J. Ruthenium-Catalyzed Hydroxylation of Unactivated Tertiary C–H Bonds. *J. Am. Chem. Soc.*, **2010**, *132* (29), 10202-10204.
- ¹⁸ McNeill, E.; Du Bois, J. Catalytic C–H oxidation by a triazamacrocyclic ruthenium complex. *Chem. Sci.*, **2012**, *3* (6), 1810-1813.
- ¹⁹ Mack, J.B.; Gipson, J.D.; Du Bois, J.; Sigman, M.S. Ruthenium-catalyzed C–H hydroxylation in aqueous acid enables selective functionalization of amine derivatives. *J. Am. Chem. Soc.*, **2017**, *139* (28), 9503-9506.
- ²⁰ McNeill, E. M. Ph.D. Dissertation, Stanford University, Stanford, CA, **2012**.
- ²¹ Groves, J. T.; McClusky, G. A. Aliphatic hydroxylation via oxygen rebound. Oxygen transfer catalyzed by iron. *J. Am. Chem. Soc.*, **1976**, *98* (3), 859-861.
- ²² Groves, J. T.; Nemo, T. E.; Myers, R. S. Hydroxylation and epoxidation catalyzed by iron-porphine complexes. Oxygen transfer from iodosylbenzene. *J. Am. Chem. Soc.*, **1979**, *101* (4) 1032-1033.

-
- ²³ Chen, K.; Que Jr, L. Evidence for the participation of a high-valent iron–oxo species in stereospecific alkane hydroxylation by a non-heme iron catalyst. *Chem. Commun.*, **1999**, *15*, 1375-1376.
- ²⁴ Chen, M.S.; White, M.C. A Predictably Selective Aliphatic C-H Oxidation Reaction for Complex Molecule Synthesis. *Science*, **2007**, *318*, 783-787.
- ²⁵ Bigi, M. A.; Reed, S. A.; White, M. C. Directed metal (oxo) aliphatic C–H hydroxylations: overriding substrate bias. *J. Am. Chem. Soc.*, **2012**, *134* (23), 9721-9726.
- ²⁶ Gormisky, P. E.; White, M. C. Catalyst-controlled aliphatic C–H oxidations with a predictive model for site-selectivity. *J. Am. Chem. Soc.*, **2013**, *135* (38), 14052-14055.
- ²⁷ Howell, J. M.; Feng, K.; Clark, J. R.; Trzepakowski, L. J.; White, M. C. Remote oxidation of aliphatic C–H bonds in nitrogen-containing molecules. *J. Am. Chem. Soc.*, **2015**, *137* (46), 14590-14593.
- ²⁸ Nanjo, T.; de Lucca Jr, E. C.; White, M. C. Remote, late-stage oxidation of aliphatic C–H bonds in amide-containing molecules. *J. Am. Chem. Soc.*, **2017**, *139* (41), 14586-14591.
- ²⁹ Milan, M.; Bietti, M.; Costas, M. Highly enantioselective oxidation of nonactivated aliphatic C–H bonds with hydrogen peroxide catalyzed by manganese complexes. *ACS Cent. Sci.*, **2017**, *3* (3), 196-204.
- ³⁰ Zhao, J.; Nanjo, T.; de Lucca, E. C.; White, M. C. Chemoselective methylene oxidation in aromatic molecules. *Nat. Chem.*, **2019**, *11* (3), 213–221.
- ³¹ Chambers, R.K.; Zhao, J.; Delaney, C.P.; White, M.C. Chemoselective tertiary C–H hydroxylation for late-stage functionalization with Mn(PDP)/chloroacetic acid catalysis. *Adv. Synth. Catal.*, **2020**, *362* (2), 417-423.
- ³² Mello, R. W.; Fiorentino, M.; Sciacovelli, O.; Curci, R. On the isolation and characterization of methyl (trifluoromethyl) dioxirane. *J. Org. Chem.*, **1988**, *53* (16), 3890-3891.
- ³³ Bovicelli, P.; Lupattelli, P.; Mincione, E. Oxidation of natural targets by dioxiranes. 2. Direct hydroxylation at the side chain C-25 of cholestane derivatives and of vitamin D3 Windaus-Grundmann ketone. *J. Org. Chem.*, **1992**, *57* (19), 5052-5054.
- ³⁴ Wender, P. A.; Hilinski, M. K.; Mayweg, A. V. Late-stage intermolecular CH activation for lead diversification: a highly chemoselective oxyfunctionalization of the C-9 position of potent bryostatin analogues. *Org. Lett.*, **2005**, *7* (1), 79–82.
- ³⁵ Yang, D.; Wong, M. K.; Yip, Y. C. Epoxidation of olefins using methyl (trifluoromethyl) dioxirane generated in situ. *J. Org. Chem.*, **1995**, *60* (12), 3887-3889.

-
- ³⁶ Yang, D.; Yip, Y. C.; Tang, M. W.; Wong, M. K.; Zheng, J. H.; Cheung, K. K. A C₂ symmetric chiral ketone for catalytic asymmetric epoxidation of unfunctionalized olefins. *J. Am. Chem. Soc.*, **1996**, *118* (2), 491–492.
- ³⁷ Yang, D.; Tang, M. W.; Wang, X.C.; Tang, Y.C. Regioselective Intramolecular Oxidation of Unactivated C–H Bonds by Dioxiranes Generated in Situ. *J. Am. Chem. Soc.*, **1998**, *120* (26), 6611–6612.
- ³⁸ Zou, L.; Paton, R. S.; Eschenmoser, A.; Newhouse, T. R.; Baran, P. S.; Houk, K. N. Enhanced Reactivity in Dioxirane C–H Oxidations via Strain Release: A Computational and Experimental Study. *J. Org. Chem.*, **2013**, *78* (8), 4037–4048.
- ³⁹ Pierce, C. J.; Hilinski, M. K. Chemoselective hydroxylation of aliphatic sp³ C–H bonds using a ketone catalyst and aqueous H₂O₂. *Org. Lett.*, **2014**, *16* (24), 6504–6507.
- ⁴⁰ Shuler, W. G.; Johnson, S. L.; Hilinski, M. K. Organocatalytic, Dioxirane-Mediated C–H Hydroxylation under Mild Conditions Using Oxone. *Org. Lett.*, **2017**, *19* (18), 4790–4793.
- ⁴¹ Dantignana, V.; Milan, M.; Cussó, O.; Company, A.; Bietti, M.; Costas, M. Chemoselective Aliphatic C–H Bond Oxidation Enabled by Polarity Reversal. *ACS Cent. Sci.*, **2017**, *3* (12), 1350–1358.
- ⁴² Brodsky, B. H.; Du Bois, J. Oxaziridine-mediated catalytic hydroxylation of unactivated 3° C–H bonds using hydrogen peroxide. *J. Am. Chem. Soc.*, **2005**, *127* (44), 15391–15393.
- ⁴³ Adams, A. M.; Du Bois, J. Organocatalytic C–H hydroxylation with Oxone® enabled by an aqueous fluoroalcohol solvent system. *J. Am. Chem. Sci.*, **2014**, *5* (2), 656–659.
- ⁴⁴ Wang, D.; Shuler, W. G.; Pierce, C. J.; Hilinski, M. K. An iminium salt organocatalyst for selective aliphatic C–H hydroxylation. *Org. Lett.*, **2016**, *18* (15), 3826–3829.
- ⁴⁵ Hahn, P. L.; Lowe, J. M.; Xu, Y.; Burns, K. L.; Hilinski, M. K. Amine Organocatalysis of Remote, Chemoselective C(sp³)–H Hydroxylation. *ACS Catal.*, **2022**, *12* (8), 4302–4309.
- ⁴⁶ Wong, M. K.; Ho, L. M.; Zheng, Y. S.; Ho, C. Y.; Yang, D. Asymmetric epoxidation of olefins catalyzed by chiral iminium salts generated in situ from amines and aldehydes. *Org. Lett.*, **2001**, *3* (16), 2587–2590.
- ⁴⁷ Breslow, R.; Gellman, S. H. Tosylamidation of cyclohexane by a cytochrome P-450 model. *J. Chem. Soc. Chem. Commun.*, **1982**, *24*, 1400–1401.
- ⁴⁸ Breslow, R.; Gellman, S. H. Intramolecular nitrene carbon-hydrogen insertions mediated by transition-metal complexes as nitrogen analogs of cytochrome P-450 reactions. *J. Am. Chem. Soc.*, **1983**, *105*, 6728–6729.

-
- ⁴⁹ Nägeli, I.; Baud, C.; Bernadelli, G.; Jacquier, Y.; Moran, M.; Müller, P. Rhodium (II)-Catalyzed CH Insertions with {[4-Nitrophenyl] sulfonyl} imino} phenyl- λ^3 -iodane. *Helv. Chim. Acta.*, **1997**, *80* (4), 1087.
- ⁵⁰ Espino, C. G.; Du Bois, J. A Rh-Catalyzed C–H Insertion Reaction for the Oxidative Conversion of Carbamates to Oxazolidinones. *Angew. Chem., Int. Ed.*, **2001**, *40*, 598–600.
- ⁵¹ Espino, C. G. Expanding the scope of C–H amination through catalyst design. *J. Am. Chem. Soc.*, **2004**, *126* (47), 15378–15379.
- ⁵² Du Bois, J. Rhodium-catalyzed C–H amination. An enabling method for chemical synthesis. *Org. Process Res. Dev.*, **2011**, *15* (4), 758–762.
- ⁵³ Chiappini, N. D.; Mack, J. B. C.; Du Bois, J. Intermolecular C(sp³)–H amination of complex molecules. *Angew. Chem. Int. Ed.*, **2018**, *57* (18), 4956–4959.
- ⁵⁴ Mulcahy, J. V.; Du Bois, J. A stereoselective synthesis of (+)-gonyautoxin 3. *J. Am. Chem. Soc.*, **2008**, *130*, 12630–12631.
- ⁵⁵ Hurski, A.L.; Kukel, A.G.; Liubina, A.I.; Baradzenka, A.G.; Straltsova, D.; Demidchik, V.; Drašar, P.; Zhabinskii, V.N.; Khripach, V.A.; Regio- and stereoselective C–H functionalization of brassinosteroids. *Steroids*, **2019**, *146*, 92–98.
- ⁵⁶ Nasrallah, A.; Boquet, V.; Hecker, A.; Retailleau, P.; Darses, B.; Dauban, P.; Catalytic enantioselective intermolecular benzylic C(sp³)–H amination. *Angew. Chem. Int. Ed.*, **2019**, *58* (24), 8192–8196.
- ⁵⁷ Lindsay, V.N.G.; Lin, W.; Charette, A.B.; Experimental Evidence for the All-Up Reactive Conformation of Chiral Rhodium(II) Carboxylate Catalysts: Enantioselective Synthesis of cis-Cyclopropane α -Amino Acids. *J. Am. Chem. Soc.*, **2009**, *131* (45), 16383–16385.
- ⁵⁸ Erwan, B.; Vincent, B.; Elsa, E.V.; Tanguy S.; Philippe, D.; Catalytic Intermolecular C(sp³)–H Amination: Selective Functionalization of Tertiary C–H Bonds vs Activated Benzylic C–H Bonds. *J. Am. Chem. Soc.*, **2021**, *143* (17), 6407–6412.
- ⁵⁹ Vine, L. E.; Zerull, E. E.; Schomaker, J. M.; Taming nitrene transfer with silver catalysts. *Synlett.*, **2021**, *32* (01), 30–44.
- ⁶⁰ Dolan, N. S.; Scamp, R. J.; Yang, T.; Berry, J. F.; Schomaker, J. M. Catalyst-Controlled and Tunable, Chemoselective Silver-Catalyzed Intermolecular Nitrene Transfer: Experimental and Computational Studies. *J. Am. Chem. Soc.*, **2016**, *138* (44), 14658–14667.
- ⁶¹ Alderson, J. M.; Corbin, J. R.; Schomaker, J. M. Investigation Of Transition Metal-Catalyzed Nitrene Transfer Reactions In Water. *Bioorg. Med. Chem.*, **2018**, *26*, 5270–5273.

-
- ⁶² Paradine, S.M.; White, M.C.; Iron-catalysed Intramolecular Allylic C–H Amination. *J. Am. Chem. Soc.*, **2012**, *134* (4), 2036–2039.
- ⁶³ Clark, J. R.; Feng, K.; Sookezian, A.; White, M. C. Manganese-catalysed benzylic C(sp³)–H amination for late-stage functionalization. *Nat. Chem.*, **2018**, *10* (6), 583-591.
- ⁶⁴ Washington, I.; Houk, K.N.; Armstrong, A. Strategies for the design of organic aziridination reagents and catalysts: Transition structures for alkene aziridinations by NH transfer. *J. Org. Chem.*, **2003**, *68*, 6497-6501.
- ⁶⁵ Allen, J.M.; Lambert, T.H. Synthesis and characterization of a diaziridinium ion. Conversion of 3, 4-dihydroisoquinolines to 4, 5-dihydro-3H-benzo [2,3] diazepines via a formal N-insertion process. *Tetrahedron*, **2014**, *70* (27-28), 4111-4117.
- ⁶⁶ Combee, L.A.; Raya, B.; Wang, D.; Hilinski, M.K. Organocatalytic nitrenoid transfer: metal-free selective intermolecular C(sp³)–H amination catalyzed by an iminium salt. *Chem. Sci.*, **2018**, *9*, 935-939.

Chapter Two

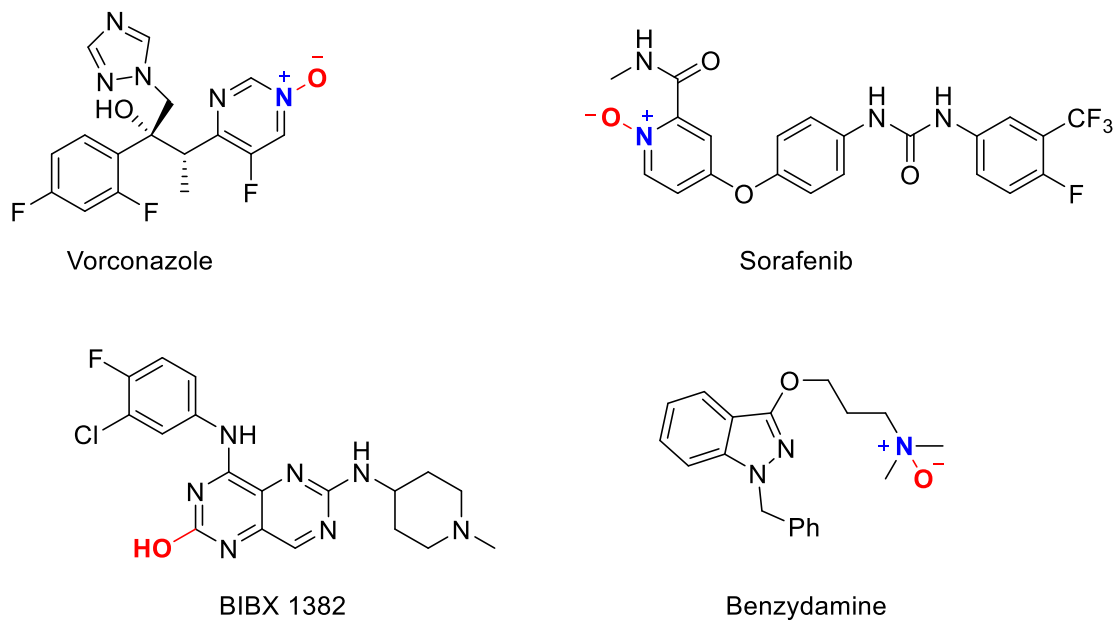
Chemoselective Oxidation of Nitrogen

2.1 Enzymatic Metabolism

Oxidative transformations represent one of the largest portions of transformations for phase I drug metabolism, wherein cytochromes P450 (CYPs) play a dominant role.¹ Incorporation of hydroxyl groups and other polar functional groups make molecules less lipid soluble and create sites for glucuronidation and other processes in Phase II drug metabolism that designate the molecule to be excreted.²

Although a large portion of metabolism is mediated by CYPs through C–H hydroxylation, other metabolic transformations by CYPs and other families of enzymes are critical to drug discovery. Nitrogen functionality, such as heterocycles, are abundant in substrates like natural product targets and therapeutic compounds with 59% of small-molecule drugs containing a nitrogen heterocycle.³ The metabolism of nitrogen functionality is generally divided into two transformations: direct N-oxidation mediated by CYP (**2.1**, **2.2**) or flavin-containing monooxygenase (FMO) family of enzymes (**2.4**), and C(sp²) –H hydroxylation adjacent to the nitrogen mediated by aldehyde oxidase (AO) family of enzymes (**2.3**).^{4,5,6} Several drug compounds and their sites of metabolism (SOM) are shown in **Figure 2.1**.

Figure 2.1: Oxidized nitrogen containing drugs by CYPs, FMOs and AO



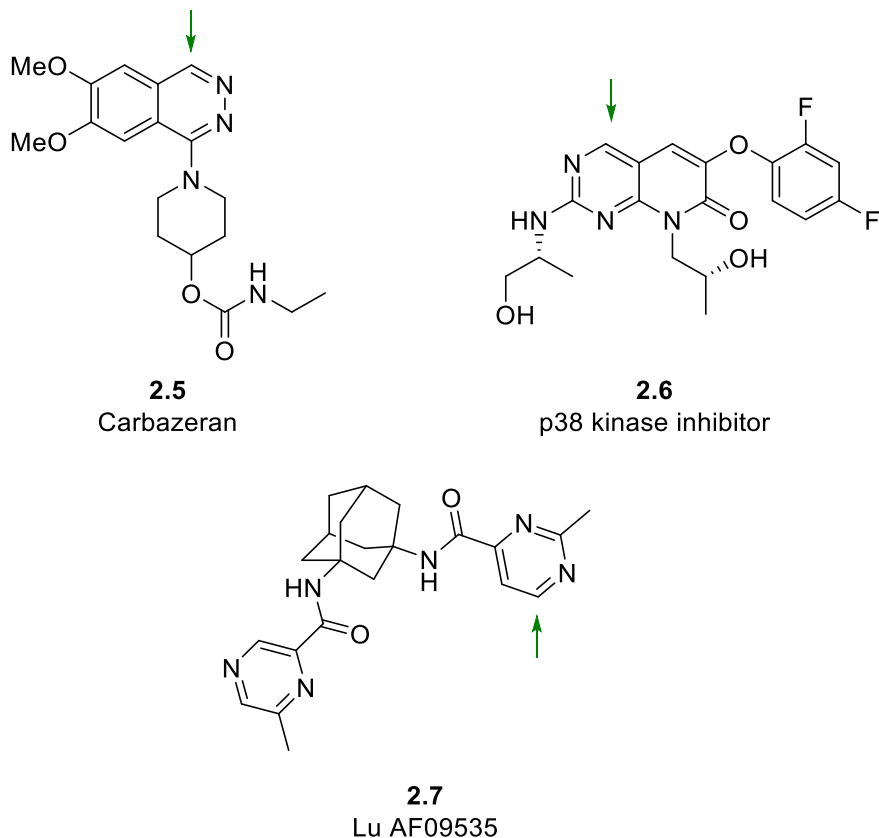
2.2 Metabolism and Drug Discovery

Understanding the metabolic fate of drug candidates remains an important and necessary aspect of drug development for pharmaceutical companies as metabolism relates to toxicity, drug clearance, and identification of the therapeutic active species.⁷ Pharmaceutical companies need to rapidly identify and characterize biological metabolites as they continue to develop a potential drug. Guidelines by the FDA require that metabolites circulating as >10% of the original parent drug must undergo safety testing, creating a strong demand for identification and understanding of metabolites.⁸ Identifying these metabolites remains a challenging task as drug compounds tend to be complex molecules containing a wide variety of functionality, wherein a number of metabolic enzymes can chemoselectively catalyze site-selective functionalization providing a multitude of potential metabolites. *In vitro* biotransformations continue to be the primary method of synthesizing these metabolites, even though synthetic methods would have potential advantages including scale, efficiency, and selectivity.⁹

2.3 Aldehyde Oxidase

Although there has been considerable research aimed at understanding CYPs for drug metabolism, other metabolic enzymes have received less attention. In particular, AO has become a more prominent issue for addressing drug metabolism due to its inherent reactivity targeting common scaffolds found in drug compounds.¹⁰ Investigations into the mechanism of AO suggest that oxidation occurs by nucleophilic attack at the aromatic carbon adjacent to the nitrogen by a molybdenum-oxo species present in the active site.¹¹ AO metabolism has been the main cause of several drug candidates failing trials due to unanticipated high clearance due to metabolic activity that went unnoticed in pharmaceutical models.^{12,13,14} In **Figure 2.2**, the green arrows indicates the unanticipated SOM for three known drug candidates to have failed due to AO. Given these issues, there have been more efforts of late to better understand the role this enzyme plays in drug metabolism.

Figure 2.2: Failed drug candidates due to AO metabolism



Efforts have been undertaken to better predict what drug candidates might be substrates for AO and the relevant SOM, thereby reducing the occurrence of this form of drug metabolism. Work by the Olsen lab utilized computational methods to analyze several known AO metabolites to help predict AO reactivity and sites of metabolism of potential drug compounds. The SOM can be reasonably predicted by calculating the lowest activation barrier of the transition state between the substrate and molybdenum active site of the enzyme.¹⁵ In 2020, computational predictions of AO activity and SOM of known and unknown AO substrates were evaluated and the computational data was corroborated with in vitro experiments to better demonstrate the validity of their predictive model.¹⁶ Based on the mechanistic understanding of AO, the Baran lab developed a

simple litmus test using the nucleophilic radical source, bis-(((difluoromethyl)sulfinyl)oxy)zinc (DFMS), to react with azaheteroarenes and thereby approximate susceptibility to AO-catalyzed metabolism. This method enabled both a straightforward analysis by LC-MS to determine potential reactivity and straightforward synthetic method to functionalize compounds near the AO site of metabolism.¹⁷

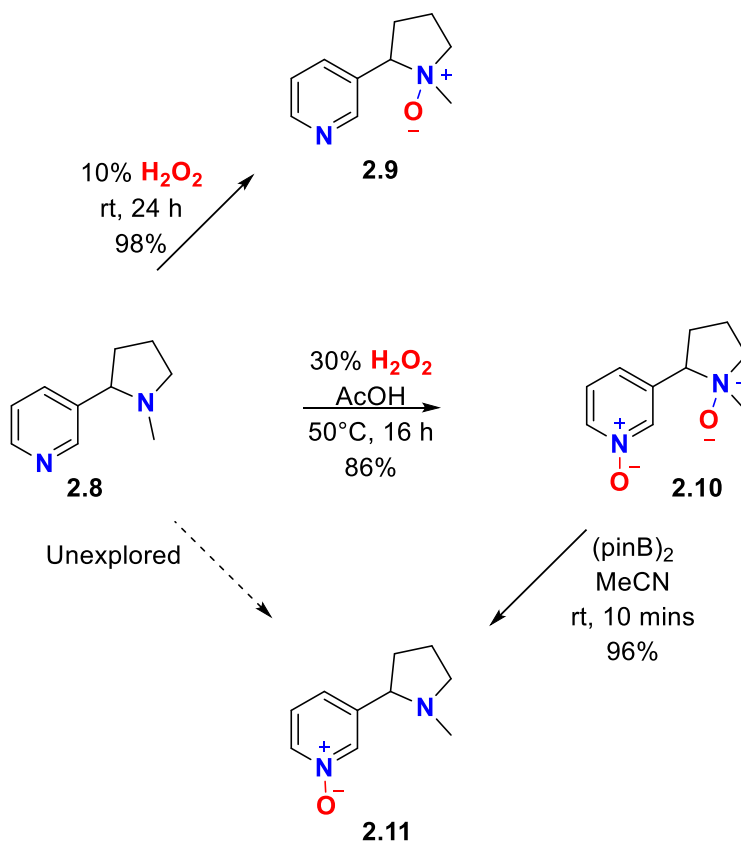
Most synthetic catalytic methods for oxidation cannot compete with the selectivity of enzymes, which have the advantage of highly evolved active sites. Enzymes use their large and complex structure to position a substrate into their active site optimizing electronic factors to enable chemoselective oxidations of these drug molecules. Given these continued efforts and attention to AO, synthetic methods that mimic late-stage AO transformations will hopefully expand the capability of medicinal chemistry.

2.4 Chemoselective Catalytic N-Oxidation

Even relatively simple molecules such as nicotine (**2.8**) highlight the need for methods for chemoselective nitrogen oxidation, as it contains two nucleophilic nitrogens, a pyridine and pyrrolidine. Under oxidative conditions, the more nucleophilic pyrrolidine nitrogen can be oxidized with high chemoselectivity (**2.9**). In contrast, chemoselective oxidations of less nucleophilic pyridyl nitrogens in the presence of aliphatic amines had not been reported (**2.11**). To address this challenge and selectively obtain pyridine N-oxides in the presence of more nucleophilic sp^3 nitrogens, a two-step protocol was adopted. The current synthetic strategy involves exhaustive oxidation of both nitrogens (**2.10**) followed by selective reduction to obtain the N-oxide of the less nucleophilic nitrogen (**2.11**). This continued to be the method of choice for obtaining the selectively oxidized heterocycle for nicotine since its development in the 1950s.¹⁸ Newer methods have been developed for the reduction of N-oxides using milder reagents like

diboron reagents that are even viable in cells, but the same synthetic principle of exhaustive oxidation and chemoselective reduction has remained (**Scheme 2.1**).^{19,20}

Scheme 2.1: Synthetic strategy to access pyridyl N-oxides

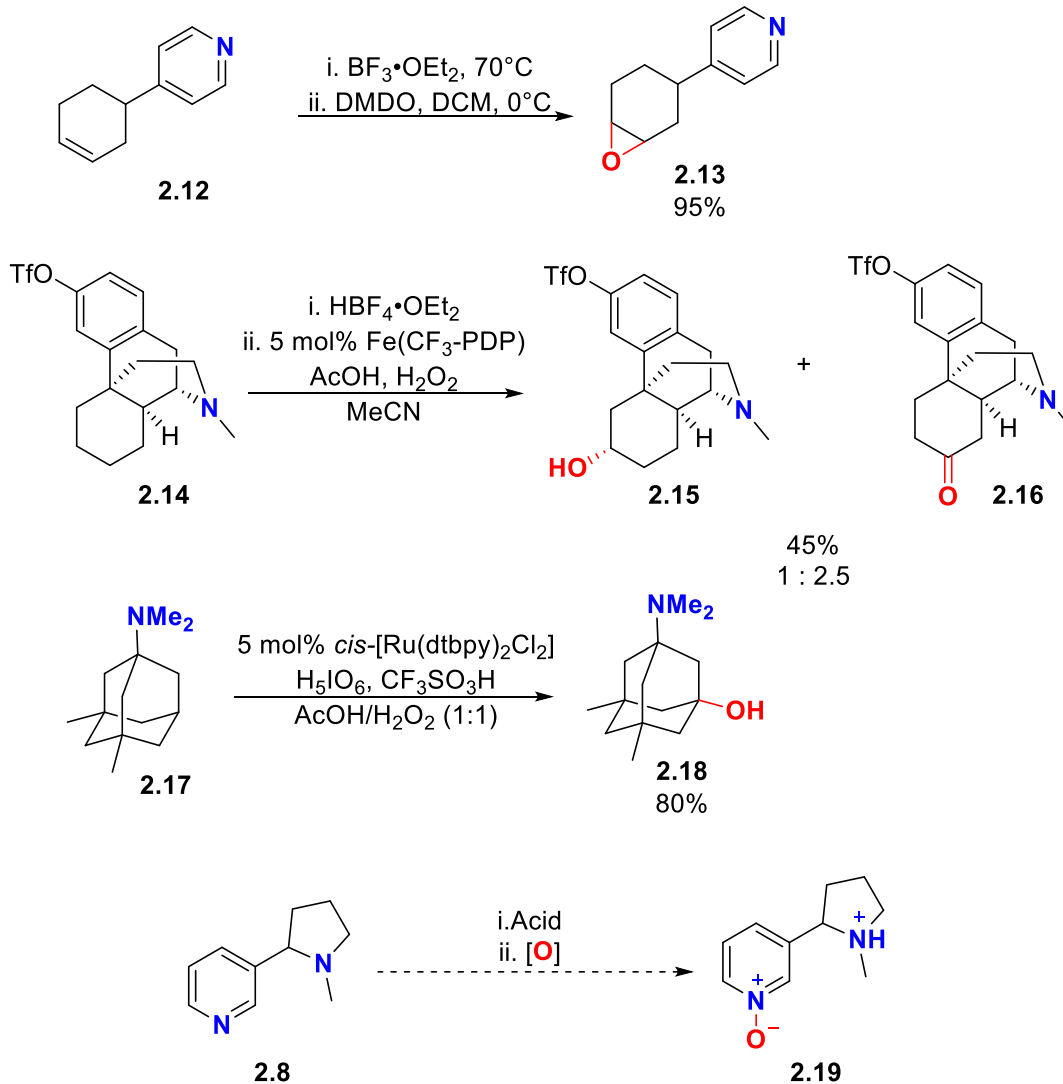


Given the exhaustive oxidation required, this method presents challenges to more complex drug compounds that contain more than two nucleophilic nitrogen atoms or other functional groups susceptible to oxidation. We therefore concluded that a method for chemoselectively oxidizing the less nucleophilic nitrogen on a complex molecule under mild conditions would be a considerable advancement in this field.

Looking to other site selective oxidation methods for inspiration, we hypothesized that the use of Brønsted acids could deactivate the more nucleophilic aliphatic amine. This in situ

protection strategy of nucleophilic amines has been prevalent in oxidative strategies for epoxidation and C–H oxidation. One of the first examples demonstrated selective oxidation of alkenes in the presence of nucleophilic nitrogen under acidic conditions with dioxiranes, such as the oxidation of alkene **2.12** to epoxide **2.13**.²¹ This approach was further advanced for terminal C–H hydroxylation of amines by the Sanford group with Pt catalysis using sulfuric acid to protonate the amine.²² That same year, the White group used a Brønsted acid to allow for selective oxidation of tertiary C–H bonds in nitrogen containing compounds with their Fe(PDP) catalyst. This transformation was demonstrated on the dextromethorphan analog **2.14** to form the alcohol **2.15** and ketone **2.16**.²³ Several years later, the Du Bois group used their Ru complex in triflic acid to oxidize amine **2.17** to **2.18**.²⁴ (**Scheme 2.2**).

Scheme 2.2: Strategy for chemoselective oxidations in the presence of free amines



Based on this precedent, we sought to apply the same concept to compounds containing multiple nucleophilic nitrogens. Due to nucleophilicity correlating with basicity, we hypothesized that we could take advantage of the relative differences in basicity and selectively oxidize the less nucleophilic pyridine in the presence of a single equivalent of Brønsted acid.²⁵

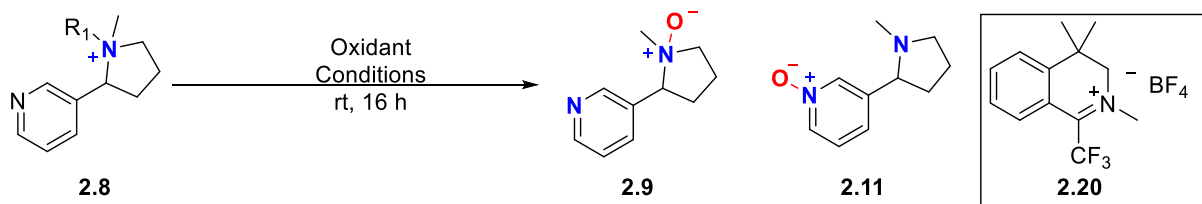
With this protonation strategy in mind, we investigated oxidation conditions that would tolerate an acidic environment. Our lab had previously developed an iminium salt catalyst **2.22**, capable of forming an oxaziridinium salt when exposed to hydrogen peroxide.²⁶ This

oxaziridinium was an effective catalyst for selective aliphatic C–H hydroxylation. In addition, the developed method exhibited chemoselectivity for remote C–H hydroxylation in the presence of primary and secondary alcohols. These previously developed conditions involved an acidic aqueous environment with the use of a fluorinated cosolvent, 1,1,1,3,3,3-hexafluoroisopropanol (HFIP). We hypothesized that this catalyst would be capable of oxidizing the desired azaheteroarenes in an acidic environment.

2.4.1 Reaction Development

To test our hypothesis, we utilized nicotine (**2.8**) as our substrate. Our initial investigations began with screening commercially available oxidants on a preformed nicotine HBF₄ salt with known oxidants capable of forming the pyrrolidine N-oxide (**Table 2.1**).²⁷

Table 2.1: Optimization of N-oxidation conditions



Entry	R ₁	Conditions	Oxidant ^b	Product Ratios ^a 2.8:2.9:2.11
1	HBF ₄	0.2 M DCM	<i>m</i> -CPBA	1:5:0
2	HBF ₄	0.2 M DCM	TBHP	1:0:0
3	HBF ₄	0.2 M DCM	DMDO	11:0:1
4	HBF ₄	Oxone, NaHCO ₃ , HFIP:H ₂ O, 4 °C	1,1,1-trifluorohexan-2-one (20 mol %)	1:19:0
5	HBF ₄	50% H ₂ O ₂ ; 5:1 DCM: HFIP	2.20 (20 mol%)	77% ^c 2.11
6	-	HBF ₄ ·OEt ₂ , 50% H ₂ O ₂ ; 5:1 DCM: HFIP	2.20 (20 mol%)	77% ^c 2.11
7	-	HBF ₄ ·OEt ₂ , 5:1 DCM: HFIP	DMDO	15% ^c 2.11
8	-	HBF ₄ ·OEt ₂ , 5:1 DCM: HFIP	50% H ₂ O ₂	1:0:0
9	-	HBF ₄ ·OEt ₂ , 5:1 DCM: HFIP	<i>m</i> -CPBA	2:5:0
10	-	H ₂ SO ₄ , 50% H ₂ O ₂ ; 5:1 DCM: HFIP	2.20 (20 mol%)	66% ^c 2.11
11	-	50% H ₂ O ₂ ; 5:1 DCM: HFIP	2.20 (20 mol%)	0:1:0

^aDetermine by integration of LC-MS chromatogram ^b1 equivalent of oxidant used unless otherwise stated

^cIsolated yield

Several oxidants used routinely for N-oxidation were screened including *m*-chloroperoxybenzoic acid (*m*-CPBA) and *tert*-butyl hydrogen peroxide (TBHP) (**entries 1 and 2**).

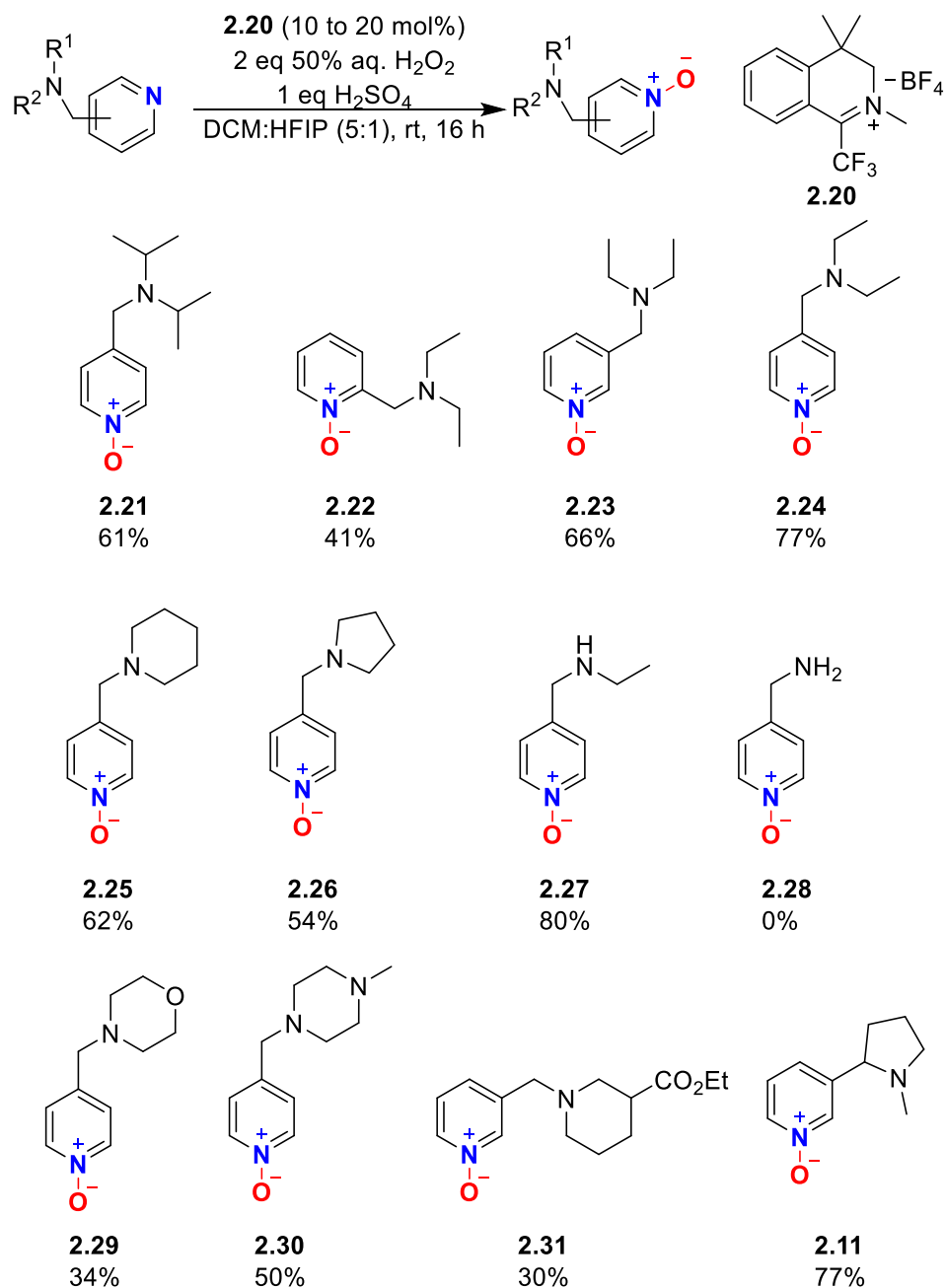
The use of *m*-CPBA and TBHP resulted in either unreacted starting material or pyrrolidine oxidation, suggesting that a stronger oxidant might be required to enable pyridine oxidation. When using a stoichiometric amount of dimethyldioxirane (DMDO), we observed the first evidence of selective pyridine N-oxidation, albeit in low yield (**entry 3**). Catalytic trifluoroketones were investigated (**entry 4**), but unsurprisingly resulted in pyrrolidine oxidation given the necessary basic conditions for their catalytic activity.²⁸ Following this trend, we then investigated the use of iminium salt catalyst **2.20**, which provided an isolated yield of 77% of the nicotine pyridine N-oxide (**entry 5**). Pre-preparation of the amine salt could be avoided via the addition of 1 equivalent of HBF₄•OEt₂ to the reaction mixture with no change in yield (**entry 6**). Given the unique properties of HFIP in promoting oxidation reactions, several control experiments were conducted to determine its effect on the reaction with other oxidants (**entry 7-9**).²⁹ Leaving out the iminium salt results in no oxidation (**entry 8**). Another strong acid, sulfuric acid, was also shown to be effective, albeit with a slightly lower yield (**entry 10**). The exclusion of acid results in a mixture of pyrrolidine N-oxide and some di-N-oxide (**entry 11**).

2.4.2 Reaction Scope

With optimized conditions in hand, we synthesized substrates incorporating pyridines with different substituted aliphatic amines. We found for the majority of our substrates; the reactions resulted in product with high selectivity for oxidation and moderate conversion of over 50% (**Scheme 2.3**).³⁰ Secondary (**2.27**) and tertiary amines were well tolerated, while primary amine **2.28** resulted in none of the desired pyridinyl N-oxide and trace oxidation of the primary amine to the imine. Cyclic and acyclic amines (**2.21-2.24**) worked with minimal effect from either a 5- or 6-membered ring (**2.26, 2.25**). Ethers (**2.29**) and esters (**2.31**) were both tolerated with this method. A piperazine substrate (**2.30**) was effectively oxidized using only one equivalent of acid,

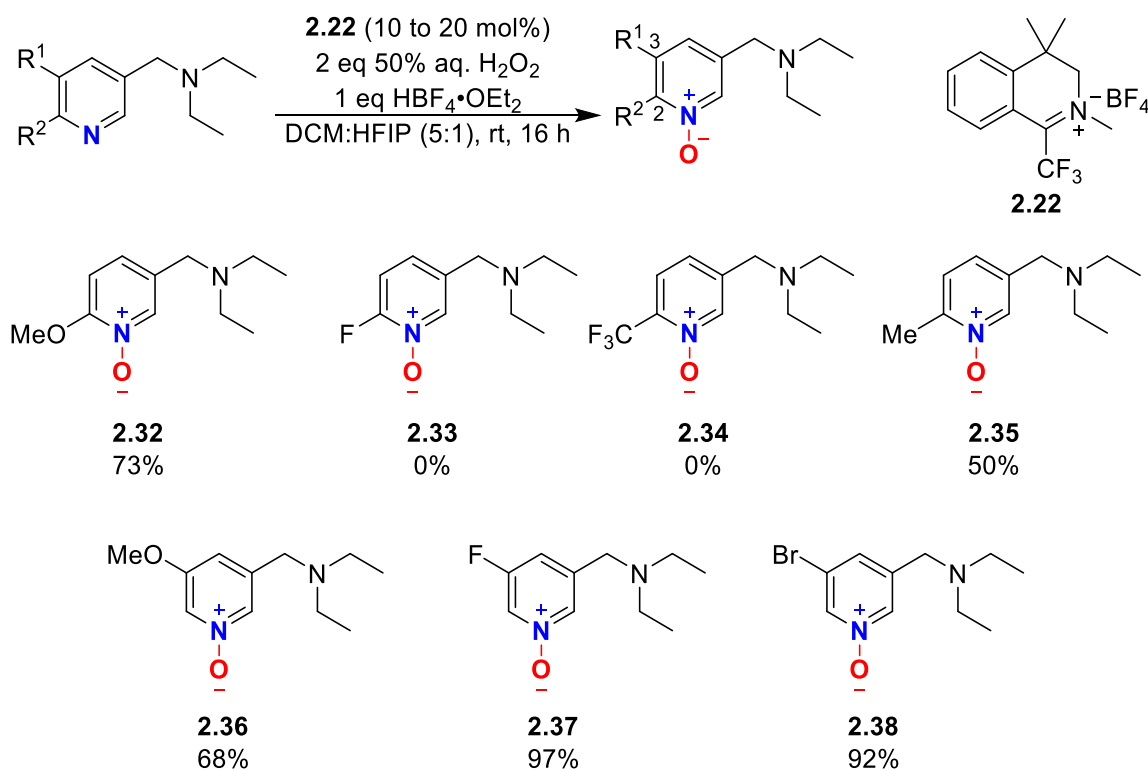
suggesting that protonation of only one nitrogen atom is sufficient to deactivate the piperazine ring toward oxidation. The initial screening demonstrated the broad applicability of protonation of the aliphatic nitrogen.

Scheme 2.3: N-Oxidation substrate scope: Amines

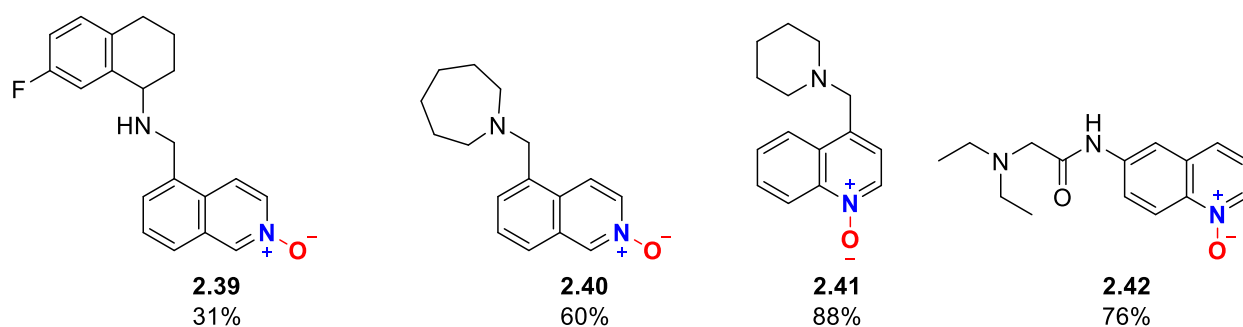


To better understand the scope of the reaction with respect to the heteroarene, we synthesized substrates with functional groups at the 2- and 3- positions of the aromatic ring (**Scheme 2.4**). Compounds bearing σ -withdrawing substituents at the 2-position were not reactive (**2.33**, **2.34**), whereas electron-neutral groups at the 2-position were tolerated with moderate yields (**2.32**, **2.35**). All groups are tolerated at the 3-position and electron-donating groups resulted in some of the highest yields (**2.37**, **2.28**). Other nitrogen aromatic heterocycles including isoquinolines (**2.39**, **2.40**) and quinolones (**2.41**, **2.42**) were also effectively oxidized demonstrating other pharmaceutically relevant heterocycles amenable to this method (**Scheme 2.5**).

Scheme 2.4: N-Oxidation substrate scope: Functionalized Pyridines

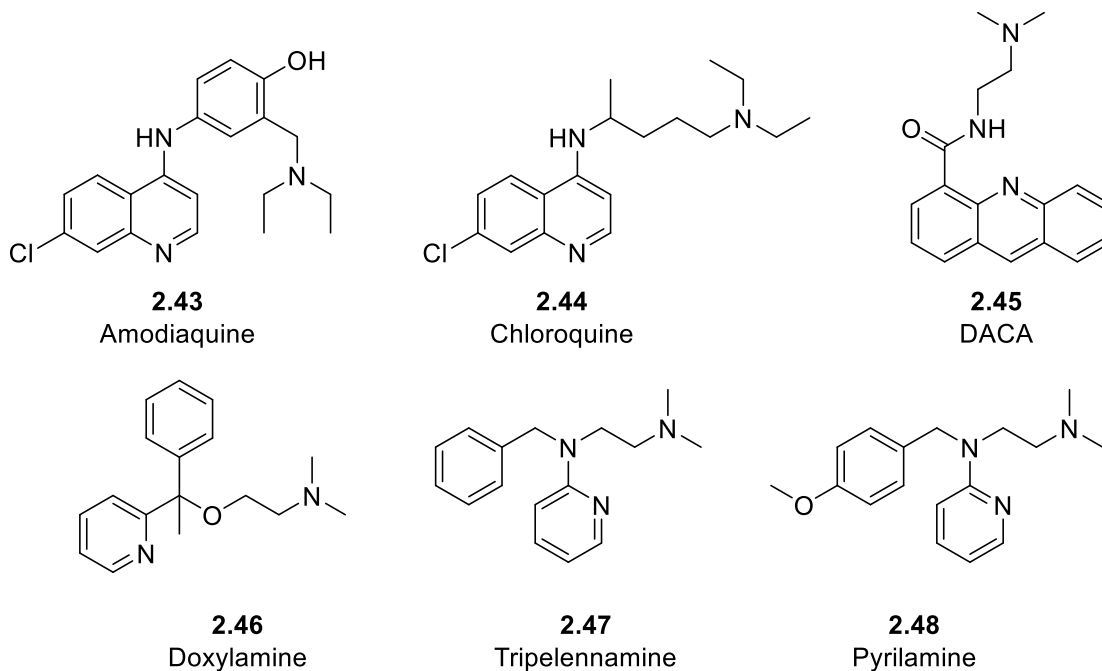


Scheme 2.5: N-Oxidation substrate scope: Azaheterocycles

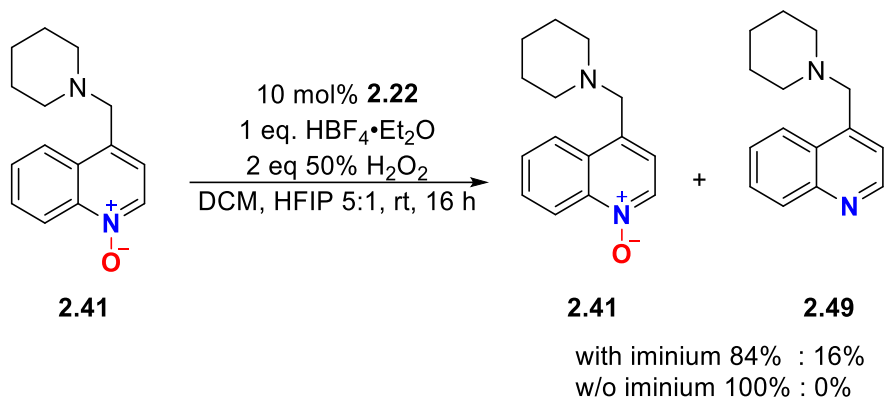


We ran into difficulty expanding our scope to applying this concept to several compounds approved as drugs or previously involved in clinical trials (**Scheme 2.6**). Despite structural similarity to other model substrates, the compounds were not oxidized efficiently. The lack of reactivity observed for amodiaquine (**2.43**) and chloroquine (**2.44**) was somewhat surprising given the expectation for enhanced nucleophilicity arising from the amine at the 4-position. The lack of reactivity for DACA, doxylamine, tripeleminamine and pyrilamine (**2.45-2.48**) suggest that the method is sensitive to steric effects. We further tested doxylamine (**2.46**) and pyrilamine (**2.48**) without any acid additive to determine if the di-N-oxide could be formed, but observed only a single oxidation of the aliphatic amine (not shown). The lack of di-N-oxide and sole formation of the aliphatic N-oxide suggests that the nitrogen heterocycles of **2.46** and **2.48** are inherently unreactive to these oxidative conditions regardless of the acid additive.

Scheme 2.6: Drug-like substrates with 0% yield of heteroaryl N-oxidation



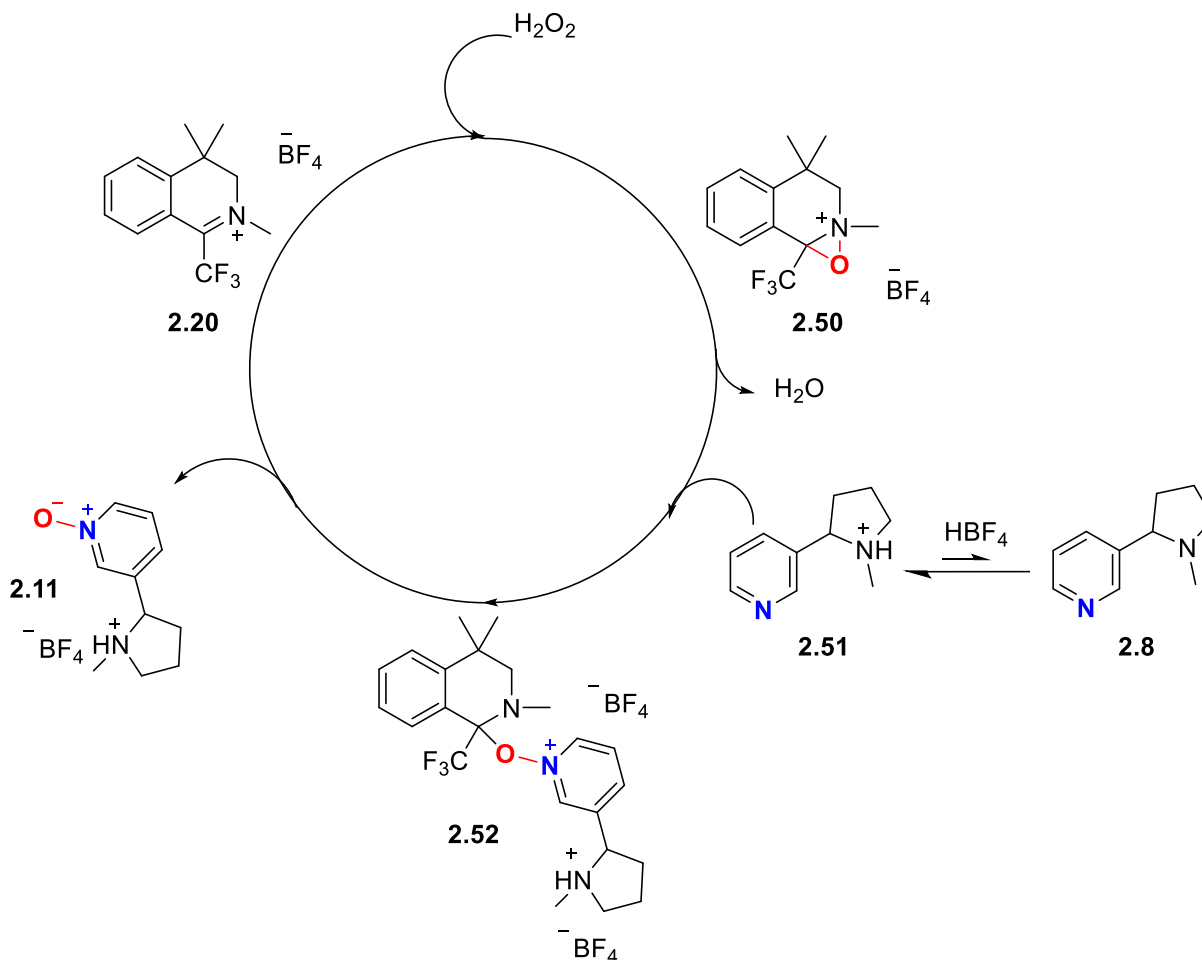
We hypothesized that our N-oxide products might be consumed under the reaction conditions, which might account for some of the poorly performing substrates. Studies of oxidations of heteroarenes with DMDO have identified the formation of singlet oxygen in solution.³¹ By resubjecting N-oxide **2.41** to the reaction conditions, we isolated the reduced pyridine **2.49** and **2.41**, in a ratio (84:16) similar to the initial reaction's yield of 88% (**Scheme 2.7**). Our reaction vessels also have been observed to release gas when opened, further corroborating the hypothesis that the oxaziridinium reacts with the N-oxide to regenerate the starting material with concomitant formation of O₂. This might suggest the poor results for **2.33** and **2.34**, wherein the N-oxide is formed but quickly consumed under the reaction conditions.

Scheme 2.7: N-oxide reversion experiment

2.4.3 Catalytic Cycle

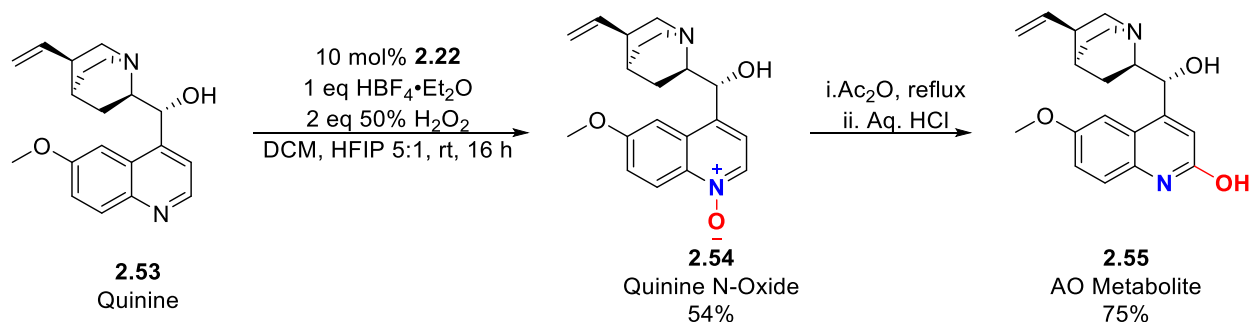
Given the similarity of the optimized conditions to our original hydroxylation reactions, we believe an oxaziridinium to be the active oxidant in our reaction (**Scheme 2.8**). Analogous oxidations of nitrogen heteroarenes with DMDO have been shown to undergo an $\text{S}_{\text{N}}2$ mechanism so it is reasonable to suspect that a similar case might be occurring with the proposed oxaziridinium species.³²

Scheme 2.8: Proposed catalytic cycle of pyridyl oxidation



2.4.4 Mimicking AO metabolism

Finally, this strategy can mimic the enzymatic oxidation of AO, an area of synthetic chemistry that has not yet been addressed. Quinine (**2.53**), a known AO substrate, can be synthesized into its AO metabolite (**2.55**) using this strategy with a subsequent oxidation step.³³ This method enables an efficient two step pathway to AO metabolites for further pharmaceutical testing (**Scheme 2.9**).

Scheme 2.9: Mimicking AO through selective N-oxidation

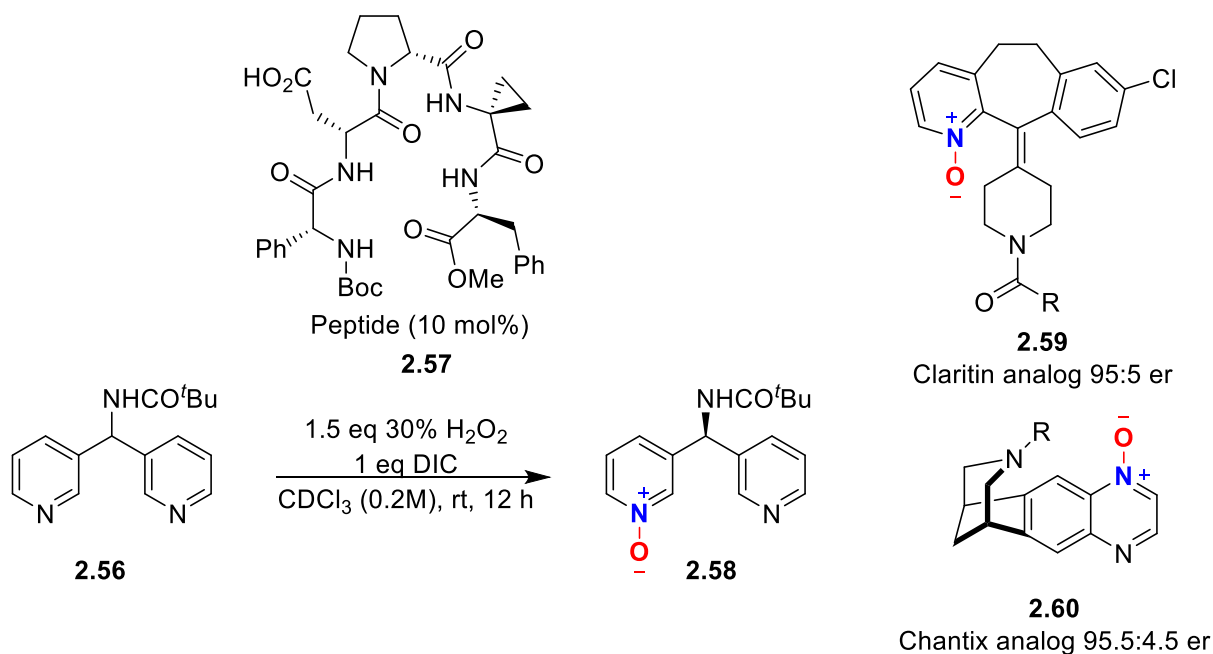
2.5 Conclusions and outlook for selective N-oxidation

Expanding the substrate scope towards other heterocycles would greatly enhance the applicability of this method as we have only been able to demonstrate its utility towards pyridines, quinolines, and isoquinolines. Other heterocycles such as purine present new challenges as heterocycles containing a greater number of nitrogen atoms are generally more deactivated towards oxidation and present issues of selectivity. Furthermore, substrates containing multiple heteroarenes and aliphatic amines represent a unique challenge as the differences in basicity might not be substantial enough to easily be utilized to selectively oxidize one heteroarene demonstrating a limitation to this strategy for certain complex compounds.

Peripheral to site-selective synthesis of N-oxides has been work addressing stereoselective oxidations. Notable examples include Sharpless's work in 1983 wherein chiral Ti-based complexes were employed to effect kinetic resolution of tertiary amines. These methods were stoichiometric, however, and only worked with β -amino alcohols containing substrates to enable the enantioselectivity.³⁴ This was only recently expanded to work with γ -amino alcohols.³⁵ The Miller Lab has focused on this area to expand a broader range of substrates in recent years by leveraging the steric restraints of enzymes in tandem with established organocatalytic methods.³⁶

They were able to modify some of their peptide-based catalysts (**2.57**) with an aspartate side chain capable of oxidation in its peracid form. Through a hydrogen-bonding interaction, the substrate (**2.56**) is selectively oxidized and subsequently desymmetrizes the bispyridine compound (**2.58**) enabling further functionalization (**Scheme 2.10**).

Scheme 2.10: Peptide-based chemoselective nitrogen oxidation and desymmetrization



This work is particularly interesting given its ability to work on derivatives of approved pharmaceuticals Claritin and Chantix (**2.59**, **2.60**), providing chiral derivatives of both in moderate yields. Stereoselective protocols, like from the Miller lab, are particularly valuable given the importance of enantiopure compounds as bioactive compounds. These methods and further work towards chemoselective nitrogen oxidation can enable another approach to efficient late-stage functionalization by focusing on differentiating several nitrogen functionalities in a molecule rather than the numerous C–H bonds.

2.7 References

-
- ¹ Guengerich, F.P. Cytochrome P450s and other enzymes in drug metabolism and toxicity. *AAPS J.* **2006**; 8 (1): E101-11.
- ² Williams J.A.; Hyland R.; Jones B.C.; Smith D.A.; Hurst S.; Goosen T.C.; Peterkin V.; Koup J.R.; Ball S.E. Drug-drug interactions for UDP-glucuronosyltransferase substrates: a pharmacokinetic explanation for typically observed low exposure (AUC_i/AUC) ratios. *Drug Metab. Dispos.*, **2004**; 32 (11):1201-1208.
- ³ Vitaku, E.; Smith, D. T.; Njardarson, J. T. Analysis of the Structural Diversity, Substitution Patterns, and Frequency of Nitrogen Heterocycles among U.S. FDA Approved Pharmaceuticals. *J. Med. Chem.*, **2014**, 57 (24), 10257–10274.
- ⁴ Lewis, D. F. V. Human Cytochromes P450 Associated with the Phase 1 Metabolism of Drugs and Other Xenobiotics: A Compilation of Substrates and Inhibitors of the CYP1, CYP2 and CYP3 Families. *Curr. Med. Chem.*, **2003**, 10 (19), 1955–1972.
- ⁵ Krueger, S. K.; Williams, D. E. Mammalian Flavin-Containing Monooxygenases: Structure/Function, Genetic Polymorphisms and Role in Drug Metabolism. *Pharmacol. Ther.*, **2005**, 106 (3), 357–387.
- ⁶ Hutzler, J. M.; Cerny, M. A.; Yang, Y. S.; Asher, C.; Wong, D.; Frederick, K.; Gilpin, K. Cynomolgus Monkey as a Surrogate for Human Aldehyde Oxidase Metabolism of the Egfr Inhibitor Bibx1382. *Drug Metab. Dispos.*, **2014**, 42 (10), 1751– 1760.
- ⁷ Obach, R. S. Pharmacologically Active Drug Metabolites: Impact on Drug Discovery and Pharmacotherapy. *Pharmacol. Rev.*, **2013**, 65 (2), 578– 640.
- ⁸ Smith, D.A.; Obach, R.S. Metabolites in safety testing (MIST): considerations of mechanisms of toxicity with dose, abundance, and duration of treatment. *Chem. Res. Toxicol.*, **2009**, 22 (2): 267– 279.
- ⁹ Genovino, J.; Lgtz, S.; Sames, D.; Tour, B.B. Complementation of Biotransformations with Chemical C–H Oxidation: Copper-Catalyzed Oxidation of Tertiary Amines in Complex Pharmaceuticals. *J. Am. Chem. Soc.*, **2013**, 135 (33), 12346 – 12352.
- ¹⁰ Pryde, D. C.; Dalvie, D.; Hu, Q.; Jones, P.; Obach, R. S.; Tran, T. D. Aldehyde Oxidase: An Enzyme of Emerging Importance in Drug Discovery. *J. Med. Chem.*, **2010**, 53 (24), 8441–8460.
- ¹¹ Alfaro, J.F.; Jones, J.P. Studies on the mechanism of aldehyde oxidase and xanthine oxidase. *J. Org. Chem.*, **2008**, 73 (23), 9469-9472.
- ¹² Kaye, B.; Offerman, J. L.; Reid, J. L.; Elliott, H. L.; Hillis, W. S. A Species Difference in the Presystemic Metabolism of Carbazeran in Dog and Man. *Xenobiotica*, **1984**, 14 (12), 935– 945.

-
- ¹³ Zhang, X.; Liu, H. H.; Weller, P.; Zheng, M.; Tao, W.; Wang, J.; Liao, G.; Monshouwer, M.; Peltz, G. In Silico and in Vitro Pharmacogenetics: Aldehyde Oxidase Rapidly Metabolizes a P38 Kinase Inhibitor. *Pharmacogenomics J.*, **2011**, *11* (1), 15–24.
- ¹⁴ Jensen, K. G.; Jacobsen, A. M.; Bundgaard, C.; Nilausen, D. O.; Thale, Z.; Chandrasena, G.; Jorgensen, M. Lack of Exposure in a First-in-Man Study Due to Aldehyde Oxidase Metabolism: Investigated by Use of 14c-Microdose, Humanized Mice, Monkey Pharmacokinetics, and in Vitro Methods. *Drug Metab. Dispos.*, **2017**, *45* (1), 68–75.
- ¹⁵ Montefiori, M.; Jorgensen, F. S.; Olsen, L. Aldehyde Oxidase: Reaction Mechanism and Prediction of Site of Metabolism. *ACS Omega*, **2017**, *2* (8), 4237–4244.
- ¹⁶ Zhao, J.; Cui, R.; Wang, L.; Chen, Y.; Fu, Z.; Ding, X.; Cui, C.; Yang, T.; Li, X.; Xu, Y.; Chen, K.; Luo, X.; Jiang, H.; Zheng, M. Revisiting Aldehyde Oxidase Mediated Metabolism in Drug-like Molecules: An Improved Computational Model. *J. Med. Chem.*, **2020**, *63* (12), 6523–6537.
- ¹⁷ O'Hara, F.; Burns, A. C.; Collins, M. R.; Dalvie, D.; Ornelas, M. A.; Vaz, A. D.; Fujiwara, Y.; Baran, P. S. A Simple Litmus Test for Aldehyde Oxidase Metabolism of Heteroarenes. *J. Med. Chem.*, **2014**, *57* (4), 1616–1620.
- ¹⁸ Taylor, E.; Boyer, N. Notes- Pyridine-1-Oxides. IV. Nicotine-1-Oxide, Nicotine-1'-Oxide, and Nicotine-1,1'-Dioxide. *J. Org. Chem.*, **1959**, *24* (2), 275–277.
- ¹⁹ Kokatla, H.P.; Thomson, P.F.; Bae, S.; Doddi, V.R.; Lakshman, M.K. Reduction of Amine N-Oxides by Diboron Reagents. *J. Org. Chem.*, **2011**, *76* (19), 7842–7848.
- ²⁰ Kim, J.; Bertozzi, C.R. A Bioorthogonal Reaction of N-Oxide and Boron Reagents. *Angew. Chem., Int. Ed.*, **2015**, *54* (52), 15777–15781.
- ²¹ Ferrer, M.; Sánchez-Baeza, F.; Messeguer, A.; Diez, A.; Rubiralta, M. Use of Dioxiranes for the Chemoselective Oxidation of Tertiary Amines Bearing Alkene Moieties. *J. Chem. Soc. Chem. Commun.*, **1995**, *3*, 293–294.
- ²² Lee, M.; Sanford, M. S. Platinum-Catalyzed, Terminal-Selective C(sp³)-H Oxidation of Aliphatic Amines. *J. Am. Chem. Soc.*, **2015**, *137* (40), 12796–12799.
- ²³ Howell, J. M.; Feng, K.; Clark, J. R.; Trzepakowski, L. J.; White, M. C. Remote Oxidation of Aliphatic C-H Bonds in Nitrogen-Containing Molecules. *J. Am. Chem. Soc.*, **2015**, *137* (46), 14590–14593.
- ²⁴ Mack, J. B. C.; Gipson, J. D.; Du Bois, J.; Sigman, M. S. Ruthenium-Catalyzed C-H Hydroxylation in Aqueous Acid Enables Selective Functionalization of Amine Derivatives. *J. Am. Chem. Soc.*, **2017**, *139* (28), 9503–9506.

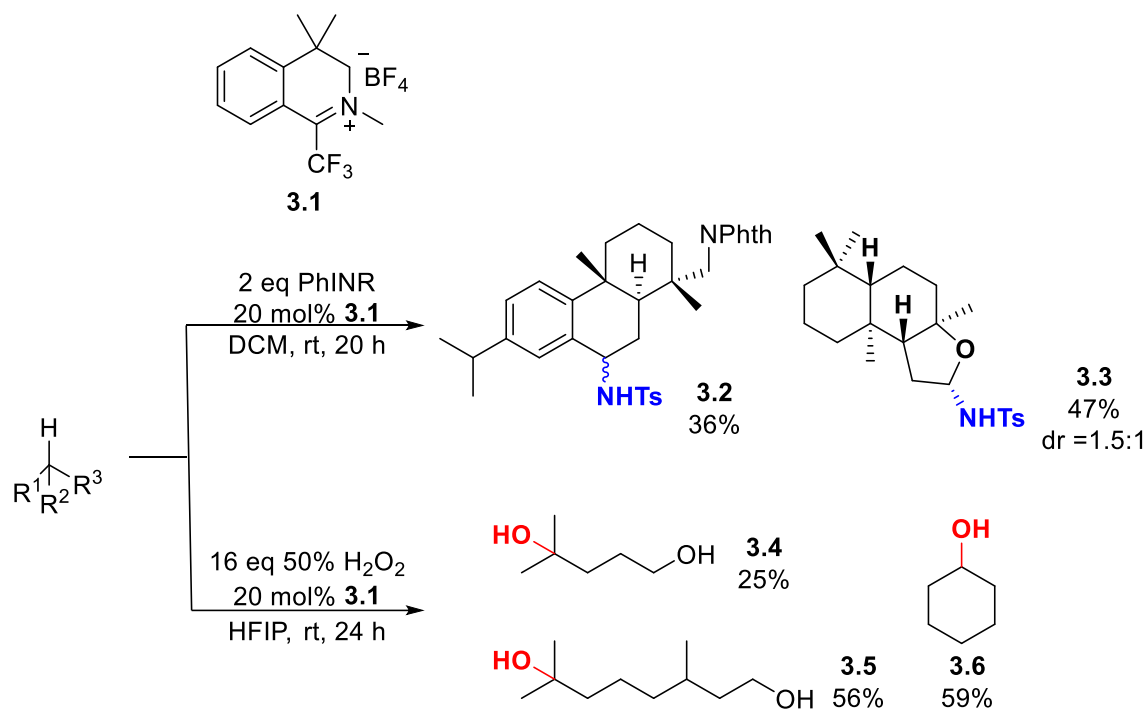
-
- ²⁵ Bordwell, F. G.; Hughes, D. L. Direct Relationship between Nucleophilicity and Basicity in SN2 Reactions of Fluorenyl Anions with Benzyl Chloride in Dimethyl Sulfoxide Solution. *J. Org. Chem.*, **1980**, *45* (16), 3314–3320.
- ²⁶ Wang, D.; Shuler, W.G.; Pierce, C. J.; Hilinski, M.K. An Iminium Salt Organocatalyst for Selective Aliphatic C–H Hydroxylation. *Org. Lett.*, **2016**, *18* (15), 3826–3829.
- ²⁷ Cymerman, Craig, J.; Purushothaman, K. K. Improved Preparation of Tertiary Amine N-Oxides. *J. Org. Chem.*, **1970**, *35* (5), 1721–1722.
- ²⁸ Shuler, W. G.; Johnson, S. L.; Hilinski, M. K. Organocatalytic, Dioxirane-Mediated C–H Hydroxylation under Mild Conditions Using Oxone. *Org. Lett.*, **2017**, *19* (18), 4790–4793.
- ²⁹ Dantignana, V.; Milan, M.; Cussó, O.; Company, A.; Bietti, M.; Costas, M. Chemoselective Aliphatic C–H Bond Oxidation Enabled by Polarity Reversal. *ACS Cent. Sci.*, **2017**, *3* (12), 1350–1358.
- ³⁰ Philip L. Hahn ran these substrates for N-oxidation.
- ³¹ Adam, W.; Briviba, K.; Duschek, F.; Golsch, D.; Kiefer, W.; Sies, H. Formation of Singlet Oxygen in the Deoxygenation of Heteroarene N-Oxides by Dimethyldioxirane. *J. Chem. Soc. Chem. Commun.*, **1995**, *18*, 1831–1832.
- ³² Adam, B. W.; Golsch, D. SN2 Reaction versus Electron Transfer in the Oxygen Transfer by Dimethyldioxirane to Nitrogen Heteroarenes. *Angew. Chem., Int. Ed.*, **1993**, *32* (5), 737–739.
- ³³ Díaz-Araújo, H.; Cook, J. M.; Christie, D. J. Synthesis of 10, 11-Dihydroxydihydroquinidine N-Oxide, a New Metabolite of Quinidine. Preparation and 1H-NMR Spectroscopy of the Metabolites of Quinine and Quinidine and Conformational Analysis via 2D COSY NMR Spectroscopy. *J. Nat. Prod.*, **1990**, *53* (1), 112–124.
- ³⁴ Miyano, S.; Lu, L. D. L.; Viti, S. M.; Sharpless, K. B. Kinetic Resolution of Racemic α -Hydroxyamines by Enantioselective N-Oxide Formation. *J. Org. Chem.*, **1983**, *48*, 3608–3611.
- ³⁵ Bhadra, S.; Yamamoto, H. Catalytic Asymmetric Synthesis of N-Chiral Amine Oxides. *Angew. Chem. Int. Ed.*, **2016**, *55* (42), 13043–13046.
- ³⁶ Hsieh, S.Y.; Tang, Y.; Crotti, S.; Stone, E.A.; Miller, S.J. Catalytic Enantioselective Pyridine N-Oxidation. *J. Am. Chem. Soc.*, **2019**, *141* (46), 18624–18629.

Chapter 3

Synthesis and Evaluation of New Iminium Salt Catalysts

Introduction

Work by the Hilinski Lab has led to significant developments in the area of organocatalytic C–H functionalization, including the use of iminium salt catalysts such as with **3.1**, which forms oxaziridinium and diaziridinium salts, both potent oxidants, when exposed to hydrogen peroxide or an iminoiodinane, respectively. Nitrogen quaternization and trifluoromethyl substitution of the iminium carbon have been found to be key features for hydroxylation and amination activity. In the context of hydroxylation, the catalyst's compatibility with the use of hexafluoroisopropanol (HFIP) as a solvent allows for chemoselective oxidations in the presence of unprotected alcohols, an unprecedented accomplishment and challenge for many C–H hydroxylation catalysts.¹ Using a preformed iminoiodinane, this same catalyst was demonstrated to be effective for a number of substrates for C–H amination of benzylic C–H bonds and aliphatic C–H bonds that are strongly activated via hyperconjugation. This method can also be applied to late-stage functionalization, as demonstrated by the natural product derivatives shown in **Scheme 3.1**.²

Scheme 3.1: Iminium salt catalyst for hydroxylation or amination of C–H bonds

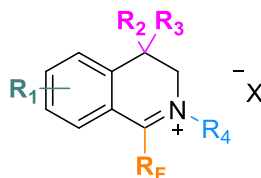
3.1.1 First-Generation Iminium Catalyst

Originally based on Lusinchi-type dihydroisoquinoliniums, additional work in the Hilinski lab has demonstrated the importance of several moieties present on the catalyst for both hydroxylation and amination activity.³ The aryl ring allows for introduction of either electron withdrawing or donating groups that can influence the electronic nature of the iminium. The benzylic gem-dimethyl substitution prevents aromatization of the catalyst under oxidative conditions, while the methyl iminium adds a positive charge to the molecule, increasing the electron deficiency. The trifluoromethyl group further decreases the electron density of the iminium carbon and enhances the rate of reaction. The importance of the tetrafluoroborate counterion is due to its non-coordinating nature. Catalyst degradation pathways were identified for

hydroxylation. Hydroxylation reactions have resulted in rearrangement to a new iminium species, maintaining a hydroxylated imine carbon.⁴

Given the critical features of **3.1** and its known limitations, several sites were targeted for modification in the attempt to develop an improved catalyst (**Figure 3.1**). Replacing the gem-dimethyl with different cycloalkyl rings to incorporate larger steric functionality in the molecule was considered. It was reasoned that doing so could limit steric issues of the catalyst given the smaller bond angles of a cyclobutyl group compared to the gem-dimethyls, while maintaining the sp³ hybridization of the benzylic carbon. The trifluoromethyl group could be replaced with fluorinated alkyl chains and aryl groups to tune the electronics of the iminium while still maintaining sufficient catalytic activity.⁵ Other functional groups could be added to the aryl ring to tune the electronics or lipophilicity of the iminium to help with solubility.⁶ Finally, the methyl group on the iminium could be modified with other alkyl or an aryl group to try to prevent catalyst decomposition via N-demethylation. With these ideas in mind, we went about identifying a synthesis for these iminium salts from a modified approach to the iminium synthesis.

Figure 3.1: Points of modulation for the Hilinski iminium catalyst



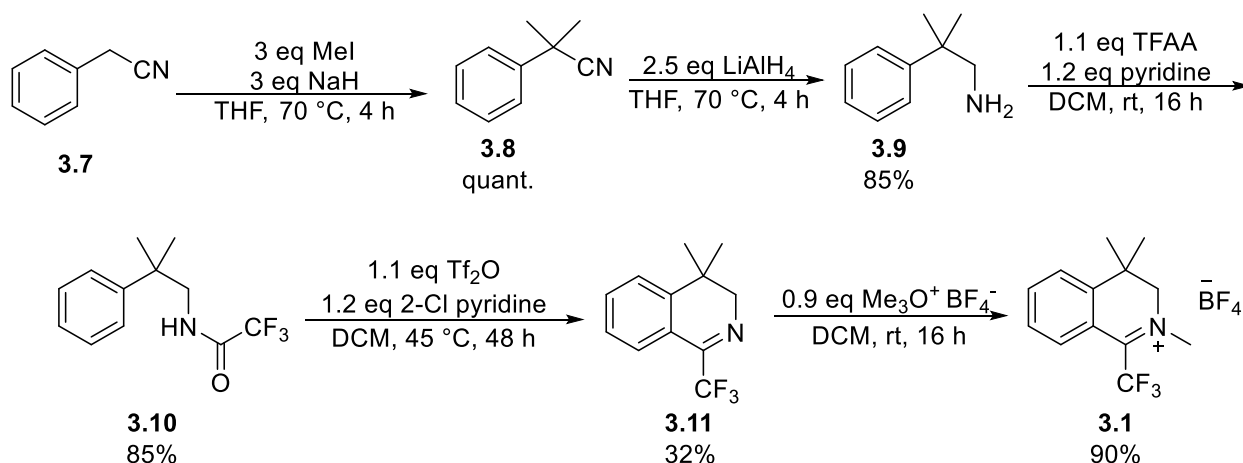
3.1.2 Iminium Synthetic Route

The iminium catalyst (**3.1**) is prepared using a modular five-step synthesis from a commercially available starting material in a 20% overall yield. The first step incorporates the gem-dimethyl group through benzylic alkylation of benzyl cyanide **3.7** with iodomethane. This is

followed by reduction of nitrile **3.8** using lithium aluminum hydride followed by a Fieser work-up to isolate the free amine. Free amine **3.9** is then acylated with trifluoroacetic anhydride to form the trifluoroacetamide (**3.10**). Acetamide **3.10** is cyclized at reflux under Bischler-Napieralski conditions giving imine **3.11** in the lowest yielding step of the synthesis.⁷ Imine **3.11** is rigorously purified before undergoing alkylation using a Meerwein salt. The Meerwein salt is the limiting reagent in this step for ease of purification, since it allows unreacted imine, as the only non-volatile byproduct, to be triturated from the product mixture, providing pure catalyst (**Scheme 3.2**).

As a modular synthesis, there are several steps at which adjustments can be made to easily access new iminiums. The benzyl cyanide can be substituted with a range of aryl functionalized benzyl cyanides in the first step. Dihaloalkanes can be used to incorporate different cycloalkyl groups at the benzyl position in the second step. While the trifluoroacetamide moiety can be replaced with other fluorinated amides by utilizing a different anhydride or acyl halide, aryl-substituted ketimines are not easily accessed through this route due to the application of the Bischler-Napieralski cyclization and requires a different synthetic route. Given these considerations, fifteen new iminiums were targeted as synthetically tractable and pursued.

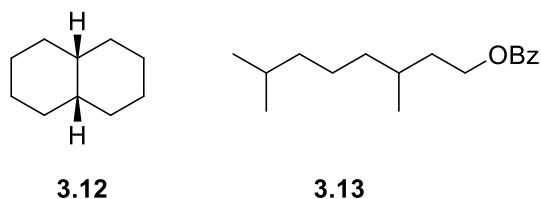
Scheme 3.2: Iminium catalyst synthetic route



3.1.3 Selection of Model Substrates

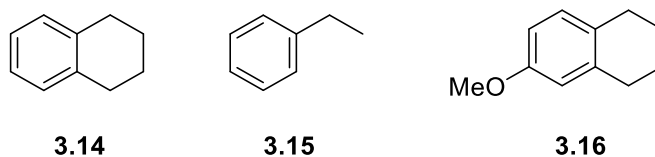
To evaluate the performance of the new catalysts, we chose several substrates to screen for hydroxylation and amination using previously developed conditions. Cis-decalin (**3.12**) and 3,7-dimethyloctyl benzoate (**3.13**) were utilized as more reactive and less reactive substrates for hydroxylation, respectively, and as an added benefit their reactions could be easily monitored by GC-FID (**Figure 3.2**). Using two substrates of widely varying reactivity allowed us to gauge the relative hydroxylation capabilities of these new catalysts.

Figure 3.2: Hydroxylation screening substrates



Tetralin (**3.14**), ethylbenzene (**3.15**) and 6-methoxytetralin (**3.16**) were identified as screening substrates for C–H amination (**Figure 3.3**). These represent moderately (**3.14**), weakly (**3.15**),^{8,9} and highly (**3.16**) reactive substrates using our original method in combination with catalyst **3.1**. Screening with **3.16**, enables us to evaluate catalyst performance with the trichloroethylsulfonamide iminoiodinane, which exhibited greatly reduced reactivity compared to PhINTs in our initial investigations.

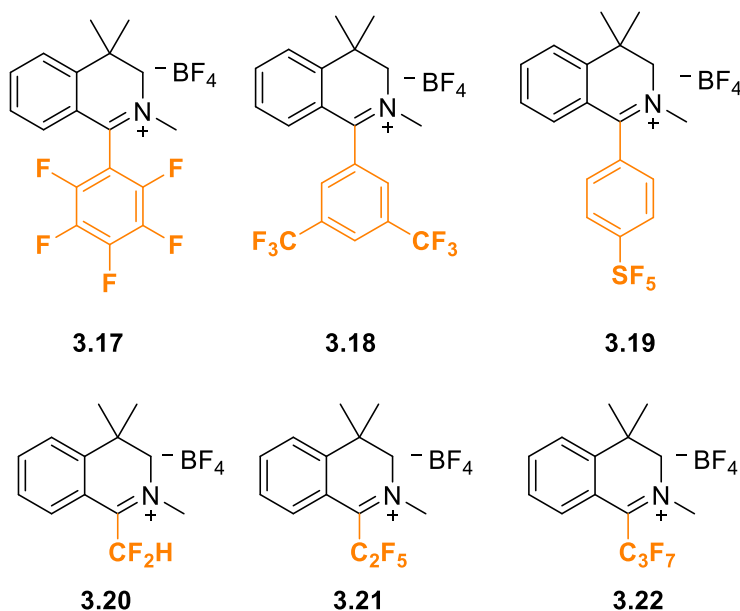
Figure 3.3: Amination screening substrates



3.2.1 Polyfluorinated Iminiums

Following a similar synthetic route as described, six different iminiums were targeted to investigate the effect of changes to the trifluoromethyl group of iminium **3.1** and activity in C–H bond hydroxylation and amination reactions (**Figure 3.4**). Although sterically larger than $-\text{CF}_3$, the fluoroarenes (**3.17-3.19**) would increase the lipophilicity of the catalyst while maintaining the electron-withdrawing character of the trifluoromethyl group.¹⁰ The perfluoroethyl (**3.21**) and perfluoropropyl (**3.23**) groups would be only slightly larger than the trifluoromethyl group, but were reasoned to provide enhanced electrophilicity and lipophilicity.

Figure 3.4: Polyfluorinated Iminiums

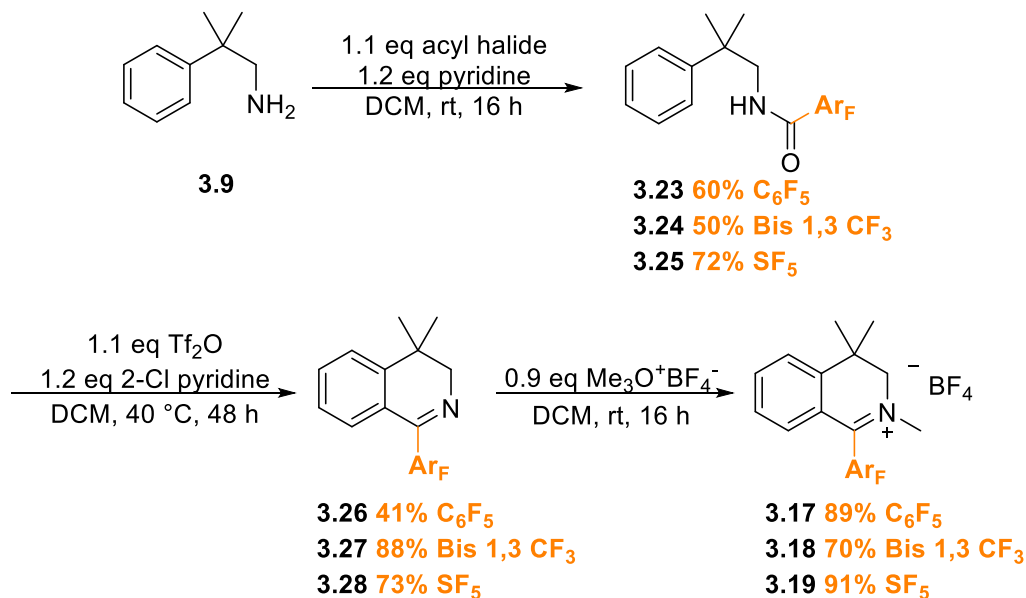


3.2.2 Polyfluorinated Aryl Iminium Synthesis

The aryl fluorinated amides (**3.18**, **3.19**, **3.20**) were synthesized in modest yields using the respective acyl halides. The Bischler-Napieralski cyclizations were higher yielding for these amides than the original iminium catalyst (>32%). The cyclization step in the mechanism is

probably aided by the more electrophilic nitrilium ion that forms compared to the CF_3 nitrilium in catalyst **3.1**, helping to encourage the ring closure (**Scheme 3.3**).

Scheme 3.3: Polyfluorinated aryl iminium synthesis

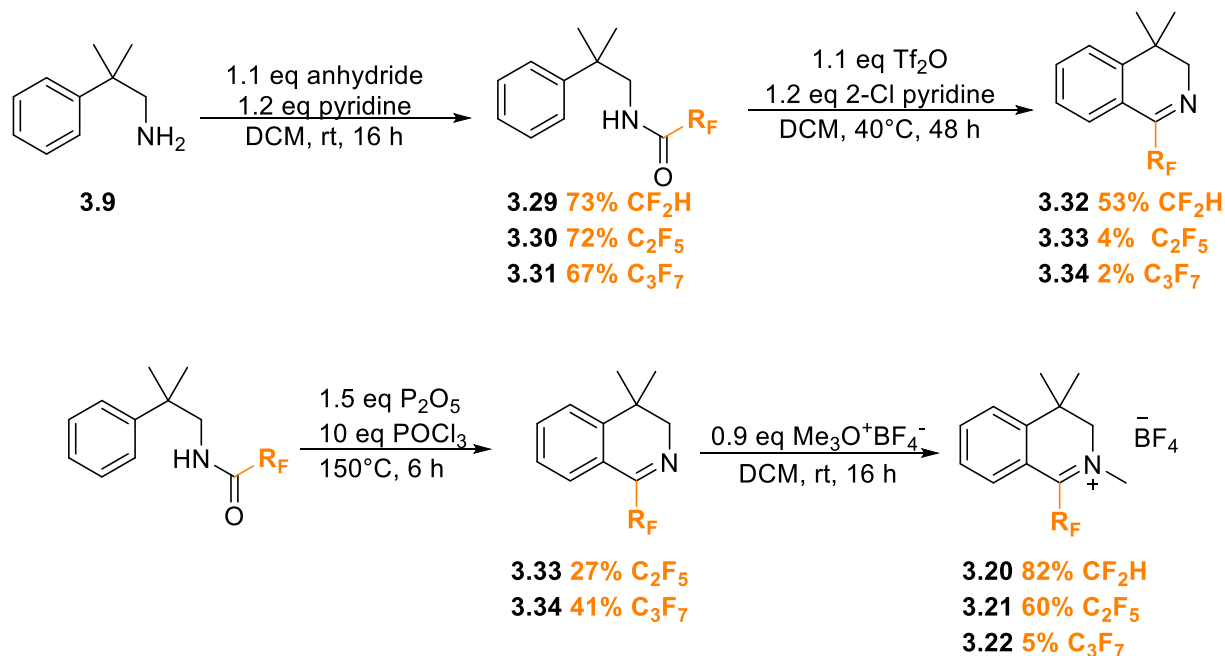


3.2.3 Polyfluorinated Alky Iminium Synthesis

The fluoroalkyl amides (**3.24**, **3.25**, **3.26**) were synthesized using their respective anhydride in good yields. The cyclizations for the perfluoroethyl and perfluoropropyl amides (**3.25** and **3.26**), however, did not provide appreciable quantities of the cyclized products under our standard conditions. These conditions provided undesired side products and unreacted starting material. The Cambon group has reported conditions utilizing phosphorus pentoxide in phosphorus oxychloride with highly elevated temperatures for a series of similar F-alkyl isoquinolines.¹¹ These conditions provided an effective method for cyclization. Under these conditions, a pyrophosphate acts as a leaving group during the nitrilium formation step, suggesting that the nitrilium formation step was problematic for this series rather than the ring closure step. The subsequent Meerwein methylation

proceeded smoothly, but the salts required a modified crystallization in cooled ether to precipitate the product (**Scheme 3.4**).

Scheme 3.4: Polyfluorinated alkyl iminium synthesis

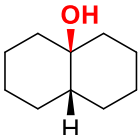
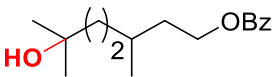
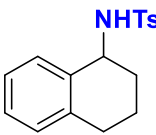
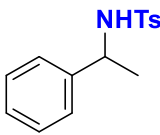
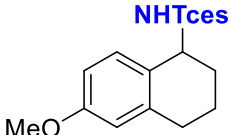


3.2.4 Polyfluorinated Aryl Iminiums Substrate Screening

With the catalysts in-hand, they were evaluated for amination and hydroxylation yields (**Table 3.1**). The fluorinated aryl iminiums (**3.17**, **3.18**, **3.19**) were not competent catalysts under our hydroxylation conditions, resulting in no conversion. We postulated this might be due to sterics, such as the aryl rings blocking attack of the carbon of the iminium by the hydrogen peroxide and preventing any oxaziridinium formation. The CF₃-iminium (**3.1**) is known to react spontaneously upon addition of *m*-CPBA to form the oxaziridinium. In support of the sterics hypothesis, an ¹H-NMR experiment demonstrated that new aryl fluorinated iminiums do not readily form the corresponding oxaziridinium salts when reacted with *m*-CPBA; we only observed the unreacted iminium. C–H amination yields were also poor using these catalysts, with no

identified conversion of ethylbenzene to **3.38**. This is consistent with the hydroxylation results; in this case we hypothesized that the large aryl groups block the nucleophilic attack trajectory of the iminoiodinane on the iminium carbon, affecting the efficiency of diaziridinium formation.

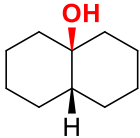
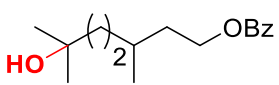
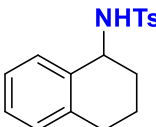
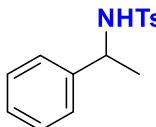
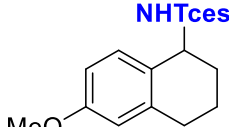
Table 3.1: Polyfluorinated aryl iminium hydroxylation and amination performance

					
	3.35	3.36	3.37	3.38	3.39
3.1	Overoxidized	57%	64%	18%	53%
3.17	0%	0%	23%	0%	20%
3.18	0%	0%	10%	0%	25%
3.19	0%	0%	0%	0%	0%

3.2.5 Polyfluorinated Alkyl Iminiums Substrate Screening

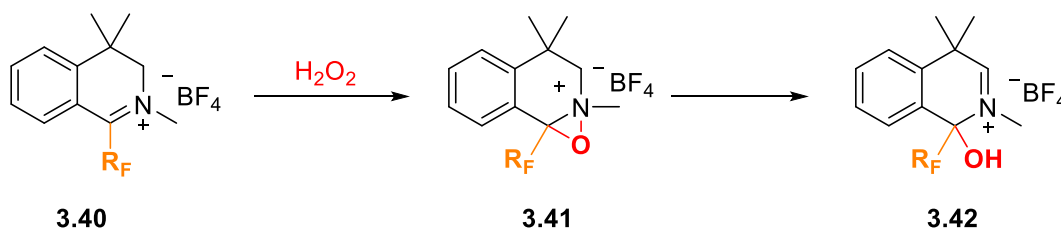
The fluorinated alkyl iminiums performed poorly under hydroxylation conditions, compared to the original trifluoromethyl catalyst. The difluorinated iminium catalyst (**3.20**) resulted in lower yields for both model substrates using our previously published reaction conditions, whereas the perfluoroethyl and perfluoropropyl fluorinated iminium catalysts (**3.21** and **3.22**) were only able to catalyze the hydroxylation of cis-decalin (**Table 3.2**). The lack of overoxidation of cis-decalin suggests that catalysts **3.21** and **3.22** provide a less reactive oxaziridinium incapable of hydroxylating the C–H bonds of 3,7-dimethyloctyl benzoate (**3.13**).

Table 3.2: Polyfluorinated alkyl iminium hydroxylation and amination performance. Yields in parentheses indicate recovered starting material.

					
	3.35	3.36	3.37	3.38	3.39
3.1	Overoxidized	57%	64%	18%	53%
3.20	0%	0%	12%	0%	23%
3.21	40%	0%	15%	0%	31%
3.22	50%	10% (78%)	20%	0%	35%

Although the electron deficiency of the iminium was speculated to increase given the more fluorinated nature of the catalyst, we might, at the same time, be increasing the rate of the degradation towards the less reactive iminium (**3.32**) given the extremely low conversion of 3,7-dimethyloctyl benzoate (**Scheme 3.5**). However, there are other factors like sterics that could be at play and it is not entirely clear what is negatively affecting performance. The amination yields were also poor when compared to **3.1** regardless of decreased or increased extent of fluorination. This suggests that the active site of the catalyst is extremely sensitive to modulation of this group.

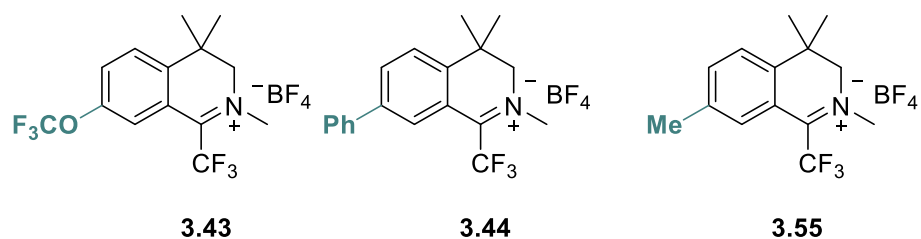
Scheme 3.5: Iminium hydroxylation degradation pathway



3.3.1 Aryl-functionalized Iminium Salts

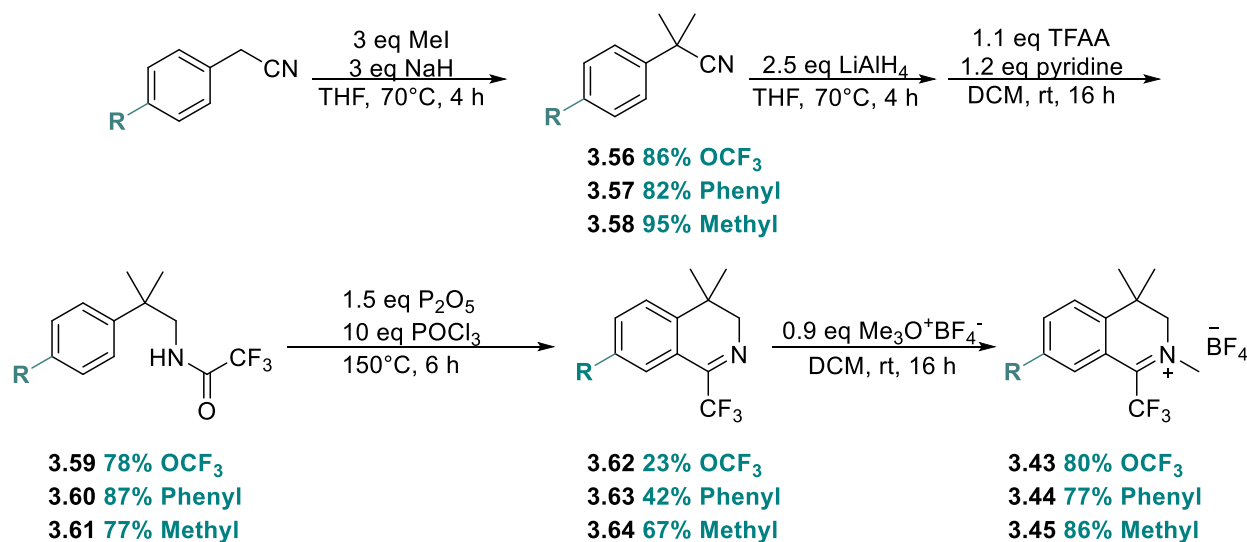
We next synthesized three catalysts with electron-donating groups in a non-resonant position relative to the iminium pi-bond (**Figure 3.5**). Evaluation of electron-donating groups in this position of the catalyst had been previously unexplored. These catalysts were synthesized following the original catalyst's synthetic route with minor modifications. Bischler-Napieralski conditions with phosphorus oxychloride and phosphorus pentoxide were utilized for the syntheses of these catalysts.

Figure 3.5: Aryl-functionalized iminium salts



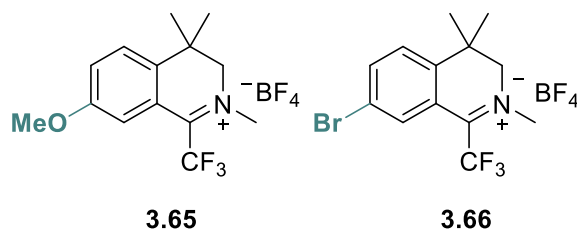
3.3.2 Aryl-functionalized Iminium Salt Synthesis

The aryl-functionalized iminium salts were synthesized utilizing their respective benzyl cyanide as the starting material. The reduction and trifluoroacetamide formation steps were telescoped, allowing for a more efficient synthesis. The new cyclization conditions dramatically improved the time for completion of the reaction and generally provided a cleaner reaction, requiring only separation of the imine from unreacted starting material (**Scheme 3.6**).

Scheme 3.6: Aryl-functionalized iminium salt synthesis

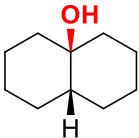
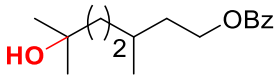
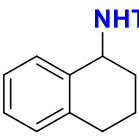
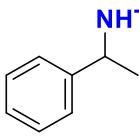
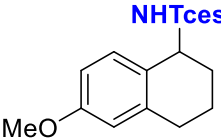
3.3.3 Aryl-functionalized Iminium Salt Substrate Screening

These catalysts performance is outlined in **Table 3.3**. Cis-decalin (**3.12**) was overoxidized using each catalyst, and yields for 3,7-dimethyloctyl benzoate (**3.13**) hydroxylation were subpar compared to **3.1**. To help provide further insight into these catalysts' performance, data from previously synthesized and tested catalysts (**Figure 3.6**) are included in **Table 3.3**.⁴

Figure 3.6: Previously synthesized aryl-functionalized iminiums

Comparing **3.43** to **3.65**, the additional electronegativity from the fluorinated methoxy provided higher yields of hydroxylation while lower yields of amination. There does not seem to be a clear correlation with inductive effects with hydroxylation yields suggesting that multiple factors are probably influencing catalyst activity. Both **3.44** and **3.45** perform about the same for hydroxylation and amination, with the methyl performing slightly better for amination. Weak electron-donating groups do not have a positive impact on catalyst performance for amination, while they only marginally lower yields for hydroxylation. The electronics of the amination seem particularly sensitive given this dramatic difference between the two oxidations. Overall, for amination, these catalysts all performed poorly compared to **3.1**, except **3.65**. The alkoxy **3.44** with the electronegative trifluoromethyl is dramatically worse than the other alkoxy catalyst **3.65**.

Table 3.3: Aryl functionalized iminium hydroxylation and amination performance. Yields in parentheses indicate recovered starting material. Dashes indicate no data available.

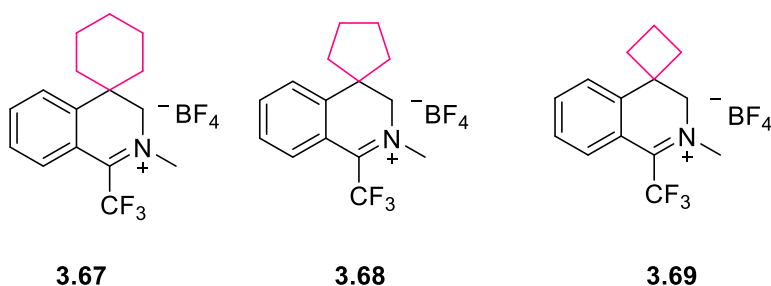
					
	3.35	3.36	3.37	3.38	3.39
3.1	Overoxidized	57%	64%	18%	53%
3.43	Overoxidized	41% (36%)	26%	10%	20%
3.44	Overoxidized	38% (55%)	13%	0%	15%
3.45	Overoxidized	36% (53%)	16%	5%	23%
3.65	-	20%	62%	-	-
3.66	-	37%	44%	-	-

3.4.1 Benzylic Cycloalkyl Iminium Salts

We next synthesized three catalysts with cycloalkyl groups in the benzylic position on the catalyst (**Figure 3.7**). We hoped to explore how ring strain and steric bulk at this position might affect the performance of our catalyst and influence site selectivity of our oxidations. Large steric

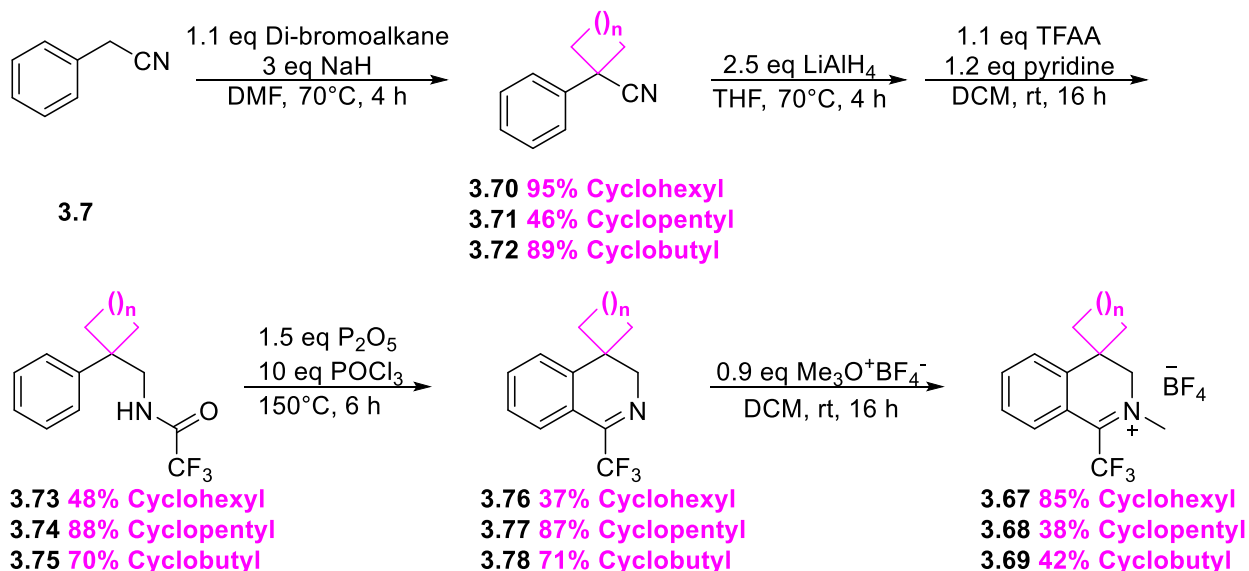
bulk might help override inherent substrate selectivity. These catalysts were synthesized following the original catalyst's synthetic route with minor modification. Bischler-Napieralski conditions with phosphorus oxychloride and phosphorus pentoxide were utilized for the syntheses of these catalysts.

Figure 3.7: Benzylic cycloalkyl iminium salts



3.4.2 Benzylic Cycloalkyl Iminium Salt Synthesis

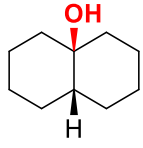
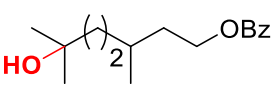
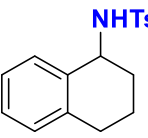
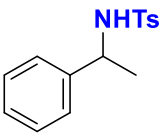
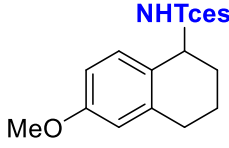
These iminium salts were synthesized utilizing their respective dibromo alkane as the alkyl halide in the initial step. The reduction and trifluoroacetamide formation steps were again telescoped. The new cyclization conditions gave moderate to high yields of the expected products and expedited the completed synthesis (**Scheme 3.7**).

Scheme 3.7: Cycloalkyl iminium salt synthesis

3.4.3 Benzylic Cycloalkyl Iminium Salt Substrate Screening

Introductions of alkyl rings appears to have negative consequences for hydroxylation and amination yields (**Table 3.4**). Of the newly synthesized catalysts, the cyclohexyl catalyst (**3.67**), whose bond angles provide no torsional strain, performed the best for amination and hydroxylation. Increased ring strain at this position correlated with poorer performance for hydroxylation reactions, possibly due to poorer catalyst stability given the correlation between ring strain and poorer performance. Amination with the new catalysts resulted in poorer yields across all substrates. Although the cyclohexyl confirmation limits the ring strain, the catalyst still performed poorly across all substrates when compared to **3.1**.

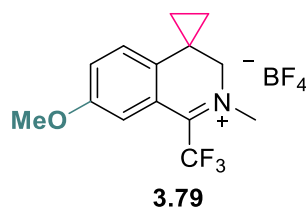
Table 3.4: Cycloalkyl iminium hydroxylation and amination performance. Yields in parentheses indicate recovered starting material.

					
	3.35	3.36	3.37	3.38	3.39
3.1	Overoxidized	57%	64%	18%	53%
3.67	Overoxidized	46% (37%)	36%	15%	33%
3.68	Overoxidized	30% (60%)	20%	12%	25%
3.69	14%	8% (92%)	25%	13%	16%

3.5.1 Cyclopropyl Methoxy Iminium Salt

In addition to the benzyl- and aryl-derivatized iminiums, an iminium catalyst was proposed that incorporates two features found to be beneficial (**Figure 3.8**) We had previously noted a possible rate enhancement for some amination substrates utilizing the 6-methoxy catalyst while maintaining the same yields as **3.1**. We proposed combining these modifications to ideally create a better catalyst, capable of aminating challenging substrates **3.15** in good yields.

Figure 3.8: Cyclopropyl methoxy iminium salt

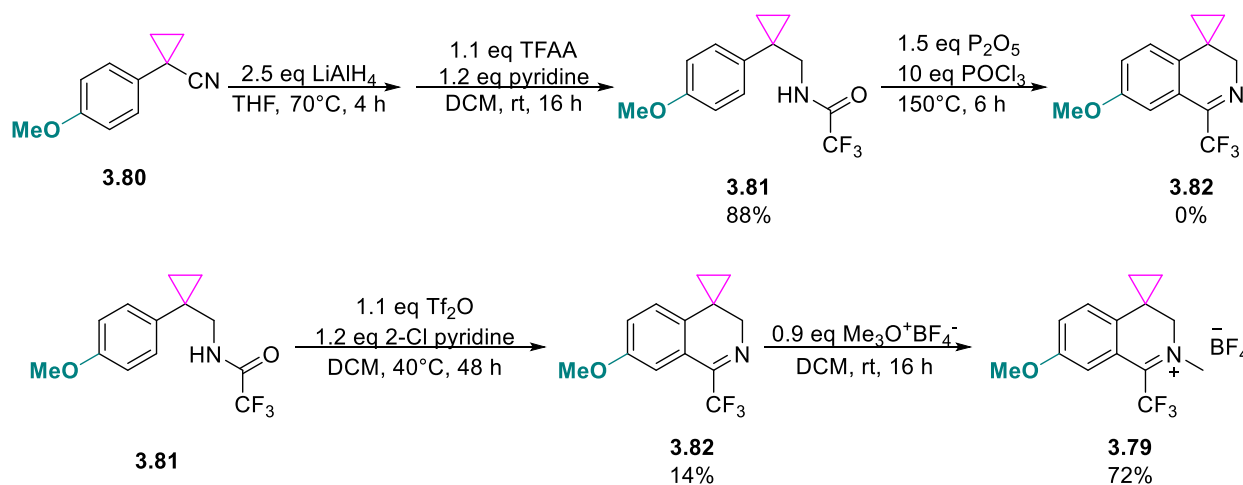


3.5.2 Cyclopropyl Methoxy Iminium Salt Synthesis

Synthesis of this iminium was expedited by purchasing phenylacetonitrile **3.80** directly and telescoping the steps of the synthesis to the trifluoroacetamide, allowing us quick access to the most difficult step in the synthesis. We tried employing the new modified Bischler-Napieralski conditions with phosphorous pentoxide in POCl₃, but were unable to ultimately get it to cyclize,

resulting in unidentified side products and unrecovered starting material. We postulated the conditions to be too harsh and cyclopropyl ring-opening might be occurring. We utilized the original and milder conditions to successfully make imine **3.82** and subsequently, the desired iminium salt (**Scheme 3.8**).

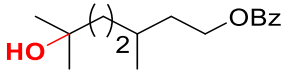
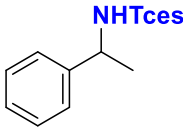
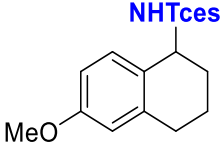
Scheme 3.8: Cyclopropyl methoxy iminium salt synthesis



3.5.3 Cyclopropyl Methoxy Iminium Salt Substrate Screening

We screened catalyst **3.79** using PhINTces for amination, which is an easier to remove protecting group, but more challenging iodine for reactivity in this method.¹² It resulted in no conversion of aminated ethylbenzene and low 6-methoxy tetralin yields, a substrate that is typically reactive for transition metal catalyzed conditions. No hydroxylation was observed and postulated to be due to the aqueous environment of our conditions (**Table 3.5**). A previously target iminium with just the cyclopropyl group was found to be unstable to moisture.

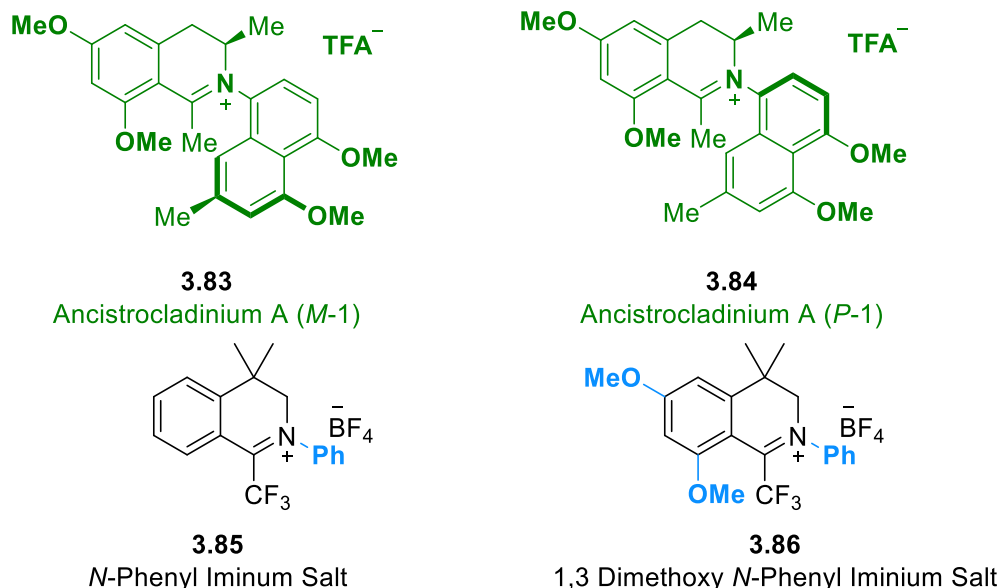
Table 3.5: Cyclopropyl methoxy iminium hydroxylation and amination performance comparison

			
	3.36	3.81	3.39
3.1	57%	0%	53%
3.79	0%	0%	16%

3.6.1 Phenyl *N*-Iminium Salts

Our final target was an *N*-aryl iminium incorporating an aryl ring onto the iminium nitrogen. We hoped that incorporation of an aryl group would prevent degradation of the iminium, wherein **3.1** is demethylation under our amination conditions. We identified the total synthesis of Ancistrocladinium A (**3.83**) as inspiration for our synthetic route given the closely analogous structure to our iminium and the future prospect of using this scaffold to introduce axial chirality close to the active site.¹³ Two phenyl iminium salts that resembled catalyst **3.1** and **3.83** were proposed (**Figure 3.9**).

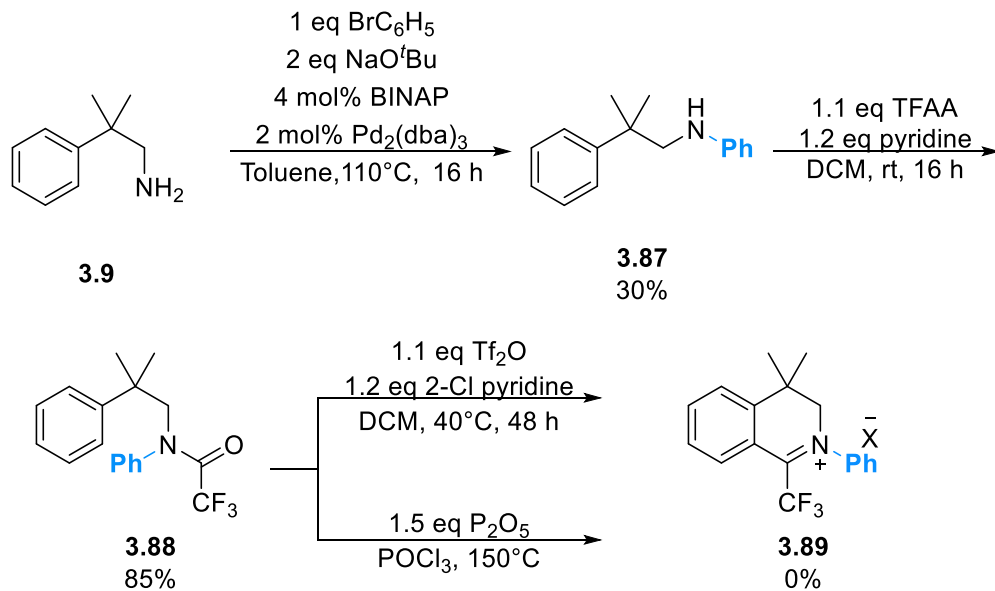
Figure 3.9: *N*-Phenyl iminium salts

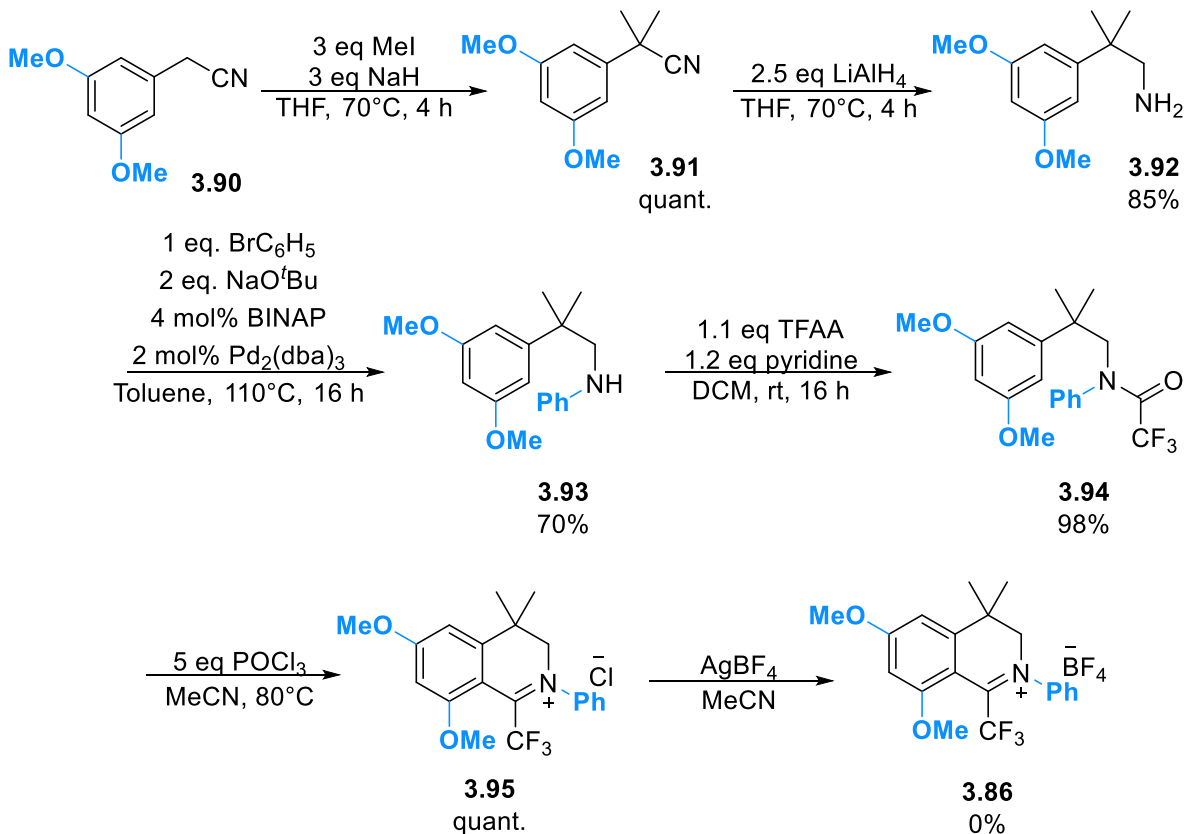


3.6.2 Synthesis of *N*-phenyl Iminium Salts

We followed a similar synthetic route to our other iminiums but deviated with a Buchwald-Hartwig coupling to amine **3.9** before our initial trifluoroacetamide formation (**Scheme 3.9**). This coupling step enables future modulation using other bromoarenes to tune catalyst activity. The formation of acetamide **3.87** proceeded smoothly in 85% yield. However, our previously employed cyclization methods failed to furnish iminium **3.89**.

We hypothesized that a more electron-rich arene scaffold would allow for a successful cyclization step by increasing arene nucleophilicity. To test this, we attempted a synthesis of an *N*-phenyl iminium catalysts starting from dimethoxyphenylacetonitrile **3.90** and were able to access the cyclized product, iminium **3.95** (**Scheme 3.10**). Unfortunately, we were unable to exchange the chloride counterion for the less coordinating tetrafluoroborate after trying with silver salt exchange to form **3.86**. Reactions with this material were not pursued further.

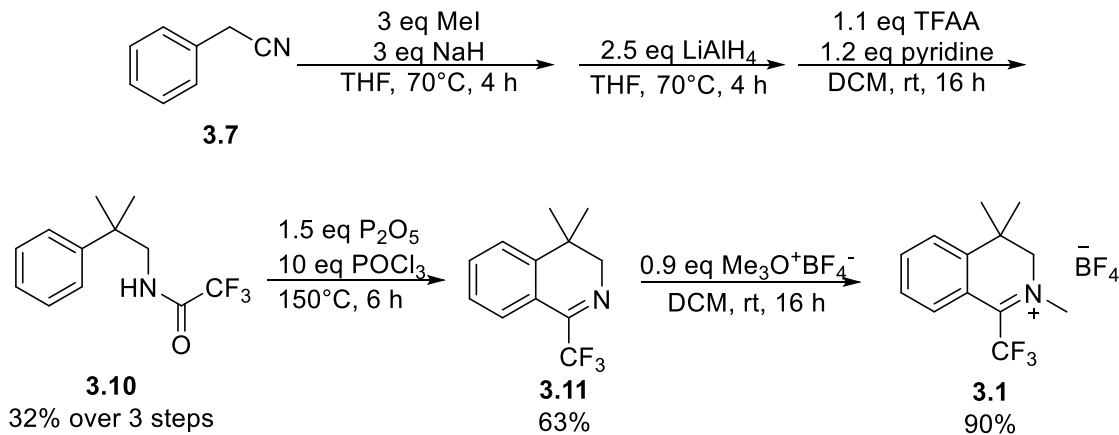
Scheme 3.9: N-phenyl iminium synthesis

Scheme 3.10: 1,3 Dimethoxy N-phenyl iminium synthesis

This iminium proves to be a good proof-of-concept for forming a new class of phenyl iminiums, allowing for another point of modulation that is directly at the active site of the catalyst. Further efforts will be needed to pursue a synthetic route to other counterions.

3.7 Improved Synthesis of the First-Generation Iminium Catalyst

Having synthesized iminium catalysts using modified conditions, we were able to incorporate these improvements into the original synthesis of the catalyst. The first three reactions, benzylic methylation, reduction, and trifluoroacetamide formation were found to be amenable to telescoping. Trifluoroacetamide **3.10** was then purified by flash chromatography; however, crystallization might be a viable alternative based on the observation of a crystalline white solid that forms in the crude reaction mass on standing. The cyclization step has been improved in both time and ease of purification under the conditions with phosphorus pentoxide and phosphorus oxychloride, where only starting material remains and imine **3.11** can be distilled under vacuum for high purity. This material can be treated with Meerwein salt to form the iminium salt **3.1**. Overall, one is able to make our iminium catalyst in multi-gram scale in a matter of days with minimal silica purification (**Scheme 3.11**). Such a streamlined synthesis might prove to be useful for scaleup production of the catalyst **3.1**.

Scheme 3.11: Improved synthesis of the iminium catalyst

3.8 Conclusions

Ultimately, a catalyst capable of providing higher yields with the chosen model substrates was not synthesized. However, significant improvements in the synthetic route of this class of catalysts have been realized, allowing for the potential of expedited generation of a large supply of iminium catalyst. The development of a synthetic pathway to *N*-phenyl iminiums has also been laid out and remains an unexplored area of catalyst modification. *N*-phenyl iminium catalysts might provide the most influential modifications of the catalyst and help specifically address the amination degradation pathway towards demethylation and incorporate stereoselectivity through axial chirality like **3.85** and **3.86**. Furthermore, there was only one instance of dual modification of the catalyst. Multiple modifications might be necessary to significantly improve the iminium's capabilities but have been relatively unexplored in this work. With a clearly laid out pathway with higher yields for iminium synthesis, it would be good to explore these catalysts with a broader substrate scope to more fully determine the capabilities of these catalysts. Computational data might also help provide clearer guidance for which catalyst designs might best improve our

reactions and which structures to prioritize, especially as we better understand factors influencing our amination and hydroxylation mechanisms.¹⁴

3.9 References

-
- ¹ Wang, D.; Shuler, W. G.; Pierce, C. J.; Hilinski, M. K. An iminium salt organocatalyst for selective aliphatic C–H hydroxylation. *Org. Lett.*, **2016**, *18* (15), 3826-3829.
- ² Combee, L.A.; Raya, B.; Wang, D.; Hilinski, M.K. Organocatalytic nitrenoid transfer: metal-free selective intermolecular C(sp³)–H amination catalyzed by an iminium salt. *Chem. Sci.*, **2018**, *9*, 935-939.
- ³ Hanquet, G.; Lusinchi, X. Action of an Oxaziridinium Tetrafluoroborate on Amines and Imines *Tetrahedron*, **1994**, *50* (42), 12185-12200.
- ⁴ Shuler, W.G. Ph.D. Thesis, University of Virginia, Charlottesville, VA, **2018**.
- ⁵ Brodsky, B. H.; Du Bois, J. Oxaziridine-mediated catalytic hydroxylation of unactivated 3 C–H bonds using hydrogen peroxide. *J. Am. Chem. Soc.*, **2005**, *127* (44), 15391-15393.
- ⁶ Litvinas, N.D.; Brodsky, B.H.; Du Bois, J. C–H Hydroxylation Using a Heterocyclic Catalyst and Aqueous H₂O₂. *Angew. Chem. Int. Ed.*, **2009**, *48*, 4513- 4516.
- ⁷ Movassaghi, M.; Hill, M.D. A versatile cyclodehydration reaction for the synthesis of isoquinoline and β-carboline derivatives. *Org. Lett.*, **2008**, *10* (16), 3485-3488.
- ⁸ Fiori, K. W.; Du Bois, J. Catalytic intermolecular amination of C–H bonds: method development and mechanistic insights. *J. Am. Chem. Soc.*, **2007**, *129* (3), 562–568.
- ⁹ Clark, J. R.; Feng, K.; Sookezian, A.; White, M. C. Manganese-catalysed benzylic C(sp³)–H amination for late-stage functionalization. *Nat. Chem.*, **2018**, *10* (6), 583-591.
- ¹⁰ Kirsch, P. *Modern fluoroorganic chemistry: synthesis, reactivity, applications*. John Wiley & Sons, **2013**.
- ¹¹ Pastor, R.; Cambon, A. Synthèse d'isoquinoléines F-alkyl substituées. *J. Fluor. Chem.*, **1979**, *13* (4), 279-296.
- ¹² K. Guthikonda, K.; Du Bois, J.; A Unique and Highly Efficient Method for Catalytic Olefin Aziridination. *J. Am. Chem. Soc.*, **2002**, *124* (46), 13672-13673.
- ¹³ Kim, K. H.; Cheon, C. H.; Concise catalytic asymmetric total syntheses of ancistrocladinium A and its atropdiastereomer. *Org. Chem. Front.*, **2017**, *4* (7), 1341-1349.

¹⁴ Rotella, M. E.; Dyer, R. M.B.; Hilinski, M. K.; Gutierrez, O. Mechanism of Iminium Salt-Catalyzed C(sp³)-H Amination: Factors Controlling Hydride Transfer versus H-Atom Abstraction. *ACS Catal.*, **2020**, *10* (1) 897-906.

Chapter Four

New Iminoiodinanes For C–H Amination

Introduction

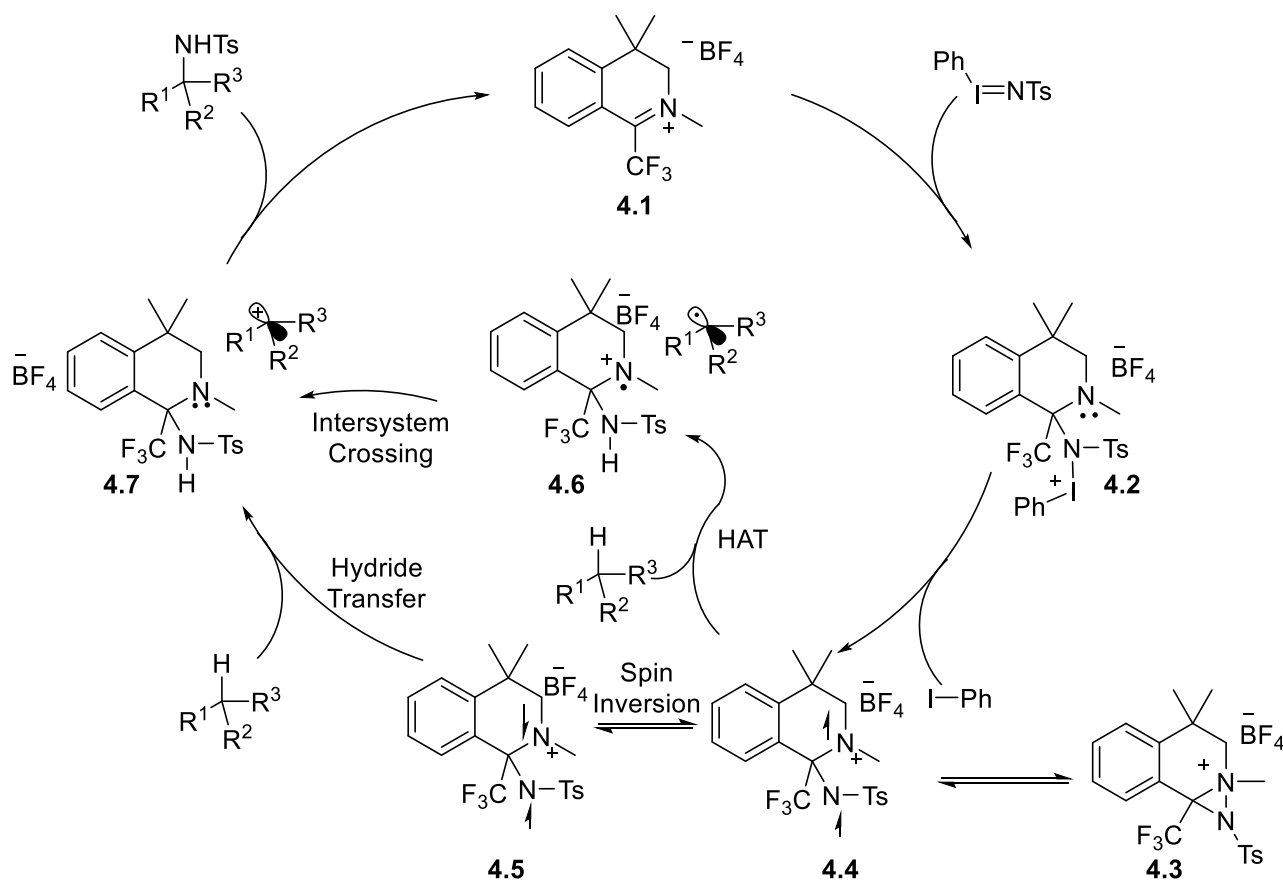
The development of catalytic methods for the direct functionalization of C–H bonds has allowed chemists to reimagine practical synthetic routes to complex molecules.¹ The amination of C–H bonds is one such transformation. Formation of carbon-nitrogen bonds has drawn significant attention due to the importance of nitrogen-based functionality in FDA-approved pharmaceuticals, which contain an average of 2.3 nitrogen atoms per small-molecule drug, as well as other biologically relevant molecules such as bioactive natural products.² Chemical properties such as hydrogen bonding ability and hydrophilicity can be greatly enhanced by the addition of more nitrogen functionality to molecules. As such, methods for the amination of C–H bonds to incorporate this functionality rapidly and efficiently are eagerly sought.

4.1 Organocatalytic C–H Amination

The Hilinski lab was the first to successfully demonstrate a method for organocatalytic atom-transfer C–H amination. The method employed iminium salt catalyst **4.1**, previously developed for C–H hydroxylation, and iminoiodinanes (e.g. PhINTs and PhINTces) as nitrenoid precursors.³ This method was amenable to the amination of benzylic C–H bonds and weak aliphatic C–H bonds. In looking for ways to increase the scope and practicality of this reaction, one area identified for improvement was the iminoiodinane reagent. The requirement to pre-synthesize these reagents creates a barrier to adoption compared to methods that are compatible with in situ formation of iminoiodinanes, for example from the corresponding sulfonamides and carbamates.⁴ In addition, intramolecular reactions generally require compatibility with in situ iminoiodinane formation.^{5,6}

In collaboration with the Gutierrez group, computational efforts were undertaken to better understand the mechanism and reactivity of the amination reaction.⁷ Using quantum mechanical calculations and molecular dynamics simulations, we were able to corroborate our mechanistic understandings from our original work that our system has a preference for benzylic amination and otherwise non-benzylic C–H bonds only when a resonance or hyperconjugation stabilized carbocation would form. The initially proposed diaziridinium (**4.3**) is an off-cycle intermediate, whereas an open amidyl biradical form (**4.4**) is the active oxidant. The computationally calculated mechanism is described in **Figure 4.1**. The iminium **4.1** initially undergoes nucleophilic attack from PhINTs to form species **4.2**. The rate determining step is the loss of iodobenzene from **4.2** to form the open amidyl biradical species, which can interconvert between its singlet (**4.4**) and triplet (**4.5**) biradical forms through spin inversion. Triplet **4.4** reacts with the C–H via H-atom abstraction (HAT) to form **4.6**. Whereas, **4.5** reacts with the C–H of a substrate via hydride transfer to form **4.7**. **4.6** then undergoes intersystem crossing to form **4.7** before the aminated product is released and **4.1** is reformed. Given that the rate-determining step was calculated to involve breaking of the N–I bond, we hypothesized that modification of the nitrogen protecting group along with electronic modification of the iodobenzene should impact the rate of amination.

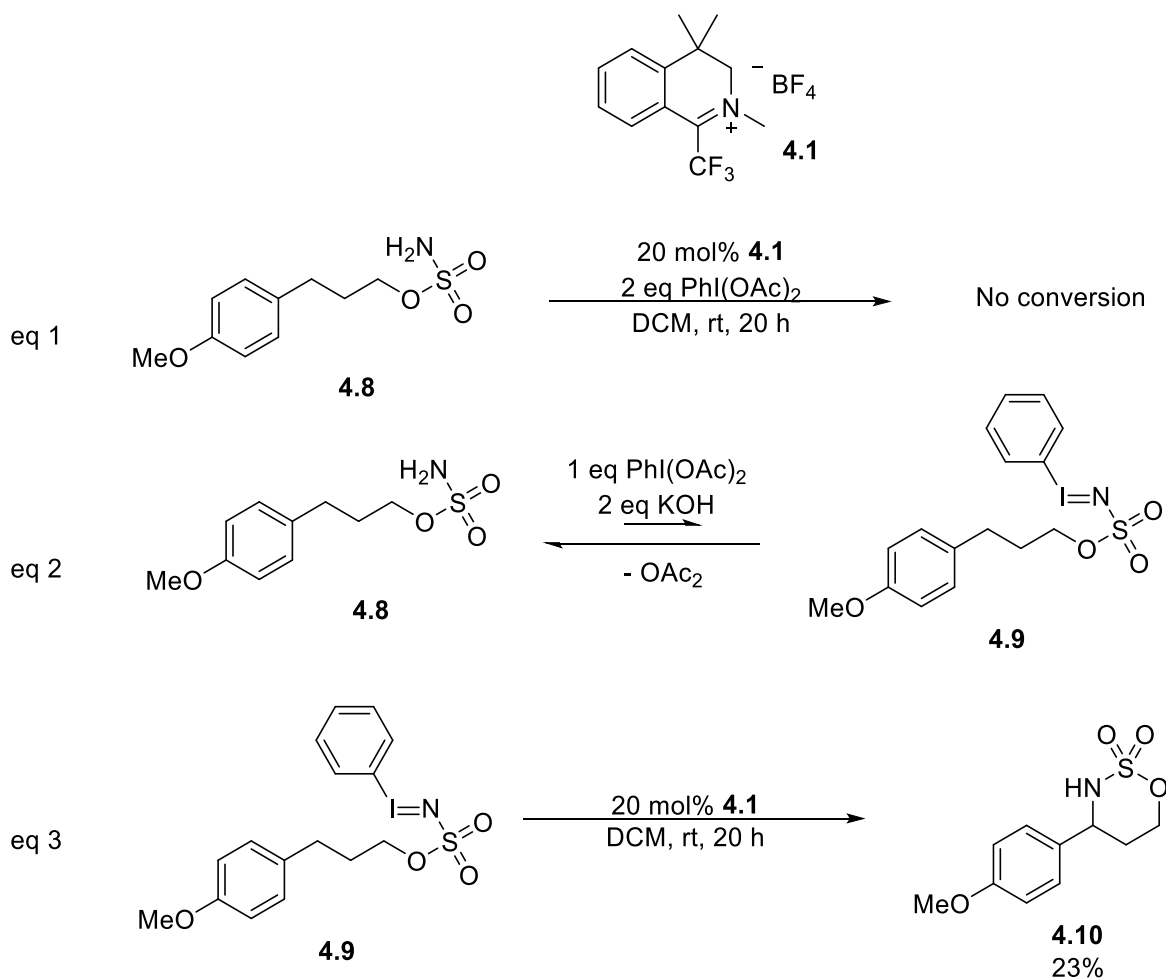
Figure 4.1: Proposed catalytic cycle of organocatalytic C–H amination based on DFT and molecular dynamics calculations.



4.2.1 Intramolecular Amination with a preformed iodine

Given this computational data and having already explored some catalyst development (see Chapter 3), we then focused on the iodine to expand our amination capabilities given that calculations suggest the rate determining step of our amination mechanism is the conversion of **4.2** to **4.4**, which involves cleavage of the N–I bond. As mentioned above, practical intramolecular C–

H amination reactions would need compatibility with in situ formation of the iminoiodinane. As shown in **Scheme 4.1**, attempted iminium-catalyzed intramolecular amination of sulfamate **4.8** using $\text{PhI}(\text{OAc})_2$, which has been used commonly as an oxidant in metal-catalyzed intramolecular amination, failed to provide any of the desired product.⁸ We were not certain the iminoiodinane was being formed under these in situ conditions as iminoiodinanes are generally very low in concentration with the equilibrium of the reaction between the sulfonamide and $\text{PhI}(\text{OAc})_2$ favoring the free sulfonamide (**eq 2, Scheme 4.1**).⁹ To evaluate the relative impacts of iminoiodinane formation we synthesized and isolated the iminoiodinane (**4.9**) expected to be formed from the reaction between **4.1** and $\text{PhI}(\text{OAc})_2$. This substrate would enable a six-membered oxathiazinane amination which is generally the favored structure versus the five-membered oxathiazinane. This preference is rationalized by comparing metrical parameters (in particular, the N–S–O bond angle) between the starting sulfamate and product heterocycle.¹⁰ Treatment with catalyst **4.1** resulted in modest yield of intramolecular amination product **4.10**. This confirmed that our catalyst is capable of promoting intramolecular amination of pre-formed iminoiodinanes, suggesting that under the right conditions intramolecular amination via in situ iodine formation is a possibility.

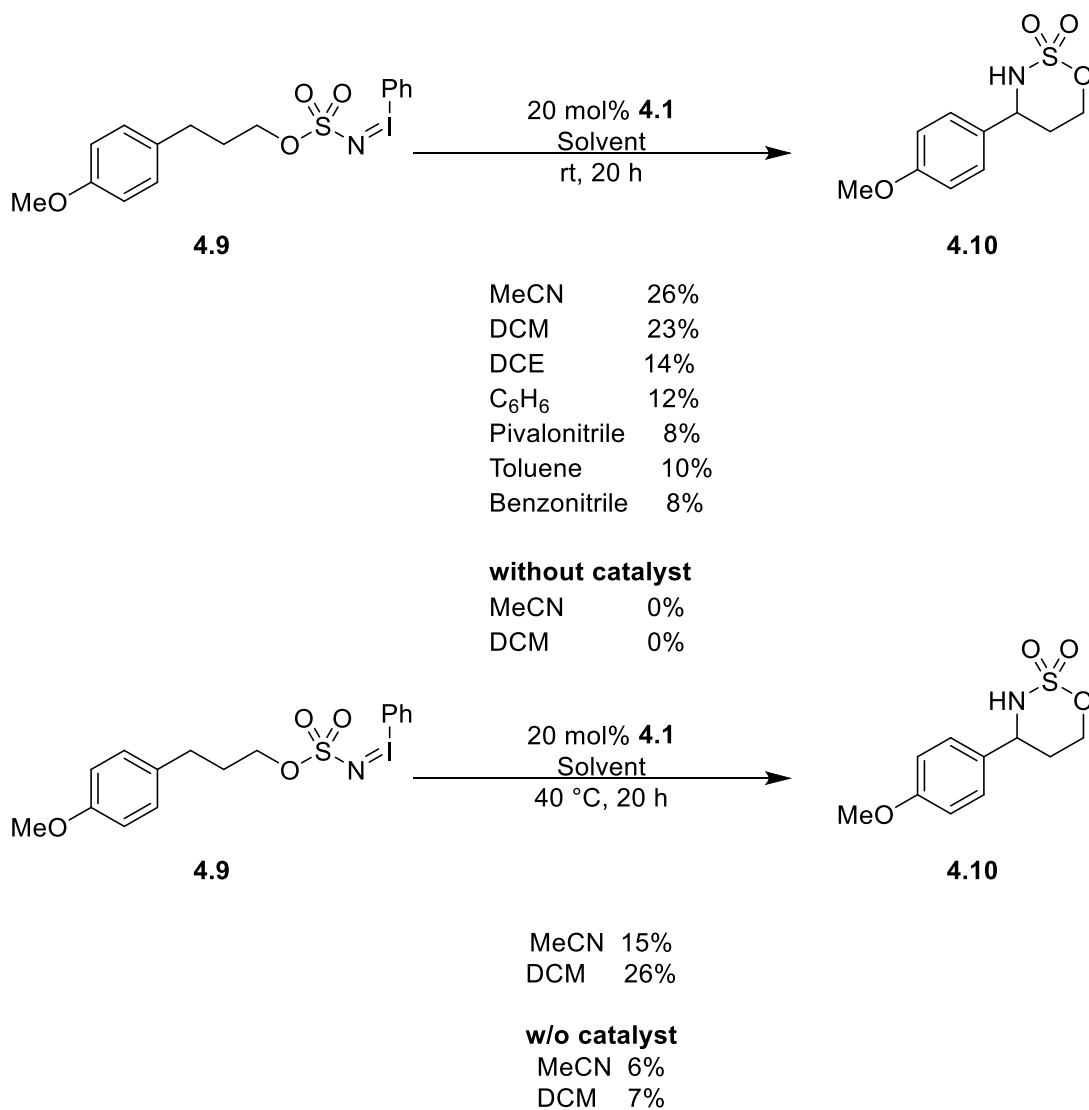
Scheme 4.1: Intramolecular amination with preformed iminoiodinane

4.2.1 Solvent Screening

With the viable substrate **4.9** in hand, we began screening solvents to possibly help increase our yields. We tried several nitrile solvents that had found to be beneficial for rhodium-catalyzed nitrene aminations by mitigating solvent oxidation, and found that the use of acetonitrile provided slightly higher yields than DCM.⁴ Dichloroethane, benzene, and toluene all worked poorly compared to DCM. Under slightly elevated temperatures, the reaction proceeds only marginally better in DCM and worse in MeCN, possibly due to the poor thermal stability of the preformed

iminoiodinane **4.9**, which we have observed, decomposes at temperatures as low as 30 °C. Control reactions without catalyst demonstrated the necessity of the iminium for the reaction to proceed, unless otherwise heated wherein some background amination occurs.

Scheme 4.2: Solvent screening of preformed iminoiodinane amination

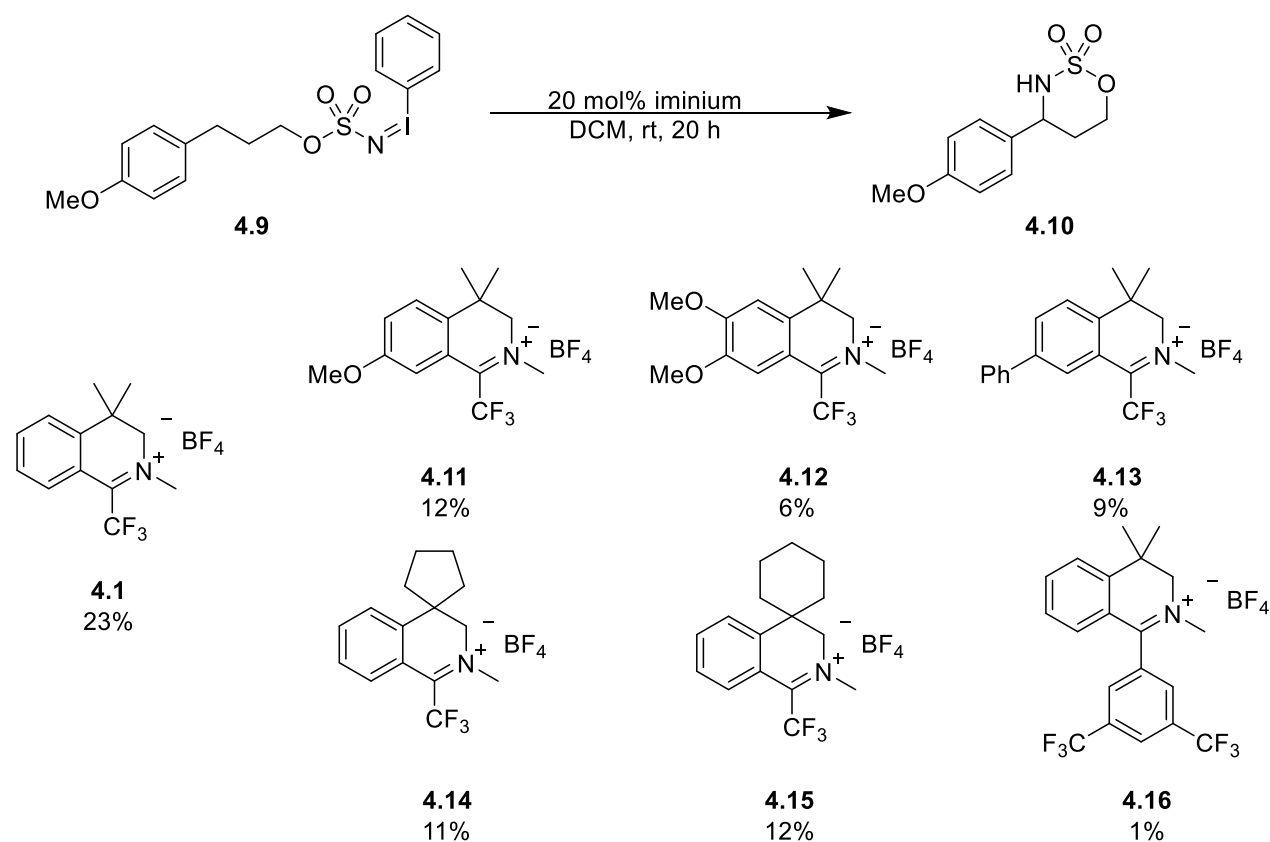


4.2.2 Catalyst Screening

In addition, an assessment of our previously synthesized catalysts was undertaken. Catalyst structure showed no improvement on the efficiency of the amination reaction. This is not surprising

given that these catalysts had already been screened for intermolecular C–H amination and shown to perform poorly (see Chapter 3). Catalysts **4.11** and **4.12** had shown comparable results to **4.1** for intermolecular amination but performed worse with this iminoiodinane.³ Catalysts with minimal or no ring strain at the benzylic position, **4.14** and **4.15**, also performed worse than **4.1**. The use of catalyst **4.16** resulted in almost no conversion. One likely reason is the larger aryl substituent blocking the attack trajectory of the iminoiodinane on the iminium carbon.

Scheme 4.3: Catalyst screening of preformed iminoiodinane amination



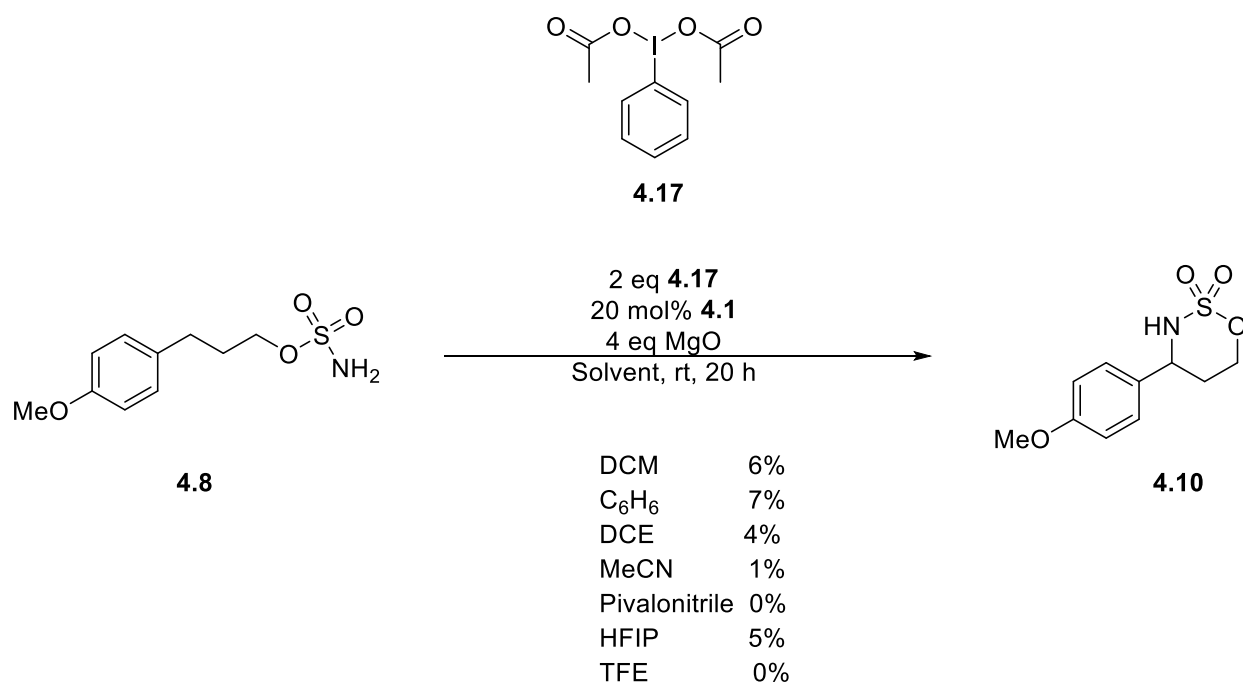
4.3.1 Intramolecular amination via in situ iminoiodinane formation

Having confirmed the feasibility of intramolecular aminations with our iminium catalyst, we worked to establish conditions for in situ iminoiodinane formation compatible with this family

of catalysts. The first example of iminoiodinane synthesis is from 1975, when PhINTs was isolated following the reaction of diacetoxy iodobenzene with tosylamide in MeOH under basic conditions.¹¹ It is well established that the polymeric structure of iminoiodinanes make them relatively insoluble in organic solvents.¹² For solvents in which it does dissolve completely, it can be the result of a reaction between the ylide and the solvent, such as when PhINTs undergoes solvolysis to tosylamide and (dimethoxyiodo)benzene when dissolved in MeOH.¹¹ It was not until 2000 that the first example of in situ generation of iminoiodinanes was utilized for C–H amination by Che utilizing metal porphyrin complexes to aminate ethyl benzene, indane, and adamantane.¹³ This implementation enabled higher yields of amination for several of these substrates and allowed for efficient exploration of the effect of sulfonamide structure. We hypothesized that there is a relatively low concentration of iminoiodinane in solution under in the conditions evaluated, which was detrimental to our attempts at organocatalysis. Therefore, we decided to evaluate new conditions that might increase the concentration.¹⁴

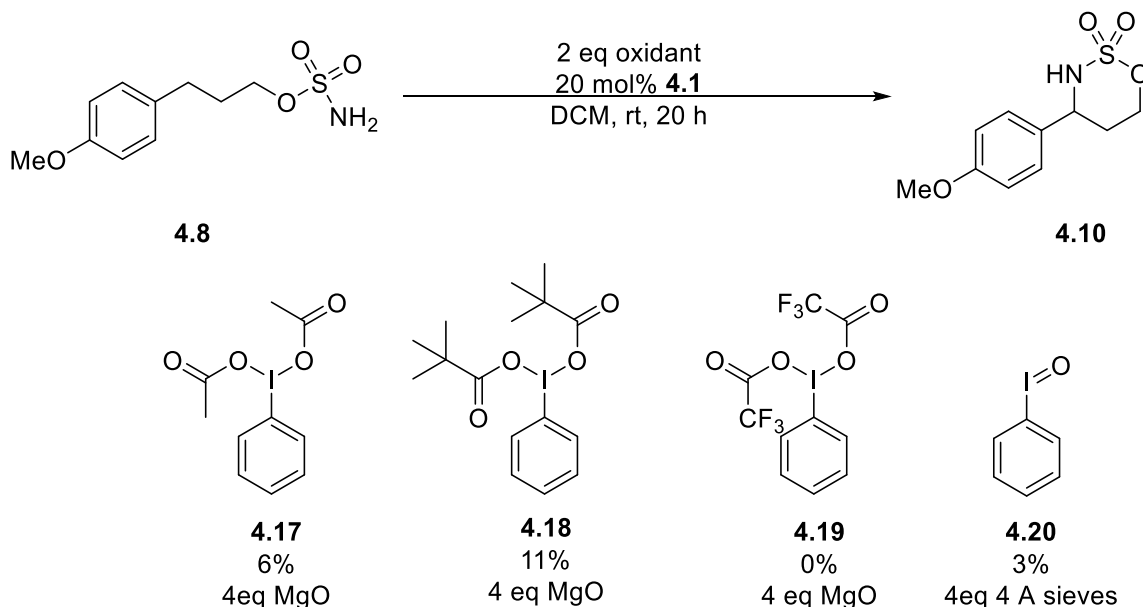
4.3.2 Solvent Screening for in situ intramolecular amination

We began with initially screening solvents for reactions using diacetoxy iodobenzene (**4.17**) to evaluate the effect on yield. We added the inorganic base, MgO, to neutralize any acetic acid formed from the formation of the iminoiodinane. Benzene resulted in the marginally highest yield with other non-polar solvents forming a similarly low amount of product. However, most of these solvents did not lead to any meaningful improvement in yields.

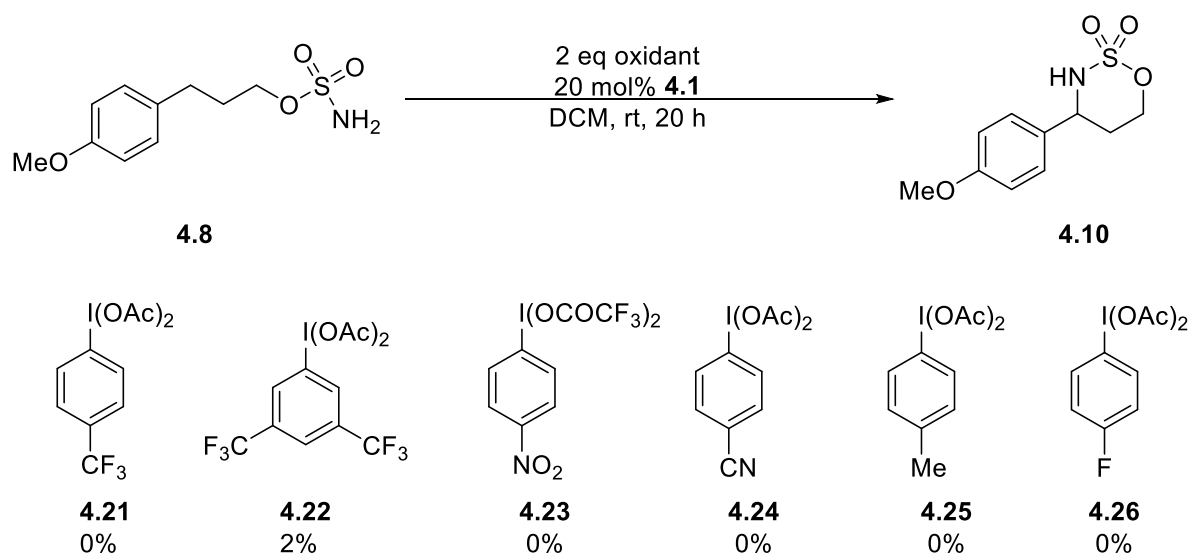
Scheme 4.4: Intramolecular amination with diacetoxy iodobenzene

4.3.3 Oxidant screening

Given the poor response to solvent screening, we next investigated the effect of changes to the carboxylate present in $\text{PhI}(\text{OAc})_2$. We hypothesized that different ligands might help form the iminoiodinane in solution. Modification had minor effects on our reaction yield with the pivalate analog (**4.18**) providing a modest increase in yield. The pivalate might help increase solubility of the iodine and enhance the formation of the iminoiodinane.¹⁵ The trifluoroacetate (**4.19**) provided no conversion to product **4.10**. Iodosobenzene (**4.20**), used for silver-catalyzed reactions, also performed poorly.¹⁶

Scheme 4.5: Intramolecular amination with oxidized iodobenzenes

We also synthesized diacetoxy iodobenzenes containing substitution on the benzene ring, to examine how tuning the electronics might improve our amination mechanism (**Scheme 4.6**). In particular, we thought that tuning the electronics might help with the proposed rate determining step involving the cleavage of the N-I bond. Ultimately, all of these proved to be extremely poor oxidants with little to no amination observed regardless of changes in the electron-withdrawing or -donating groups. Given the poor performance of screening so far, we looked to try a new oxidant beyond iodanes to enable intramolecular amination.

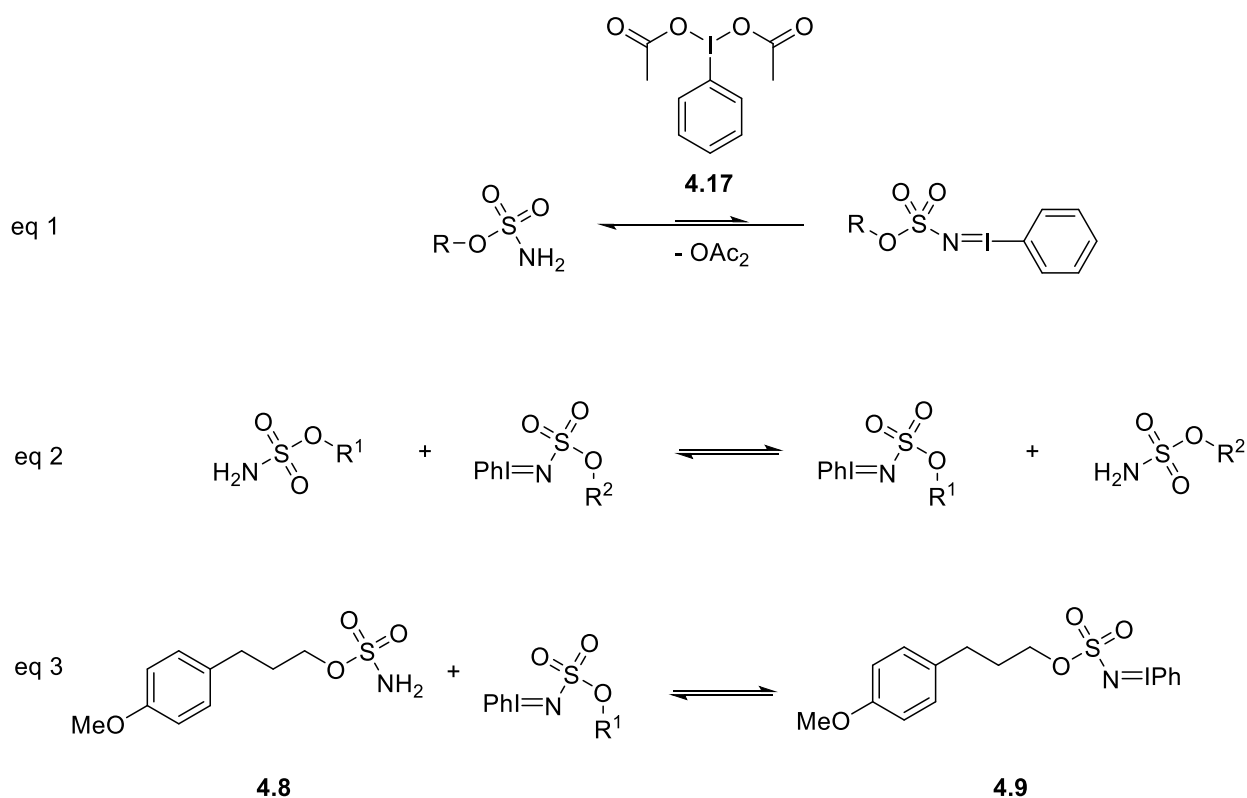
Scheme 4.6: Intramolecular amination screening of functionalized diacetoxy iodobenzenes

4.4.1 Iminoiodinane Exchange for intramolecular amination

The Du Bois lab had shown that in the presence of iminoiodinanes, sulfonamides form an equilibrium with the corresponding iminoiodinane arising from the exchange of iodobenzene with release of the sulfonamide originally present as part of the iminoiodinane (eq 2, Figure 4.2). They were able to use a preformed iminoiodinane in place of iodobenzene dicarboxylates for intramolecular amination, with a 2.5-fold increase in rate of product formation.⁹ Furthermore, they showed that the rate of equilibrium between free sulfonamide and iminoiodinane of the sulfonamide is dramatically increased from over 30 minutes to less than 15 minutes with the presence of a pre-formed iminoiodinane additive. We decided to investigate this exchange as a means to activate our intramolecular substrate to enable benzylic C–H amination (Figure 4.2). Iminoiodinanes formed under in situ conditions are generally very low in concentration with the equilibrium favoring the free sulfonamide (eq 1, Figure 4.2). Based on Fiori's dissertation, the equilibrium established between sulfonamides and iminoiodinanes ought to be more quickly established with a preformed iminoiodinane being present in the mixture (eq 2, Figure 4.2) than

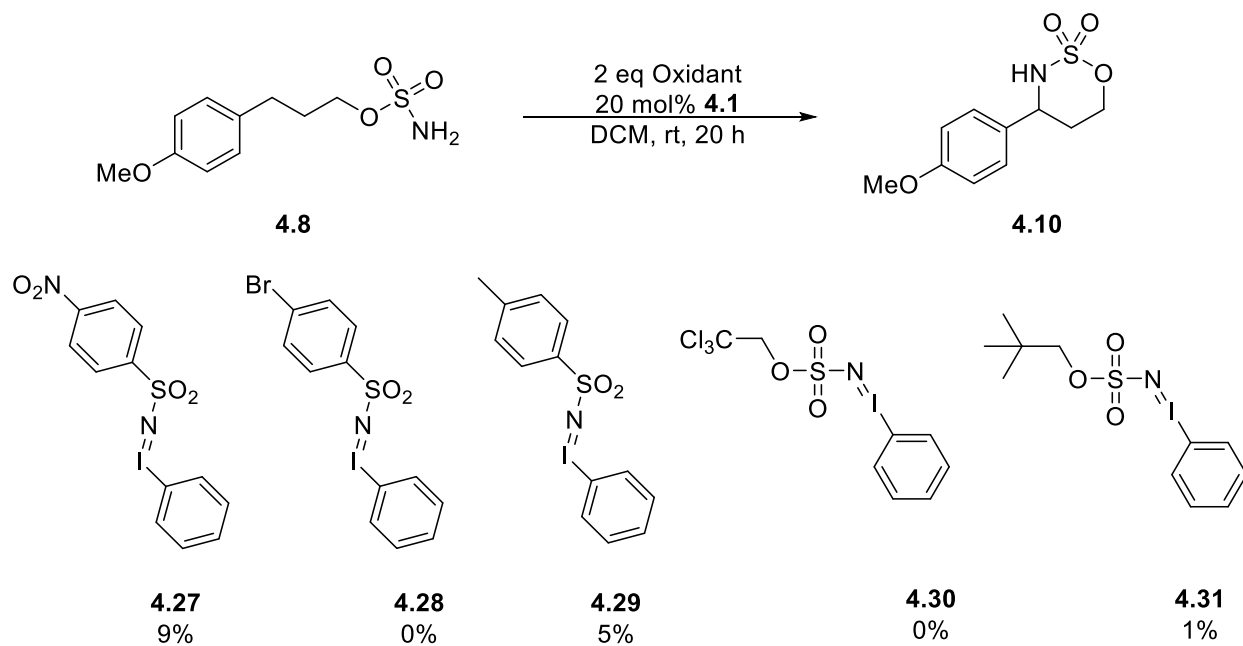
simply in the presence of **4.17**. We hoped to leverage this by using a preformed iodine in the presence of a free sulfonamide capable of intramolecular amination (**eq 3, Figure 4.2**). This would enable the in situ formation of the desired iminoiodinane of our intramolecular substrate.

Figure 4.2: Iminoiodinane exchange equilibrium



4.4.2 Iminoiodinane Screening

Given this hypothesis, we tried several iminoiodinanes (**4.27-4.31**) that have been previously utilized for intermolecular amination reactions (**Scheme 4.7**). These iminoiodinanes were not effective for this amination resulting in little to no conversion. Therefore, we decided to explore modifying the iodoarene to influence the reactivity of our intramolecular reaction.

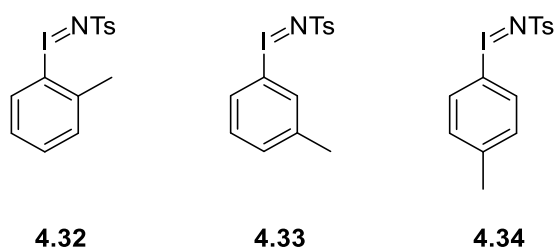
Scheme 4.7: Screening of iminoiodinanes as oxidants for intramolecular amination

4.4.3 Development of new more soluble iminoiodinanes

Given the low yields of our initial iminoiodinanes, we wanted to try more soluble iminoiodinanes to see how that might influence the nature of the exchange reaction and subsequent amination. Although these iminoiodinanes might require more synthetic steps, we hypothesized that they would be beneficial for expanding the capabilities of our catalyst and we investigated the literature to determine appropriate iminoiodinanes to synthesize and test. We hoped that more soluble iodinananes might enable a higher concentration of the intermediate involved in the rate determining step and subsequently increase the rate of amination. Furthermore, these iodinananes might help decrease the barrier for N–I bond cleavage. Introducing electron-donating groups on the iodobenzene would make the iodide more electron rich, and electron withdrawing groups on the sulfonamide would make a more electron deficient nitrogen atom and ultimately reduce double bond character on the N–I bond.

X-ray powder diffraction studies have shown the nature of the PhINTs to be polymeric.¹⁸ This polymeric structure is formed by I–N intermolecular non-bonding attractions. Intermolecular electrostatic interactions and ionic bonding between individual iminoiodinanes enable highly aggregated polymeric networks. Subtle changes in the structure of the iminoiodinane have influences into the nature of these polymeric networks. Protasiewicz showed that the addition of an ortho methyl group to form (tosyliminoiodo)-*o*-toluene (**4.32**, **Figure 4.3**) disrupted the secondary bonding affecting the polymeric structure.¹⁹ The methyl group disrupted I–N and I–O non-bonding attractions resulting in the formation of a different polymeric structure while maintaining the same analogous electrophilicity of the iodine center, as tested by cyclic voltammetry.²⁰ Further work was done by the Protasiewicz group to understand the supramolecular structure of other iminoiodinanes including the tosyliminoiodo-*m*-toluene (**4.33**) and tosyliminoiodo-*p*-toluene (**4.34**).²¹ Each of these iminoiodinanes had different supramolecular structures demonstrating the dramatic influence that minor structural changes can cause.

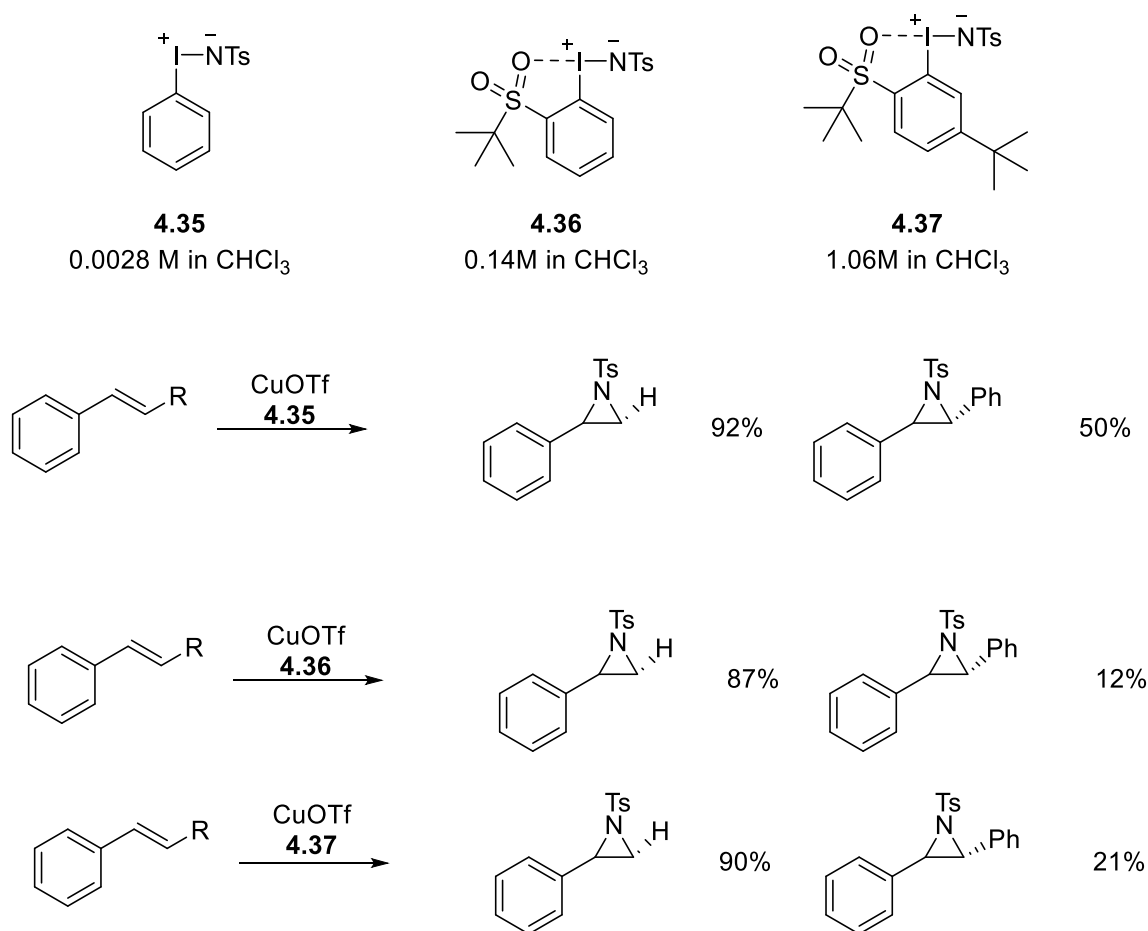
Figure 4.3: Methylated (tosyliminoiodo) toluenes



With a better understanding of the intermolecular bonding of the polymeric structure of these iminoiodinanes, the Protasiewicz group developed a new iminoiodinane that includes intramolecular bonding to help dissociate the monomer iminoiodinanes from the supramolecular polymer.²² This iminoiodinane has a sulfonyl group at the ortho position (**4.36**, **Figure 4.4**), wherein a sulfonyl oxygen can directly interact with iodine and limit secondary intermolecular

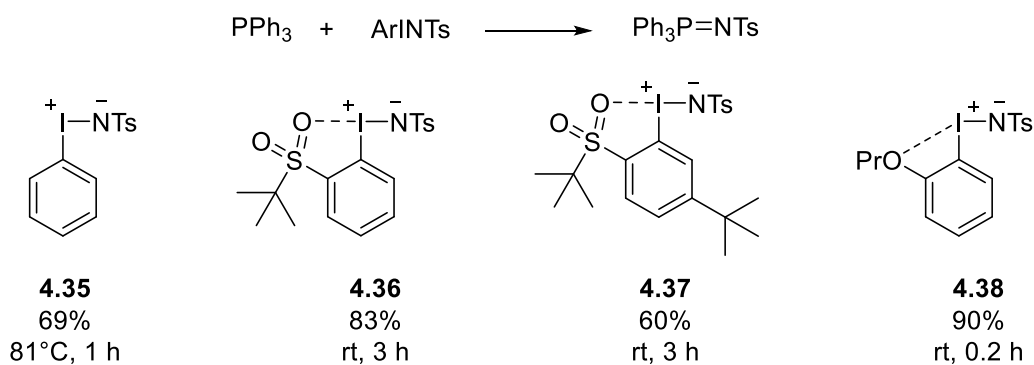
electrostatic I–O bonding that form the supramolecular structures. This feature greatly enhanced the solubility of the iminoiodinanes in organic solvents such as chloroform, by over 50-fold compared to **4.35**. This solubility was even further enhanced by the introduction of a tert-butyl group on the iminoiodinane, as in **4.37** whose solubility in chloroform is increased 8-fold compared to **4.36**.²³ Unfortunately, none of these solubility increases seemingly correlated with significant increase to yields for the aziridination reactions they tested (**Figure 4.4**). In fact, these modifications appeared worse for the aziridation of stilbene under the tested Cu conditions suggesting factors other than solubility of the iodine controlling the reactivity for aziridination.

Figure 4.4: Soluble tert-butyl sulfonyl iminoiodinanes



Studies were also later conducted by Zhdankin to create other more soluble iminoiodinanes. Instead of a *tert*-butyl sulfonyl group, they utilized alkoxy substituents ortho to the iodoarene to disrupt the intermolecular bonding of the polymeric structure.²⁴ A series of *o*-alkoxyphenyliminoiodanes were synthesized and evaluated for reactivity with the propyl alkoxy (**4.38**) being the most soluble of the alkoxy derivatives. When compared directly with the Protasiewicz iminoiodinanes in noncatalyzed reactions, the alkoxy iodinananes provide higher yields and increased rates in the transylation reaction with triphenyl phosphine (**Figure 4.4**).

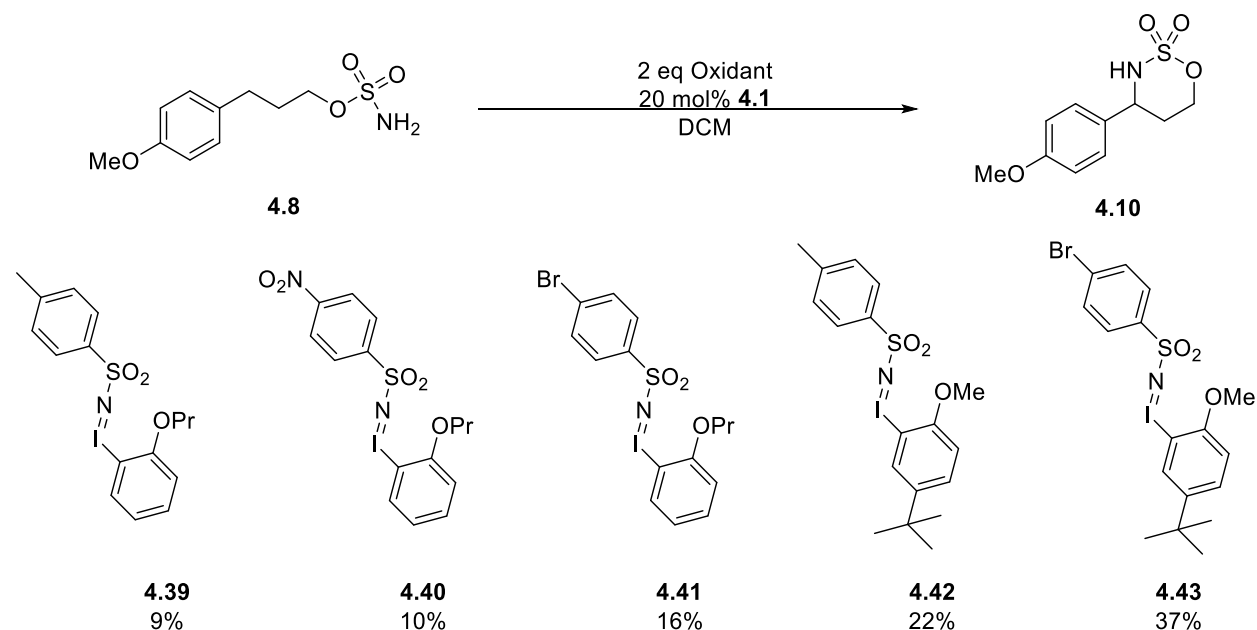
Figure 4.4: Comparison of soluble iminoiodinanes reactivity with triphenyl phosphine



Given this information, we explored the capabilities of several functionalized iodoarene iminoiodinanes to tune the solubility and reactivity of our aminations (**Scheme 4.8**). We first synthesized several iminoiodinanes containing propoxy iodoarenes (**4.39-4.43**). These performed poorly, however, the brosyl sulfonamide (**4.41**) provided the highest yield. This might be due to high electronegativity of the bromine from the sulfonamide helping withdraw electron density and destabilize the N–I bond. As a result, the intramolecular iminoiodinane is more thermodynamically stable and favored in the equilibrium. We next synthesized several iodoarenes that incorporated the alkoxy at the 2-position and *tert*-butyl substituent at the 5-position (**4.42** and **4.43**) to enhance solubility. The solubility of these iodinananes could be improved by including functionality from both the Zhdankin and Protasiewicz iminoiodinanes. The resulting iminoiodinanes worked well

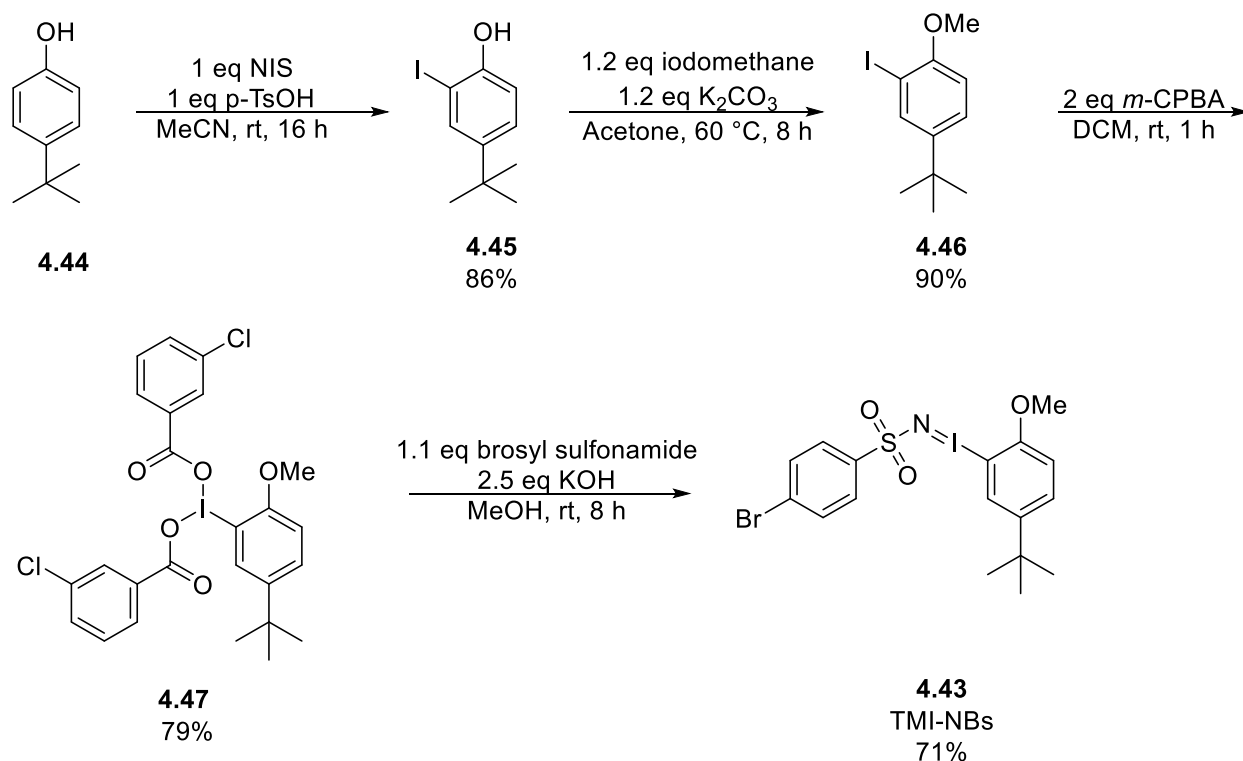
with the brosyl 5-*tert*-butyl 2-methoxy iminoiodinane (TMI-NBs, **4.43**) enabling our highest yields yet.

Scheme 4.8: Soluble iminoiodinane screening for intramolecular amination



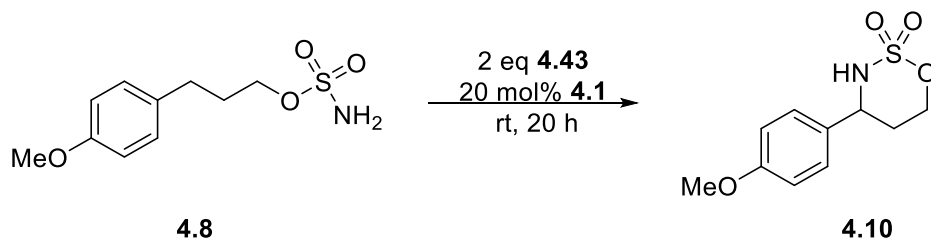
4.4.1 TMI-NBs Synthesis

Synthesis of this class of iminoiodinane (**Scheme 4.9**) began with iodination of *tert*-butyl phenol (**4.44**) using N-iodosuccinimide providing **4.45** in 86% yield. The phenol **4.45** was then alkylated with iodomethane to form **4.46** and subsequently oxidized. The use of *m*-CPBA was required to ensure full conversion of iodoarene **4.46** to iodine **4.47**; more commonly used oxidation methods for this step resulted in poor conversion and/or problematic isolation.²⁵ The iodine was subsequently carried on to form the brosyl sulfonamide iminoiodinane **4.43** utilizing a method modified from one reported by the White group to extract and precipitate the iminoiodinane.²⁶

Scheme 4.9: Synthesis of *tert*-butyl methoxy iodobenzene iminoiodinanes

4.4.2 Solvent Screen with TMI-NBs

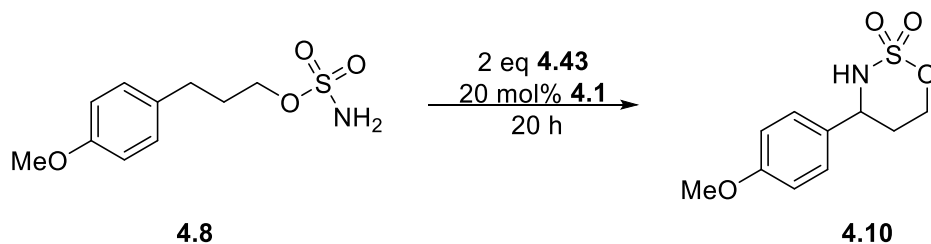
With a superior oxidant in hand, we then attempted to identify the best solvent for our reaction (**Scheme 4.10**). Compared to dichloromethane, other non-polar aprotic solvents like chloroform, benzene, and dichloroethane provided moderate yields but performed poorly. We again tried several nitrile-based solvents including pivalonitrile and benzonitrile. The reaction also performed poorly in benzotrifluoride, a greener solvent replacement for dichloromethane.²⁷

Scheme 4.10: TMI-NBs solvent screening

C ₆ H ₆	18%
DCE	24%
MeCN	25%
DCM	37%
CHCl ₃	22%
PhCF ₃	6%
Pivalonitrile	6%
Benzonitrile	9%

4.4.3 Temperature Screening

We also wanted to explore different reaction temperatures with these iminoiodinanes (**Scheme 4.11**). Previously, iminoiodinanes had to be heated to help solubilize them into their monomer forms and slightly elevated temperatures are used for some transition metal catalysis like the Mn(ClIPc).²⁵ We initially tried DCM at 40 °C which led to improved yields. Chloroform allowed for higher temperatures but led to lower yields. Both DCE and acetonitrile were tested at 70 °C and provided our best yields. However, at elevated temperatures we have observed a large amount of uncatalyzed reaction occurring. Control reactions without catalyst showed a substantial amount of background activity above 40 °C in all solvents screened.

Scheme 4.11: TMI-NBs solvent screening at elevated temperatures

40°C DCM	45%
60°C CHCl ₃	35%
70°C DCE	50%
70°C MeCN	56%
50°C MeCN	37%

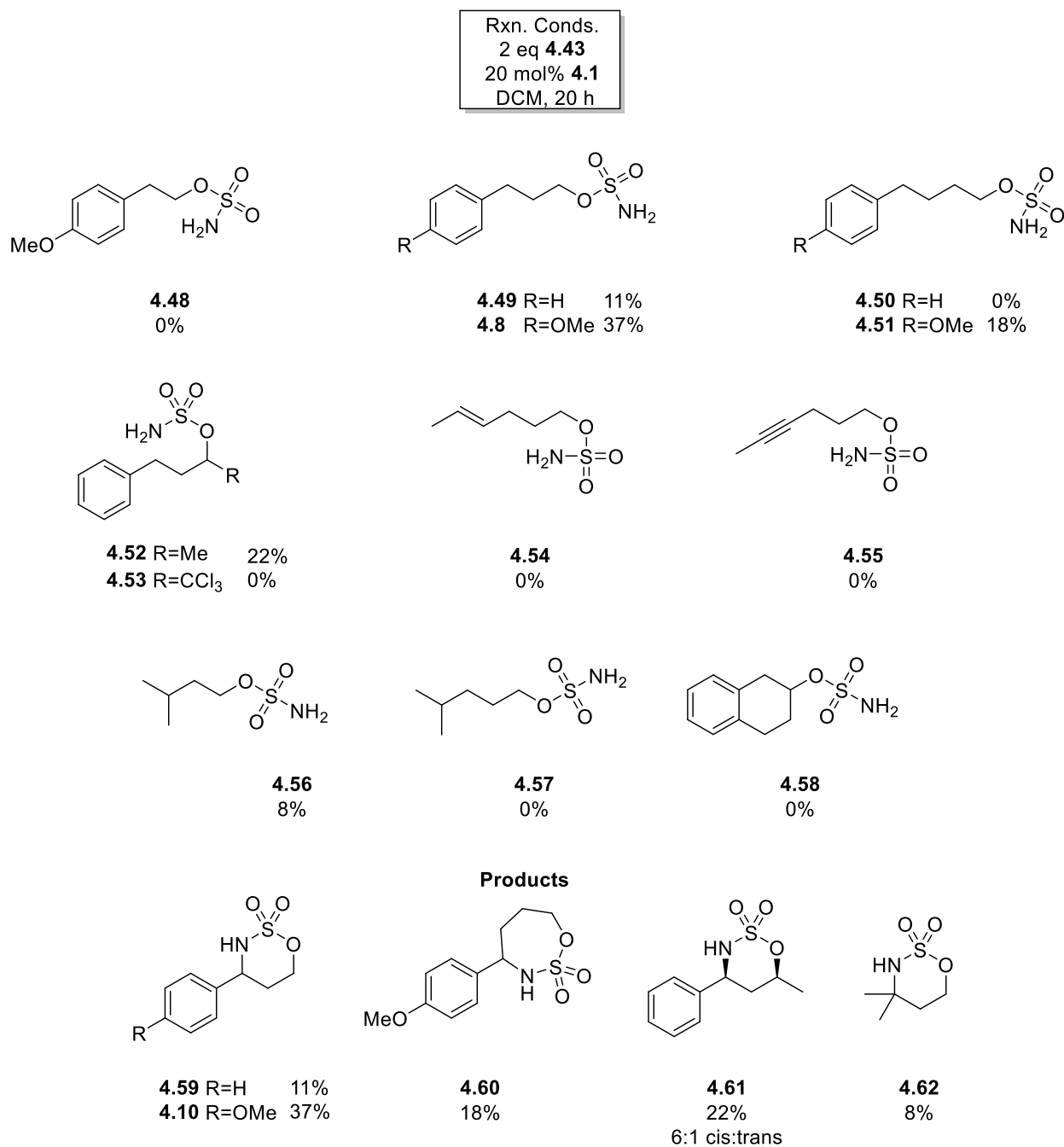
without catalyst

40°C DCM	24%
50°C MeCN	20%
70°C MeCN	22%
70°C DCE	21%
rt DCM	4%
rt MeCN	1%

4.4.4 Screening for Intramolecular Reactions

With an initial exploration of conditions, we investigated the potential to expand our substrate scope to other sulfonamides (**Scheme 4.12**). The phenylpropyl sulfonamide (**4.49**) provided low conversion to the oxathiazinane confirming the effects that the *p*-methoxy group has to activate the benzylic C–H bond (**4.8**) by stabilizing build-up of positive charge. We explored several sulfonamides that would be expected to lead to larger (**4.50** and **4.51**) and smaller (**4.48**) ring sizes of products. However, only the activated benzylic C–H substrate (**4.51**) forming the oxathiazepane **4.60** worked, albeit in low yield, whereas other oxathiazepane and oxathiazolidine rings failed to form. We hypothesized that the addition of the methyl or trichloromethyl group on substrates **4.52** and **4.53** would result in higher yields by decreasing the preference for an all-anti conformer expected for compounds like **4.49**. In support of this hypothesis, **4.47** provided some increase in yield over **4.44**, whereas **4.48** failed to react, presumably due to a negative electronic

influence of the trichloromethyl group. Allylic (**4.54**) and propargylic (**4.55**) intramolecular substrates were explored with no conversion identified. We were able to get low conversion of a tertiary C–H amination **4.56** to form the oxathiazinane **4.62**, but not the oxathiazepane sulfamate precursor **4.57**. Our intermolecular conditions are generally reactive towards cyclic benzylic C–H bonds, but cyclic intermolecular substrate **4.58** resulted in no conversion. Ultimately, we were unable to get a broad scope of intramolecular aminations to effectively work under these conditions. Our reaction products were mainly limited to benzylic C–H and one tertiary C–H amination, suggesting that our current catalytic system is not sufficient for these stronger C–H bonds that should react through the HAT mechanism occurring after our rate determining step.

Scheme 4.12: Intramolecular amination substrates and respective product yields

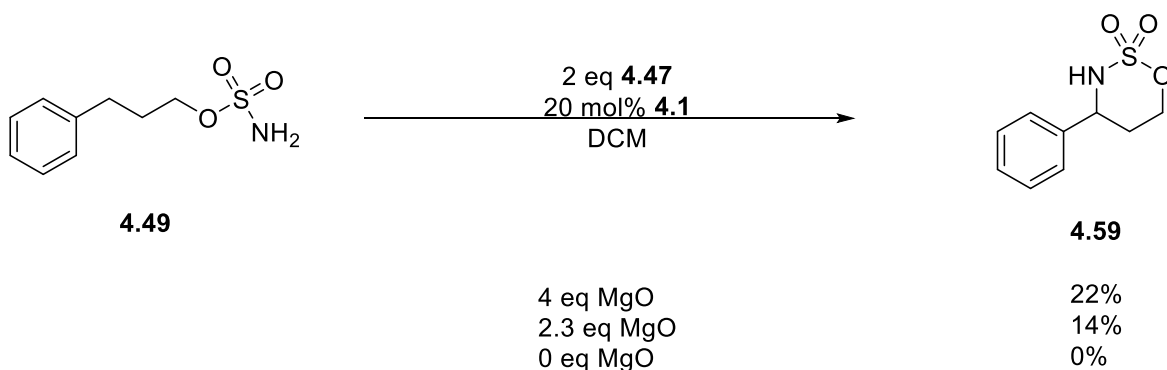
4.6 Conclusions

Although intramolecular aminations do not appear to be effective with these new iodinanones, we have found an iodinanone that enables intramolecular amination for a limited number of

substrates utilizing **4.1**. We are continuing to explore the substrates unlocked with this new iminoiodinane and other reactivity it might enable such as improved intermolecular aminations and cycloaddition chemistry that we have previously explored.²⁸ Further work on iminoiodinane design might enable intramolecular aminations to be more broadly applicable to our system utilizing iminoiodinanes as viable oxidants for intramolecular aminations.

In addition, we explored the newly developed iodine precursor (**4.47**), as a potential oxidant for our intramolecular reaction yielding an initial promising result and highest yield yet for iodine oxidations (**Scheme 4.13**). The addition of *m*-CBA to the iodoarene doubled the yield over previously best pivalate iodine oxidant. The role of the benzoate or acetate has a substantial effect on the formation of the intramolecular iminoiodinane and further exploration of appropriate benzoate or acetates is needed. Furthermore, the optimization of appropriate base should be explored as the equivalents had a profound effect on reactivity possibly due to helping promote formation of the iminoiodinane in solution.

Scheme 4.13 *m*-CBA iodine amination



We have only explored a relatively small number of potential iodoarene and sulfonamide and acetate/benzoate combinations for our intramolecular aminations. There are large number of potential options and combinations to investigate to further optimize and elucidate the best conditions to promote intra- and intermolecular amination under our catalytic system. In addition,

there are a number of transition metal systems that utilize these iminoiodinanes that might also be improved with the application of these new iminoiodinanes towards improved yields or more functional group tolerance. Computational work might also help direct which iodine structures to prioritize for synthesis and unlock amination with carbamates and other analogous structures.

4.7 References

-
- ¹ White, M.C.; Zhao, J. Aliphatic C–H Oxidations for Late-Stage Functionalization. *J. Am. Chem. Soc.*, **2018**, *140* (43), 13988-14009.
- ² Vitaku, E.; Smith, D. T.; Njardarson, J. T. Analysis of the structural diversity, substitution patterns, and frequency of nitrogen heterocycles among US FDA approved pharmaceuticals: miniperspective. *J. Med. Chem.*, **2014**, *57* (24), 10257–10274.
- ³ Combee, L.A.; Raya, B.; Wang, D.; Hilinski, M.K. Organocatalytic nitrenoid transfer: metal-free selective intermolecular C(sp³)–H amination catalyzed by an iminium salt. *Chem. Sci.*, **2018**, *9*, 935-939.
- ⁴ Chiappini, N. D.; Mack, J. B. C.; Du Bois, J. Intermolecular C(sp³)–H amination of complex molecules. *Angew. Chem. Int. Ed.*, **2018**, *57* (18), 4956–4959.
- ⁵ Fiori, K.W.; Fleming, J.J.; Du Bois, J. Rh-Catalyzed Amination of Etheral C^α–H Bonds: A Versatile Strategy for the Synthesis of Complex Amines. *Angew. Chem. Int. Ed.*, **2004**, *43* (33), 4349-4352.
- ⁶ Kim, M.; Mulcahy, J.V.; Espino, C.G.; Du Bois, J. Expanding the Substrate Scope for C–H Amination Reactions: Oxidative Cyclization of Urea and Guanidine Derivatives. *Org. Lett.*, **2006**, *8* (6), 1073–1076.
- ⁷ Rotella, M. E.; Dyer, R. M.B.; Hilinski, M. K., Gutierrez, O. Mechanism of Iminium Salt-Catalyzed C(sp³)–H Amination: Factors Controlling Hydride Transfer versus H-Atom Abstraction. *ACS Catal.*, **2020**, *10* (1), 897-906.
- ⁸ Du Bois, J. Rhodium-Catalyzed C–H Amination. An Enabling Method for Chemical Synthesis. *Org. Process Res. Dev.*, **2011**, *15* (4), 758–762.
- ⁹ Fiori, K.W. Ph.D. Thesis, Stanford University, Stanford, CA, **2007**.
- ¹⁰ Espino, C. G. Ph.D. Thesis, Stanford University, Stanford, CA, **2004**.
- ¹¹ Yamada, Y.; Yamamoto, T.; Okawara, M. Synthesis and Reaction of New type I–N ylide, n-Tosyliminoiodinane. *Chem. Lett.*, **1975**, *4* (4), 361-362.

-
- ¹² White, R. E. Methanolysis of ((tosylimino)iodo)benzene. *Inorg. Chem.*, **1987**, *26* (23), 3916-3919.
- ¹³ Yu, X.Q.; Huang, J.S.; Zhou, X.G.; Che, C.M. Amidation of saturated C–H bonds catalyzed by electron-deficient ruthenium and manganese porphyrins. A highly catalytic nitrogen atom transfer process. *Org. Lett.*, **2000**, *2* (15), 2233-2236.
- ¹⁴ Fiori, K.W.; Espino, C.G.; Brodsky, B.H.; Du Bois, J. A mechanistic analysis of the Rh-catalyzed intramolecular C–H amination reaction. *Tetrahedron*, **2009**, *65* (16), 3042-3051.
- ¹⁵ Fiori, K. W.; Du Bois, J. Catalytic Intermolecular Amination of C–H Bonds: Method Development and Mechanistic Insights. *J. Am. Chem. Soc.*, **2007**, *129* (3), 562–568.
- ¹⁶ Dolan, N. S.; Scamp, R. J.; Yang, T.; Berry, J. F.; Schomaker, J. M. Catalyst-Controlled and Tunable, Chemoselective Silver-Catalyzed Intermolecular Nitrene Transfer: Experimental and Computational Studies. *J. Am. Chem. Soc.*, **2016**, *138* (44), 14658–14667.
- ¹⁸ Carmalt, C. J.; Crossley, J. G.; Knight, J. G.; Lightfoot, P.; Martin, A.; Muldowney, M. P.; Norman, N. C.; Orpen, A. G. An examination of the structures of iodosylbenzene (PhIO) and the related imido compound, PhINSO 2-4-Me-C 6 H 4, by X-ray powder diffraction and EXAFS (extended X-ray absorption fine structure) spectroscopy. *J. Chem. Soc. Chem. Commun.*, **1994**, *20*, 2367-2368.
- ¹⁹ Cicero, R. L.; Zhao, D.; Protasiewicz, J. D. Polymorphism of ((tosylimino)iodo)-o-toluene: Two new modes of polymeric association for ArINTs. *Inorg. Chem.*, **1996**, *35*, 275–276.
- ²⁰ Kokkinidis, G.; Papadopoulou, M.; Varvoglis, A. Electrochemical reduction of [bis(acyloxy)iodo]arenes. *Electrochem. Acta.*, **1989**, *34* (2), 133-139.
- ²¹ Boucher, M.; Macikenas, D.; Ren, T.; Protasiewicz, J.D. Secondary Bonding as a Force Dictating Structure and Solid-State Aggregation of the Primary Nitrene Sources (Arylsulfonylimino) iodoarenes (ArINSO₂Ar). *J. Am. Chem. Soc.*, **1997**, *119* (40), 9366-9376.
- ²² Macikenas, D.; Skrzypczak-Jankun, E.; Protasiewicz, J. D. A new class of iodonium ylides engineered as soluble primary oxo and nitrene sources. *J. Am. Chem. Soc.*, **1999**, *121* (30), 7164-7165.
- ²³ Mephrathu, B.V.; Protasiewicz, J. D. Enhancing the solubility for hypervalent ortho-sulfonyl iodine compounds. *Tetrahedron*, **2010**, *66* (31), 5768 – 5774.
- ²⁴ Yoshimura, A.; Nemykin, V.N.; Zhdankin, V.V. Alkoxyphenyliminoiodanes: highly efficient reagents for the catalytic aziridination of alkenes and the metal-free amination of organic substrates. *Chem. Eur. J.*, **2011**, *17* (38), 10538.

-
- ²⁵ Iinuma, M.; Moriyama, K.; Togo, H. Simple and Practical Method for Preparation of [(Diacetoxy)iodo] arenes with Iodoarenes and *m*-Chloroperoxybenzoic Acid. *Synlett*, **2012**, 23 (18), 2663-2666.
- ²⁶ Clark, J. R.; Feng, K.; Sookezian, A.; White, M. C. Manganese-catalysed benzylic C (sp³)-H amination for late-stage functionalization. *Nat. Chem.*, **2018**, 10 (6), 583-591.
- ²⁷ Ogawa, A.; Curran, D.P.; Benzotrifluoride: A Useful Alternative Solvent for Organic Reactions Currently Conducted in Dichloromethane and Related Solvents. *J. Org. Chem.*, **1997**, 62 (3), 450-451.
- ²⁸ Combee, L.A.; Johnson, S.L.; Laudenschlager, J.E.; Hilinski, M.K. Rh(II)-catalyzed nitrene-transfer [5+ 1] cycloadditions of aryl-substituted vinylcyclopropanes. *Org. Lett.*, **2019**, 21 (7), 2307-2311.

Appendix One:

Chapter Two Supporting Information

1.1 General Information

All reagents were obtained commercially in the highest available purity and used without further purification. 1,1,1,3,3,3-hexafluoropropan-2-ol (HFIP) were purchased from Oakwood Chemical Company. Anhydrous solvents were obtained from an aluminum oxide solvent purification system. Flash column chromatography was performed using silica gel or alumina gel (230 - 400 mesh) purchased from Fisher Scientific. Elution of compounds was monitored by UV. ^1H and ^{13}C NMR spectra were measured on a Varian Inova 600 (600 MHz) or Bruker Avance DRX 600 (600 MHz) or Bruker Avance III 800 (800 MHz) spectrometer and acquired at 300 K. Chemical shifts are reported in parts per million (ppm δ) referenced to the residual ^1H or ^{13}C resonance of the solvent. The following abbreviations are used singularly or in combination to indicate the multiplicity of signals: s - singlet, d - doublet, t - triplet, q - quartet, m - multiplet and br - broad. IR spectra were recorded on a Shimadzu IR Affinity-1S. HRMS data were obtained from the School of Chemical Sciences Mass Spectrometry Laboratory at the University of Illinois at Urbana-Champaign and are accurate to within 5 ppm.

1.2 Screening of Oxidant Conditions

Reaction conditions and potential substrates were screened on a 0.1 mmol scale. A general procedure is as follows: the nicotine salt or nicotine was measured in a 2 dram vial with a stir bar, followed by .5 mL of dichloromethane, HFIP (if included), and the acid additive (if necessary). The oxidant was then added and the vial capped and allowed to stir for 16 hrs. The organic layer was extracted with 5 mL of DCM 3x, dried with magnesium sulfate, and concentrated under vacuum. The sample was then analyzed by LC-MS or crude ^1H NMR.

1.3 General Reductive Amination Procedure: Aldehyde (2.50 mmol, 1 eq), amine (2.75 mmol, 1.1 eq), were measured out into a 50 mL round bottom with a stir bar. Dichloroethane (20mL) was

added and the suspension was gently mixed for 5 minutes. Sodium triacetoxyborohydride (3.50 mmol, 1.4 eq) was weighed out and then added to the mixture. The reaction stirred for 16 hrs or until complete by TLC. Upon reaction completion, the reaction mixture was basified with 1M NaOH (10mL). The layers were separated, and extracted with 5x15 mL EtOAc. The resulting organic layers were combined, dried with sodium sulfate, concentrated on a rotary evaporator, and purified by flash chromatography as noted.

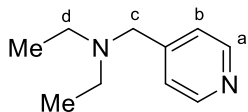
1.4 Oxidation Reactions

General Procedure A: Substrate (0.5 mmol 1 eq) was measured out into a 2 dram screw top vial equipped with a stir bar. Dichloromethane (2.5 mL) was added and the suspension was gently mixed. 1M H₂SO₄ (1 eq) was added, followed by HFIP. Iminium catalyst (0.030g, 20 mol%) was weighed out and then added to the mixture. Finally 50% H₂O₂ (2 eq) was added to vial. The reaction stirred for 16 hrs. Upon reaction completion, the reaction mixture was basified with 6M NaOH (10mL). Brine (10 mL) was added to salt out N-oxide product. The layers were separated, and extracted with 3x10 mL DCM. The resulting organic layers were combined and dried with magnesium sulfate, concentrated on a rotary evaporator, and purified by flash chromatography as noted.

General Procedure B: Substrate (0.5 mmol 1 eq) was measured out into a 2 dram screw top vial equipped with a stir bar. Dichloromethane (2.5 mL) was added and the suspension was gently mixed. 50% Tetrafluoroboric acid diethyl ether complex (1 eq) was added, followed by HFIP. Iminium catalyst (0.015g, 10 mol%) was weighed out and then added to the mixture. Finally 50% H₂O₂ (2 eq) was added to vial. The reaction stirred for 16 hrs. Upon reaction completion, the reaction mixture was basified with 6M NaOH (10mL). Brine (10 mL) was added to salt out N-oxide product. The layers were separated, and extracted with 3x10 mL DCM. The resulting organic layers were combined and dried with magnesium sulfate, concentrated on a rotary evaporator, and purified by flash chromatography as noted.

1.5 Compounds

N-ethyl-N-(pyridin-4-ylmethyl)ethanamine (S1.1)



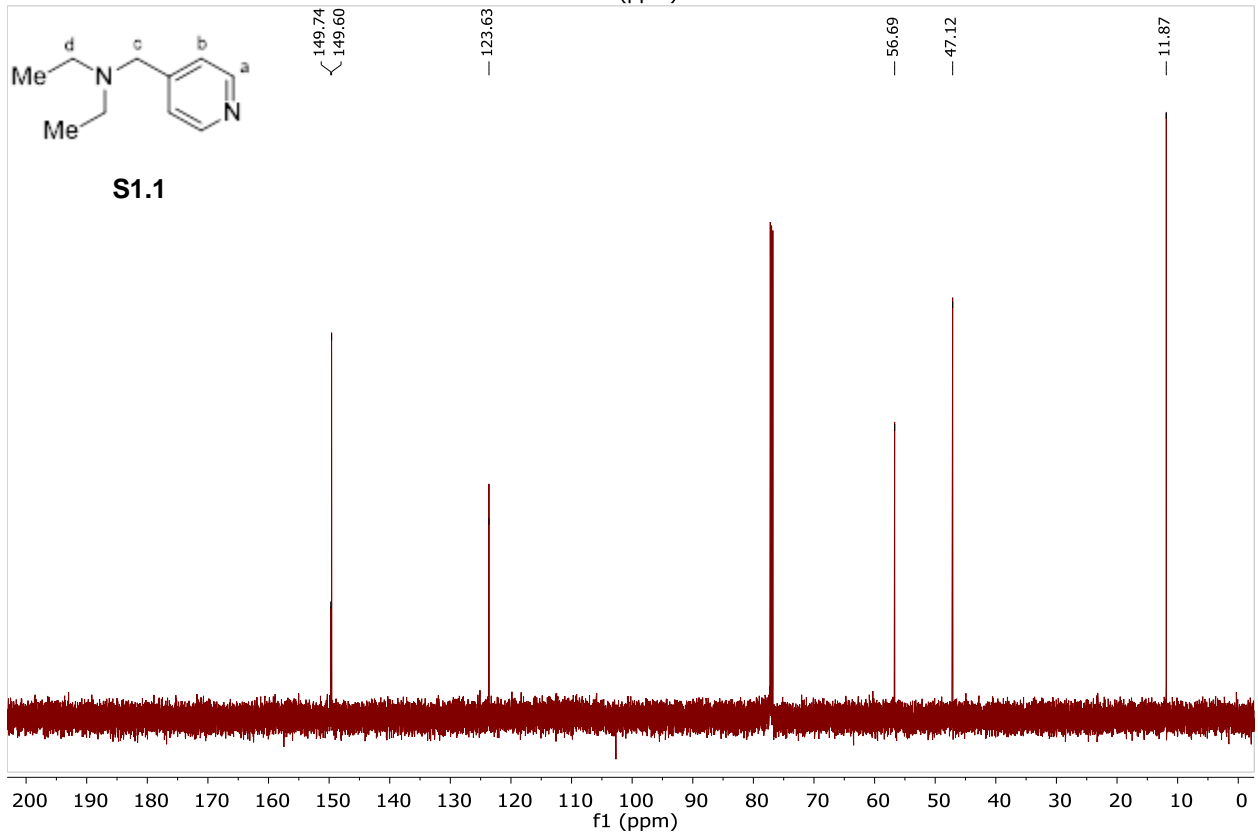
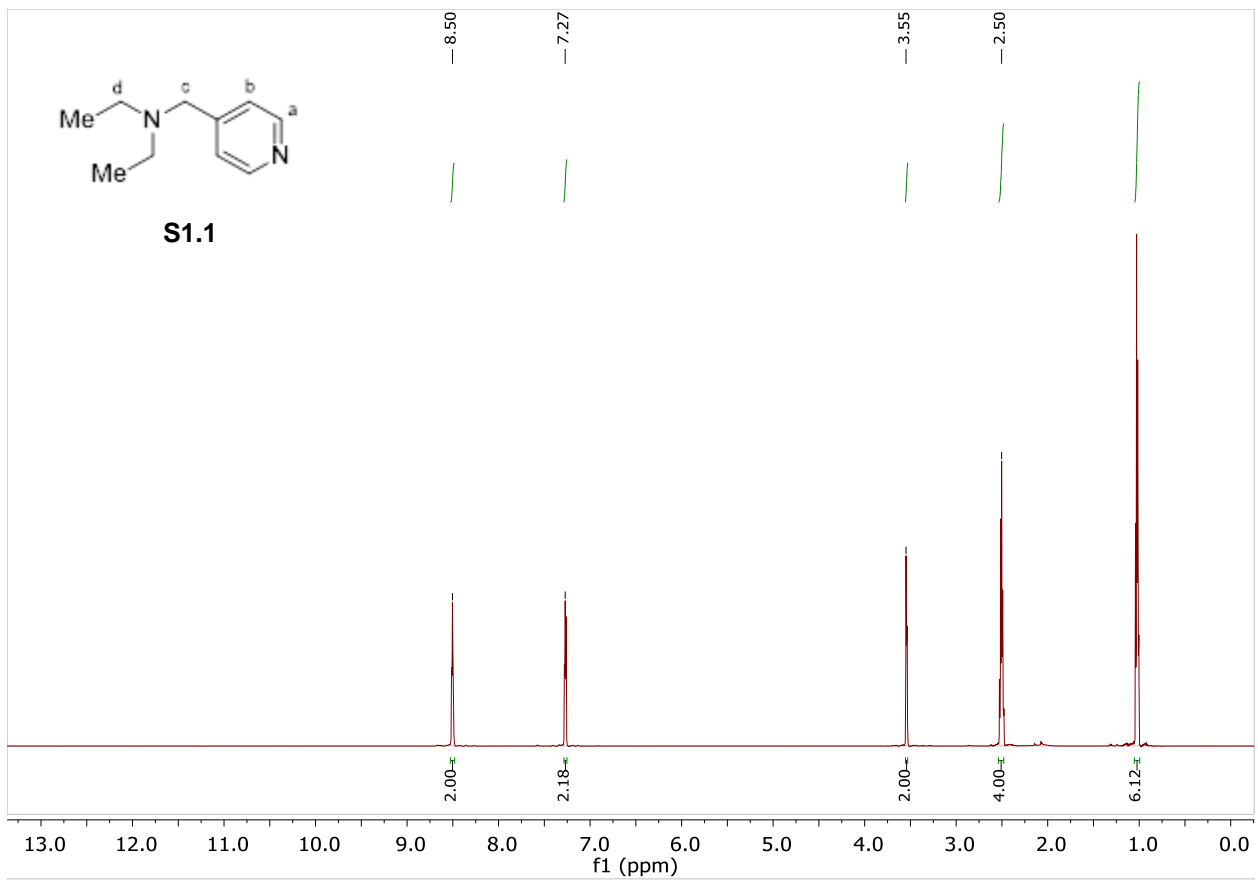
N-ethyl-N-(pyridin-4-ylmethyl)ethanamine was synthesized using the general reductive amination procedure on a 2.50 mmol scale relative to the aldehyde. The reaction mixture was purified after workup using alumina flash chromatography (20% to 40% to 60% EtOAc/hexanes) to give product as 0.0941 g of orange oil (0.570 mmol 22 % yield).

¹H NMR (600 MHz, CDCl₃): δ 8.51 (H_a, d, *J* = 6.0 Hz, 2H), 7.28 (H_b, d, *J* = 6.0 Hz, 2H), 3.55 (H_c, s, 2H), 2.51 (H_d, q, *J* = 7.1 Hz, 4H), 1.03 (Me, t, *J* = 7.1 Hz, 6H) ppm.

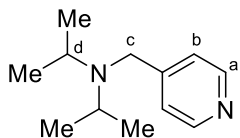
¹³C NMR (150 MHz, CDCl₃) δ 149.7, 123.8, 123.4, 59.3, 54.8, 23.5 ppm.

IR (ATR) 2800.64, 1602.85, 1548.84, 1417.68, 1375.72, 1227.87, 1062.78, 1033.85 cm⁻¹.

HRMS (ESI/QTOF) *m/z*: [M + H]⁺ Calcd for C₁₀H₁₇N₂ 165.1392, found 165.1396



N-isopropyl-N-(pyridin-4-ylmethyl)propan-2-amine (S1.2)



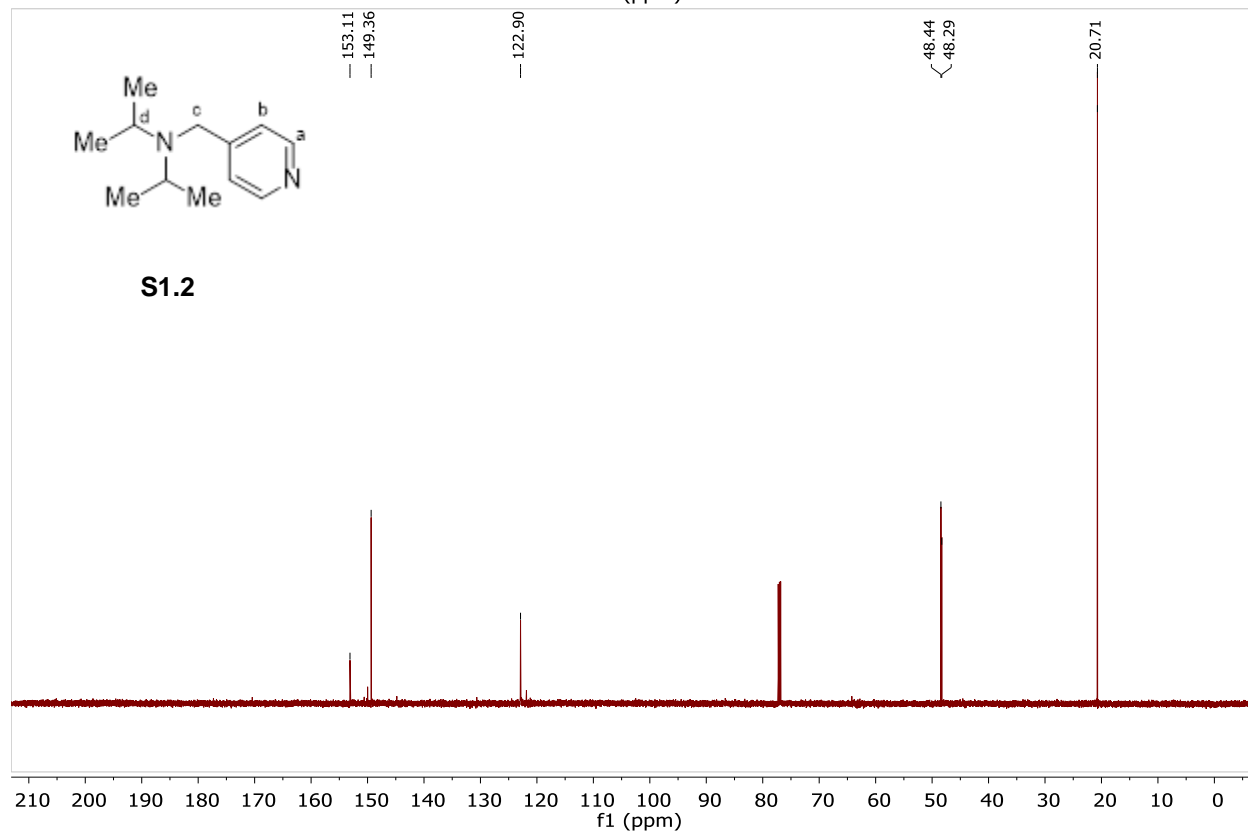
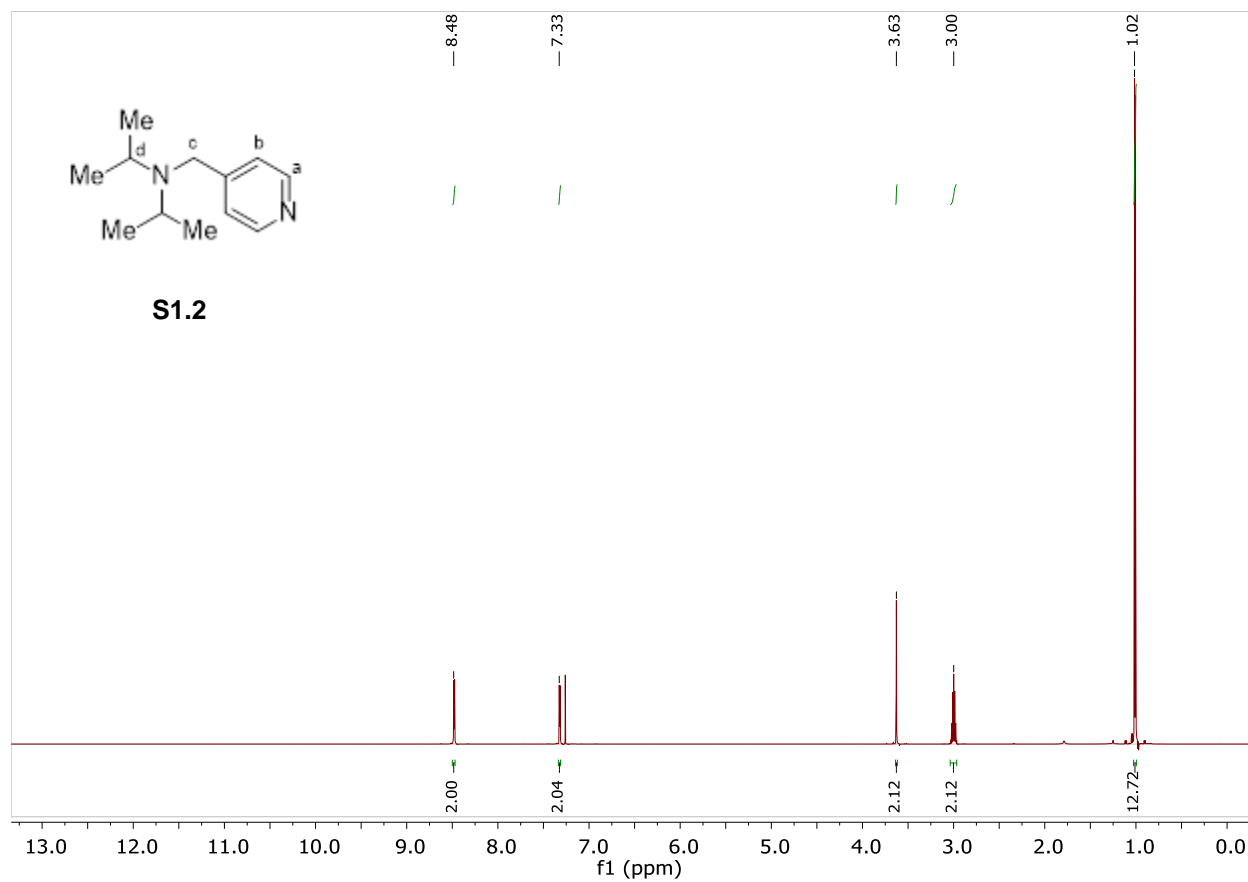
N-isopropyl-N-(pyridin-4-ylmethyl)propan-2-amine was synthesized using General reductive amination procedure A using isonicotinaldehyde (0.240 mL, 2.50 mmol), diisopropylamine (0.390 mL, 2.75 mmol), and sodium triacetoxyborohydride (0.780g, 3.50 mmol). The reaction mixture was purified after workup using alumina flash chromatography (10% to 30% EtOAc/hexanes) to give product as 23.0 mg of clear oil (0.119 mmol 4.7% yield).

¹H NMR (600 MHz, CDCl₃): δ 8.48 (H_a, d, *J* = 6.0 Hz, 2H), 7.32 (H_b, d, *J* = 6.0 Hz, 2H), 3.63 (H_c, s, 2H), 3.00 (H_d, hept, *J* = 6.5 Hz, 2H), 1.01 (Me, d, *J* = 6.6 Hz, 12H) ppm.

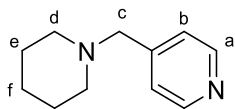
¹³C NMR (150 MHz, CDCl₃) δ 153.1, 149.4, 122.9, 48.4, 48.3, 20.7. ppm.

IR (ATR) 2964.59, 1749.44, 1597.06, 1463.97, 1382.96, 1139.93, 1031.92 cm⁻¹.

HRMS (ESI/QTOF) *m/z*: [M + H]⁺ Calcd for C₁₂H₂₁N₂ 193.1705; Found 193.1710.



4-(piperidin-1-ylmethyl)pyridine (S1.3)



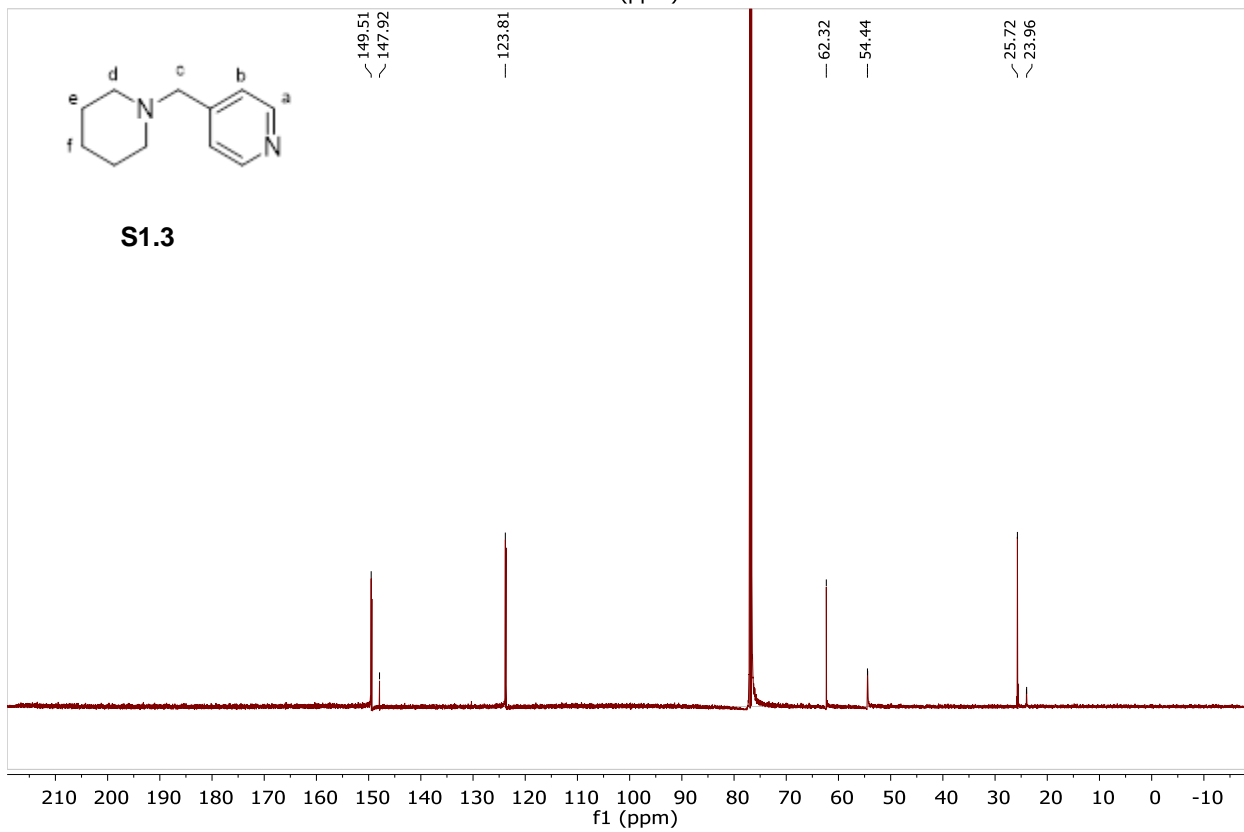
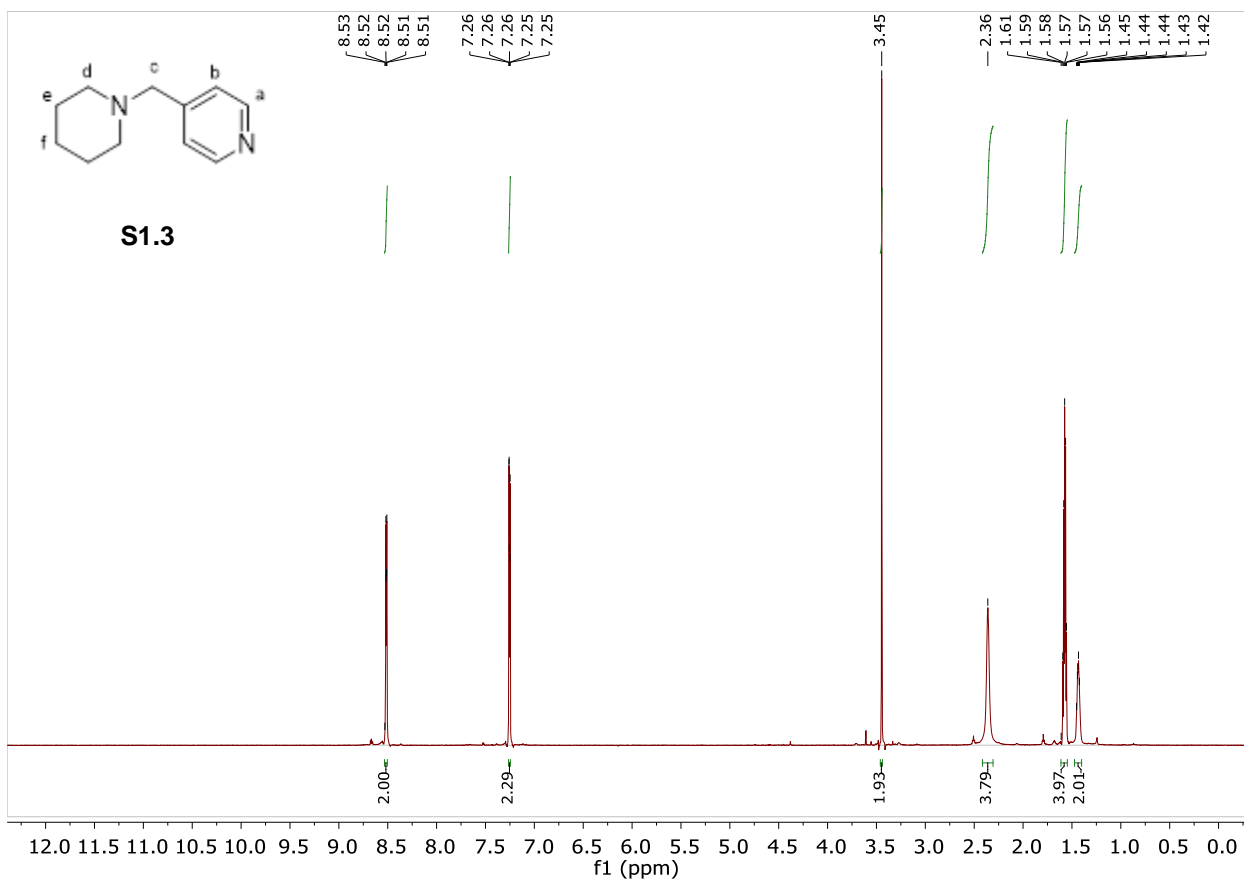
4-(piperidin-1-ylmethyl)pyridine was synthesized using the general reductive amination procedure on a 5 mmol scale relative to the aldehyde. The reaction mixture was purified after workup using silica flash chromatography (1% NH₄OH/10% MeOH/89%DCM) to give product as 0.590 g of yellow oil (3.34 mmol 67%)

¹H NMR (600 MHz, CDCl₃): δ 8.51 (H_a, d, *J* = 6.0 Hz, 2H), 7.26 (H_b, d, *J* = 6.0 Hz, 2H), 3.46 (H_c, s, 2H), 2.44 – 2.30 (H_d, m, 4H), 1.58 (H_e, p, *J* = 5.6 Hz, 4H), 1.46 – 1.40 (H_f, m, 2H) ppm.

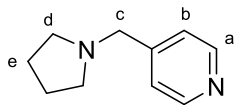
¹³C NMR (150 MHz, CDCl₃) δ 149.6, 148.1, 123.9, 62.5, 54.6, 25.9, 24.1 ppm.

IR (ATR) 2794.85, 2758.21, 1602.85, 1412.82, 993.34, 804.32 cm⁻¹.

HRMS (ESI/QTOF) *m/z*: [M + H]⁺ Calcd for C₁₁H₁₇N₂ 177.1392, found 177.1394



4-(pyrrolidin-1-ylmethyl)pyridine (S1.4)



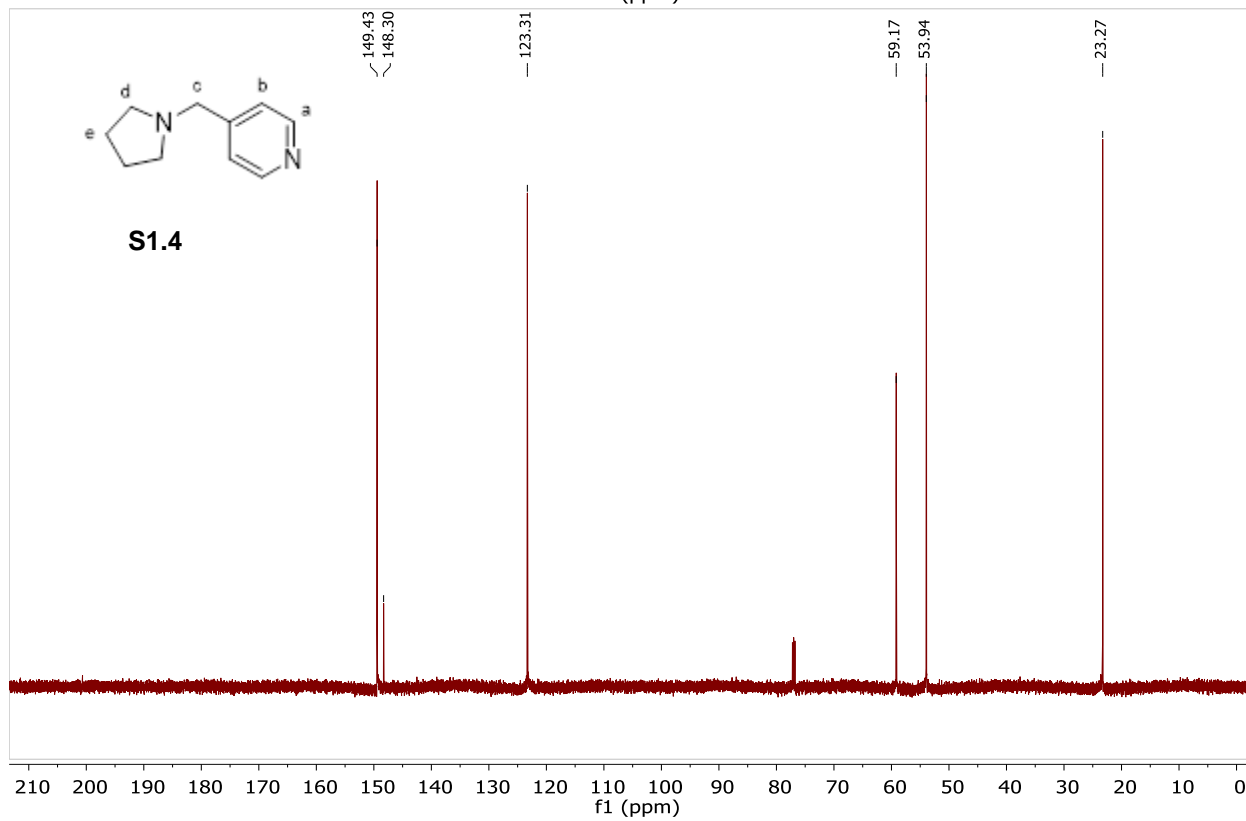
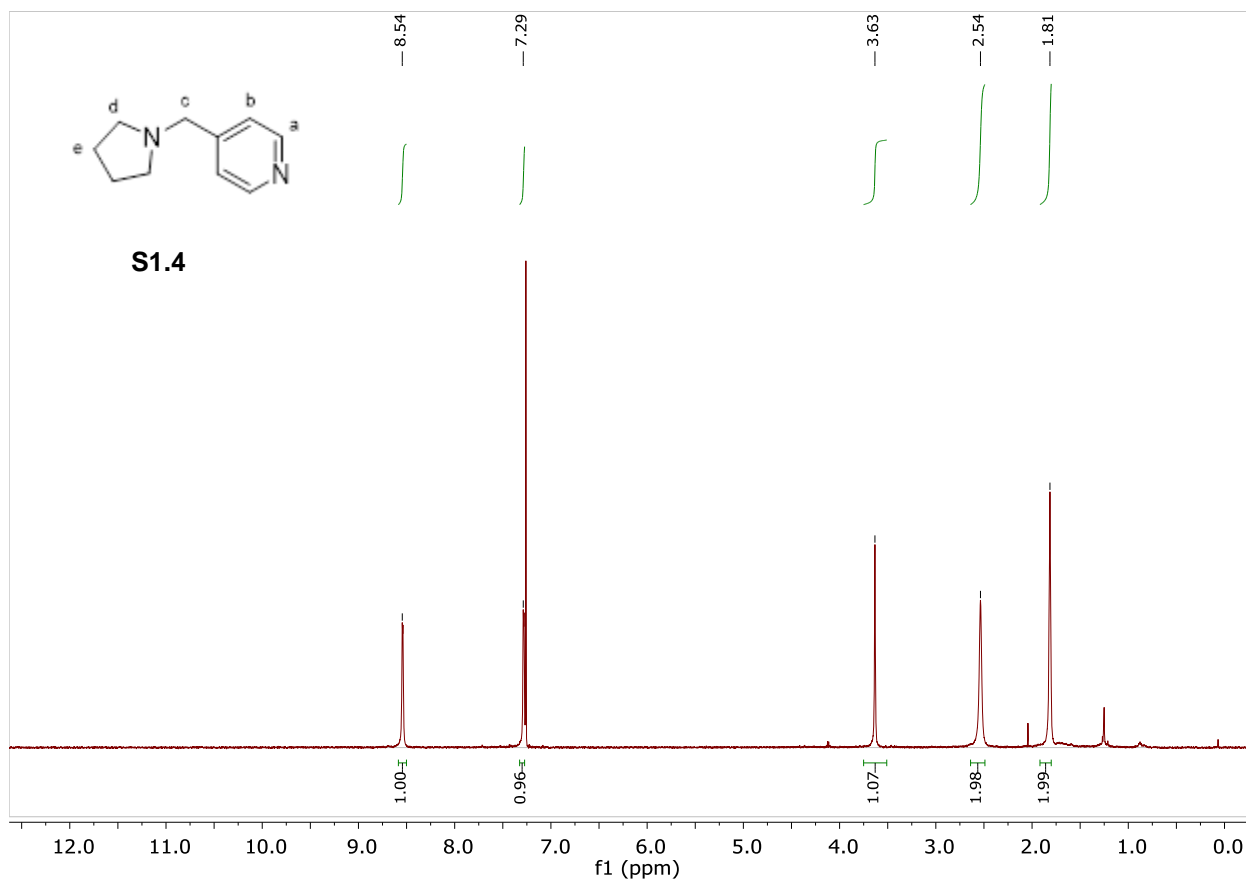
4-(pyrrolidin-1-ylmethyl)pyridine was synthesized using the general reductive amination procedure on a 10 mmol scale relative to the aldehyde. The reaction mixture was purified after workup using alumina flash chromatography (20% to 40% EtOAc/hexanes) to give as 1.59 g of yellow oil (9.80 mmol 98% yield)

¹H NMR (600 MHz, CDCl₃): δ 8.60 (H_a, d, *J* = 6.0 Hz, 2H), 7.35 (H_b, d, *J* = 6.0 Hz, 2H), 3.71 (H_c, s, 2H), 2.62 – 2.60 (H_d, m, 4H), 1.89 – 1.87 (H_e, m, 4H) ppm.

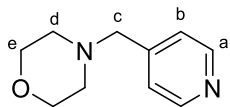
¹³C NMR (150 MHz, CDCl₃) δ 149.4, 148.3, 123.3, 59.2, 53.9, 23.3 ppm.

IR (ATR) 2783.28, 2735.08, 1600.92, 1413.82, 933.34, 800.46 cm⁻¹.

HRMS (ESI/QTOF) *m/z*: [M + H]⁺ Calcd for C₁₀H₁₅N₂ 163.1235; Found 163.1235



4-(pyridin-4-ylmethyl)morpholine (S1.5)



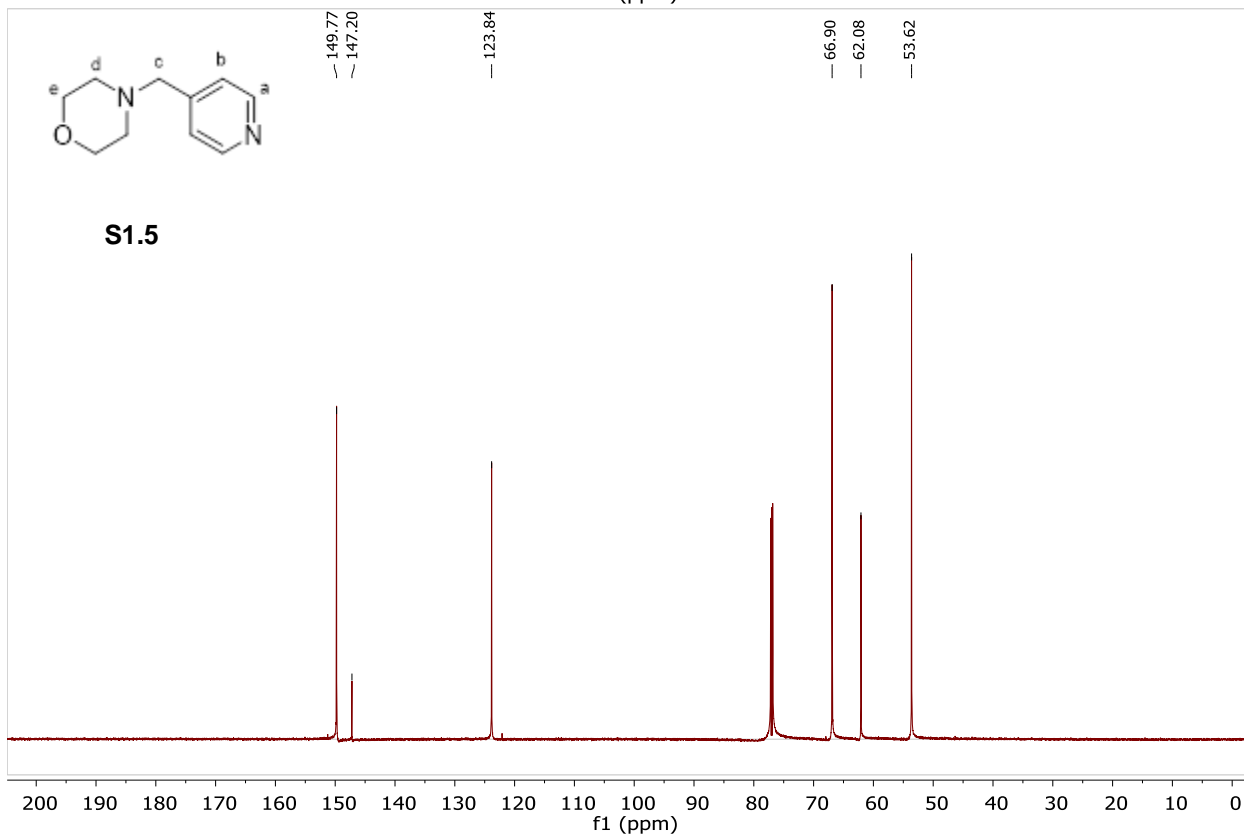
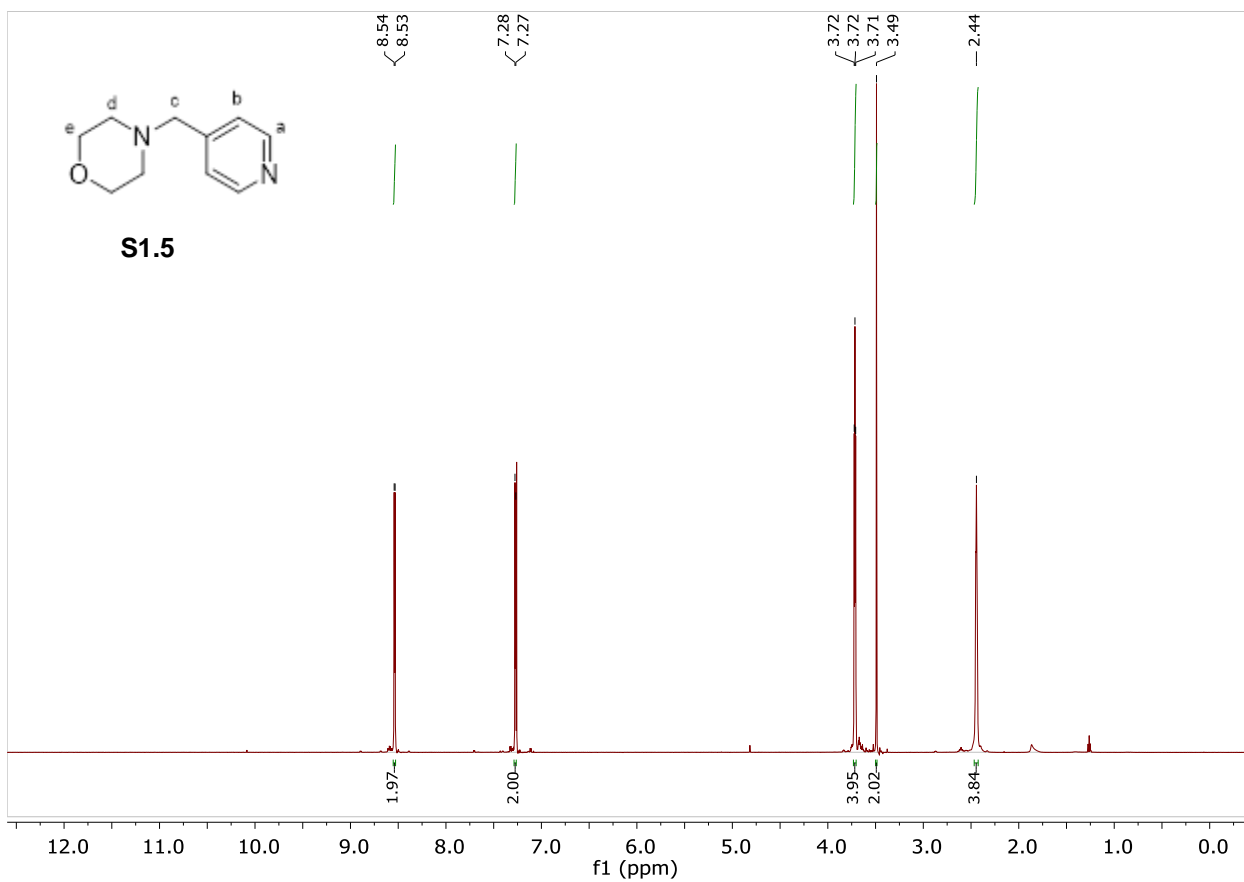
4-(pyridin-4-ylmethyl)morpholine was synthesized using the general reductive amination procedure on a 2.25 mmol scale relative to the aldehyde. The reaction mixture was purified after workup using alumina flash chromatography (solvent gradient: 20% to 40% EtOAc/hexanes) to give product as 0.331 g of yellow-brown oil (1.86 mmol, 74% yield).

¹H NMR (600 MHz, CDCl₃): δ 8.54 (H_a, d, *J* = 6.0 Hz, 2H), 7.28 (H_b, d, *J* = 6.0 Hz, 2H), 3.72 (H_e, t, *J* = 4.7 Hz, 4H), 3.49 (H_c, s, 2H), 2.48 – 2.45 (H_d, m, 4H) ppm.

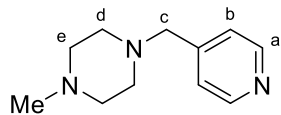
¹³C NMR (150 MHz, CDCl₃) δ 149.8, 147.2, 123.9, 66.9, 62.1, 53.6 ppm.

IR (ATR) 2854.65, 2808.36, 1602.85 1454.33, 1415.75, 1114.86, 1008.77, 866.04cm⁻¹.

HRMS (ESI/QTOF) *m/z*: [M + H]⁺ Calcd for C₁₀H₁₅N₂O 179.1184, found 179.1189



1-methyl-4-(pyridin-4-ylmethyl)piperazine (S1.6)



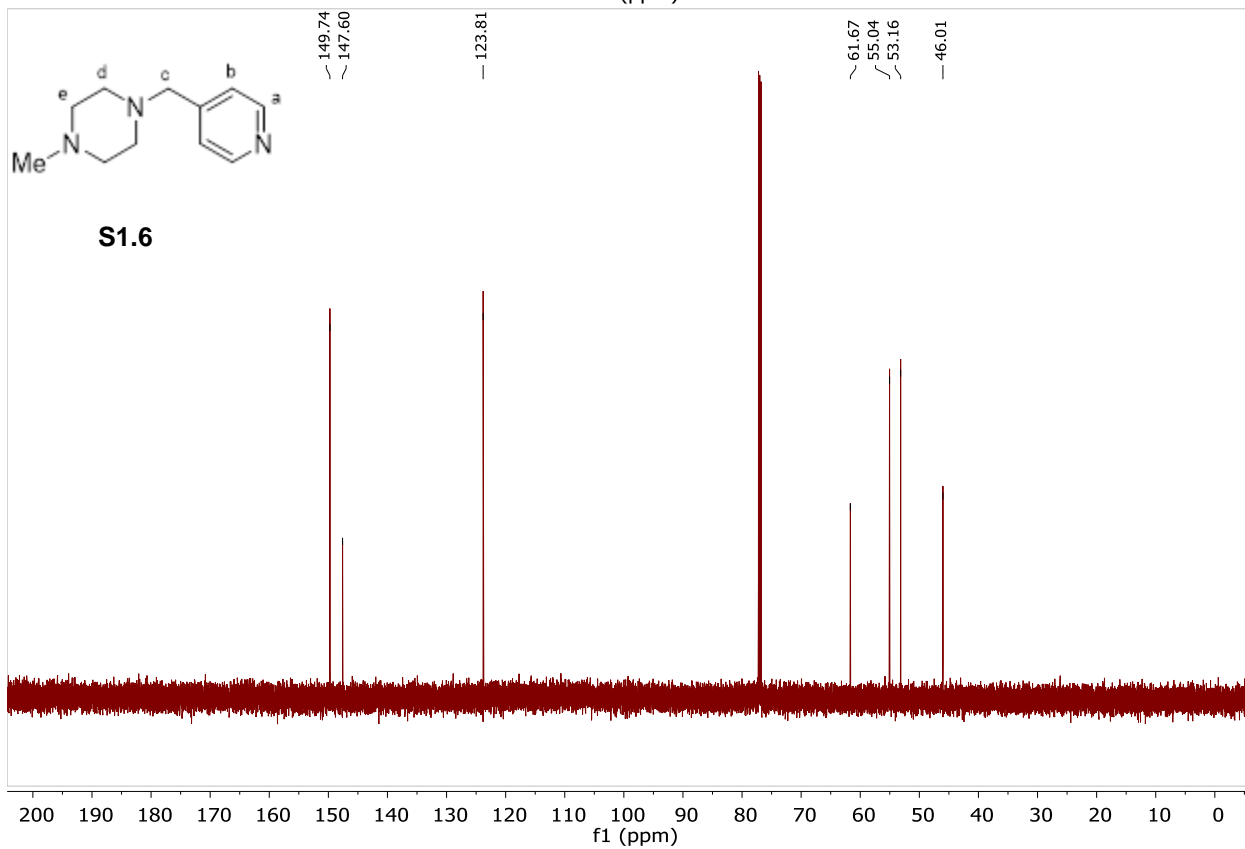
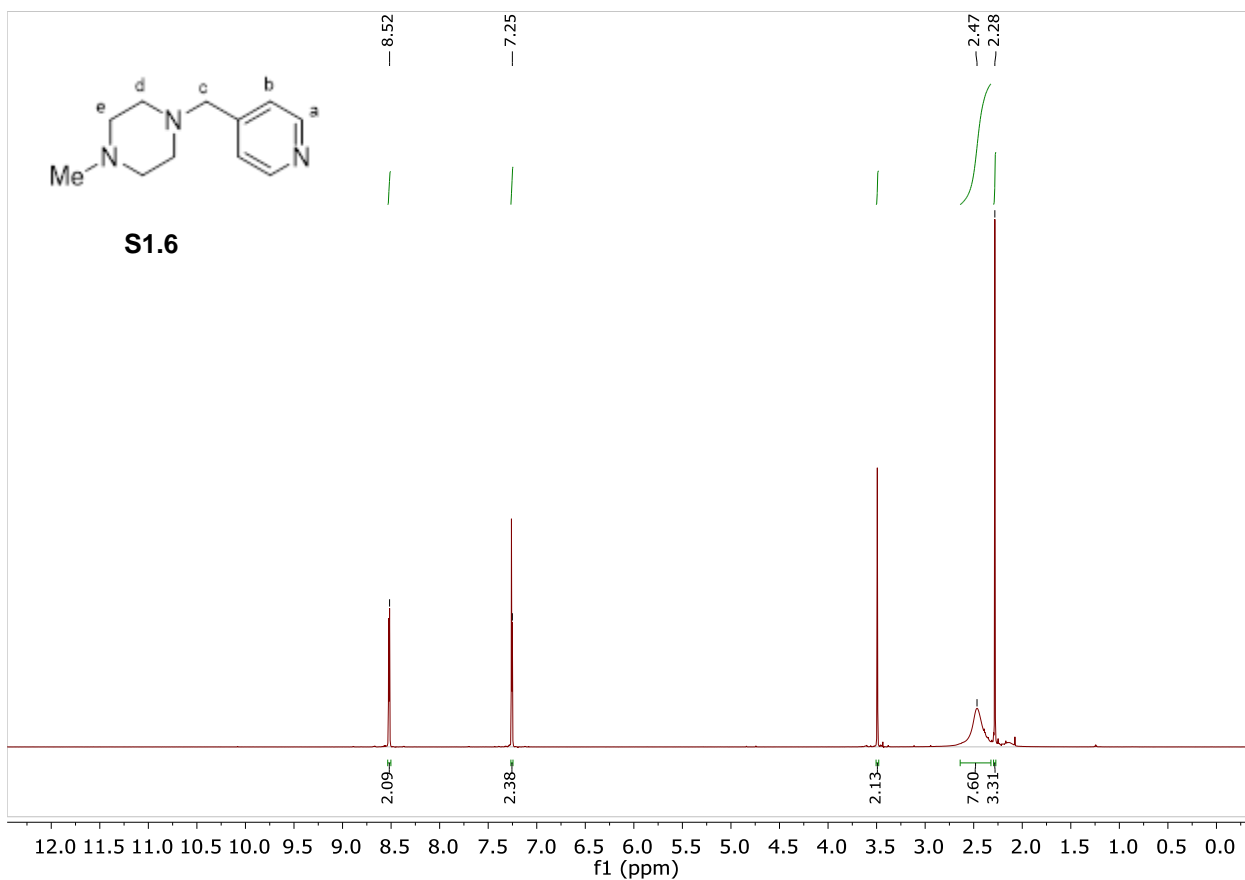
1-methyl-4-(pyridin-4-ylmethyl)piperazine was synthesized using the general reductive amination procedure on a 5 mmol scale relative to the aldehyde. The reaction mixture was purified after workup using alumina flash chromatography (80% EtOAc/hexanes to 100%) to give product as 0.535 g of yellow oil (2.80 mmol, 56% yield).

¹H NMR (600 MHz, CDCl₃): δ 8.52 (H_a, d, J = 4.4 Hz, 2H), 7.26 (H_b, d, J = 4.4 Hz, 2H), 3.49 (H_c, s, 2H), 2.46 (H_d and H_e, br s, 8H), 2.28 (Me, s, 3H) ppm.

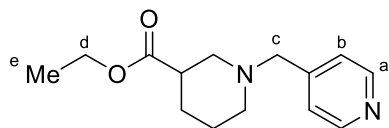
¹³C NMR (151 MHz, CDCl₃): δ 149.7, 147.6, 123.8, 61.7, 55.0, 53.2, 46.0 ppm.

IR (ATR) 2792.93, 1602.85, 1560.41, 1456.26, 1413.92, 1290.38, 1165.00, 1139.93, 1012.63, 827.46, 794.67 cm⁻¹.

HRMS (ESI/QTOF) m/z: [M + H]⁺ Calcd for C₁₁H₁₈N₃ 192.1501, found 192.1500



Ethyl 1-(pyridin-4-ylmethyl)piperidine-3-carboxylate (S1.7)



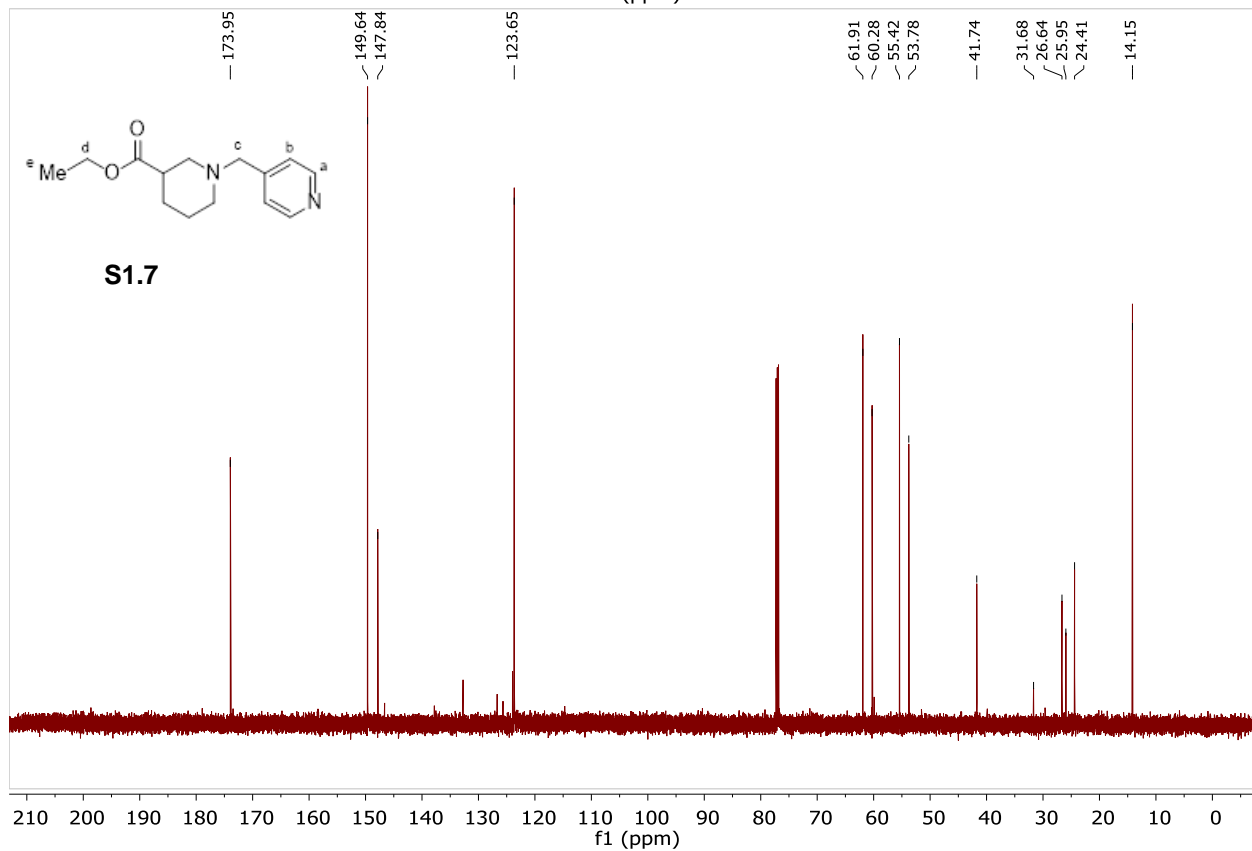
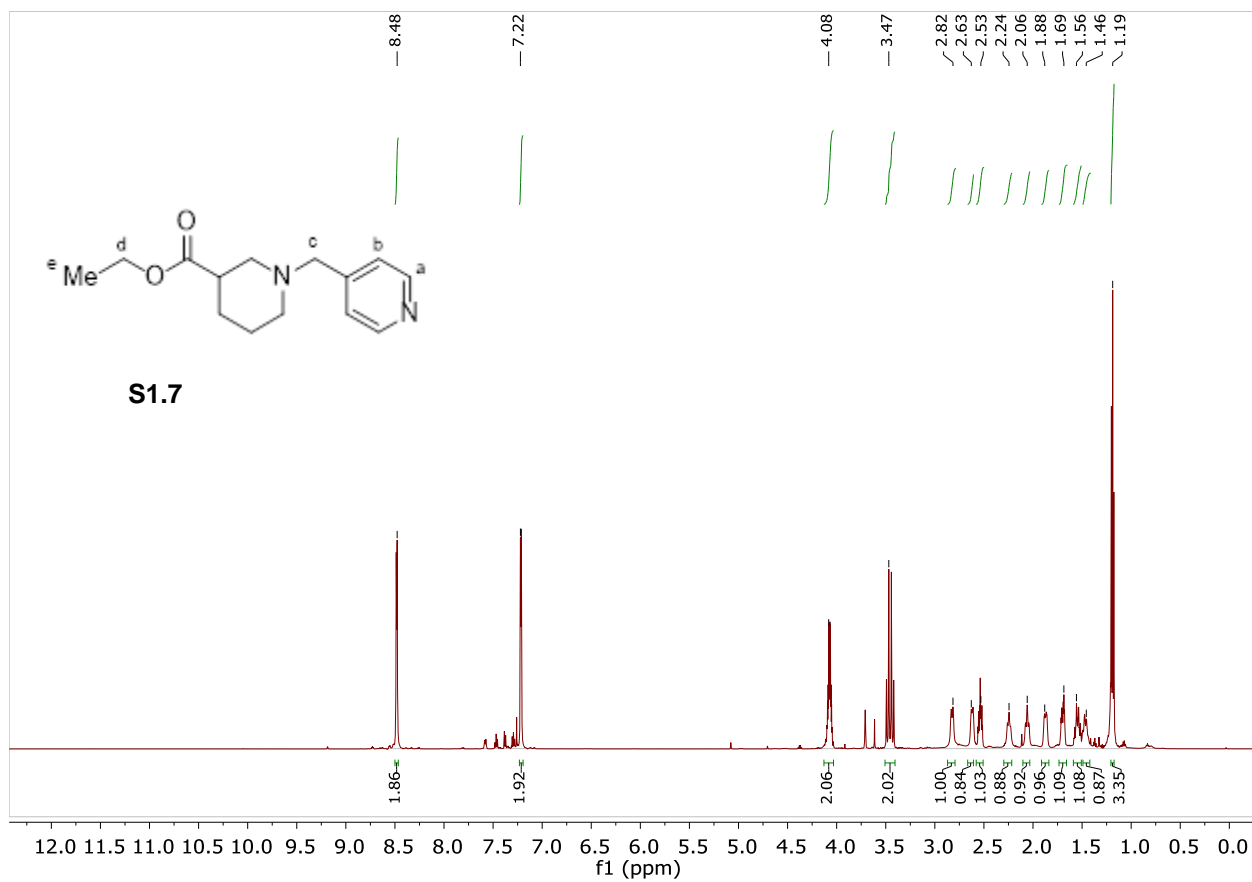
Ethyl 1-(pyridin-4-ylmethyl)piperidine-3-carboxylate was synthesized using general reductive amination procedure on a scale of 4 mmol relative to the aldehyde. The reaction mixture was purified after workup using alumina flash chromatography (20% to 60% EtOAc/hexanes) to give product as 45.3 mg of yellow oil (0.180 mmol, 4.5% yield).

¹H NMR (600 MHz, CDCl₃): δ 8.48 (H_a, d, *J* = 6.1 Hz, 2H), 7.22 (H_b, d, *J* = 6.1 Hz, 2H), 4.12 – 4.01 (H_c, m, 2H), 3.46 (H_d, q, *J* = 14.3 Hz, 2H), 2.82 (d, *J* = 11.4 Hz, 1H), 2.62 (d, *J* = 11.0 Hz, 1H), 2.57 – 2.50 (m, 1H), 2.28 – 2.20 (m, 1H), 2.09 – 2.04 (m, 1H), 1.91 – 1.84 (m, 1H), 1.73 – 1.67 (m, 1H), 1.59 – 1.52 (m, 1H), 1.51 – 1.44 (m, 1H), 1.19 (H_e, t, *J* = 7.6 Hz, 3H) ppm.

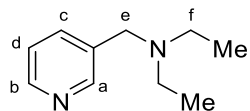
¹³C NMR (151 MHz, CDCl₃): δ 174.0, 149.6, 147.8, 123.7, 61.9, 60.3, 55.4, 53.8, 41.7, 26.6, 26.0, 24.4, 14.2 ppm.

IR (ATR) 2805.50, 1726.29, 1600.92, 1413.82, 1367.53, 1180.55, 1028.06, 991.41 cm⁻¹.

HRMS (ESI/QTOF) *m/z*: [M + H]⁺ Calcd for C₁₄H₂₁N₂O₂ 249.1603, found 249.1602



N-ethyl-N-(pyridin-3-ylmethyl)ethanamine (S1.8)



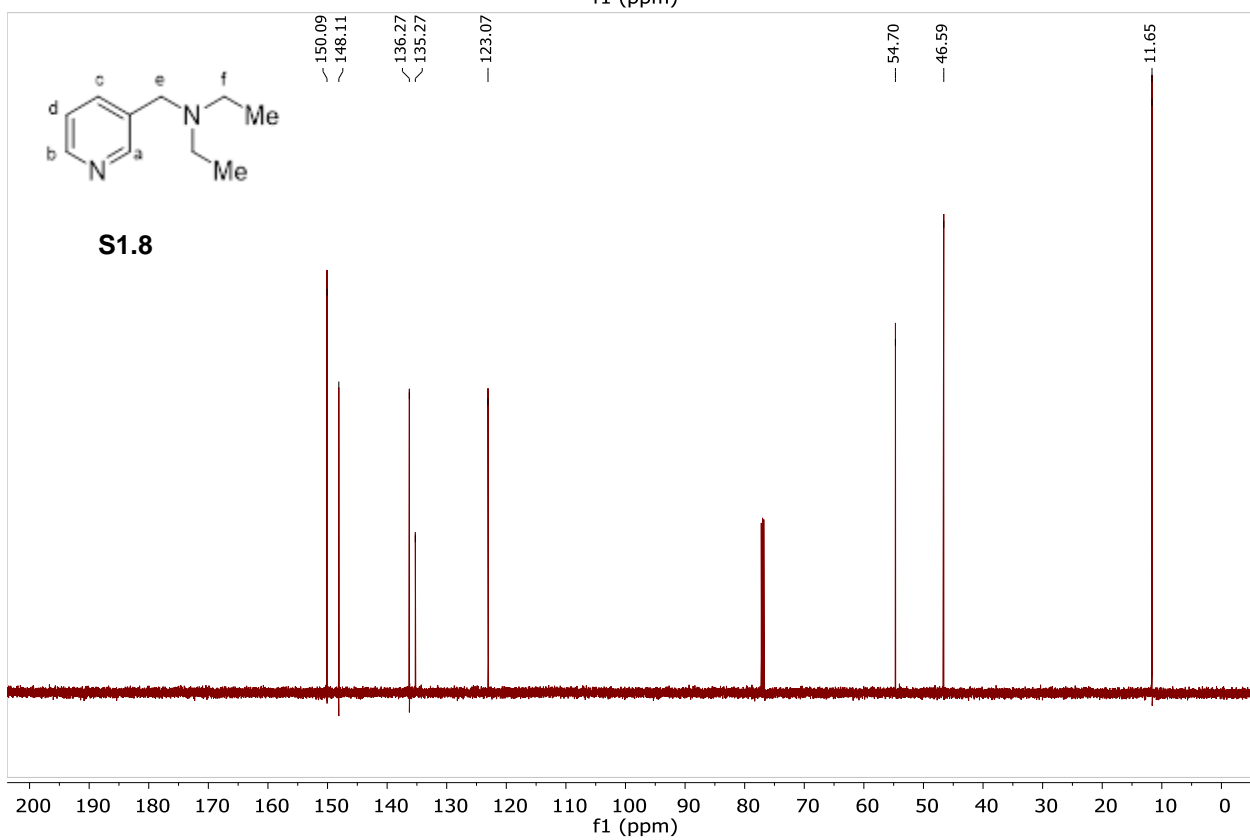
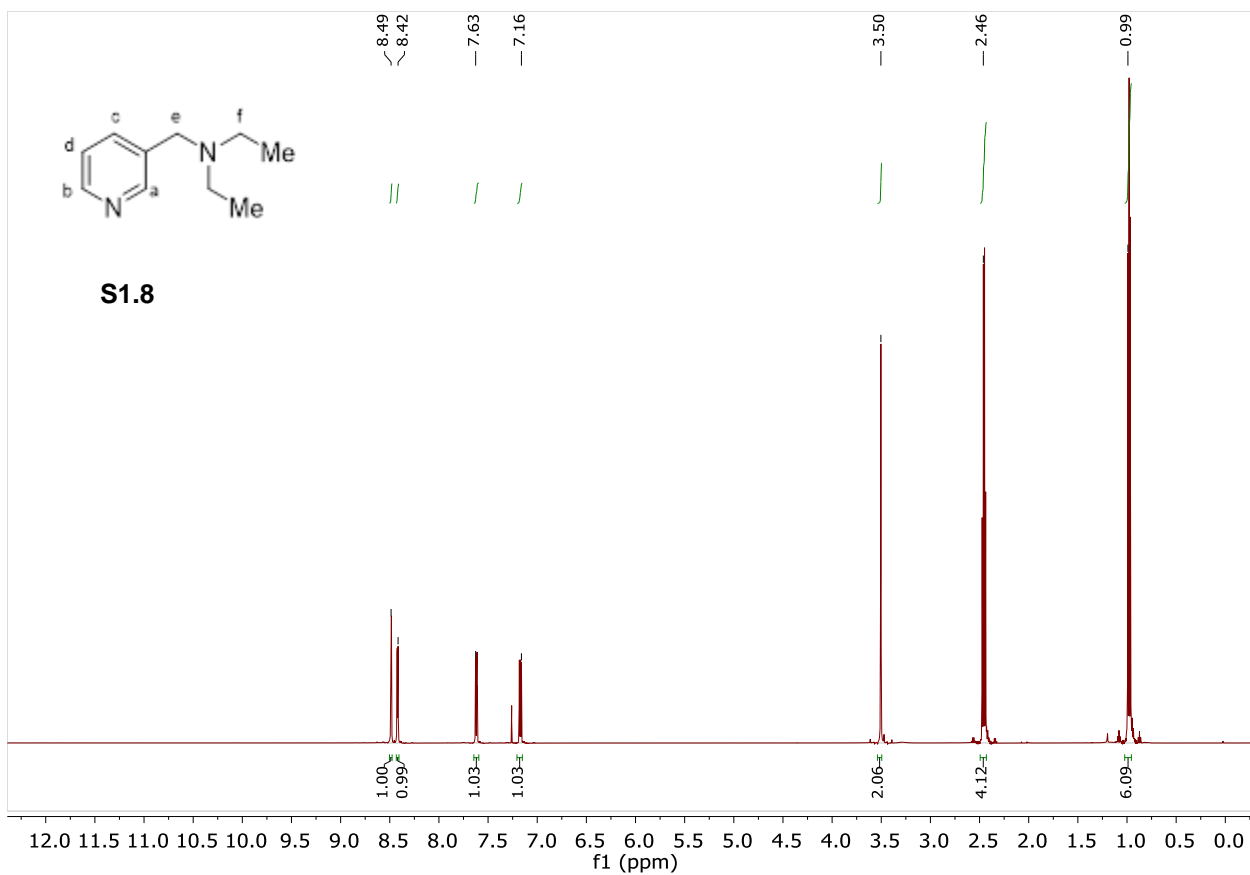
N-ethyl-N-(pyridin-3-ylmethyl)ethanamine was synthesized using the general reductive amination procedure on a 2 mmol scale relative to the aldehyde. The reaction mixture was purified after workup using alumina flash chromatography (20% to 30% to 40% EtOAc/hexanes) to give product as .045 g of white oil (0.330 mmol, 16% yield)

¹H NMR (600 MHz, CDCl₃): δ 8.48 (H_a, s, 1H), 8.42 (H_b, d, *J* = 5.4 Hz, 1H), 7.62 (H_c, d, *J* = 7.4 Hz, 1H), 7.17 (H_d, dd, *J* = 7.4, 5.4 Hz, 1H), 3.50 (H_e, s, 2H), 2.46 (H_f, q, *J* = 7.2 Hz, 4H), 0.98 (Me, d, *J* = 7.2 Hz, 6H) ppm.

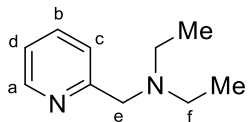
¹³C NMR (150 MHz, CDCl₃) δ 150.1, 148.1, 136.3, 135.3, 123.1, 54.7, 46.6, 11.7 ppm.

IR (ATR) 2804.50, 1575.84, 1423.47, 1028.06 cm⁻¹.

HRMS (ESI/QTOF) *m/z*: [M + H]⁺ Calcd for C₁₀H₁₇N₂ 165.1392, found 165.1396



N-ethyl-N-(pyridin-2-ylmethyl)ethanamine (S1.9)



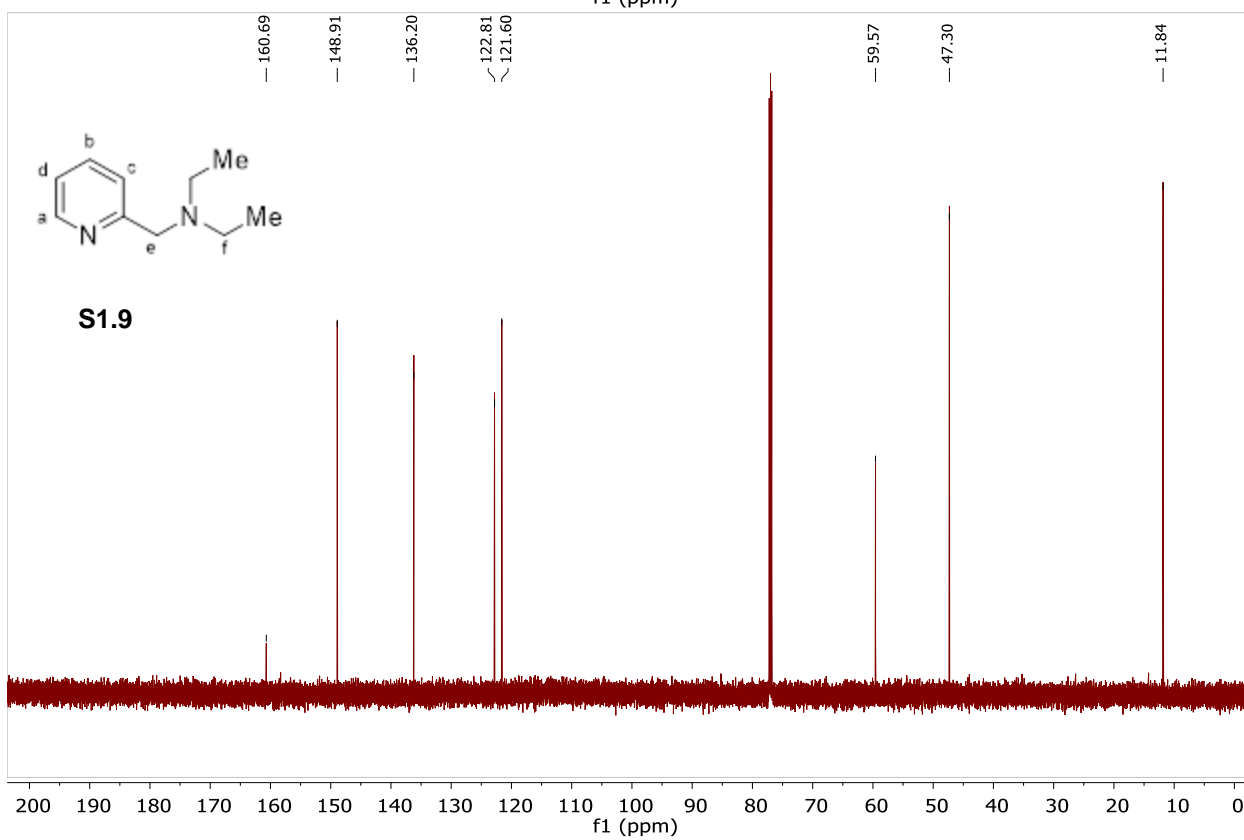
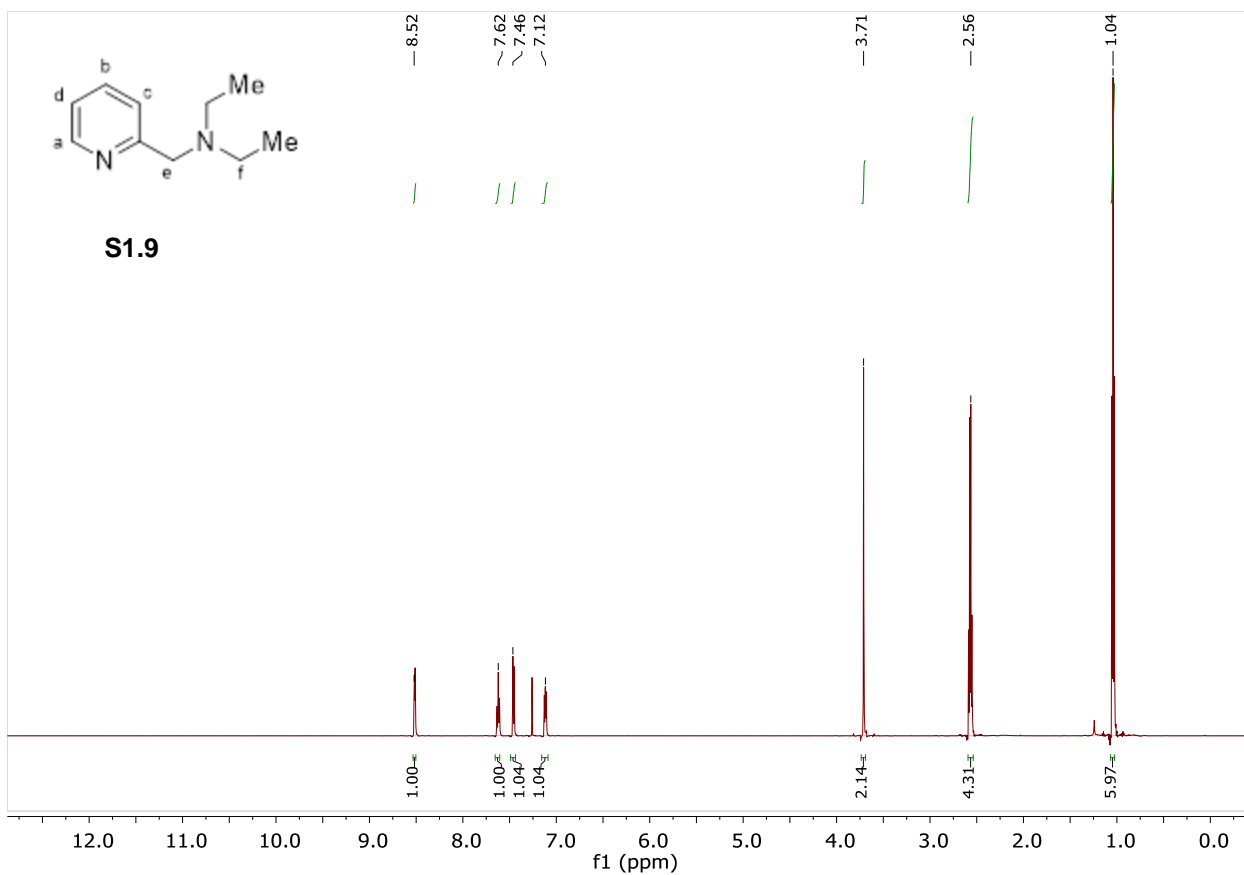
N-ethyl-N-(pyridin-2-ylmethyl)ethanamine was synthesized using the general reductive amination procedure on a scale of 2.5 mmol of the aldehyde. The reaction mixture was purified after workup using alumina flash chromatography (10% to 20% EtOAc/hexanes) to give product as 0.276 g of brown oil (1.68 mmol 67% yield)

¹H NMR (600 MHz, CDCl₃): δ 8.52 (H_a, d, *J* = 4.9 Hz, 1H), 7.62 (H_b, dd, *J* = 7.7, 1.9 Hz, 1H), 7.46 (H_c, d, *J* = 7.7 Hz, 1H), 7.13 – 7.10 (H_d, m, 1H), 3.71 (H_e, s, 2H), 2.57 (H_f, q, *J* = 7.1 Hz, 4H), 1.04 (Me, t, *J* = 7.1 Hz, 6H) ppm.

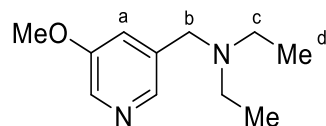
¹³C NMR (150 MHz, CDCl₃) δ 160.7, 148.9, 136.2, 122.8, 121.6, 59.6, 47.3, 11.8 ppm.

IR (ATR) 2804.50, 1589.34, 1431.18, 991.41, 754.17 cm⁻¹.

HRMS (ESI/QTOF) *m/z*: [M + H]⁺ Calcd for C₁₀H₁₇N₂ 165.1392, found 165.1395.



N-ethyl-N-((5-methoxypyridin-3-yl)methyl)ethanamine (S1.10)



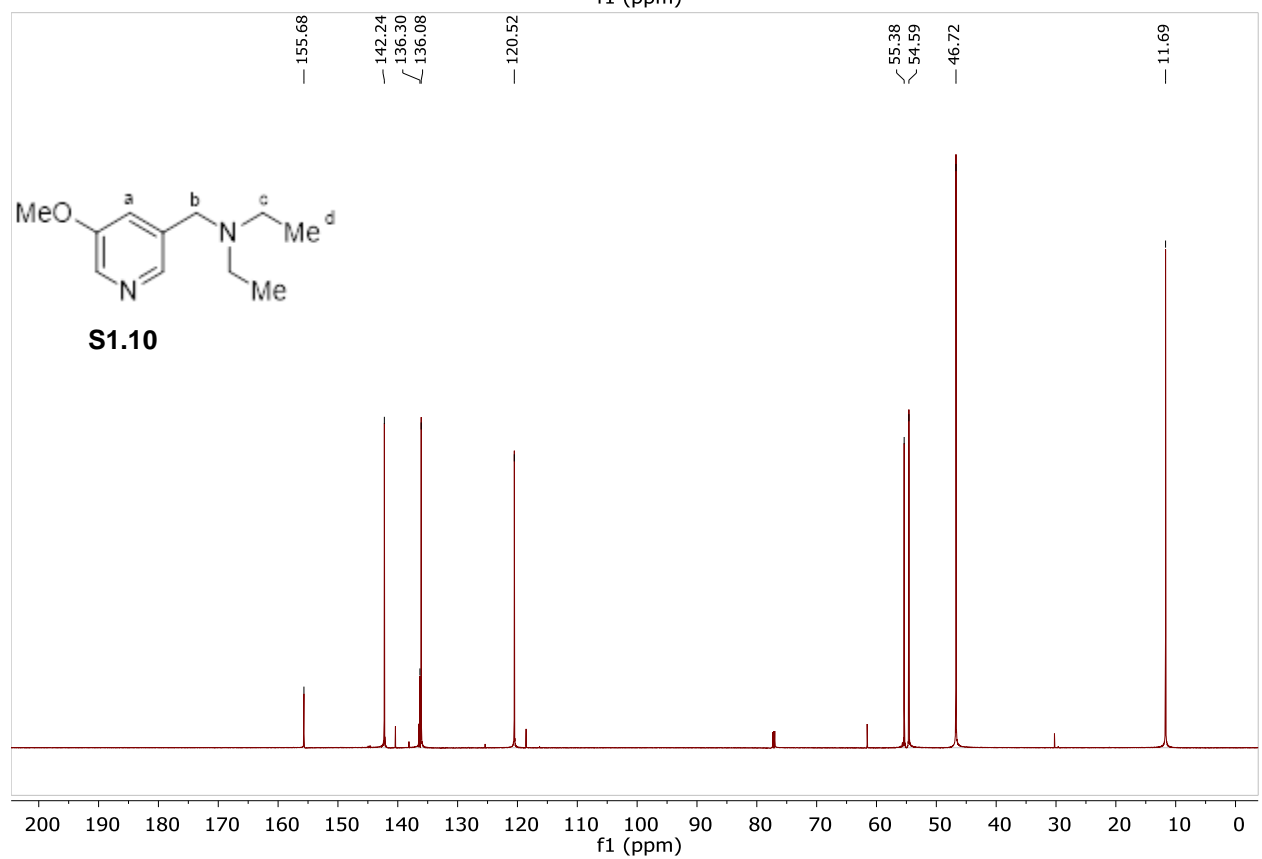
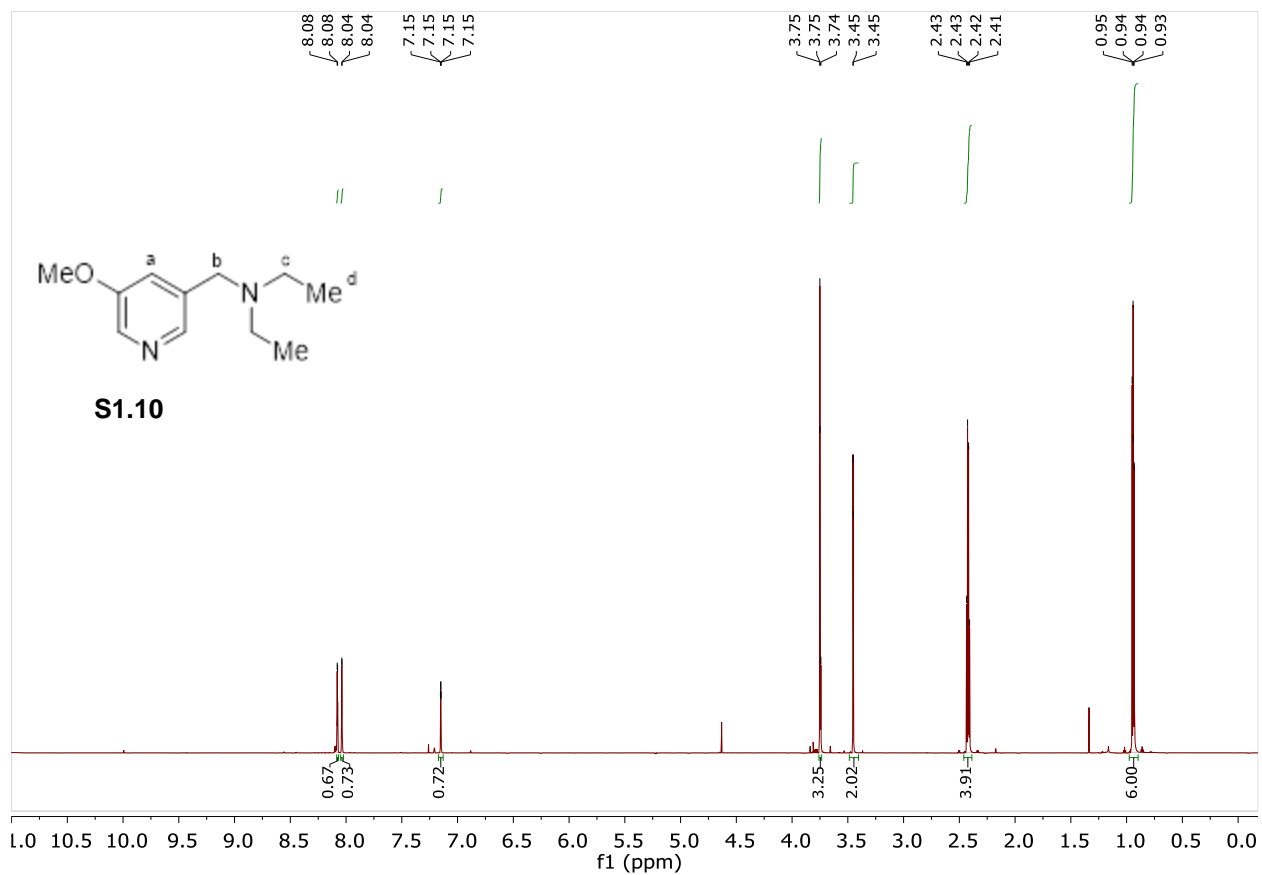
N-ethyl-N-((5-methoxypyridin-3-yl)methyl)ethanamine was synthesized using the general reductive amination procedure. The reaction mixture was purified after workup using alumina flash chromatography (90% Et₂O/MeOH) to give product as 0.340 g of a chunky, clear oil (1.46 mmol, 49%).

¹H NMR (800 MHz, CDCl₃) δ 8.08 (d, *J* = 2.9 Hz, 1H), 8.04 (d, *J* = 1.7 Hz, 1H), 7.15 (H_a, dd, *J* = 2.9, 1.7 Hz, 1H), 3.75 (OMe, s, 3H), 3.45 (H_b, s, 2H), 2.42 (H_c, q, *J* = 7.1 Hz, 4H), 0.94 (H_d, t, *J* = 7.1 Hz, 6H) ppm.

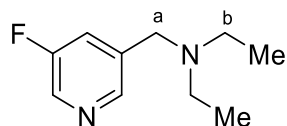
¹³C NMR (201 MHz, CDCl₃) δ 155.7, 142.2, 136.3, 136.1, 120.5, 55.4, 54.6, 46.7, 11.7 ppm.

IR (ATR) 2968.45, 2802.57, 1587.42, 1463.97, 1425.40, 1282.66, 1157.29, 1041.56, 866.04, 707.88 cm⁻¹.

HRMS (ESI/QTOF) *m/z*: [M + H]⁺ Calcd for C₁₁H₁₉N₂O 195.1497; Found 195.1493



N-ethyl-N-((5-fluoropyridin-3-yl)methyl)ethanamine (S.11)



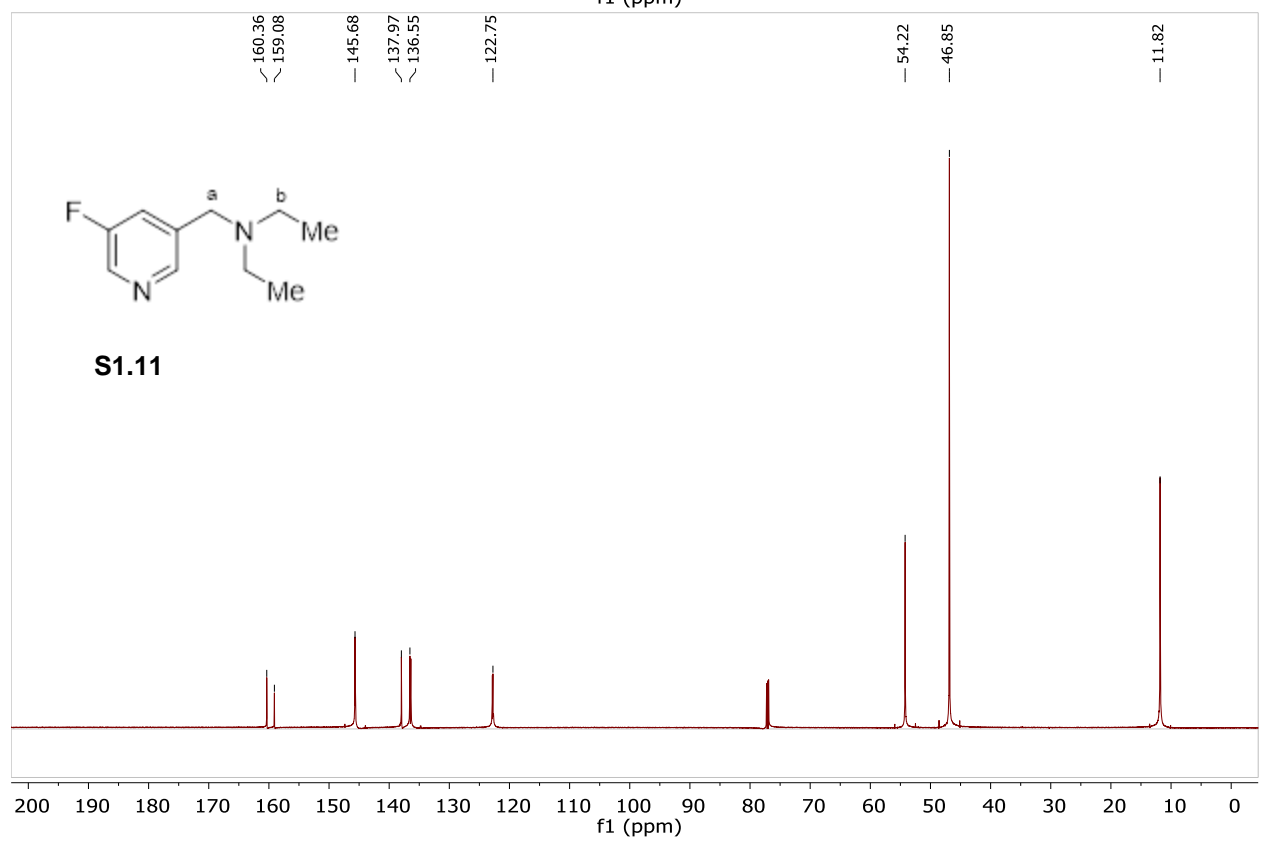
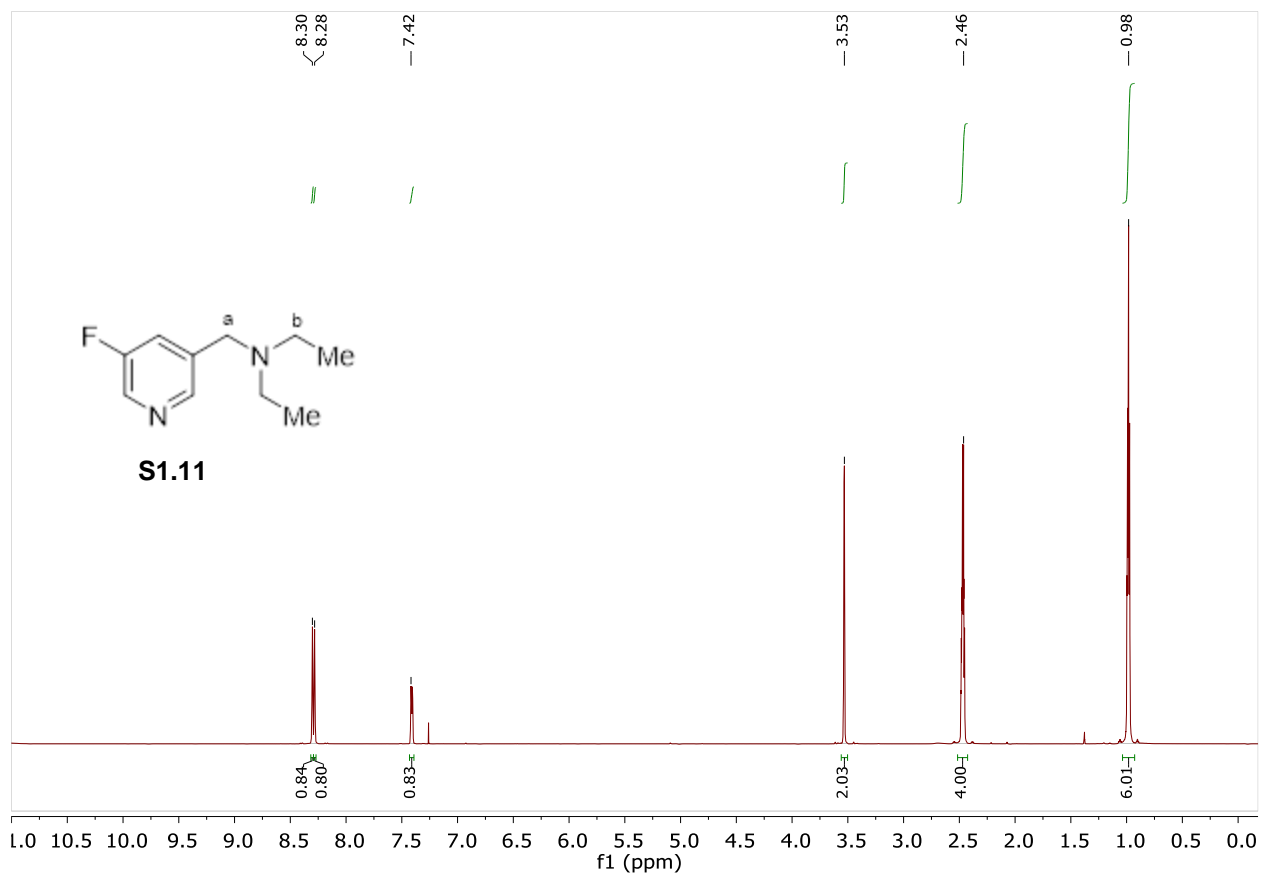
N-ethyl-N-((5-fluoropyridin-3-yl)methyl)ethanamine was synthesized using the general reductive amination procedure. The reaction mixture was purified after workup using alumina flash chromatography (Et₂O) to give product as 0.140 g of pale yellow oil (0.769 mmol, 31%)

¹H NMR (800 MHz, CDCl₃) δ 8.30 (ArH, q, J = 2.1 Hz, 1H), 8.28 (ArH, p, J = 2.1 Hz, 1H), 7.42 (d, J = 9.4 Hz, 1H), 3.53 (H_a, d, J = 2.6 Hz, 2H), 2.48 – 2.43 (H_b, m, 4H), 1.00 – 0.95 (Me, m, 6H) ppm.

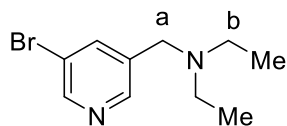
¹³C NMR (201 MHz, CDCl₃) δ 159.7 (d, J = 256.0 Hz), 145.7 (dd, J = 7.5, 3.9 Hz), 138.0 (d, J = 3.6 Hz), 136.5 (dd, J = 23.5, 8.2 Hz), 122.8 (dd, J = 18.4, 8.1 Hz), 54.2, 46.9, 11.8 (d, J = 4.9 Hz) ppm.

IR (ATR) 2970.38, 2804.50, 1600.92, 1577.77, 1429.25, 1265.30, 1026.13, 875.68, 744.52, 700.16 cm⁻¹.

HRMS (ESI/QTOF) m/z: [M + H]⁺ Calcd for C₁₀H₁₆FN₂ 183.1298; Found 183.1304



N-((5-bromopyridin-3-yl)methyl)-N-ethylethanamine (S.12)



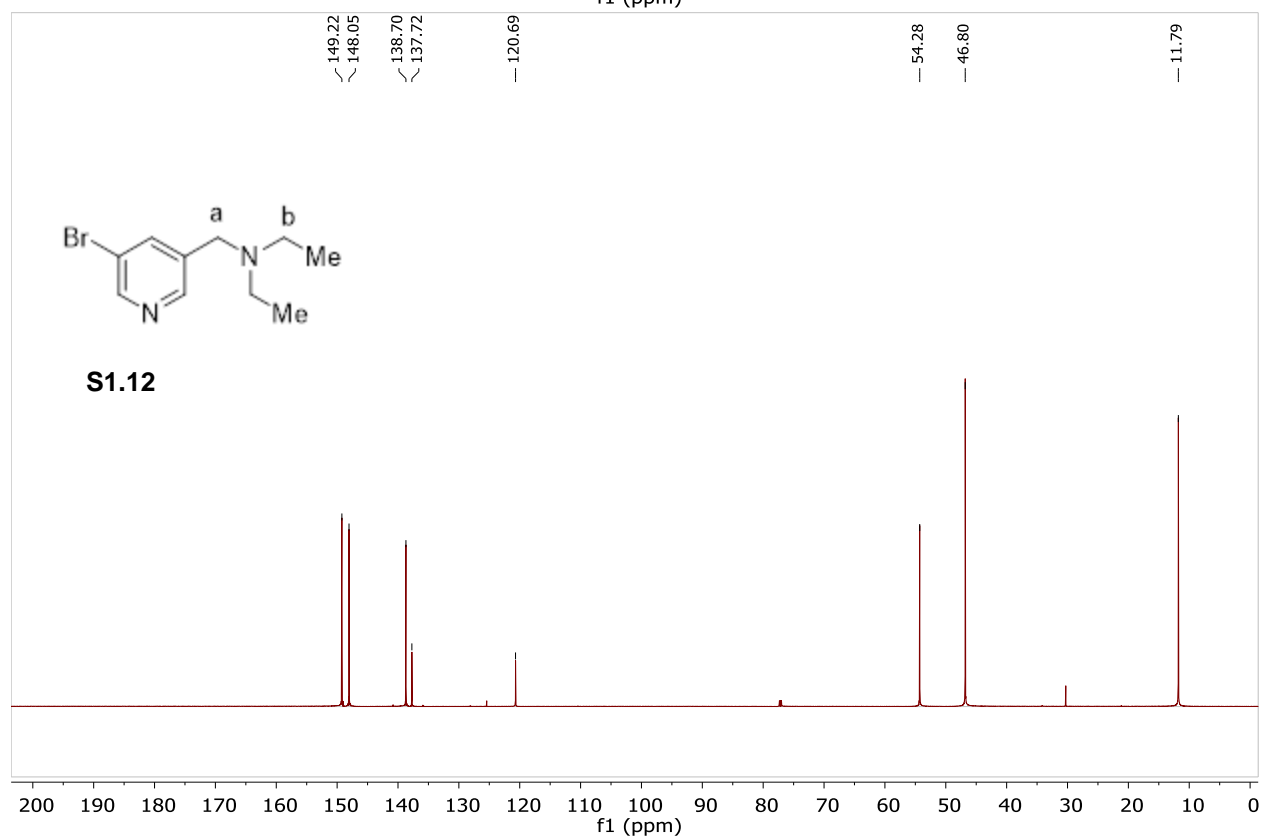
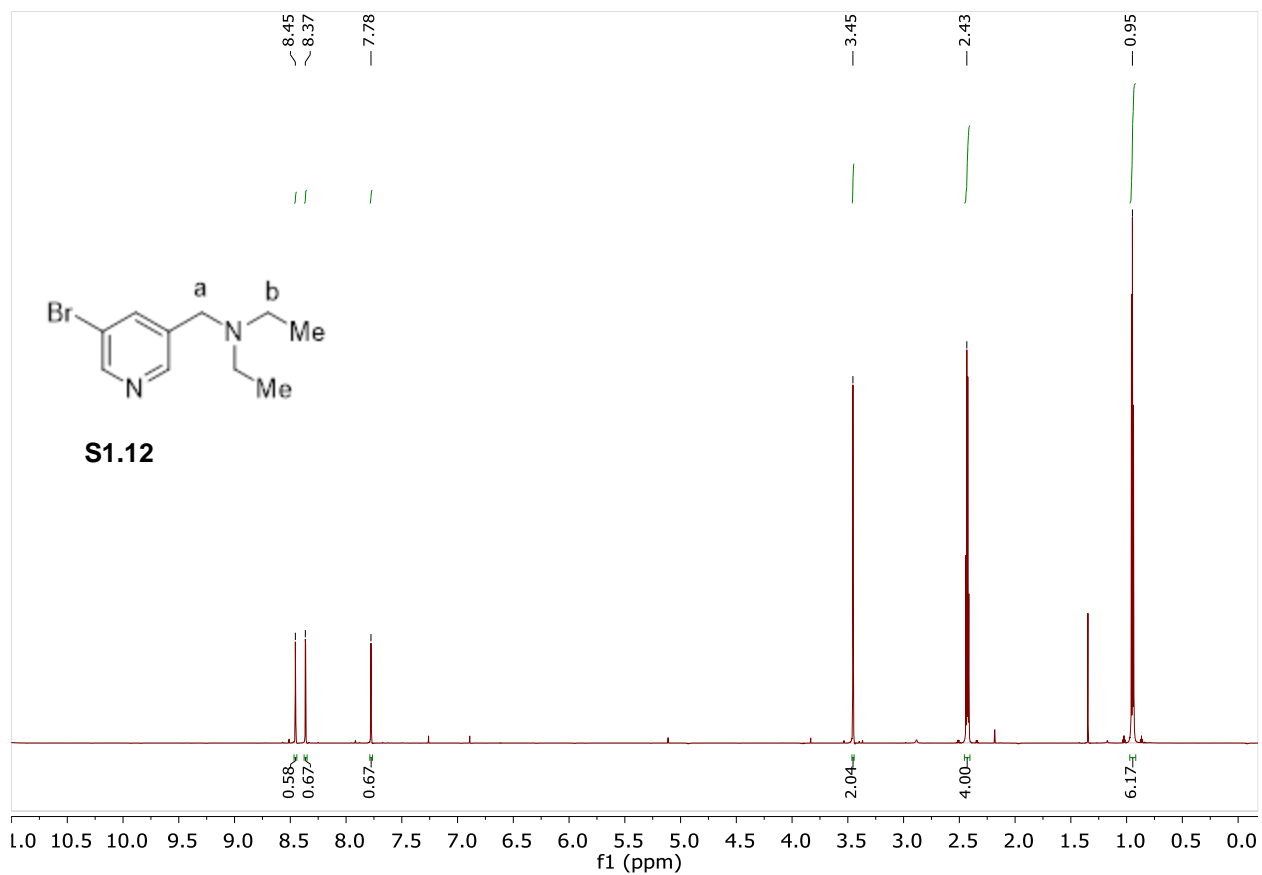
N-((5-bromopyridin-3-yl)methyl)-N-ethylethanamine was synthesized using the general reductive amination procedure on a 2.70 mmol of aldehyde. The reaction mixture was purified after workup using alumina flash chromatography (Et₂O) to give product as 0.184 g of clear oil (0.757 mmol, 28%)

¹H NMR (800 MHz, CDCl₃) δ 8.45 (ArH, d, J = 2.0 Hz, 1H), 8.37 (ArH, d, J = 2.0 Hz, 1H), 7.78 (ArH, t, J = 2.0 Hz, 1H), 3.45 (H_a, s, 1H), 2.43 (H_b, q, J = 7.1 Hz, 4H), 0.95 (Me, t, J = 7.1 Hz, 6H) ppm.

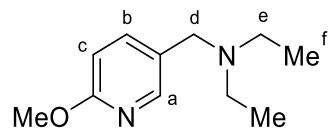
¹³C NMR (201 MHz, CDCl₃) δ 149.2, 148.1, 138.7, 137.7, 120.7, 54.3, 46.8, 11.8 ppm.

IR (ATR) 2968.45, 2800.64, 1579.70, 1556.55, 1419.61, 1290.38, 1203.58, 1166.93, 1087.85, 1022.27, 860.25, 702.09, 678.94 cm⁻¹.

HRMS (ESI/QTOF) m/z: [M + H]⁺ Calcd for C₁₀H₁₆BrN₂ 243.0497; Found 243.0490



N-((5-bromopyridin-3-yl)methyl)-N-ethylethanamine (S1.13)



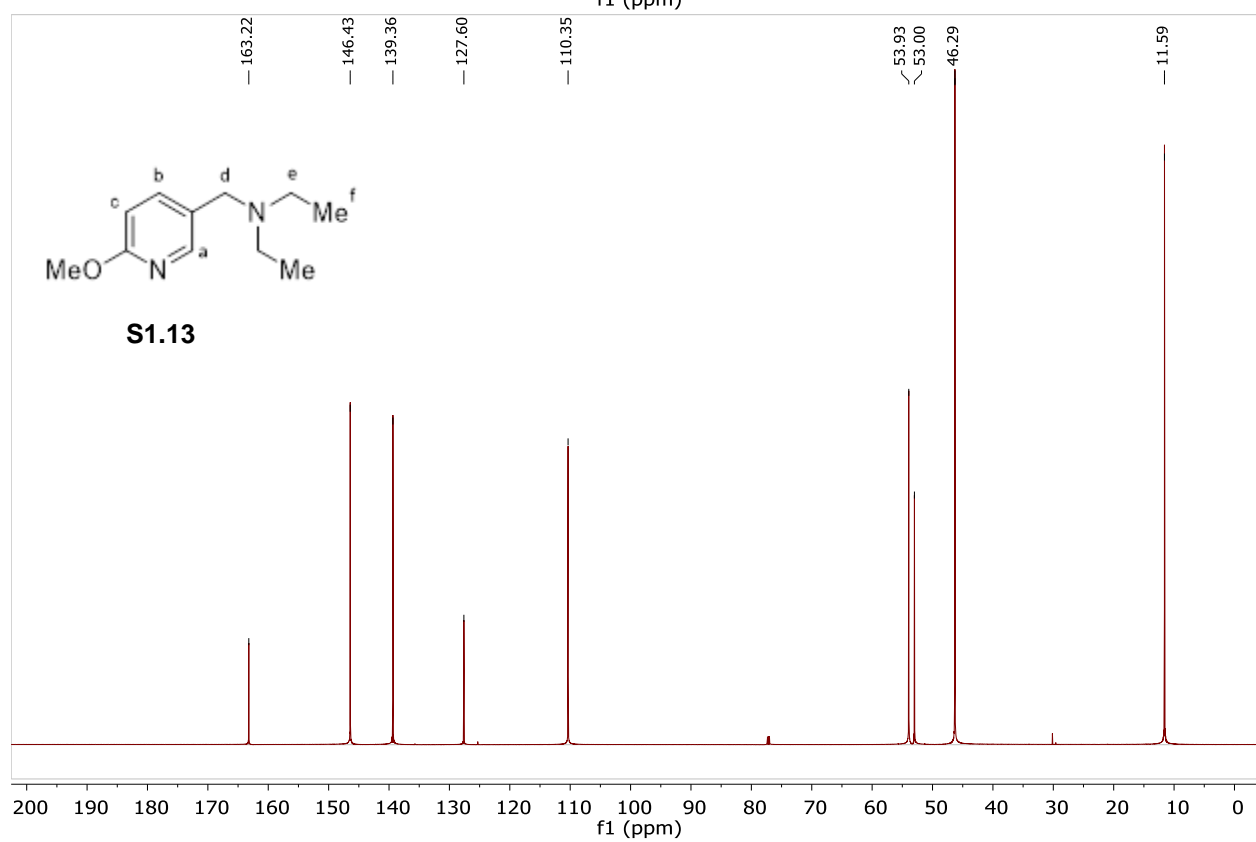
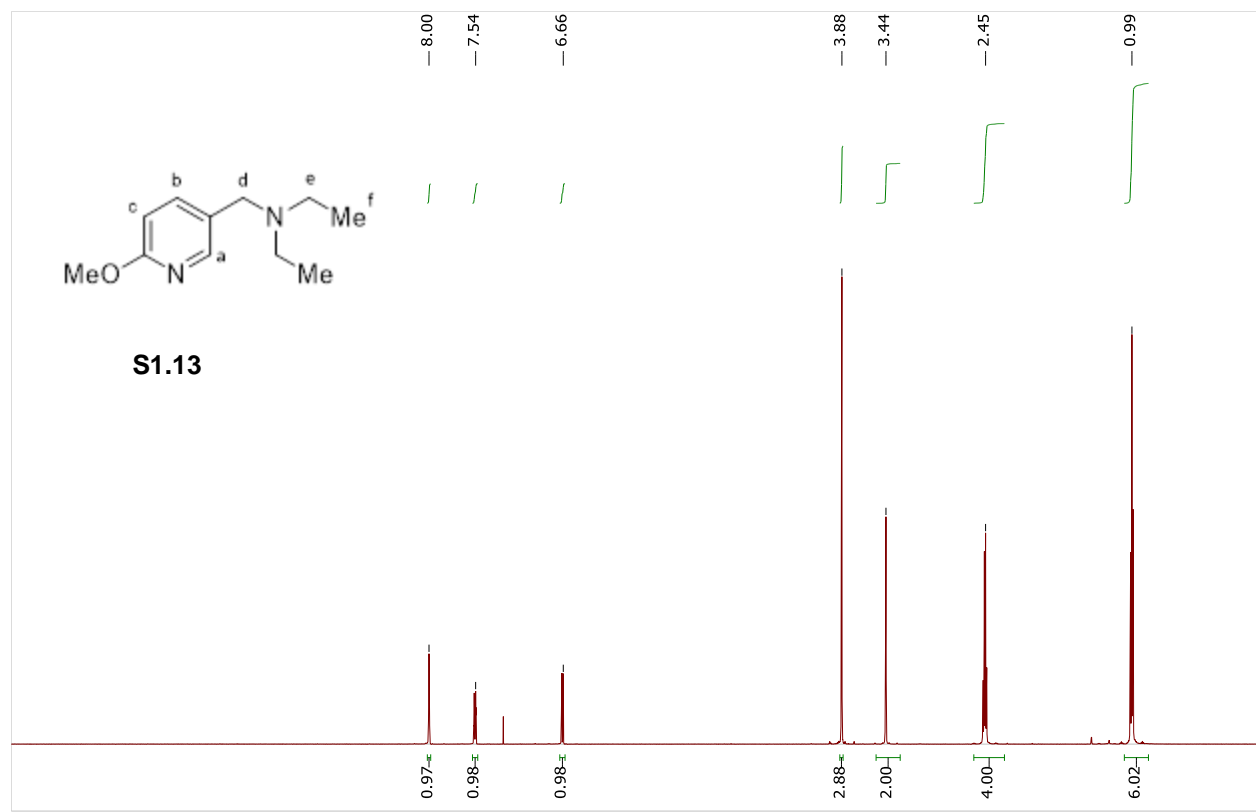
N-ethyl-N-((6-methoxypyridin-3-yl)methyl)ethanamine was synthesized using the general reductive amination procedure on scale of 3.65 mmol of aldehyde. The reaction mixture was purified after workup using alumina flash chromatography (Et₂O) to give product as 0.366 g of pale yellow oil (1.88 mmol, 52%)

¹H NMR (800 MHz, CDCl₃) δ 8.00 (H_a, d, *J* = 2.5 Hz, 1H), 7.54 (H_b, dd, *J* = 8.5, 2.5 Hz, 1H), 6.66 (H_c, d, *J* = 8.5 Hz, 1H), 3.88 (OMe, s, 3H), 3.44 (H_d, s, 2H), 2.45 (H_e, q, *J* = 7.1 Hz, 4H), 0.99 (H_f, t, *J* = 7.1 Hz, 6H) ppm.

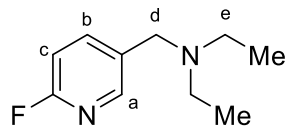
¹³C NMR (201 MHz, CDCl₃) δ 163.2, 146.4, 139.4, 127.6, 110.4, 53.9, 53.0, 46.3, 11.6 ppm.

IR (ATR) 2986.45, 2800.64, 1608.63, 1573.91, 1490.97, 1458.18, 1392.61, 1355.96, 1307.74, 1288.45, 1259.52, 1199.72, 1166.93, 1116.78, 1058.92, 1026.13, 829.39, 775.38, 613.36 cm⁻¹.

HRMS (ESI/QTOF) *m/z*: [M + H]⁺ Calcd for C₁₁H₁₉N₂O 195.1497; Found 195.1498



N-ethyl-N-((6-fluoropyridin-3-yl)methyl)ethanamine (S1.14)



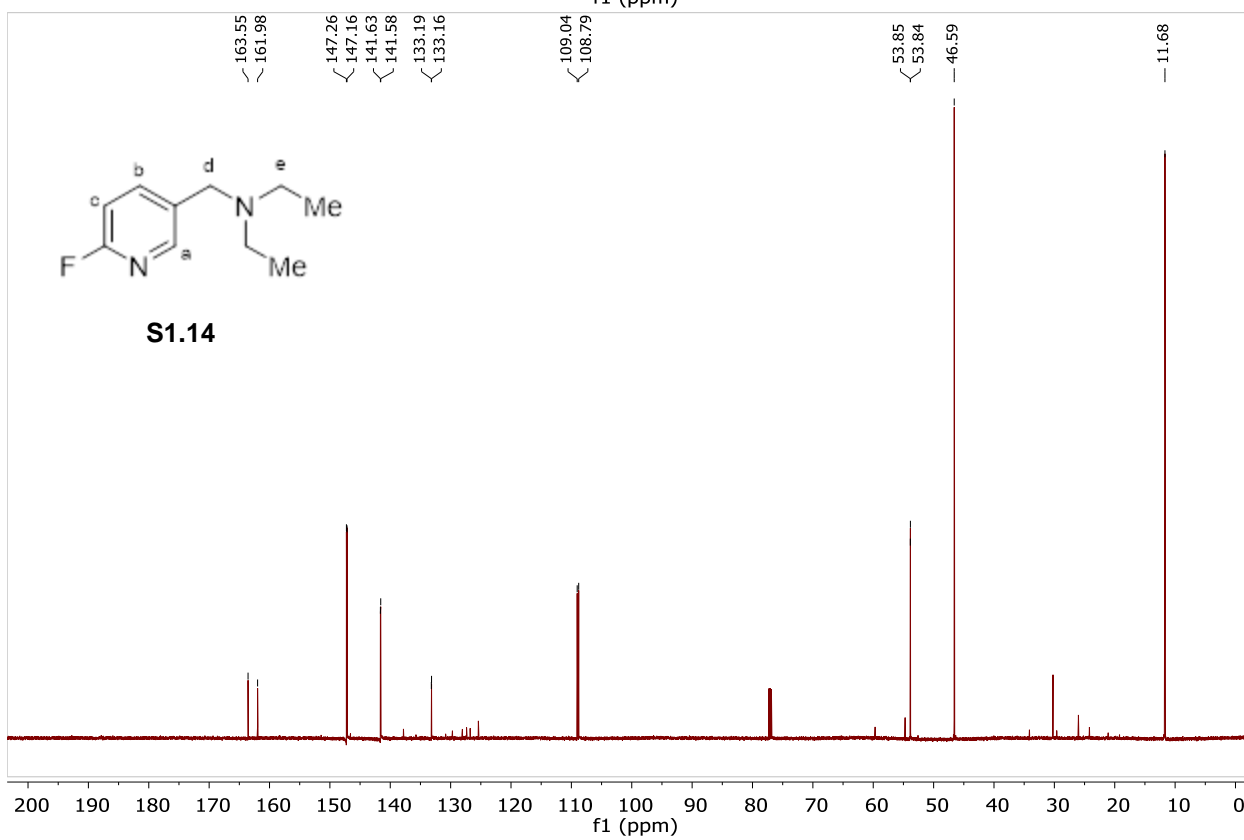
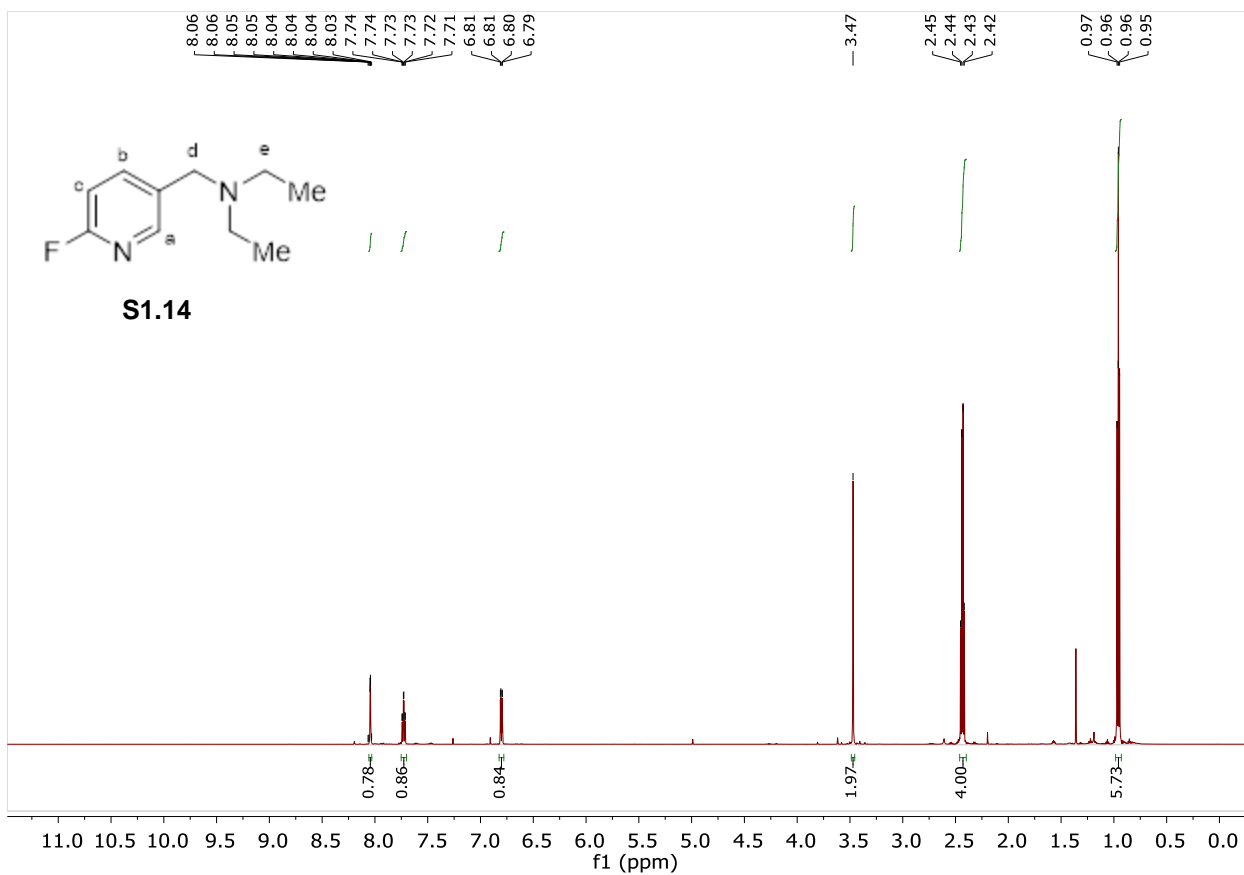
N-ethyl-N-((6-fluoropyridin-3-yl)methyl)ethanamine was synthesized using the general reductive amination procedure on a scale of 4.00 mmol of aldehyde. The reaction mixture was purified after workup using alumina flash chromatography (Et₂O) to give 0.0989 g of product as a pale yellow oil (0.543 mmol, 14%).

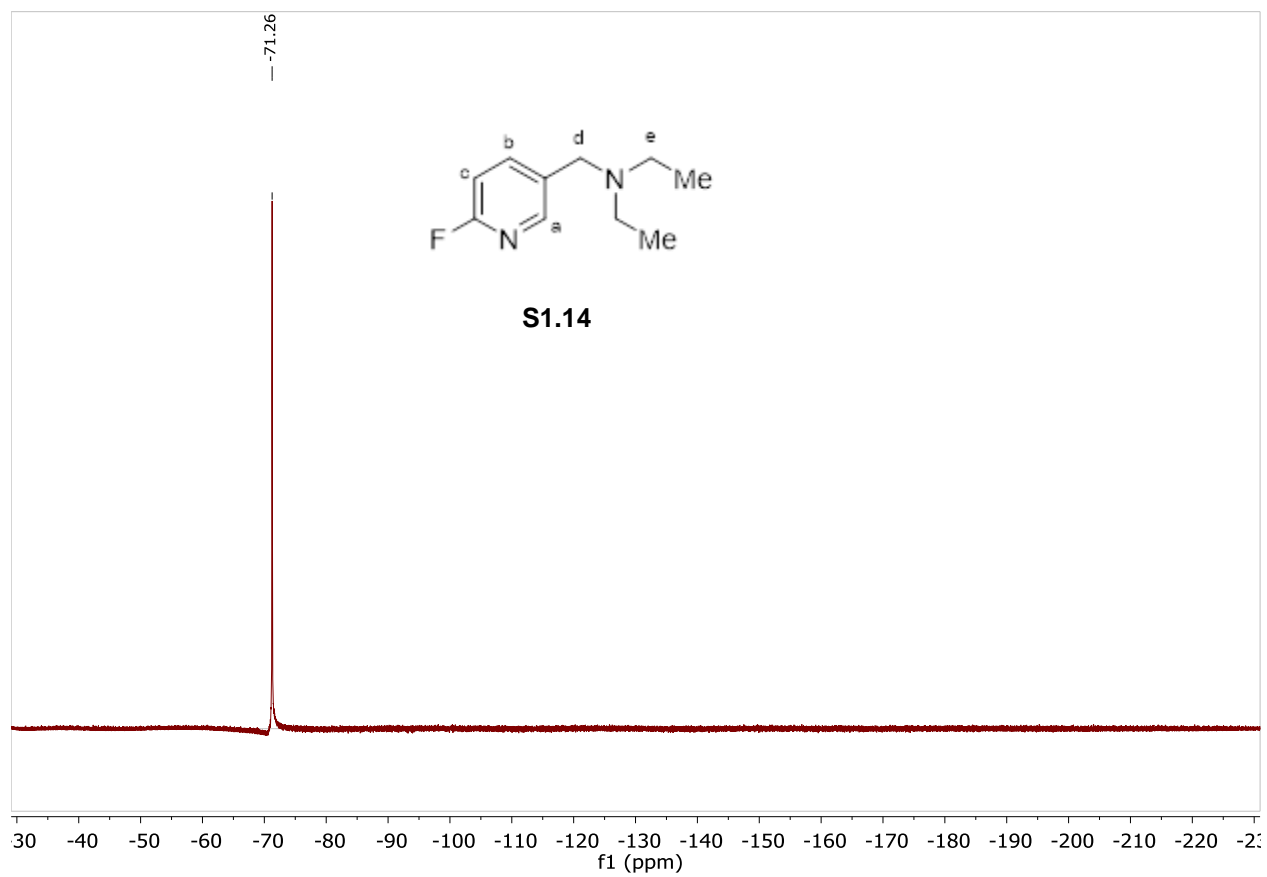
¹H NMR (598 MHz, CDCl₃) δ 8.04 (H_a, d, *J* = 1.9 Hz, 1H), 7.73 (H_b, td, *J* = 8.2, 2.7 Hz, 1H), 6.80 (H_c, dd, *J* = 8.2, 2.7 Hz, 1H), 3.47 (H_d, s, 2H), 2.43 (H_f, q, *J* = 7.1 Hz, 4H), 0.96 ppm (Me, t, *J* = 7.1 Hz, 6H) ppm.

¹³C NMR (150 MHz, CDCl₃) δ 162.8 (d, *J* = 237.5 Hz), 147.2 (d, *J* = 14.4 Hz), 141.6 (d, *J* = 7.7 Hz), 133.2 (d, *J* = 4.5 Hz), 108.9 (d, *J* = 37.4 Hz), 53.9 (d, *J* = 1.4 Hz), 46.6, 11.7 ppm.

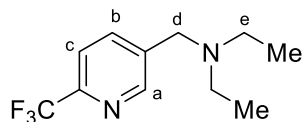
IR (ATR) 2968.45, 2935.66, 2873.94, 2810.28, 1595.13, 1481.33, 1382.96, 1288.45, 1242.16, 1201.65, 1166.93, 1114.86, 1060.85, 1024.20, 831.32, 775.38 cm⁻¹.

HRMS (ESI/QTOF) *m/z*: [M + H]⁺ Calcd for C₁₀H₁₅FN₂ 183.1298; Found 183.1304





N-ethyl-N-((6-(trifluoromethyl)pyridin-3-yl)methyl)ethanamine (S1.15)



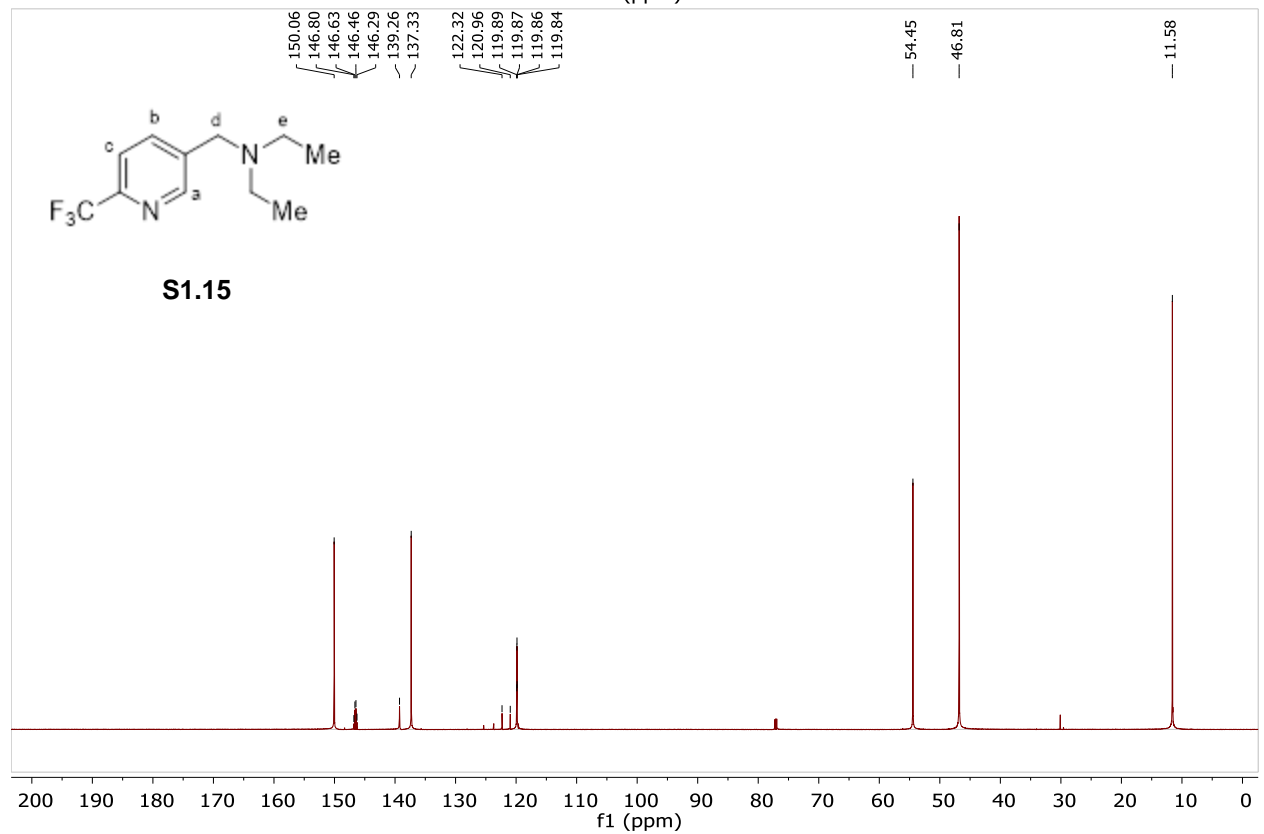
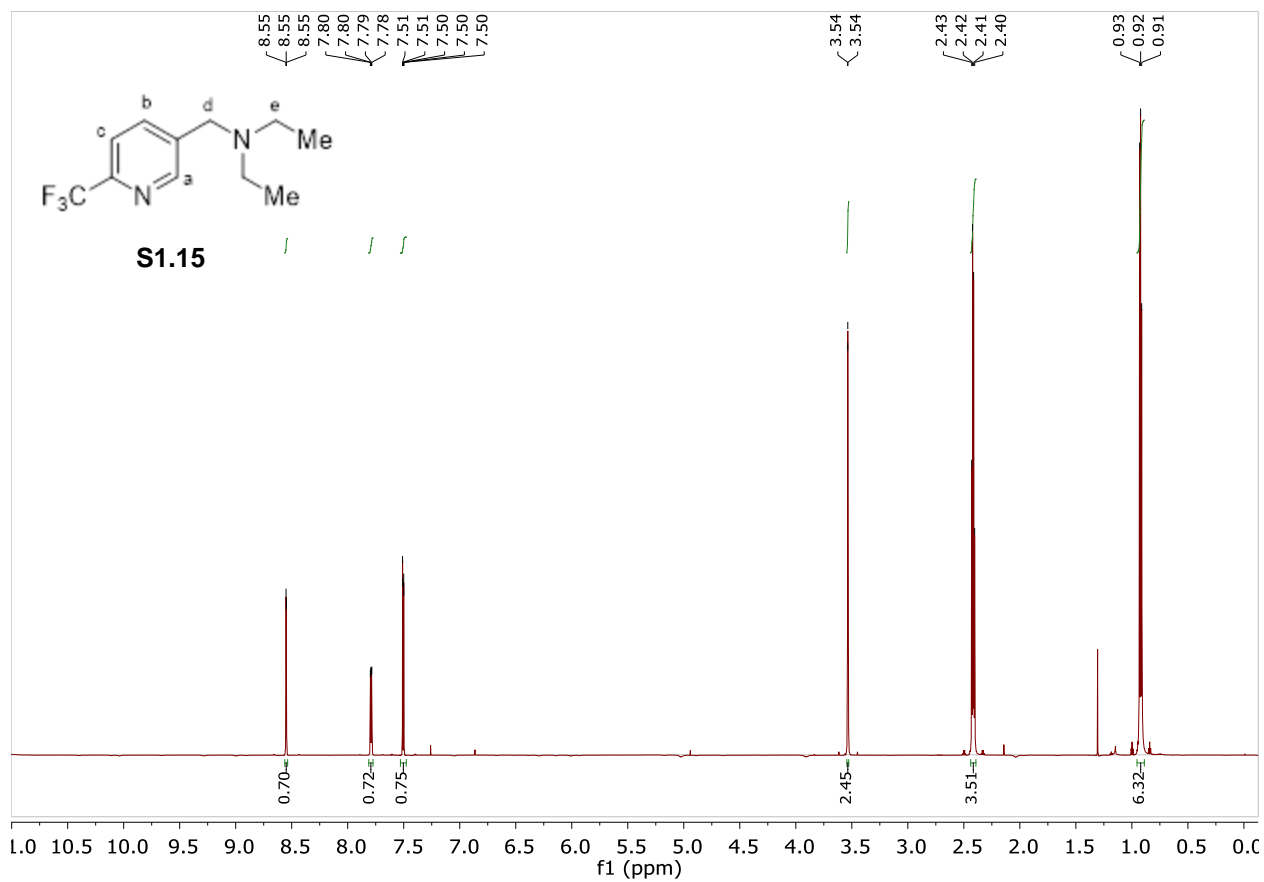
N-ethyl-N-((6-(trifluoromethyl)pyridin-3-yl)methyl)ethanamine was synthesized using the general reductive amination procedure on scale of 2.38 mmol of aldehyde. The reaction mixture was purified after workup using silica flash chromatography (Et₂O) to give product as 0.463 g of pale yellow oil (2.00 mmol, 84%).

¹H NMR (800 MHz, CDCl₃) δ 8.55 (H_a, d, *J* = 1.9 Hz, 1H), 7.79 (H_b, dd, *J* = 8.2, 1.9 Hz, 1H), 7.51 (H_c, d, *J* = 8.2 Hz, 1H), 3.54 (H_d, s, 2H), 2.42 (H_e, q, *J* = 7.1 Hz, 4H), 0.92 (Me, t, *J* = 7.1 Hz, 6H) ppm.

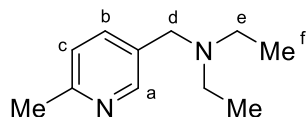
¹³C NMR (201 MHz, CDCl₃) δ 150.1, 146.5 (q, *J* = 34.5 Hz), 139.3, 137.3, 121.6 (d, *J* = 273.9 Hz), 119.9 (q, *J* = 3.0 Hz), 54.5, 46.8, 11.6 ppm.

IR (ATR) 2972.31, 2937.59, 2814.14, 1456.26, 1384.89, 1330.88, 1292.31, 1238.30, 1168.86, 1132.21, 1083.99, 1026.13, 850.61, 837.11, 752.24, 634.58, 592.15 cm⁻¹.

HRMS (ESI/QTOF) *m/z*: [M + H]⁺ Calcd for C₁₁H₁₅F₃N₂ 233.1266; Found 233.1270



N-ethyl-N-((6-methylpyridin-3-yl)methyl)ethanamine (S1.16)



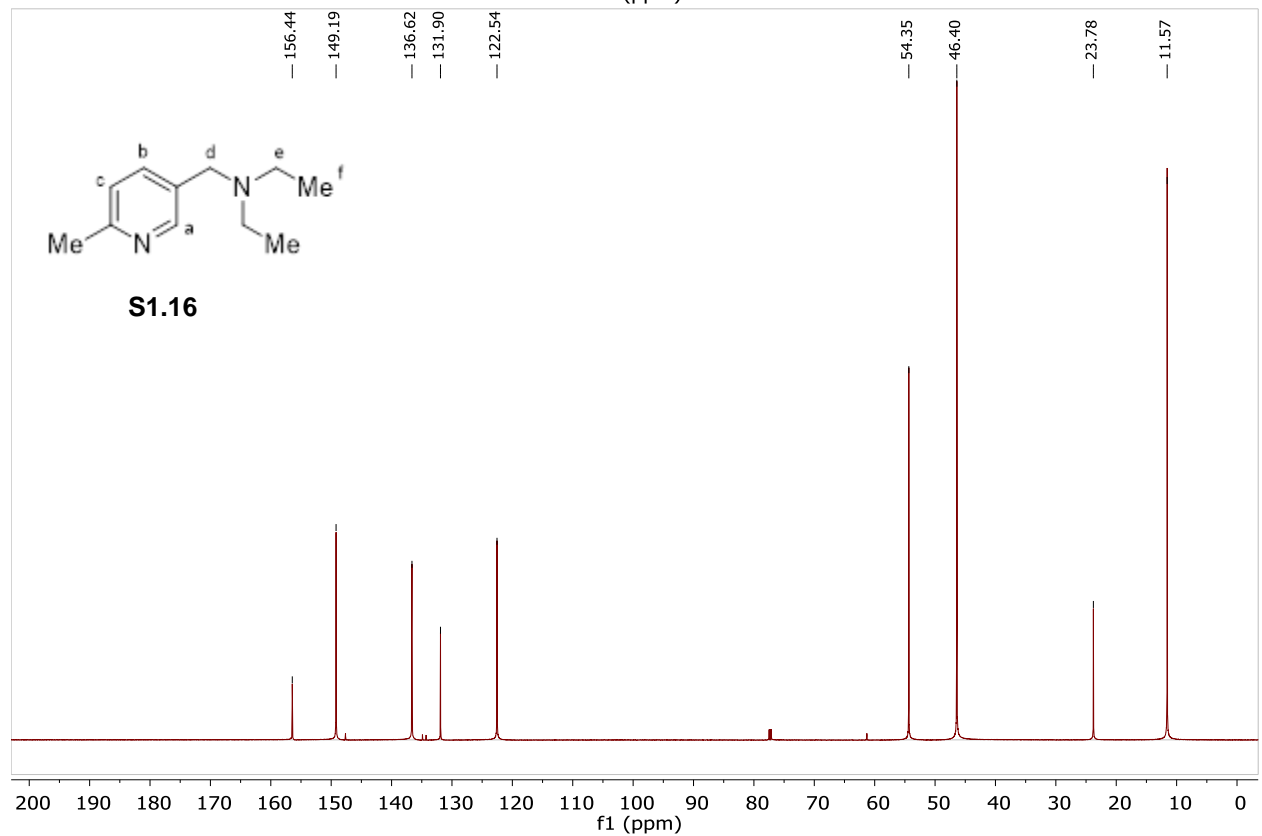
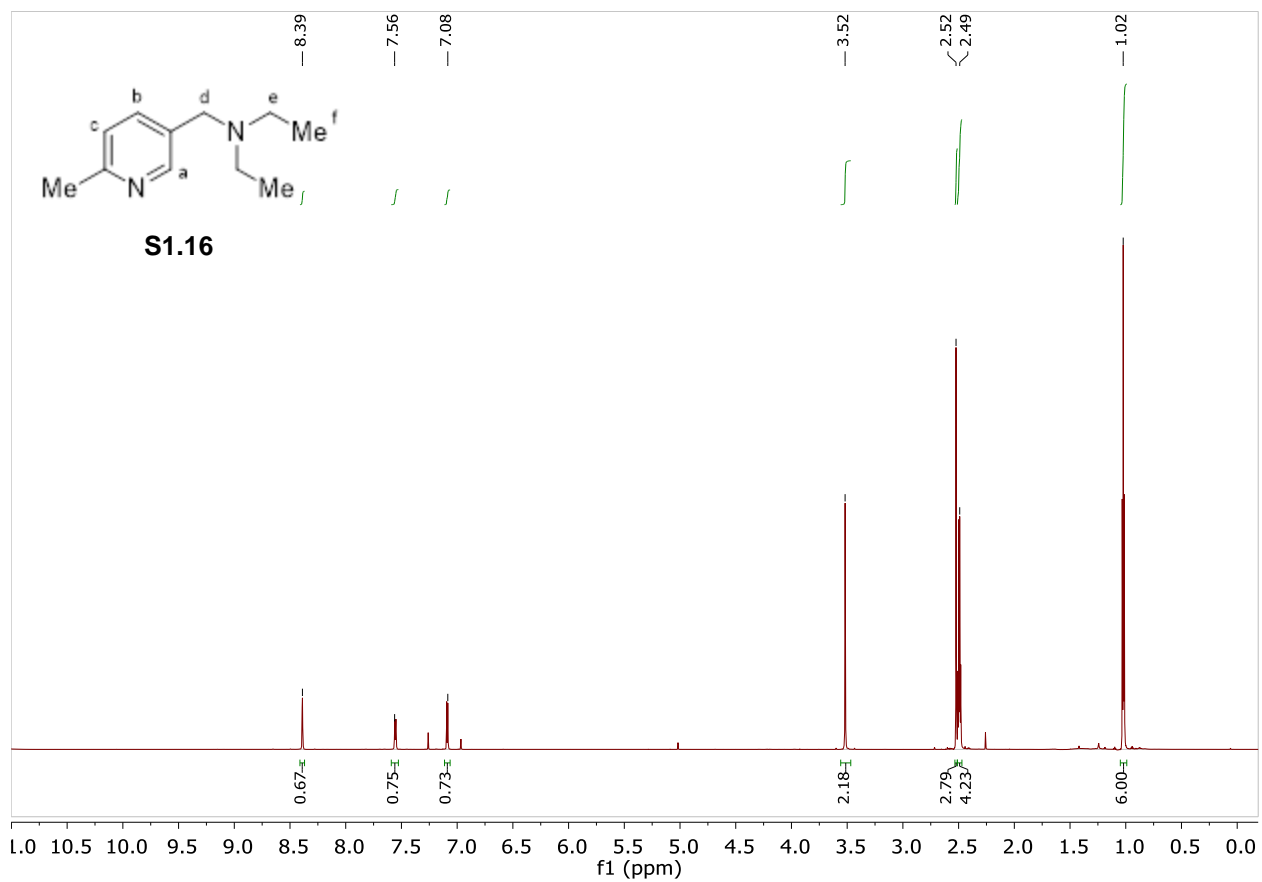
N-ethyl-N-((6-methylpyridin-3-yl)methyl)ethanamine was synthesized using the general reductive amination procedure on scale of 3.94 mmol of aldehyde. The reaction mixture was purified after workup using alumina flash chromatography (10% MeOH/Et₂O) to give product as 0.219 g of pale yellow solid (1.23 mmol, 31%).

¹H NMR (800 MHz, CDCl₃) δ 8.39 (H_a, d, *J* = 2.3 Hz, 1H), 7.56 (H_b, dd, *J* = 8.0, 2.3 Hz, 1H), 7.08 (H_c, d, *J* = 8.0 Hz, 1H), 3.52 (H_d, s, 2H), 2.52 (ArMe, s, 3H), 2.49 (H_e, q, *J* = 7.2 Hz, 4H), 1.02 (H_f, d, *J* = 7.2 Hz, 6H) ppm.

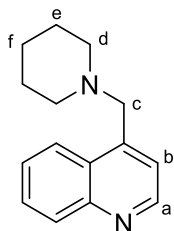
¹³C NMR (201 MHz, CDCl₃) δ 157.5, 149.3, 138.0, 128.9, 123.2, 53.6, 45.9, 23.6, 10.4 ppm.

IR (ATR) 2972.31, 2569.18, 2497.82, 1604.77, 1568.13, 1490.97, 1381.03, 1296.16, 1267.23, 1172.72, 1028.06, 727.16, 578.64 cm⁻¹.

HRMS (ESI/QTOF) *m/z*: [M + H]⁺ Calcd for C₁₁H₁₈N₂ 179.1548; Found 179.1551



4-(piperidin-1-ylmethyl)quinoline (S1.17)



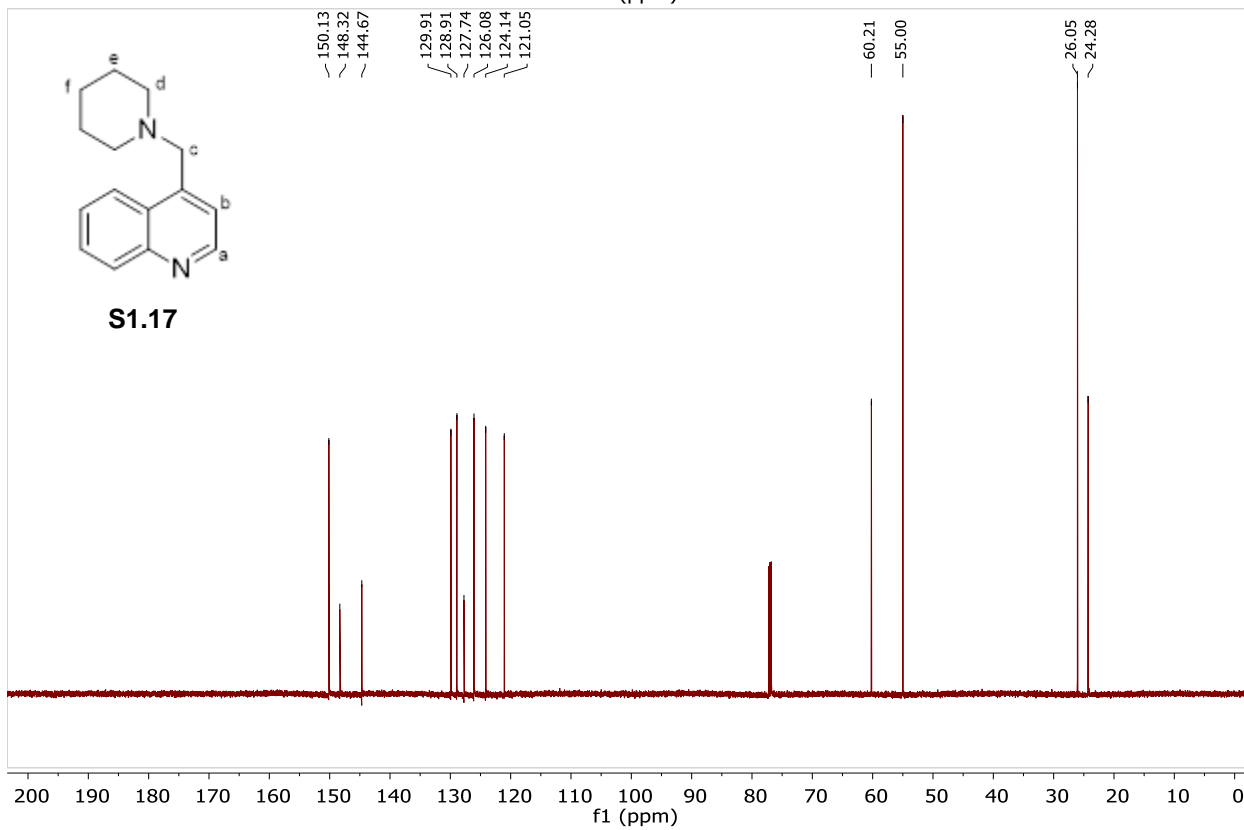
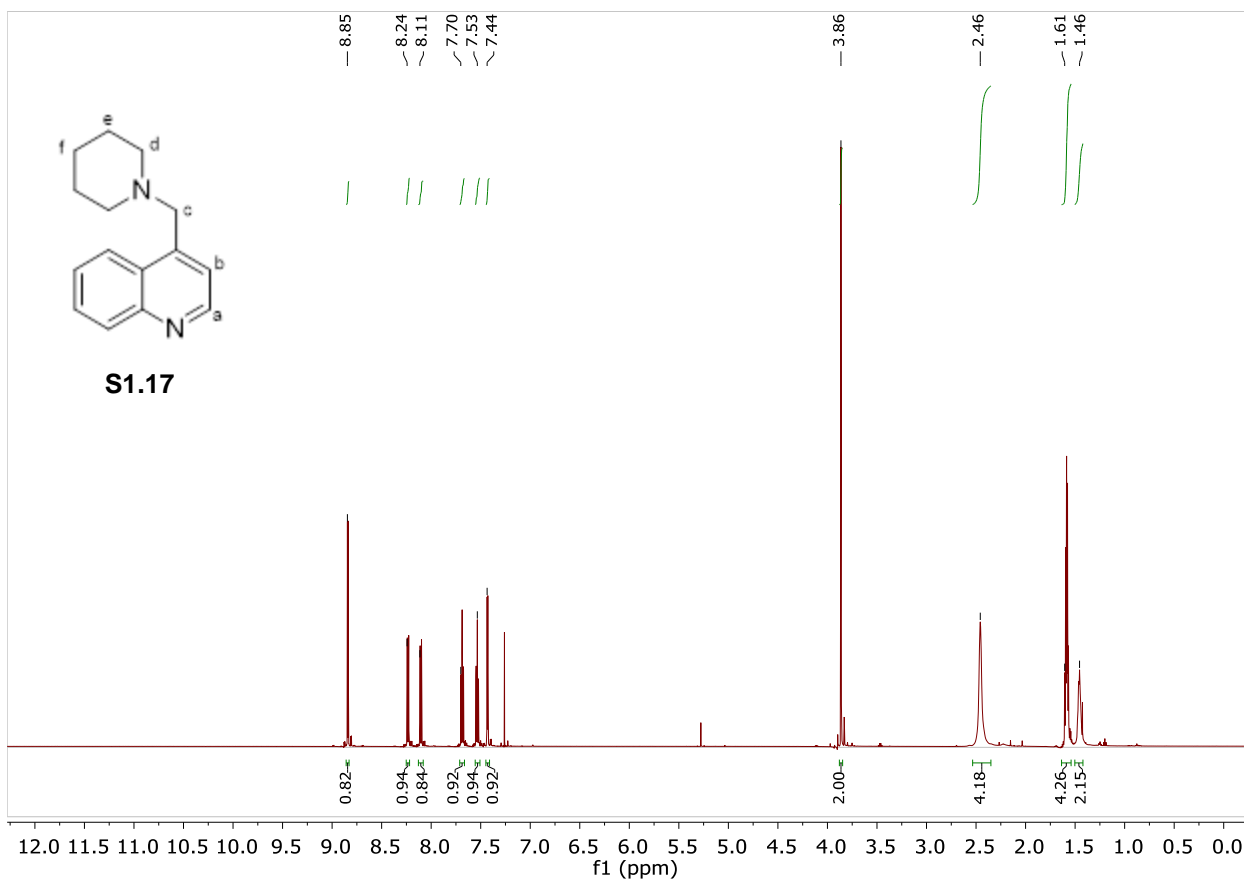
4-(piperidin-1-ylmethyl)quinoline was synthesized using the general reductive amination procedure on scale of 11.5 mmol of aldehyde. The reaction mixture was purified after workup using alumina flash chromatography (Et₂O) to give product as 1.69 g of greenish-yellow oil (7.48 mmol, 65%).

¹H NMR (598 MHz, CDCl₃) δ 8.84 (H_a, d, J = 4.3 Hz, 1H), 8.23 (ArH, dd, J = 8.4, 1.3 Hz, 1H), 8.11 (ArH, dt, J = 8.3, 1.2 Hz, 1H), 7.69 (ArH, ddd, J = 8.3, 6.8, 1.2 Hz, 1H), 7.53 (ArH, ddd, J = 8.4, 6.8, 1.3 Hz, 1H), 7.43 (H_b, d, J = 4.3 Hz, 1H), 3.86 (H_c, s, 2H), 2.51 – 2.36 (H_d, m, 4H), 1.61 – 1.55 (H_e, m, 4H), 1.49 – 1.42 (H_f, m, 2H) ppm.

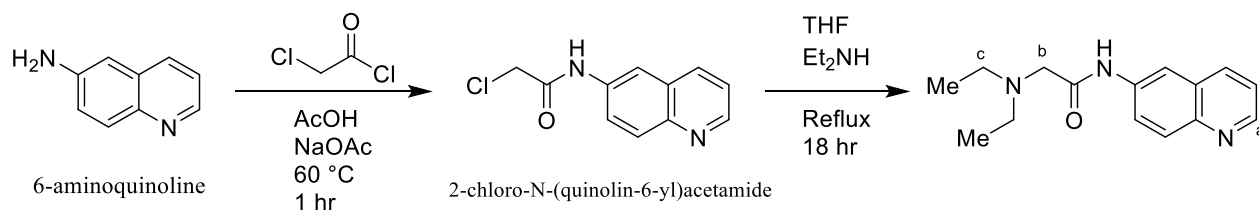
¹³C NMR (150 MHz, cdcl₃) δ 150.1, 148.3, 144.7, 129.9, 128.9, 127.7, 126.1, 124.1, 121.1, 60.2, 55.0, 26.1, 24.3 ppm.

IR (ATR) 2931.80, 2850.79, 2798.71, 2756.28, 1591.27, 1568.13, 1508.33, 1344.38, 1296.16, 1236.37, 1107.14, 867.97, 842.89, 752.24 cm⁻¹.

HRMS (ESI/QTOF) m/z: [M + H]⁺ Calcd for C₁₅H₁₉N₂ 227.1548; Found 227.1559



2-(diethylamino)-N-(quinolin-6-yl)acetamide (S1.18)



2-chloro-N-(quinolin-6-yl)acetamide was prepared as follows. 6-aminoquinoline (1.19 g, 8.25 mmol) was dissolved in 35 mL of glacial acetic acid in a 100 mL round-bottom flask equipped with a stir bar. α -chloroacetylchloride (1.5 eq., 1.31 mL, 16.5 mmol) was added dropwise and reaction was heated to 60 °C for 10 min. Sodium acetate (6.00 g, 73.1 mmol in 45.0 mL of water) was added. After 1 hr reaction was brought to RT. 6 M NaOH (50.0 mL) added until product precipitated out. Collected by vacuum filtration to yield 0.184 g of a brown, clay-like solid (7.04 mmol, 85%)

¹H NMR (800 MHz, CDCl₃) δ 8.87 (dd, J = 4.2, 1.7 Hz, 1H), 8.48 (s, 1H), 8.35 (d, J = 2.4 Hz, 1H), 8.15 (d, J = 8.2 Hz, 1H), 8.09 (d, J = 9.0 Hz, 1H), 7.65 (dd, J = 9.0, 2.4 Hz, 1H), 7.41 (dd, J = 8.2, 4.2 Hz, 1H), 4.26 (s, 2H) ppm.

2-chloro-N-(quinolin-6-yl)acetamide (1.56 g, 7.04 mmol) was dissolved in 150 mL dry THF in a 250 mL round-bottom flask equipped with a stir bar. Diethylamine (5 eq., 3.64 mL, 35.2 mmol) was added. Flask was equipped with a condenser and brought to reflux for 18 hr. Solvent evaporated and diluted with 20 mL EtOAc. Extracted with 3x 20 mL of 1 M HCl. Combined fractions basified with 15 mL of 6 M NaOH. Extracted with 5x 20 mL DCM. Combined fractions washed with brine and dried over Na₂SO₄ to give the title compound as 1.72 g of brown powder (6.69 mmol, 95%)

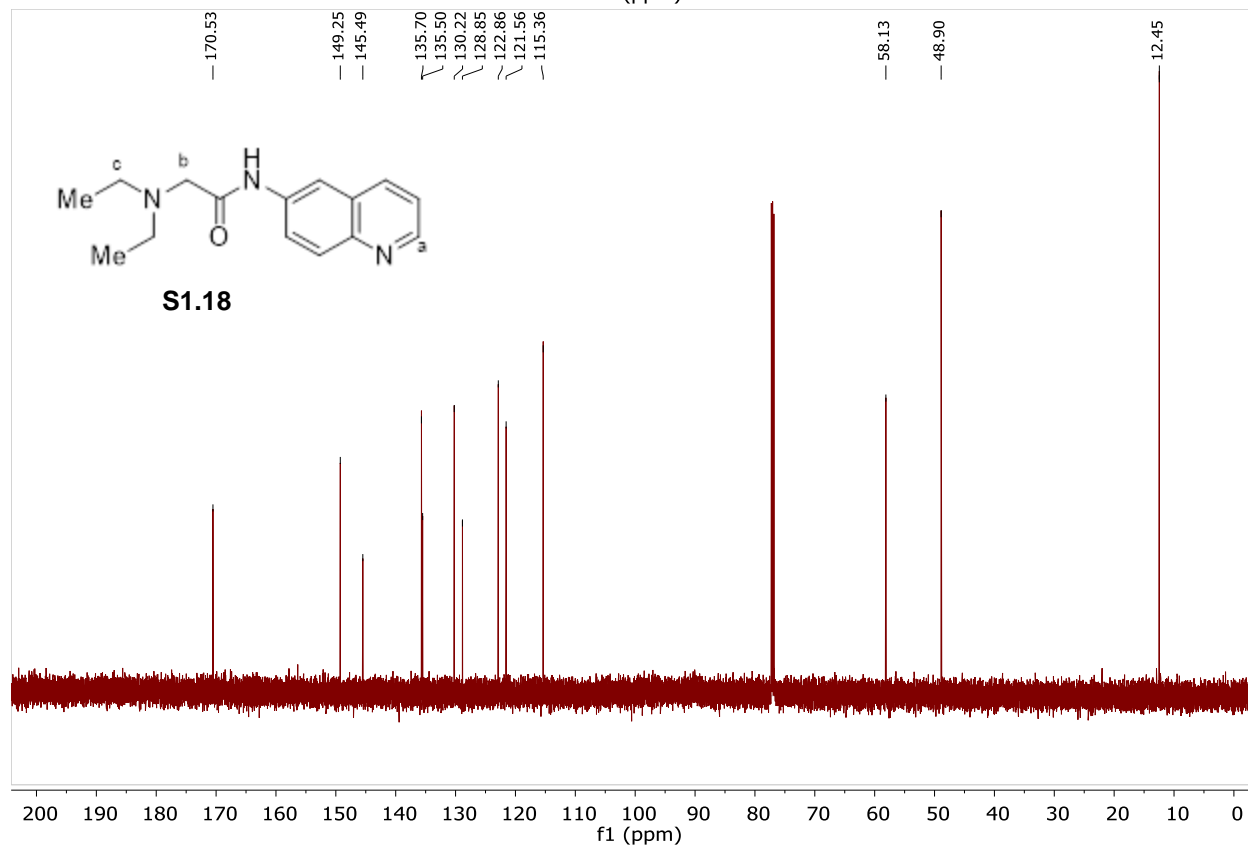
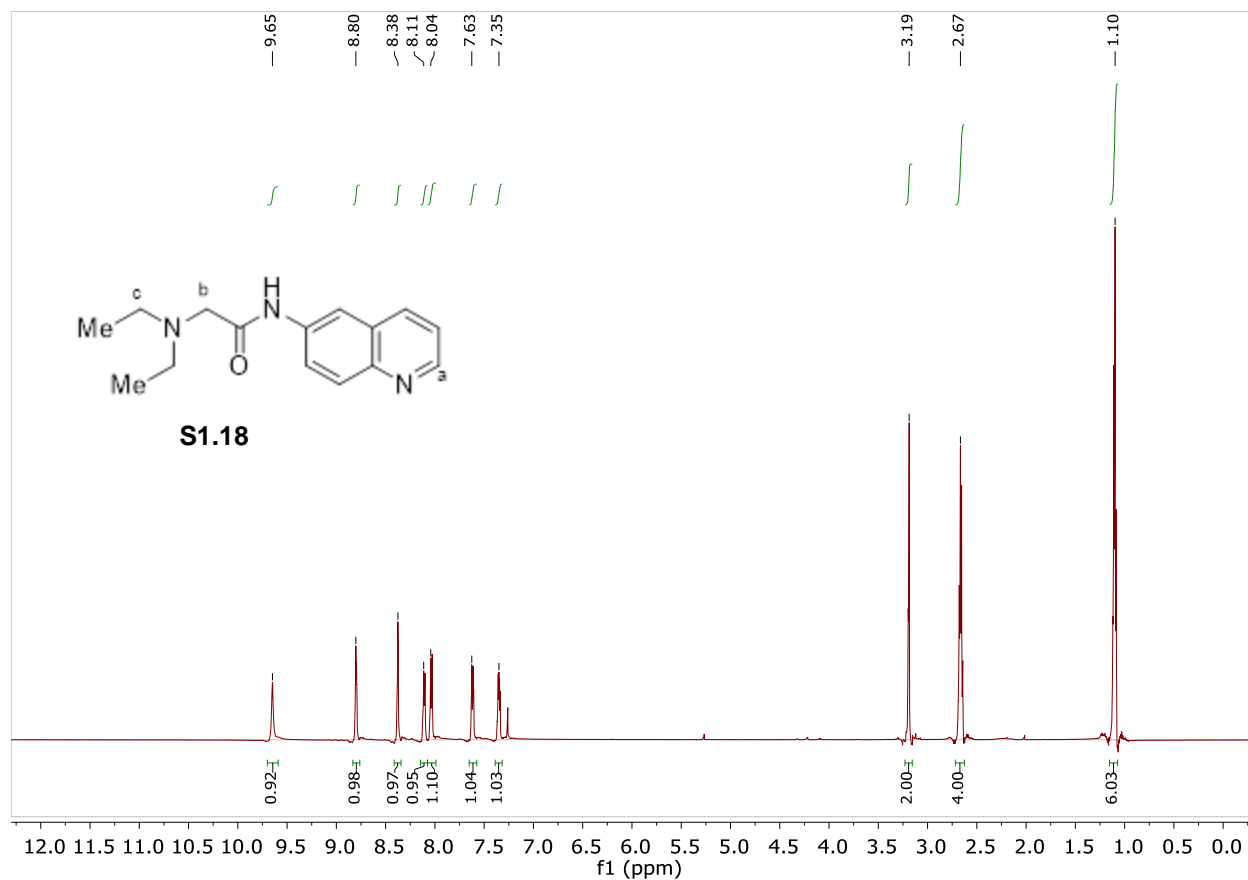
¹H NMR (600 MHz, CDCl₃) δ 9.65 (NH, s, 1H), 8.81 – 8.79 (H_a, m, 1H), 8.37 (ArH, t, J = 2.4 Hz, 1H), 8.11 (ArH, d, J = 8.3 Hz, 1H), 8.03 (ArH, d, J = 8.9 Hz, 1H), 7.62 (ArH, dt, J = 8.9, 2.4 Hz,

1H), 7.35 (ArH, dd, J = 8.3, 4.1 Hz, 1H), 3.19 (H_b, s, 2H), 2.66 (H_c, q, J = 7.1 Hz, 4H), 1.10 (Me, t, J = 7.1 Hz, 6H) ppm.

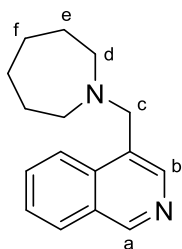
¹³C NMR (151 MHz, CDCl₃) δ 170.4, 149.2, 145.4, 135.6, 135.4, 130.1, 128.8, 122.8, 121.5, 115.3, 58.0, 48.8, 12.4 ppm.

IR (ATR) 3259.70, 2972.31, 2929.87, 2791.00, 1683.86, 1525.69, 1490.97, 1363.67, 1207.44, 1116.78, 877.61, 831.32, 792.74, 748.38, 611.43 cm⁻¹.

HRMS (ESI/QTOF) m/z: [M + H]⁺ Calcd for C₁₅H₂₀N₃O 258.1606; Found 258.1604



4-(azepan-1-ylmethyl)isoquinoline (S1.19)



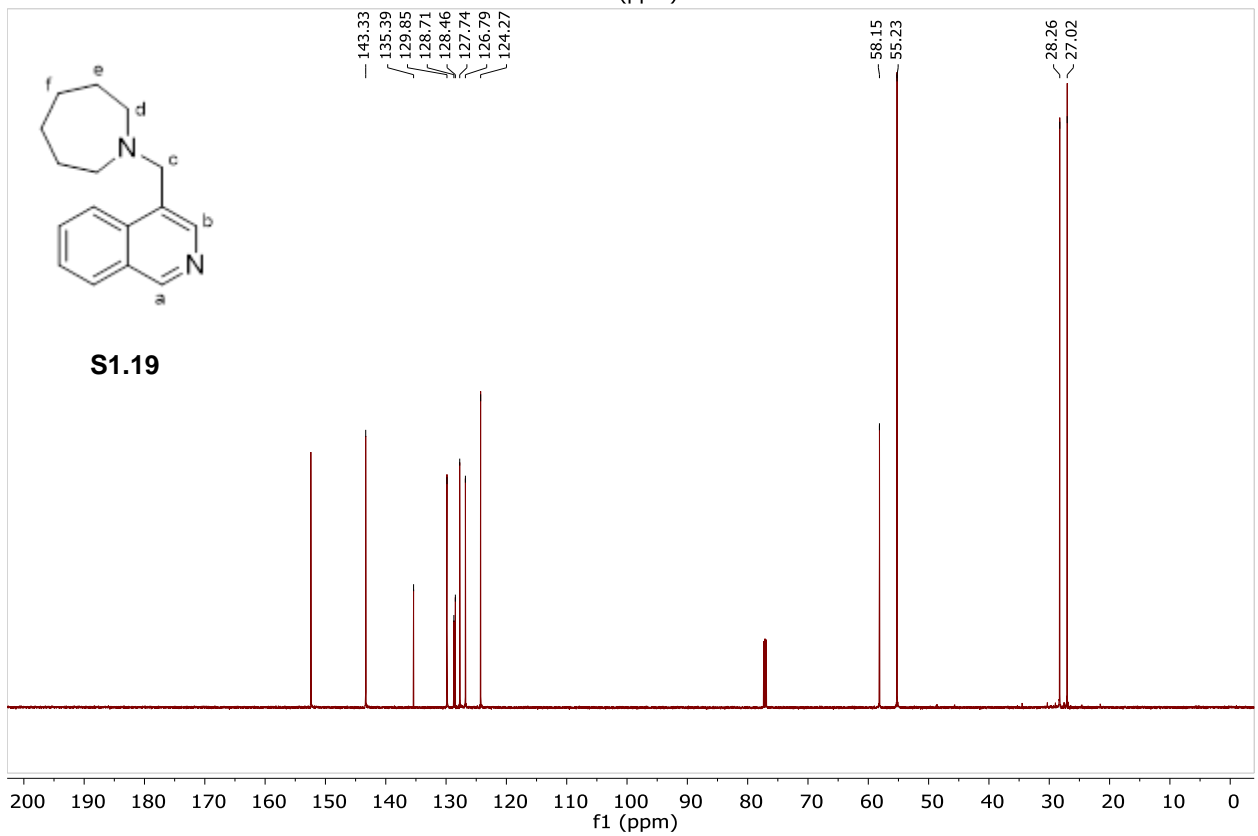
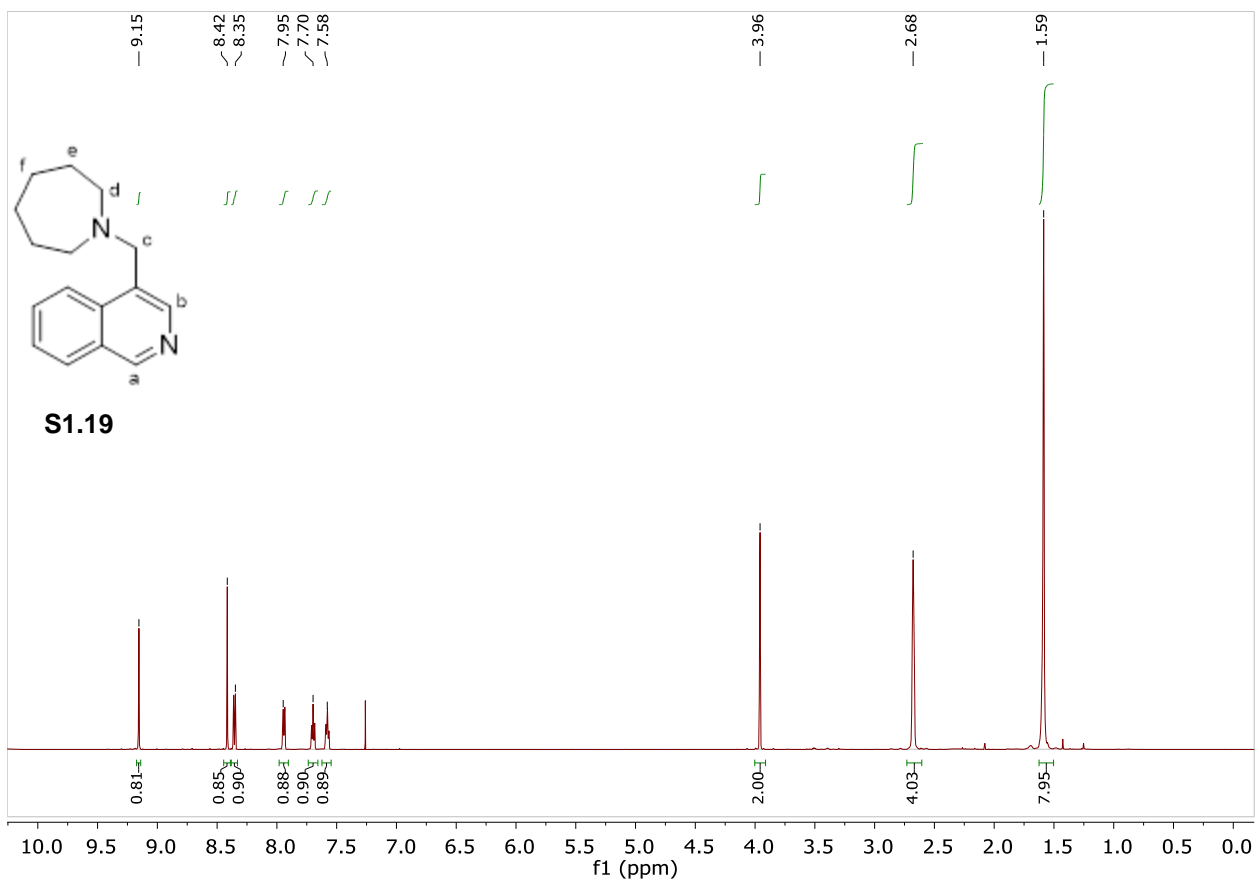
4-(azepan-1-ylmethyl)isoquinoline was synthesized using the general reductive amination procedure on scale with 2.0 mmol of aldehyde. The reaction mixture was purified after workup using alumina flash chromatography (60% Et₂O/hexanes) to give product as 0.330 g of orange oil (1.37 mmol, 69%)

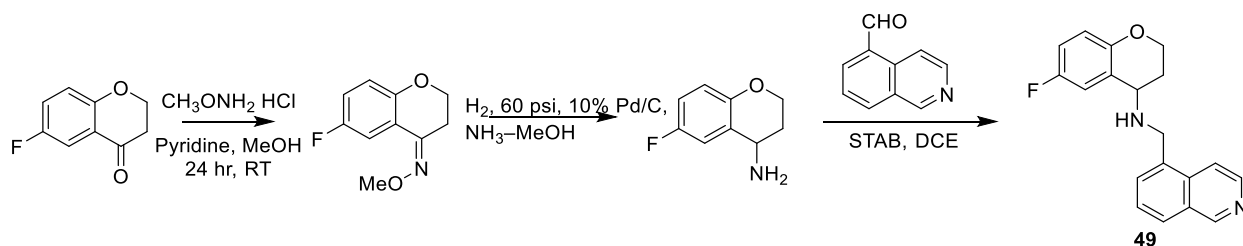
¹H NMR (600 MHz, CDCl₃) δ 9.15 (H_a, s, 1H), 8.42 (H_b, s, 1H), 8.35 (ArH, d, *J* = 7.6 Hz, 1H), 7.94 (ArH, d, *J* = 7.6 Hz, 1H), 7.70 (ArH, t, *J* = 7.6 Hz, 1H), 7.58 (t, *J* = 7.6 Hz, 1H), 3.96 (H_c, s, 2H), 2.68 (H_d, m, 4H), 1.59 (H_e and H_f, m, 8H) ppm.

¹³C NMR (151 MHz, CDCl₃) δ 152.4, 143.3, 135.4, 129.9, 128.7, 128.5, 127.7, 126.8, 124.3, 58.2, 55.2, 28.3, 27.0.

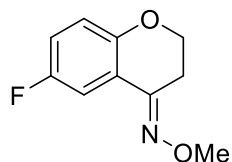
IR (ATR) 2922.16, 2850.79, 1622.13, 1583.56, 1500.62, 1450.47, 1355.96, 1220.94, 1147.65, 1078.21, 904.61, 887.26, 783.10, 748.38, 727.16, 626.87 cm⁻¹.

HRMS (ESI/QTOF) *m/z*: [M + H]⁺ Calcd for C₁₆H₂₁N₂ 241.1705; Found 241.1709





(-E)-6-fluorochroman-4-one O-methyl oxime (S1.20)



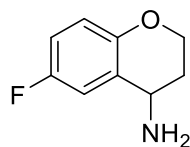
(-E)-6-fluorochroman-4-one O-methyl oxime was synthesized using 6-fluorochroman-4-one (0.253 g, 1.5 mmol), methoxyamine hydrochloride (0.124 g, 1.50 mmol), and pyridine (0.60 mL, 7.5 mmol). The reagents were combined together and allowed to stir for 24 hrs. The reaction mixture was reduced, 10 mL of 1M HCl was added, and the organic layer was extracted 3x with 10 mL DCM. The combined organics were dried with magnesium sulfate and reduced to give 0.219 g (1.12 mmol, 80% yield) of product.

¹H NMR (600 MHz, CDCl₃) δ 7.57 (dd, *J* = 9.4, 3.1 Hz, 1H), 6.95 (ddd, *J* = 9.1, 7.7, 3.1 Hz, 1H), 6.83 (dd, *J* = 9.0, 4.7 Hz, 1H), 4.18 (t, *J* = 6.2 Hz, 2H), 3.99 (s, 3H), 2.87 (t, *J* = 6.2 Hz, 2H) ppm.

¹³C NMR (201 MHz, CDCl₃) δ 157.5, 156.3, 150.4, 127.7, 117.8, 115.4, 114.4, 63.1, 45.4, 32.2 ppm.

HRMS (ESI/QTOF) *m/z*: [M + H]⁺ Calcd for C₁₀H₁₁NO₂F 196.0774; Found 196.0778.

6-fluorochroman-4-amine (S1.21)



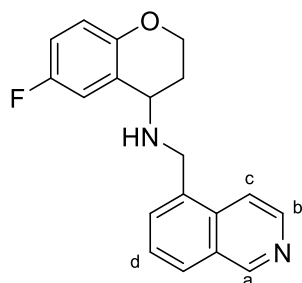
6-fluorochroman-4-amine was synthesized using (.E)-6-fluorochroman-4-one O-methyl oxime (0.822g, 4.21 mmol), 10% Pd/C (0.448g, 10 mol%), and MeOH-NH₂ (15 mL). The reagents were combined in a pressure reactor and pressurized with 60 psi H₂ for 48 hrs. Afterwards, the reaction mixture was filtered through celite, the filtrate was collected and reduced under pressure to give 0.326 g (1.95 mmol, 46% yield) of product.

¹H NMR (600 MHz, CDCl₃) δ 7.03 (dd, *J* = 9.1, 3.1 Hz, 1H), 6.86 – 6.82 (m, 1H), 6.76 – 6.73 (m, 1H), 4.25 (ddd, *J* = 11.3, 8.4, 2.9 Hz, 1H), 4.19 (ddd, *J* = 11.2, 6.9, 3.1 Hz, 1H), 4.01 (t, *J* = 5.6 Hz, 1H), 2.18 – 2.12 (m, 1H), 1.86 – 1.80 (m, 1H), 1.59 (s, 2H) ppm.

¹³C NMR (151 MHz, CDCl₃) δ 157.7, 156.1, 150.3, 117.7 (d, *J* = 7.7 Hz), 115.3 (d, *J* = 23.3 Hz), 114.5 (d, *J* = 22.8 Hz), 63.1, 45.3, 32.2 ppm.

HRMS (ESI/QTOF) *m/z*: [M + H]⁺ Calcd for C₉H₁₁NOF 168.0825; Found 168.0819.

6-fluoro-N-(isoquinolin-5-ylmethyl)chroman-4-amine (S1.22)³



6-fluoro-N-(isoquinolin-5-ylmethyl)chroman-4-amine was synthesized using the general reductive amination procedure on a 1.95 mmol scale relative to the aldehyde. The reaction mixture was purified after workup using alumina flash chromatography (1% MeOH/99%DCM to 2% MeOH/98%DCM) to give product as .354 g of thick orange oil (1.14 mmol, 59% yield).

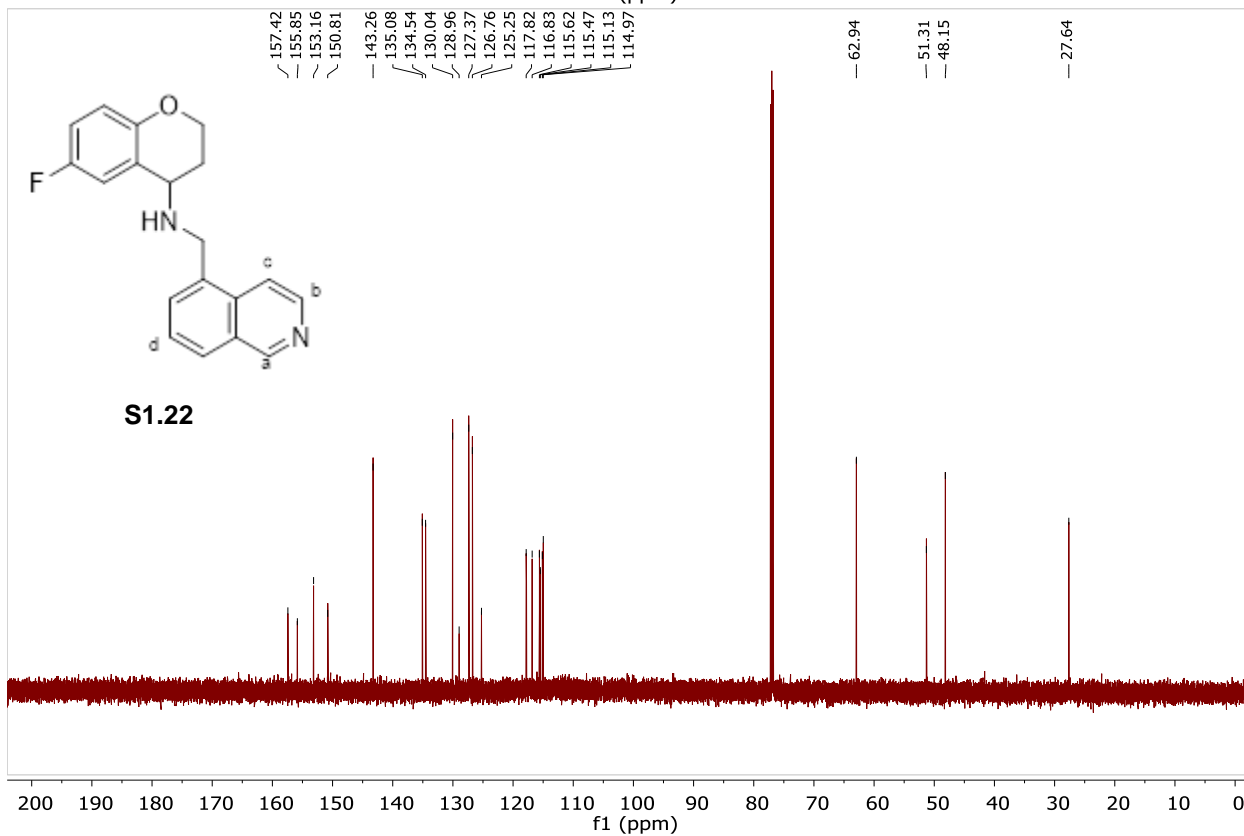
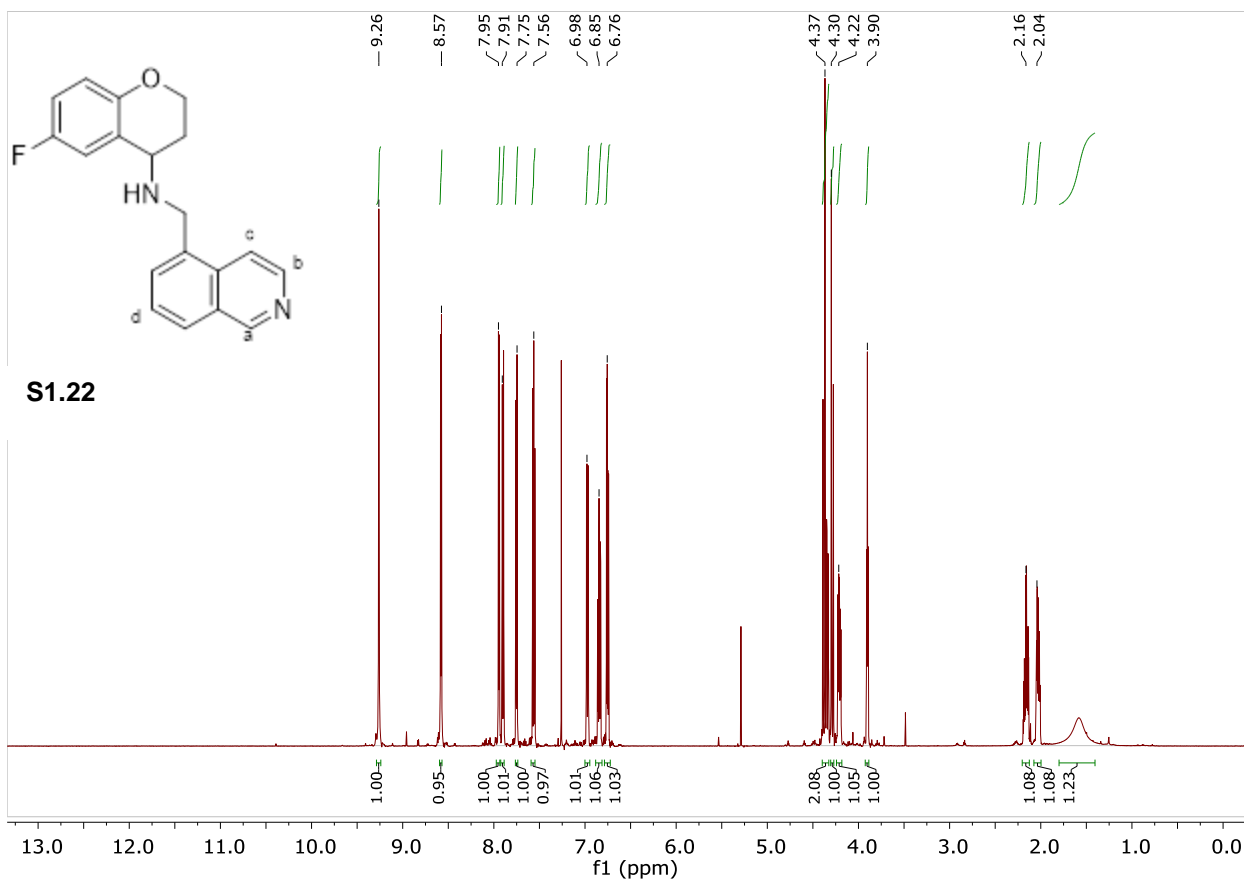
¹H NMR (600 MHz, CDCl₃) δ 9.26 (H_a, s, 1H), 8.58 (H_b, d, *J* = 6.0 Hz, 1H), 7.94 (H_c, d, *J* = 6.0 Hz, 1H), 7.90 (Ar_{isoquinoline}H, d, *J* = 8.2 Hz, 1H), 7.75 (Ar_{isoquinoline}H, d, *J* = 7.1 Hz, 1H), 7.56 (H_d, dd, *J* = 8.2, 7.1 Hz, 1H), 6.97 (ArH, dd, *J* = 9.0, 3.1 Hz, 1H), 6.84 (ArH, dd, *J* = 9.0, 8.0, 3.1 Hz,

1H), 6.75 (ArH, dd, J = 9.0, 4.8 Hz, 1H), 4.40 – 4.27 (m, 3H), 4.23 – 4.19 (m, 1H), 3.90 (t, J = 4.8 Hz, 1H), 2.20 – 2.12 (m, 1H), 2.07 – 2.01 (m, 1H) ppm.

¹³C NMR (151 MHz, CDCl₃) δ 157.4, 155.9, 153.2, 150.8, 143.3, 135.1, 134.6, 130.1, 129.0, 127.4, 126.8, 125.3, 117.8, 116.9, 115.6, 115.2, 62.9, 51.3, 48.2, 27.7 ppm.

IR (ATR) 1622.13, 1589.91, 1573.91, 1489.05, 1460.11, 1309.67, 1255.66, 873.75, 742.59, cm⁻¹.

HRMS (ESI/QTOF) m/z: [M + H]⁺ Calcd for C₁₉H₁₈N₂O 309.1403, found 309.1400

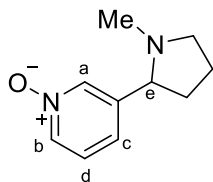


1.4 Oxidation Reactions

General Procedure A: Substrate (0.5 mmol 1 eq) was measured out into a 2 dram screw top vial equipped with a stir bar. Dichloromethane (2.5 mL) was added and the suspension was gently mixed. 1M H₂SO₄ (1 eq) was added, followed by HFIP. Iminium catalyst (0.030g, 20 mol%) was weighed out and then added to the mixture. Finally 50% H₂O₂ (2 eq) was added to vial. The reaction stirred for 16 hrs. Upon reaction completion, the reaction mixture was basified with 6M NaOH (10mL). Brine (10 mL) was added to salt out N-oxide product. The layers were separated, and extracted with 3x10 mL DCM. The resulting organic layers were combined and dried with magnesium sulfate, concentrated on a rotary evaporator, and purified by flash chromatography as noted.

General Procedure B: Substrate (0.5 mmol 1 eq) was measured out into a 2-dram screw top vial equipped with a stir bar. Dichloromethane (2.5 mL) was added and the suspension was gently mixed. 50% Tetrafluoroboric acid diethyl ether complex (1 eq) was added, followed by HFIP. Iminium catalyst (10 mol%) was weighed out and then added to the mixture. Finally, 50% H₂O₂ (2 eq) was added to vial. The reaction stirred for 16 hrs. Upon reaction completion, the reaction mixture was basified with 6M NaOH (10mL). Brine (10 mL) was added to salt out N-oxide product. The layers were separated, and extracted with 3x10 mL DCM. The resulting organic layers were combined and dried with magnesium sulfate, concentrated on a rotary evaporator, and purified by flash chromatography as noted.

3-(1-methylpyrrolidin-2-yl)pyridine 1-oxide 2.11



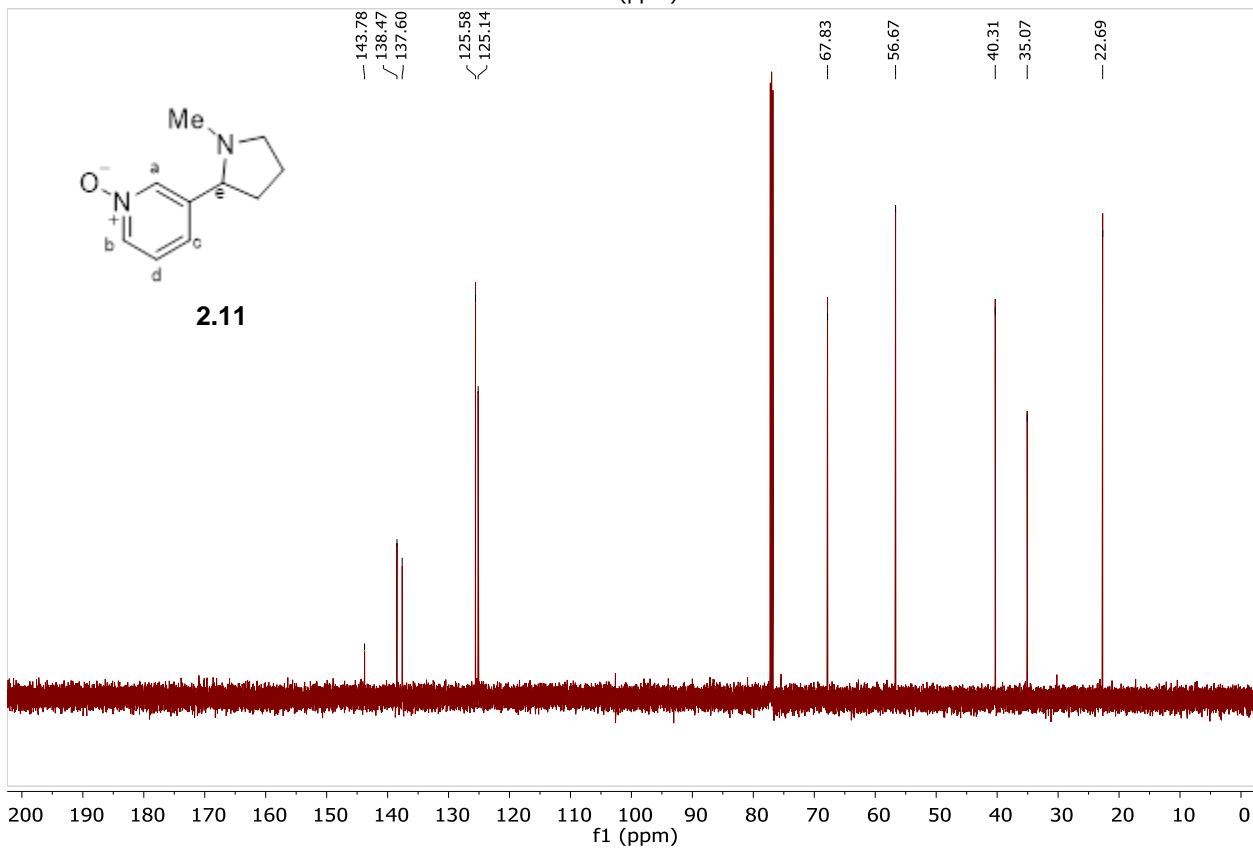
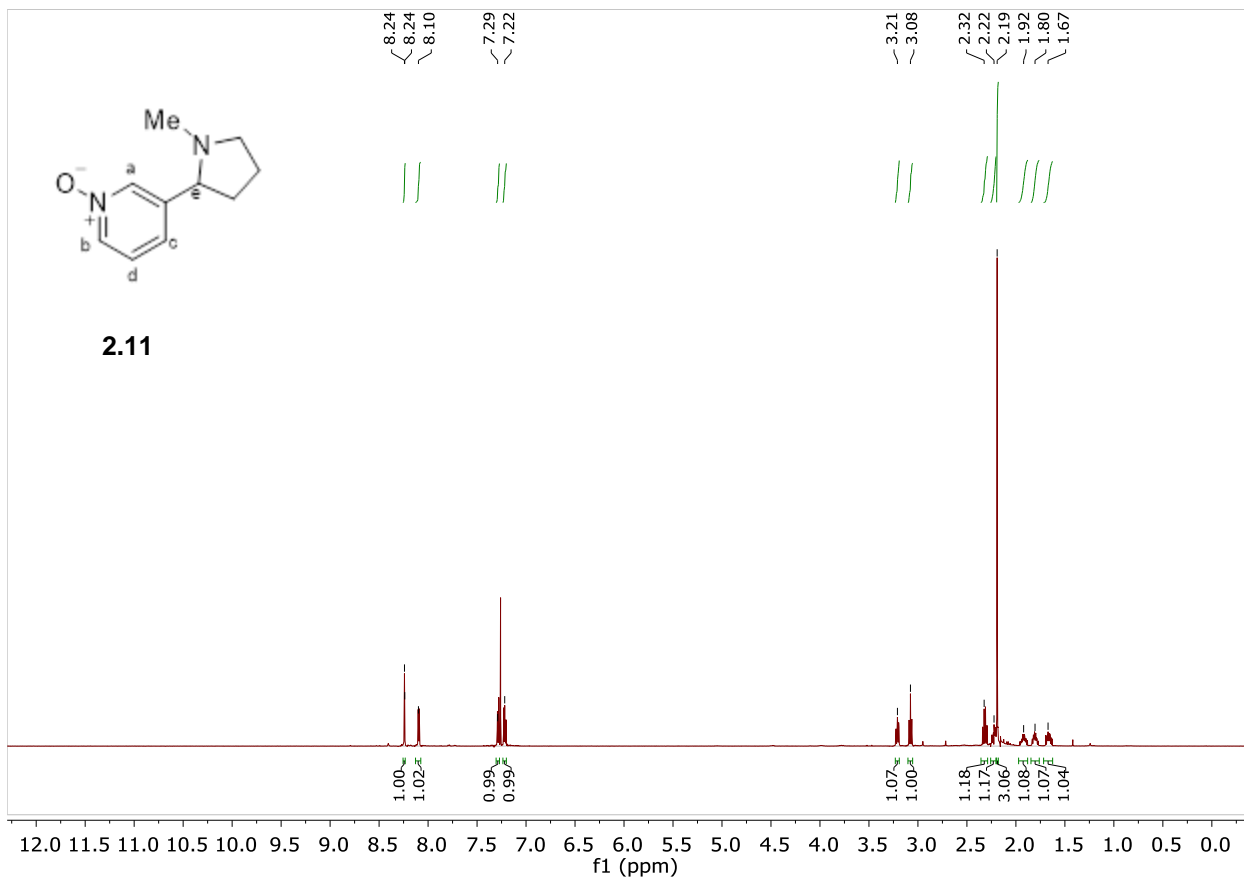
3-(1-methylpyrrolidin-2-yl)pyridine 1-oxide was synthesized using general procedure A. The reaction mixture was purified after workup using alumina flash chromatography (10% MeOH/Et₂O) to give product as 68.5 mg of clear oil (0.385 mmol, 77%)

¹H NMR (600 MHz, CDCl₃) δ 8.24 (H_a, s, 1H), 8.10 (H_b, d, *J* = 6.3 Hz, 1H), 7.29 (H_c, d, *J* = 8.0 Hz, 1H), 7.24 – 7.20 (H_d, m, 1H), 3.21 (H_e, dd, *J* = 9.7, 7.9 Hz, 1H), 3.08 (t, *J* = 8.2 Hz, 1H), 2.32 (ddd, *J* = 9.4, 8.2 Hz, 1H), 2.26 – 2.20 (m, 1H), 2.19 (Me, s, 3H), 1.96 – 1.88 (m, 1H), 1.85 – 1.76 (m, 1H), 1.70 – 1.63 (m, 1H) ppm.

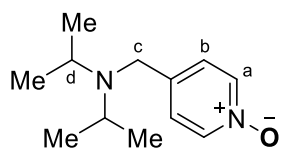
¹³C NMR (151 MHz, CDCl₃) δ 143.9, 137.7, 125.7, 125.3, 67.9, 56.8, 40.4, 35.2, 22.8 ppm.

IR (ATR) 2779.41, 1602.85, 1435.00, 1269.16, 1149.57, 1012.63, 794.67, 547.78, 486.06 cm⁻¹.

HRMS (ESI/QTOF) *m/z*: [M + H]⁺ Calcd for C₁₀H₁₅N₂O 179.1184, Found 179.1184.



4-((diisopropylamino)methyl)pyridine 1-oxide (2.21)



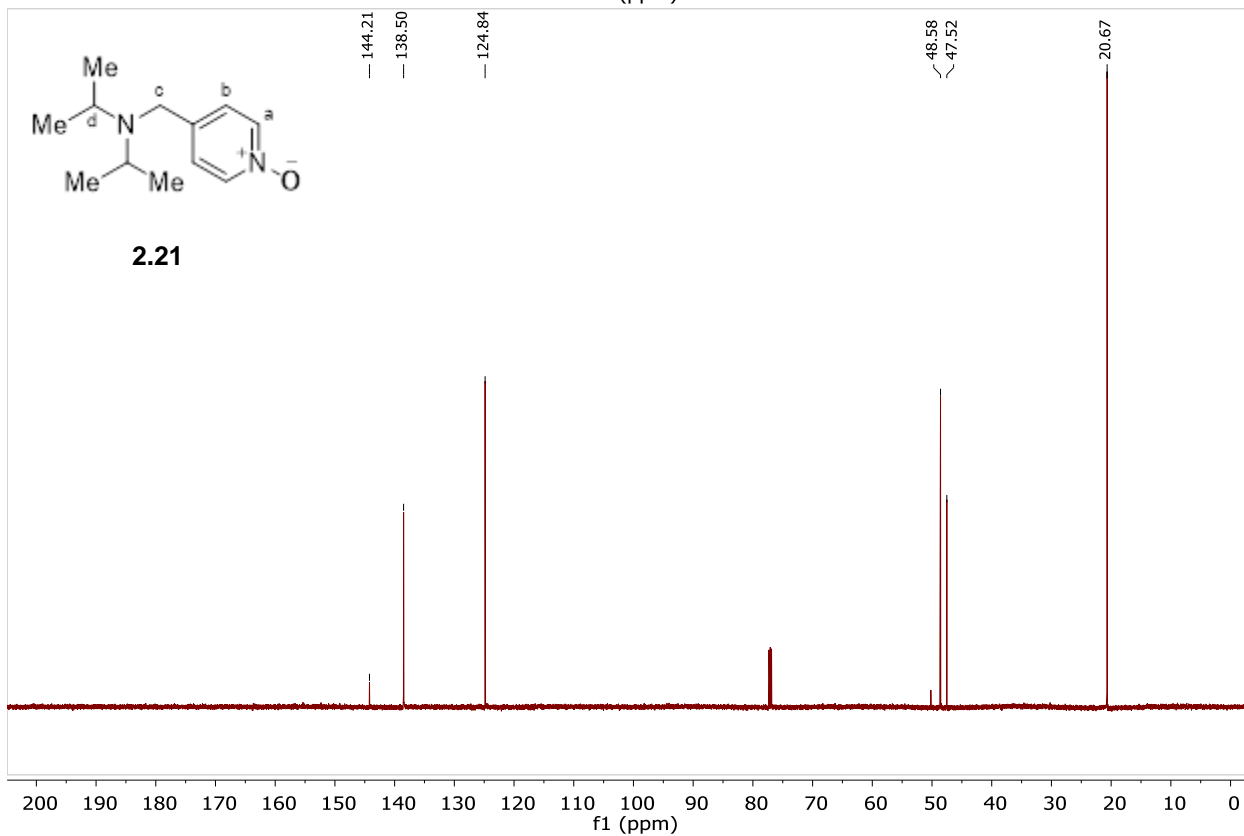
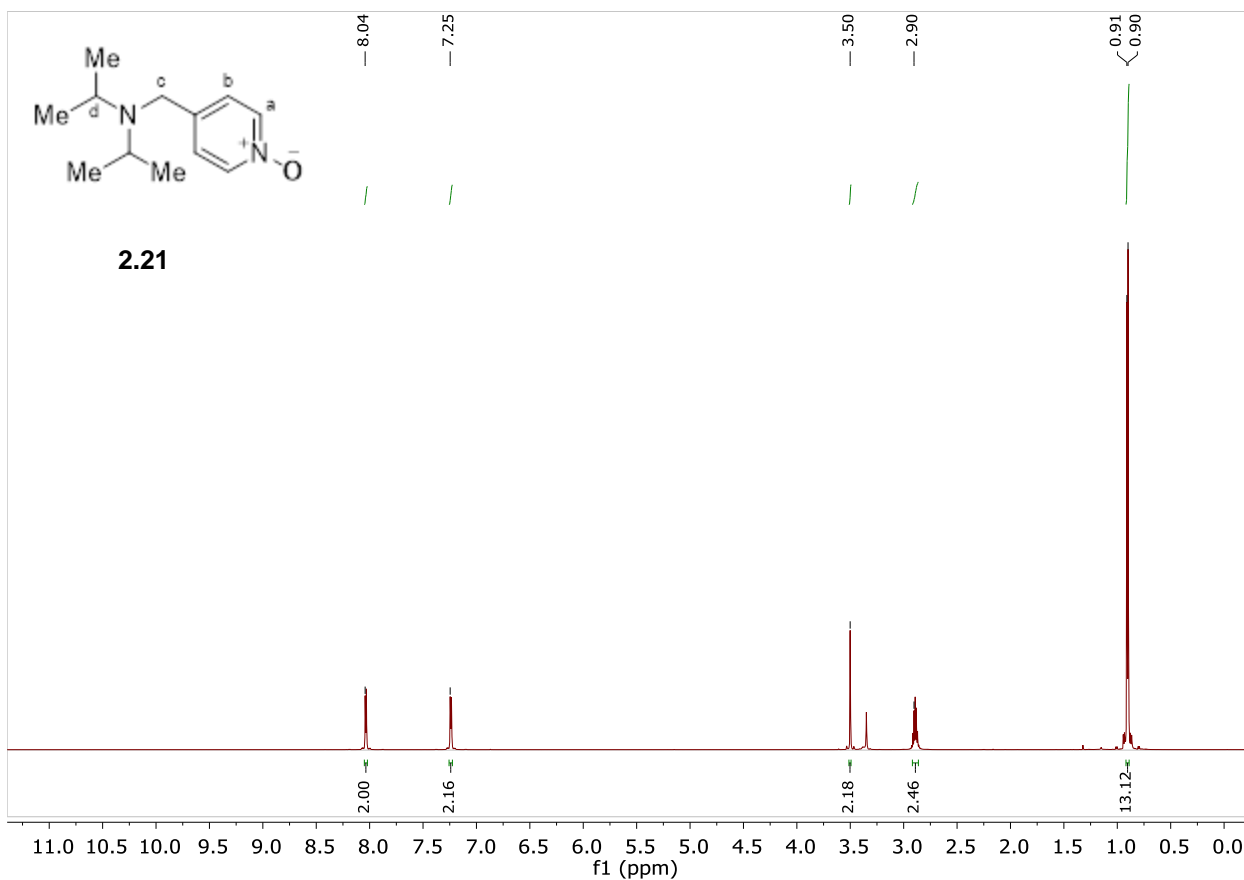
4-((diisopropylamino)methyl)pyridine 1-oxide was synthesized using general procedure A. The reaction mixture was purified after workup using alumina flash chromatography (10% to 40% MeOH/Et₂O) to give product as 64.0 mg of yellow oil (0.306 mmol 61% yield)

¹H NMR (600 MHz, CDCl₃): δ 8.04 (H_a, d, *J* = 6.9 Hz, 2H), 7.24 (H_b, d, *J* = 6.9 Hz, 2H), 3.50 (H_c, s, 2H), 2.89 (H_d, hept, *J* = 6.6 Hz, 2H), 0.90 (Me, d, *J* = 6.6 Hz, 6H) ppm.

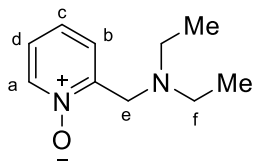
¹³C NMR (150 MHz, CDCl₃) δ 144.1, 138.4, 124.8, 48.5, 47.4, 20.6 ppm.

IR (ATR) 1489.05, 1381.03, 1361.74, 1242.16, 1203.58, 1174.65, 947.05, 831.32, 790.81⁻¹.

HRMS (ESI/QTOF) *m/z*: [M + H]⁺ Calcd for C₁₂H₂₁N₂O 209.1654, found 209.1652



2-((diethylamino)methyl)pyridine 1-oxide (2.22)



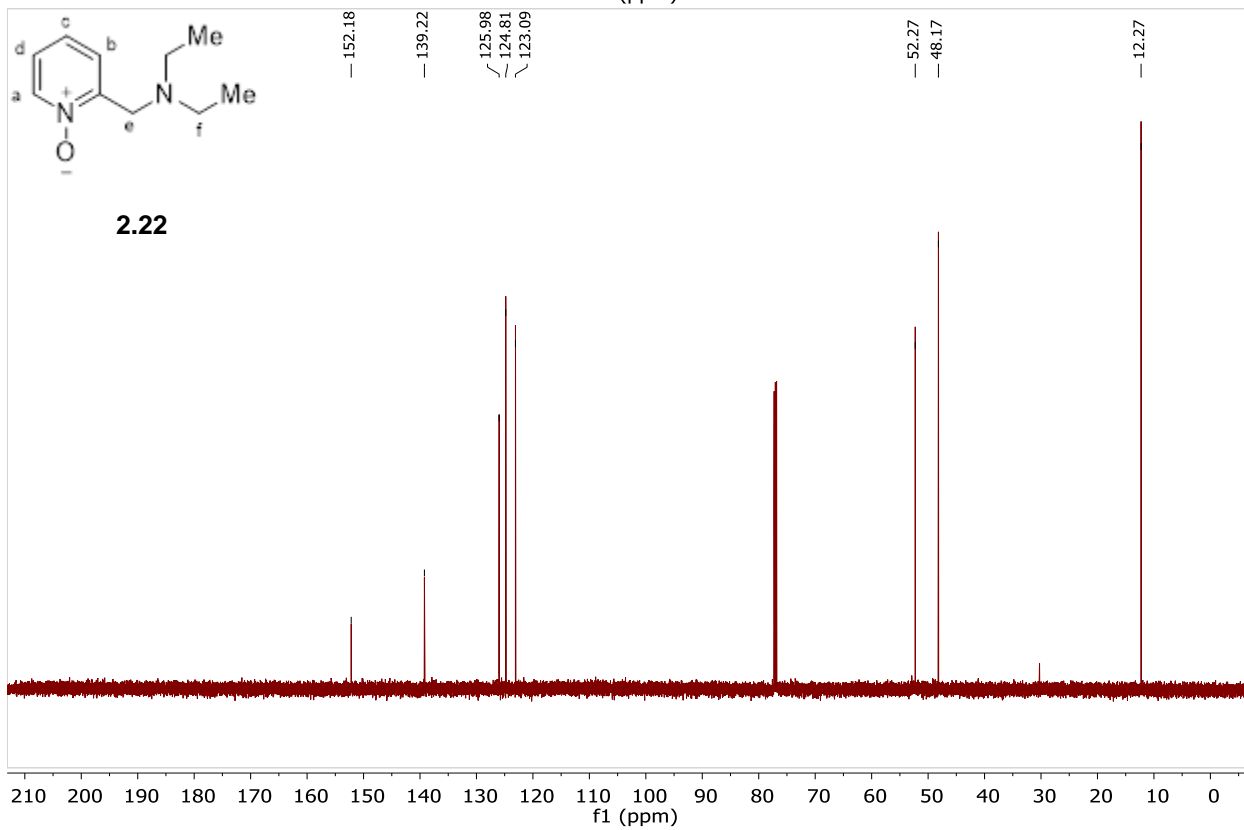
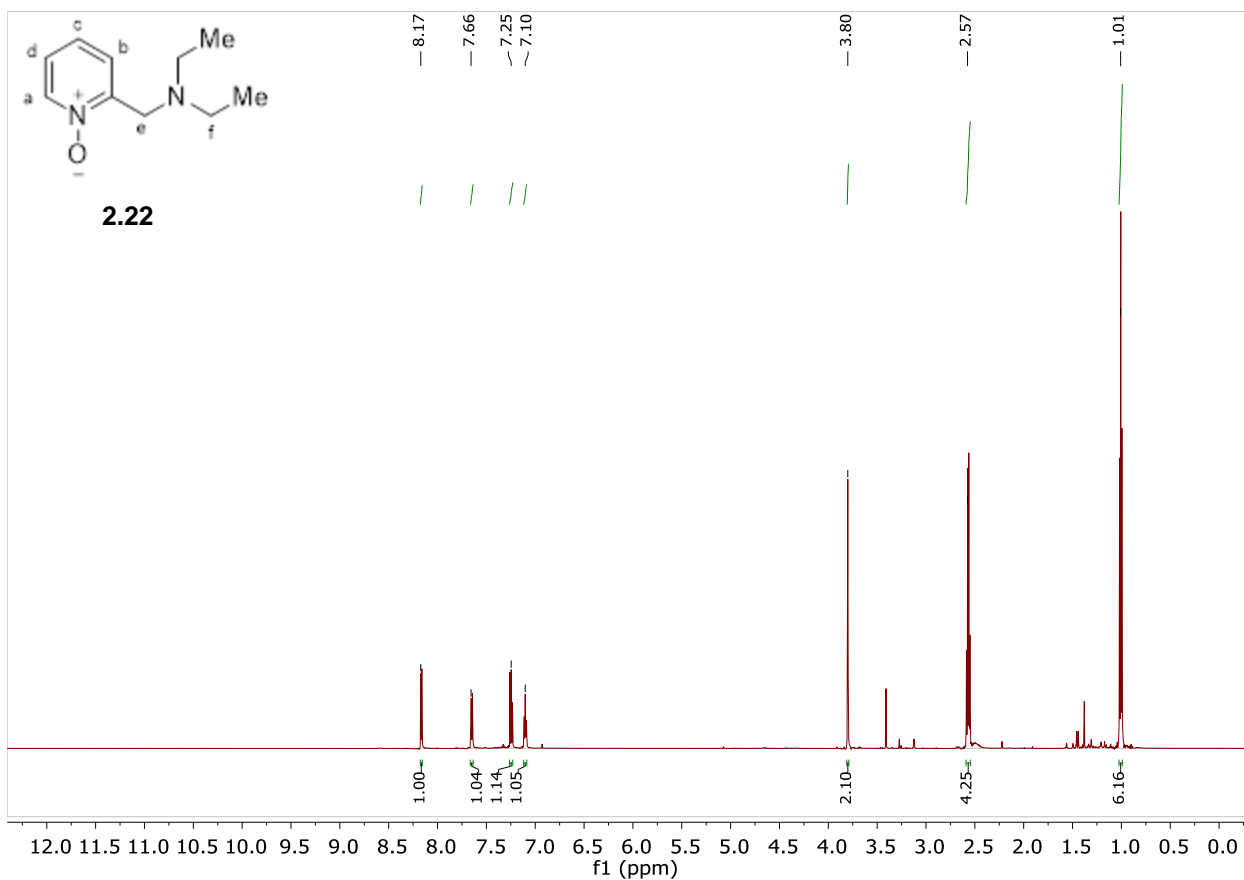
2-((diethylamino)methyl)pyridine 1-oxide was synthesized using general procedure A. The reaction mixture was purified after workup using alumina flash chromatography (10% MeOH/Et₂O) to give product as 37.0 mg of yellow oil (0.206 mmol, 41%)

¹H NMR (600 MHz, CDCl₃): δ 8.17 (H_a, d, *J* = 6.4 Hz, 1H), 7.65 (H_b, d, *J* = 7.8 Hz, 1H), 7.24 (H_c, t, *J* = 7.8 Hz, 1H), 7.10 (H_d, t, *J* = 6.4 Hz, 1H), 3.80 (H_e, s, 2H), 2.57 (H_f, q, *J* = 7.1 Hz, 4H), ppm
1.01 (Me, t, *J* = 7.1 Hz, 6H) ppm.

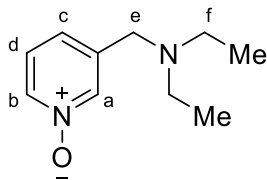
¹³C NMR (150 MHz, CDCl₃) δ 152.1, 139.1, 125.9, 124.8, 123.0, 52.2, 48.1, 12.2 ppm.

IR (ATR) 2968.45, 2810.28, 1487.12, 1431.18, 1228.66, 1186.22, 852.54, 767.67 cm⁻¹.

HRMS (ESI/QTOF) *m/z*: [M + H]⁺ Calcd for C₁₀H₁₇N₂O 181.1341, found 181.1344



3-((diethylamino)methyl)pyridine 1-oxide (2.23)



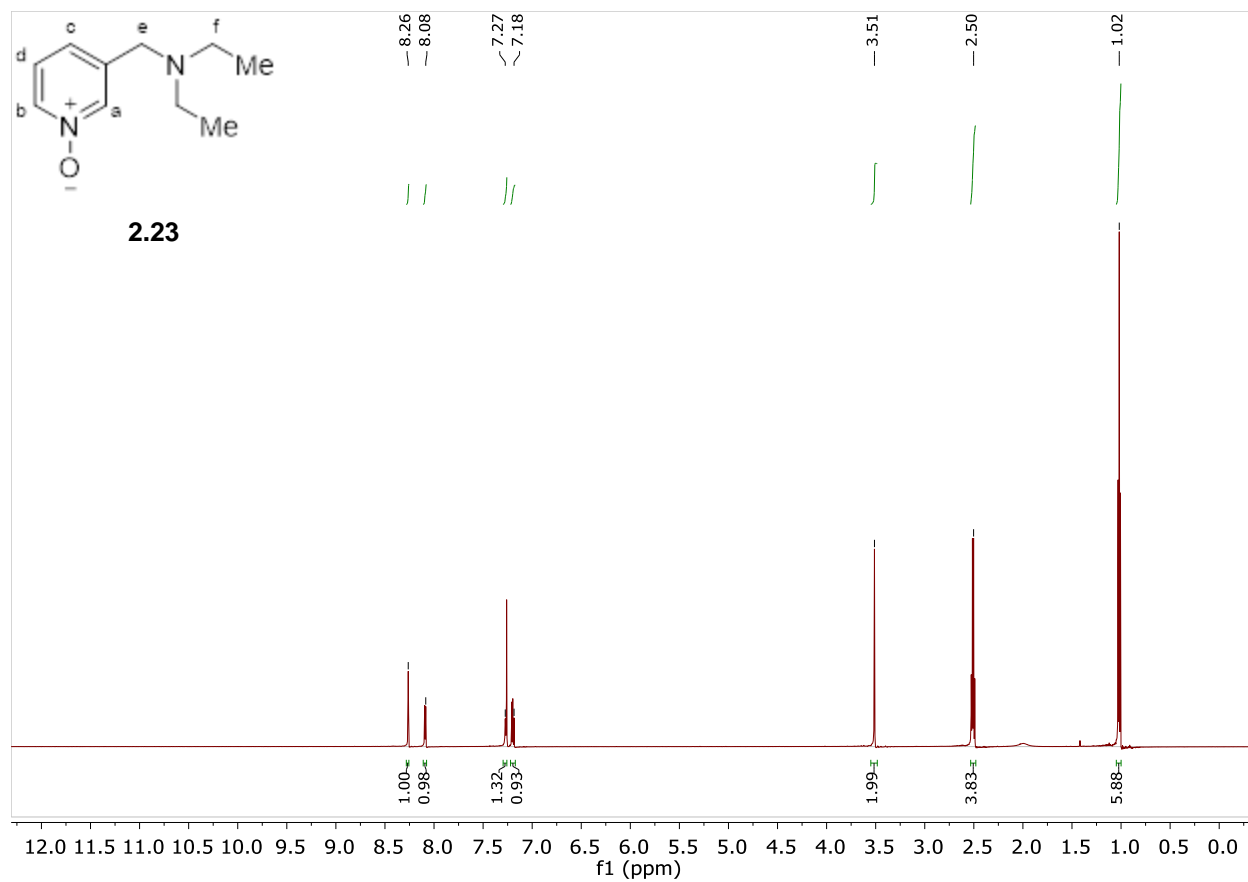
3-((diethylamino)methyl)pyridine 1-oxide was synthesized using general procedure A. The reaction mixture was purified after workup using alumina flash chromatography (10% MeOH/Et₂O) to give product as 60.0 mg of an oil (0.331 mmol, 66% yield)

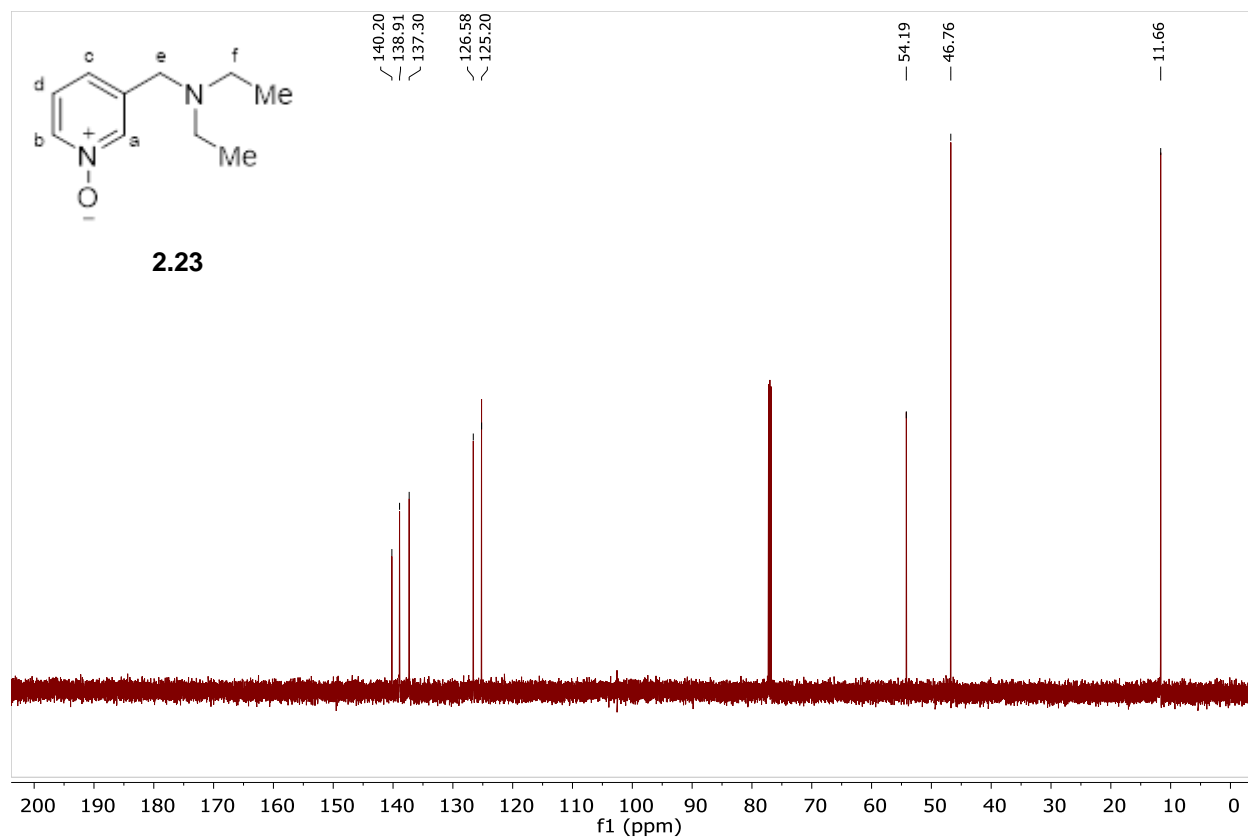
¹H NMR (600 MHz, CDCl₃): δ 8.27 – 8.26 (H_a, s, 1H), 8.09 (H_b, d, J = 6.5 Hz, 1H), 7.27 (H_c, d, J = 8.1 Hz, 1H), 7.20 (H_d, dd, J = 8.1, 6.5 Hz, 1H), 3.51 (H_e, s, 2H), 2.51 (H_f, q, J = 7.1 Hz, 4H), 1.02 (Me, t, J = 7.1 Hz, 6H) ppm.

¹³C NMR (150 MHz, CDCl₃): δ 140.2, 138.9, 137.3, 126.6, 125.2, 54.2, 46.8, 11.7 ppm.

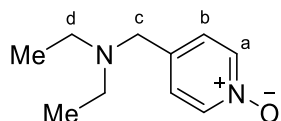
IR (ATR) 2804.50, 1602.85, 1431.19, 1273.02, 1147.65, 1012.63, 792.74, 759.95, 678.84 cm⁻¹.

HRMS (ESI/QTOF) m/z: [M + H]⁺ Calcd for C₁₀H₁₇N₂O 181.1341, found 181.1346





4-((diethylamino)methyl)pyridine 1-oxide (2.24)



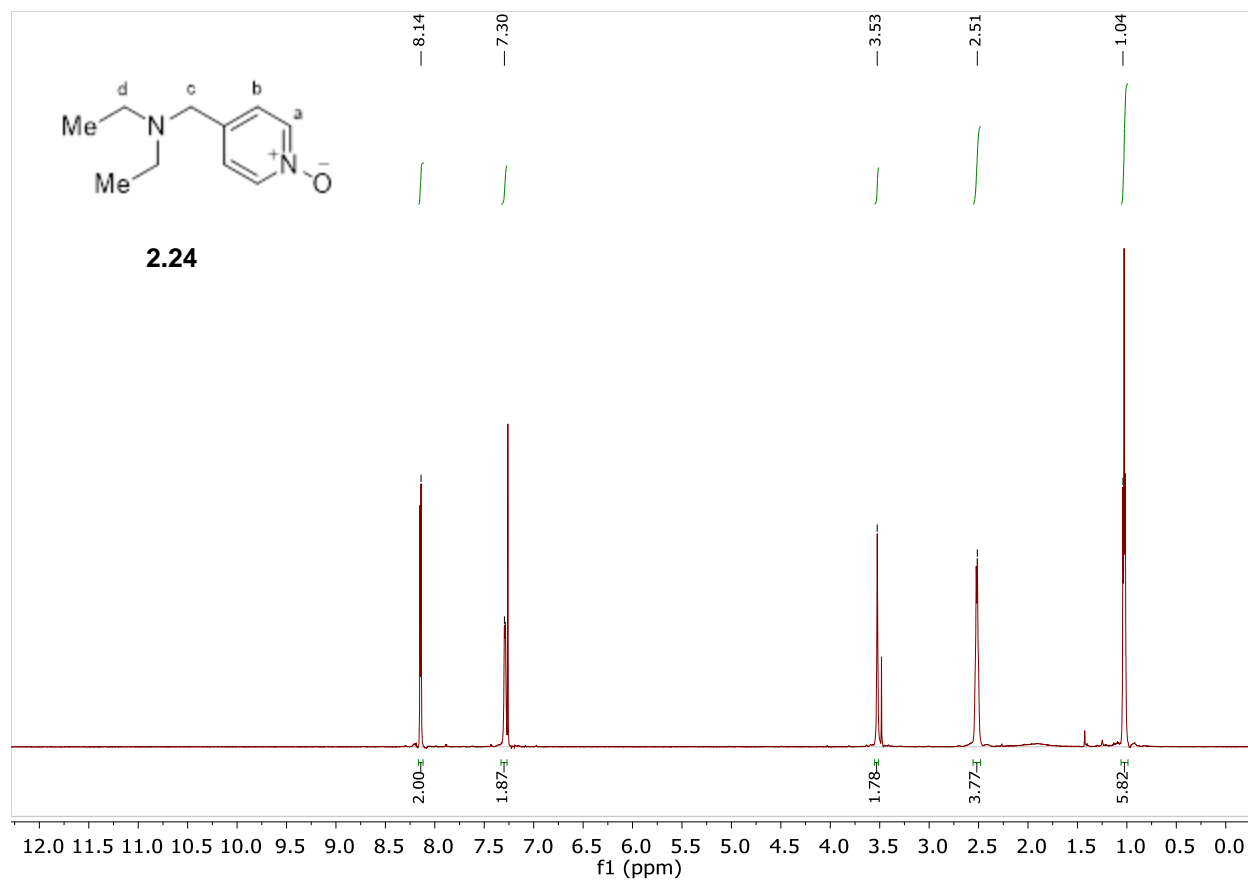
4-((diethylamino)methyl)pyridine 1-oxide was synthesized using general procedure A. The reaction mixture was purified after workup using alumina flash chromatography (10% to 20% to 30% MeOH/Et₂O) to give product as 70.0 mg of orange/yellow oil (0.387 mmol 77% yield)

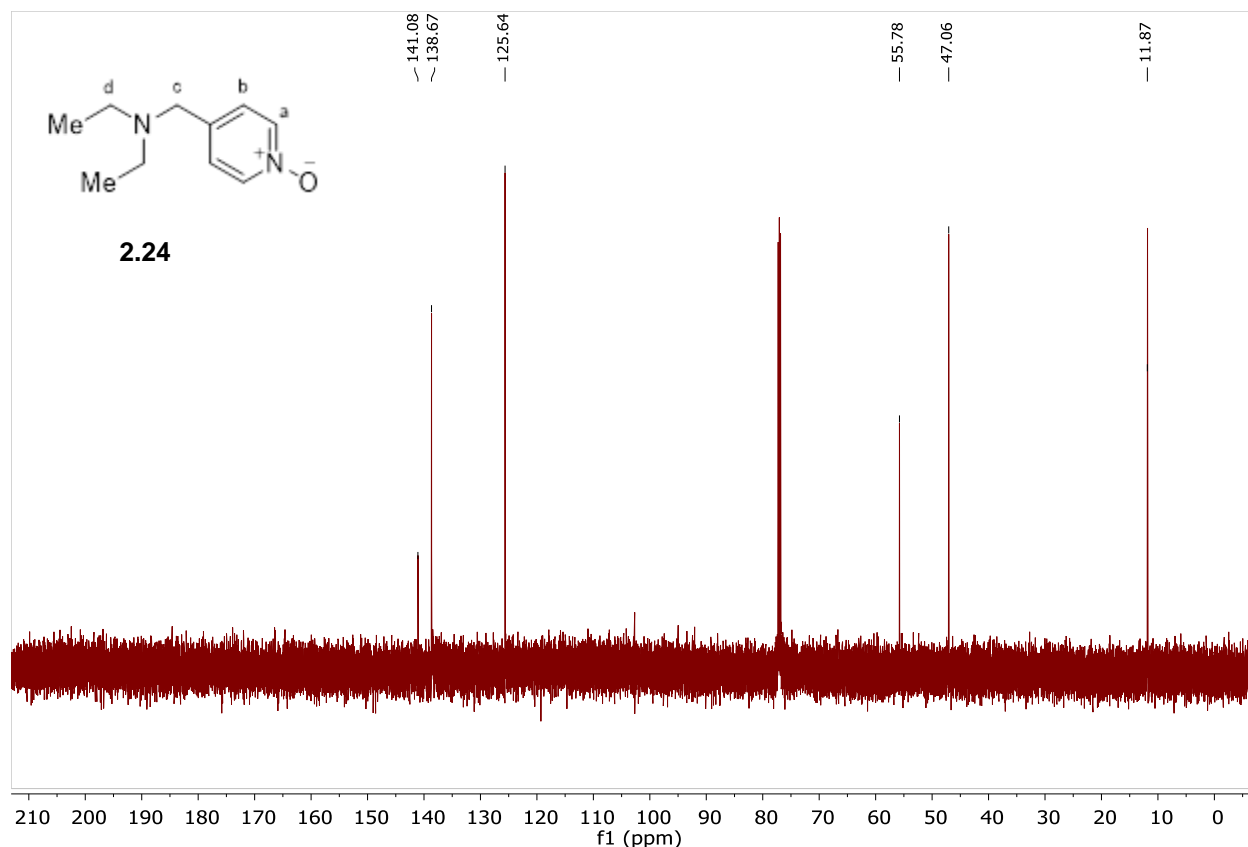
¹H NMR (600 MHz, CDCl₃): 8.15 (H_a, d, J = 6.5 Hz, 2H), 7.29 (H_b, d, J = 6.5 Hz, 2H), 3.52 (H_c, s, 2H), 2.52 (H_d, q, J = 7.1 Hz, 4H), 1.03 (Me, t, J = 7.1 Hz, 6H) δ ppm.

¹³C NMR (150 MHz, CDCl₃) 141.1, 138.7, 125.6, 55.8, 47.1, 11.9 δ ppm.

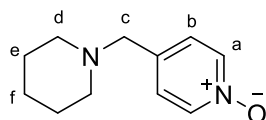
IR (ATR) 1483.26, 1232.51 1170.79, 786.96, cm⁻¹.

HRMS (ESI/QTOF) m/z: [M + H]⁺ Calcd for C₁₀H₁₇N₂O 181.1341, found 181.1344





4-(piperidin-1-ylmethyl)pyridine 1-oxide (2.25)



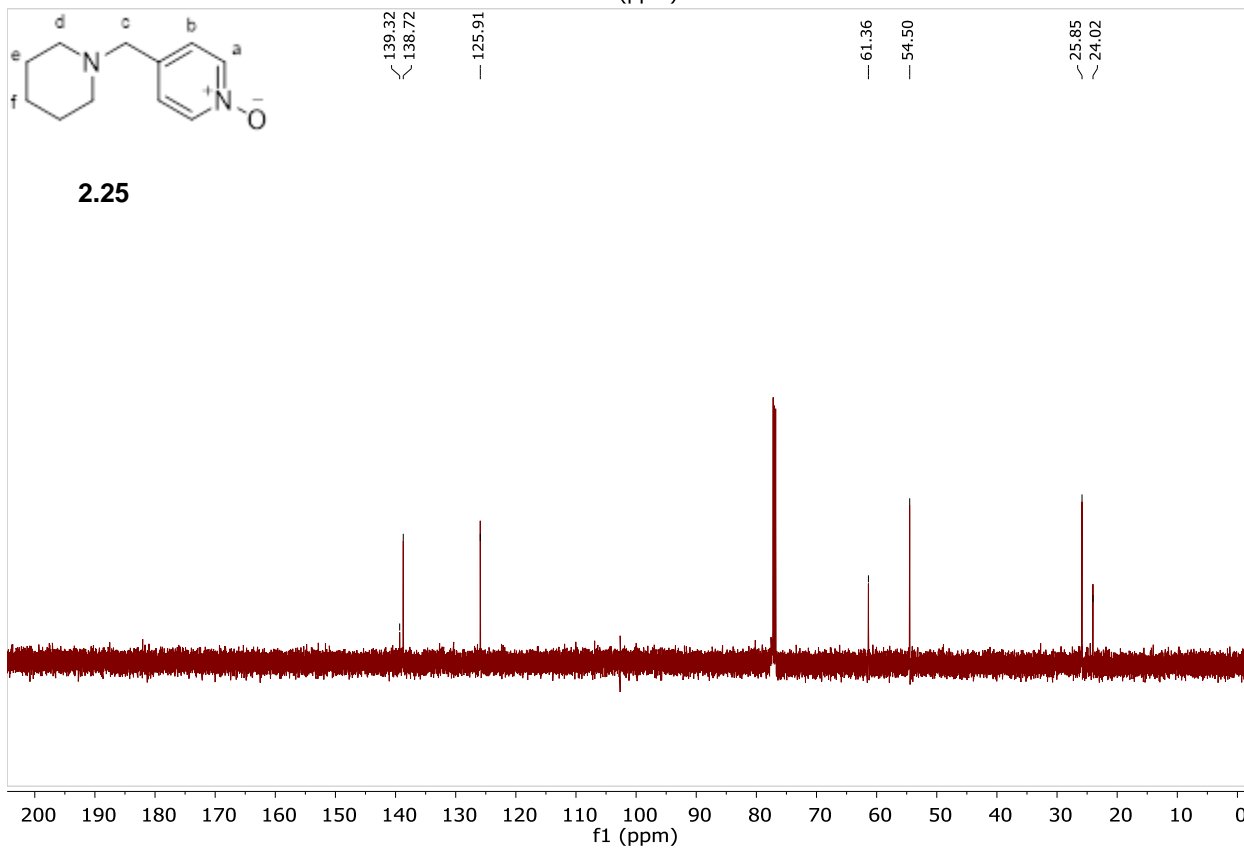
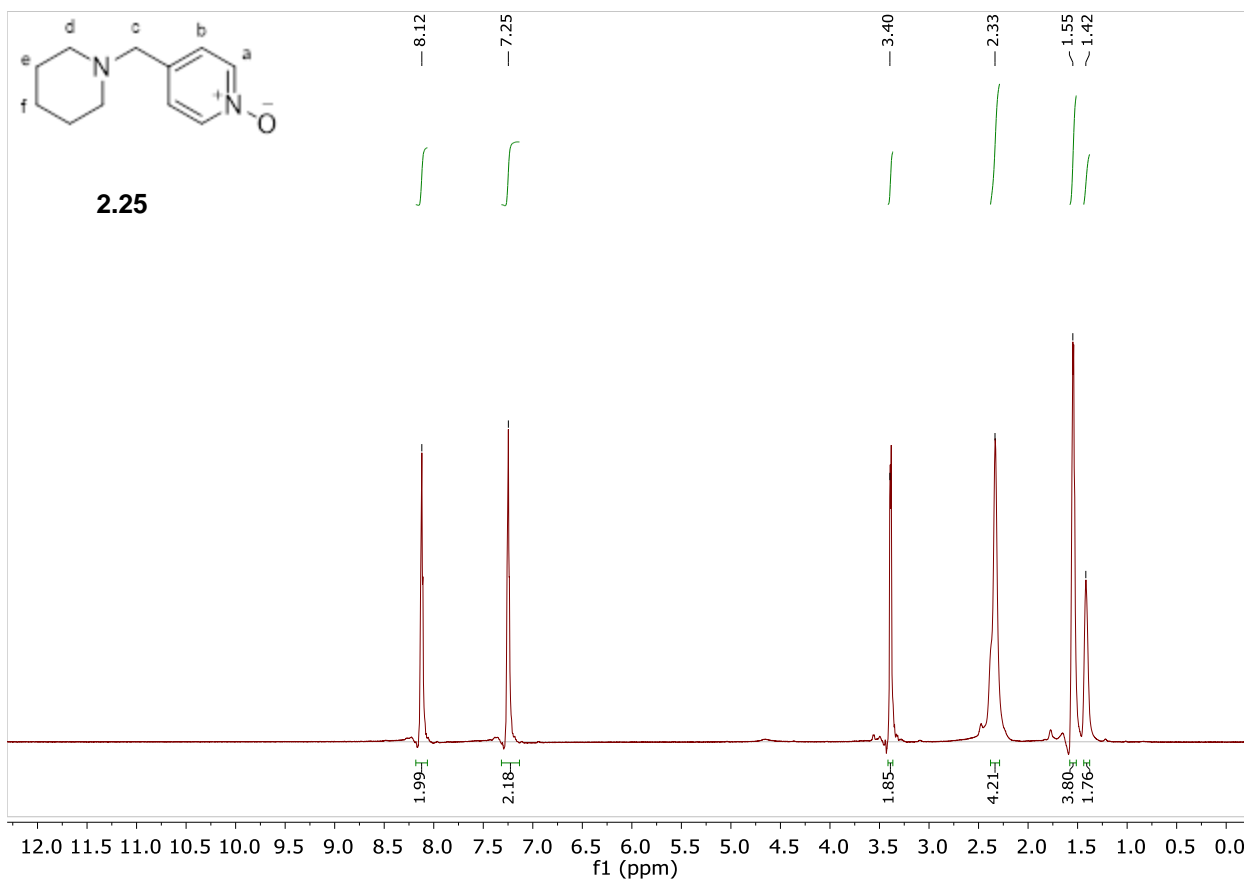
4-(piperidin-1-ylmethyl)pyridine 1-oxide was synthesized using general procedure A. The reaction mixture was purified after workup using alumina flash chromatography (10% MeOH/Et₂O) to give product as 60.0 mg of yellow oil (0.314 mmol, 62% yield)

¹H NMR (600 MHz, CDCl₃): δ 8.15 – 8.09 (H_a, m, 2H), 7.28 – 7.23 (H_b, m, 2H), 3.39 (H_c, s, 1H), 2.39 – 2.31 (H_d, m, 4H), 1.58 – 1.51 (H_e, m, 4H), 1.45 – 1.37 (H_f, m, 2H) ppm.

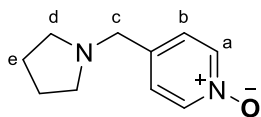
¹³C NMR (150 MHz, CDCl₃) δ 139.4, 138.8, 125.9, 61.4, 54.5, 25.9, 24.1. ppm.

IR (ATR) 1483.26, 1446.61, 1234.44, 1172.72, 1037.00, 783.10 cm⁻¹.

HRMS (ESI/QTOF) m/z: [M + H]⁺ Calcd for C₁₁H₁₇N₂O 193.1341; found 193.1343



4-(pyrrolidin-1-ylmethyl)pyridine 1-oxide (2.26)



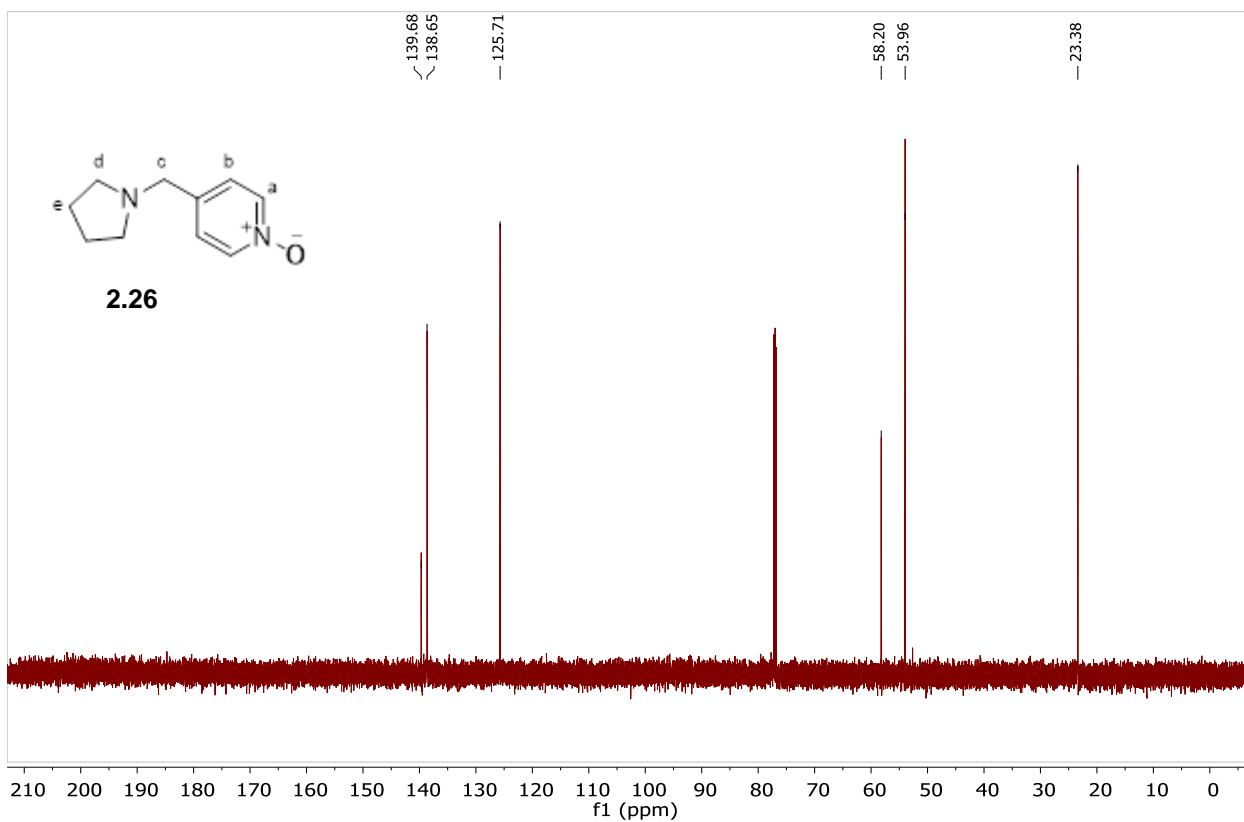
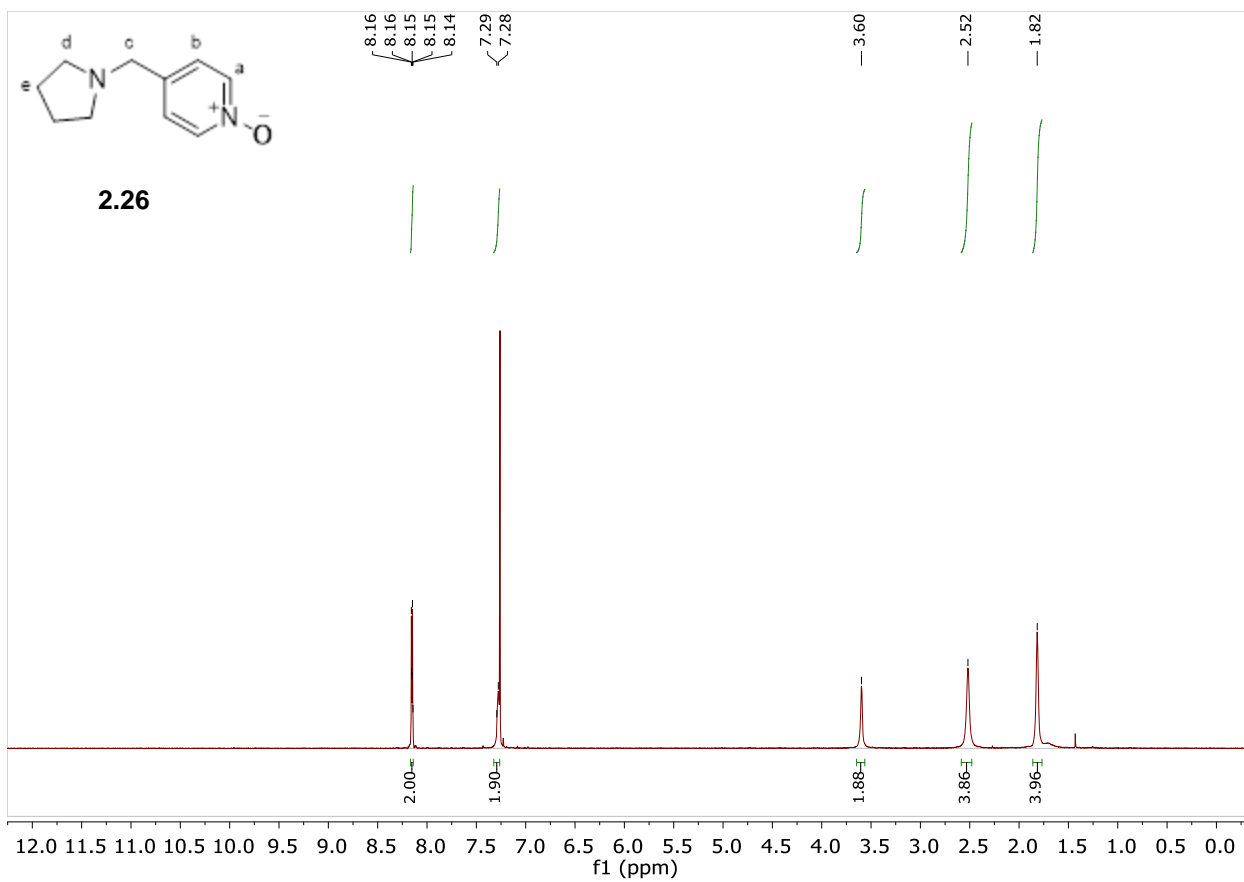
4-(pyrrolidin-1-ylmethyl)pyridine 1-oxide was synthesized using general procedure A. The reaction mixture was purified after workup using alumina flash chromatography (10% to 40% MeOH/Et₂O) to give product as 48.2 mg of yellow oil (0.271 mmol, 54% yield)

¹H NMR (600 MHz, CDCl₃): δ 8.13 (H_a, d, *J* = 6.5 Hz, 2H), 7.26 (H_b, d, *J* = 6.5 Hz, 2H), 3.57 (H_c, s, 3H), 2.51 – 2.47 (H_e, m, 4H), 1.80 – 1.76 (H_f, m, 4H) ppm.

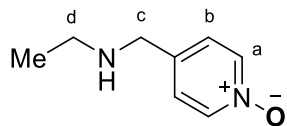
¹³C NMR (150 MHz, CDCl₃) δ 139.8, 138.8, 125.8, 58.3, 54.1, 23.5 ppm.

IR (ATR) 2789.07, 1481.33, 1446.61, 1246.02, 1168.86, 1033.85, 786.96 cm⁻¹.

HRMS (ESI/QTOF) *m/z*: [M + H]⁺ Calcd for C₁₀H₁₅N₂O 179.1184, found 179. 1188.



4-((ethylamino)methyl)pyridine 1-oxide (2.27)



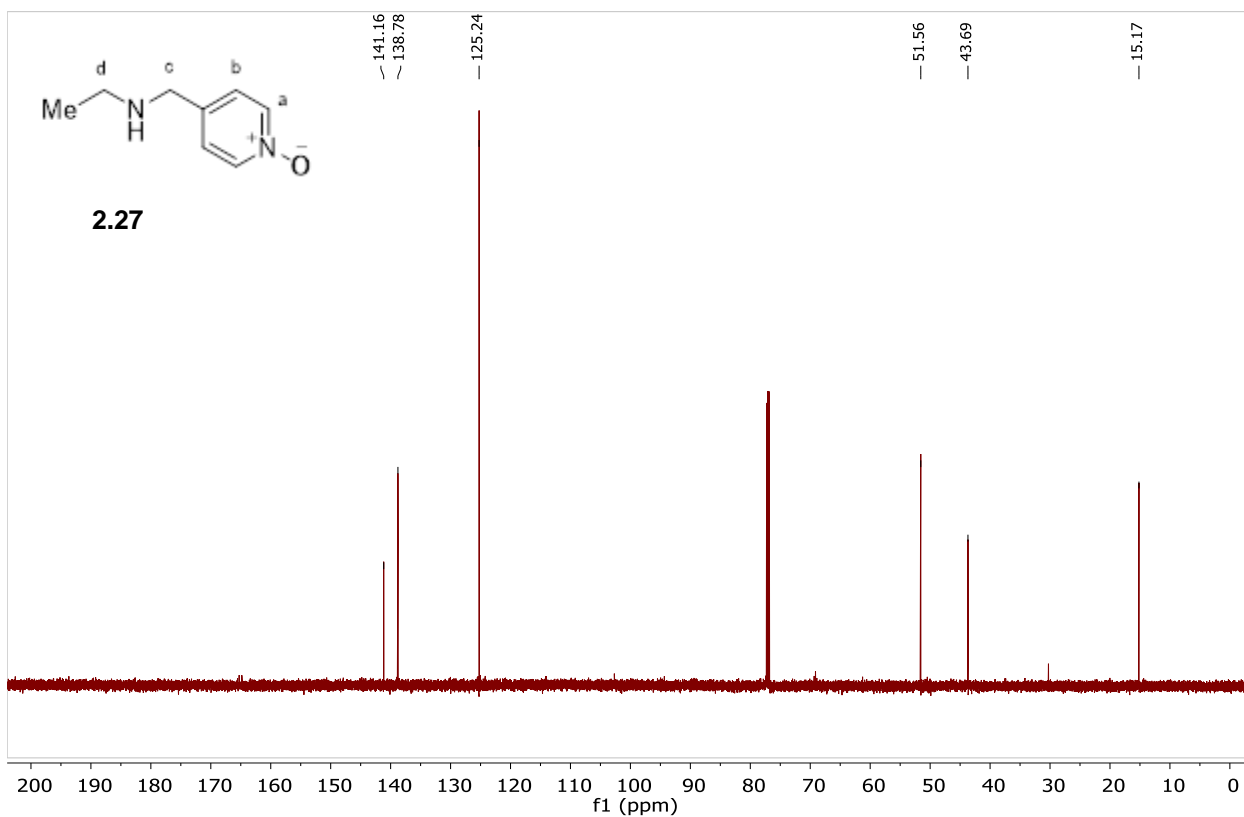
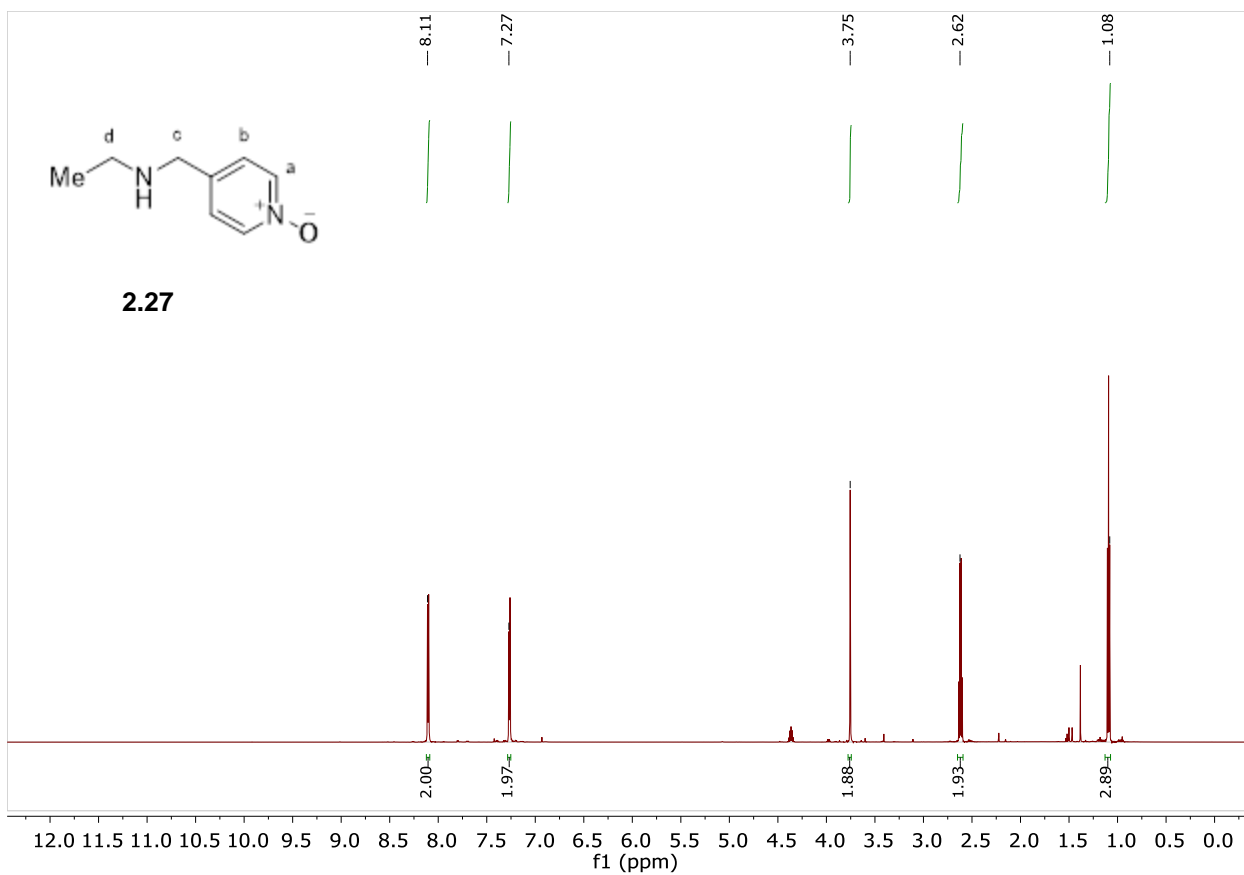
4-((ethylamino)methyl)pyridine 1-oxide was synthesized using general procedure A. The reaction mixture was purified after workup using alumina flash chromatography (10% to 20% MeOH/Et₂O) to give product as 61.3 mg of clear oil (0.403 mmol, 80% yield)

¹H NMR (600 MHz, CDCl₃) δ 8.11 (H_a, d, *J* = 7.0 Hz, 2H), 7.27 (H_b, d, *J* = 7.0 Hz, 2H), 3.76 (H_c, s, 2H), 2.62 (H_d, q, *J* = 7.1 Hz, 2H), 1.09 (Me, t, *J* = 7.1 Hz, 3H) ppm.

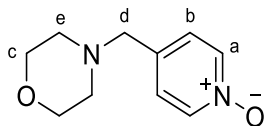
¹³C NMR (151 MHz, CDCl₃) δ 141.1, 138.7, 125.2, 51.5, 43.6, 15.1 ppm.

IR (ATR) 2966.52, 1483.26, 1284.59, 1176.55, 1099.34, 840.96 cm⁻¹.

HRMS (ESI/QTOF) *m/z*: [M + H]⁺ Calcd for C₈H₁₃N₂O 153.1028; Found 153.1033.



4-(morpholinomethyl)pyridine 1-oxide (2.29)

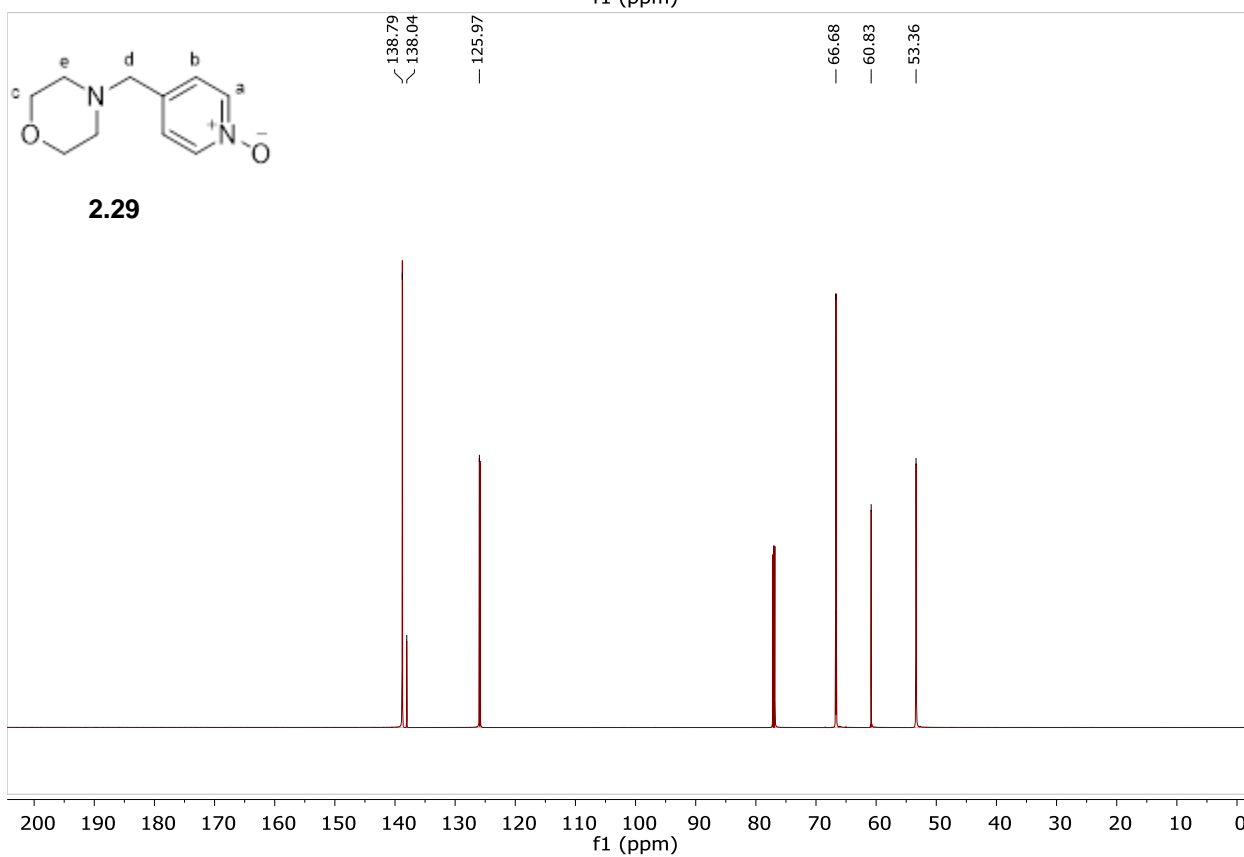
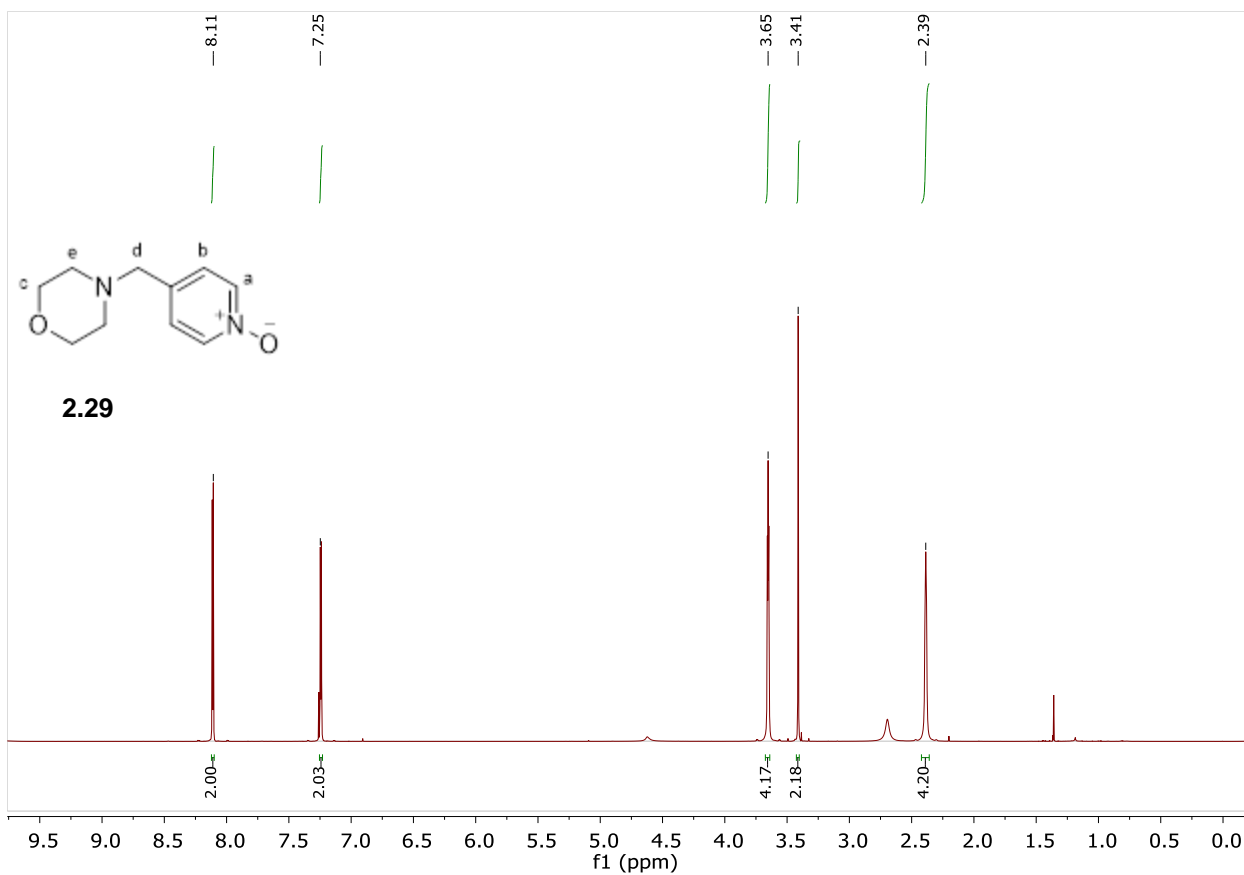


4-(morpholinomethyl)pyridine 1-oxide was synthesized using the general procedure. The reaction mixture was purified after workup using alumina flash chromatography (10% to 30% MeOH/Et₂O) to give product as 33.1 mg of white oil (0.206 mmol, 34% yield).

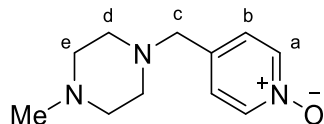
¹H NMR (600 MHz, CDCl₃): δ 8.11 (H_a, d, *J* = 7.0 Hz, 2H), 7.25 (H_b, d, *J* = 7.0 Hz, 2H), 3.65 (H_c, t, *J* = 4.5 Hz, 4H), 3.41 (H_d, s, 2H), 2.39 (H_e, t, *J* = 4.5 Hz, 4H) ppm.

¹³C NMR (150 MHz, CDCl₃) δ 138.8, 138.0, 126.0, 66.7, 60.8, 53.4 ppm.

HRMS (ESI/QTOF) *m/z*: [M + H]⁺ Calcd for C₁₀H₁₅N₂O₂ 195.1134, found 195.1131



4-((4-methylpiperazin-1-yl)methyl)pyridine 1-oxide (2.30)



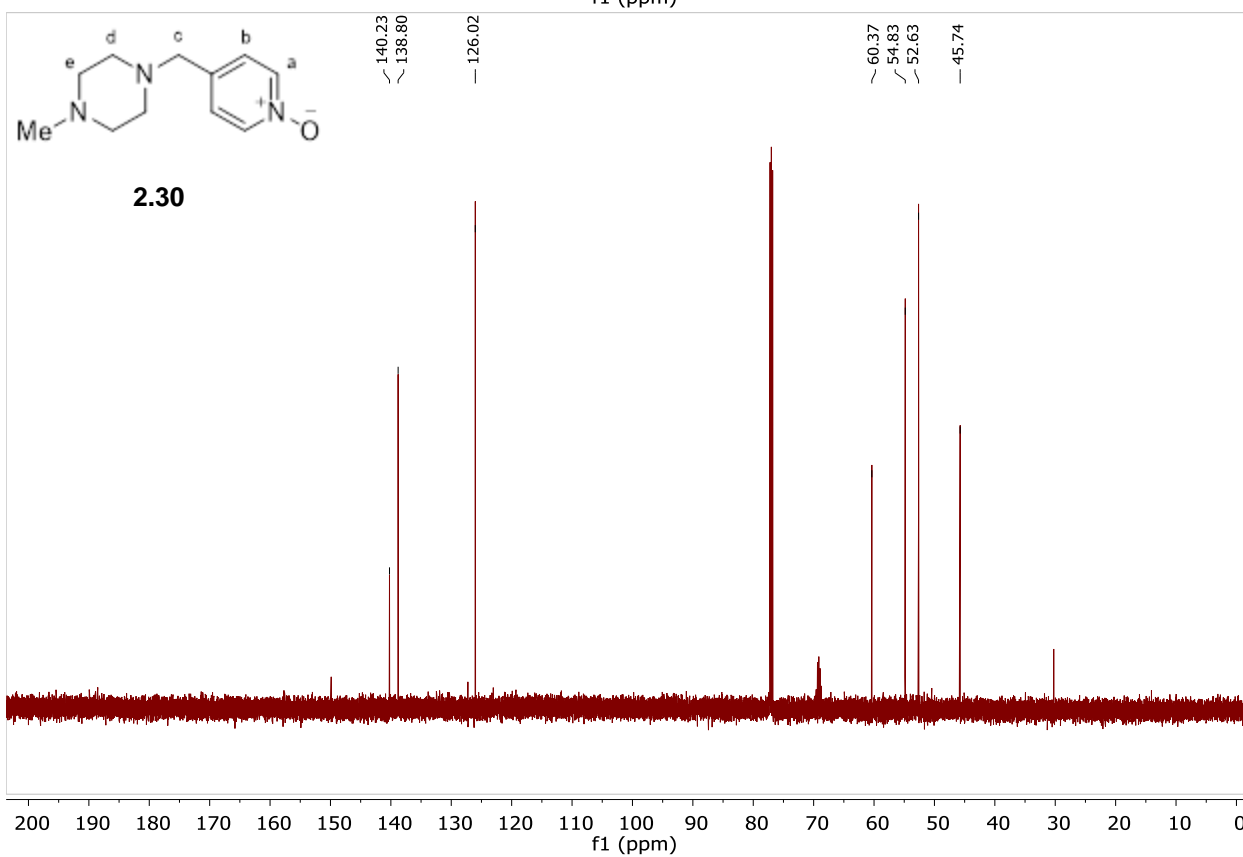
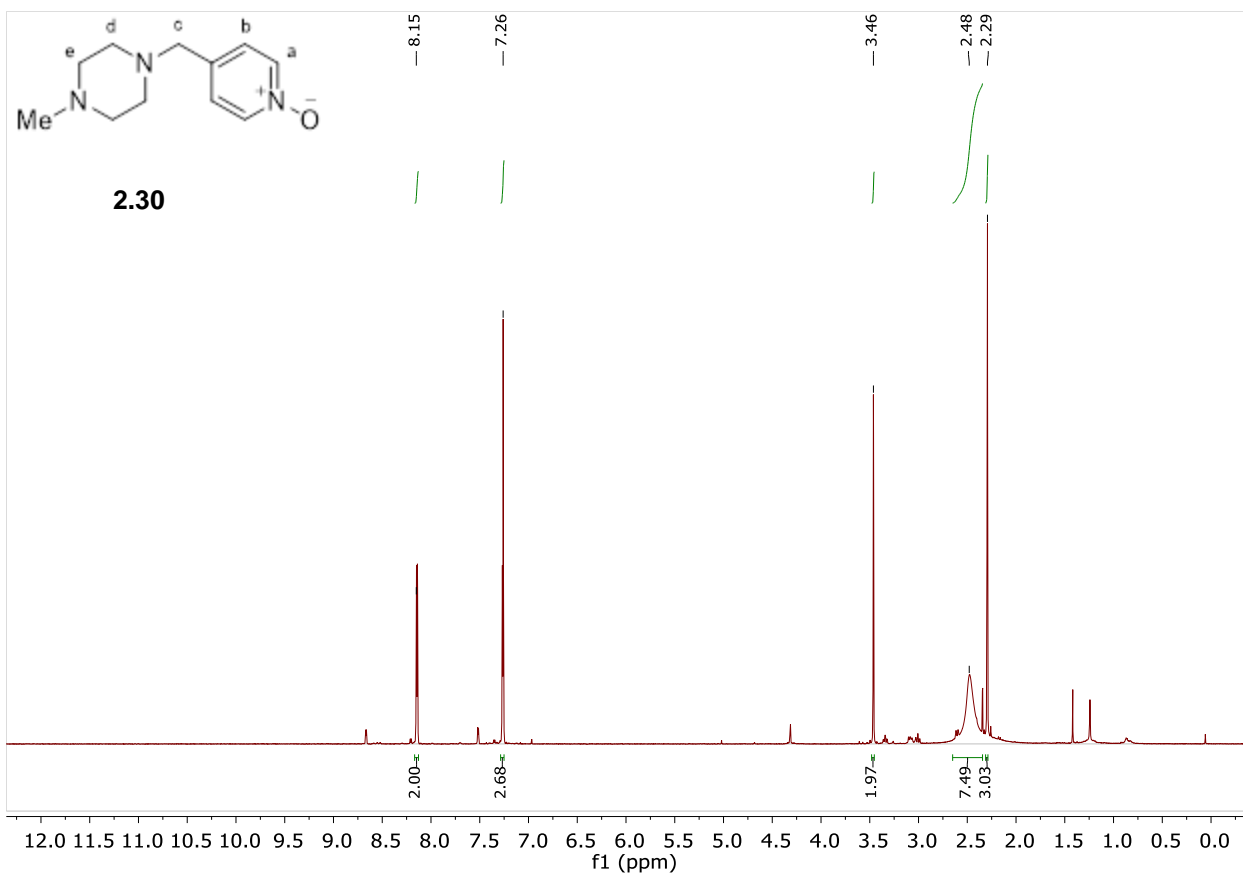
4-((4-methylpiperazin-1-yl)methyl)pyridine 1-oxide was synthesized using general procedure A. The reaction mixture was purified after workup using alumina flash chromatography (10% to 30% MeOH/Et₂O) to give product as 36.6 mg of clear oil (0.177 mmol, 50% yield).

¹H NMR (600 MHz, CDCl₃) δ 8.14 (H_a, d, *J* = 7.1 Hz, 2H), 7.31 (H_b, d, *J* = 7.1 Hz, 2H), 3.48 (H_c, s, 2H), 2.59 – 2.37 (H_d and H_e, m, 8H), 2.28 (Me, s, 3H) ppm.

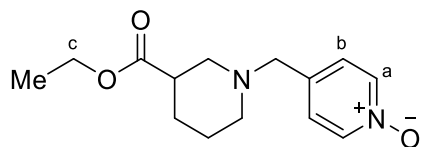
¹³C NMR (151 MHz, CDCl₃) δ 140.2, 138.8, 126.0, 60.4, 54.8, 52.6, 45.7 ppm.

IR (ATR) 2796.78, 1483.26, 1456.26, 1282.66, 1213.23, 1138.00, 1099.43, 1010.70, 842.89 cm⁻¹.

HRMS (ESI/QTOF) *m/z*: [M + H]⁺ Calcd for C₁₁H₁₈N₃O 208.1450; Found 208.1451.



4-((3-(ethoxycarbonyl)piperidin-1-yl)methyl)pyridine 1-oxide (2.31)



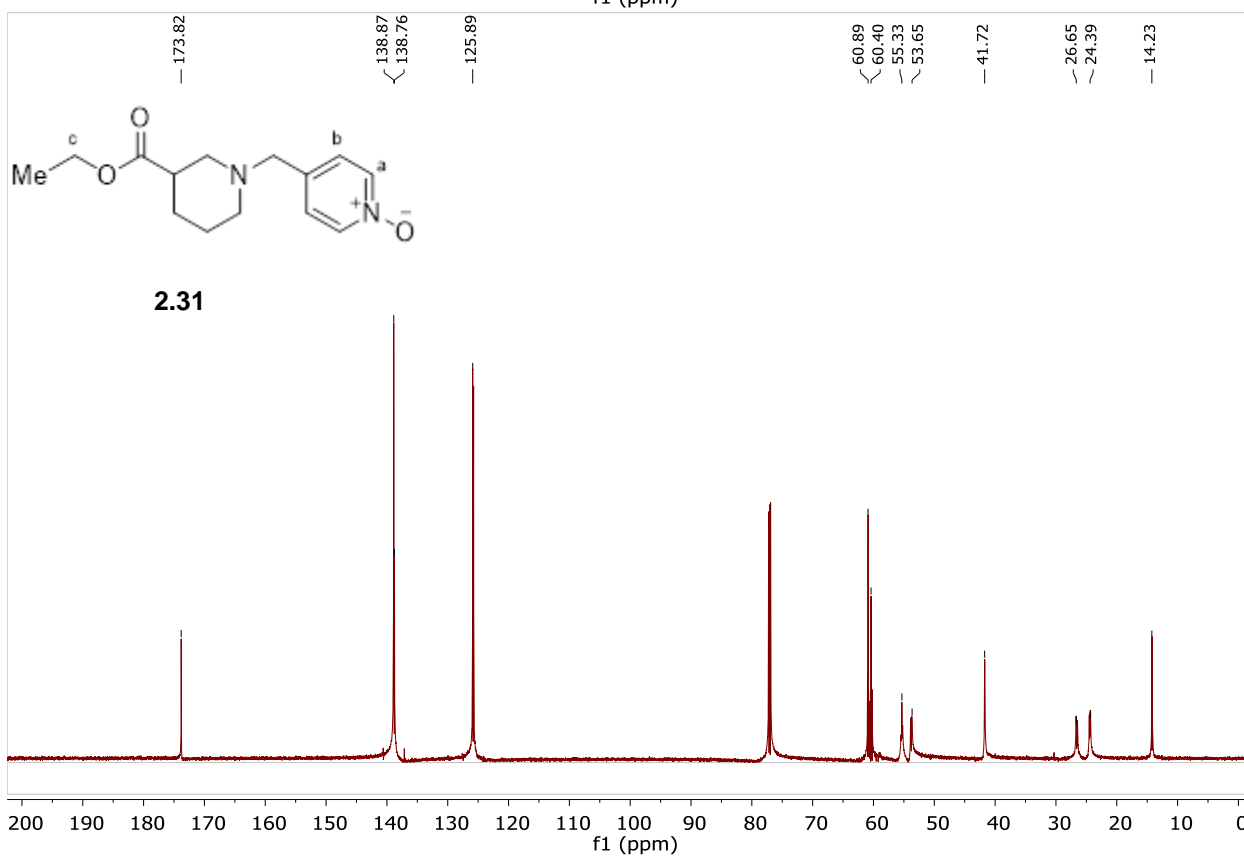
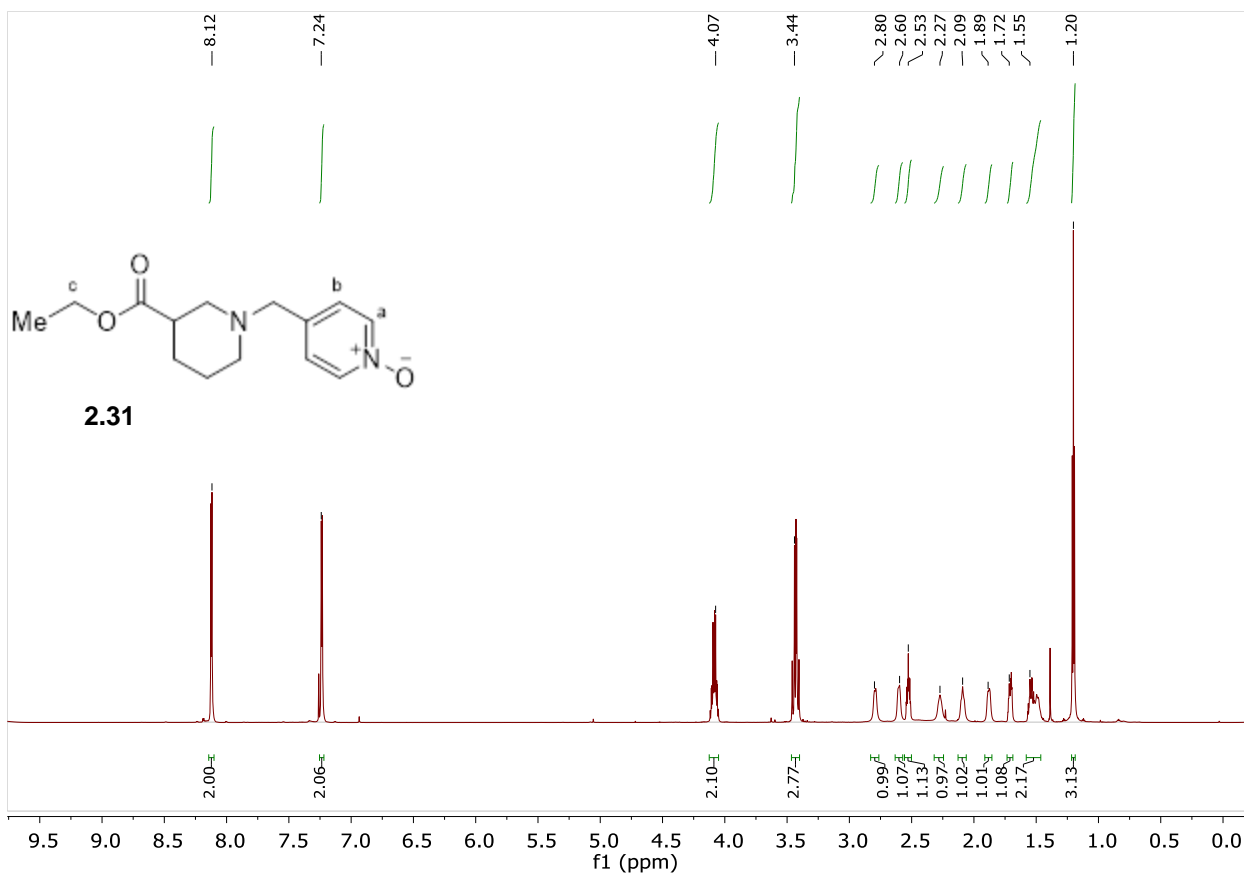
4-((3-(ethoxycarbonyl)piperidin-1-yl)methyl)pyridine 1-oxide was synthesized using general procedure A. The reaction mixture was purified after workup using alumina flash chromatography (10% to 20% MeOH/Et₂O) to give product as 39.0 mg of yellow oil (0.148 mmol 30% yield)

¹H NMR (600 MHz, CDCl₃): δ 8.12 (H_a, d, J = 6.7 Hz, 2H), 7.24 (H_b, d, J = 6.7 Hz, 2H), 4.12 – 4.05 (m, 2H), 3.43 (H_c, q, J = 14.4, 2H), 2.83 – 2.75 (m, 1H), 2.64 – 2.57 (m, 1H), 2.55 – 2.50 (m, 1H), 2.33 – 2.24 (m, 1H), 2.13 – 2.05 (m, 1H), 1.91 – 1.86 (m, 1H), 1.73 – 1.69 (m, 1H), 1.58 – 1.45 (m, 2H), 1.20 (Me, t, J = 7.2 Hz, 3H) ppm.

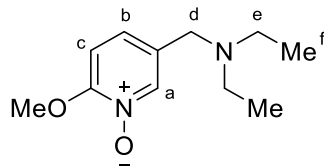
¹³C NMR (150 MHz, CDCl₃) δ 173.7, 138.7, 138.6, 125.7, 60.8, 60.3, 55.2, 53.7, 41.6, 26.5, 24.3, 14.1 ppm

IR (ATR) 1724.36, 1481.33, 1446.61, 1234.44, 1170.79, 1031.92 cm⁻¹.

HRMS (ESI/QTOF) m/z: [M + H]⁺ Calcd for C₁₄H₂₁N₂O₃ 265.1552; Found 265.1553.



5-((diethylamino)methyl)-2-methoxypyridine 1-oxide (2.32)



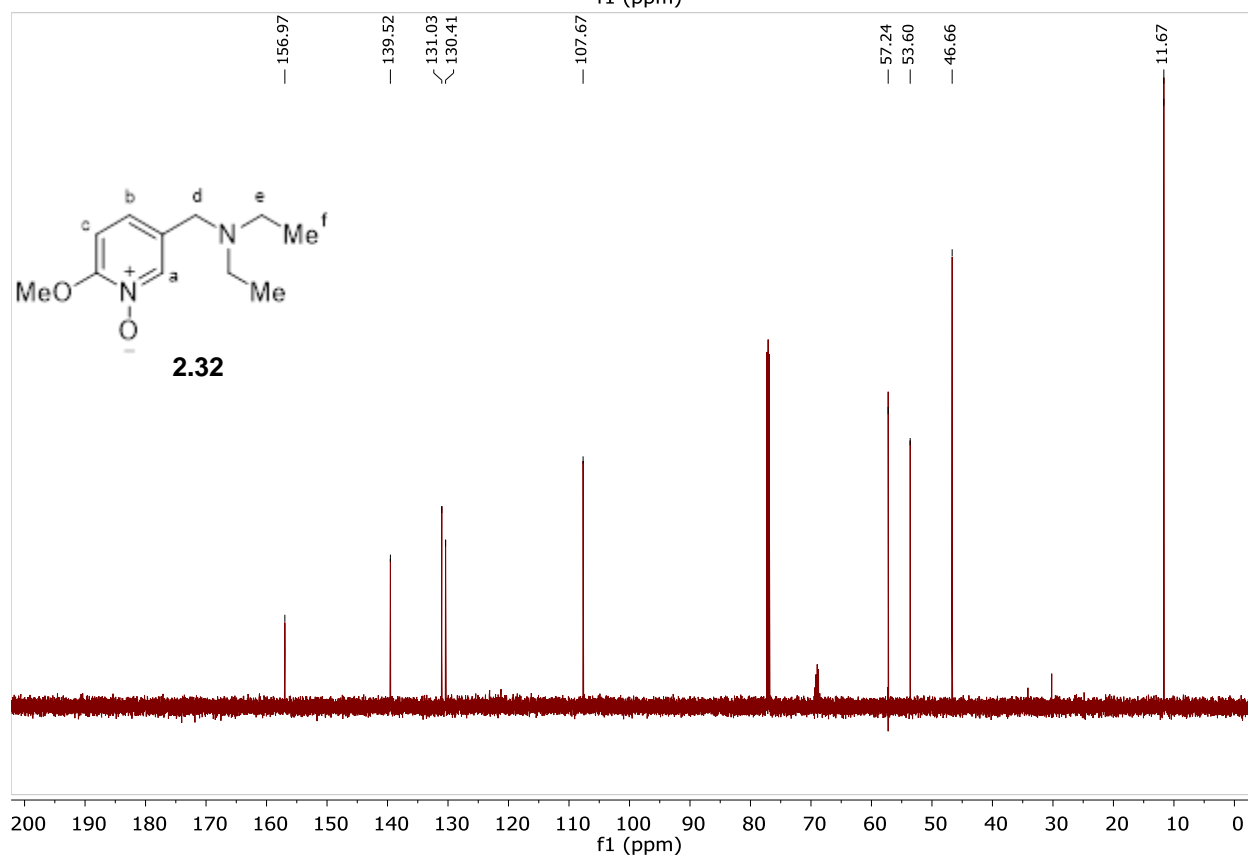
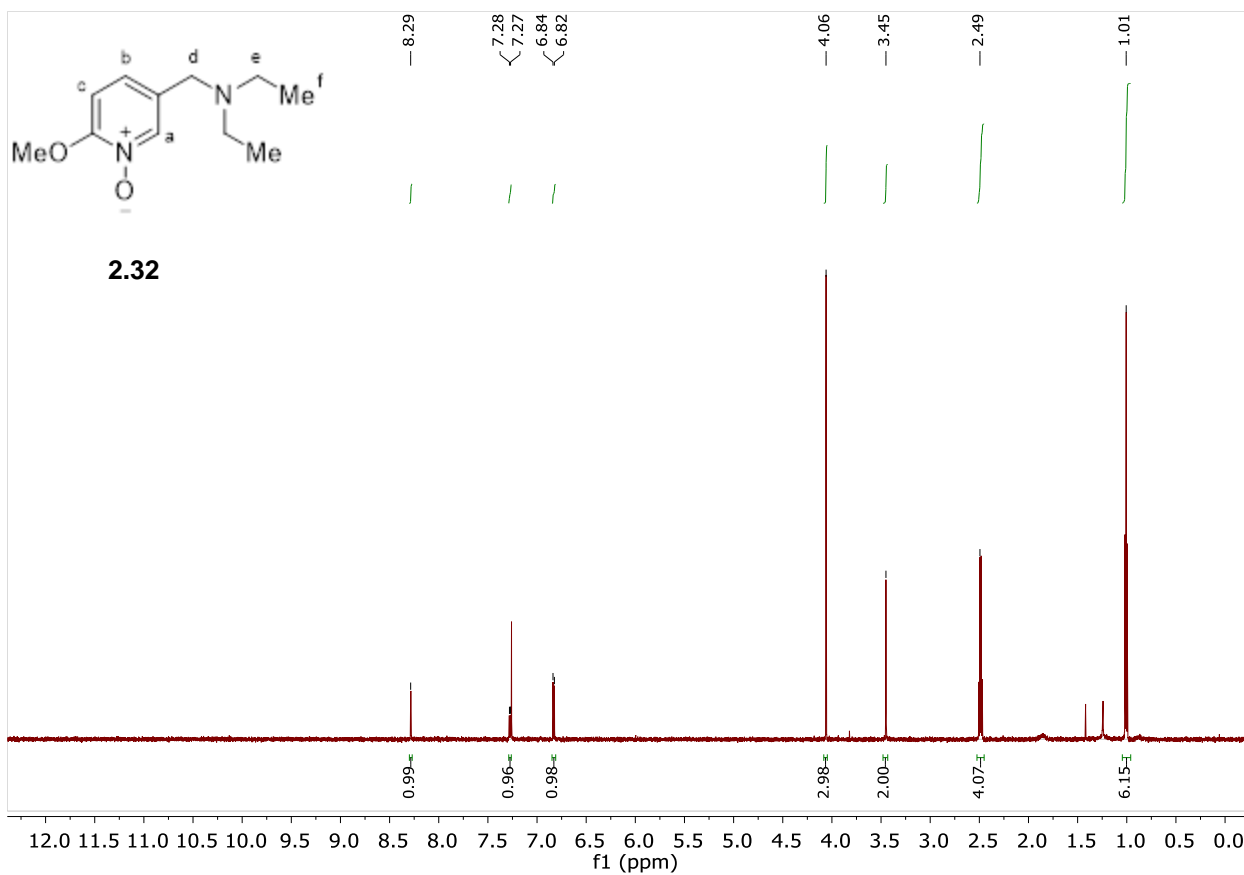
5-((diethylamino)methyl)-2-methoxypyridine 1-oxide was synthesized using general procedure B. The reaction mixture was purified after workup using alumina flash chromatography (10% MeOH/Et₂O) to give product as 0.770 g of a pale-yellow oil (0.366, mmol 73%)

¹H NMR (600 MHz, CDCl₃) δ 8.29 (H_a, d, J = 1.8 Hz, 1H), 7.28 (H_b, dd, J = 8.6, 1.8 Hz, 1H), 6.83 (H_c, d, J = 8.6 Hz, 1H), 4.06 (OMe, s, 3H), 3.45 (H_d, s, 2H), 2.49 (H_e, q, J = 7.2 Hz, 4H), 1.01 (H_f, t, J = 7.2 Hz, 6H) ppm.

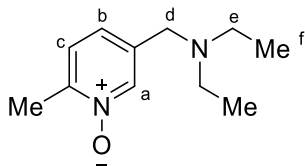
¹³C NMR (151 MHz, CDCl₃) δ 157.0, 139.5, 131.0, 130.4, 107.7, 57.2, 53.6, 46.7, 11.7 ppm.

IR (ATR) 2970.38, 1614.42, 1517.98, 1458.18, 1444.68, 1382.96, 1307.74, 1282.66, 1213.23, 1176.58, 1120.64, 1097.50, 1018.41, 891.11, 783.10, 734.88, 684.73, 613.36 cm⁻¹.

HRMS (ESI/QTOF) m/z: [M + H]⁺ Calcd for C₁₁H₁₉N₂O₂ 211.1447; Found 211.1452



5-((diethylamino)methyl)-2-methylpyridine 1-oxide (2.35)



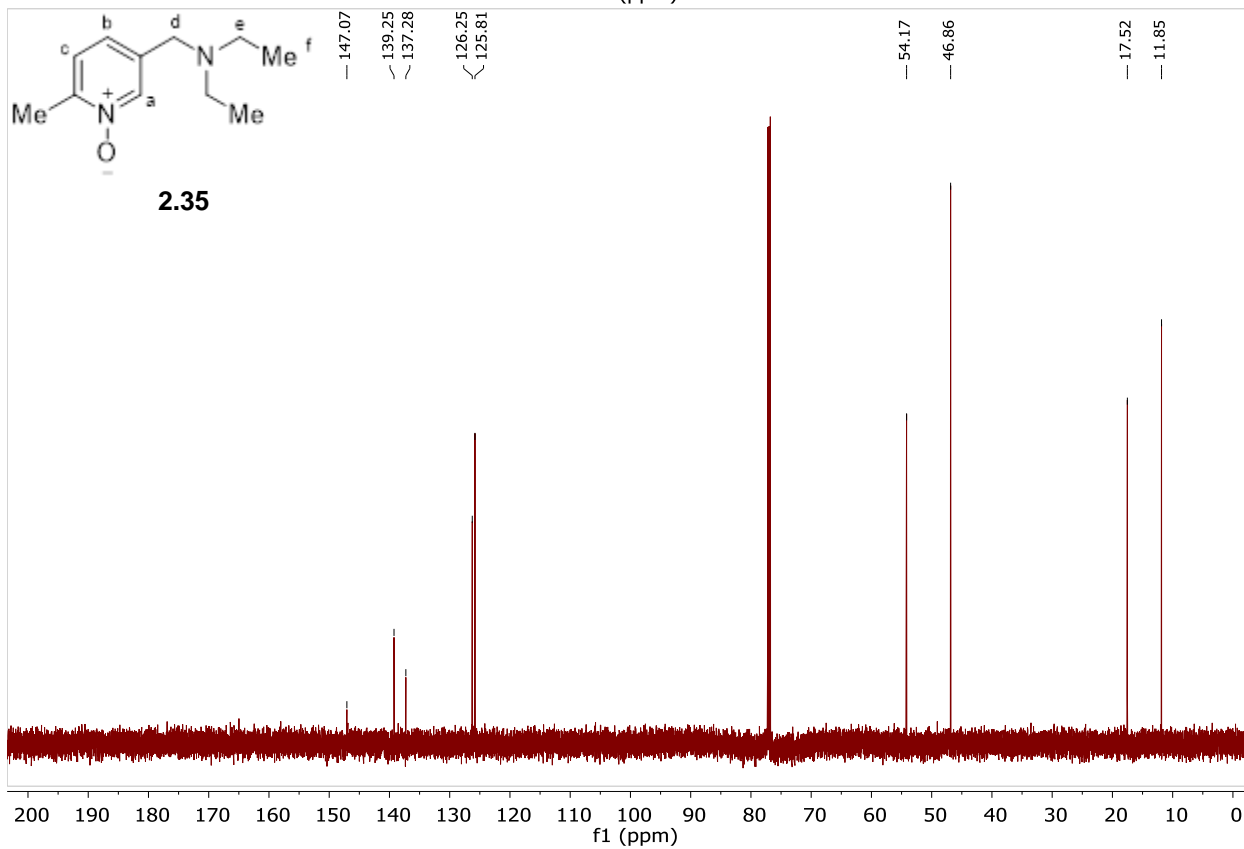
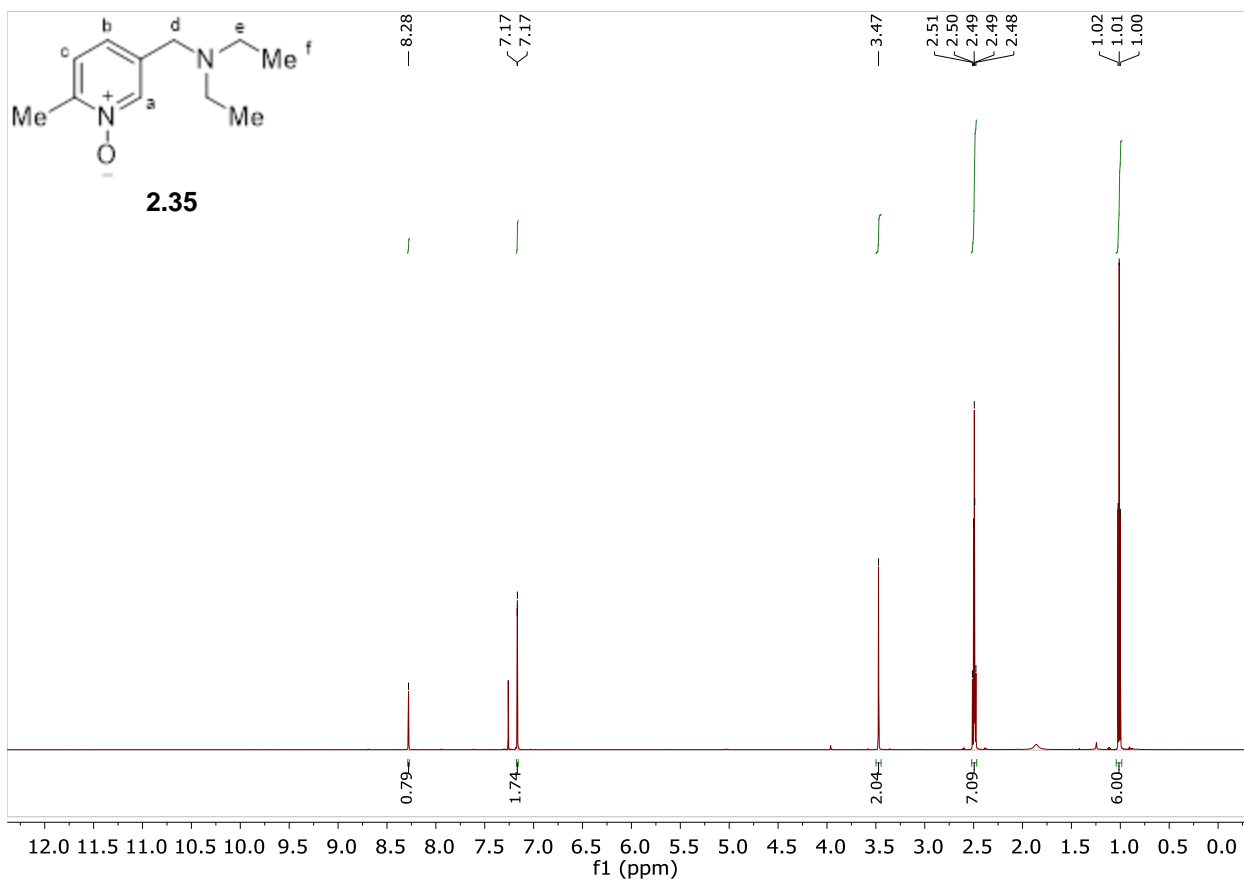
5-((diethylamino)methyl)-2-methylpyridine 1-oxide was synthesized using general procedure B on scale with 0.1 mmol of substrate. The reaction mixture was purified after workup using silica flash chromatography (10% MeOH/CH₂Cl₂) to give product as 11.8 mg of pale yellow oil (0.0607 mmol, 51%)

¹H NMR (600 MHz, CDCl₃) δ 8.28 (H_a, s, 1H), 7.18 – 7.16 (H_b and H_c, m, 2H), 3.47 (H_d, s, 2H), 2.52 – 2.47 (ArMe and H_e, m, 7H), 1.01 (H_f, t, *J* = 7.1 Hz, 6H) ppm.

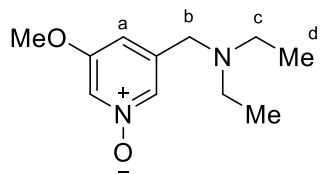
¹³C NMR (150 MHz, CDCl₃) δ 147.1, 139.3, 137.3, 126.3, 125.8, 54.2, 46.9, 17.5, 11.9 ppm.

IR (ATR) 2966.52, 2926.01, 2808.36, 1616.35, 1506.41, 1448.54, 1375.25, 1354.03, 1265.30, 1217.08, 1163.08, 1116.78, 1062.78, 1002.98, 939.33, 810.10, 754.17, 586.36 cm⁻¹.

HRMS (ESI/QTOF) *m/z*: [M + H]⁺ Calcd for C₁₁H₁₈N₂O 195.1497; Found 195.1500



3-((diethylamino)methyl)-5-methoxypyridine 1-oxide 2.36



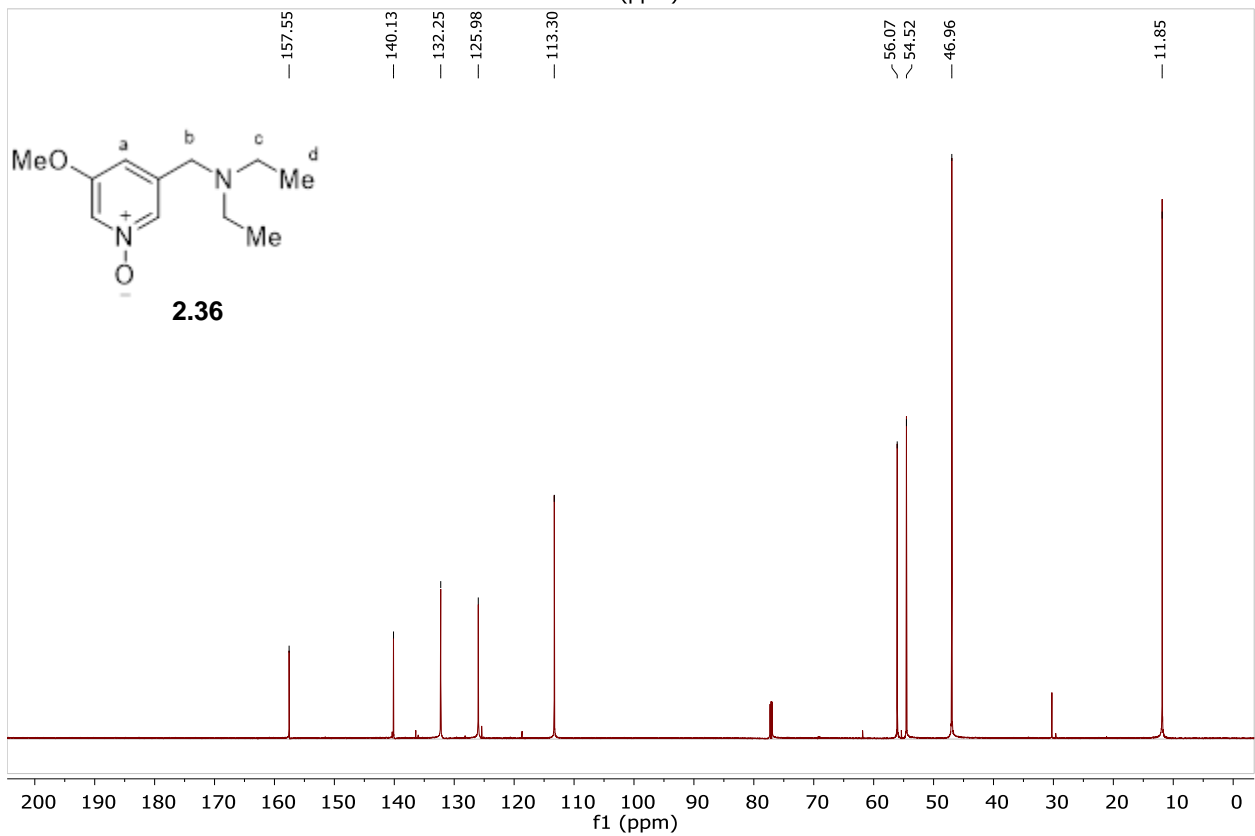
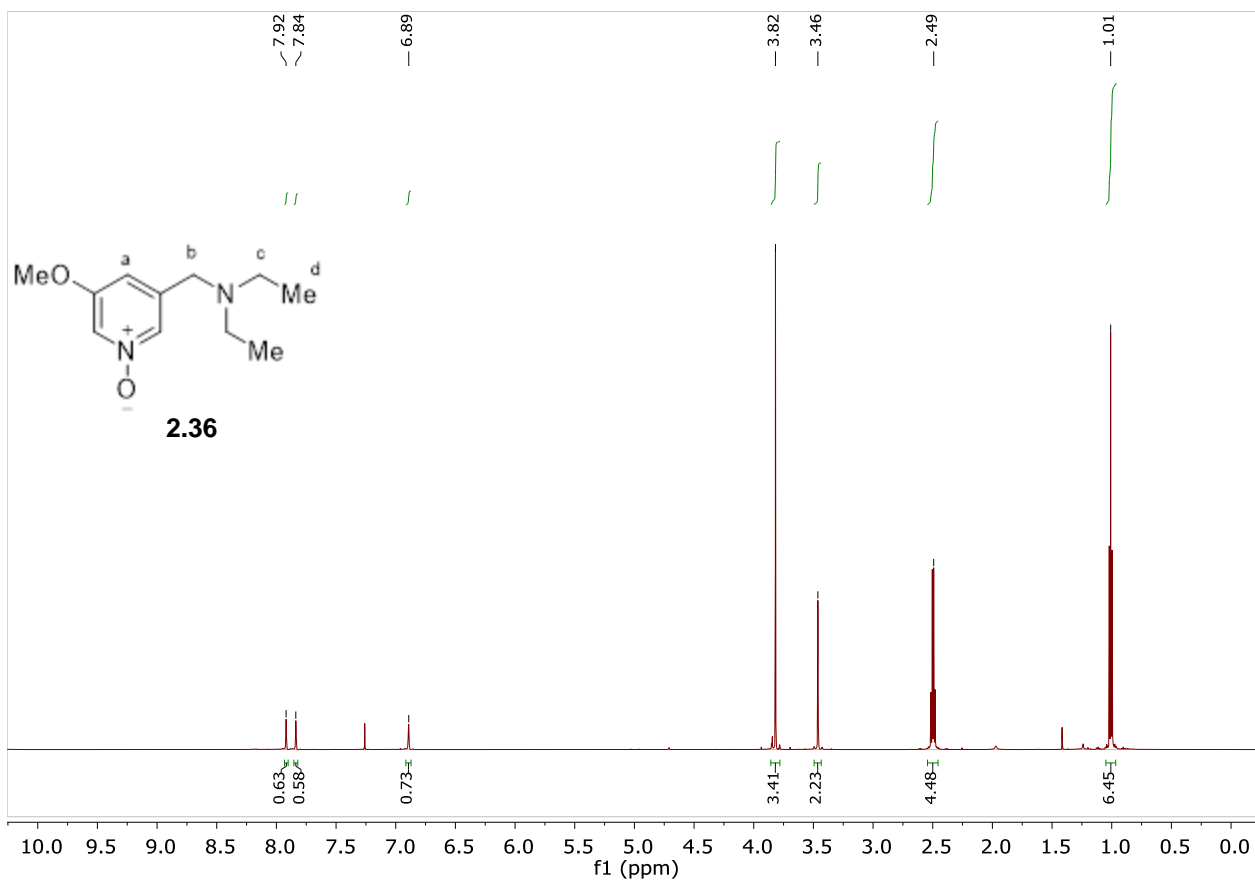
3-((diethylamino)methyl)-5-methoxypyridine 1-oxide was synthesized using general procedure B. The reaction mixture was purified after workup using alumina flash chromatography (10% MeOH/Et₂O) to give product as 0.0712 g of a clear oil (0.339 mmol, 68%)

¹H NMR (800 MHz, CDCl₃) δ 7.93 – 7.92 (ArH, s, 1H), 7.84 (ArH, s, 1H), 6.89 (H_a, s, Hz, 1H), 3.82 (OMe, s, 3H), 3.46 (H_b, s, 2H), 2.49 (H_c, q, J = 7.1 Hz, 4H), 1.01 (H_d, t, J = 7.1 Hz, 6H) ppm.

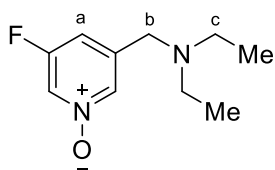
¹³C NMR (201 MHz, CDCl₃) δ 157.6, 140.1, 132.3, 126.0, 113.3, 56.1, 54.5, 47.0, 11.9 ppm.

IR (ATR) 2968.45, 2810.28, 1573.91, 1469.76, 1425.40, 1327.03, 1286.52, 1263.37, 1228.66, 1193.94, 1159.22, 1058.92, 1004.91, 840.96, 667.37 cm⁻¹.

HRMS (ESI/QTOF) m/z: [M + H]⁺ Calcd for C₁₁H₁₉N₂O₂ 211.1447; Found 211.1440



3-((diethylamino)methyl)-5-fluoropyridine 1-oxide (2.37)



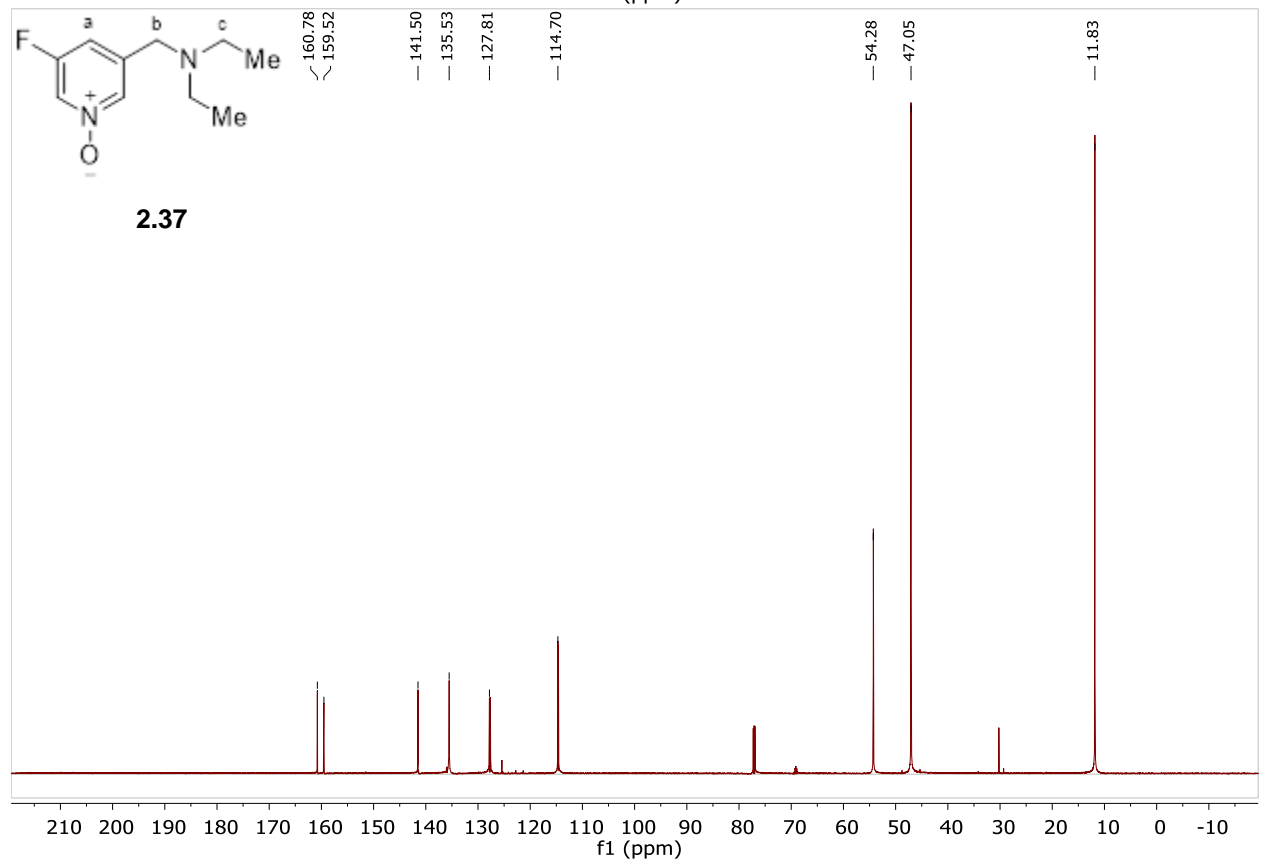
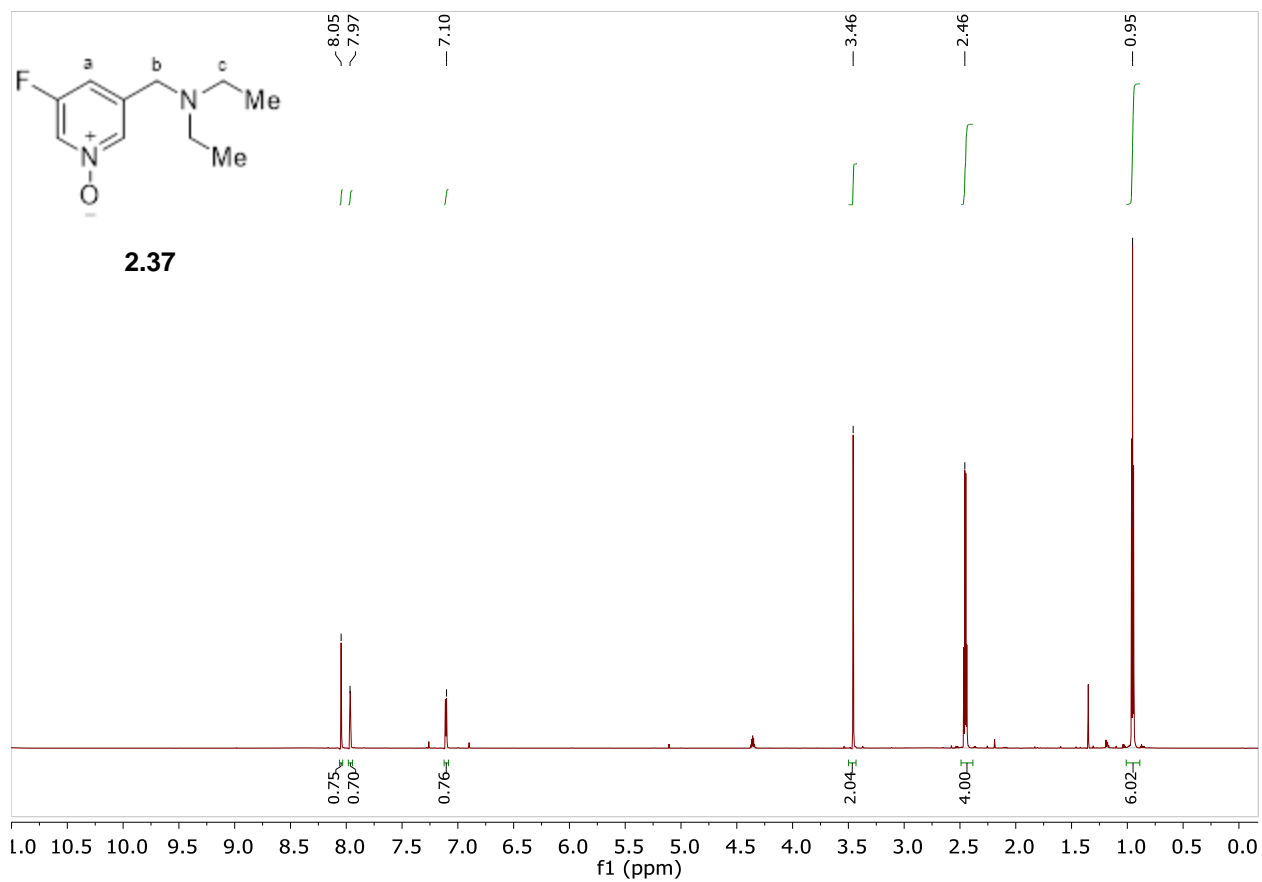
3-((diethylamino)methyl)-5-fluoropyridine 1-oxide was synthesized using general procedure B. The reaction mixture was purified after workup using alumina flash chromatography (10% MeOH/Et₂O) to give product as 0.0963 g of a pale yellow oil (0.486 mmol, 97%)

¹H NMR (800 MHz, CDCl₃) δ 8.05 (ArH, s, 1H), 7.97 (ArH, s, 1H), 7.10 (H_a, d, J = 7.7 Hz, 1H), 3.46 (H_b, d, J = 1.7 Hz, 2H), 2.46 (H_c, q, J = 7.1 Hz, 4H), 0.95 (Me, t, J = 7.1 Hz, 6H) ppm.

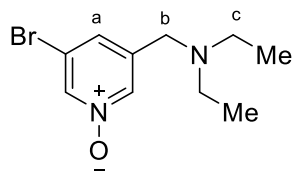
¹³C NMR (201 MHz, CDCl₃) δ 160.2 (d, J = 252.9 Hz), 141.5 (d, J = 8.0 Hz), 135.5 (d, J = 4.4 Hz), 127.7 (d, J = 36.6 Hz), 114.7 (d, J = 20.2 Hz), 54.3, 47.1, 11.8 ppm.

IR (ATR) 2970.38, 2810.28, 1614.42, 1573.91, 1431.18, 1327.03, 1286.52, 1213.23, 1157.29, 1010.70, 840.96 cm⁻¹.

HRMS (ESI/QTOF) m/z: [M + H]⁺ Calcd for C₁₀H₁₆FN₂O 199.1247; Found 199.1268



3-bromo-5-((diethylamino)methyl)pyridine 1-oxide (2.38)



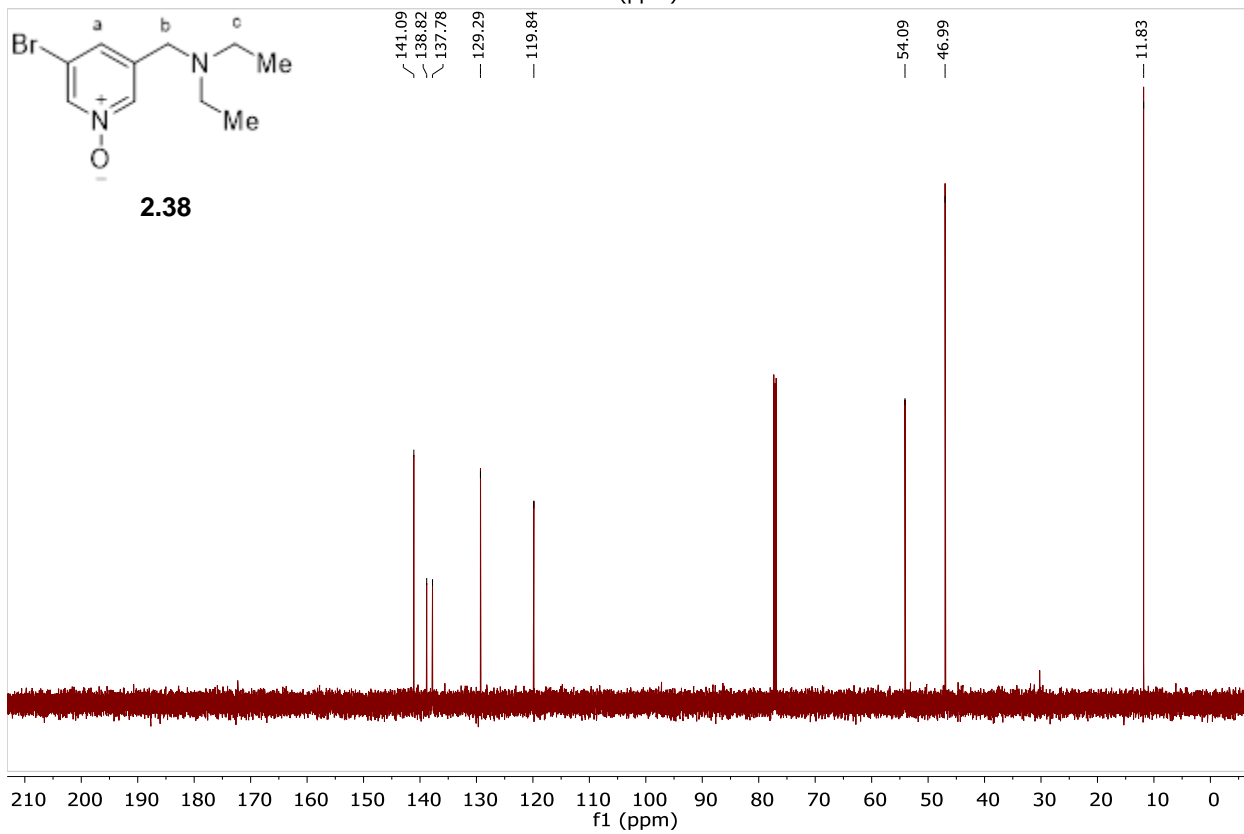
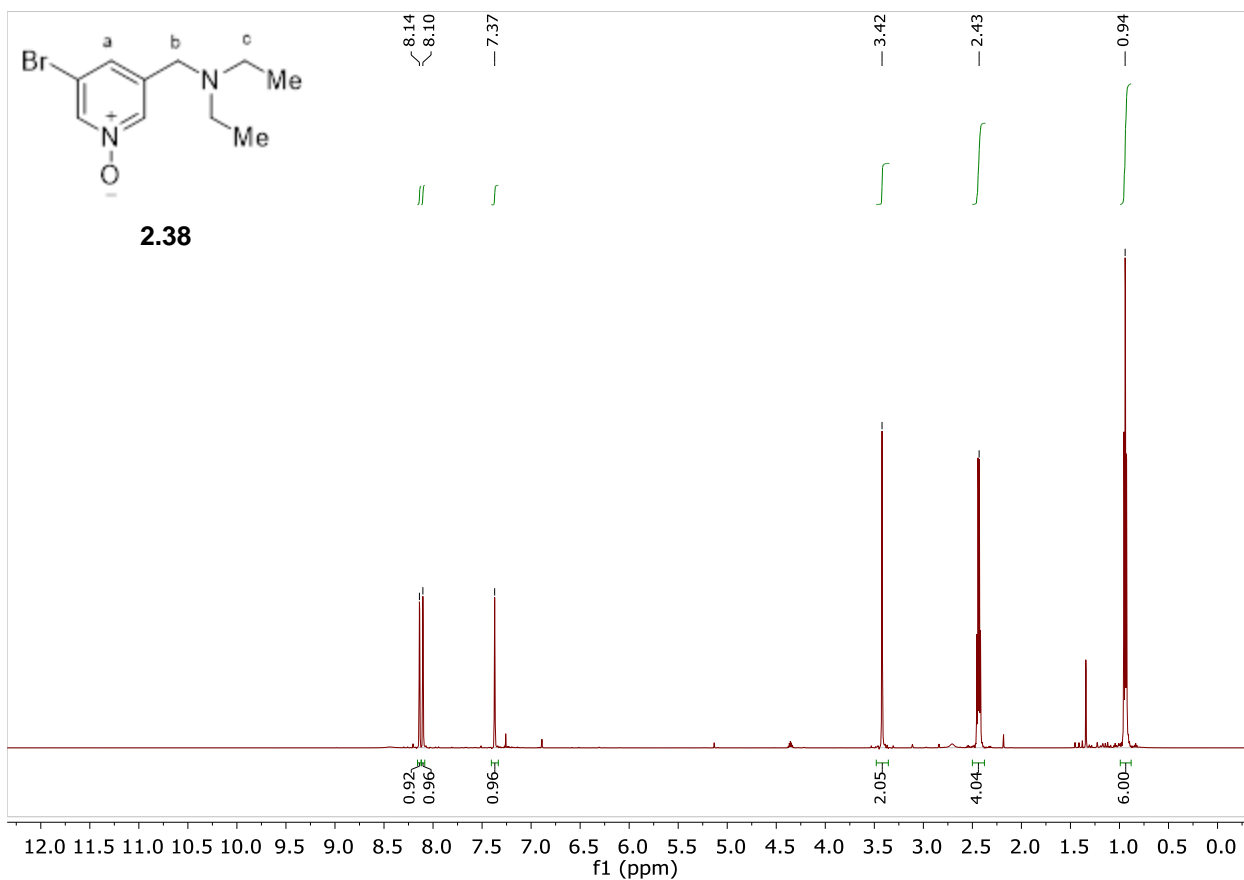
3-bromo-5-((diethylamino)methyl)pyridine 1-oxide was synthesized using general procedure B. The reaction mixture was purified after workup using alumina flash chromatography (5% MeOH/Et₂O) to give product as 0.120 g of a clear oil (0.462 mmol, 92%)

¹H NMR (600 MHz, CDCl₃) δ 8.14 (ArH, s, 1H), 8.10 (ArH, s, 1H), 7.37 (H_a, s, 1H), 3.42 (H_b, s, 2H), 2.44 (H_c, q, J = 7.2 Hz, 4H), 0.94 (Me, t, J = 7.2 Hz, 6H) ppm.

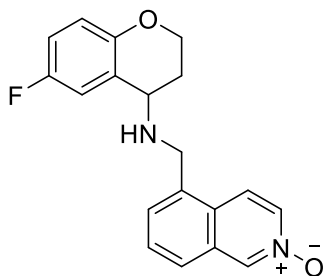
¹³C NMR (151 MHz, CDCl₃) δ 141.1, 138.8, 137.8, 129.3, 119.8, 54.1, 47.0, 11.8 ppm.

IR (ATR) 2966.52, 2931.80, 2804.50, 1589.34, 1541.12, 1454.33, 1408.04, 1284.59, 1201.65, 1153.43, 1118.71, 1064.71, 1002.98, 970.19, 840.96, 769.60, 669.30 cm⁻¹.

HRMS (ESI/QTOF) m/z: [M + H]⁺ Calcd for C₁₀H₁₆BrN₂O 259.0446; Found 259.0443



5-(((6-fluorochroman-4-yl)amino)methyl)isoquinoline 2-oxide (2.39)



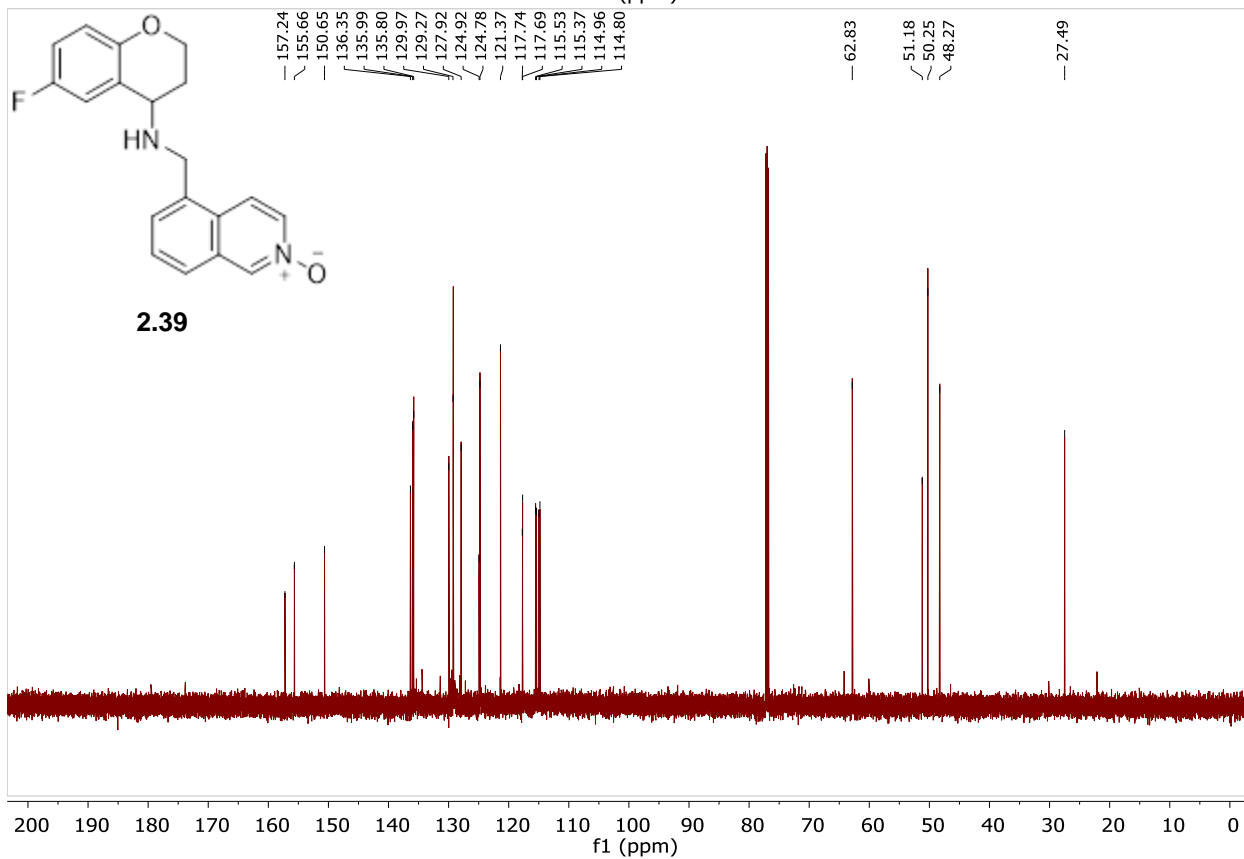
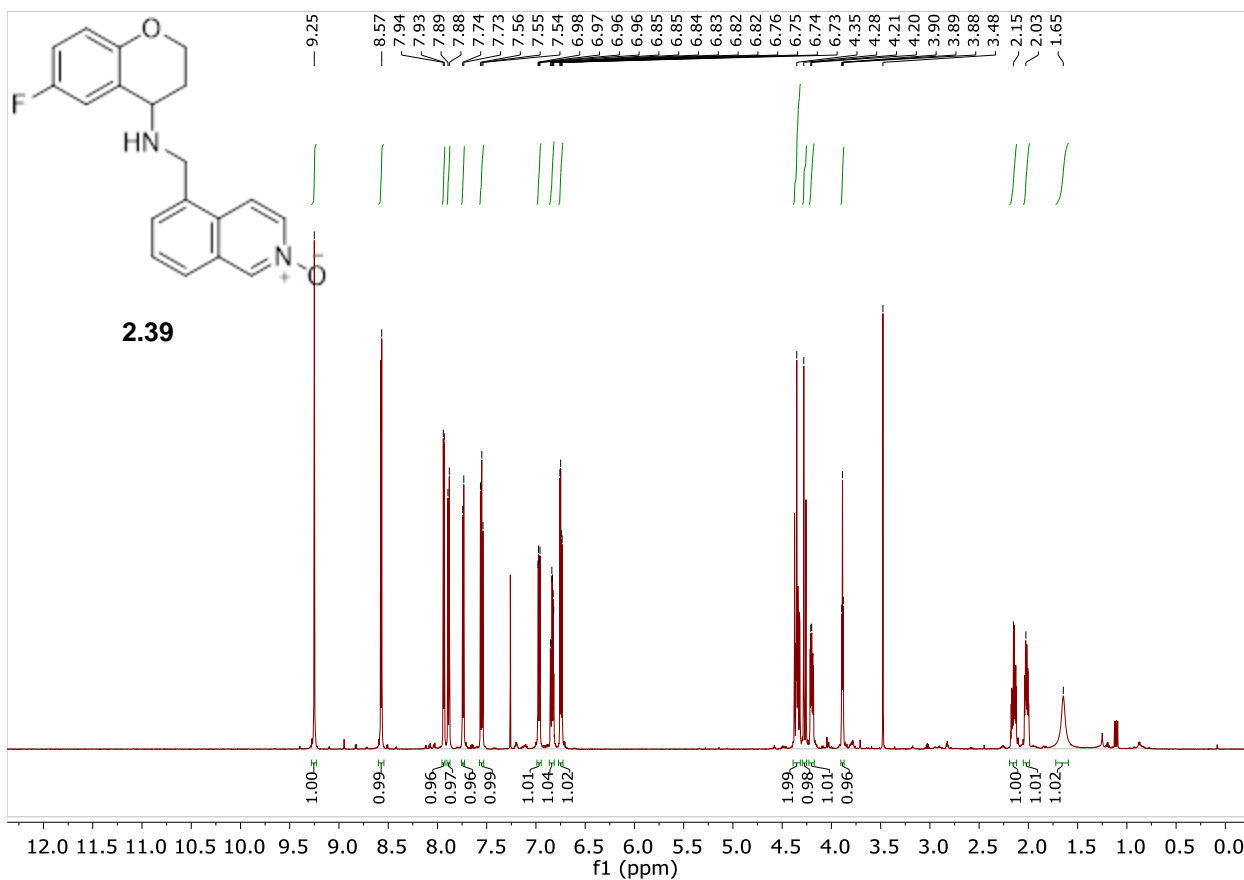
5-(((6-fluorochroman-4-yl)amino)methyl)isoquinoline 2-oxide was synthesized using general procedure A. The reaction mixture was purified after workup using alumina flash chromatography twice (1% MeOH/99%DCM and 10% MeOH/90% Et₂O) to give 0.123 g of product (.380 mmol, 57% yield) of white solid.

¹H NMR (600 MHz, CDCl₃) δ 8.79 (d, J = 1.9 Hz, 1H), 8.21 (dd, J = 7.3, 1.9 Hz, 1H), 8.15 (d, J = 7.3 Hz, 1H), 7.71 – 7.68 (m, 2H), 7.63 (dd, J = 8.2, 7.1 Hz, 1H), 7.06 – 7.03 (m, 1H), 6.91 (ddd, J = 9.0, 7.9, 3.1 Hz, 1H), 6.82 (dd, J = 9.0, 4.7 Hz, 1H), 4.42 – 4.37 (m, 2H), 4.32 (d, J = 13.5 Hz, 1H), 4.27 (ddd, J = 11.0, 6.0, 3.1 Hz, 1H), 3.95 (t, J = 5.0 Hz, 1H), 2.28 – 2.21 (m, 1H), 2.07 (dtd, J = 13.5, 5.6, 3.1 Hz, 1H), 1.65 (s, 1H) ppm.

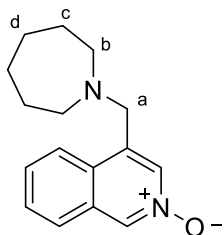
¹³C NMR (151 MHz, CDCl₃) δ 157.2, 155.7, 150.7, 136.4, 136.0, 135.8, 130.0, 129.3, 127.9, 124.9, 124.8, 121.4, 117.7, 117.7, 115.5, 115.4, 115.0, 114.8, 62.8, 51.2, 50.3, 48.3, 27.5 ppm.

IR (ATR) 2881.65, 1483.26, 1425.50, 1319.31, 1247.94, 1165.0, 1139.93, 1112.93, 1082.07, 933.55, 750.31, 729.09, 644.22 cm⁻¹.

HRMS (ESI/QTOF) m/z: [M + H]⁺ Calcd for C₁₉H₁₈N₂O₂F 325.1352, found 325.1343



4-(azepan-1-ylmethyl)isoquinoline 2-oxide (2.40)



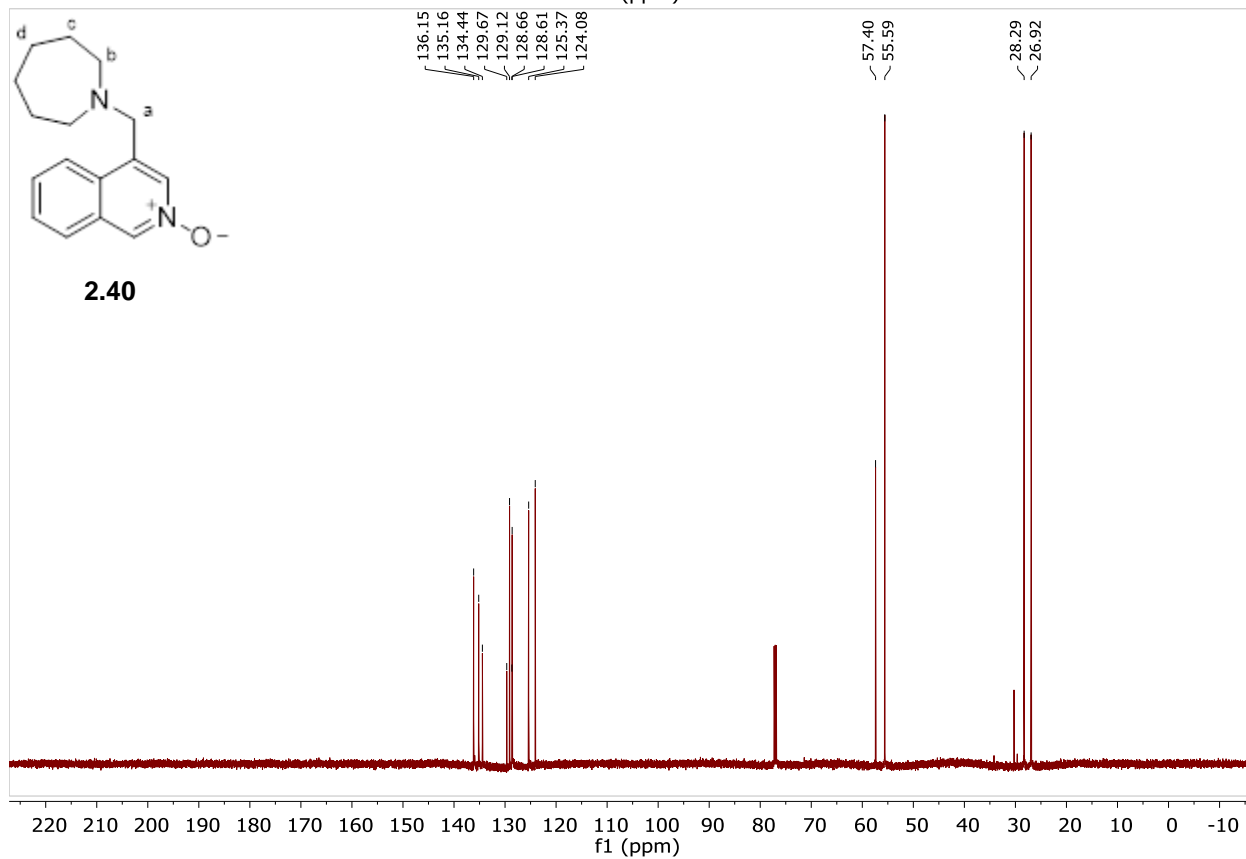
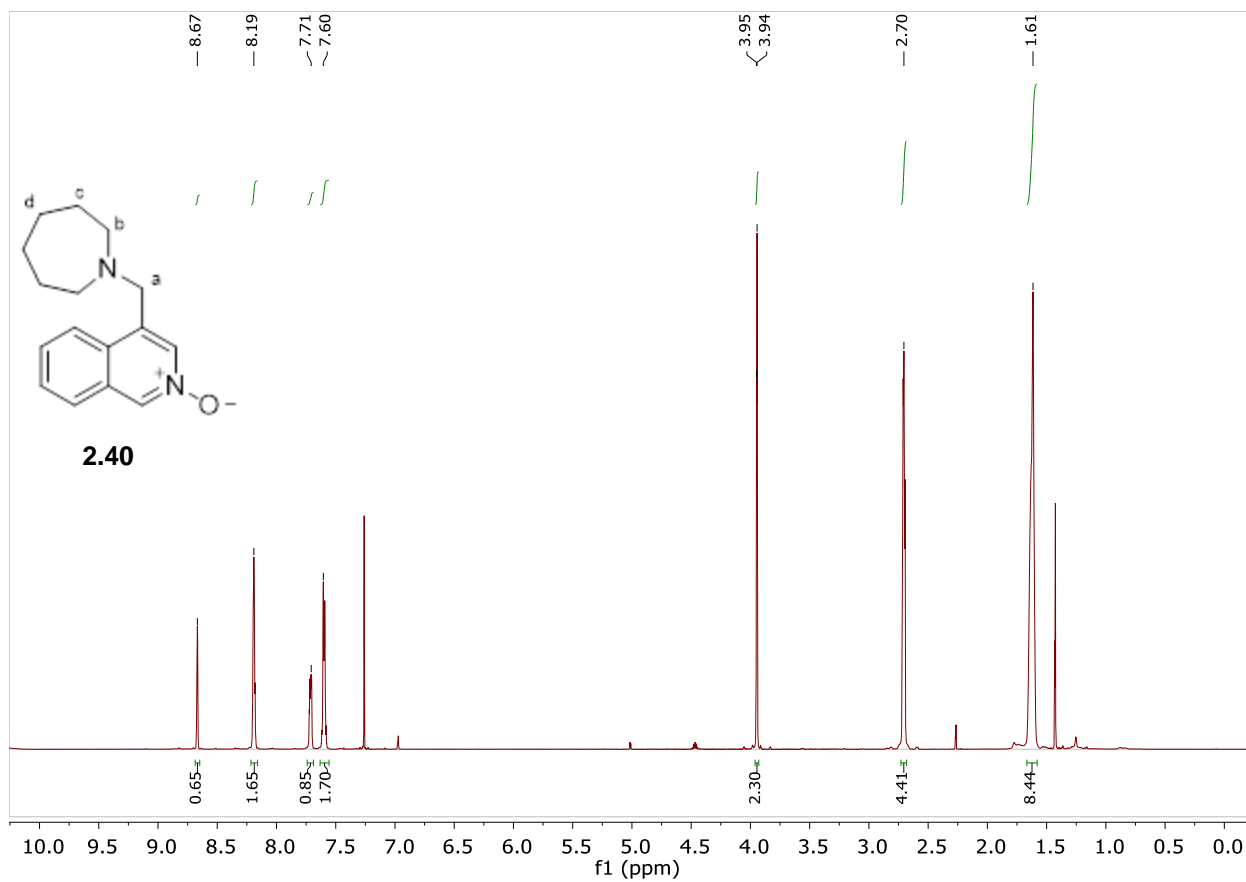
4-(azepan-1-ylmethyl)isoquinoline 2-oxide was synthesized using general procedure B. The reaction mixture was purified after workup using alumina flash chromatography (10% MeOH/Et₂O) to give product as 076.8 mg of white solid (0.300 mmol, 60%)

¹H NMR (600 MHz, CDCl₃) δ 8.67 (ArH, s, 1H), 8.21 – 8.17 (ArH, m, 2H), 7.73 – 7.69 (ArH, m, 1H), 7.62 – 7.58 (ArH, m, 2H), 3.94 (H_a, s, 2H), 2.73 – 2.68 (H_b, m, 4H), 1.67 – 1.59 (H_c and H_d, m, 8H) ppm.

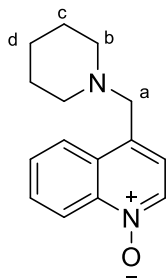
¹³C NMR (150 MHz, CDCl₃) δ 136.2, 135.2, 134.4, 129.7, 129.1, 128.7, 128.6, 125.4, 124.1, 57.4, 55.6, 28.3, 26.9 ppm.

IR (ATR) 2918.30, 2831.50, 1624.06, 1600.92, 1560.41, 1454.33, 1438.90, 1388.75, 1346.31, 1336.67, 1305.81, 1280.73, 1246.02, 1222.87, 1172.72, 1155.36, 1122.57, 1105.21, 1083.99, 977.91, 966.34, 898.83, 856.39, 779.24, 761.88, 754.17, 731.02, 692.44, 634.58 cm⁻¹.

HRMS (ESI/QTOF) m/z: [M + H]⁺ Calcd for C₁₆H₂₁N₂O 257.1654; Found 257.1644



4-(piperidin-1-ylmethyl)quinoline 1-oxide (2.41)



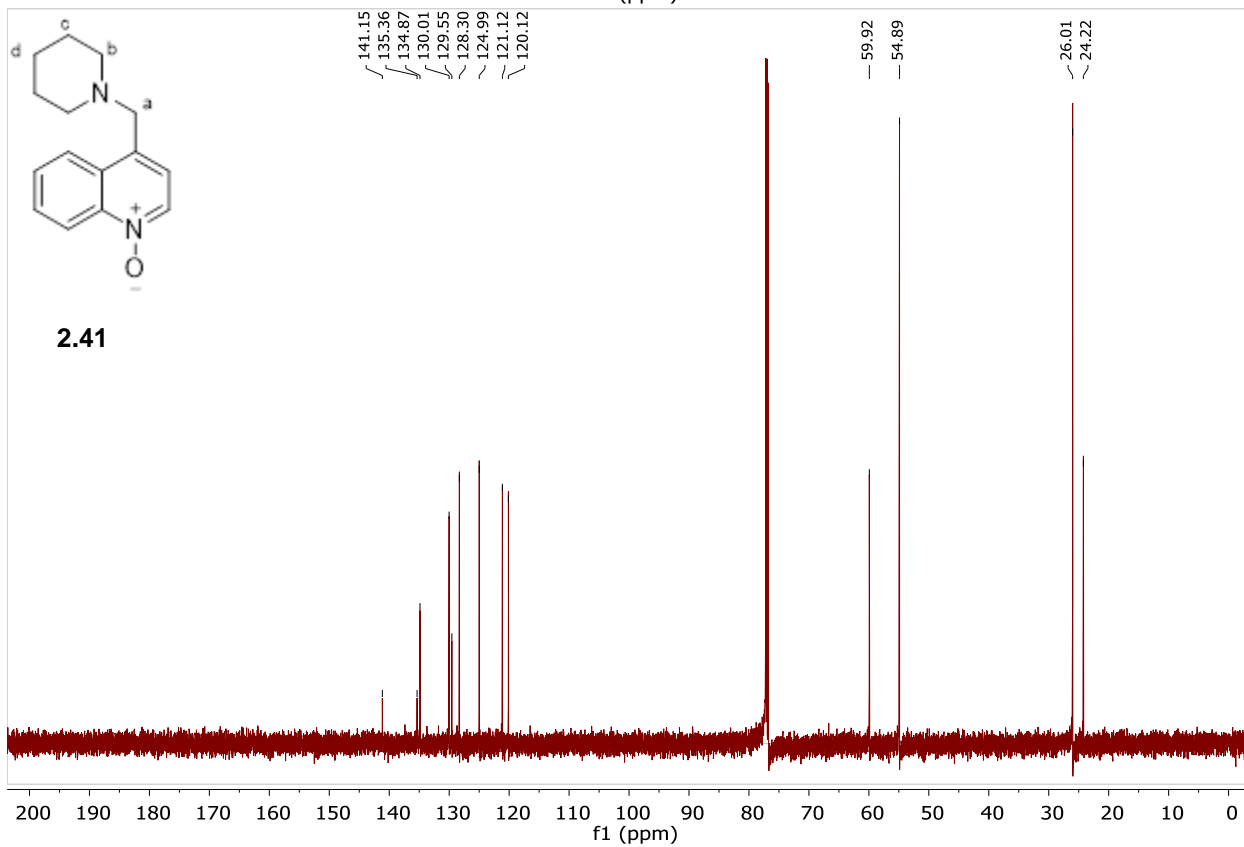
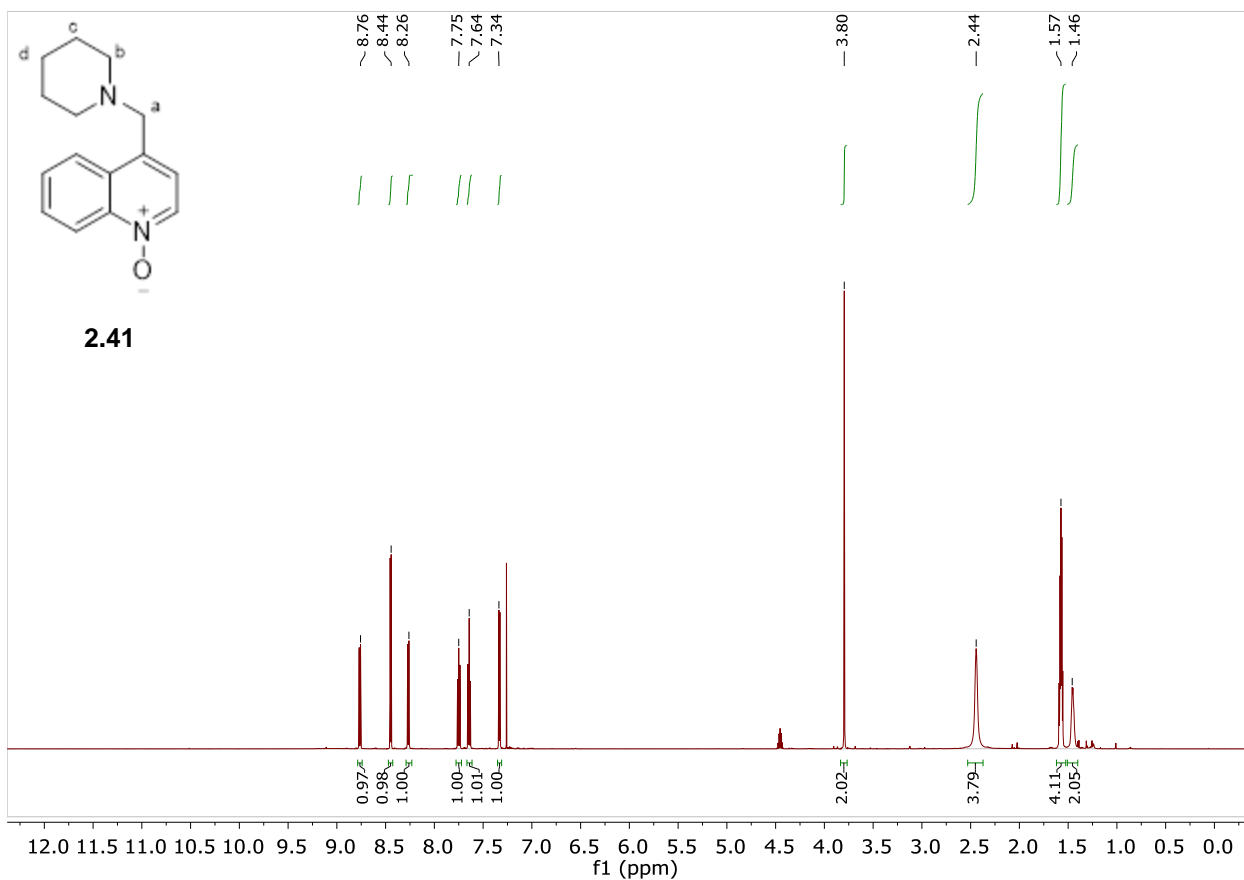
4-(piperidin-1-ylmethyl)quinoline 1-oxide was synthesized using general procedure B. The reaction mixture was purified after workup using alumina flash chromatography (EtOAc) to give product as 99.6 mg of white solid (0.411 mmol, 82%)

¹H NMR (600 MHz, CDCl₃) δ 8.76 (ArH, dt, J = 8.8, 1.3 Hz, 1H), 8.45 (ArH, d, J = 6.2 Hz, 1H), 8.27 (ArH, dd, J = 8.4, 1.3 Hz, 1H), 7.75 (ArH, ddd, J = 8.8, 6.9, 1.3 Hz, 1H), 7.64 (ArH, ddd, J = 8.4, 6.9, 1.3 Hz, 1H), 7.33 (ArH, dt, J = 6.2, 1.0 Hz, 1H), 3.80 (H_a, s, 2H), 2.50 – 2.38 (H_b, m, 4H), 1.57 (H_c, p, J = 5.6 Hz, 5H), 1.48 – 1.42 (H_d, m, 2H) ppm.

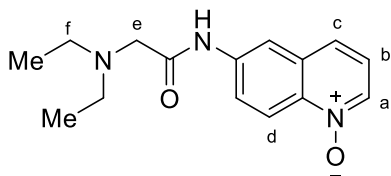
¹³C NMR (151 MHz, CDCl₃) δ 151.0, 146.5, 137.7, 130.8, 129.7, 128.0, 127.3, 127.3, 126.7, 59.7, 54.7, 26.0, 24.2 ppm.

IR (ATR) 3061.03, 2927.94, 2798.71, 2754.35, 1566.20, 1512.19, 1394.53, 1367.53, 1344.38, 1313.52, 1282.66, 1247.94, 1209.37, 1153.43, 1043.49, 842.89, 763.81 cm⁻¹.

HRMS (ESI/QTOF) m/z: [M + H]⁺ Calcd for C₁₅H₁₉N₂O 243.1497; Found 253.1497



6-(2-(diethylamino)acetamido)quinoline 1-oxide (2.42)



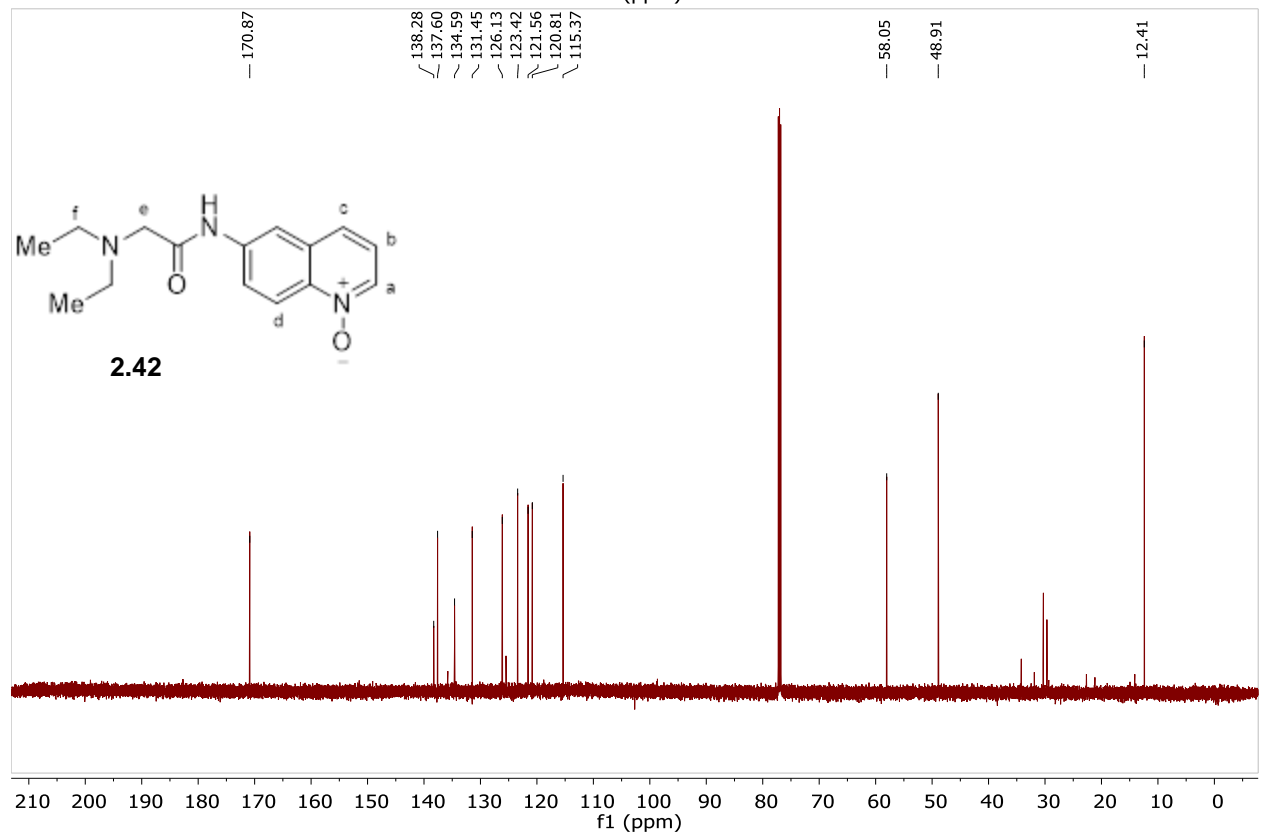
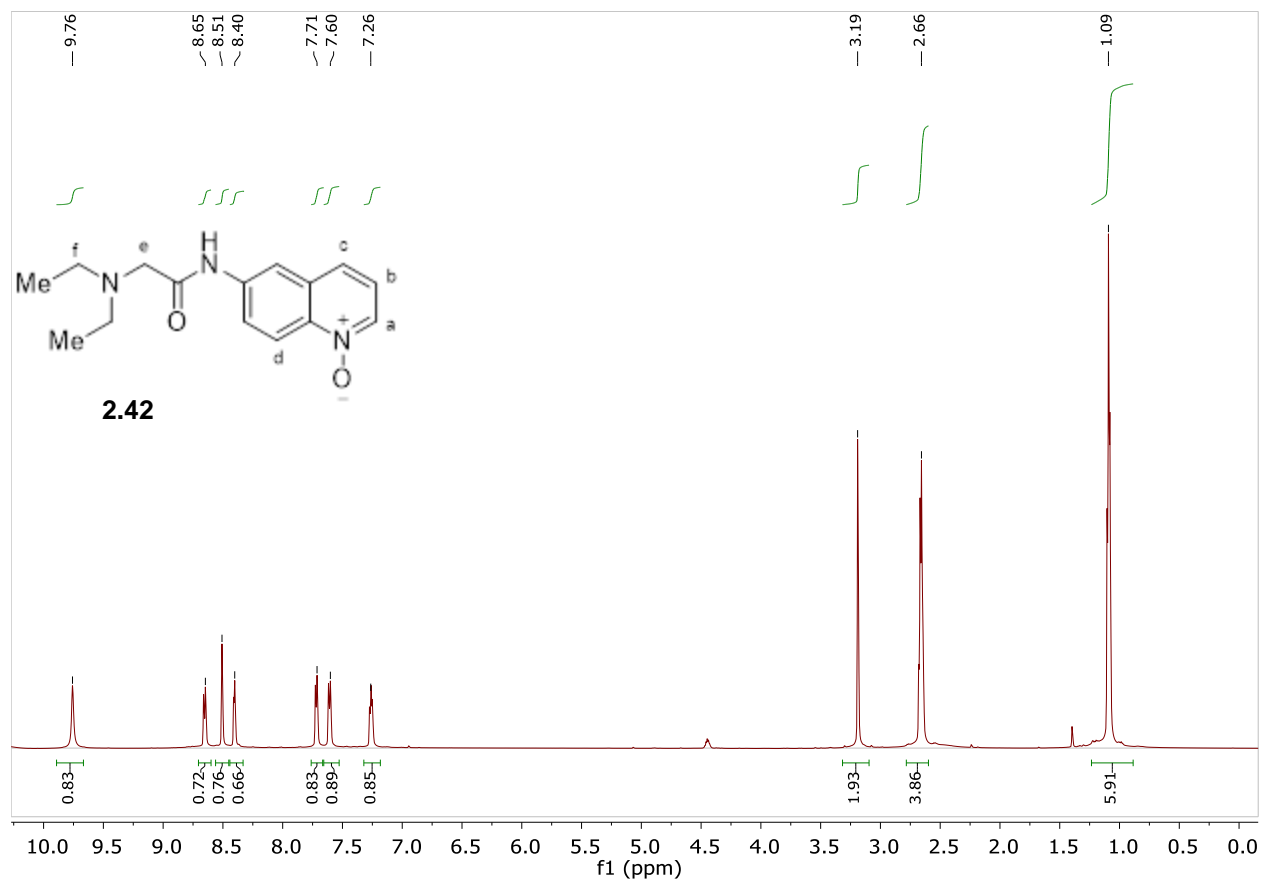
6-(2-(diethylamino)acetamido)quinoline 1-oxide was synthesized using general procedure B on scale with 1.5 mmol of substrate. The reaction mixture was purified after workup using alumina flash chromatography (5% MeOH/Et₂O) to give product as 0.308 g of white solid (1.13 mmol, 75%)

¹H NMR (600 MHz, CDCl₃) δ 9.76 (NH, s, 1H), 8.65 (H_a, d, *J* = 9.3 Hz, 1H), 8.51 (H_c, d, *J* = 2.3 Hz, 1H), 8.40 (H_d, d, *J* = 5.8 Hz, 1H), 7.71 (ArH d, *J* = 8.2 Hz, 1H), 7.60 (H_b, dd, *J* = 9.3, 2.3 Hz, 1H), 7.26 (ArH, dd, *J* = 8.2, 5.8 Hz, 1H), 3.19 (H_e, s, 2H), 2.66 (H_f, q, *J* = 7.2 Hz, 4H), 1.09 (Me, t, *J* = 7.2 Hz, 6H).

¹³C NMR (151 MHz, CDCl₃) δ 170.9, 138.3, 137.6, 134.6, 131.5, 126.1, 123.4, 121.6, 120.8, 115.4, 58.1, 48.9, 12.4 ppm.

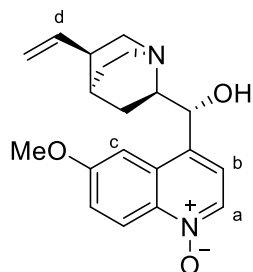
IR (ATR) 3269.34, 3051.39, 2966.52, 2927.54, 2854.65, 2791.00, 1670.35, 1575.84, 1523.76, 1489.05, 1367.53, 1271.09, 1203.58, 1182.36, 866.04, 823.60, 731.02 cm⁻¹.

HRMS (ESI/QTOF) *m/z*: [M + H]⁺ Calcd for C₁₅H₂₀N₃O₂ 274.1556; Found 274.1545



4-((R)-hydroxy((1S,2R,4S,5R)-5-vinylquinuclidin-2-yl)methyl)-6-methoxyquinoline 1-oxide

2.53



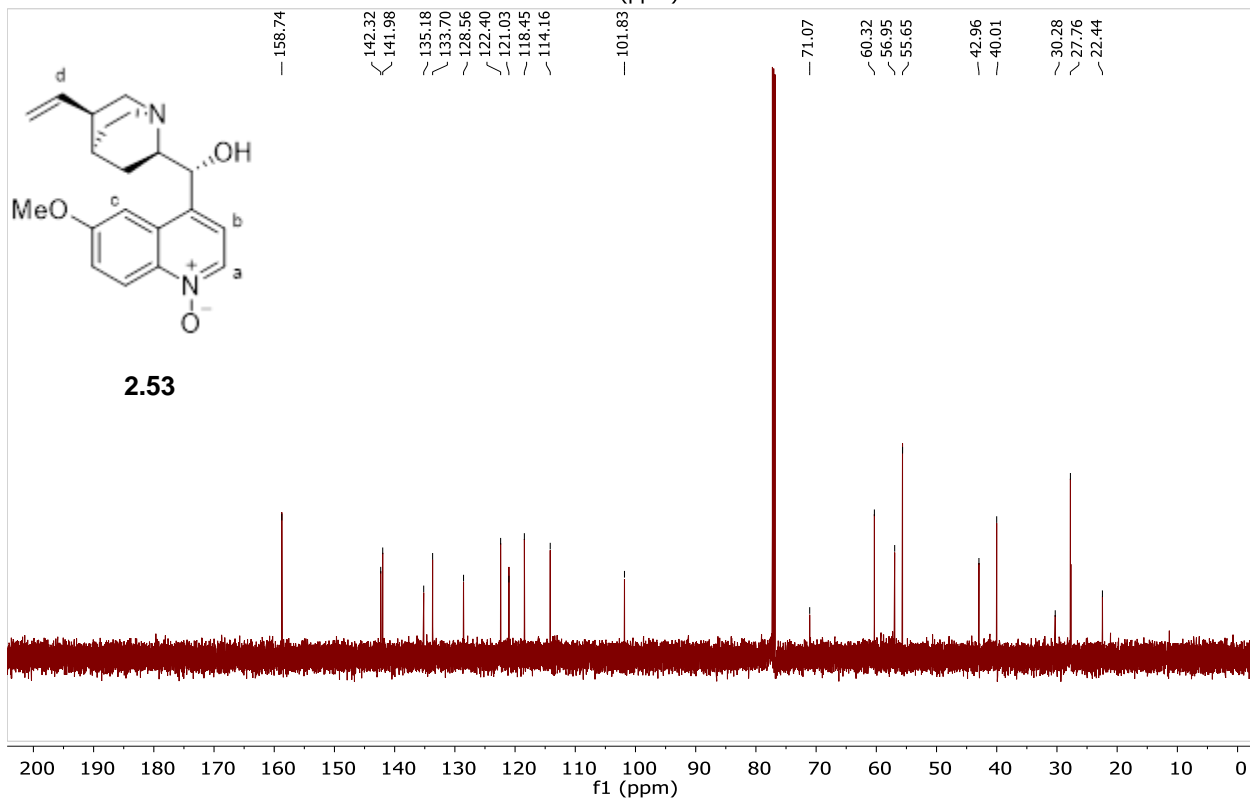
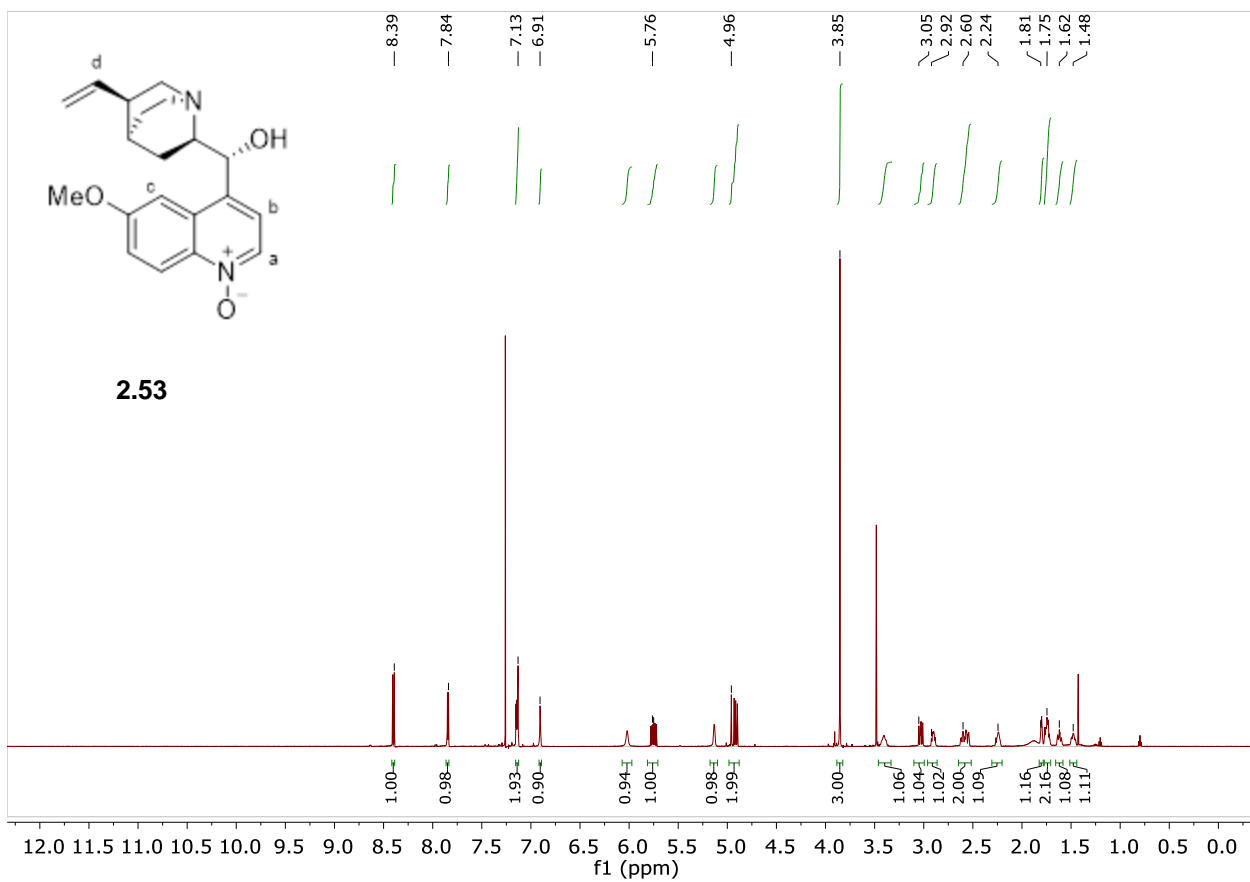
4-((R)-hydroxy((1S,2R,4S,5R)-5-vinylquinuclidin-2-yl)methyl)-6-methoxyquinoline 1-oxide was synthesized using general procedure A. The reaction mixture was purified after workup using alumina flash chromatography (10% MeOH/Et₂O) to give product as 0.930 mg of white solid. (.274 mmol 54% yield)

¹H NMR (600 MHz, CDCl₃) δ 8.35 (H_a, d, *J* = 9.5 Hz, 1H), 7.85 (ArH, d, *J* = 6.3 Hz, 1H), 7.14 (ArH, d, *J* = 6.3 Hz, 1H), 7.11 (H_b, dd, *J* = 9.5, 2.6 Hz, 1H), 6.82 (d, *J* = 2.6 Hz, 1H), 6.20 (H_c, s, 1H), 6.05-5.99 (m, 1H), 5.67 (H_d, ddd, *J* = 17.1, 10.4, 7.6 Hz, 1H), 5.18 – 5.11 (m, 1H), 4.96 – 4.89 (m, 2H), 3.85 (OMe, s, 3H), 3.45 – 3.37 (m, 1H), 3.00 (dd, *J* = 13.8, 10.1 Hz, 1H), 2.78 (td, *J* = 10.1, 9.0, 4.5 Hz, 1H), 2.62 – 2.55 (m, 1H), 2.53 – 2.49 (m, 1H), 2.23 – 2.19 (m, 1H), 1.82 – 1.69 (m, 3H), 1.51 – 1.44 (m, 1H) ppm.

¹³C NMR (150 MHz, CDCl₃) δ 158.6, 142.1, 141.8, 135.0, 133.5, 128.4, 122.3, 120.9, 118.3, 114.0, 101.7, 70.9, 60.1, 56.8, 55.5, 42.8, 39.8, 30.1, 27.6, 22.3 ppm.

IR (ATR) 3076.45, 2920.23, 1616.35, 1571.99, 1431.18, 1249.87, 1213.23, 1195.87, 1165.00, 1022.27, 829.39, cm⁻¹.

HRMS (ESI/QTOF) *m/z*: [M + H]⁺ Calcd for C₂₀H₂₅N₂O₃ 341.1865, found 341.1863



1.6 References

- (1) Wang, D.; Shuler, W. G.; Pierce, C. J.; Hilinski, M. K. An Iminium Salt Organocatalyst for Selective Aliphatic C–H Hydroxylation. *Org. Lett.*, **2016**, *18* (15), 3826–3829.
- (2) Atwell, G. J.; Rewcastle, G. W.; Baguley, B. C.; Denny, W. A. Potential Antitumor Agents. 50. In Vivo Solid-Tumor Activity of Derivatives of N-[2-(Dimethylamino)Ethyl]Acridine-4-Carboxamide. *J. Med. Chem.*, **1987**, *30* (4), 664–669.
- (3) Schmidt, R. G.; Bayburt, E. K.; Latshaw, S. P.; Koenig, J. R.; Daanen, J. F.; McDonald, H. A.; Bianchi, B. R.; Zhong, C.; Joshi, S.; Honore, P.; Marsh, K. C.; Lee, C.-H.; Faltynek, C. R.; Gomtsyan, A. Chroman and Tetrahydroquinoline Ureas as Potent TRPV1 Antagonists. *Bioorg. & Med. Chem. Lett.*, **2011**, *21* (5), 1338–1341.

Appendix Two:

Chapter Three Supporting Information

2.1 General Information

All reagents were obtained commercially in the highest available purity and used without further purification. Anhydrous solvents were obtained from an aluminum oxide solvent purification system. Flash column chromatography was performed using silica gel or alumina gel (230 - 400 mesh) purchased from Fisher Scientific. Elution of compounds was monitored by UV. ^1H and ^{13}C and ^{19}F NMR spectra were measured on a Varian Inova 600 (600 MHz) or Bruker Avance DRX 600 (600 MHz) or Bruker Avance III 800 (800 MHz) spectrometer and acquired at 300 K. Chemical shifts are reported in parts per million (ppm δ) referenced to the residual ^1H or ^{13}C resonance of the solvent. The following abbreviations are used singularly or in combination to indicate the multiplicity of signals: s - singlet, d - doublet, t - triplet, q - quartet, m - multiplet and br - broad.

2.2 General Procedures

Benzylic Alkylation General Procedure

Under N_2 atmosphere, benzyl nitrile (87.0 mmol, 1 eq.) was added into a 500 mL round bottom with a stir bar. Tetrahydrofuran (200 mL) was added and the suspension was gently mixed for 5 minutes and cooled to 0 °C. 60% sodium hydride (261 mmol, 3 eq) was weighed out and then added to the mixture carefully. The reaction stirred for 1 hour. Iodomethane or other alkyl halide (261 mmol, 3 eq) was added dropwise to the solution at 0°C and the solution stirred overnight. The reaction mixture was quenched with ice after cooling in an ice bath. The organic layer was extracted using 3x75 mL ethyl acetate, and the combined organics were washed with brine 75 mL. The resulting organic layers were combined, dried with sodium sulfate, concentrated on a rotary evaporator, and purified by flash chromatography as noted.

Nitrile Reduction General Procedure

Under N_2 atmosphere, Benzyl Nitrile (80 mmol, 1 eq) was dissolved in a 500 mL round bottom with a stir with tetrahydrofuran (200 ml). The solution was cooled to 0°C and 84 mL of 2.4 M solution of lithium aluminum hydride (200 mmol, 2.5 eq) was added by addition funnel. The solution was stirred overnight for 16 hours. The solution was cooled to 0C and diluted with 50 mL of diethyl ether. The solution was quenched with water and basified with 3M NaOH (50 mL) and stirred for 15 minutes. Another 50 mL of water was added and 2g of magnesium sulfate and stirred for additional 15 minutes. The solution was filtered off and subsequently extracted. The aqueous layer was extracted using 3x 100mL diethyl ether, combined organics were washed with brine. The combined organic layer was dried with sodium sulfate, and concentrated on a rotary evaporator. The resulting amines were carried on crude after running on GC-MS or by TLC to verify reduction of nitrile and further purified on the next step.

Aniline Formation General Procedure

A round-bottomed flask was charged with $\text{Pd}_2(\text{dba})_3$ (2 mol%), (\pm)-BINAP (4 mol%), and toluene (6 mL). The resulting solution was degassed for 10 min before being heated to 110 °C for 15 min. The reaction mixture was allowed to cool to r.t. before $\text{NaO}t\text{-Bu}$ (1.86 eq), the aryl bromide (1 eq), and amine (2 eq) were added. The resulting mixture was heated under reflux for 16 h, before being cooled to r.t. and filtered through a pad of Celite[®]. Solvents were removed under

reduced pressure and the crude material purified by column chromatography. Adapted from literature conditions.¹

Acetamide Formation General Procedure

Under N₂ atmosphere, the amine (50 mmol, 1 eq) was mixed with anhydrous dichloromethane (65 mL) in a 250 mL flask with stirring bar. Pyridine (90 mmol, 1.2 eq) was added to the stirring solution via syringe before an anhydride or acyl chloride (60 mmol, 1.1 eq) was added dropwise. The reaction mixture was stirred at room temperature overnight. The light brown solution was washed with brine, dried over sodium sulfate, and concentrated under vacuum. The residue was purified by flash chromatography as noted.

Bischler Napieralski Cyclization General Procedures:

General Procedure A for Bischler Napieralski

Under N₂ atmosphere, acetamide (15.5 mmol 1 eq), 2-chloropyridine (18.6 mmol, 1.2 eq), and anhydrous dichloromethane (75 mL) were mixed in a 250 mL two-neck flask equipped with condenser and stirring bar. The solution was cooled to -78 °C using a dry ice/acetone bath and then trifluoromethanesulfonic anhydride (17.1 mmol, 1.2 eq) was added dropwise. The solution was maintained at -78°C for 3 hours and allowed to warm to room temperature. The mixture was then warmed to 45°C and the stirring was continued for two days. The reaction mixture was cooled to room temperature before triethylamine (4.8 mL) was introduced carefully to quench the reaction. The dark solution was washed with brine, dried over sodium sulfate, and concentrated under vacuum to obtain crude product, which was purified by flash chromatography as noted.

General Procedure B for Bischler Napieralski

Under N₂ atmosphere, phosphorus pentoxide (1.5 mmol, 1.5 eq) was added to a 2-neck round bottom flask. Half the volume of phosphorus oxychloride (2.5 mmol, 2.5 eq) was added to the solution and heated to 70°C, then immediately to 120°C. The acetamide (1 mmol, 1 eq) was dissolved in half the volume (2.5 mmol, 2.5 eq) of phosphorus oxychloride and added to the solution, carefully. The solution was further heated to 150°C and let stir for 5 hours or until completion. The solution was subsequently cooled to room temperature and carefully quenched diluted with 5 mL of dichloromethane and quenched with warm water in a separate flask. The solution was basified with triethylamine. The aqueous layer was extracted with 3x 2mL of dichloromethane and the combined organic layers were washed with brine. The organic layer was dried with magnesium sulfate, filtered, and concentrated under vacuum. The residue was purified by flash chromatography as noted.

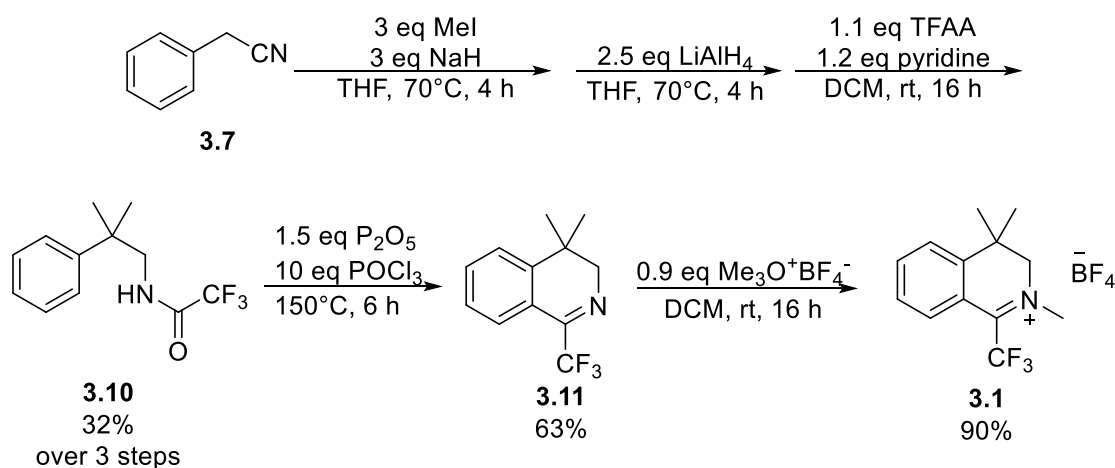
General Procedure C for Bischler Napieralski

Under N₂ atmosphere, phosphorus oxychloride (5 eq) was added to a solution of acetamide (1 mmol, 1 eq) dissolved in acetonitrile (30 mL). The reaction was heated to 80 °C and let stir for 16 hours and then cooled to r.t. The resulting reaction mixture was extracted with dichloromethane. The combined organic layers were dried over MgSO₄, filtrated and the solvent removed under reduced pressure. Adapted from Lit. Conditions.²¹

Imine Methylation General Procedure

In a nitrogen glovebox, to a solution of imine (2.2 mmol, 1 eq) in anhydrous dichloromethane (4 mL) was added trimethyloxonium tetrafluoroborate (2.0 mmol, .9 eq). The mixture was stirred at room temperature for 15 hours, then removed from the glovebox. The solvent was removed under vacuum and the resulting solid was washed with anhydrous diethyl ether (5 mL) and dried under high vacuum to give pure product.

2.3 Improved Parent Iminium Synthesis Procedure



Under N₂ atmosphere, benzyl nitrile (5.7 mL, 50 mmol, 1 eq.) was added into a flame dried round bottom with a stir bar. Tetrahydrofuran (125 mL, 0.4 M) was added and the suspension was gently mixed for 5 minutes and cooled to 0 °C. 60% sodium hydride (150 mmol, 6.0 g, 3 eq) was weighed out and then added to the mixture carefully. The reaction stirred for 1 hour. Iodomethane (150 mmol, 9.34 mL, 3 eq) was added dropwise to the solution at 0 °C and the solution was heated to 70 °C for 4 hours. The reaction mixture was quenched with ice after cooling down to 0 °C in an ice bath. The organic layer was extracted using ethyl acetate, and the combined organics were washed with brine. The resulting organic layers were combined, dried with sodium sulfate, concentrated on a rotary evaporator, and carried onto the next step.

Under N₂ atmosphere, crude benzyl nitrile (50 mmol, 1 eq) was dissolved in a round bottom with a stir bar with tetrahydrofuran (125 mL, 0.4 M). The solution was cooled to 0 °C and 2.4 M solution of Lithium Aluminum Hydride (125 mmol, 52 mL 2.5 eq) was added by addition funnel. The solution was heated to 70 °C and stirred for 4 hours. The solution was worked-up following the Fieser Method and concentrated. The resulting amines were carried on crude after running on GC-MS or by TLC to verify reduction of nitrile.

Under N₂ atmosphere, the crude amine (20.1 mmol, 3.00 g, 1 eq) was mixed with anhydrous dichloromethane (250 mL, .08M) in a flask with stirring bar. Pyridine (24.3 mmol, 1.94 mL, 1.2 eq) was added to the stirring solution via syringe before trifluoroacetic anhydride (22.1 mmol, 3.12 mL, 1.1 eq) was added dropwise. The reaction mixture was stirred at room temperature overnight or until done by TLC. The light brown solution was washed with brine, dried over sodium sulfate, and concentrated under vacuum. The residue was purified by flash chromatography with 20% ethyl acetate/hexanes to give a white solid (3.94 g, 16.1 mmol, 32% yield over 3 steps).

Under N₂ atmosphere, phosphorus pentoxide (6.85 g, 24.1 mmol, 1.5 eq) was added to a 2-neck round bottom flask. Half the volume of phosphorus oxychloride (161 mmol, 14.6 mL, 2.5 eq) was added to the solution and heated to 70 °C, then immediately heated to 120 °C. The acetamide (16.1 mmol, 3.94 g, 1 eq) was dissolved in a half volume (2.5 eq) of phosphorus oxychloride and added to the solution, carefully. The solution was further heated to 150°C and let stir for 5 hours. The solution was subsequently cooled to room temperature and carefully diluted with 5 mL of dichloromethane and quenched with warm water in a separate flask. The solution's PH was adjusted 8 with triethylamine, carefully. The aqueous layer was extracted with dichloromethane and the combined organic layers were washed with brine. The organic layer was dried with magnesium sulfate, filtered, and concentrated under vacuum. The residue was purified by flash chromatography 2% diethyl ether/hexanes to give a yellow oil (10.2 mmol, 2.32 g, 63% yield)

In a nitrogen glovebox, to a solution of imine (1 mmol, 0.227 g 1 eq) in anhydrous dichloromethane (2 mL, .5M) was added trimethyloxonium tetrafluoroborate (0.9 mmol, 0.133 g 0.9 eq). The mixture was stirred at room temperature for 15 hours, then removed from the glovebox. The solvent was removed under vacuum and the resulting solid was washed with anhydrous diethyl ether (5 mL) and dried under high vacuum to give product. Product was further purified by recrystallization from dichloromethane and diethyl ether and subsequent trituration to give a white solid (0.81 mmol, 0.266 g, 90% yield).

2.4 Substrate Screening

Hydroxylation Substrate Screening General Procedure:

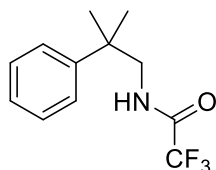
50% H₂O₂ (360 uL, 3.2 mmol, 16 equiv) was added to substrate (0.2 mmol, 1 equiv), iminium salt catalyst (20 mol%, 0.04 mmol), and HFIP (200 uL) and stirred at room temperature for 18 hours. The mixture was quenched with 2M aqueous Na₂S₂O₃ and extracted with EtOAc (1mL). 15 uL of n-dodecane was used as an internal standard and added to the organic extract before the sample was analyzed on a GC-FID.

Amination Substrate Screening General Procedure:

In a nitrogen glovebox at room temperature, the substrate (0.2 mmol, 1 equiv), iodine (0.4 mmol, 2 equiv) and iminium (0.04 mmol, 0.2 equiv) were combined in a vial equipped with a stir bar. Anhydrous dichloromethane (0.8 mL) was then added and the reaction was stirred at room temperature for 20 hours. The reaction mixture was then filtered through a silica gel plug, eluting with EtOAc. After removal of the solvent under reduced pressure, the crude reaction mixture was then purified on silica gel with 10-20% ethyl acetate in hexanes.

2.5 Compounds

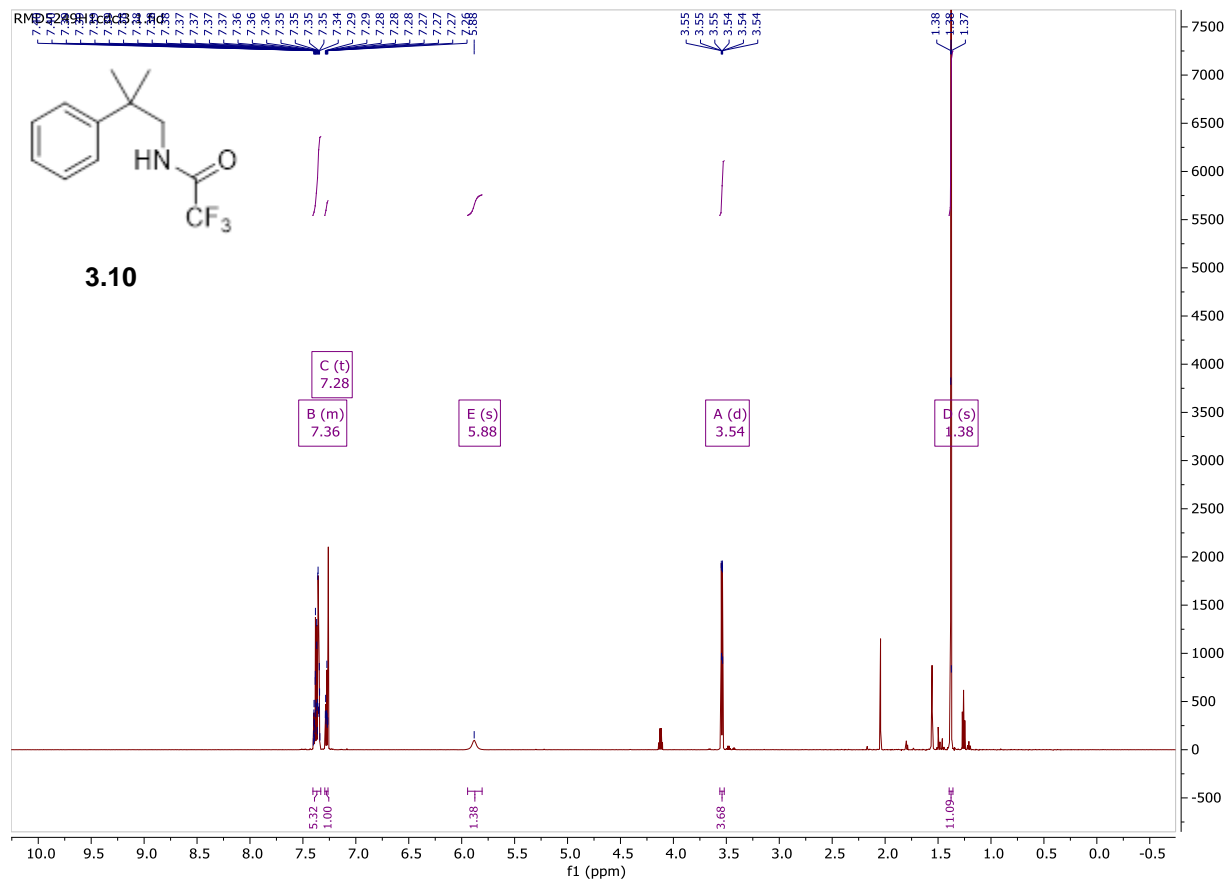
2,2,2-trifluoro-N-(2-methyl-2-phenylpropyl)acetamide (3.10)



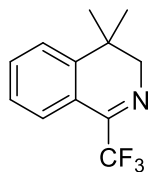
2,2,2-trifluoro-N-(2-methyl-2-phenylpropyl)acetamide was synthesized following the improved parent iminium synthesis procedure using 2-methyl-2-phenylpropan-1-amine as the respective amine.

$^1\text{H NMR}$ (600 MHz, CDCl_3) δ 7.41 – 7.33 (m, 4H), 7.28 (t, $J = 7.1$ Hz, 1H), 5.88 (s, 1H), 3.54 (d, $J = 6.2$ Hz, 2H), 1.38 (s, 6H) ppm.

Spectra are consistent with previous reports.³



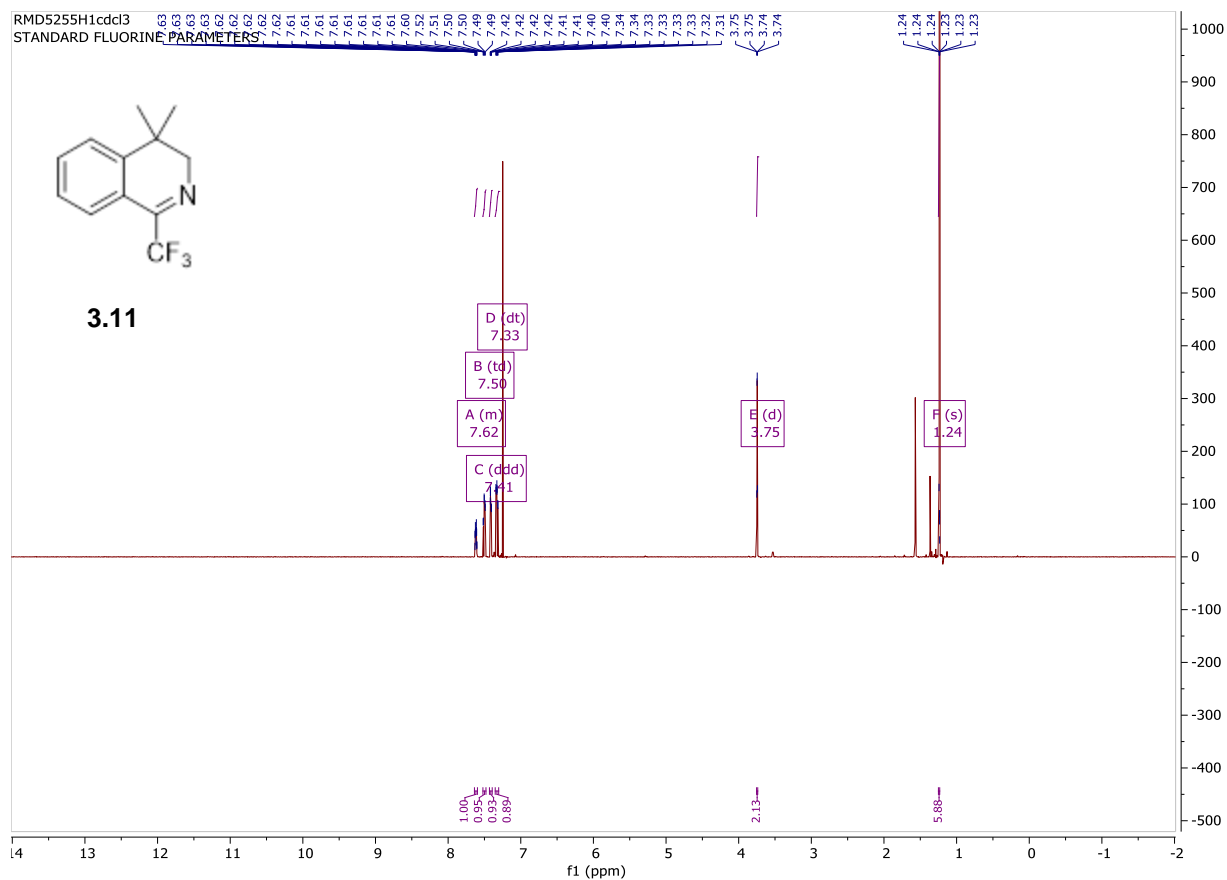
4,4-dimethyl-1-(trifluoromethyl)-3,4-dihydroisoquinoline (3.11)



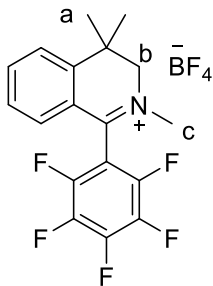
4,4-dimethyl-1-(trifluoromethyl)-3,4-dihydroisoquinoline was synthesized following the improved parent iminium synthesis procedure using 2,2,2-trifluoro-N-(2-methyl-2-phenylpropyl)acetamide as the respective acetamide.

Spectra are consistent with previous reports.³

$^1\text{H NMR}$ (600 MHz, CDCl_3) δ 7.64 – 7.60 (m, 1H), 7.50 (td, $J = 7.6$ Hz, 1H), 7.41 (dd, $J = 7.8$ Hz, 1H), 7.33 (dt, $J = 7.8$ Hz, 1H), 3.75 (q, $J = 1.9$ Hz, 2H), 1.24 (s, 6H) ppm.



2,4,4-trimethyl-1-(perfluorophenyl)-3,4-dihydroisoquinolin-2-ium tetrafluoroborate (3.17)



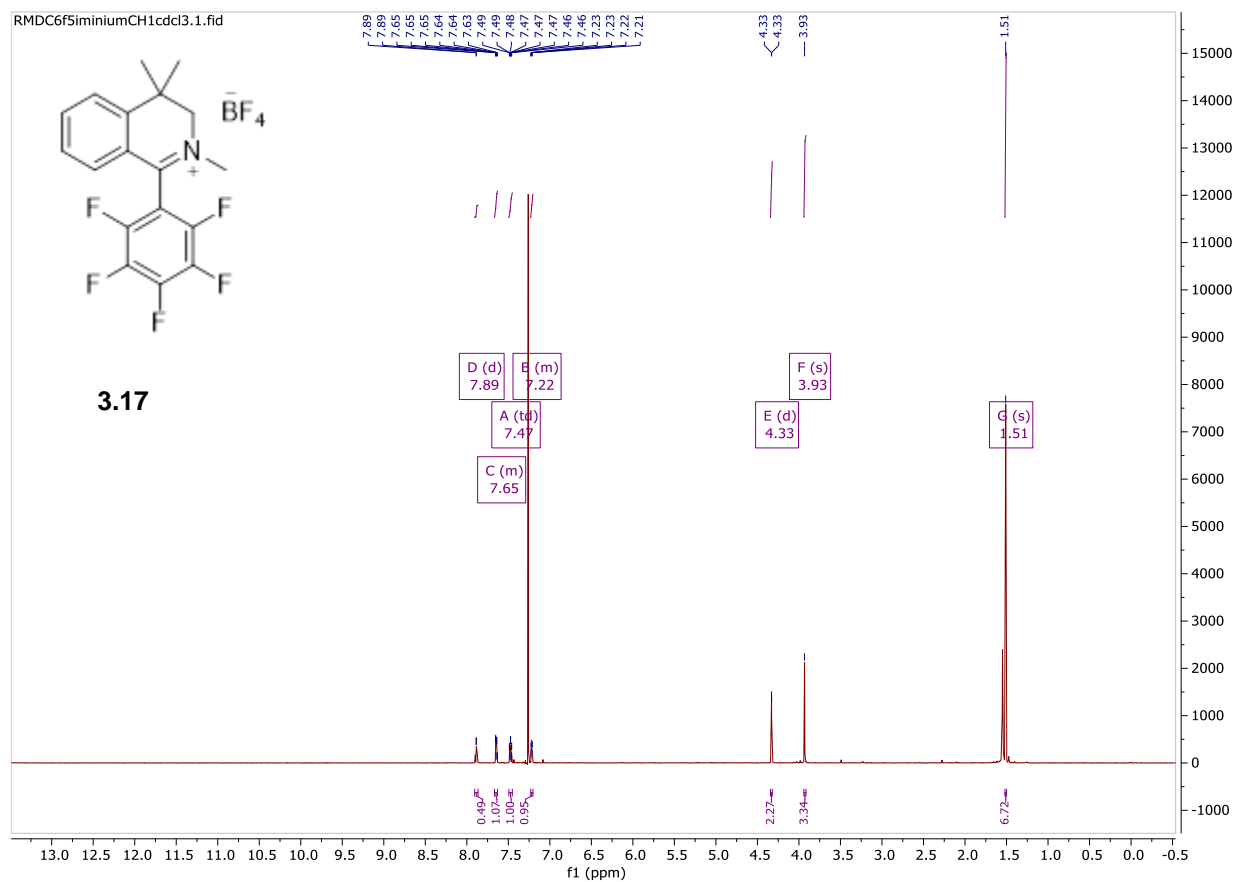
2,4,4-trimethyl-1-(perfluorophenyl)-3,4-dihydroisoquinolin-2-ium tetrafluoroborate was synthesized following general procedure for imine methylation on a 1.23 mmol scale using 4,4-dimethyl-1-(perfluorophenyl)-3,4-dihydroisoquinoline, as the respective imine, to give 0.468 g of an off white solid (1.10 mmol, 89% yield).

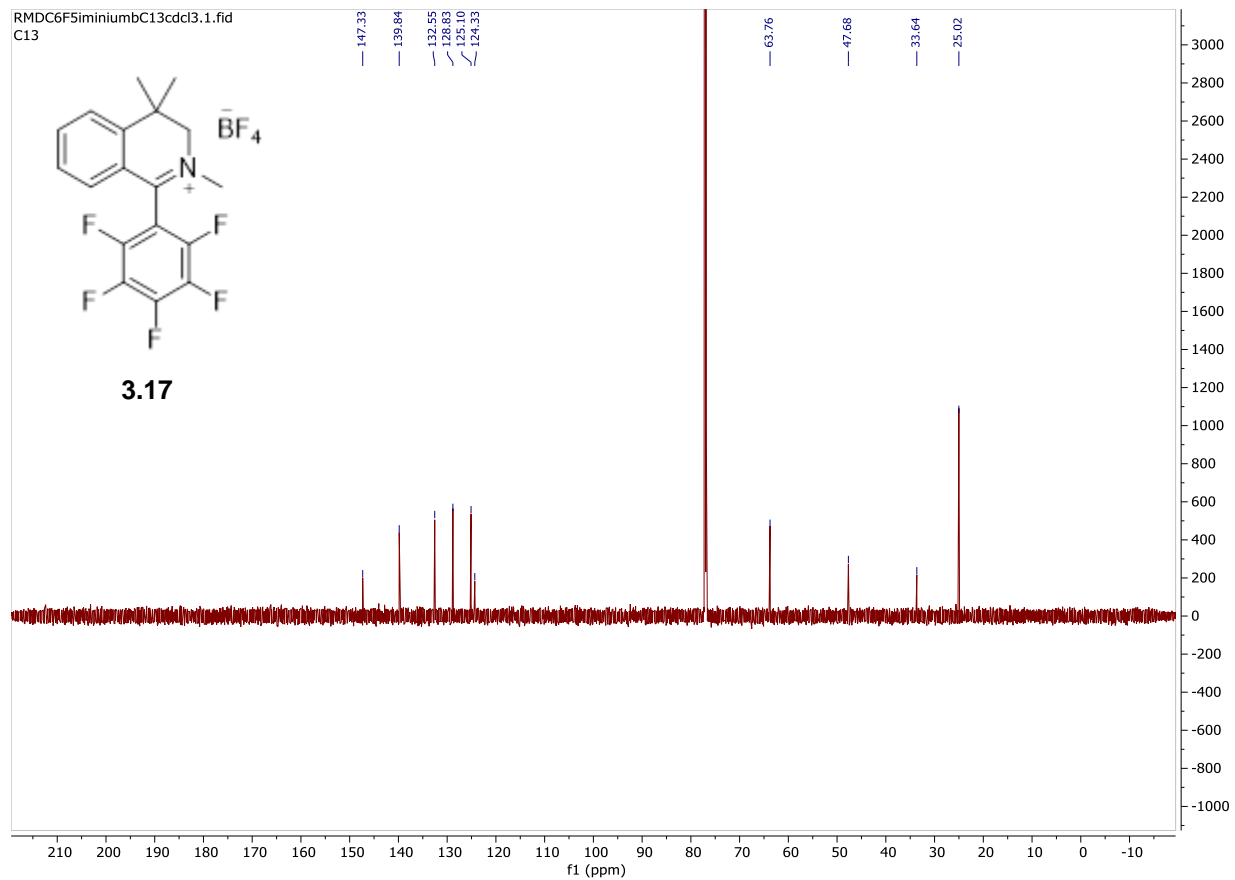
¹H NMR (600 MHz, CDCl₃) δ 7.89 (d, *J* = 1.3 Hz, 1H), 7.67 – 7.63 (m, 1H), 7.47 (td, *J* = 7.7, 1.1 Hz, 1H), 7.23 – 7.20 (m, 1H), 4.33 (H_b, d, *J* = 0.9 Hz, 2H), 3.93 (H_c, s, 3H), 1.51 (H_a, s, 6H) ppm.

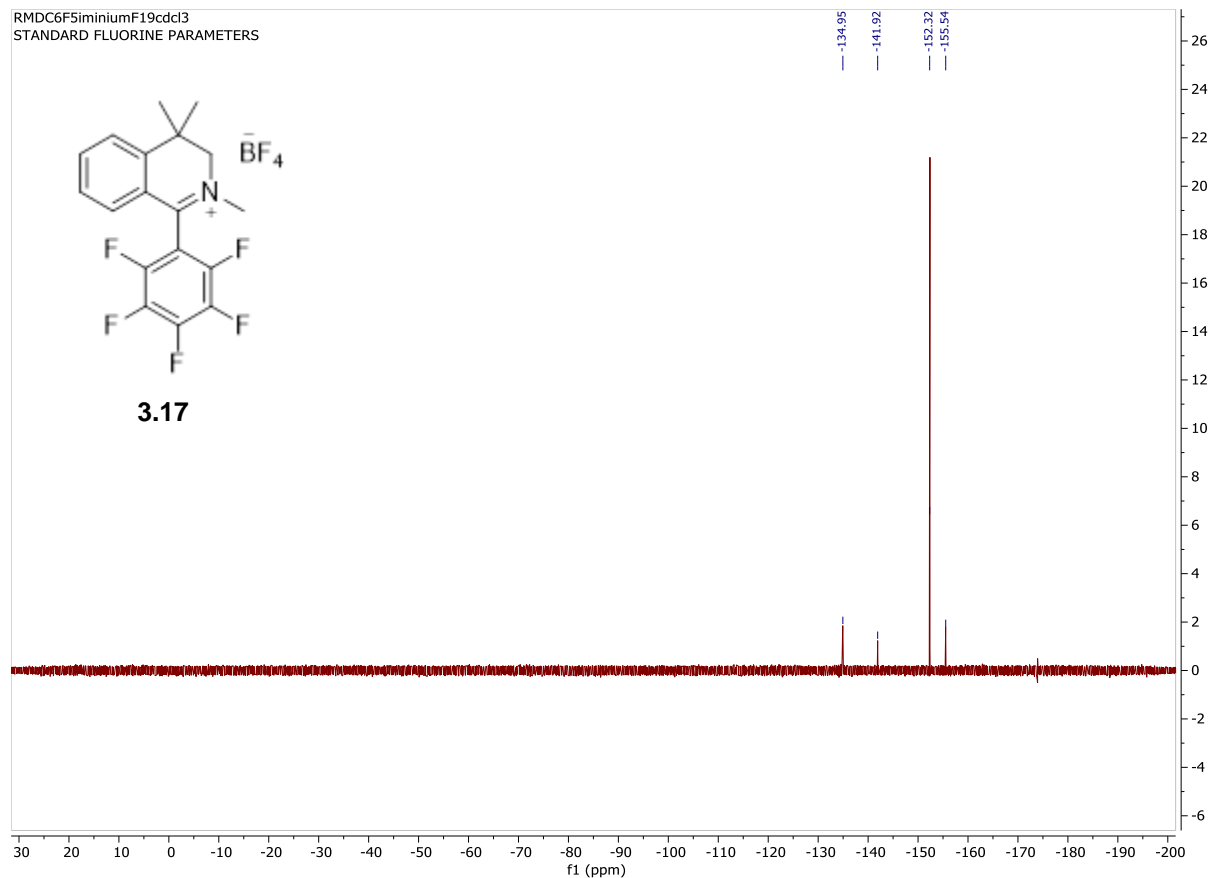
¹³C NMR (201 MHz, CDCl₃) δ 147.3, 139.8, 132.5, 128.8, 125.1, 124.3, 63.7, 47.6, 33.6, 25.0 ppm.

¹⁹F NMR (564 MHz, CDCl₃) δ -134.95, -141.92, -152.32, -155.54 ppm.

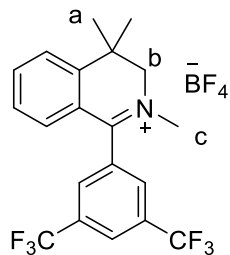
HRMS Calc'd for C₁₈H₁₅F₅N (M): 340.1125 Found: 340.1129







1-(3,5-bis(trifluoromethyl)phenyl)-2,4,4-trimethyl-3,4-dihydroisoquinolin-2-ium tetrafluoroborate (3.18)



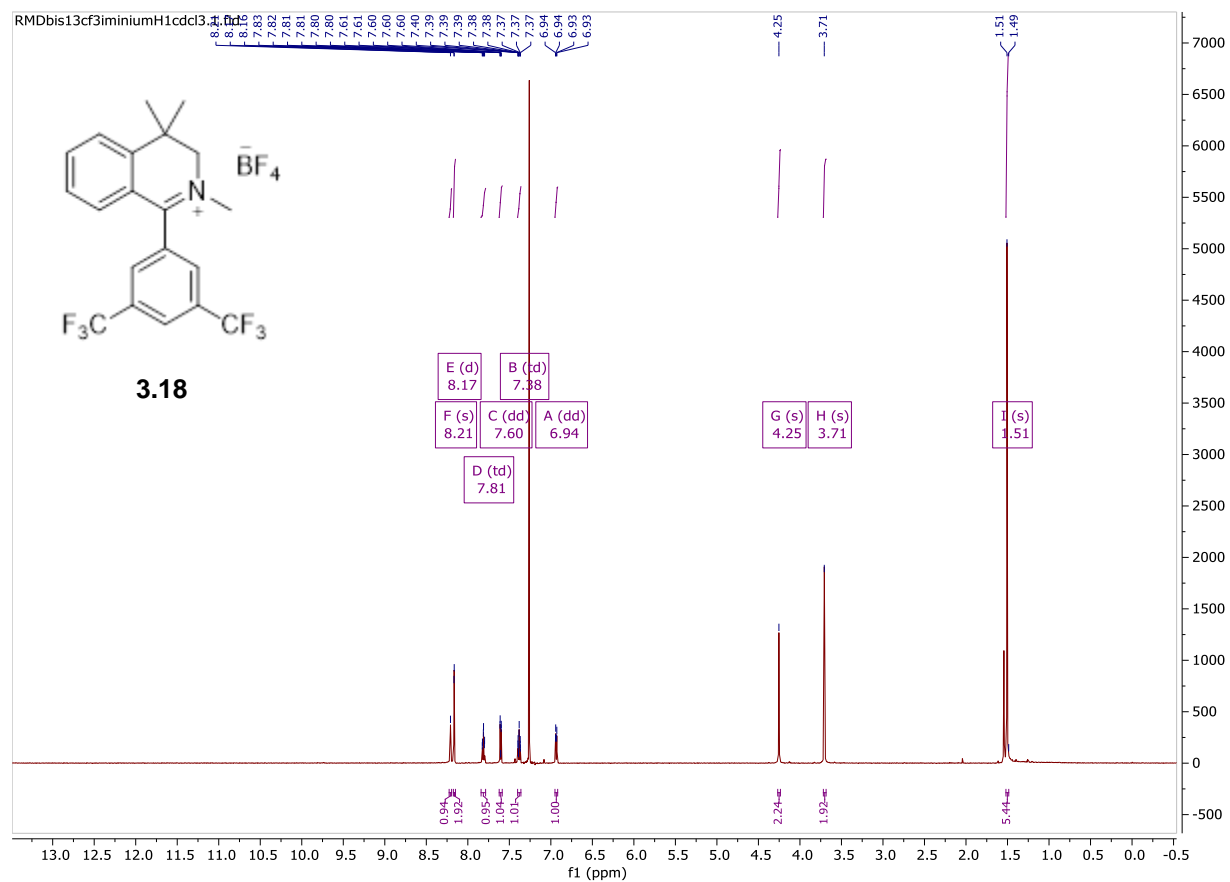
1-(3,5-bis(trifluoromethyl)phenyl)-2,4,4-trimethyl-3,4-dihydroisoquinolin-2-ium tetrafluoroborate was synthesized following general procedure for imine methylation on a 2.26 mmol scale using 1-(3,5-bis(trifluoromethyl)phenyl)-4,4-dimethyl-3,4-dihydroisoquinoline, as the respective imine, to give .748 g of an off white solid (1.58 mmol, 70% yield).

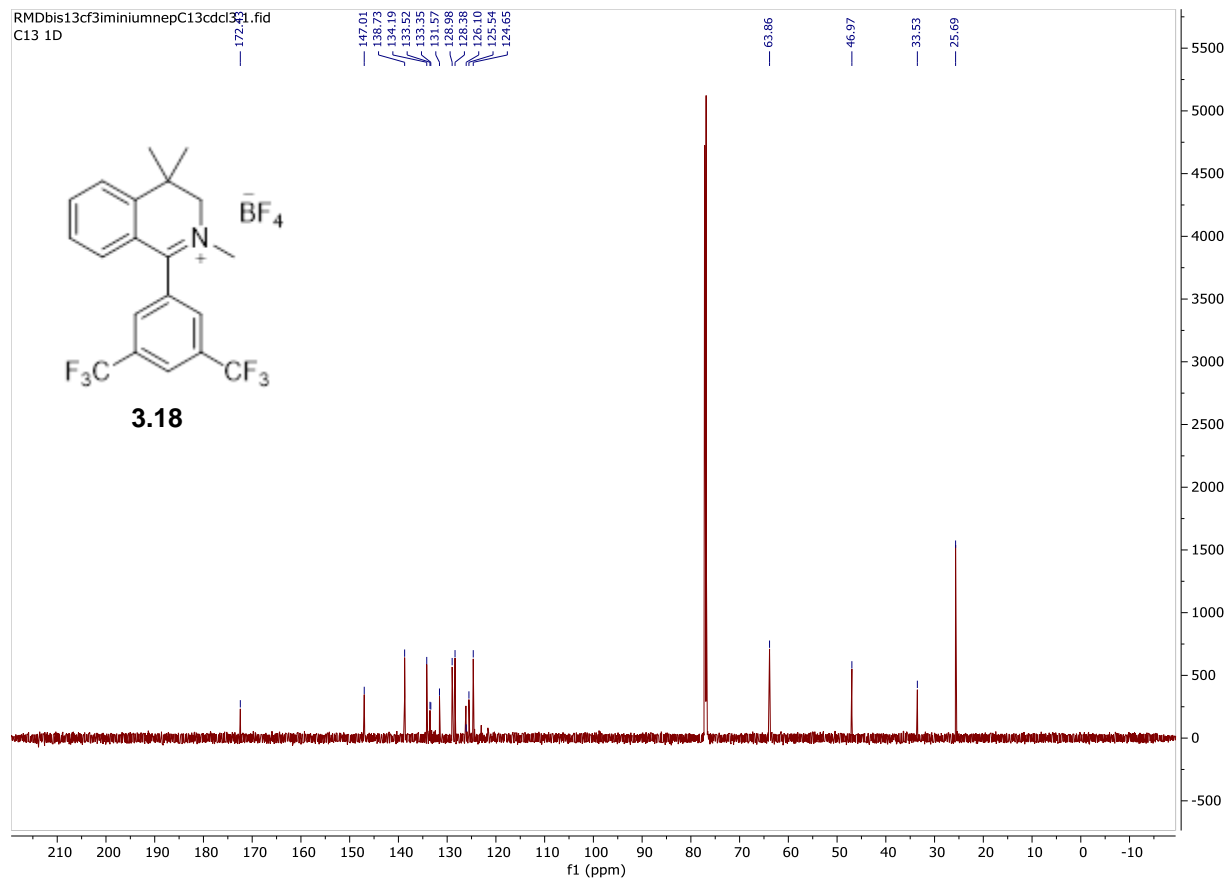
¹H NMR (600 MHz, CDCl₃) δ 8.21 (s, 1H), 8.17 (d, *J* = 1.5 Hz, 2H), 7.81 (td, *J* = 7.6, 1.3 Hz, 1H), 7.60 (dd, *J* = 7.8, 1.1 Hz, 1H), 7.38 (td, *J* = 7.6, 1.1 Hz, 1H), 6.94 (dd, *J* = 8.0, 1.3 Hz, 1H), 4.25 (H_c, s, 3H), 3.71 (H_b, s, 2H), 1.51 (H_a, s, 6H) ppm.

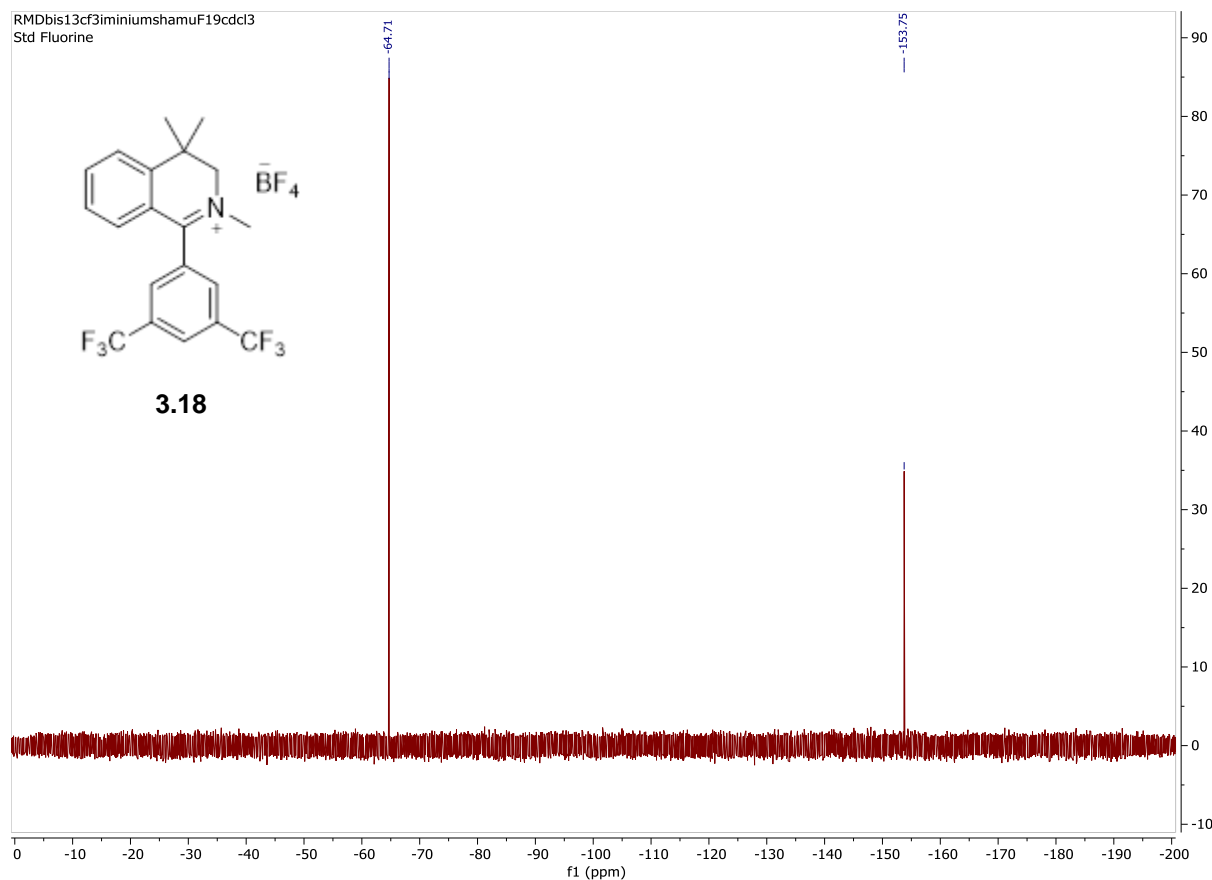
¹³C NMR (201 MHz, CDCl₃) δ 172.4, 147.0, 138.7, 134.1, 133.52, 133.35, 131.7, 128.98, 128.38, 126.1, 125.5, 124.6, 63.8, 46.9, 33.5, 25.6 ppm.

¹⁹F NMR (564 MHz, CDCl₃) δ -64.71, -153.75 ppm.

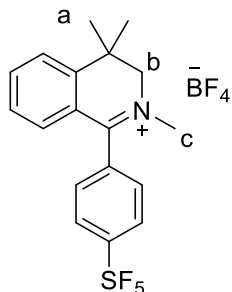
HRMS Calc'd for C₂₀H₁₈F₆N (M): 386.1338 Found: 386.1346







2,4,4-trimethyl-1-(4-(pentafluoro-*l*-6-sulfaneyl)phenyl)-3,4-dihydroisoquinolin-2-ium tetrafluoroborate (3.19)



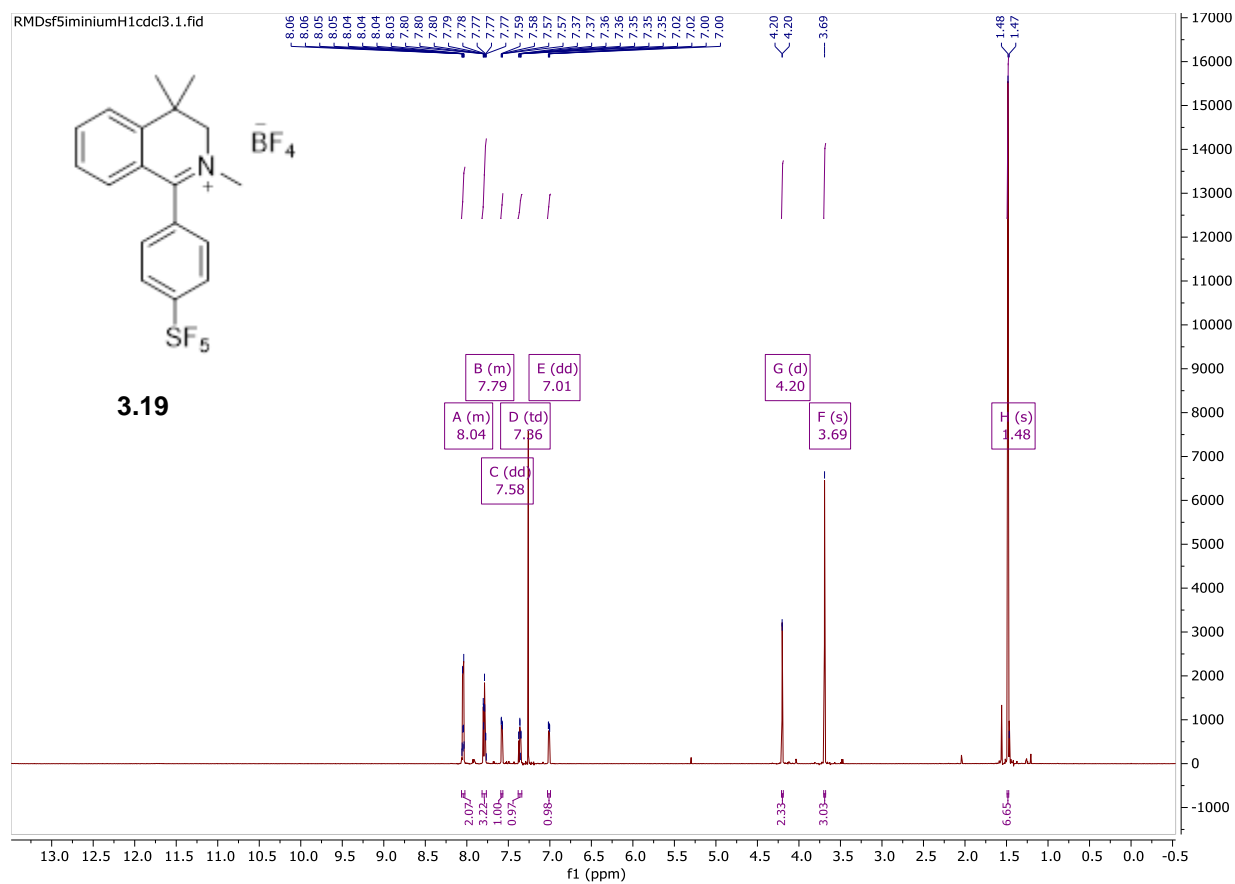
2,4,4-trimethyl-1-(4-(pentafluoro-*l*-6-sulfaneyl)phenyl)-3,4-dihydroisoquinolin-2-ium tetrafluoroborate was synthesized following general procedure for imine methylation on a 1.64 mmol scale using 4,4-dimethyl-1-(4-(pentafluoro-*l*-6-sulfaneyl)phenyl)-3,4-dihydroisoquinoline, as the respective imine, to give 0.690 g of an off white solid (1.49 mmol, 91% yield).

¹H NMR (600 MHz, CDCl₃) δ 8.06 – 8.02 (m, 2H), 7.82 – 7.76 (m, 3H), 7.58 (dd, *J* = 7.9, 1.1 Hz, 1H), 7.36 (td, *J* = 7.7, 1.1 Hz, 1H), 7.01 (dd, *J* = 7.9, 1.3 Hz, 1H), 4.20 (H_{b,d}, *J* = 0.8 Hz, 2H), 3.69 (H_c, s, 3H), 1.48 (H_a, s, 6H) ppm.

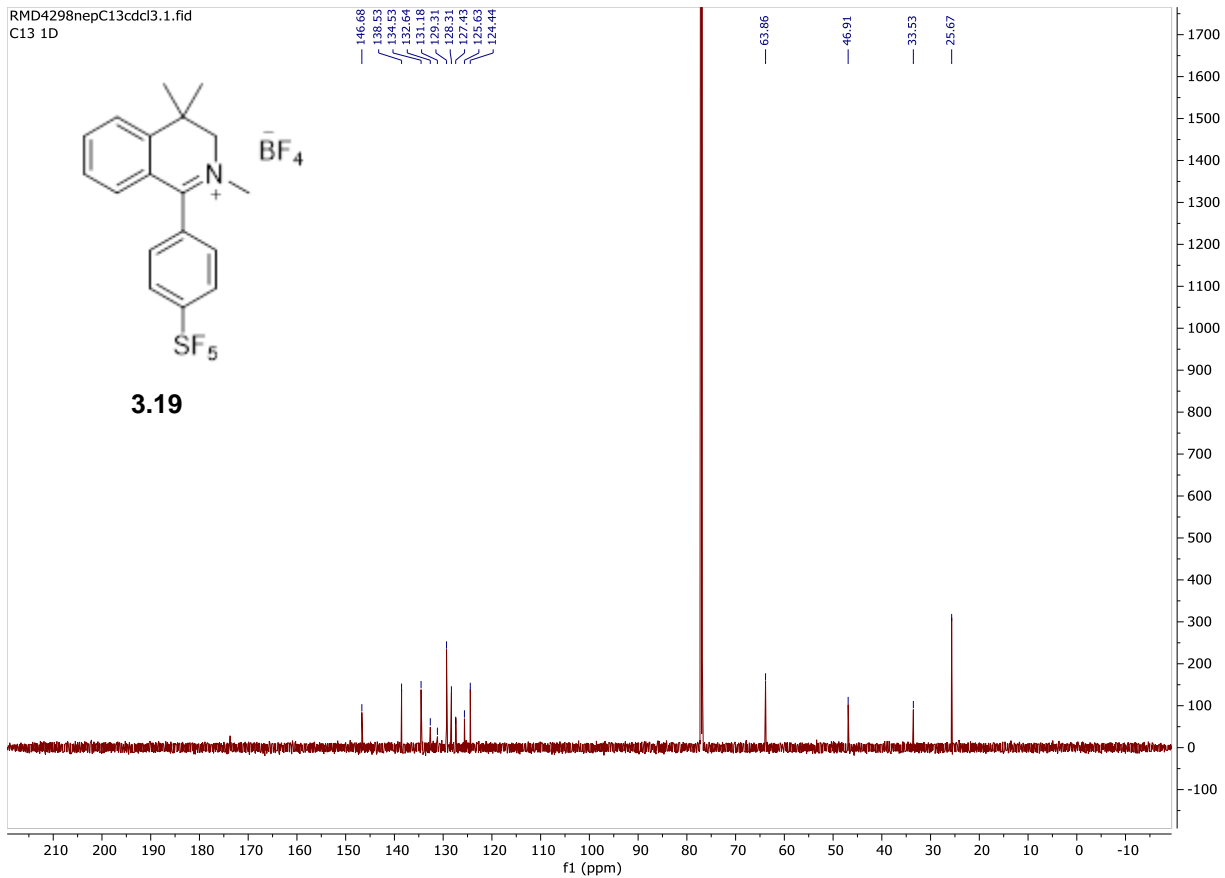
¹³C NMR (201 MHz, CDCl₃) δ 146.6, 138.5, 134.5, 132.6, 131.1, 129.3, 128.3, 127.4, 125.6, 124.4, 63.8, 46.9, 33.5, 25.6 ppm.

^{19}F NMR (564 MHz, CDCl_3) δ 81.81, 81.54, 81.27, 62.51, 62.24, -152.22 ppm.

HRMS Calc'd for $\text{C}_{18}\text{H}_{19}\text{F}_5\text{NS}$ (M): 376.1153 Found: 376.1157



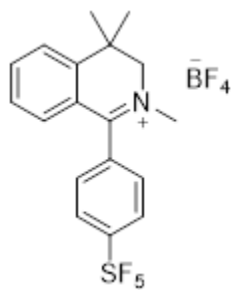
RMD4298nepC13cdcl3.1.fid
C13 1D



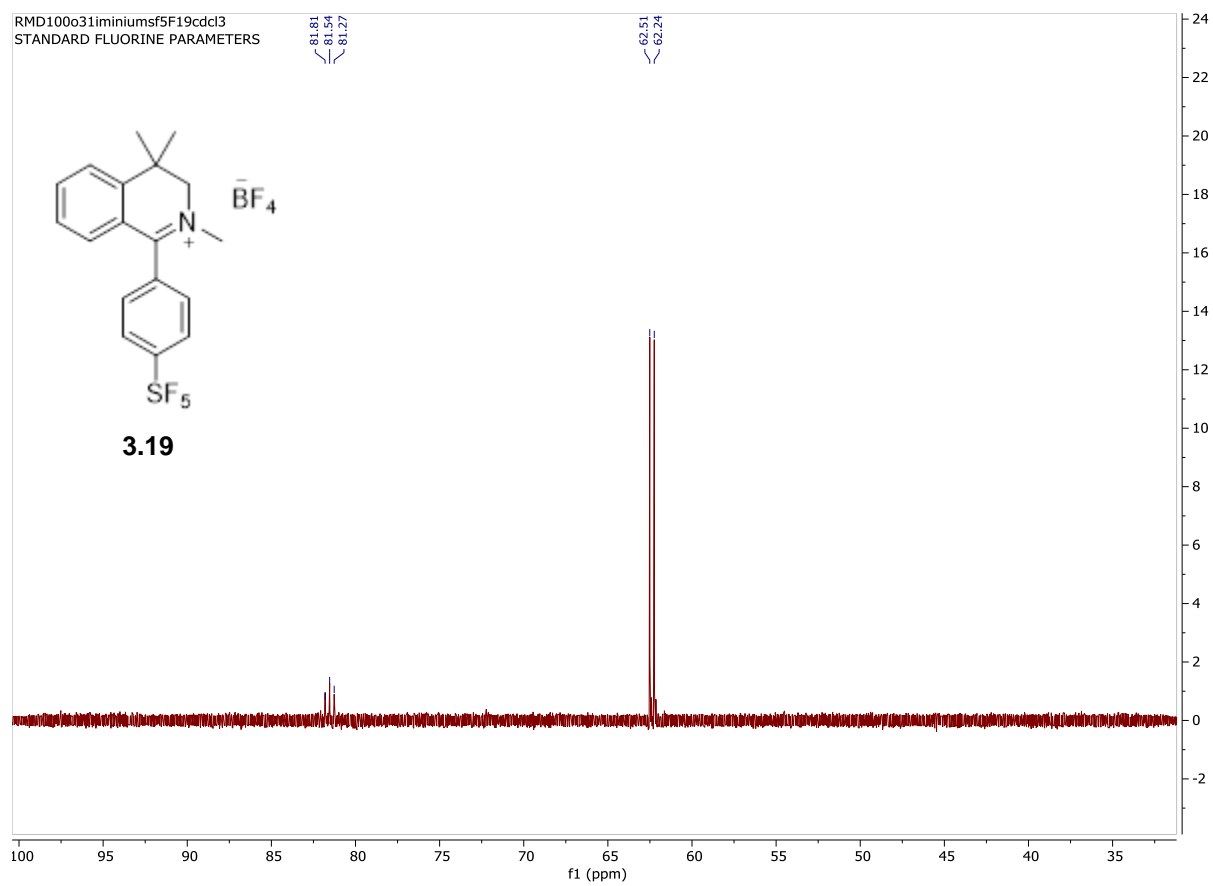
RMD100o31iminiumsf5F19cdcl3
STANDARD FLUORINE PARAMETERS

81.81
81.54
81.27

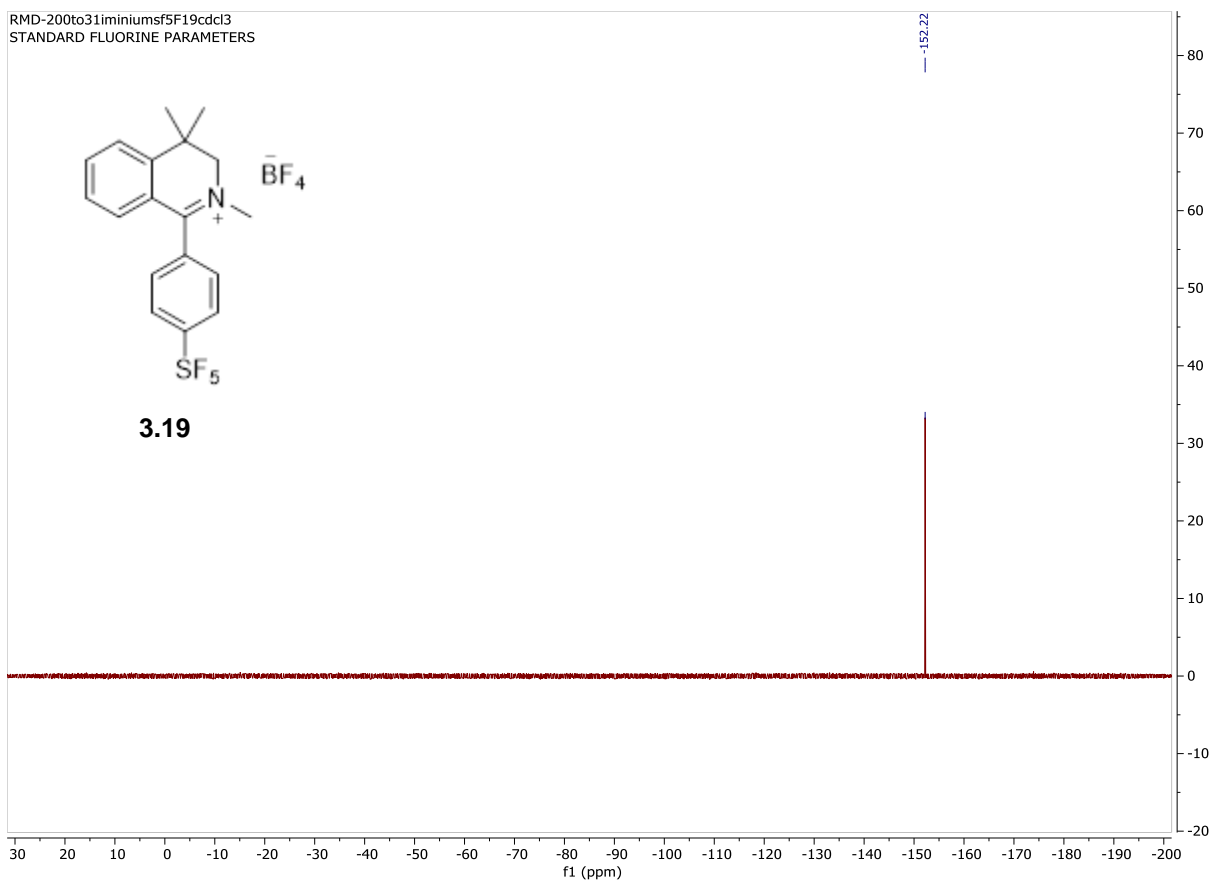
62.51
62.24



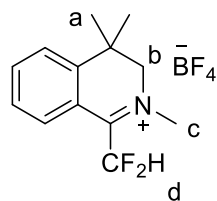
3.19



RMD-200to31iminiums5F19cdcl3
STANDARD FLUORINE PARAMETERS



1-(difluoromethyl)-2,4,4-trimethyl-3,4-dihydroisoquinolin-2-ium (3.20)



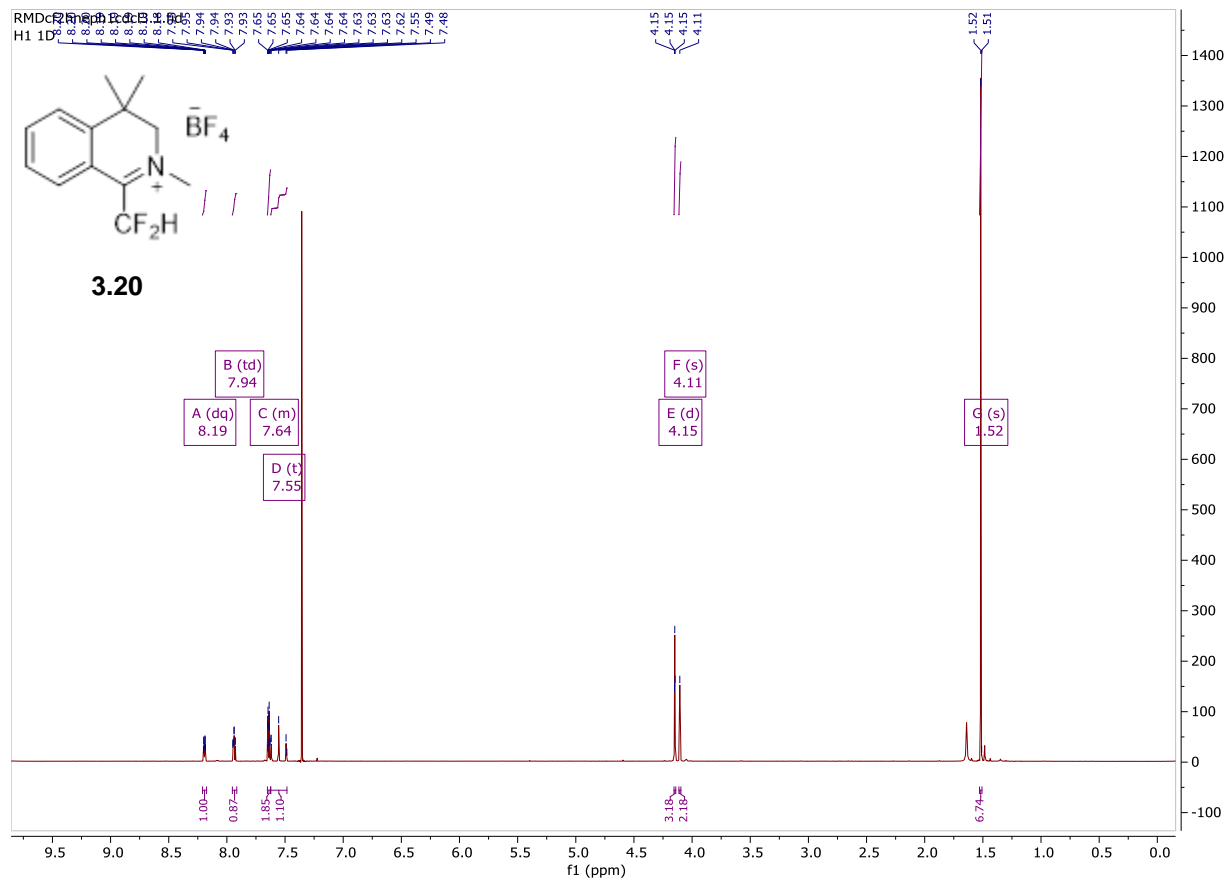
1-(difluoromethyl)-2,4,4-trimethyl-3,4-dihydroisoquinolin-2-ium tetrafluoroborate was synthesized following general procedure for imine methylation a 2.61 mmol scale using 1-(difluoromethyl)-4,4-dimethyl-3,4-dihydroisoquinoline, as the respective imine, to give 0.560 g of an off white solid (1.79 mmol, 82% yield).

¹H NMR (800 MHz, CDCl₃) δ 8.19 (dq, *J* = 8.0, 1.6 Hz, 1H), 7.94 (td, *J* = 7.7, 1.2 Hz, 1H), 7.65 – 7.62 (m, 2H), 7.55 (H_d, t, *J* = 50.9 Hz, 1H), 4.15 (H_c, s, *J* = 1.9 Hz, 3H), 4.11 (H_b, s, 2H), 1.52 (H_a, s, 6H) ppm.

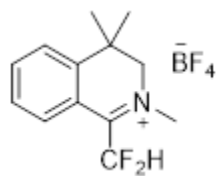
¹³C NMR (201 MHz, CDCl₃) δ 147.2, 139.0, 132.2, 128.2, 124.5, 121.7, 110.1, 108.9, 107.6, 64.9, 46.7, 33.4, 25.0 ppm.

¹⁹F NMR (564 MHz, CDCl₃) δ -117.41, -152.09 ppm.

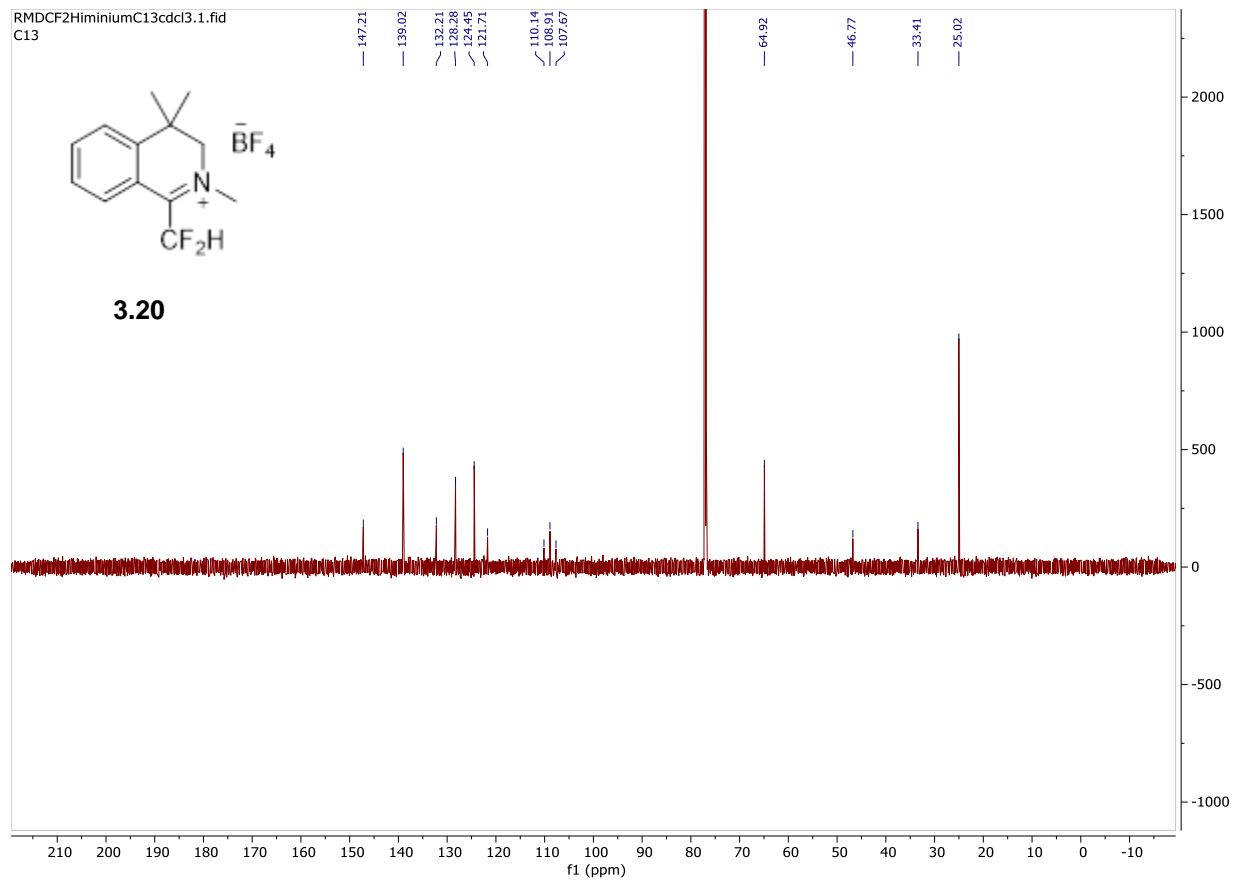
HRMS Calc'd for C₁₃H₁₆F₂N (M): 224.1245 Found: 224.1247

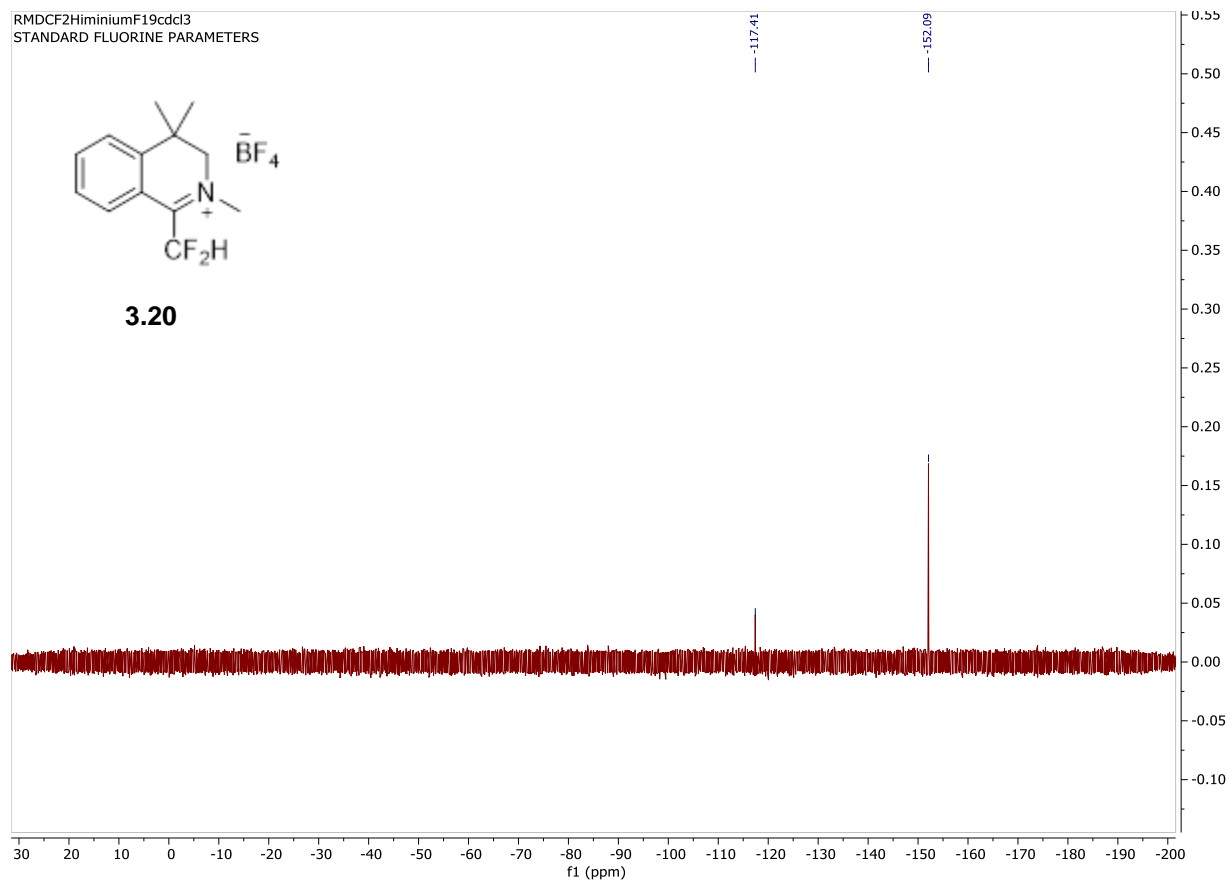


RMDCF2HiminiumC13cdcl3.1.fid
C13

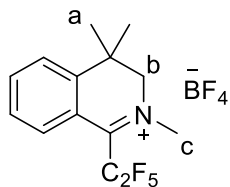


3.20





2,4,4-trimethyl-1-(perfluoroethyl)-3,4-dihydroisoquinolin-2-ium tetrafluoroborate (3.21)



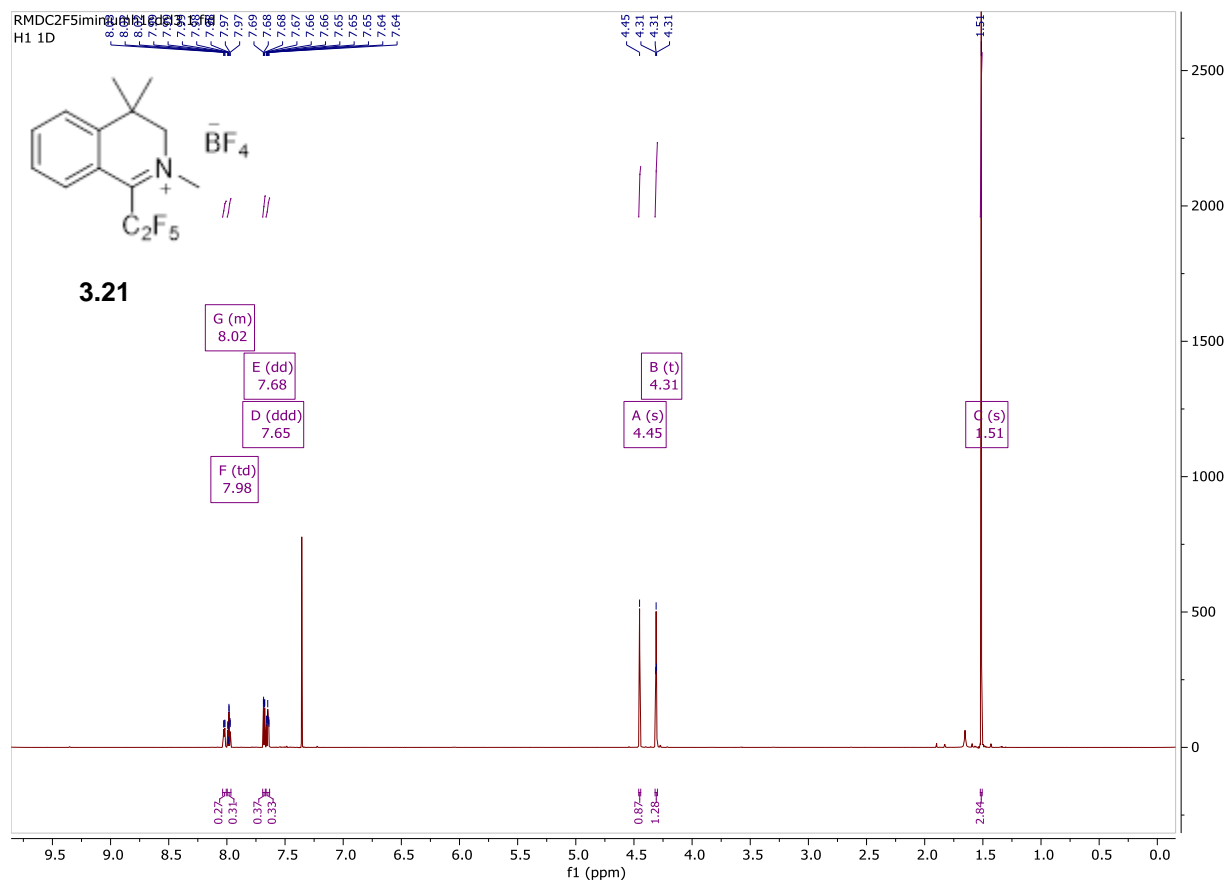
2,4,4-trimethyl-1-(perfluoroethyl)-3,4-dihydroisoquinolin-2-ium tetrafluoroborate was synthesized following general procedure for imine methylation on a .83 mmol scale using 4,4-dimethyl-1-(perfluoroethyl)-3,4-dihydroisoquinoline, as the respective imine, to give 0.190 g of an off white solid (.490 mmol, 60% yield).

¹H NMR (800 MHz, CDCl₃) δ 8.04 – 8.01 (m, 1H), 7.98 (td, *J* = 7.7, 1.2 Hz, 1H), 7.68 (dd, *J* = 7.8, 1.2 Hz, 1H), 7.65 (ddd, *J* = 8.5, 7.4, 1.2 Hz, 1H), 4.45 (H_b, s, 2H), 4.31 (H_c, t, *J* = 2.9 Hz, 3H), 1.51 (H_a, s, 6H) ppm.

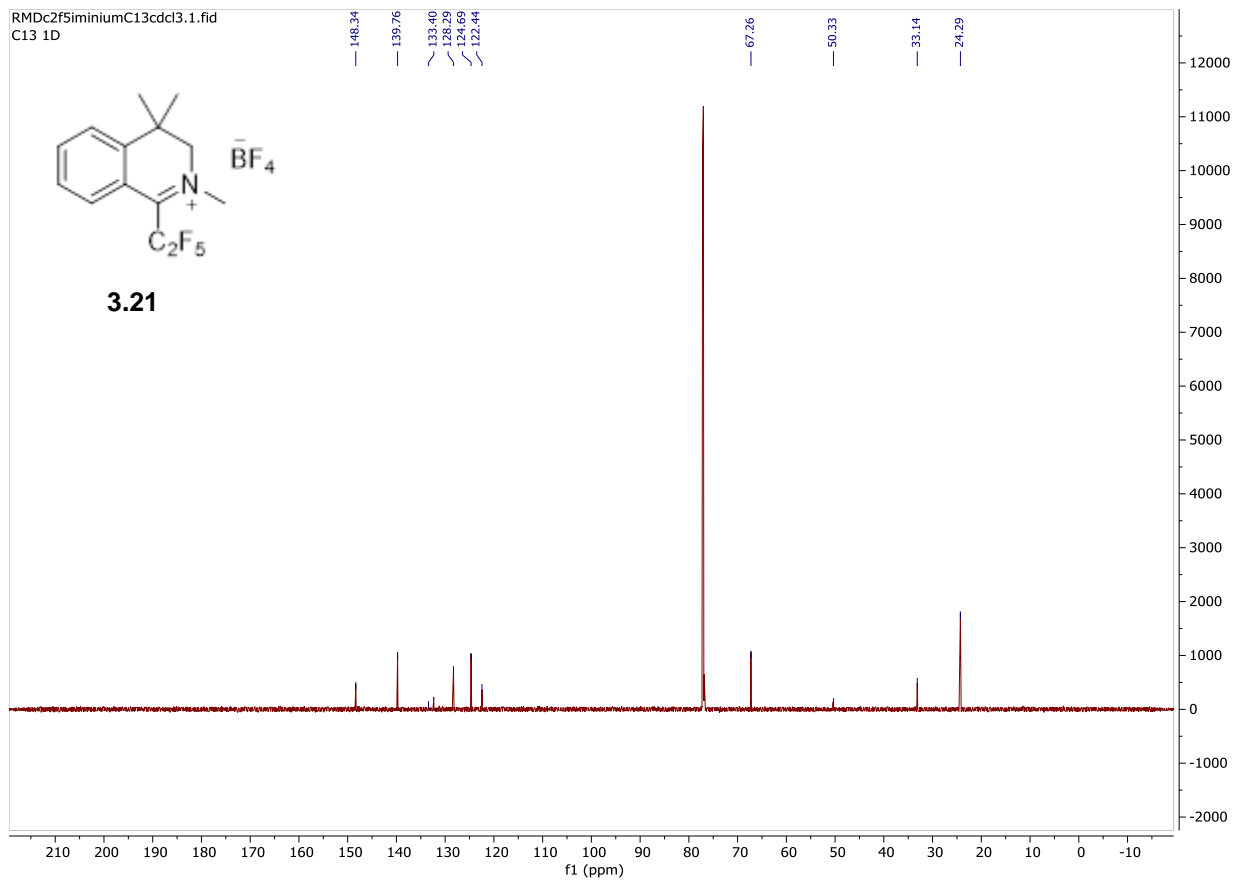
¹³C NMR (201 MHz, CDCl₃) δ 148.3, 139.7, 133.4, 128.2, 124.6, 122.4, 67.2, 50.3, 33.1, 24.2 ppm.

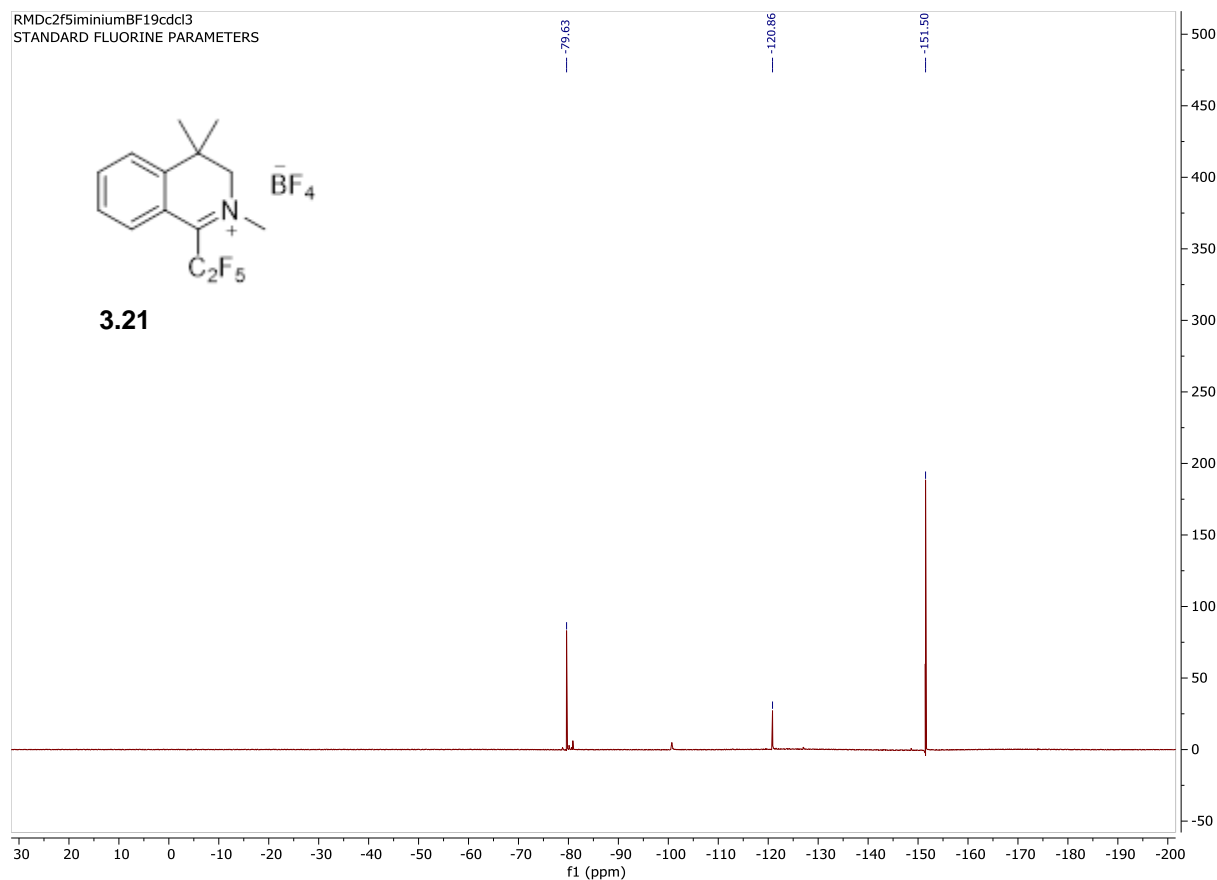
¹⁹F NMR (564 MHz, CDCl₃) δ -79.63, -120.86, -151.50 ppm.

HRMS Calc'd for C₁₄H₁₅F₅N (M): 292.1119 Found: 292.1120

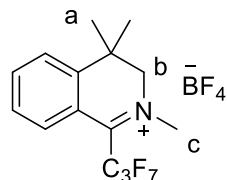


RMDc2f5iminiumC13cdcl3.1.fid
C13 1D





1-(3,3,3,3,3,3,3-heptafluoro-3l8-prop-1-yn-1-yl)-2,4,4-trimethyl-3,4-dihydroisoquinolin-2-ium tetrafluoroborate (3.22)



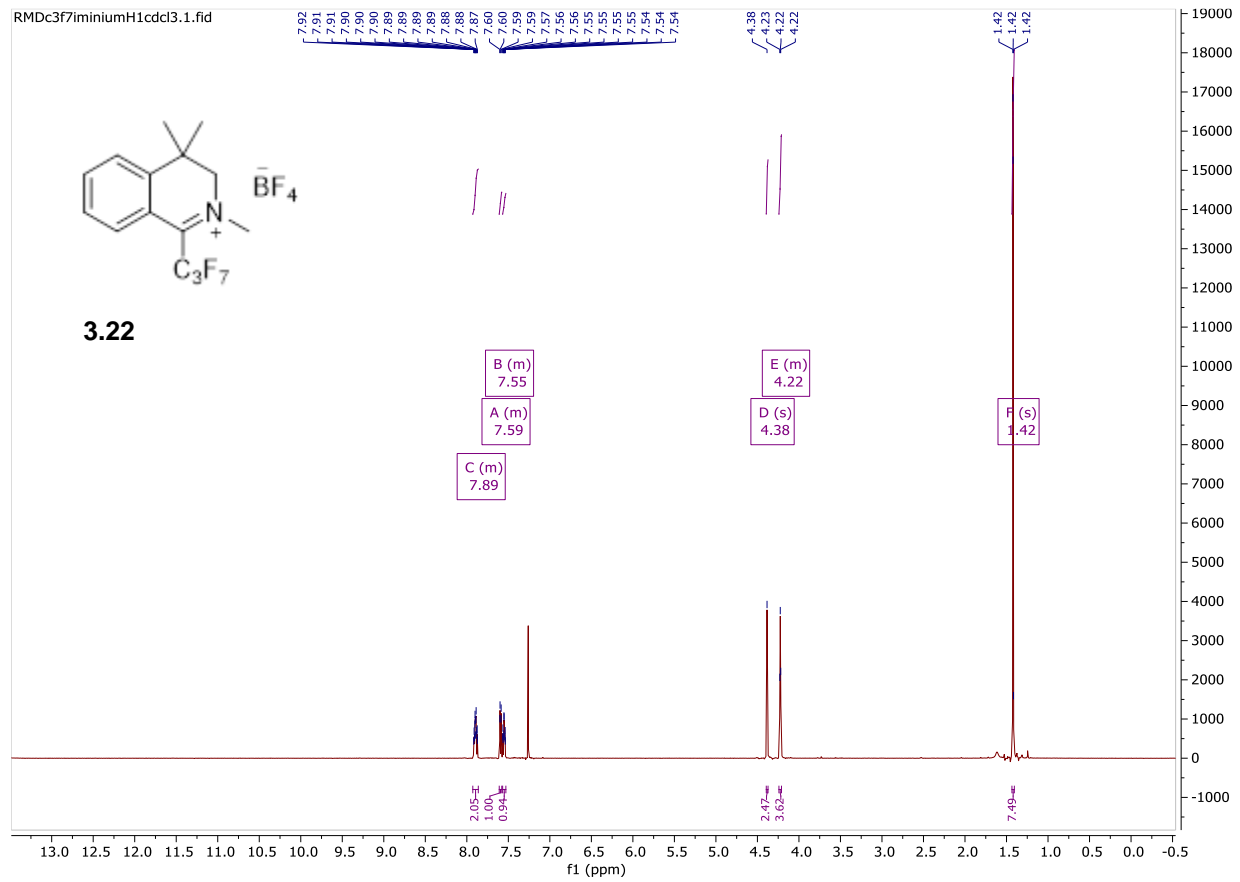
1-(3,3,3,3,3,3,3-heptafluoro-3l8-prop-1-yn-1-yl)-2,4,4-trimethyl-3,4-dihydroisoquinolin-2-ium tetrafluoroborate was synthesized following general procedure for imine methylation on a 2.67 mmol scale using 1-(3,3,3,3,3,3,3-heptafluoro-3l8-prop-1-yn-1-yl)-4,4-dimethyl-3,4-dihydroisoquinoline, as the respective imine, to give 0.058 g of an off white solid (0.134 mmol, 5% yield).

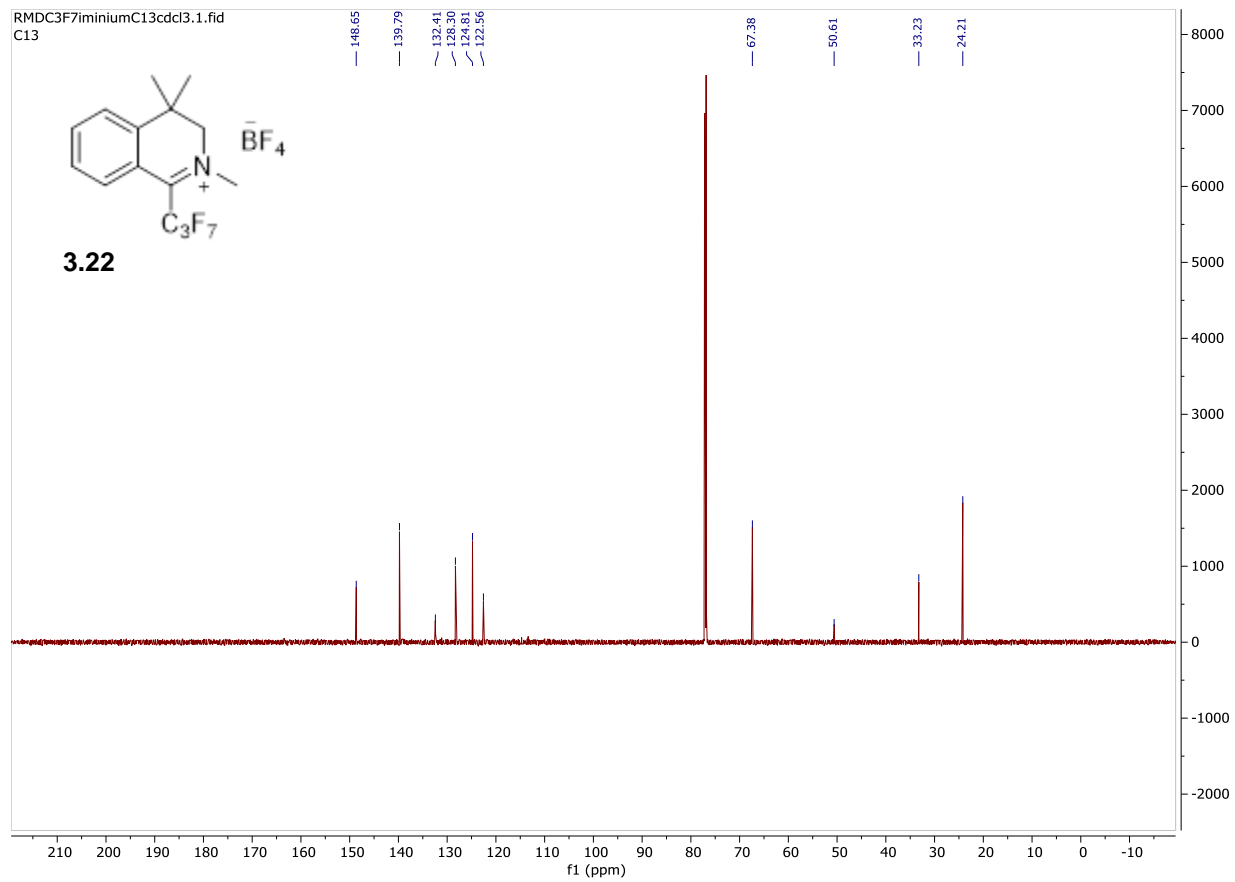
¹H NMR (600 MHz, CDCl₃) δ 7.93 – 7.86 (m, 2H), 7.61 – 7.58 (m, 1H), 7.57 – 7.53 (m, 1H), 4.38 (H_b, s, 2H), 4.24 – 4.21 (H_c, m, 3H), 1.42 (H_a, s, 6H) ppm.

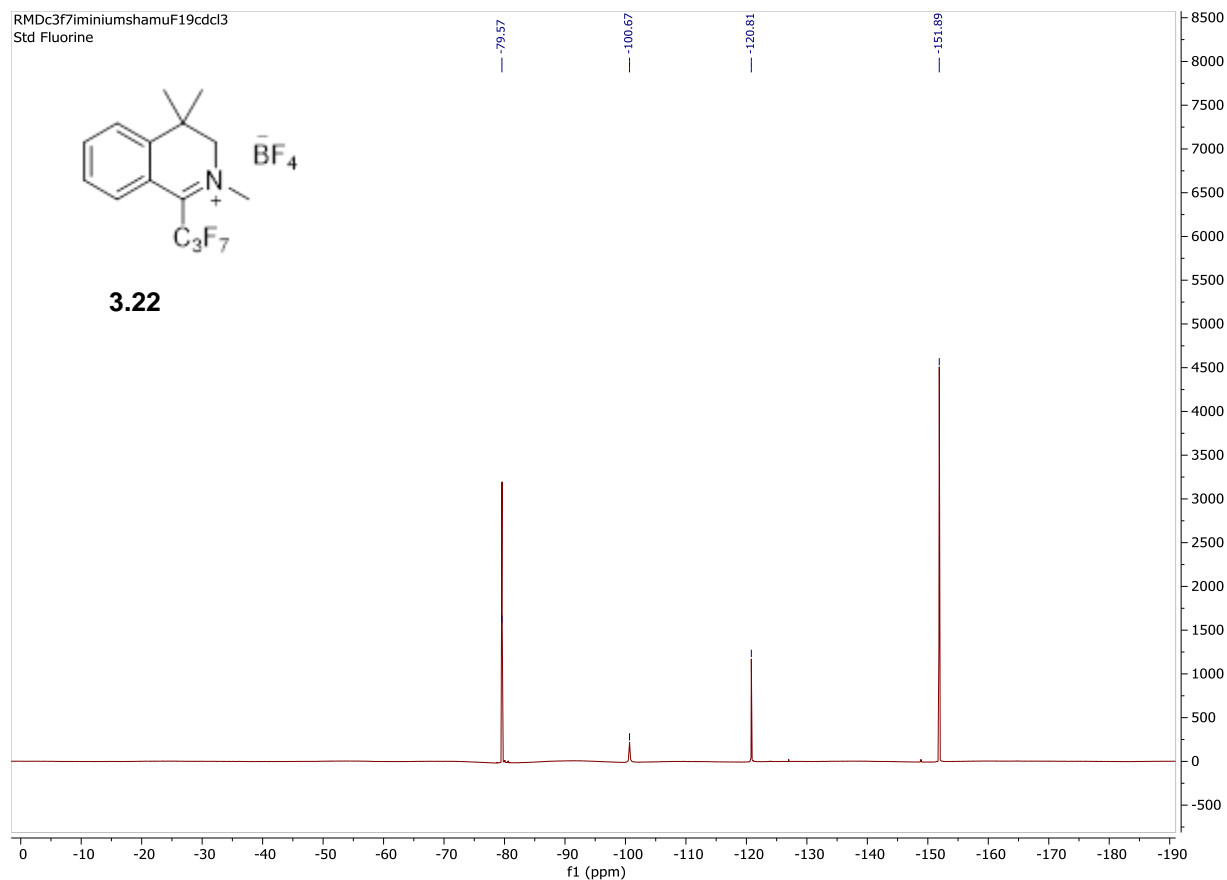
¹³C NMR (201 MHz, CDCl₃) δ 148.6, 139.7, 132.4, 128.3, 124.8, 122.5, 67.3, 50.6, 33.2, 24.2 ppm.

¹⁹F NMR (564 MHz, CDCl₃) δ -79.57, -100.67, -120.81, -151.89 ppm.

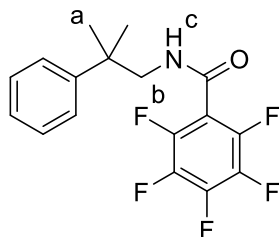
HRMS Calc'd for C₁₅H₁₅F₇N (M): 342.1087 Found: 342.1087







2,3,4,5,6-pentafluoro-N-(2-methyl-2-phenylpropyl)benzamide (3.23)



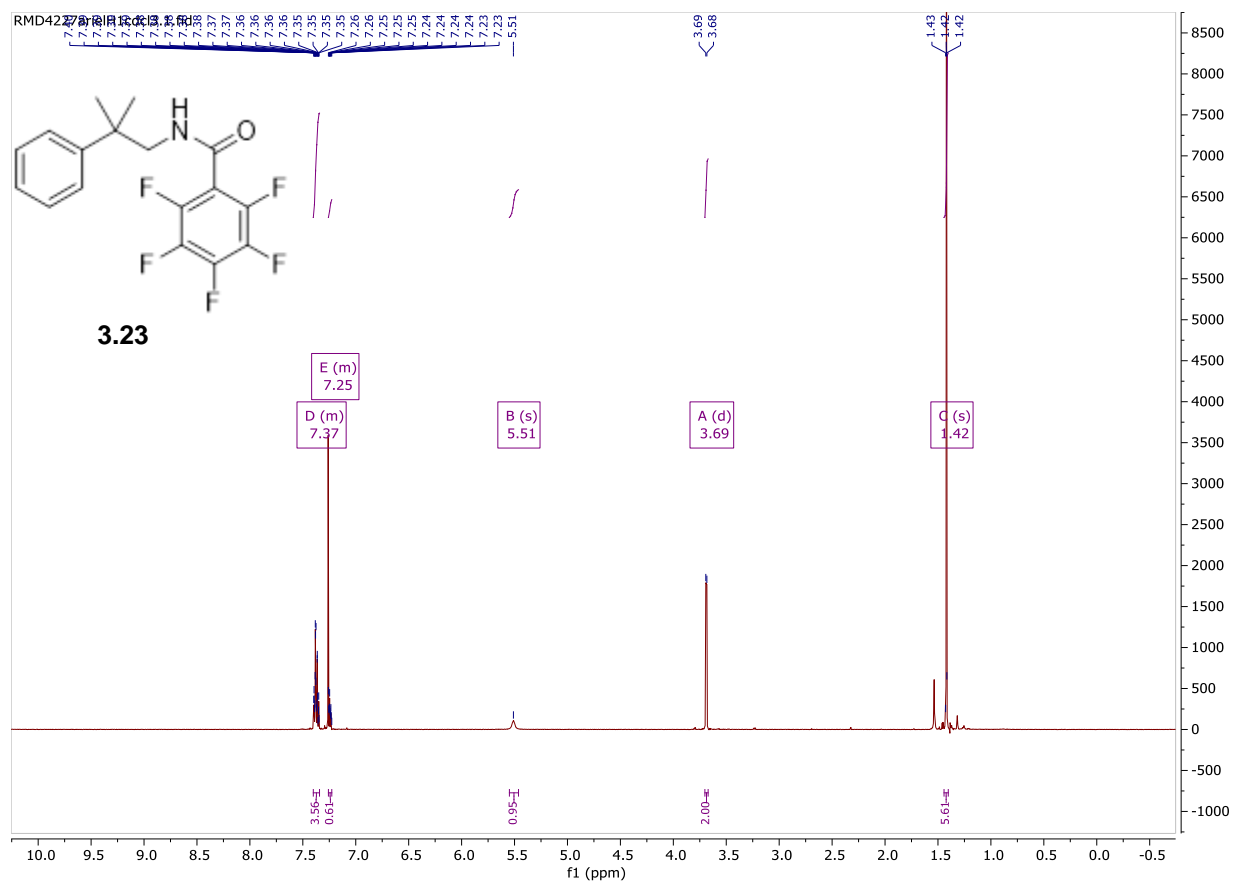
2,3,4,5,6-pentafluoro-N-(2-methyl-2-phenylpropyl)benzamide was synthesized following the general procedure for acetamide formation on a 5 mmol scale using 2-methyl-2-phenylpropan-1-amine, as the respective amine. 2,3,4,5,6-pentafluorobenzoyl chloride was used as the acyl chloride. The compound was purified using silica gel chromatography with 5% acetone/hexanes to give 1.03 g of a white solid (3.00 mmol, 60% yield).

¹H NMR (600 MHz, CDCl₃) δ 7.40 – 7.34 (m, 4H), 7.26 – 7.23 (m, 1H), 5.51 (H_c, s, 1H), 3.69 (H_b, d, *J* = 6.1 Hz, 2H), 1.42 (H_a, s, 6H) ppm.

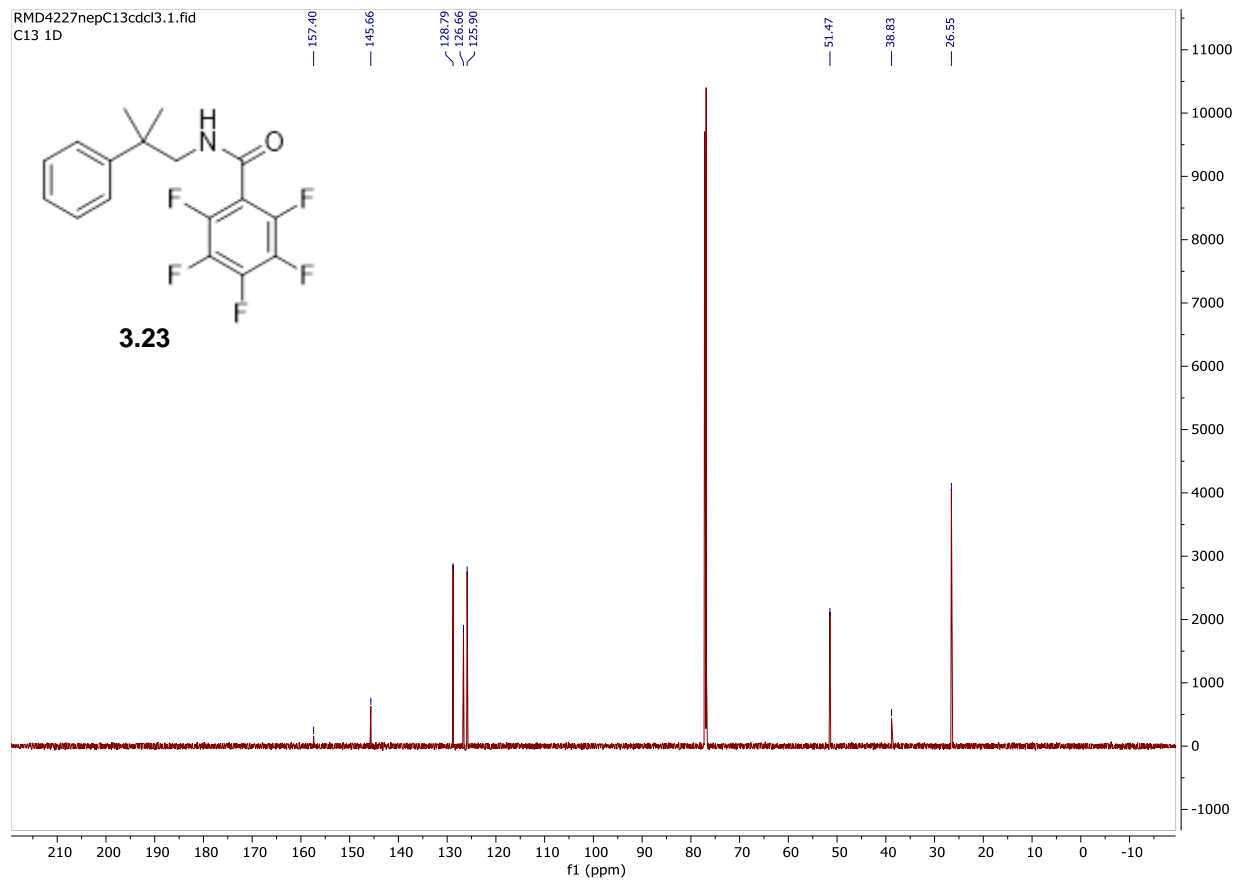
¹³C NMR (201 MHz, CDCl₃) δ 157.4, 145.6, 128.7, 126.6, 125.9, 77.18, 77.02, 76.8, 51.4, 38.8, 26.5 ppm.

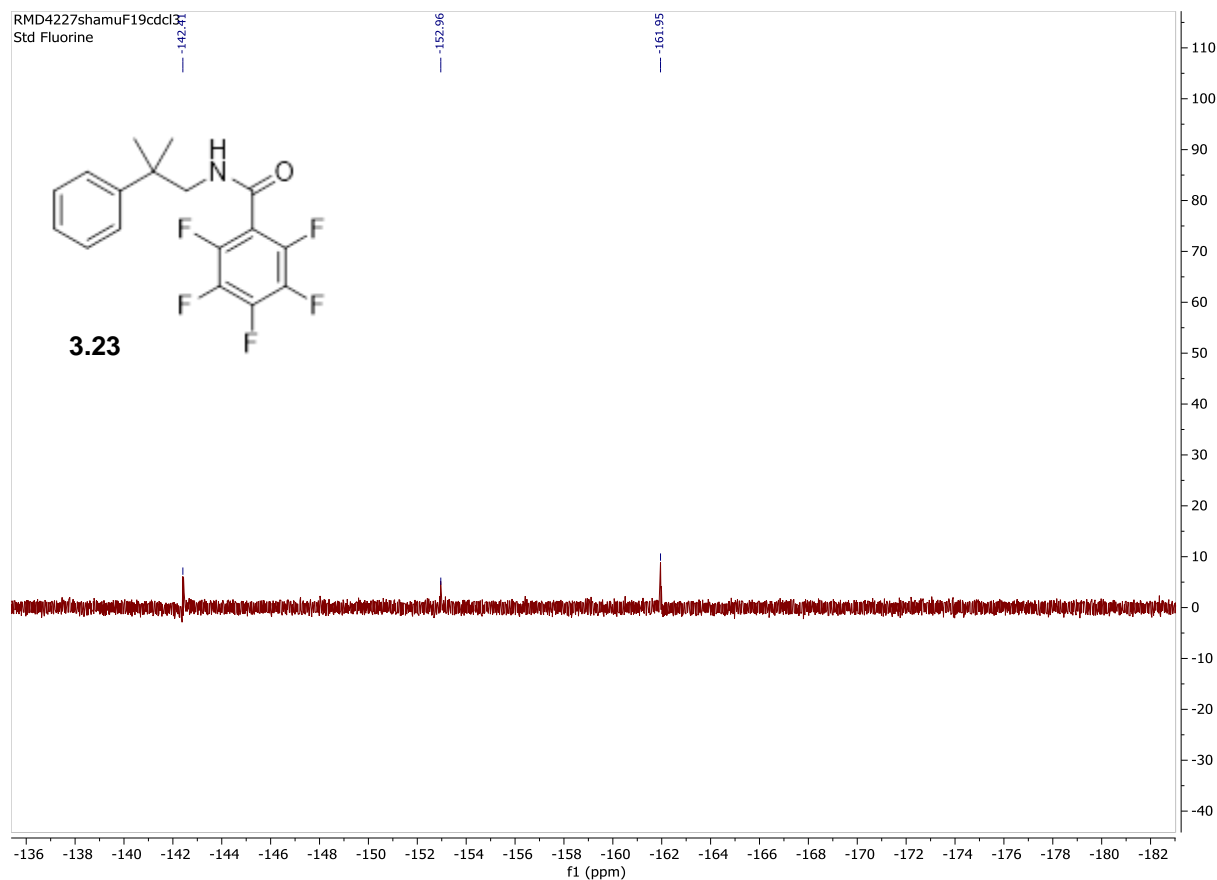
¹⁹F NMR (564 MHz, CDCl₃) δ -142.41, -152.96, -161.95 ppm.

HRMS Calc'd for C₁₇H₁₄F₅NO (M+Na): 366.0893 Found 366.0937

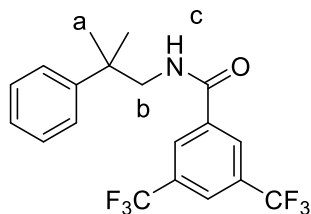


RMD4227nepC13cdcl3.1.fid
C13 1D





N-(2-methyl-2-phenylpropyl)-3,5-bis(trifluoromethyl)benzamide (3.24)



N-(2-methyl-2-phenylpropyl)-3,5-bis(trifluoromethyl)benzamide was synthesized following the general procedure for acetamide formation on a 5.1 mmol scale using 2-methyl-2-phenylpropan-1-amine, as the respective amine. 3,5-bis(trifluoromethyl)benzoyl chloride was used as the respective acyl chloride. The compound was purified using silica gel chromatography with 5% acetone/hexanes to give 1.00 g of a white solid (2.54 mmol, 50 % yield).

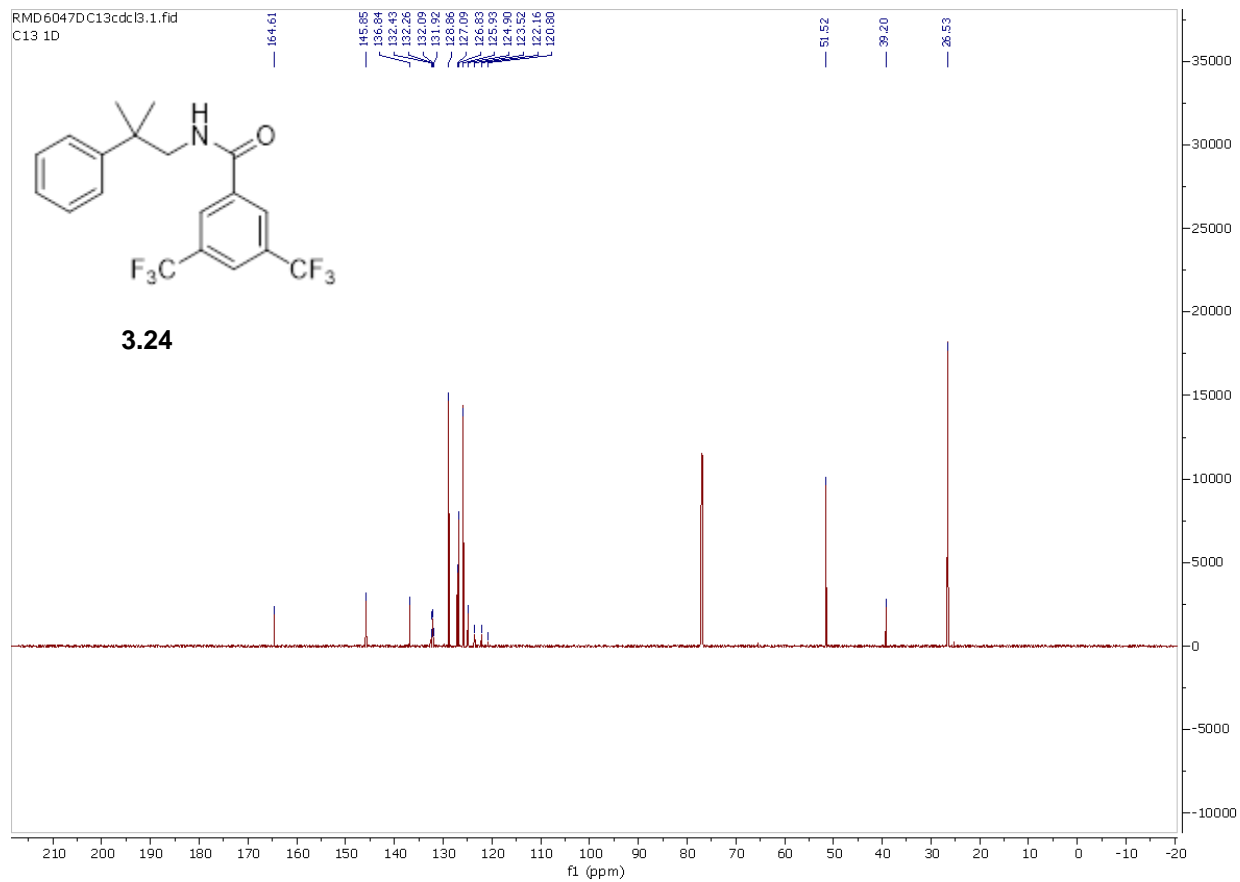
¹H NMR (600 MHz, CDCl₃) δ 7.98 – 7.93 (m, 3H), 7.44 – 7.38 (m, 4H), 7.31 – 7.27 (m, 1H), 5.78 (H_c, s, 1H), 3.67 (H_b, d, *J* = 6.1 Hz, 2H), 1.44 (H_a, s, 6H) ppm.

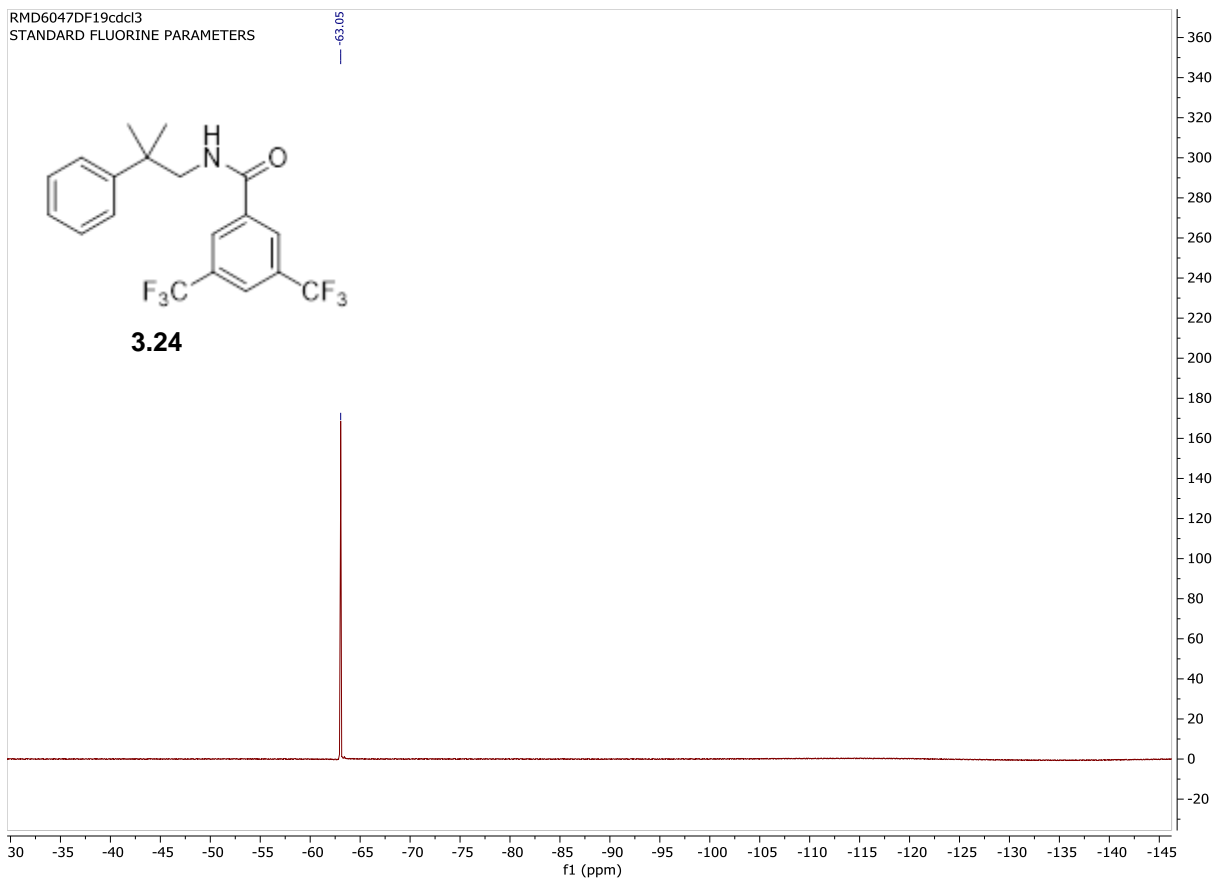
¹³C NMR (201 MHz, CDCl₃) δ 164.6, 145.8, 136.8, 132.43, 132.26, 132.09, 131.9, 128.8, 127.0, 126.8, 125.9, 124.9, 123.5, 122.1, 120.8, 51.5, 39.2, 26.5 ppm.

¹⁹F NMR (564 MHz, CDCl₃) δ -63.05 ppm.

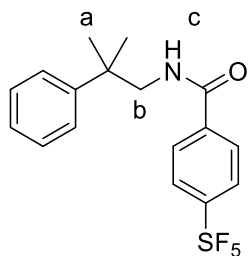
HRMS Calc'd for C₁₉H₁₇F₆NO (M+Na): 412.1111 Found: 412.1146

RMD6047DC13cdc13.1.fid
C13 1D





N-(2-methyl-2-phenylpropyl)-4-(pentafluoro-*l*-6-sulfaneyl)benzamide (3.25)



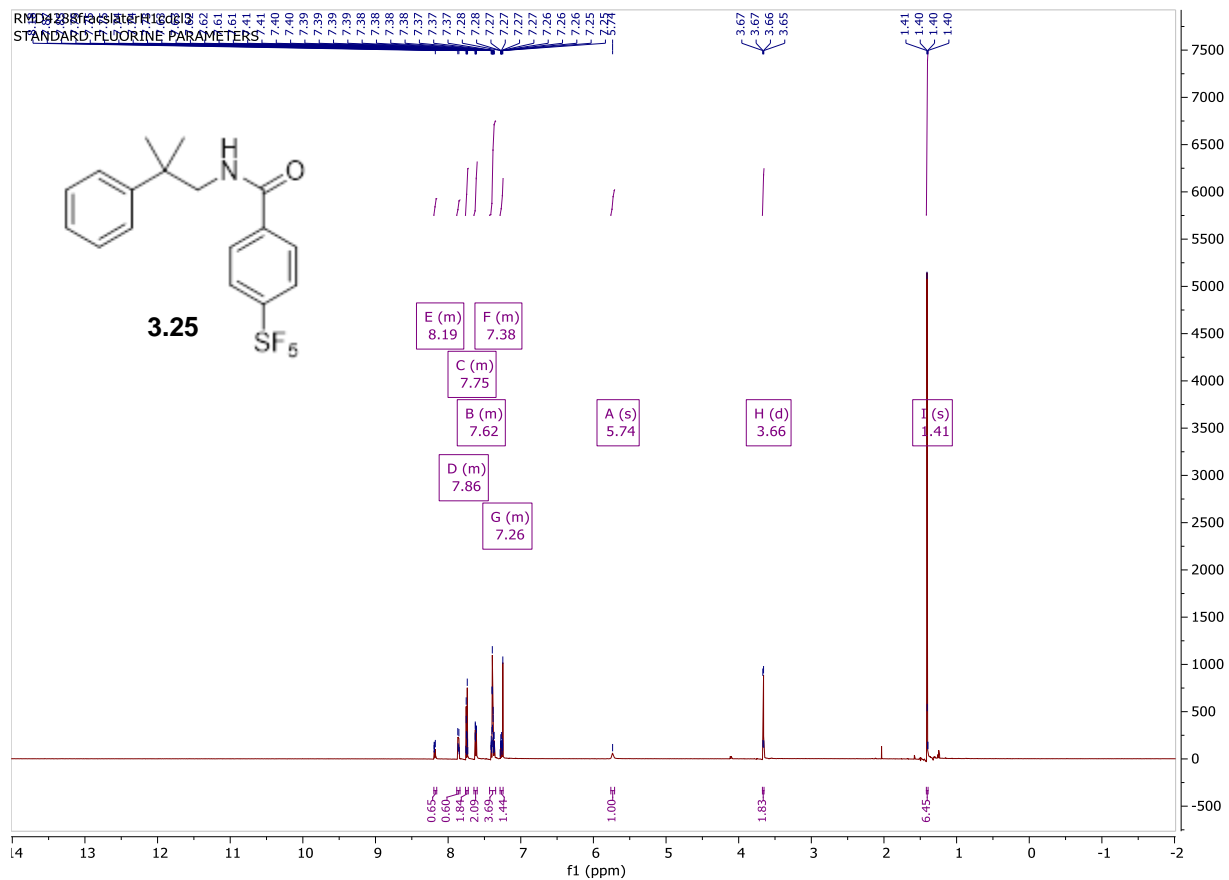
N-(2-methyl-2-phenylpropyl)-4-(pentafluoro-*l*-6-sulfaneyl)benzamide was synthesized following the general procedure for acetamide formation on a 3.12 mmol scale using 2-methyl-2-phenylpropan-1-amine, as the respective amine. 4-(pentafluoro-*l*-6-sulfaneyl)benzoyl chloride was used as the respective acyl chloride. The compound was purified using silica gel chromatography with 10% ethyl acetate/hexane to give .853 g of a white solid (2.25 mmol, 72% yield).

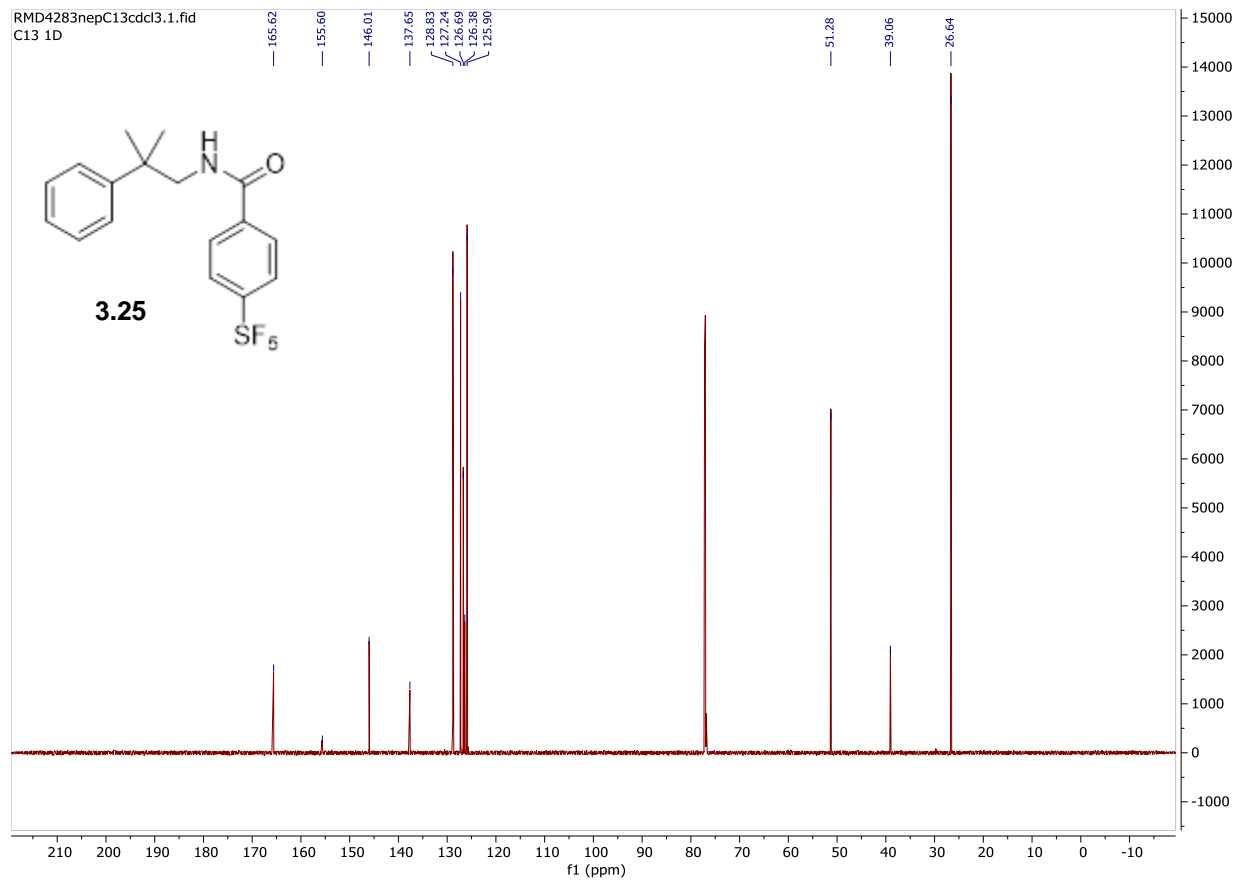
¹H NMR (600 MHz, CDCl₃) δ 8.20 – 8.16 (m, 1H), 7.88 – 7.84 (m, 1H), 7.76 – 7.72 (m, 1H), 7.64 – 7.60 (m, 1H), 7.43 – 7.35 (m, 4H), 7.28 – 7.24 (m, 1H), 5.74 (H_c, s, 1H), 3.66 (H_b, d, *J* = 6.0 Hz, 2H), 1.41 (H_a, s, 6H) ppm.

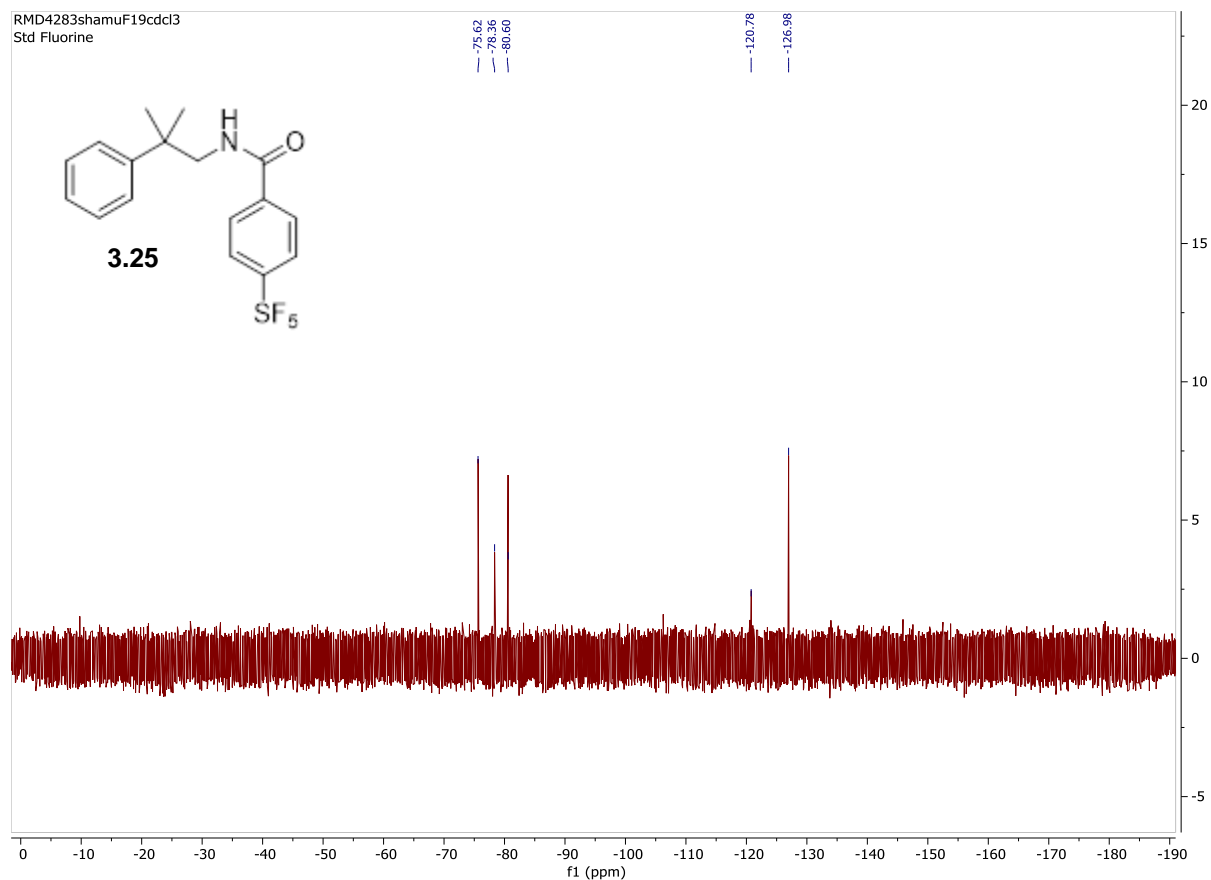
¹³C NMR (201 MHz, CDCl₃) δ 165.6, 155.6, 146.0, 137.6, 128.8, 127.2, 126.69, 126.38, 125.9, 51.2, 39.0, 26.6 ppm.

^{19}F NMR (564 MHz, CDCl_3) δ -75.62, -78.36, -80.60, -120.78, -126.98 ppm.

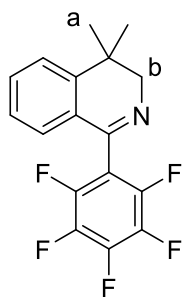
HRMS Calc'd for $\text{C}_{17}\text{H}_{18}\text{F}_5\text{NOS}$ ($\text{M}+\text{Na}$): 402.0926 Found: 402.0947







4,4-dimethyl-1-(perfluorophenyl)-3,4-dihydroisoquinoline (3.26)



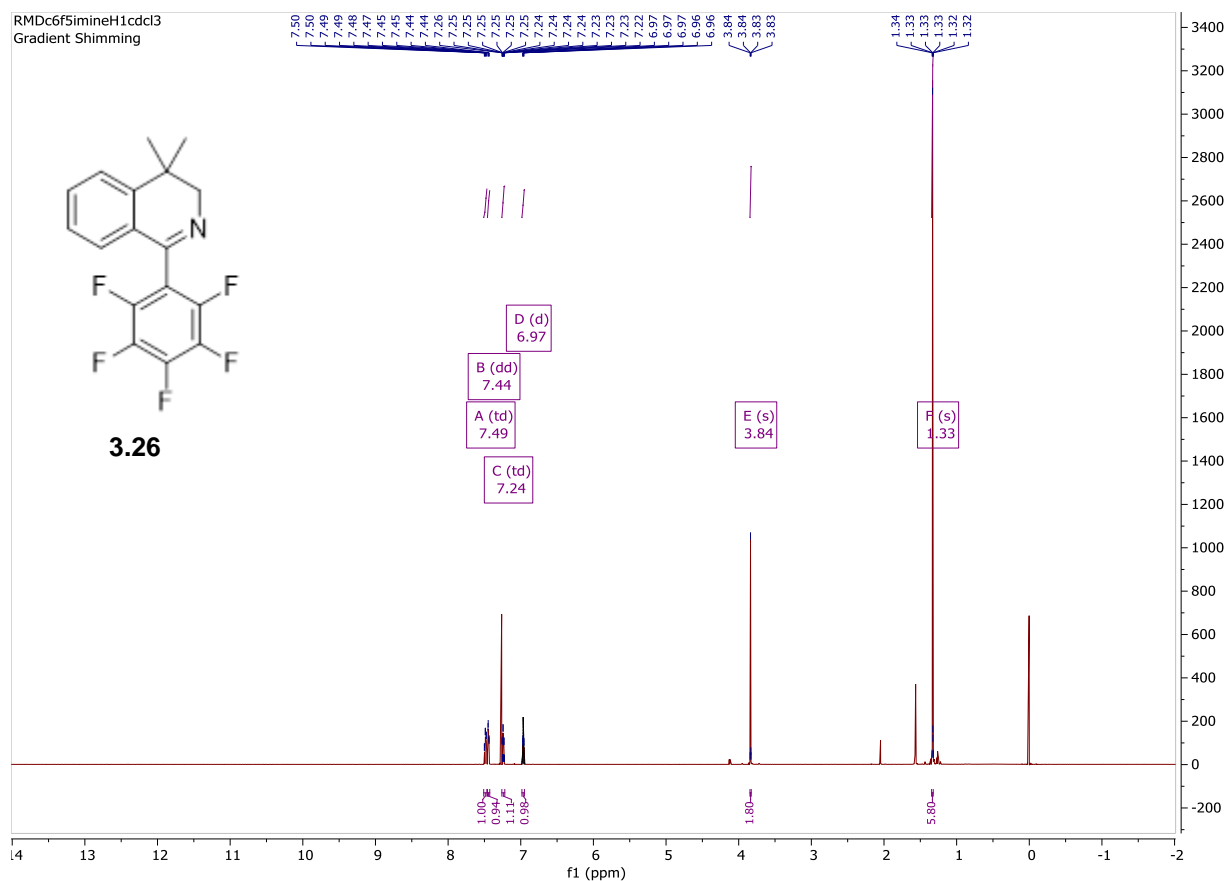
4,4-dimethyl-1-(perfluorophenyl)-3,4-dihydroisoquinoline was synthesized following general procedure A for the Bischler Naperialski reaction on a 3.0 mmol scale using 2,3,4,5,6-pentafluoro-N-(2-methyl-2-phenylpropyl)benzamide, as the respective amide. The compound was purified using silica gel chromatography with 5% acetone/hexanes to give 0.400 g of a yellow oil (1.23 mmol, 41% yield).

¹H NMR (600 MHz, CDCl₃) δ 7.49 (td, *J* = 7.5, 1.3 Hz, 1H), 7.44 (dd, *J* = 7.8, 1.4 Hz, 1H), 7.24 (td, *J* = 7.5, 1.3 Hz, 1H), 6.97 (d, *J* = 0.1 Hz, 1H), 3.84 (H_b, s, 2H), 1.33 (H_a, s, 6H) ppm.

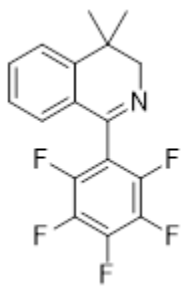
¹³C NMR (201 MHz, CDCl₃) δ 157.10, 145.99, 145.18, 144.03, 142.28, 137.00, 132.68, 126.87, 126.66, 126.25, 123.95, 61.12, 31.77, 25.99 ppm.

¹⁹F NMR (564 MHz, CDCl₃) δ -141.13 (q, *J* = 13.6, 9.1 Hz), -153.49 (t, *J* = 22.3 Hz), -161.18 – -161.38 (m) ppm.

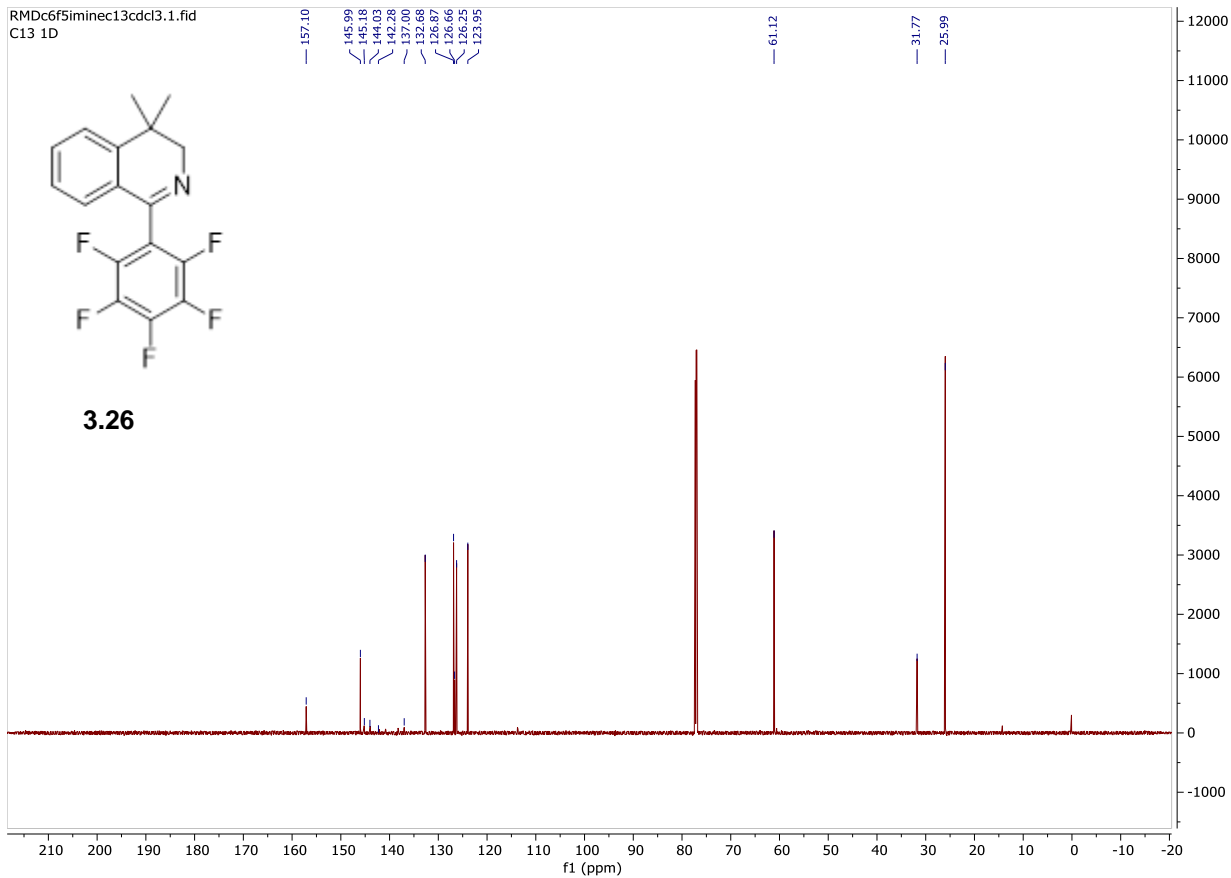
HRMS Calc'd for C₁₇H₁₂F₅N (M+H): 326.0969 Found: 326.0974

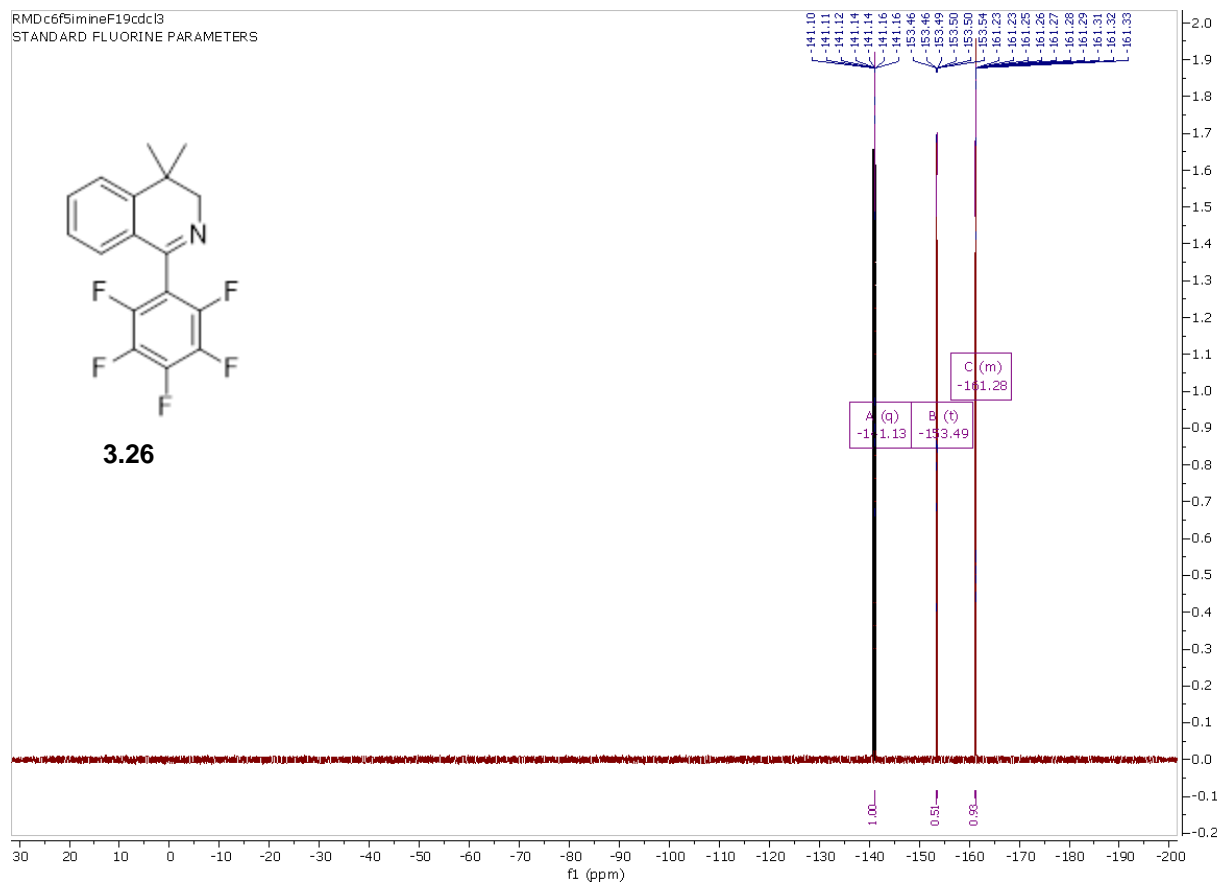


RMDc6f5iminec13cdcl3.1.fid
C13 1D

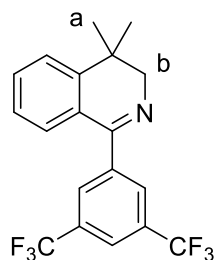


3.26





1-(3,5-bis(trifluoromethyl)phenyl)-4,4-dimethyl-3,4-dihydroisoquinoline (3.27)



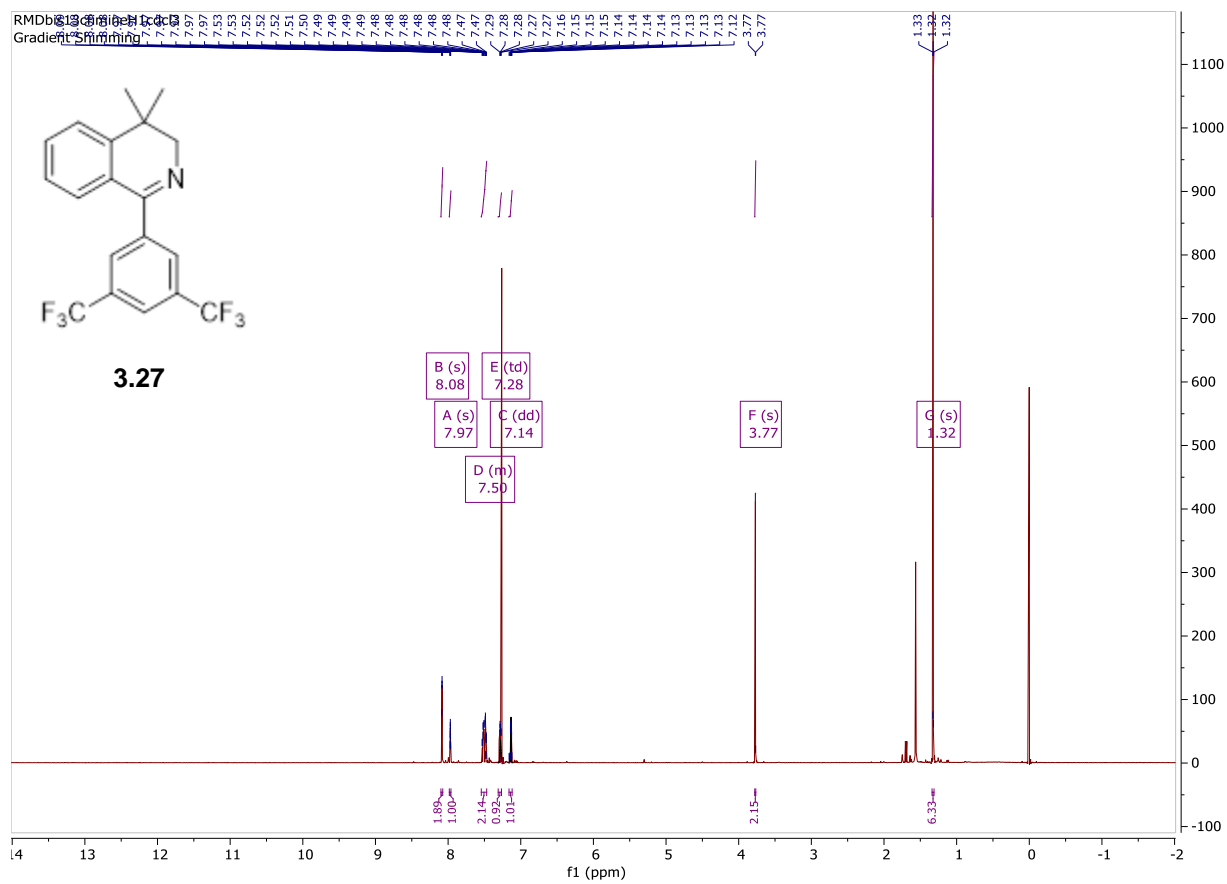
1-(3,5-bis(trifluoromethyl)phenyl)-4,4-dimethyl-3,4-dihydroisoquinoline was synthesized following general procedure A for the Bischler Naperialski reaction on a 2.57 mmol scale using N-(2-methyl-2-phenylpropyl)-3,5-bis(trifluoromethyl)benzamide, as the respective amide. The compound was purified using silica gel chromatography with 5% acetone/hexanes to give 0.840 g of a yellow oil (2.26 mmol, 88% yield).

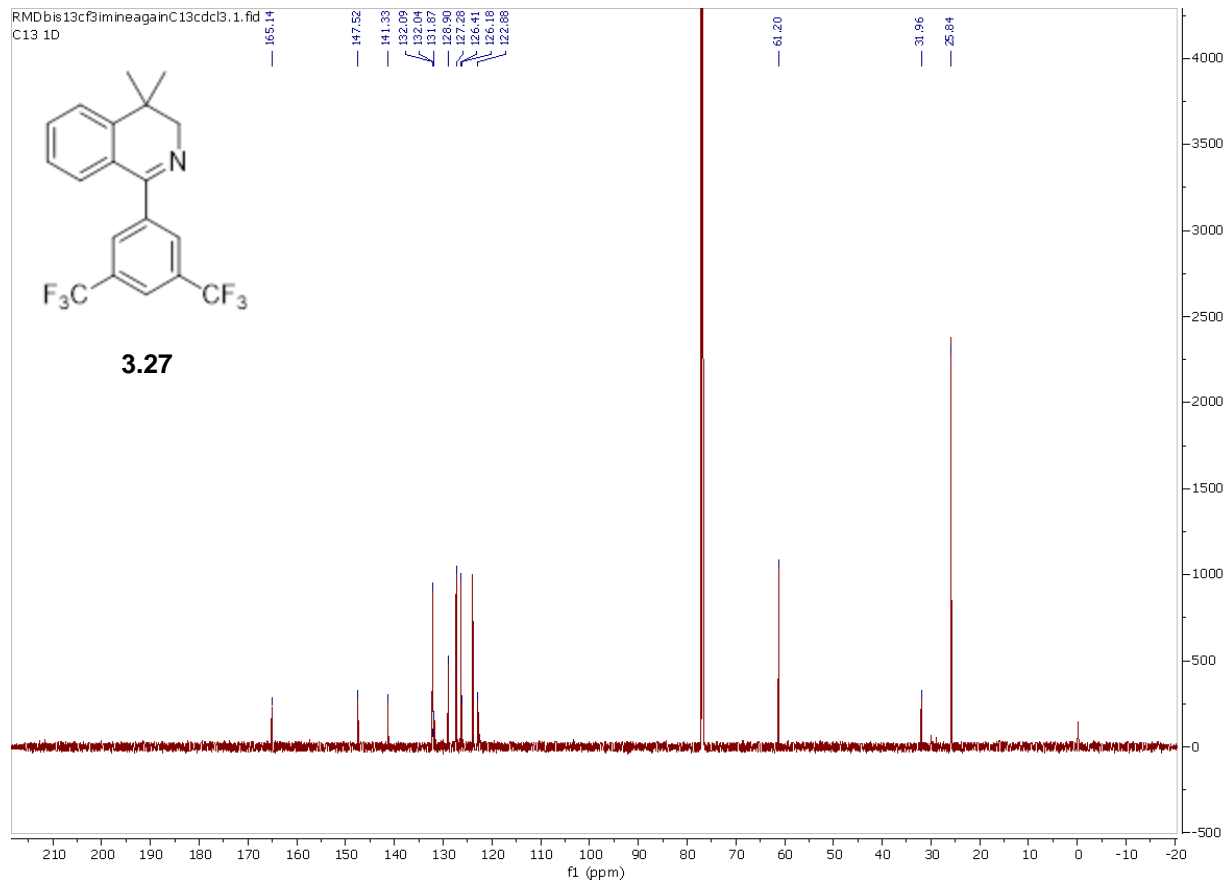
¹H NMR (600 MHz, CDCl₃) δ 8.08 (s, 2H), 7.97 (s, 1H), 7.54 – 7.47 (m, 2H), 7.28 (td, *J* = 6.4, 5.6, 1.5 Hz, 1H), 7.14 (dd, *J* = 6.4, 1.0 Hz, 1H), 3.77 (H_b, s, 2H), 1.32 (H_a, s, 6H) ppm.

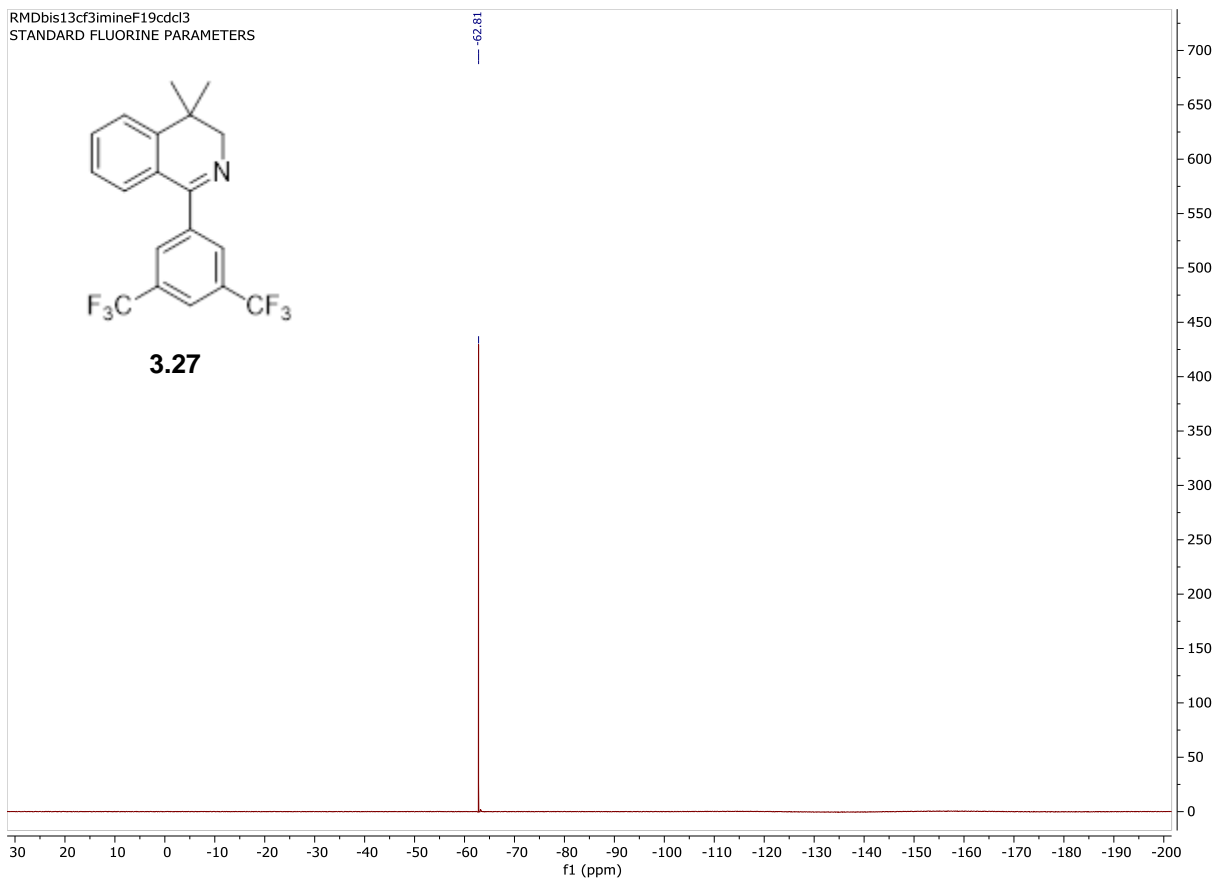
¹³C NMR (201 MHz, CDCl₃) δ 165.14, 147.52, 141.33, 132.09, 132.04, 131.87, 128.90, 127.28, 126.41, 126.18, 122.88, 61.20, 31.96, 25.84 ppm

¹⁹F NMR (564 MHz, CDCl₃) δ -62.81 ppm.

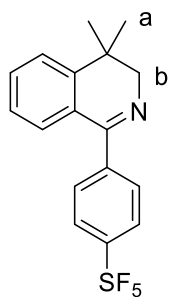
HRMS Calc'd for C₁₉H₁₅F₆N (M+H): 372.1188 Found: 372.1197







4,4-dimethyl-1-(4-(pentafluoro-*l*6-sulfaneyl)phenyl)-3,4-dihydroisoquinoline (3.28)



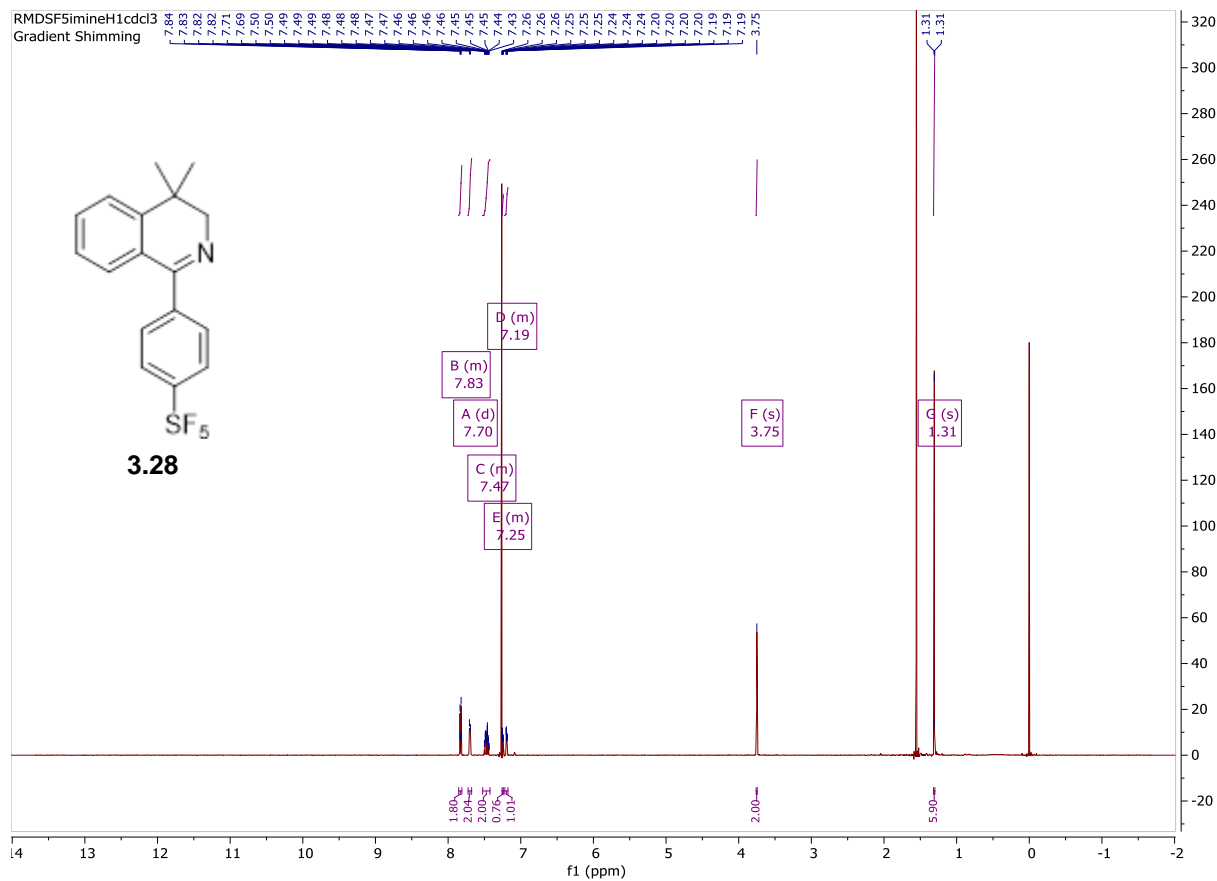
4,4-dimethyl-1-(4-(pentafluoro-*l*6-sulfaneyl)phenyl)-3,4-dihydroisoquinoline was synthesized following general procedure A for the Bischler Naperialski reaction on a 2.25 mmol scale using N-(2-methyl-2-phenylpropyl)-4-(pentafluoro-*l*6-sulfaneyl)benzamide, as the respective amide. The compound was purified using silica gel chromatography with 5% acetone/hexanes to give 0.592 g of a yellow oil (1.64 mmol, 73% yield).

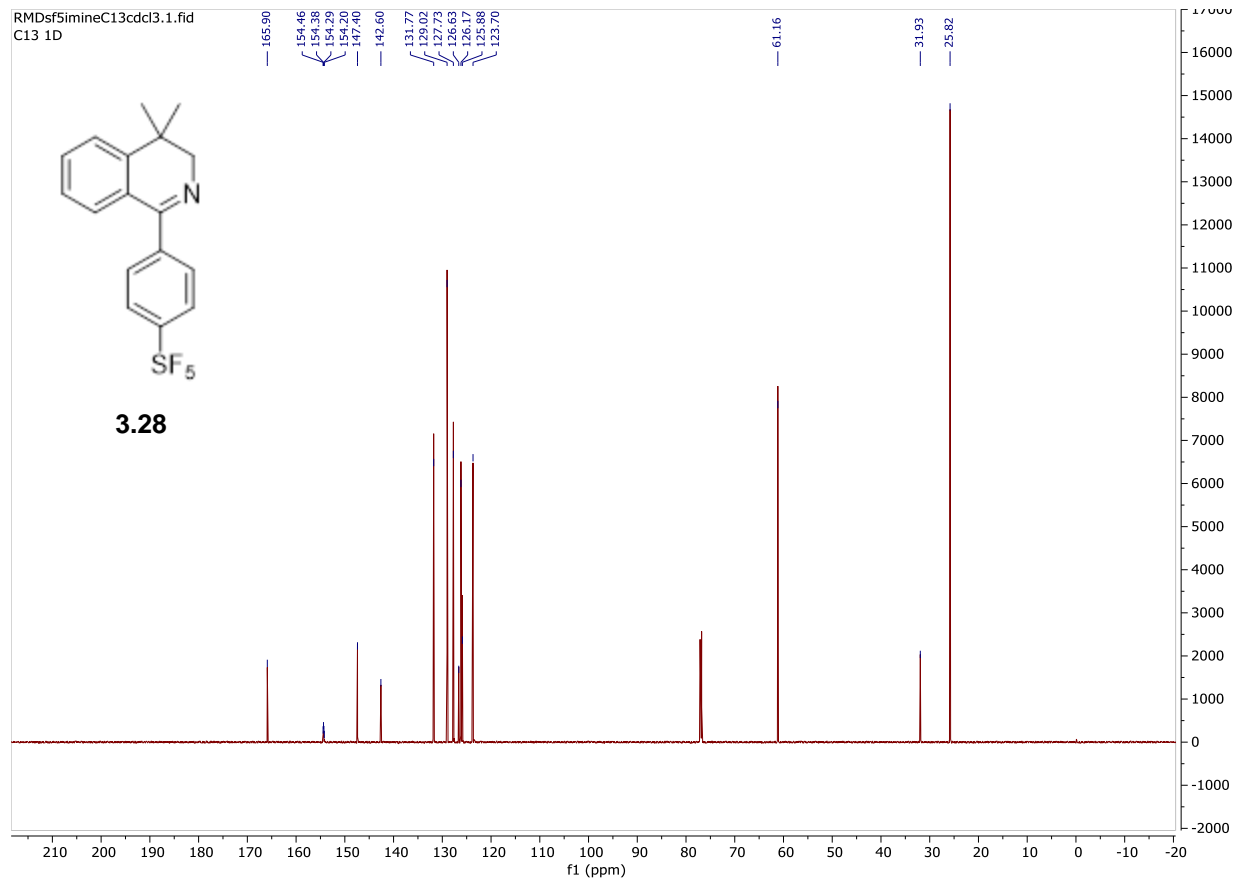
¹H NMR (600 MHz, CDCl₃) δ 7.85 – 7.81 (m, 2H), 7.70 (d, *J* = 8.3 Hz, 2H), 7.52 – 7.42 (m, 2H), 7.26 – 7.24 (m, 1H), 7.22 – 7.18 (m, 1H), 3.75 (H_b, s, 2H), 1.31 (H_a, s, 6H) ppm.

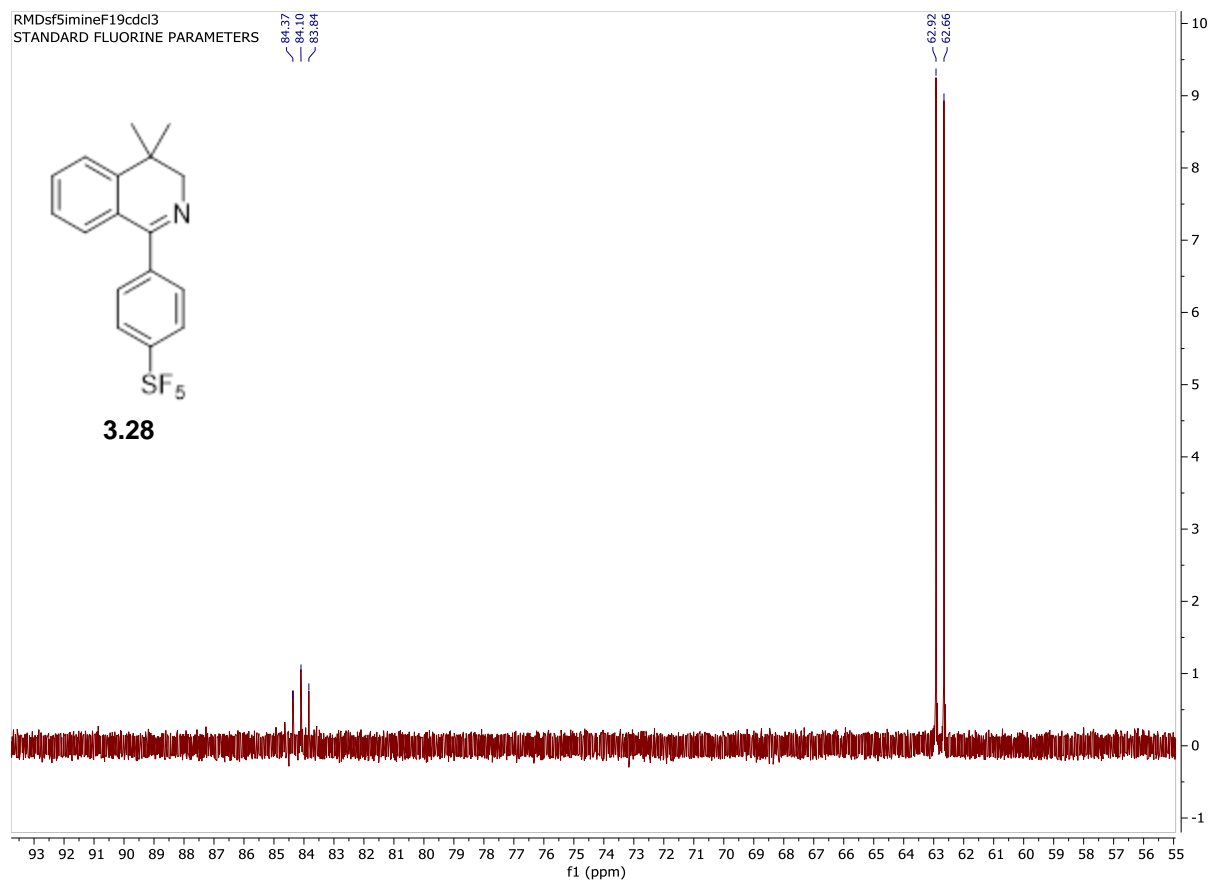
¹³C NMR (201 MHz, CDCl₃) δ 165.9, 154.46, 154.38, 154.29, 154.20, 147.4, 142.6, 131.7, 129.0, 127.7, 126.6, 126.2, 125.9, 123.7, 61.2, 31.9, 25.8 ppm.

^{19}F NMR (564 MHz CDCl_3) δ 84.37, 84.10, 83.84, 62.92, 62.66 ppm

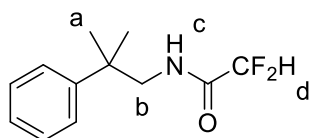
HRMS Calc'd for $\text{C}_{17}\text{H}_{16}\text{F}_5\text{NS}$ (M+H): 362.1003 Found: 362.1012







2,2-difluoro-N-(2-methyl-2-phenylpropyl) acetamide (3.29)



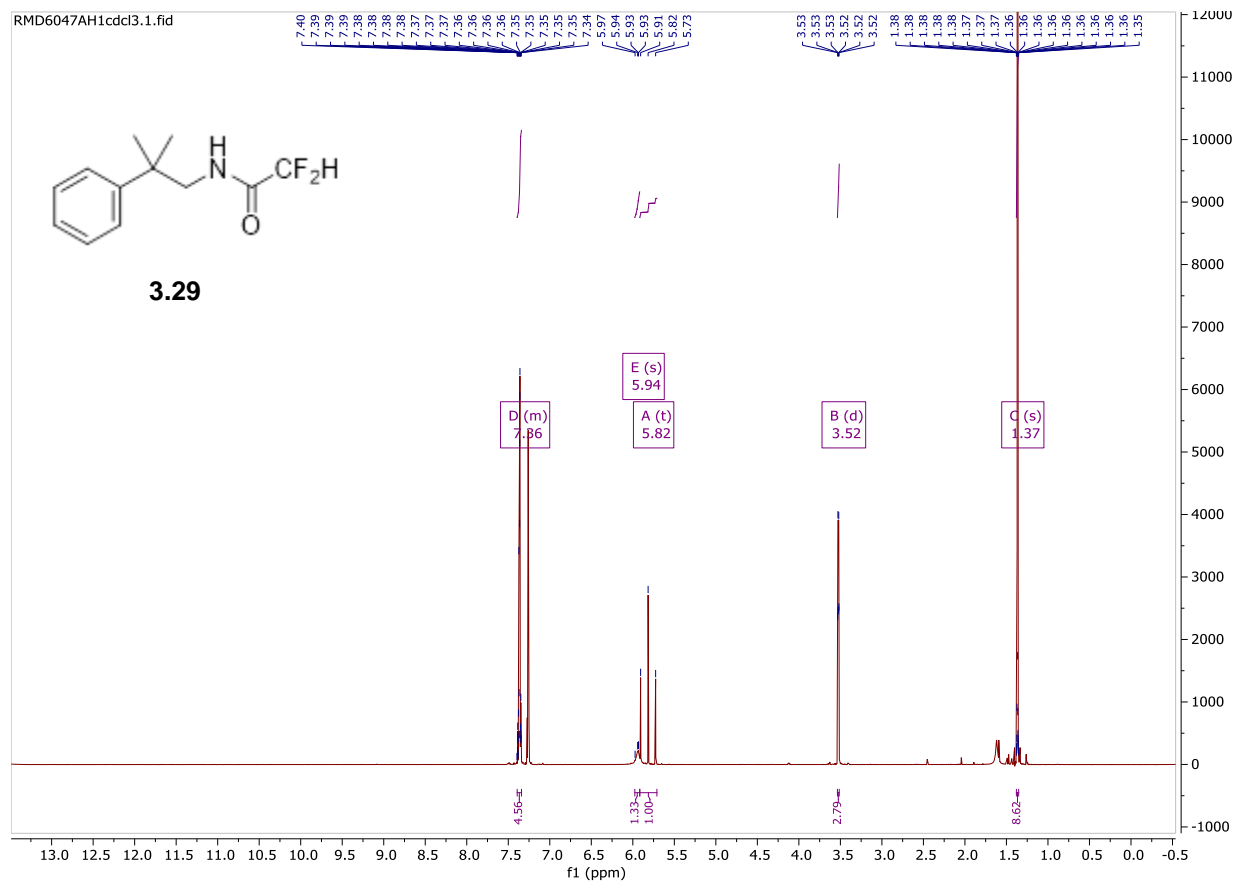
2,2-difluoro-N-(2-methyl-2-phenylpropyl) acetamide was synthesized following the general procedure for acetamide formation on a 6.7 mmol scale of 2-methyl-2-phenylpropan-1-amine, as the respective amine. 2,2-difluoroacetic anhydride was used as the anhydride. The compound was purified using silica gel chromatography with 20% diethyl ether/hexanes to give 1.11 g of a white solid (4.89 mmol, 73% yield).

^1H NMR (600 MHz, CDCl_3) δ 7.39 – 7.34 (m, 5H), 5.94 (H_c , s, 1H), 5.82 (H_d , t, $J = 54.4$ Hz, 1H), 3.52 (H_b , d, $J = 6.2$ Hz, 2H), 1.37 (H_a , s, 6H).

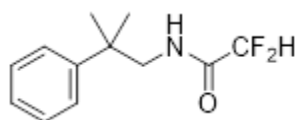
^{13}C NMR (201 MHz, CDCl_3) δ 162.6, 145.4, 128.8, 126.7, 125.7, 109.7, 108.4, 107.2, 50.3, 38.7, 26.4 ppm.

^{19}F NMR (564 MHz, CDCl_3) δ -126.18, -126.28 ppm.

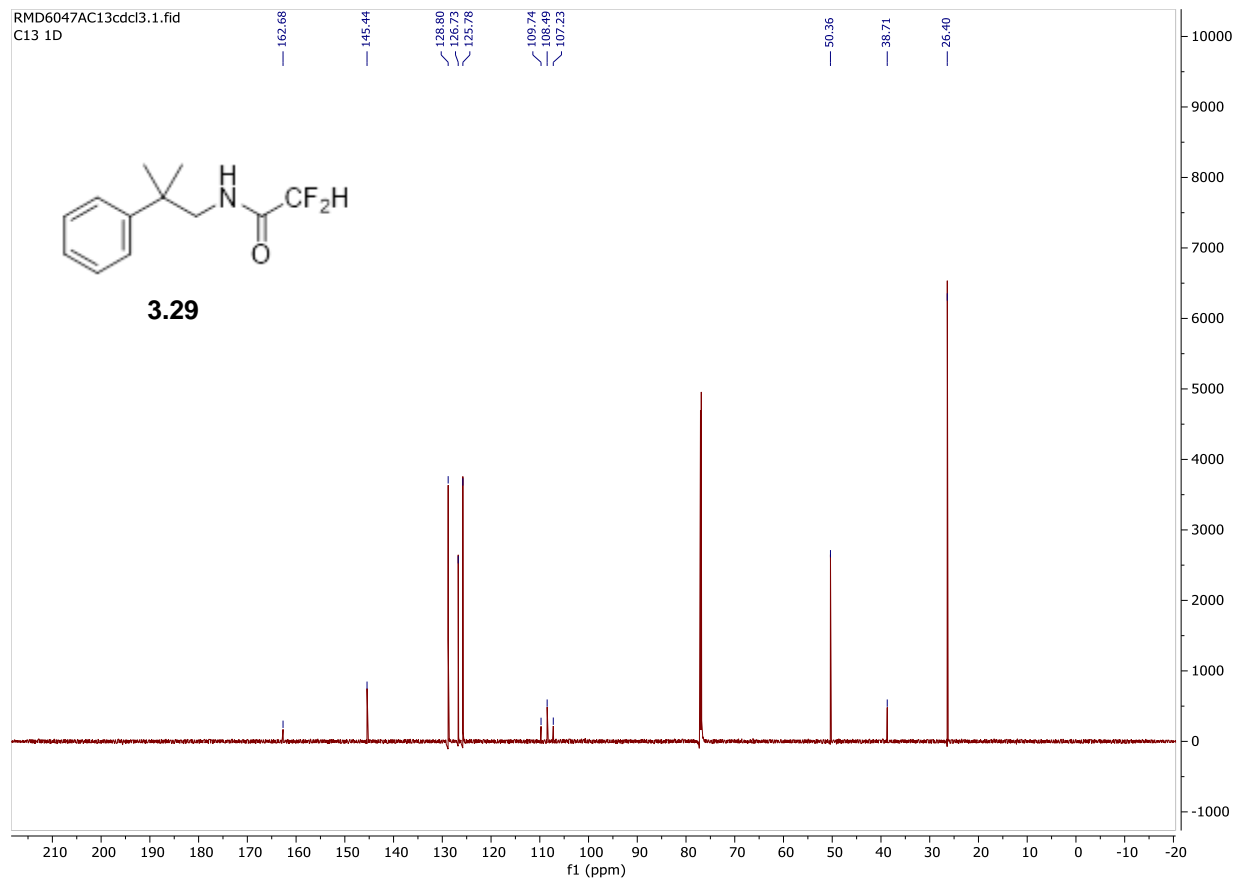
HRMS Calc'd for $\text{C}_{12}\text{H}_{15}\text{F}_2\text{NO}$ ($\text{M}+\text{Na}$): 250.1019 Found: 250.1023

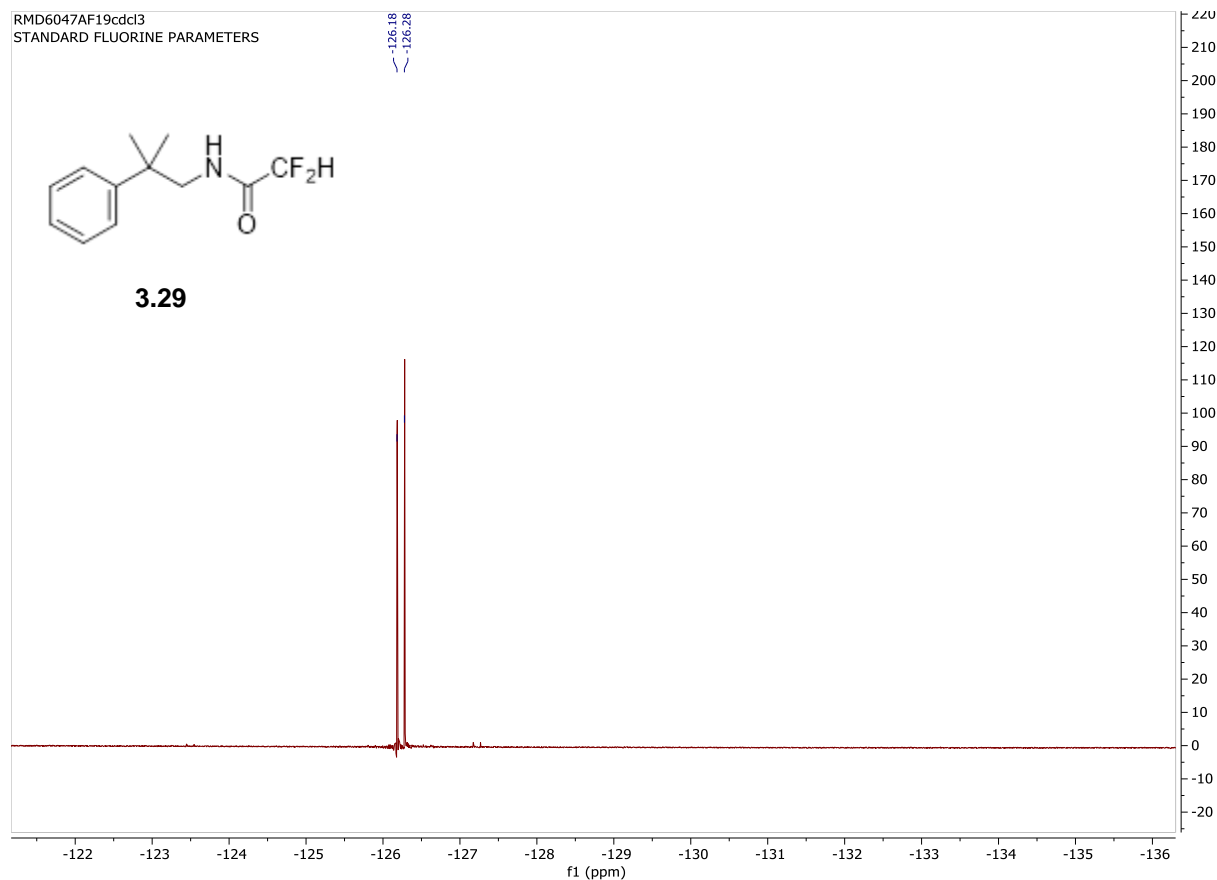


RMD6047AC13cdcl3.1.fid
C13 1D

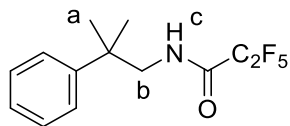


3.29





2,2,3,3,3-pentafluoro-N-(2-methyl-2-phenylpropyl)propanamide (3.30)



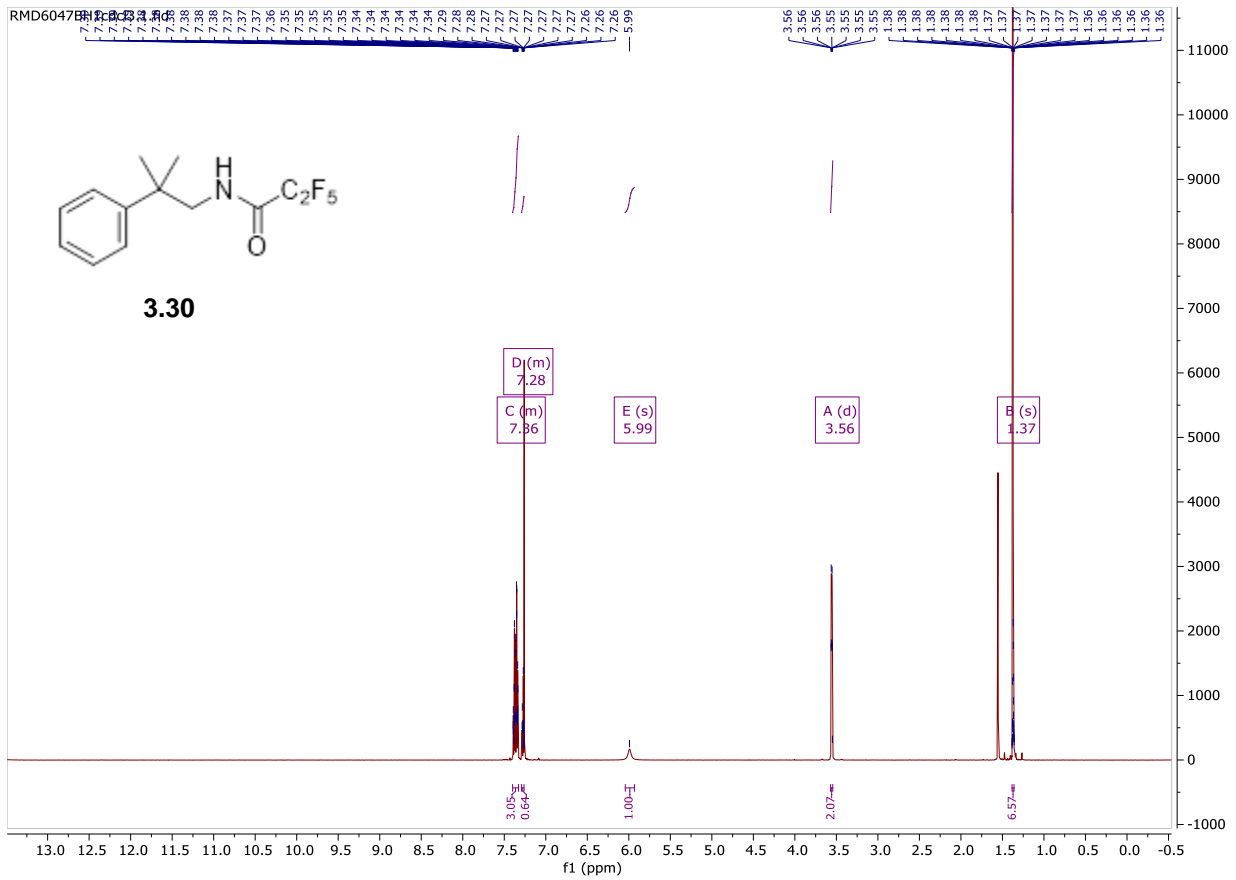
2,2,3,3,3-pentafluoro-N-(2-methyl-2-phenylpropyl)propanamide was synthesized following the general procedure for acetamide formation on a 6.7 mmol scale of 2-methyl-2-phenylpropan-1-amine, as the respective amine. 2,2,3,3,3-pentafluoropropanoic anhydride was used as the anhydride. The compound was purified using silica gel chromatography with 10% ethyl acetate/hexane to give 1.43 g of a white solid (4.85 mmol, 72% yield).

¹H NMR (600 MHz, CDCl₃) δ 7.40 – 7.33 (m, 4H), 7.29 – 7.26 (m, 1H), 5.99 (H_c, s, 1H), 3.56 (H_b, d, *J* = 6.3, 2H), 1.37 (H_a, s, 6H) ppm.

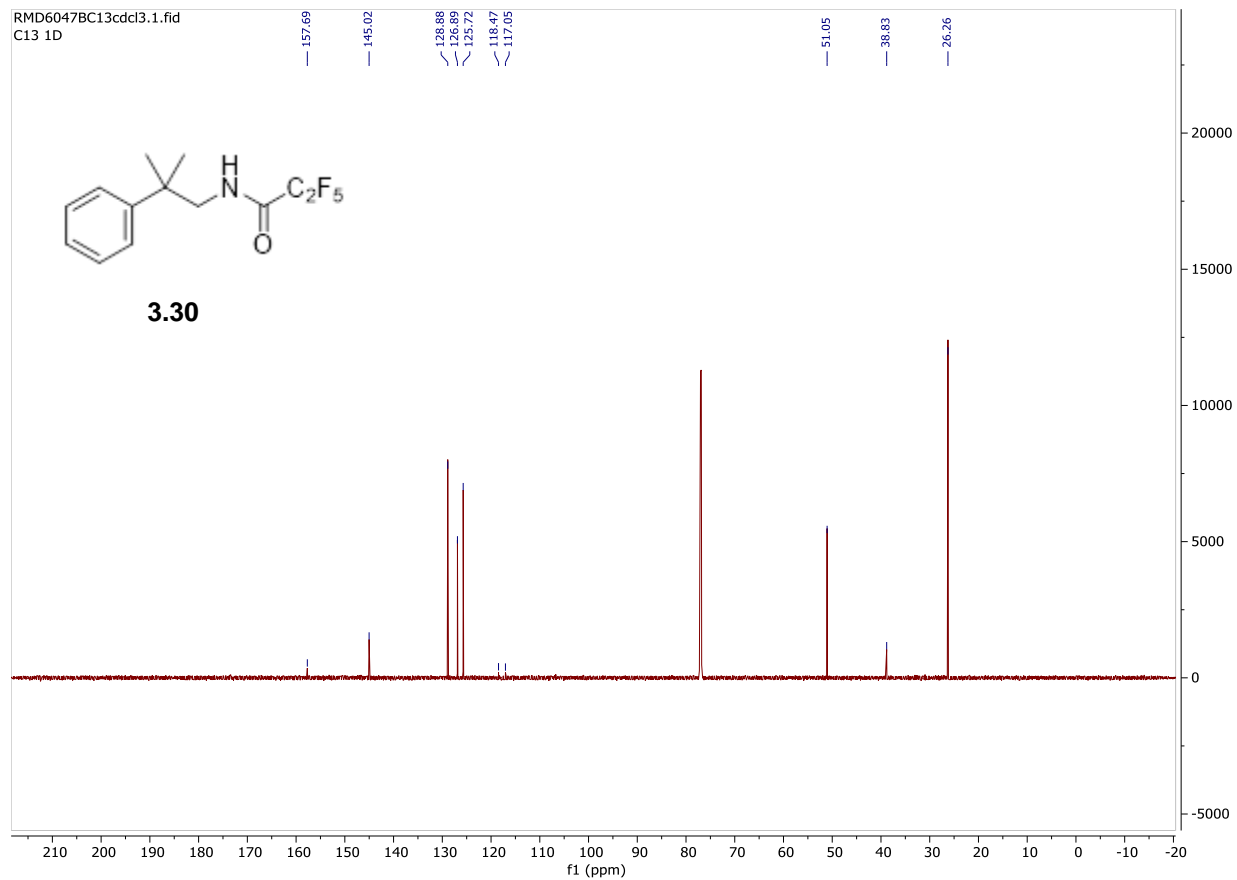
¹³C NMR (201 MHz, CDCl₃) δ 157.6, 145.0, 128.8, 126.8, 125.7, 118.4, 117.0, 51.0, 38.8, 26.2 ppm.

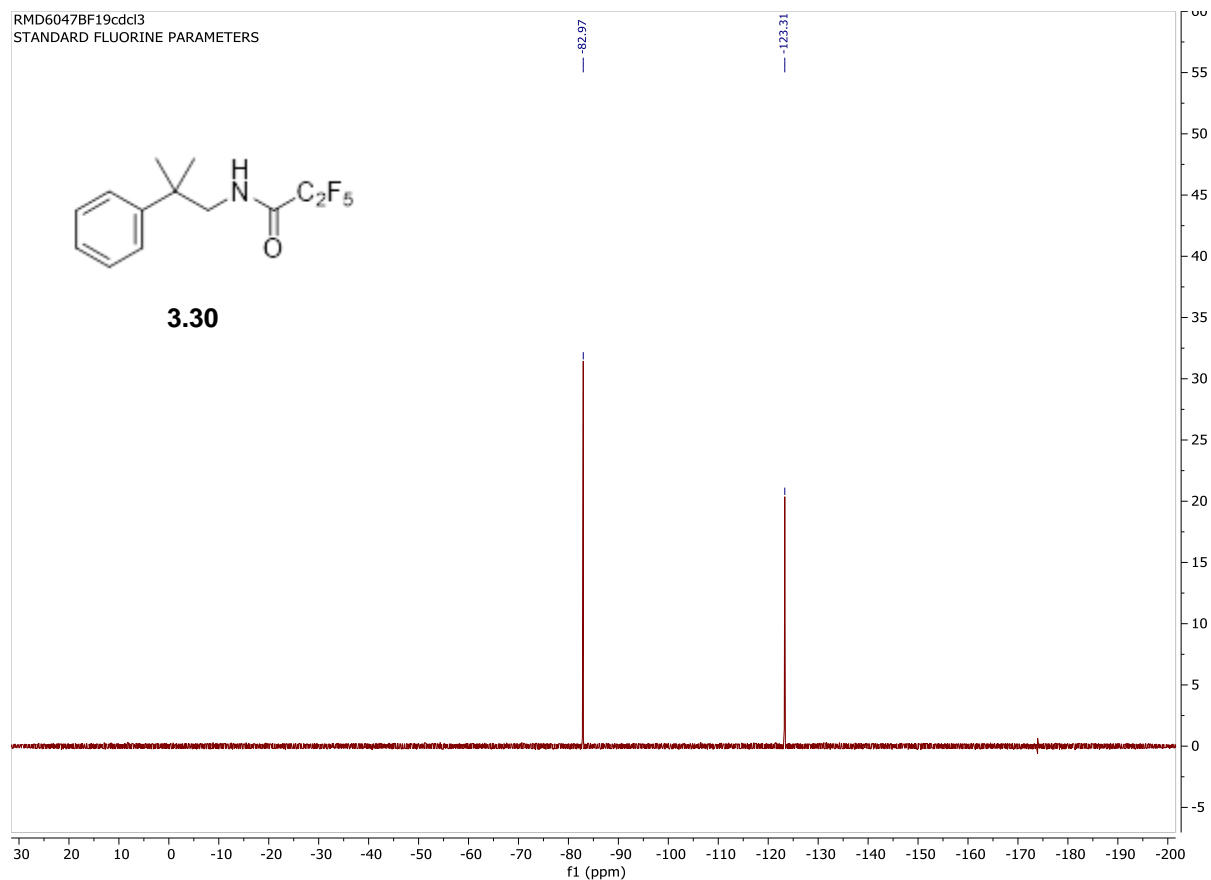
¹⁹F NMR (564 MHz, CDCl₃) δ -82.97, -123.31 ppm.

HRMS Calc'd for C₁₃H₁₄F₅NO (M+Na): 318.0893 Found: 318.0954

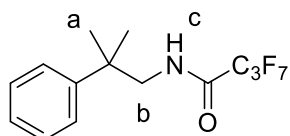


RMD6047BC13cdcl3.1.fid
C13 1D





4,4,4,4,4,4,4-heptafluoro-N-(2-methyl-2-phenylpropyl)-418-but-2-ynamide (3.31)



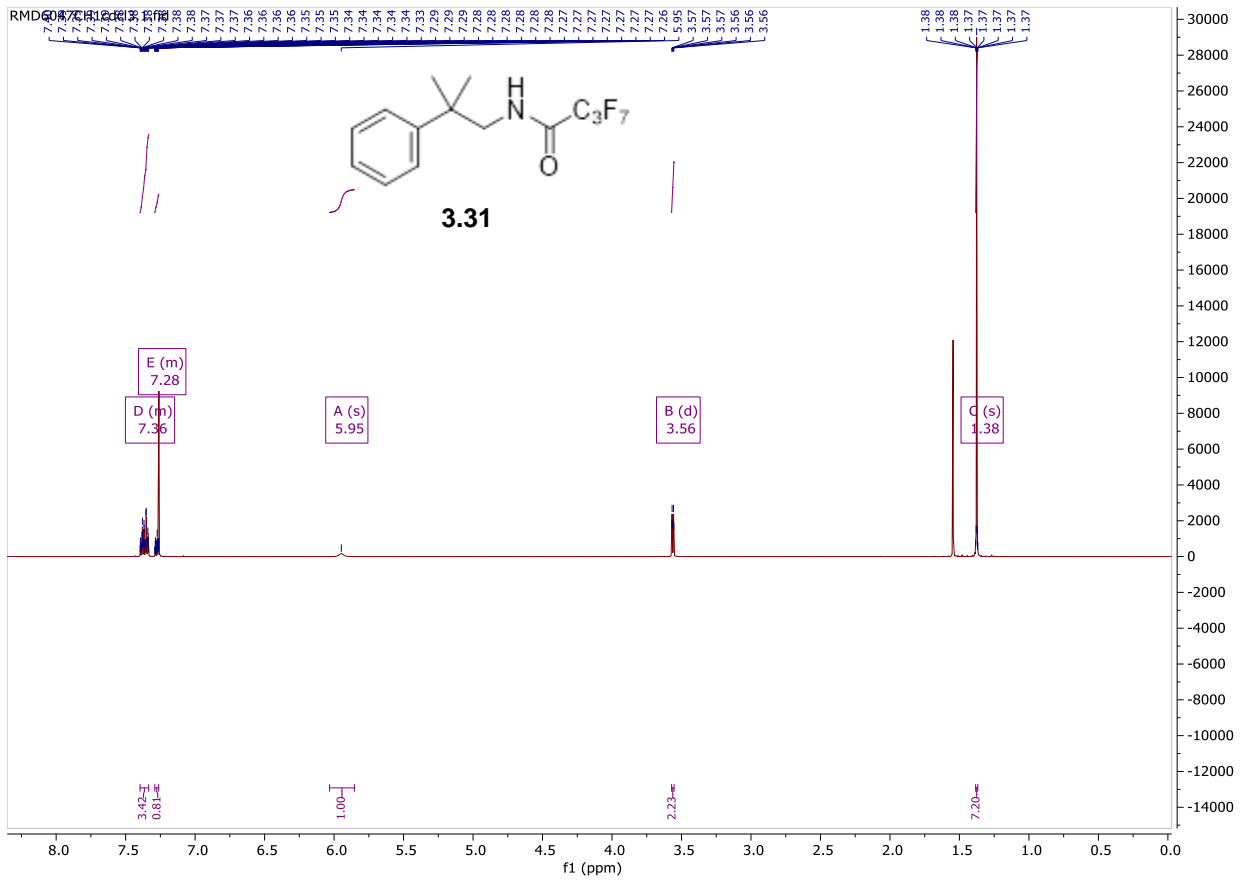
4,4,4,4,4,4,4-heptafluoro-N-(2-methyl-2-phenylpropyl)-418-but-2-ynamide was synthesized following the general procedure for acetamide formation on a 6.7 mmol scale of 2-methyl-2-phenylpropan-1-amine. 2-methyl-2-phenylpropan-1-amine was used as the anhydride. The compound was purified using silica gel chromatography with 10% ethyl acetate/hexane to give 1.55 g of a white solid (4.49 mmol, 67% yield).

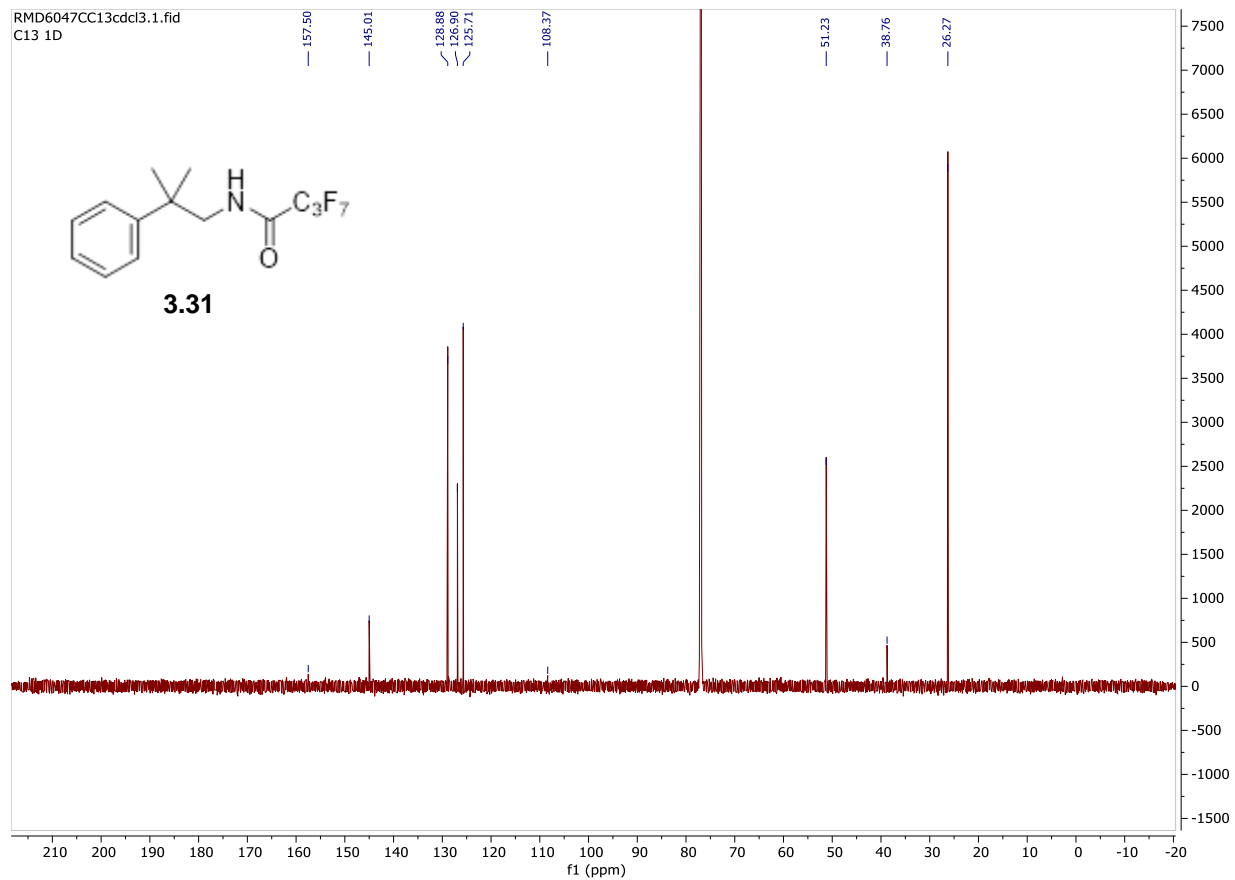
¹H NMR (600 MHz, CDCl₃) δ 7.40 – 7.33 (m, 4H), 7.29 – 7.26 (m, 1H), 5.95 (H_c, s, 1H), 3.56 (H_b, d, *J* = 6.3 Hz, 2H), 1.38 (H_a, s, 6H) ppm.

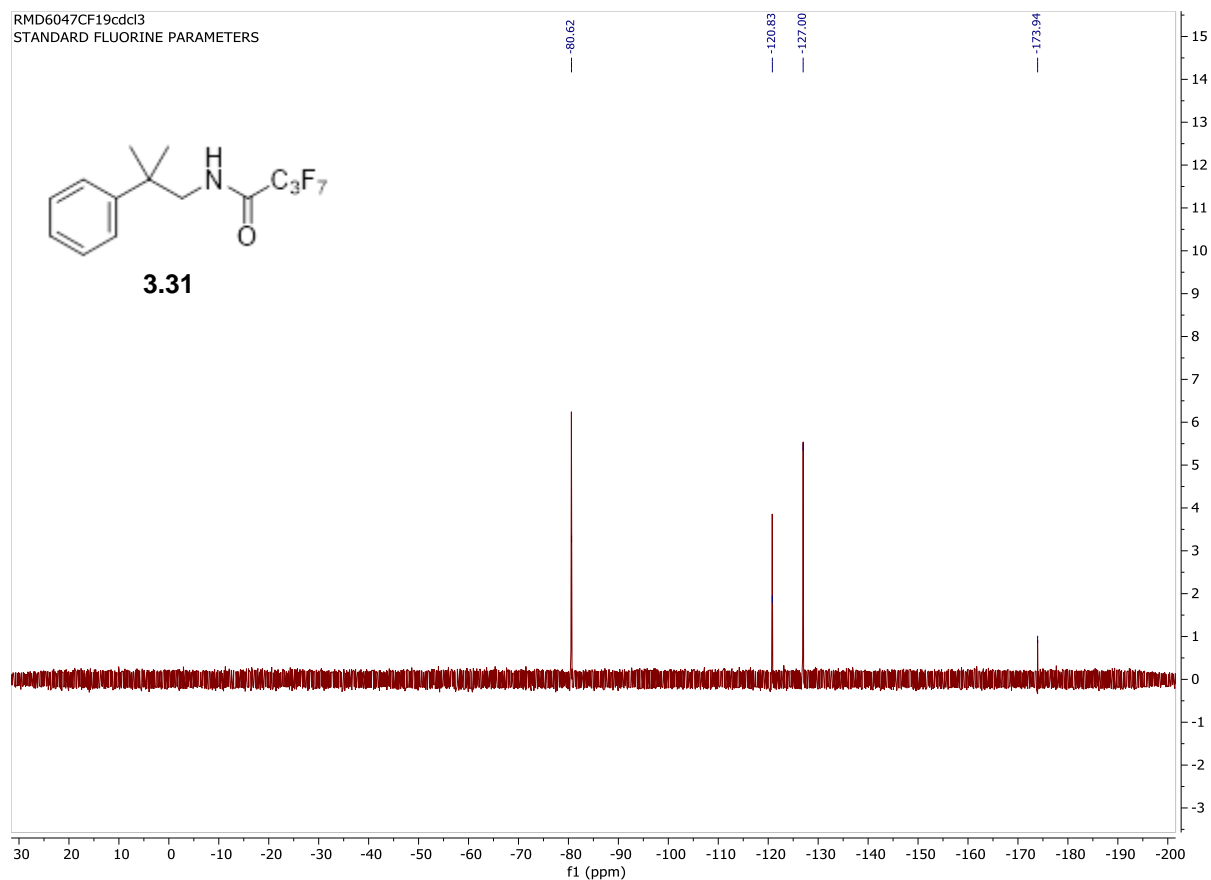
¹³C NMR (201 MHz, CDCl₃) δ 157.5, 145.0, 128.8, 126.9, 125.7, 108.3, 51.2, 38.7, 26.2 ppm.

¹⁹F NMR (564 MHz, CDCl₃) δ -80.62, -120.83, -127.00, -173.94 ppm.

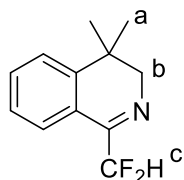
HRMS Calc'd for C₁₄H₁₄F₇NO (M+Na): 368.0861 Found: 368.0858







1-(difluoromethyl)-4,4-dimethyl-3,4-dihydroisoquinoline (3.32)



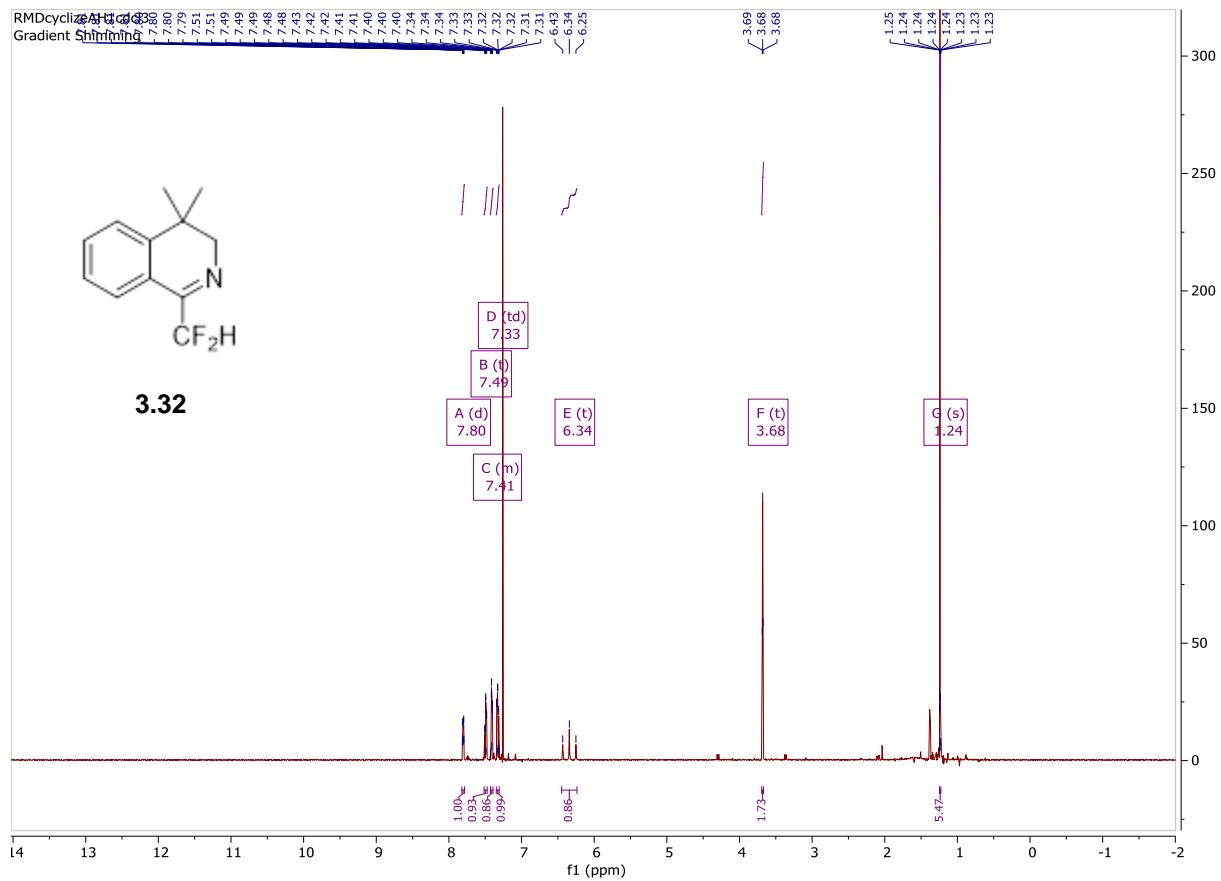
1-(difluoromethyl)-4,4-dimethyl-3,4-dihydroisoquinoline was synthesized following general procedure A for the Bischler Naperialski reaction on a 4.89 mmol scale using 2,2-difluoro-N-(2-methyl-2-phenylpropyl) acetamide, as the respective amide. The compound was purified using silica gel chromatography with 5% ethyl acetate/hexane to give 0.550 g of a yellow oil (2.61 mmol, 53% yield).

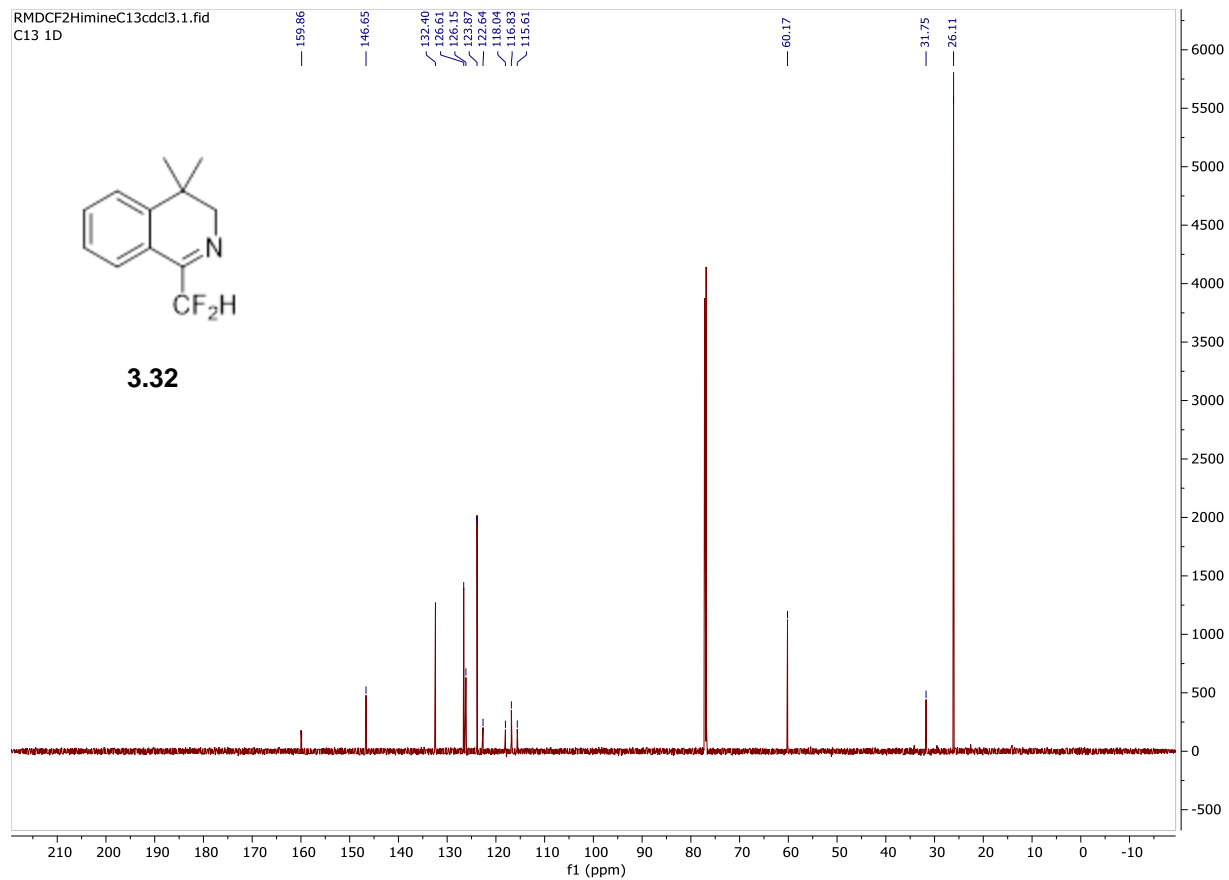
¹H NMR (600 MHz, CDCl₃) δ 7.80 (d, *J* = 7.9 Hz, 1H), 7.49 (t, *J* = 7.6 Hz, 1H), 7.43 – 7.39 (m, 1H), 7.33 (td, *J* = 7.6, 1.3 Hz, 1H), 6.34 (H_c, t, *J* = 54.5 Hz, 1H), 3.68 (H_b, t, *J* = 3.2 Hz, 2H), 1.24 (H_a, s, 6H) ppm.

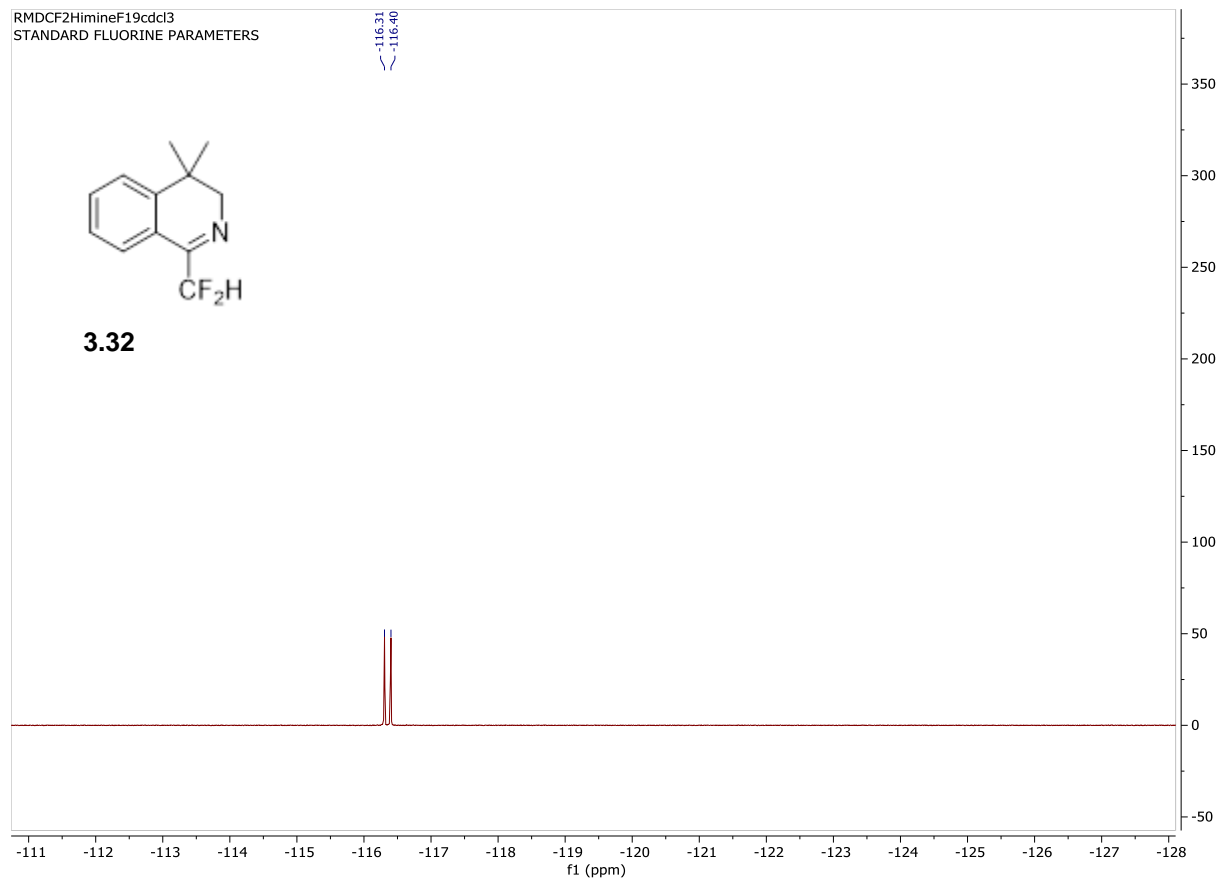
¹³C NMR (201 MHz, CDCl₃) δ 159.8, 146.6, 132.4, 126.61, 126.15, 123.8, 122.6, 118.0, 116.8, 115.6, 60.1, 31.7, 26.1 ppm.

¹⁹F NMR (564 MHz, CDCl₃) δ -116.31, -116.40 ppm.

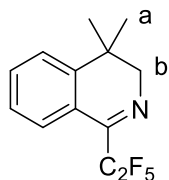
HRMS Calc'd for C₁₂H₁₃F₂N (M+H): 210.1095 Found: 210.1151







4,4-dimethyl-1-(perfluoroethyl)-3,4-dihydroisoquinoline (3.33)



4,4-dimethyl-1-(perfluoroethyl)-3,4-dihydroisoquinoline was synthesized following general procedure B for the Bischler Naperialski reaction on a 2.1 mmol scale using 2,2,3,3,3-pentafluoro-N-(2-methyl-2-phenylpropyl)propanamide, as the respective amide. The compound was purified using silica gel chromatography with 10% ethyl acetate/hexane to give 0.231 of a yellow oil (0.833 mmol, 27% yield).

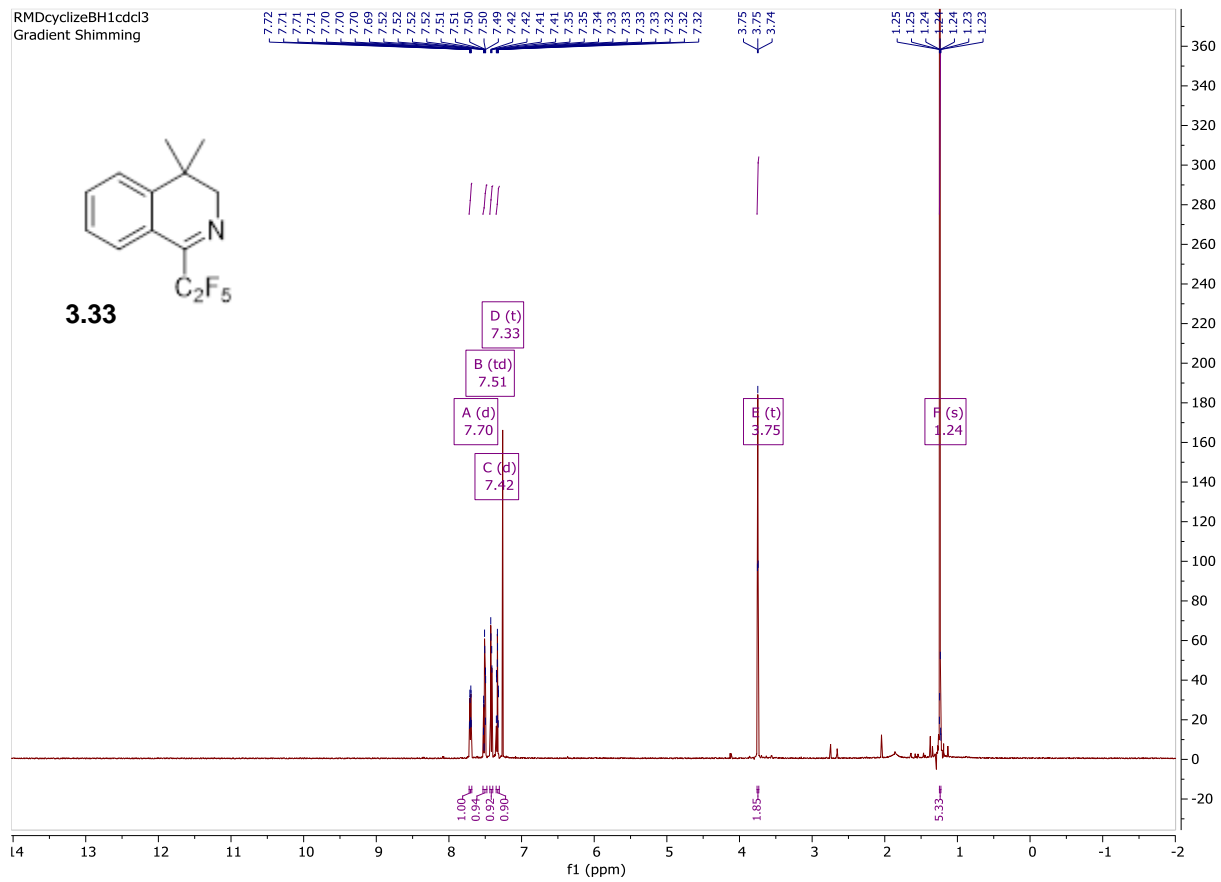
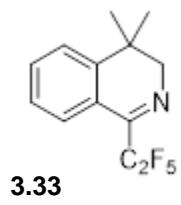
$^1\text{H NMR}$ (600 MHz, CDCl_3) δ 7.70 (d, $J = 7.8$ Hz, 1H), 7.51 (td, $J = 7.6, 1.2$ Hz, 1H), 7.42 (d, $J = 7.8$ Hz, 1H), 7.33 (t, $J = 7.7$ Hz, 1H), 3.75 (H_b , t, $J = 2.8$ Hz, 2H), 1.24 (H_a , s, 6H) ppm.

$^{13}\text{C NMR}$ (201 MHz, CDCl_3) δ 156.46, 156.33, 156.20, 146.8, 132.7, 126.6, 125.9, 123.9, 122.5, 119.4, 118.0, 59.9, 31.6, 25.7 ppm.

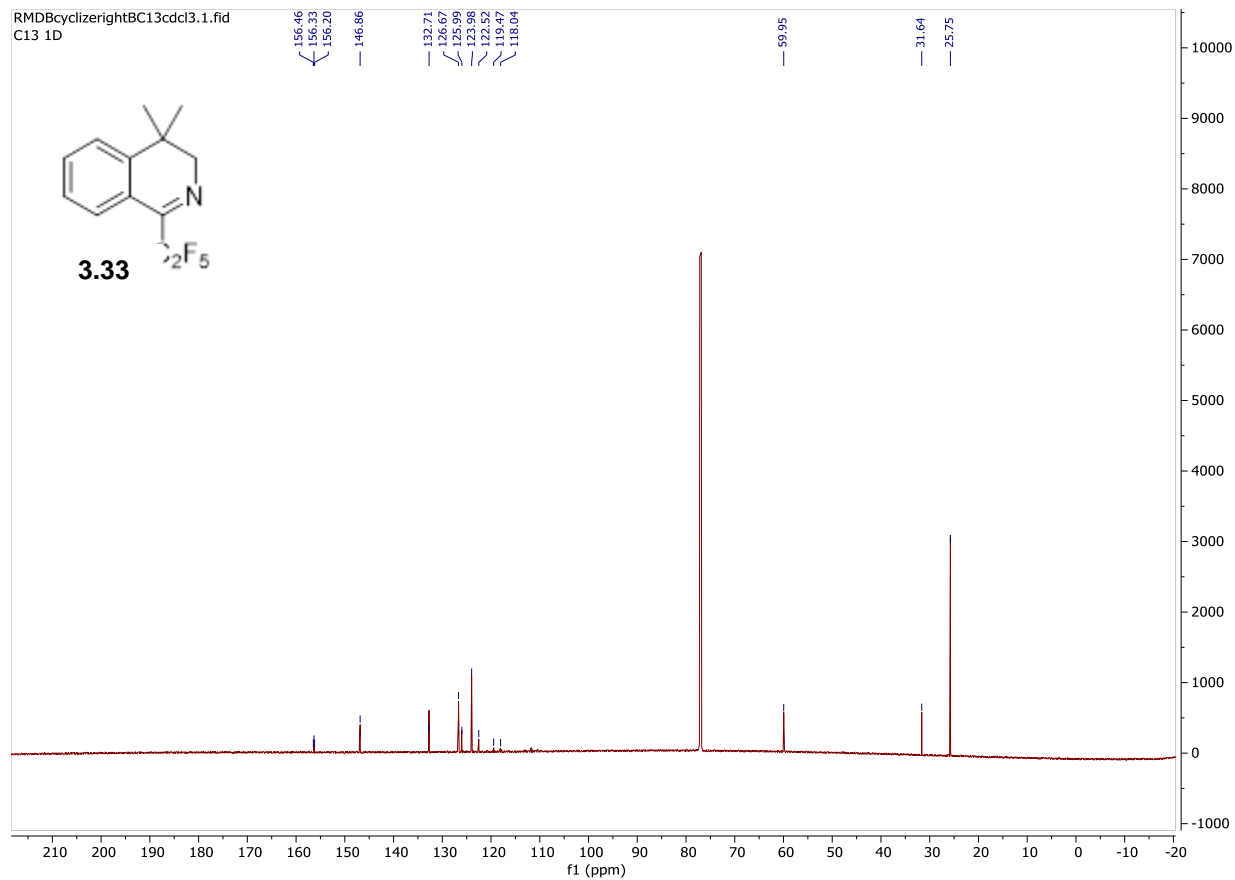
$^{19}\text{F NMR}$ (564 MHz, CDCl_3) δ -82.62, -113.73 ppm.

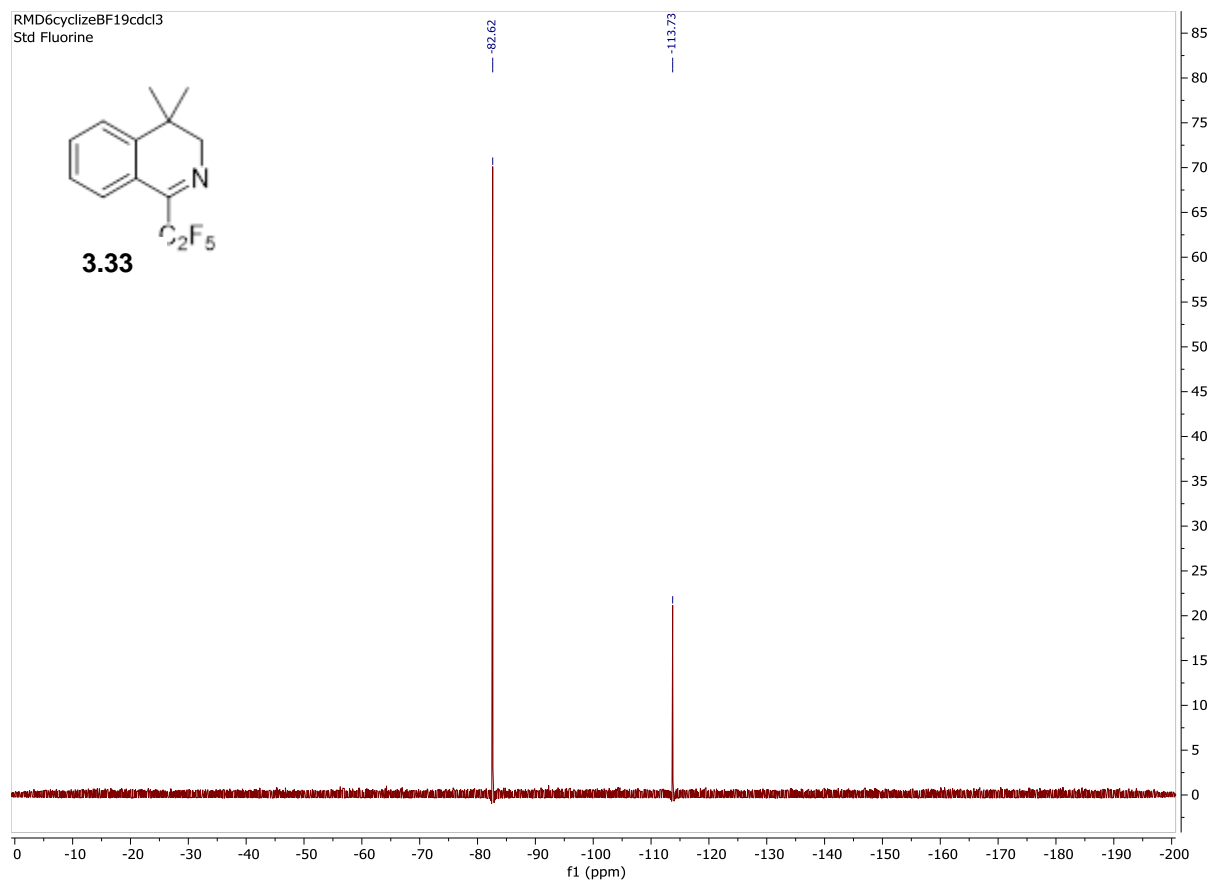
HRMS Calc'd for $\text{C}_{13}\text{H}_{12}\text{F}_5\text{N}$ (M+H): 278.0969 Found: 278.0968

RMDcyclizeBH1.cdcl3
Gradient Shimming

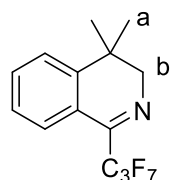


RMDBcyclizerightBC13cdcl3.1.fid
C13 1D





1-(3,3,3,3,3,3,3-heptafluoro-1-prop-1-yn-1-yl)-4,4-dimethyl-3,4-dihydroisoquinoline (3.34)



1-(3,3,3,3,3,3,3-heptafluoro-1-prop-1-yn-1-yl)-4,4-dimethyl-3,4-dihydroisoquinoline was synthesized following general procedure B for the Bischler Napieralski reaction on a 8.4 mmol scale using 4,4,4,4,4,4,4-heptafluoro-N-(2-methyl-2-phenylpropyl)-418-but-2-ynamide, as the respective amide. The compound was purified using silica gel chromatography with 40% DCM/hexanes to give 1.12 g of an orange oil (3.41 mmol, 41% yield).

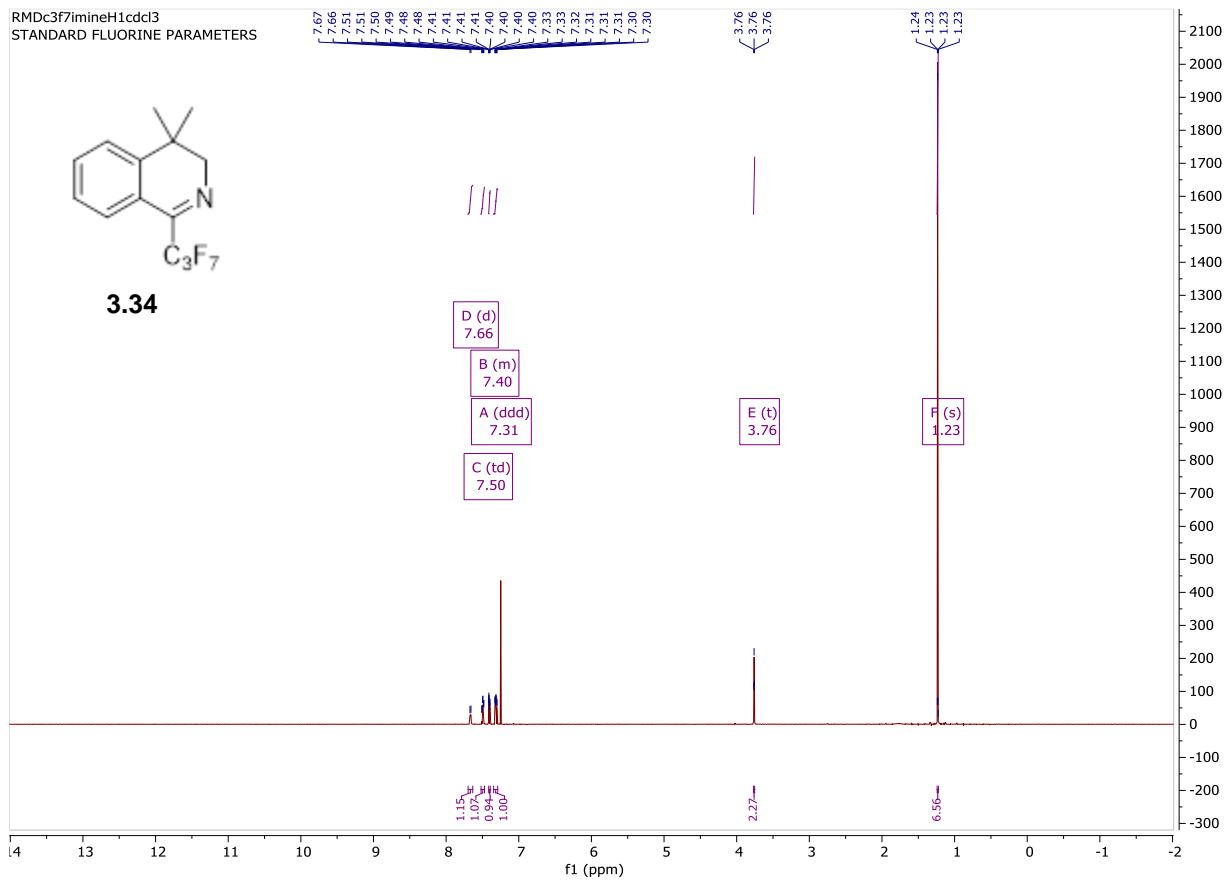
¹H NMR (600 MHz, CDCl₃) δ 7.66 (d, *J* = 8.0 Hz, 1H), 7.50 (td, *J* = 7.6, 1.3 Hz, 1H), 7.41 – 7.39 (m, 1H), 7.31 (ddd, *J* = 7.9, 7.4, 1.3 Hz, 1H), 3.76 (H_b, t, *J* = 2.5 Hz, 2H), 1.23 (H_a, s, 6H) ppm.

¹³C NMR (201 MHz, CDCl₃) δ 156.5, 146.8, 132.7, 126.67, 126.17, 124.0, 122.9, 60.1, 31.6, 25.7 ppm.

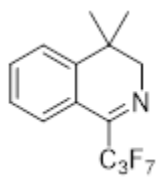
¹⁹F NMR (564 MHz, CDCl₃) δ -79.76, -109.72, -124.03 ppm.

HRMS Calc'd for C₁₄H₁₂F₇N (M+H): 328.0937 Found: 328.1070

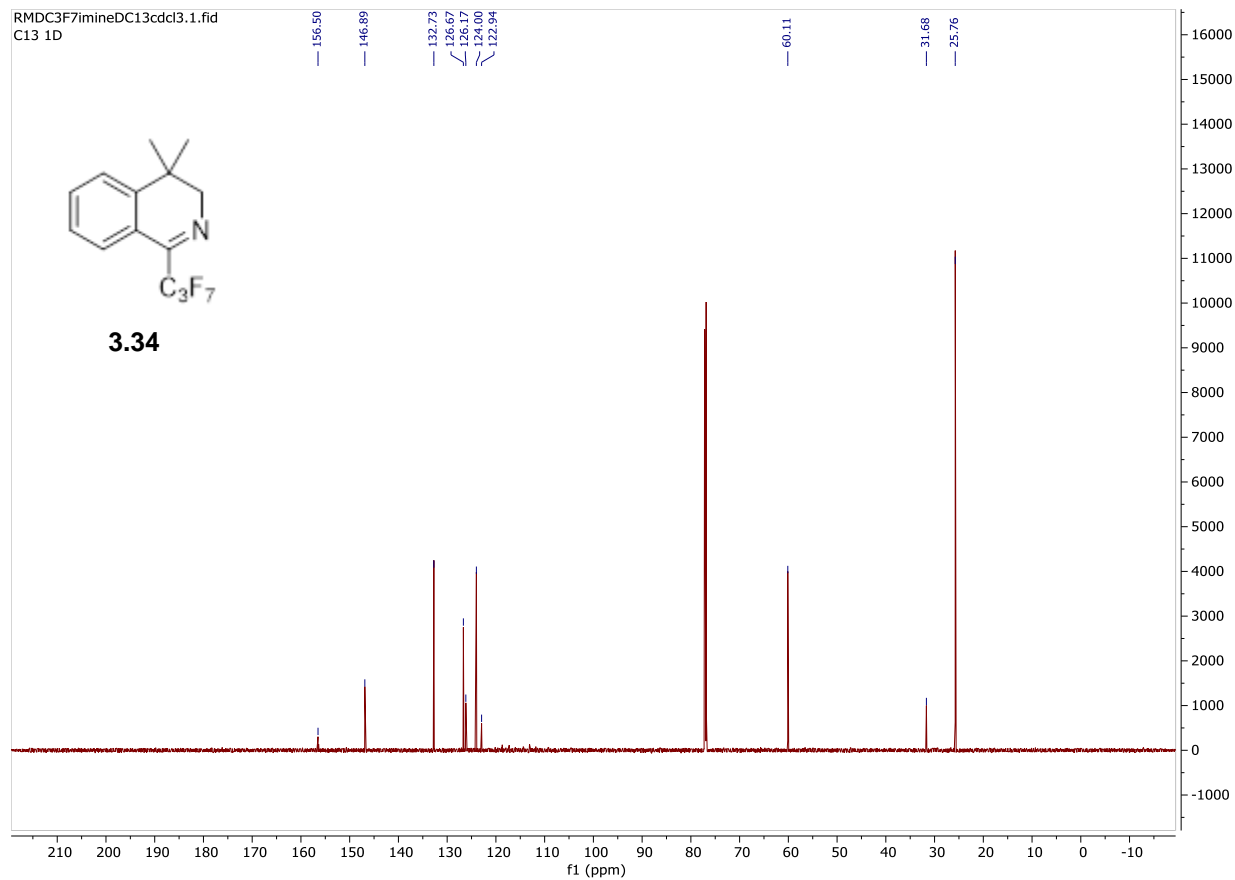
RMDC3f7imineH1cdcd3
STANDARD FLUORINE PARAMETERS

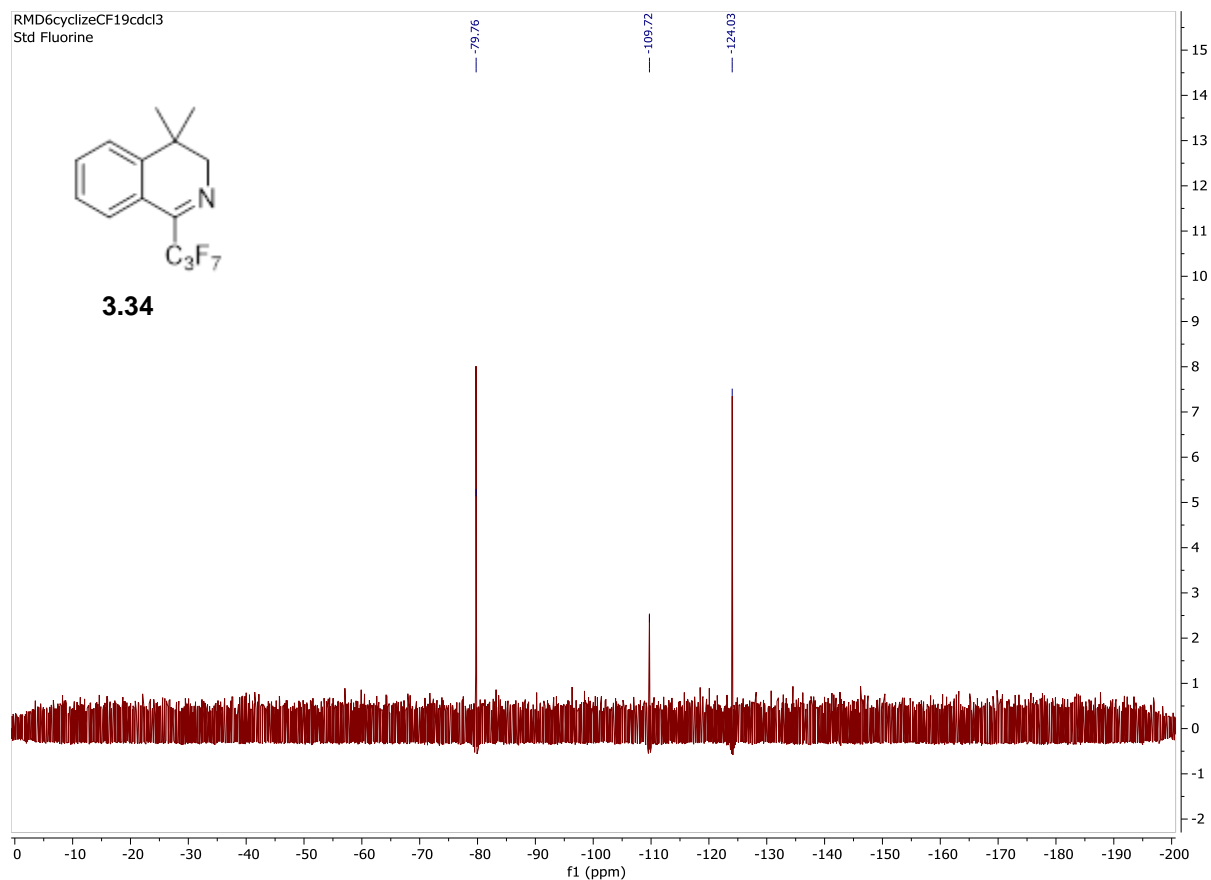


RMDC3F7imineDC13cdcl3.1.fid
C13 1D

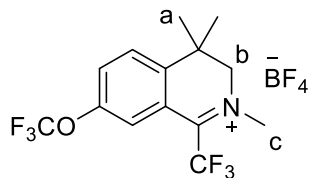


3.34





2,4,4-trimethyl-7-(trifluoromethoxy)-1-(trifluoromethyl)-3,4-dihydroisoquinolin-2-ium tetrafluoroborate (3.43)



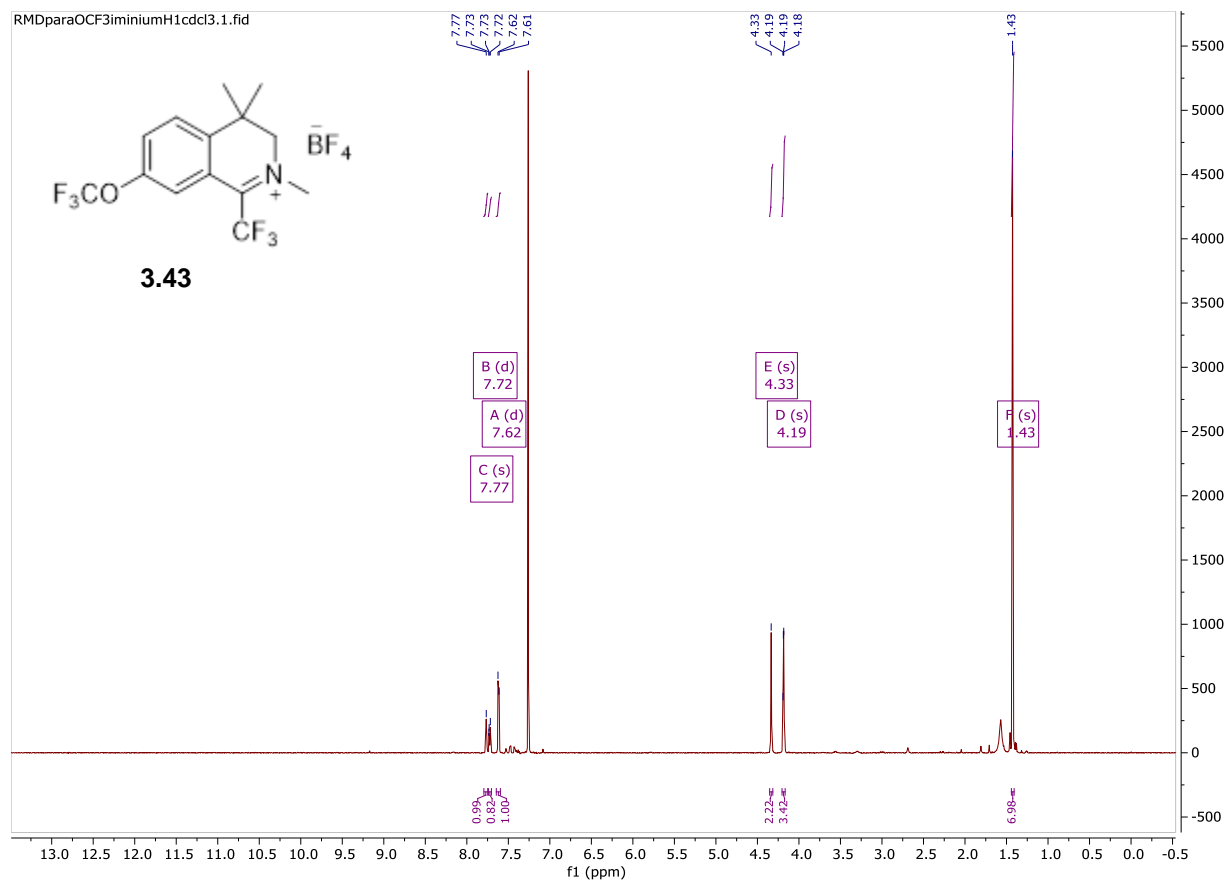
2,4,4-trimethyl-7-(trifluoromethoxy)-1-(trifluoromethyl)-3,4-dihydroisoquinolin-2-ium tetrafluoroborate was synthesized following general procedure for imine methylation a .86 mmol scale using ,4-dimethyl-7-(trifluoromethoxy)-1-(trifluoromethyl)-3,4-dihydroisoquinoline, as the respective imine, to give 0.20 g of an off white sold (0.69 mmol, 80% yield).

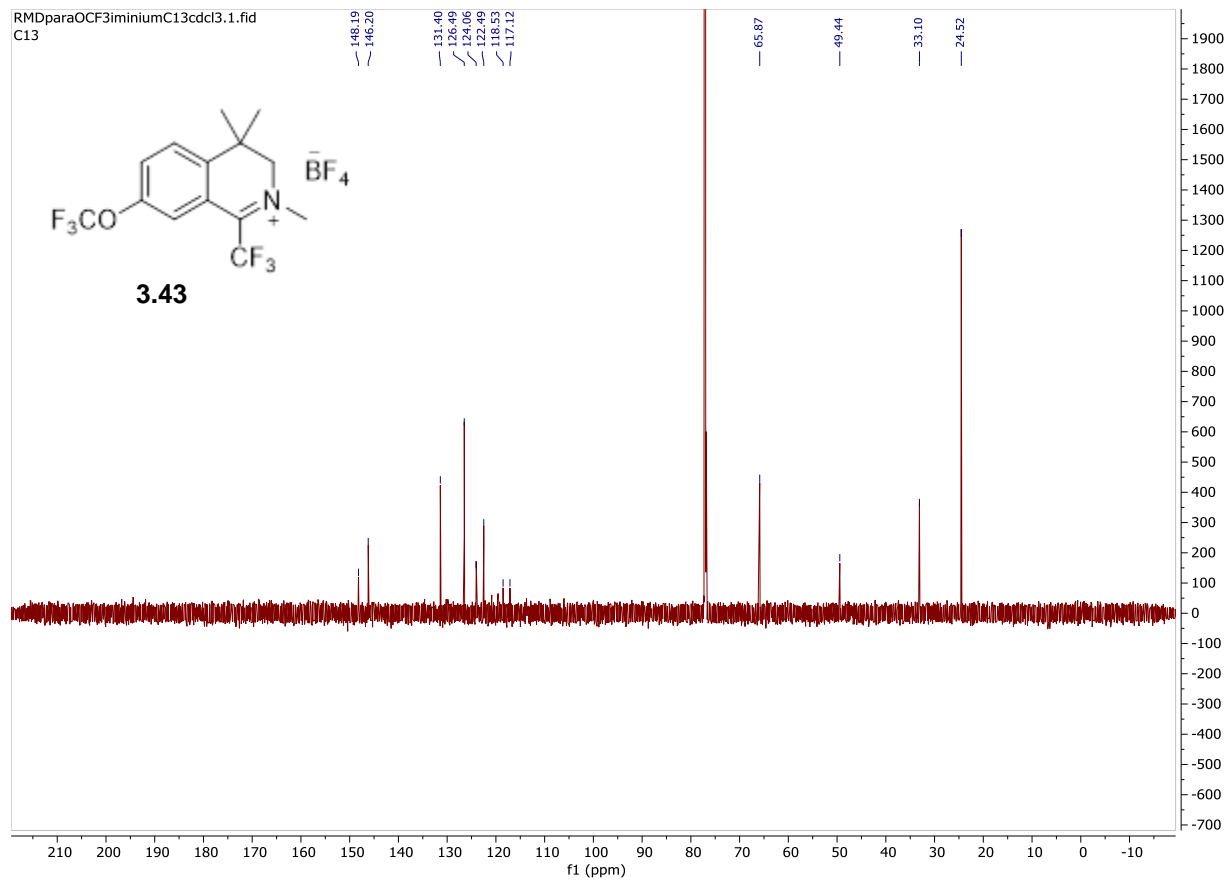
¹H NMR (600 MHz, CDCl₃) δ 7.77 (s, 1H), 7.72 (d, *J* = 8.6 Hz, 1H), 7.62 (d, *J* = 8.6 Hz, 1H), 4.33 (H_b, s, 2H), 4.19 (H_c, s, 3H), 1.43 (H_a, s, 6H) ppm.

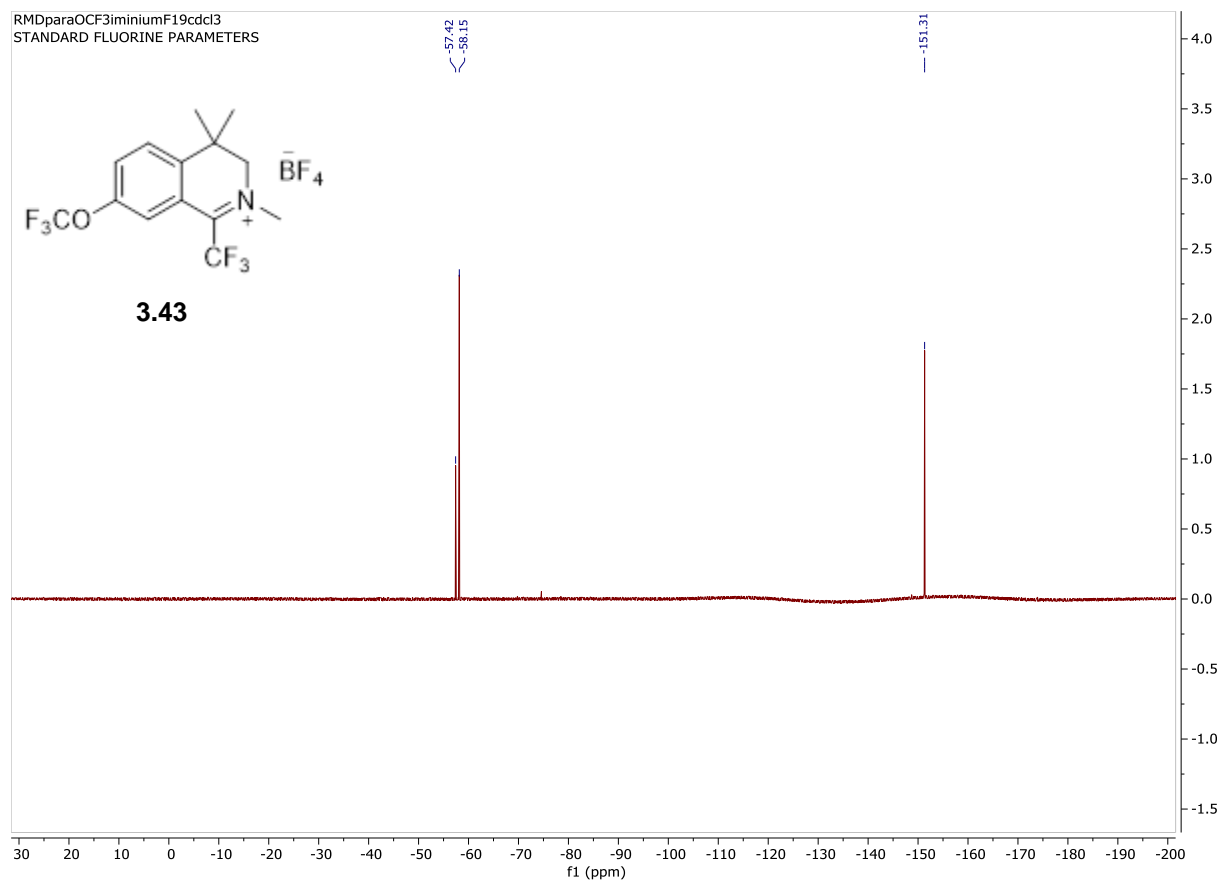
¹³C NMR (201 MHz, CDCl₃) δ 148.1, 146.2, 131.4, 126.4, 124.0, 122.4, 118.5, 117.1, 65.8, 49.4, 33.1, 24.5 ppm.

¹⁹F NMR (564 MHz, CDCl₃) δ -57.42, -58.15, -151.31 ppm.

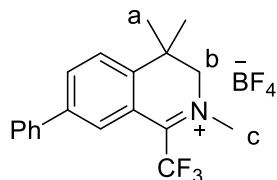
HRMS Calc'd for C₁₄H₁₄F₆NO (M+H): 327.1059 Found: 327.1042







2,4,4-trimethyl-7-phenyl-1-(trifluoromethyl)-3,4-dihydroisoquinolin-2-ium tetrafluoroborate (3.44)



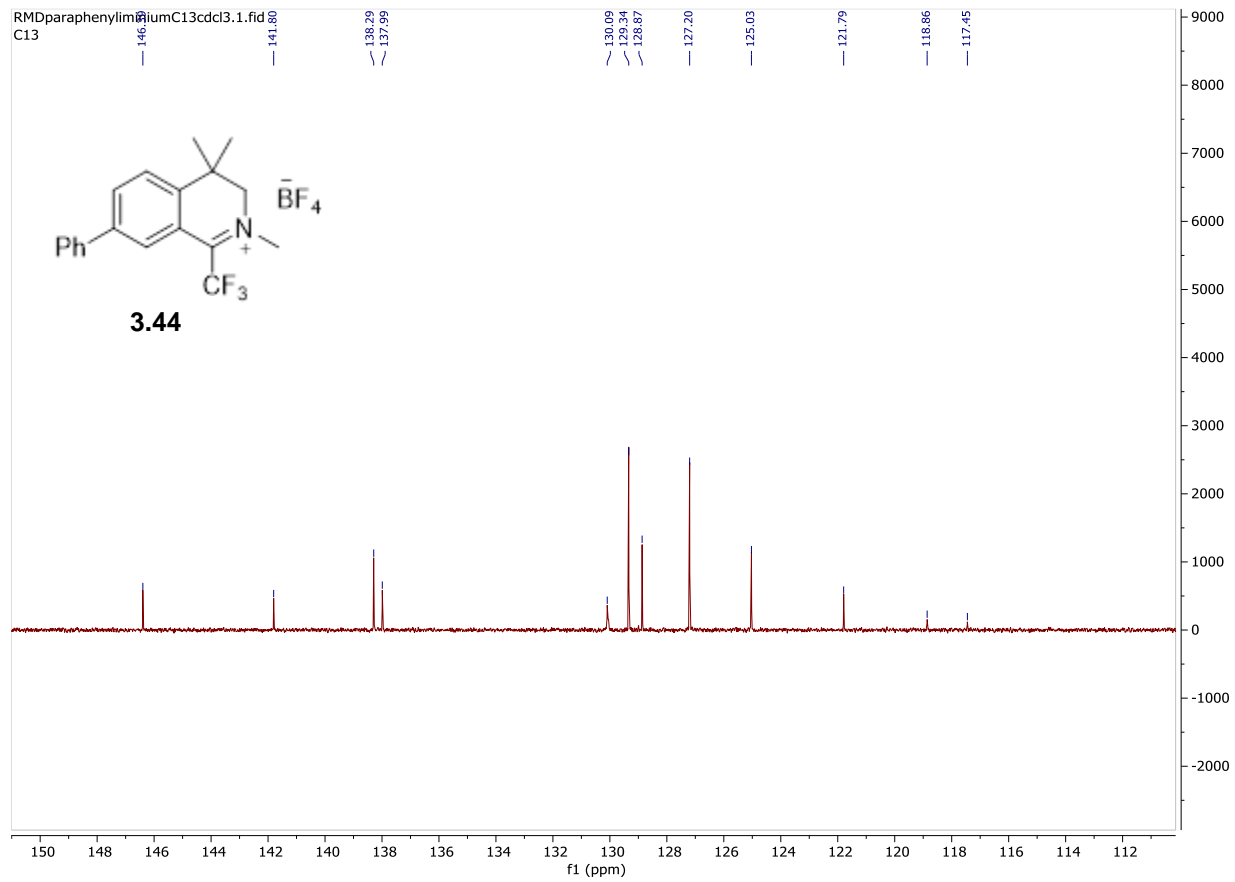
2,4,4-trimethyl-7-phenyl-1-(trifluoromethyl)-3,4-dihydroisoquinolin-2-ium tetrafluoroborate was synthesized following general procedure for imine methylation a 3.62 mmol scale using 4,4-dimethyl-7-phenyl-1-(trifluoromethyl)-3,4-dihydroisoquinoline, as the respective imine, to give 1.11 g of an off white solid (2.74 mmol, 77% yield)..

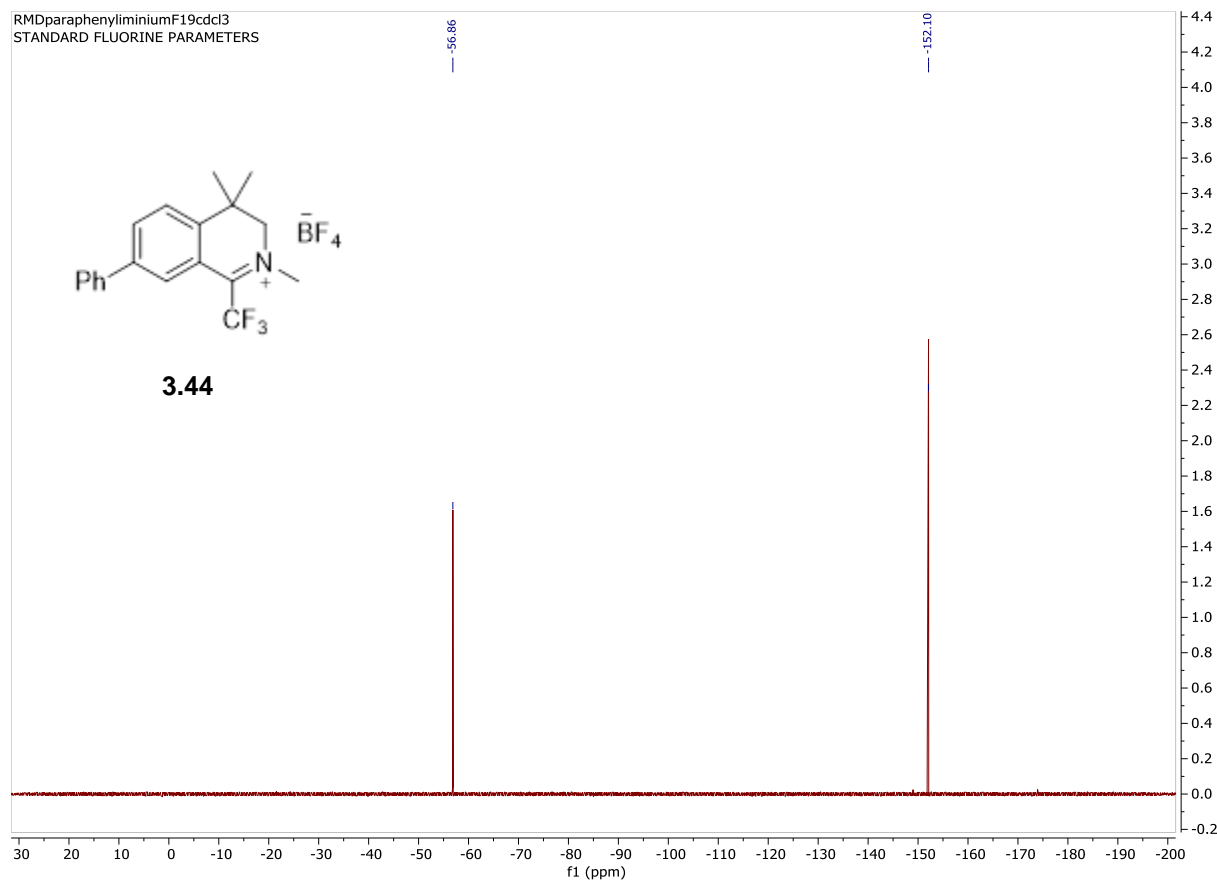
¹H NMR (600 MHz, CDCl₃) δ 8.09 – 8.03 (m, 2H), 7.64 – 7.61 (m, 1H), 7.56 – 7.52 (m, 2H), 7.52 – 7.47 (m, 2H), 7.47 – 7.43 (m, 1H), 4.31 (H_b, s, 2H), 4.19 (H_c, q, *J* = 2.5 Hz, 3H), 1.45 (H_a, s, 6H) ppm.

¹³C NMR (201 MHz, CDCl₃) δ 146.3, 141.8, 138.2, 137.9, 130.0, 129.3, 128.8, 127.2, 125.0, 121.7, 118.6, 117.4, 65.8, 49.1, 33.0, 24.5 ppm

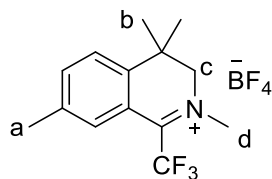
¹⁹F NMR (564 MHz, CDCl₃) δ -56.86, -152.10 ppm.

HRMS Calc'd for C₁₉H₁₉F₃N (M+H): 319.1549 Found: 319.1522





2,4,4,7-tetramethyl-1-(trifluoromethyl)-3,4-dihydroisoquinolin-2-ium tetrafluoroborate (3.45)



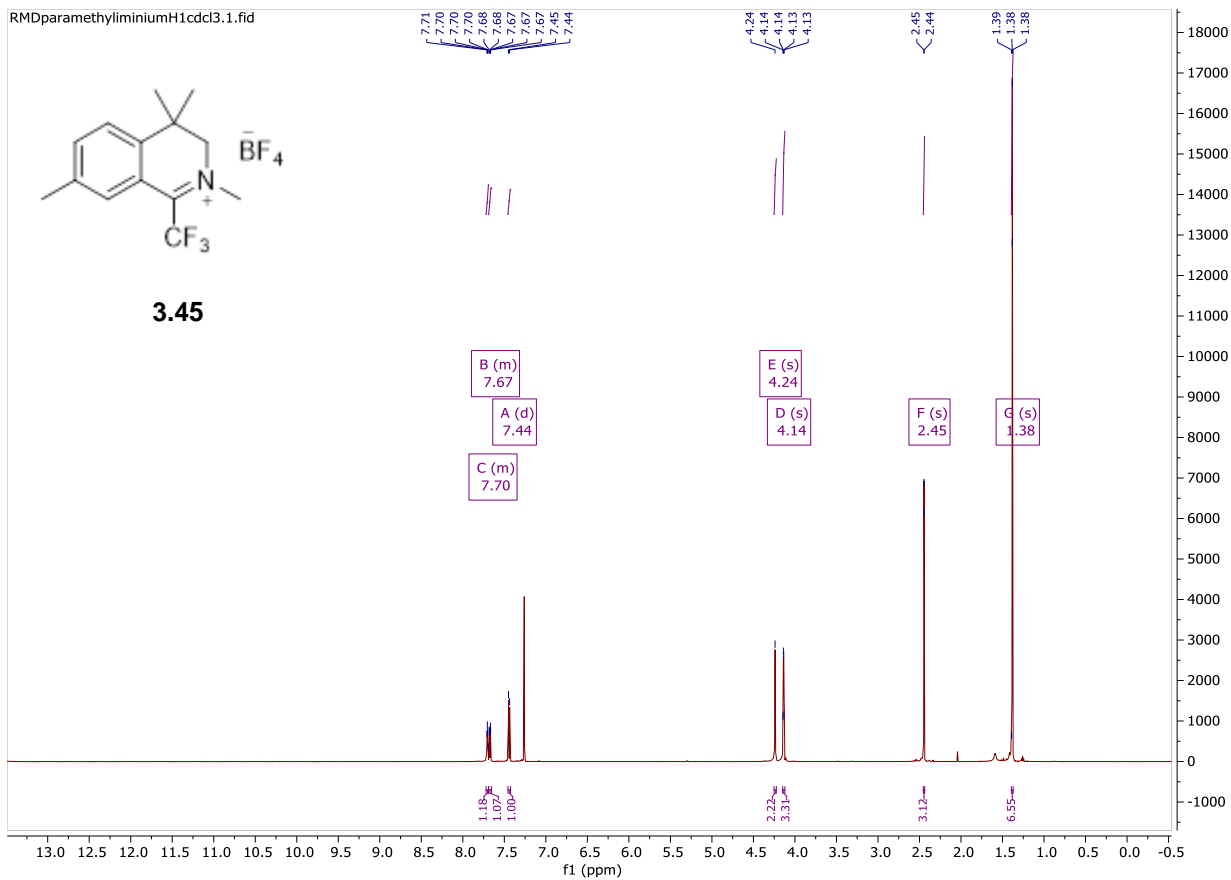
2,4,4,7-tetramethyl-1-(trifluoromethyl)-3,4-dihydroisoquinolin-2-ium tetrafluoroborate was synthesized following general procedure for imine methylation a 5.42 mmol scale using 4,4,7-trimethyl-1-(trifluoromethyl)-3,4-dihydroisoquinoline, as the respective imine, to give 1.60 g of an off yellow solid (4.66 mmol, 86% yield).

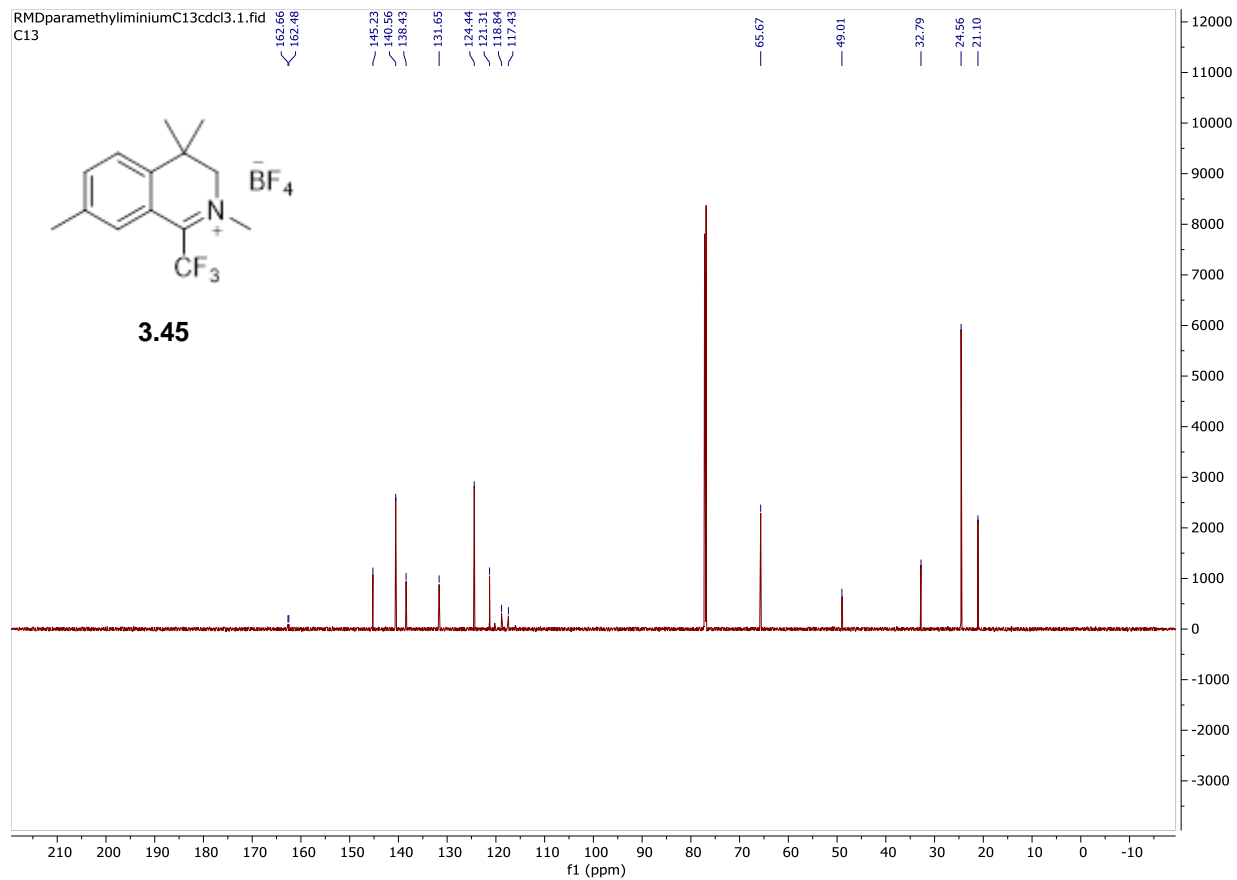
¹H NMR (600 MHz, CDCl₃) δ 7.72 – 7.69 (m, 1H), 7.69 – 7.65 (m, 1H), 7.44 (d, *J* = 8.0 Hz, 1H), 4.24 (H_c, s, 2H), 4.14 (H_d, s, 3H), 2.45 (H_a, s, 3H), 1.38 (H_b, s, 6H) ppm.

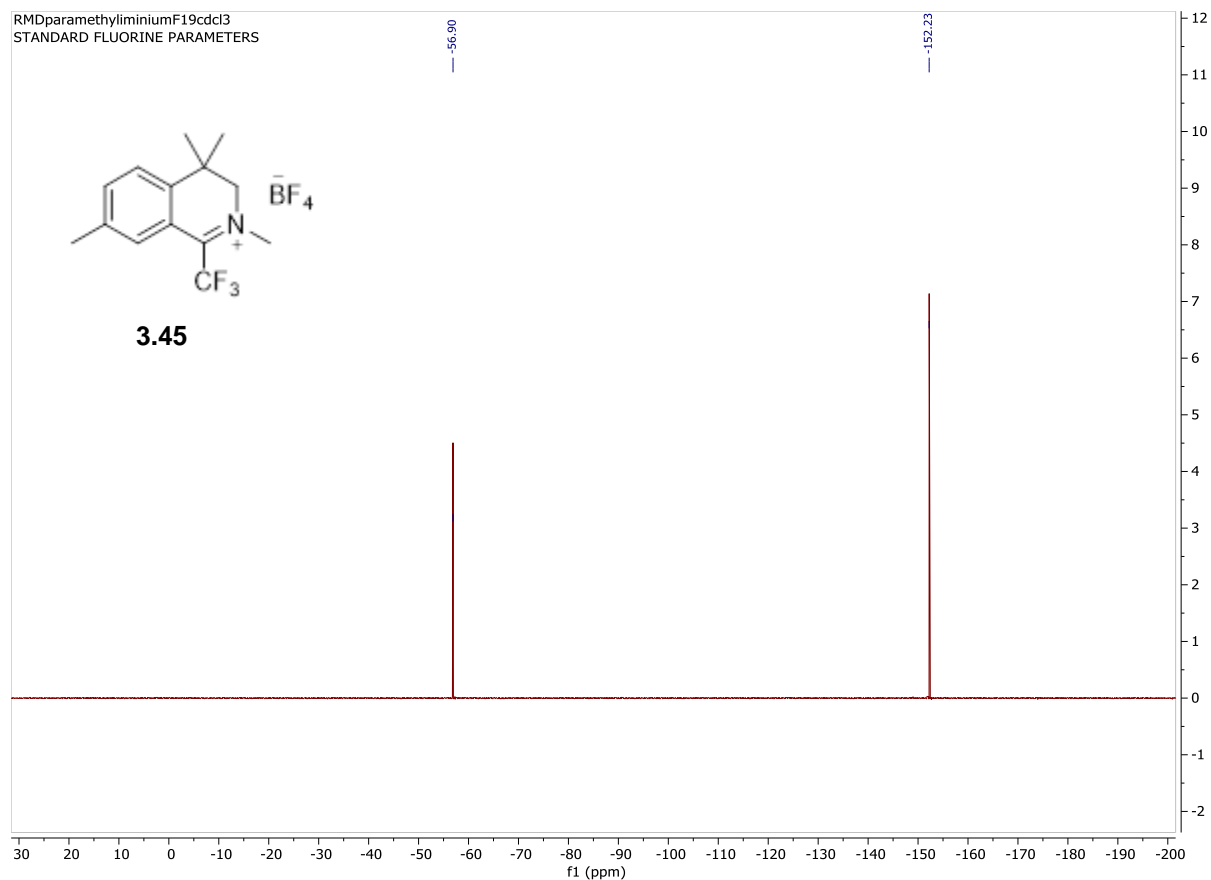
¹³C NMR (201 MHz, CDCl₃) δ 162.6, 162.4, 145.2, 140.5, 138.4, 131.6, 124.4, 121.3, 118.8, 117.3, 65.6, 49.0, 32.7, 24.5, 21.1 ppm.

¹⁹F NMR (564 MHz, CDCl₃) δ -56.90, -152.23 ppm.

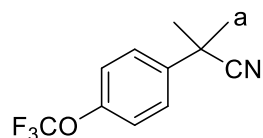
HRMS Calc'd for C₁₄H₁₇F₃N (M): 256.1308 Found: 256.1308







2-methyl-2-(4-(trifluoromethoxy)phenyl)propanenitrile (3.56)



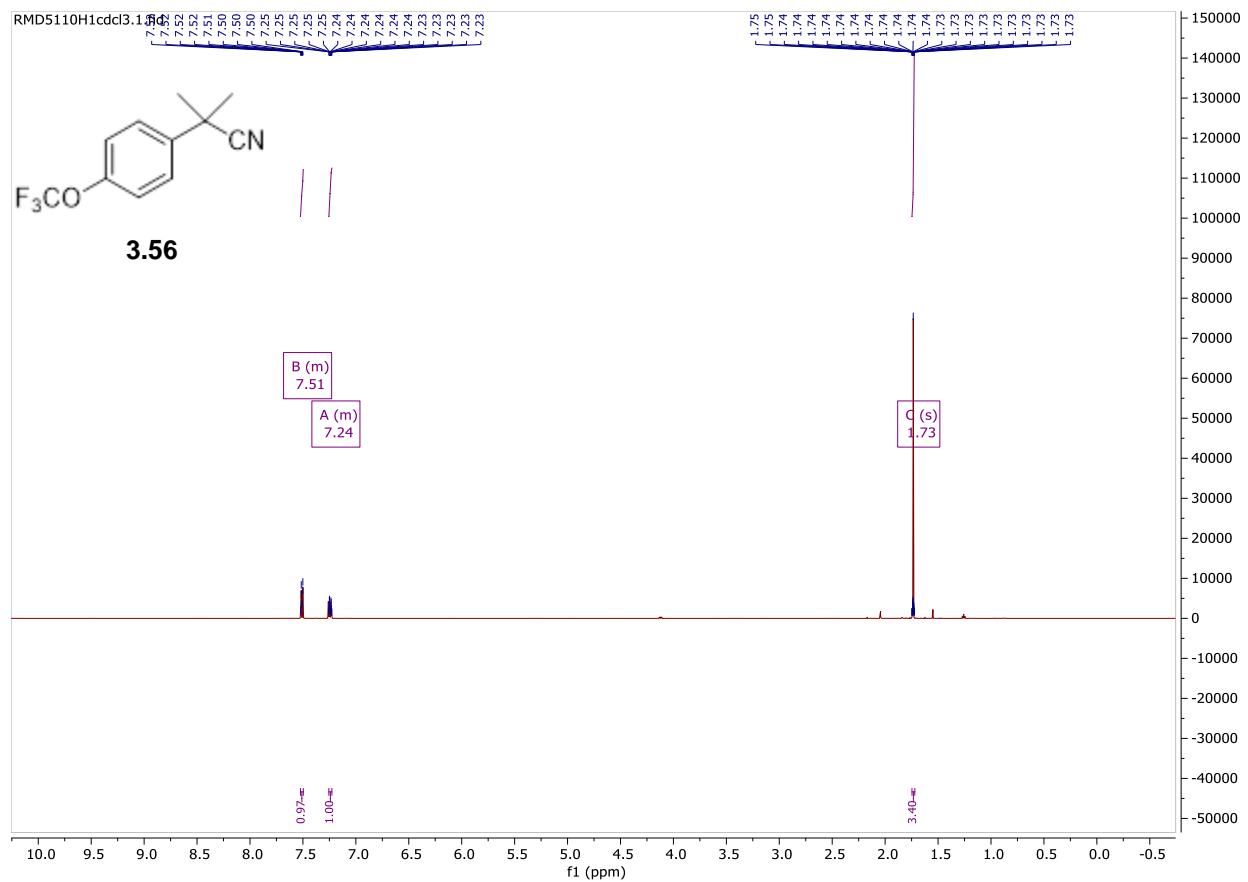
2-methyl-2-(4-(trifluoromethoxy)phenyl)propanenitrile was synthesized following the general procedure for benzylic alkylation on a 9.94 mmol scale using 2-(4-(trifluoromethoxy)phenyl)acetonitrile, as the respective nitrile. The compound was purified using silica gel chromatography with a gradient of 5% to 10% ethyl acetate/hexane to give 1.96 g of an oil. (8.57 mmol, 86% yield).

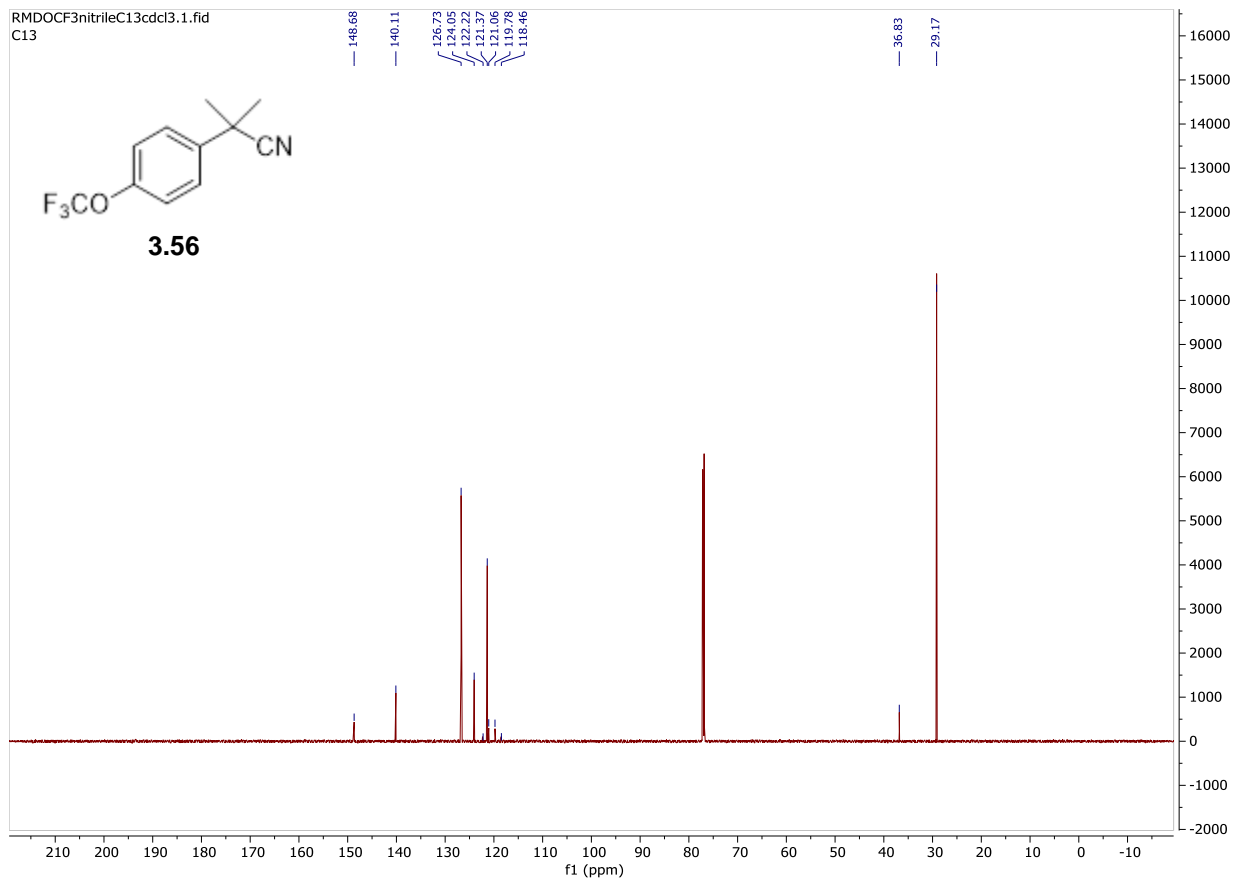
¹H NMR (600 MHz, CDCl₃) δ 7.52 – 7.50 (m, 2H), 7.25 – 7.23 (m, 2H), 1.73 (H_a, s, 6H) ppm.

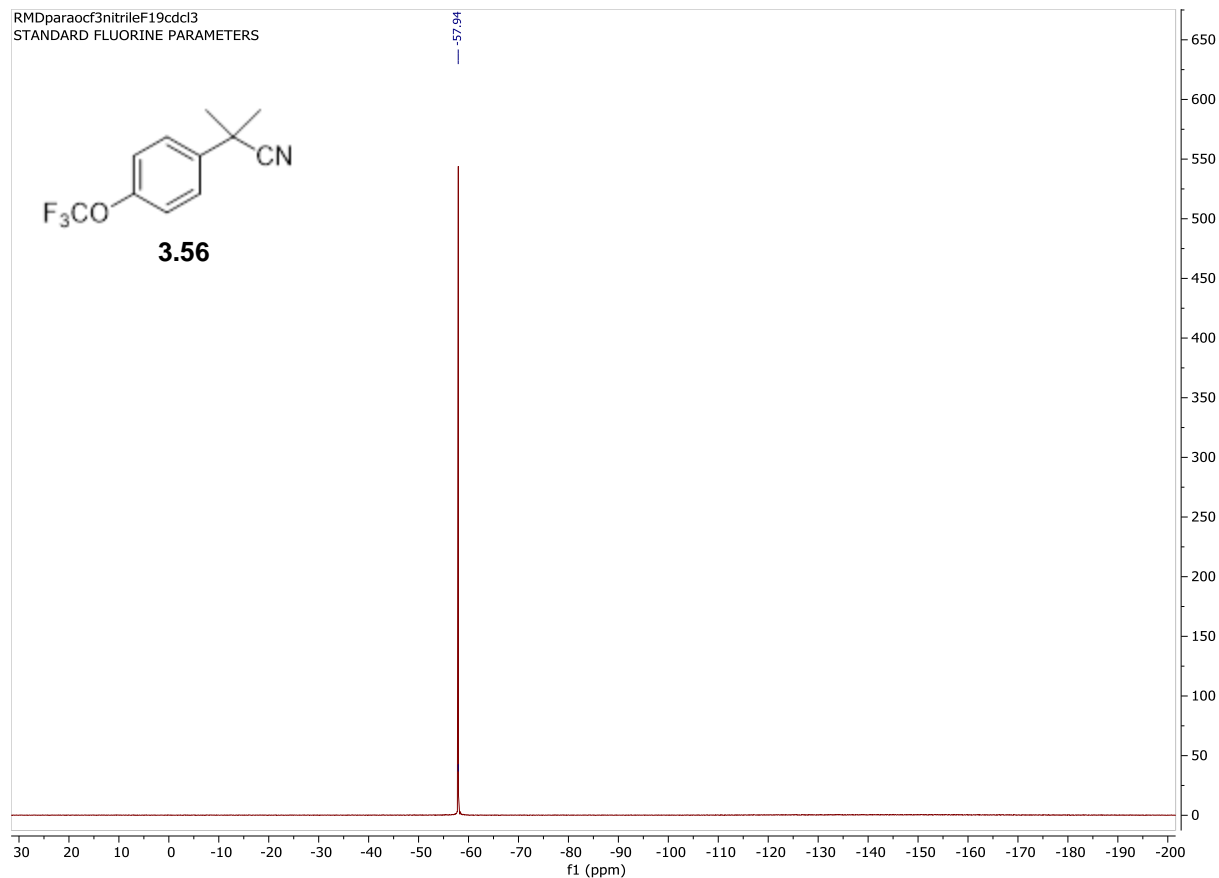
¹³C NMR (201 MHz, CDCl₃) δ 148.6, 140.1, 126.7, 124.0, 122.2, 121.3, 121.0, 119.7, 118.4, 36.8, 29.1 ppm.

¹⁹F NMR (564 MHz, CDCl₃) δ -57.94 ppm.

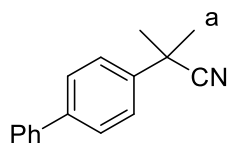
HRMS Calc'd for C₁₁H₁₀F₃NO(M+H): 229.0714 Found: 229.0718







2-([1,1'-biphenyl]-4-yl)-2-methylpropanenitrile (3.57)

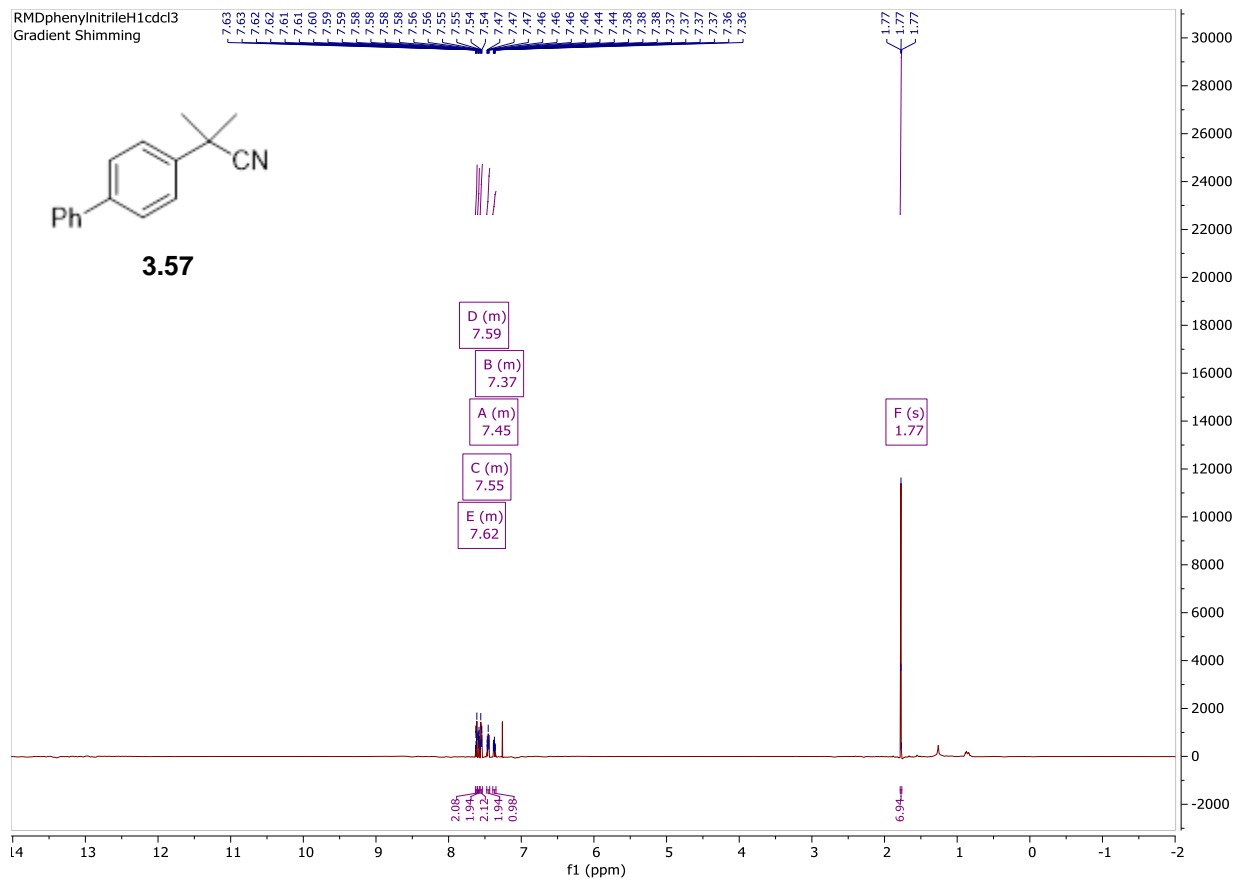


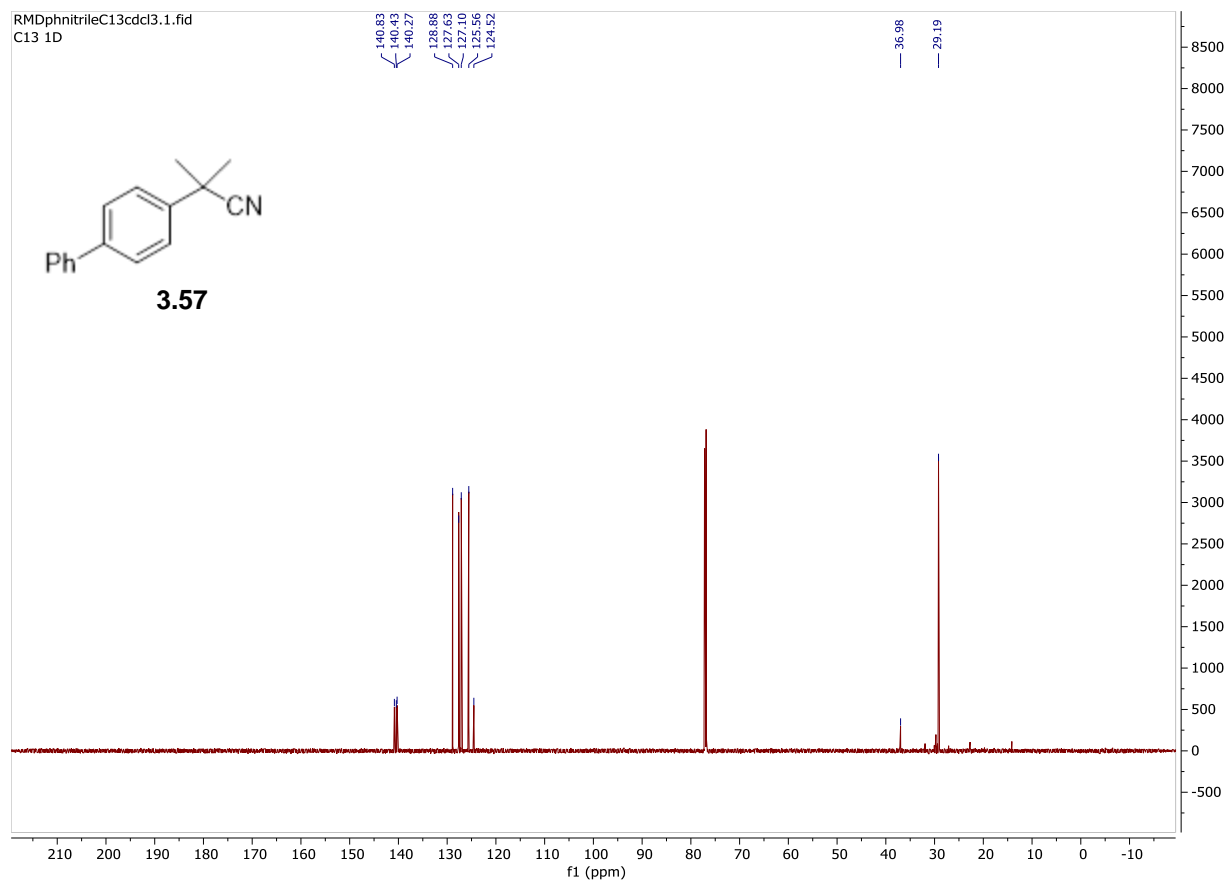
2-([1,1'-biphenyl]-4-yl)-2-methylpropanenitrile was synthesized following the general procedure for benzylic alkylation on a 20 mmol scale using 2-([1,1'-biphenyl]-4-yl)acetonitrile, as the respective nitrile. The compound was purified using silica gel chromatography with 10% ethyl acetate/hexane to give 3.63 g of a yellow oil (16.4 mmol, 82% yield).

¹H NMR (600 MHz, CDCl₃) δ 7.63 – 7.61 (m, 2H), 7.60 – 7.58 (m, 2H), 7.57 – 7.54 (m, 2H), 7.48 – 7.43 (m, 2H), 7.39 – 7.35 (m, 1H), 1.77 (H_a, s, 6H) ppm.

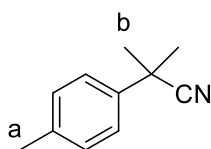
¹³C NMR (201 MHz, CDCl₃) δ 140.8, 140.4, 140.3, 128.8, 127.6, 127.1, 125.5, 124.5, 36.9, 29.1 ppm.

HRMS Calc'd for C₁₆H₁₅N (M+Na): 244.1101 Found: 244.1097





2-methyl-2-(p-tolyl) propanenitrile (3.58)

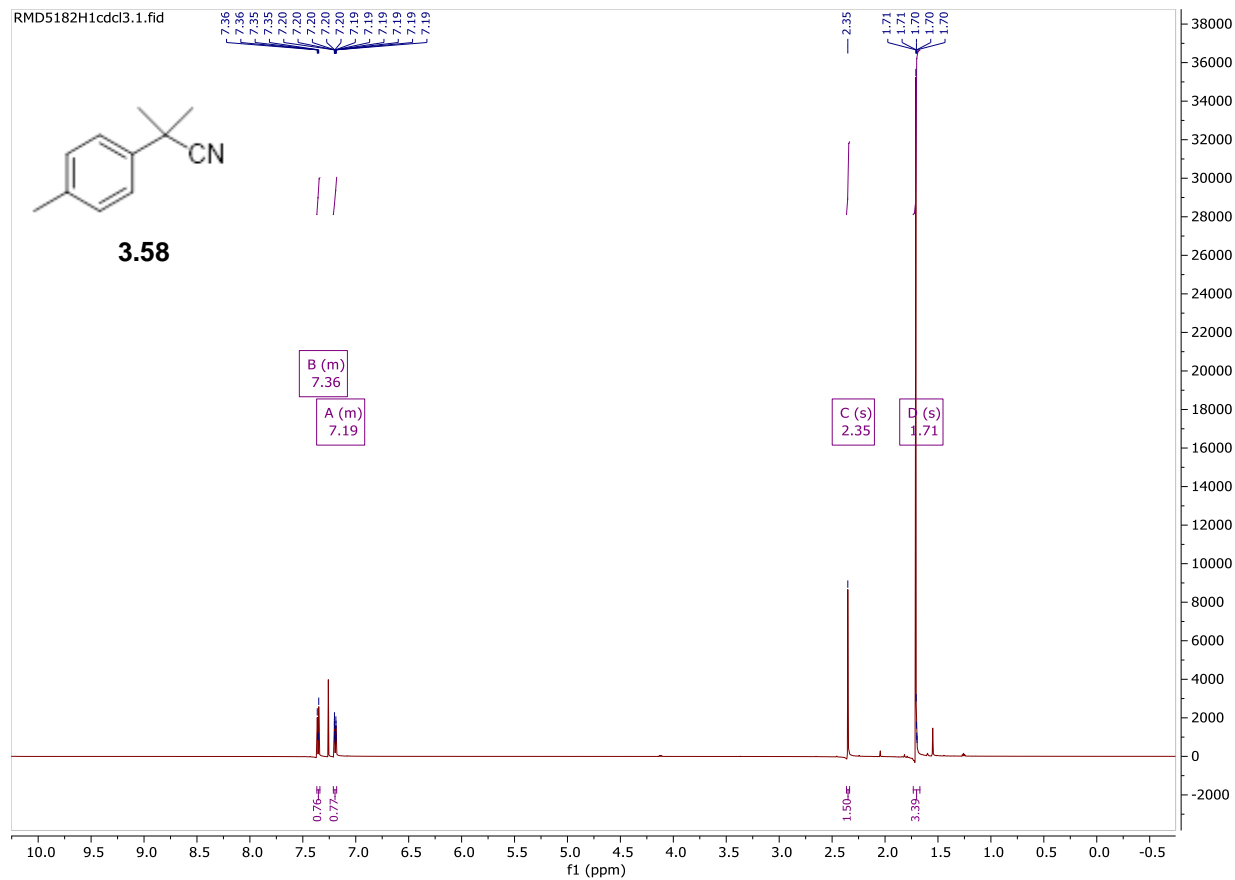


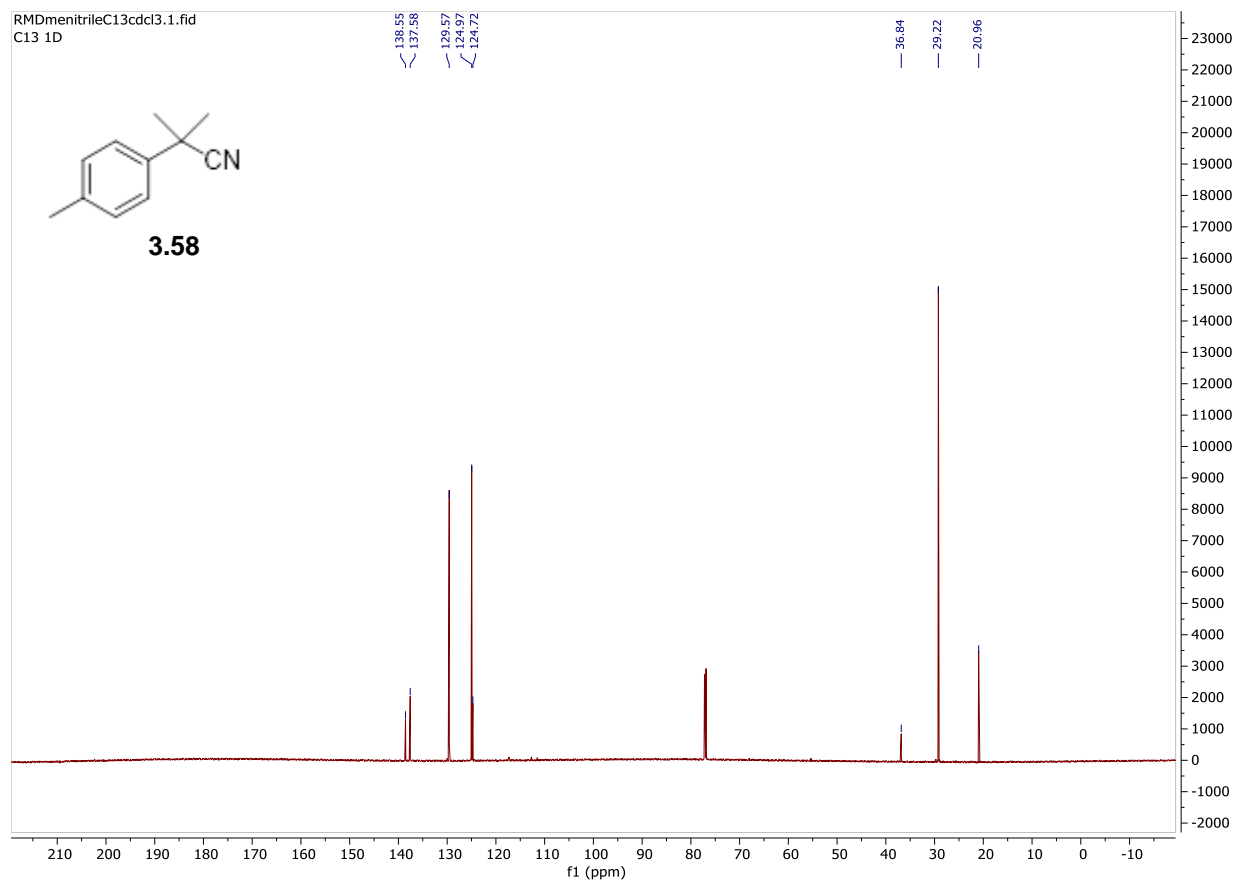
2-methyl-2-(p-tolyl) propanenitrile was synthesized following the general procedure for benzylic alkylation on a 10 mmol scale using 2-methyl-2-(p-tolyl)acetone nitrile, as the respective nitrile. The compound was purified using silica gel chromatography with 10% ethyl acetate/hexane to give 1.51 g of a clear oil (9.50 mmol, 95% yield)

¹H NMR (600 MHz, CDCl₃) δ 7.37 – 7.34 (m, 2H), 7.21 – 7.18 (m, 2H), 2.35 (H_a, s, 3H), 1.71 (H_{b,s}, 6H) ppm.

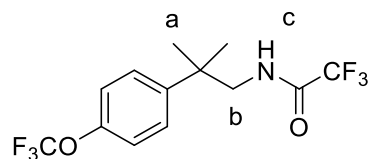
¹³C NMR (201 MHz, CDCl₃) δ 138.5, 137.6, 129.6, 125.0, 124.7, 36.8, 29.2, 21.0 ppm

HRMS Calc'd for C₁₁H₁₃N (M+NA): 182.0945 Found: 182.0938





2,2,2-trifluoro-N-(2-methyl-2-(4-(trifluoromethoxy)phenyl)propyl)acetamide (3.59)



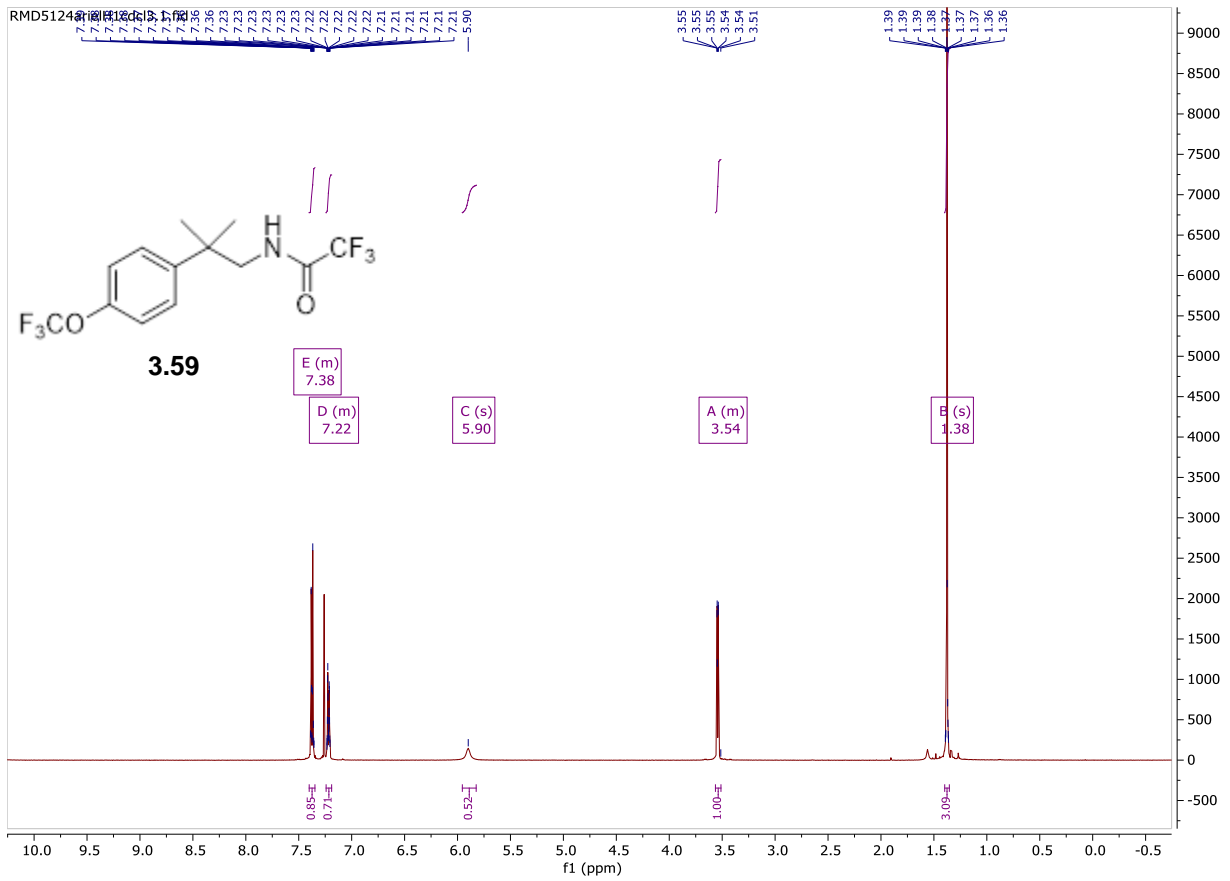
2,2,2-trifluoro-N-(2-methyl-2-(4-(trifluoromethoxy)phenyl)propyl)acetamide was synthesized following the general procedure for acetamide formation on a 10.03 mmol scale using 2-methyl-2-(4-(trifluoromethoxy)phenyl)propan-1-amine, as the respective amine. The compound was purified using silica gel chromatography with 10% ethyl acetate/hexane to give 2.57 g of a white solid (7.82 mmol, 78% yield).

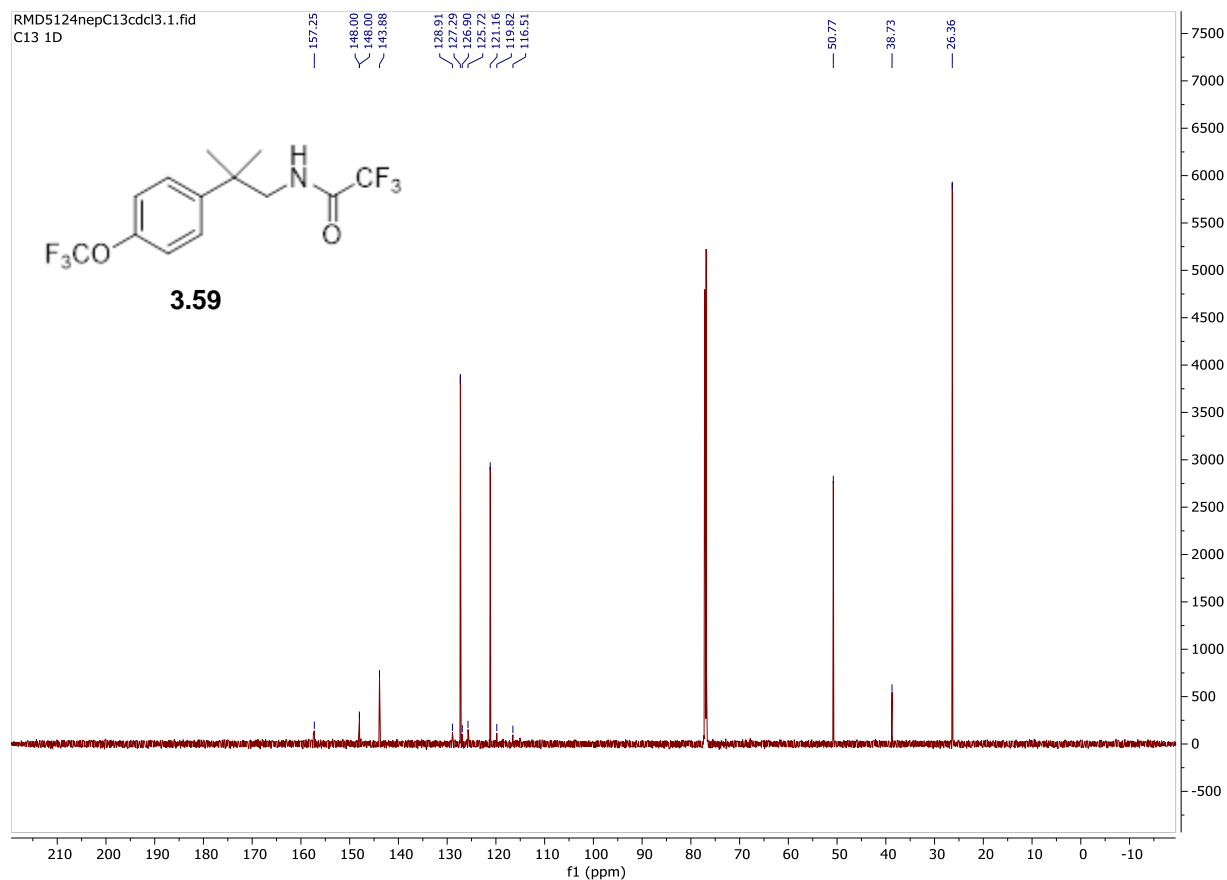
¹H NMR (600 MHz, CDCl₃) δ 7.40 – 7.35 (m, 2H), 7.24 – 7.19 (m, 1H), 5.90 (H_c, s, 1H), 3.54 (H_b, d, *J* = 6.5 Hz, 2H), 1.38 (H_a, s, 6H) ppm

¹³C NMR (201 MHz, CDCl₃) δ 157.2, 148.00, 143.8, 128.9, 127.2, 126.9, 125.7, 121.1, 119.8, 116.5, 50.7, 38.7, 26.3 ppm.

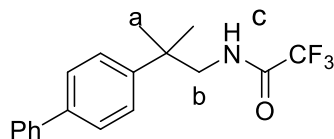
¹⁹F NMR (564 MHz, CDCl₃) δ -59.53, -77.59 ppm.

HRMS Calc'd for C₁₃H₁₃F₆NO₂ (M+Na): 352.0747 Found: 352.0758





N-(2-([1,1'-biphenyl]-4-yl)-2-methylpropyl)-2,2,2-trifluoroacetamide (3.60)



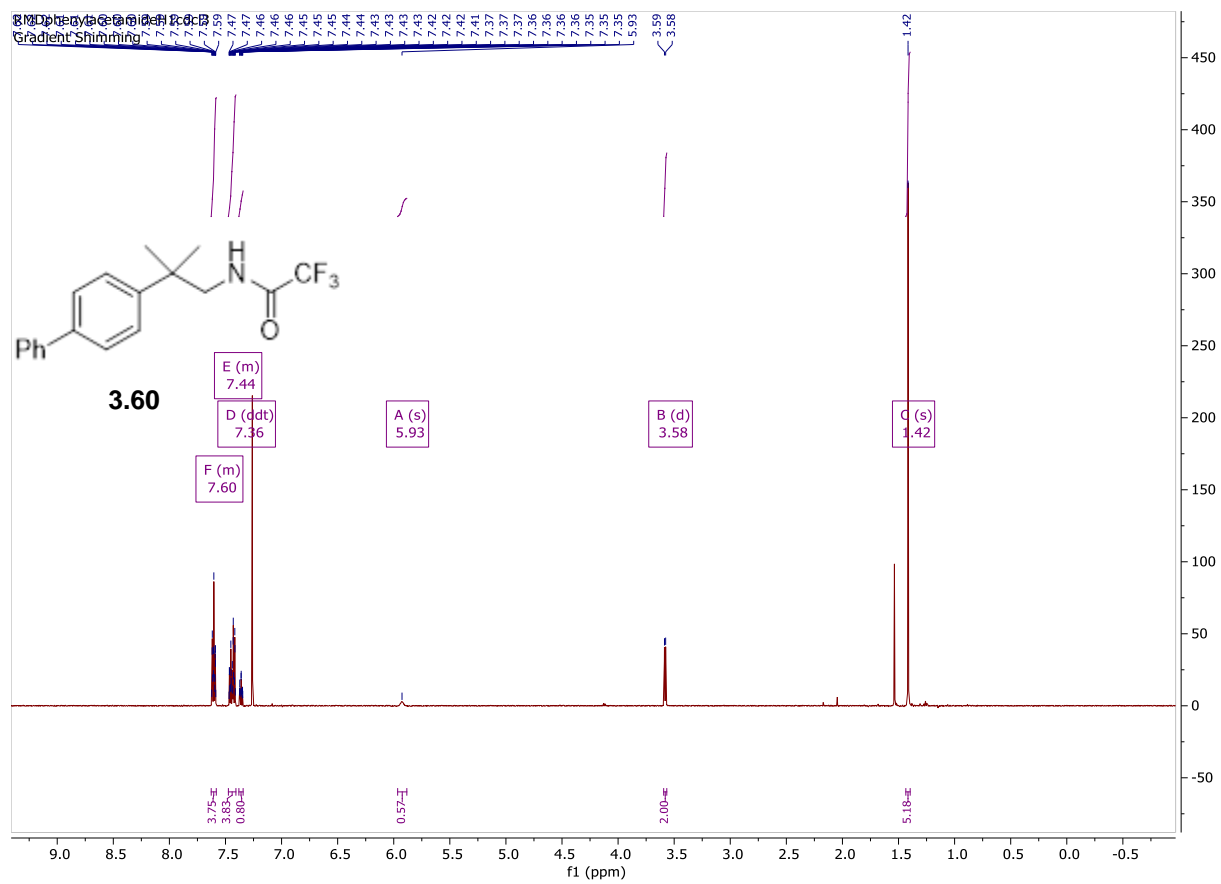
N-(2-([1,1'-biphenyl]-4-yl)-2-methylpropyl)-2,2,2-trifluoroacetamide was synthesized following the general procedure for acetamide formation on a 9.76 mmol scale using 2-([1,1'-biphenyl]-4-yl)-2-methylpropan-1-amine, as the respective amine. The compound was purified using silica gel chromatography with 10% ethyl acetate/hexane to give 2.75 g of an off-white solid (8.55 mmol, 87% yield).

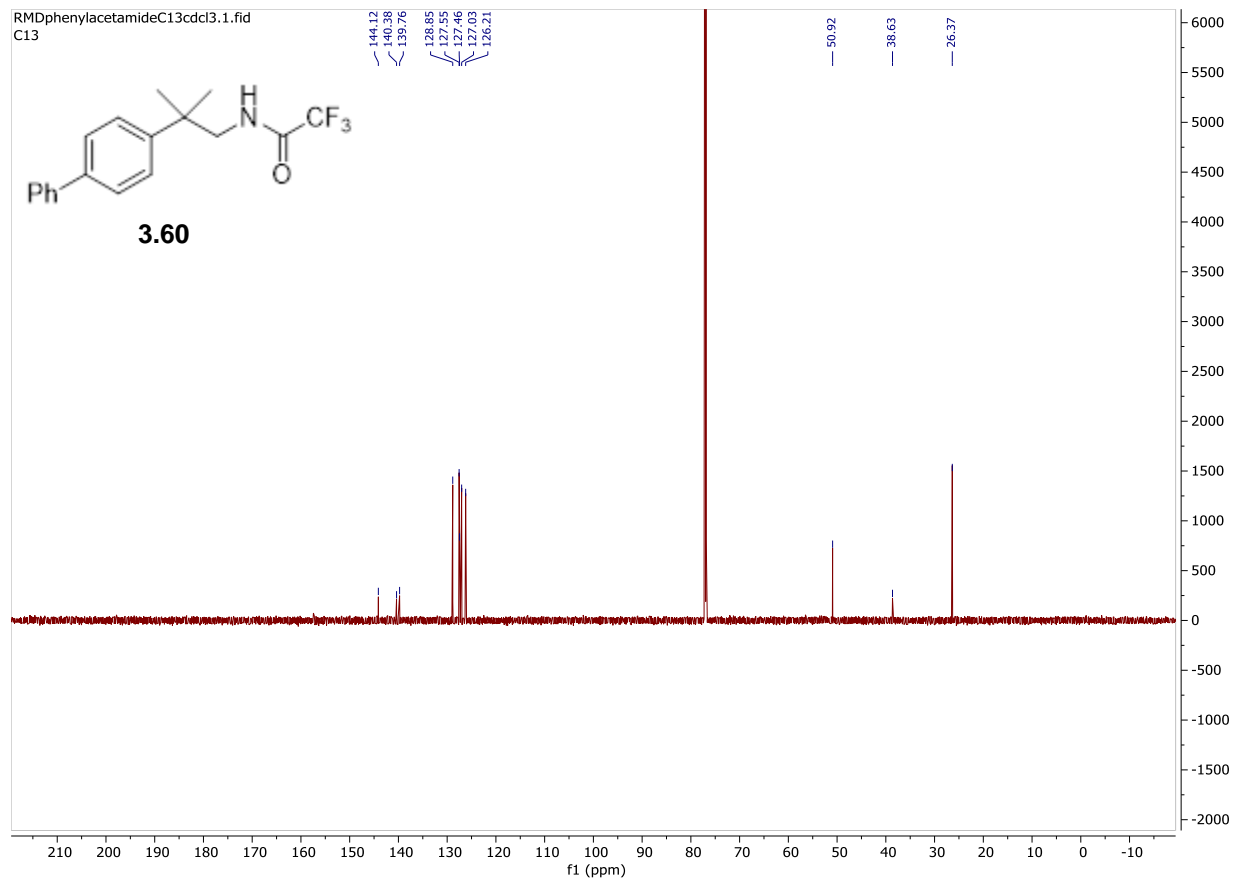
¹H NMR (600 MHz, CDCl₃) δ 7.63 – 7.58 (m, 4H), 7.47 – 7.41 (m, 4H), 7.38 – 7.34 (m, 1H), 5.93 (H_c, s, 1H), 3.58 (H_b, d, *J* = 6.2 Hz, 2H), 1.42 (H_a, s, 6H) ppm.

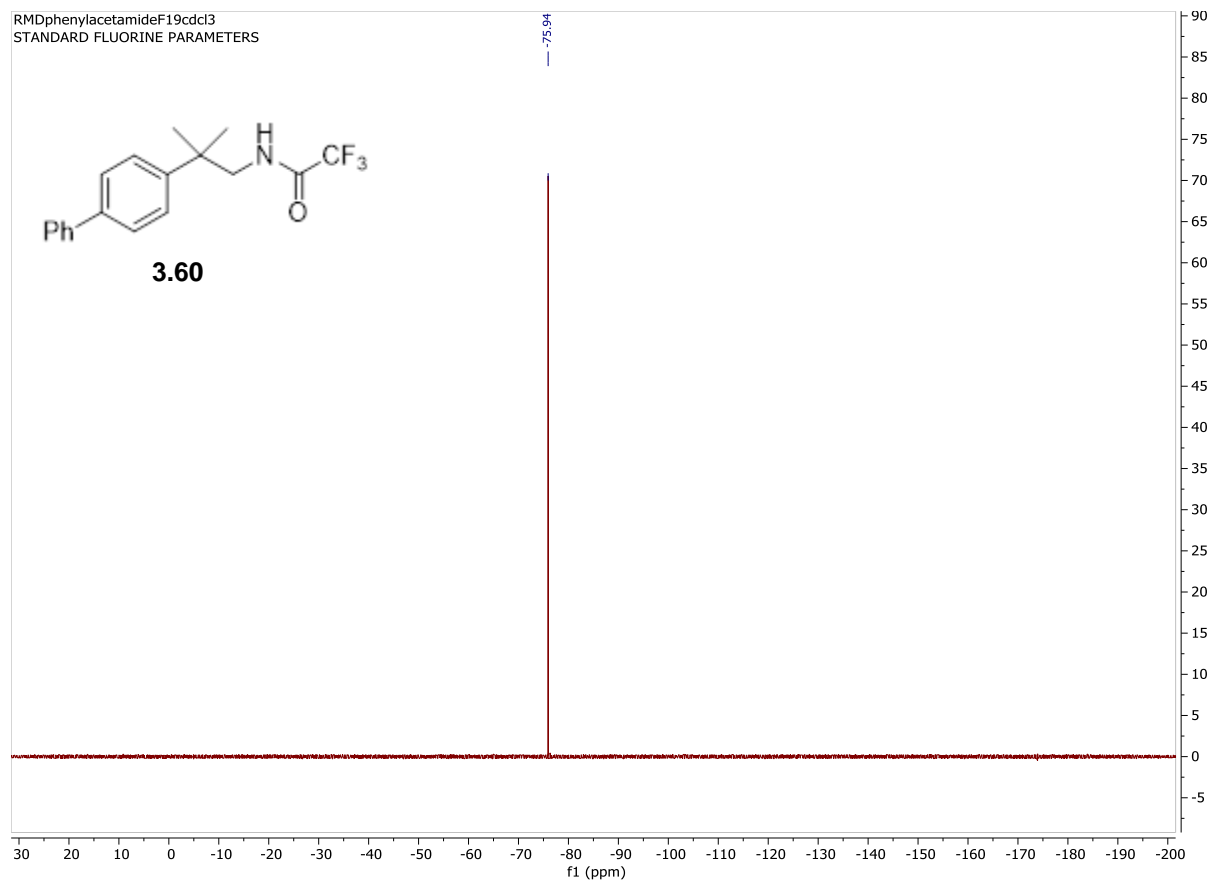
¹³C NMR (201 MHz, CDCl₃) δ 144.1, 140.3, 139.7, 128.8, 127.55, 127.46, 127.03, 126.2, 50.9, 38.6, 26.3 ppm.

¹⁹F NMR (564 MHz, CDCl₃) δ -75.94 ppm.

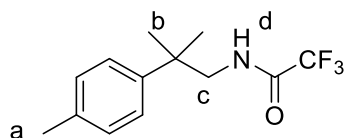
HRMS Calc'd for C₁₈H₁₈F₃NO (M+Na): 344.1237 Found: 344.1229







2,2,2-trifluoro-N-(2-methyl-2-(p-tolyl)propyl)acetamide (3.61)



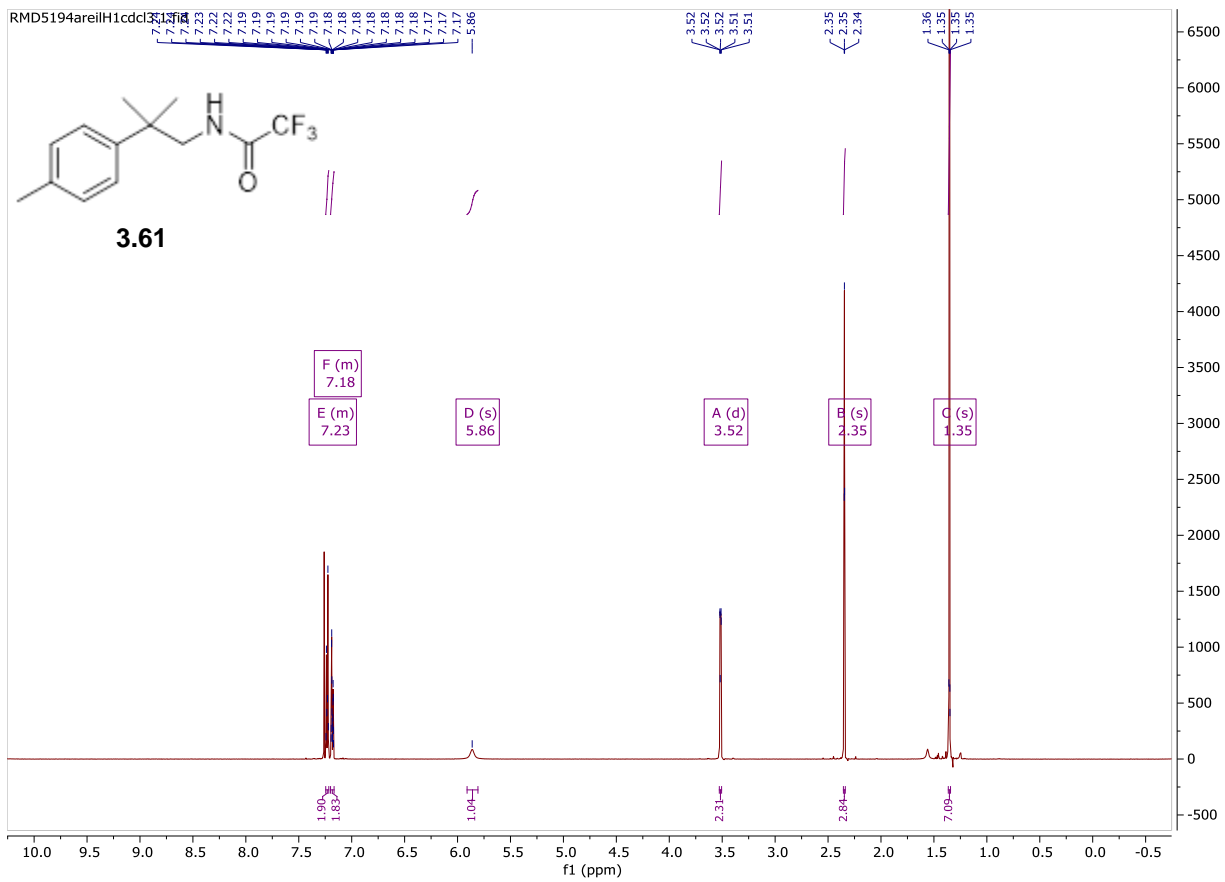
2,2,2-trifluoro-N-(2-methyl-2-(p-tolyl)propyl)acetamide was synthesized following the general procedure for acetamide formation on a 10.44 mmol scale using 2-methyl-2-(p-tolyl)propan-1-amine, as the respective amine. The compound was purified using silica gel chromatography with 10% ethyl acetate/hexane to give 2.09 g of a white solid. (8.06 mmol, 77% yield).

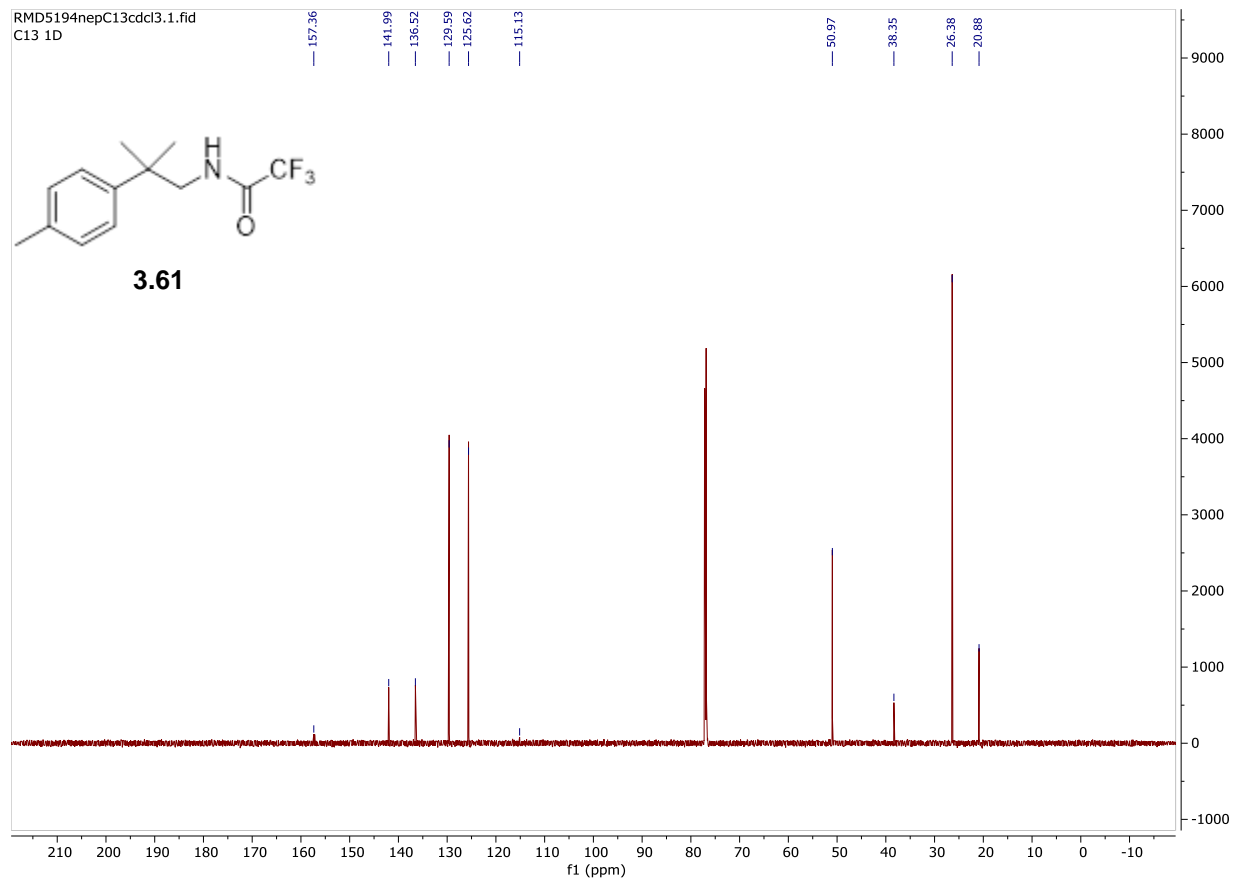
¹H NMR (600 MHz, CDCl₃) δ 7.25 – 7.22 (m, 2H), 7.20 – 7.17 (m, 2H), 5.86 (H_d, s, 1H), 3.52 (H_c, d, *J* = 6.2 Hz, 2H), 2.35 (H_a, s, 3H), 1.35 (H_b, s, 6H) ppm.

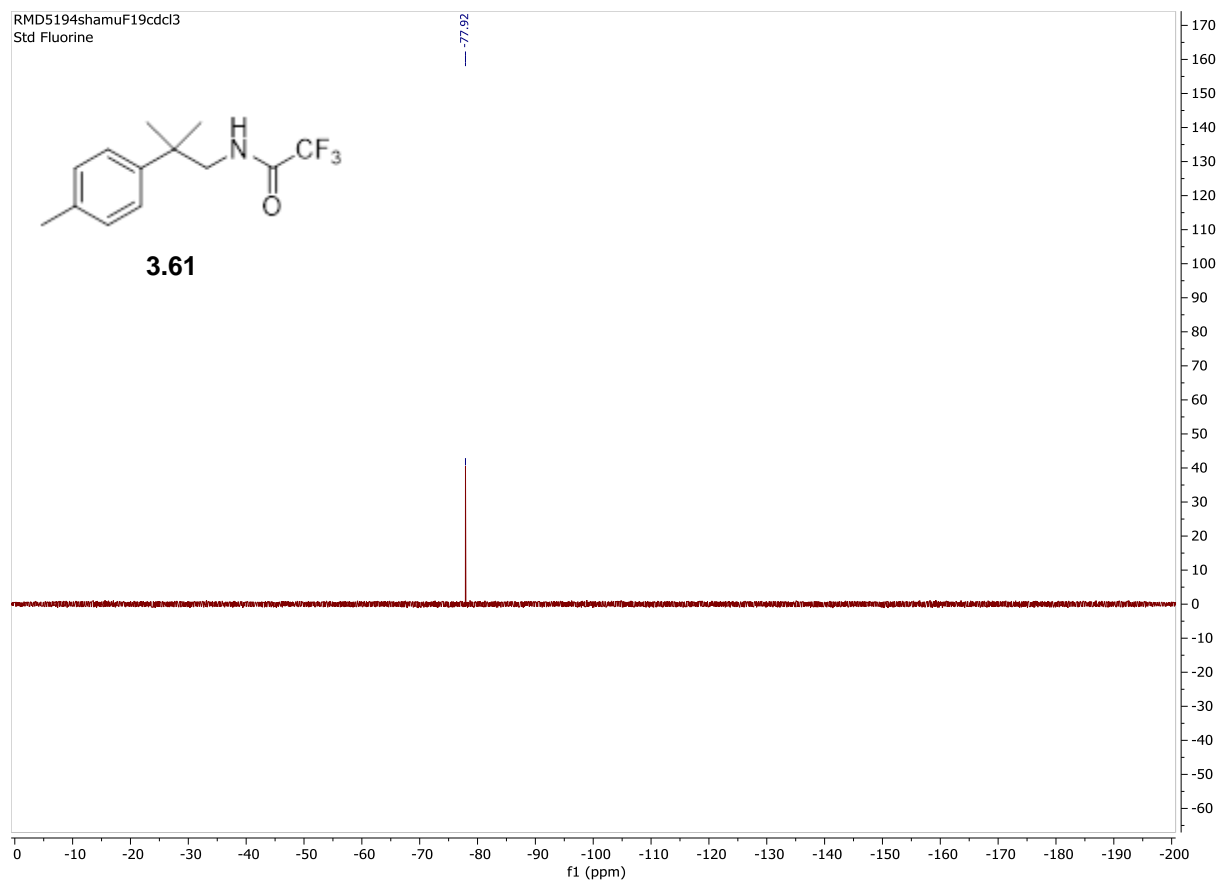
¹³C NMR (201 MHz, CDCl₃) δ 157.3, 141.9, 136.5, 129.5, 125.6, 115.1, 50.9, 38.3, 26.3, 20.8 ppm.

¹⁹F NMR (564 MHz, CDCl₃) δ -77.92 ppm.

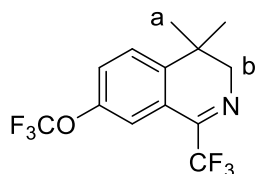
HRMS Calc'd for C₁₃H₁₆F₃NO (M+Na): 282.1081 Found 282.1080







4,4-dimethyl-7-(trifluoromethoxy)-1-(trifluoromethyl)-3,4-dihydroisoquinoline (3.62)



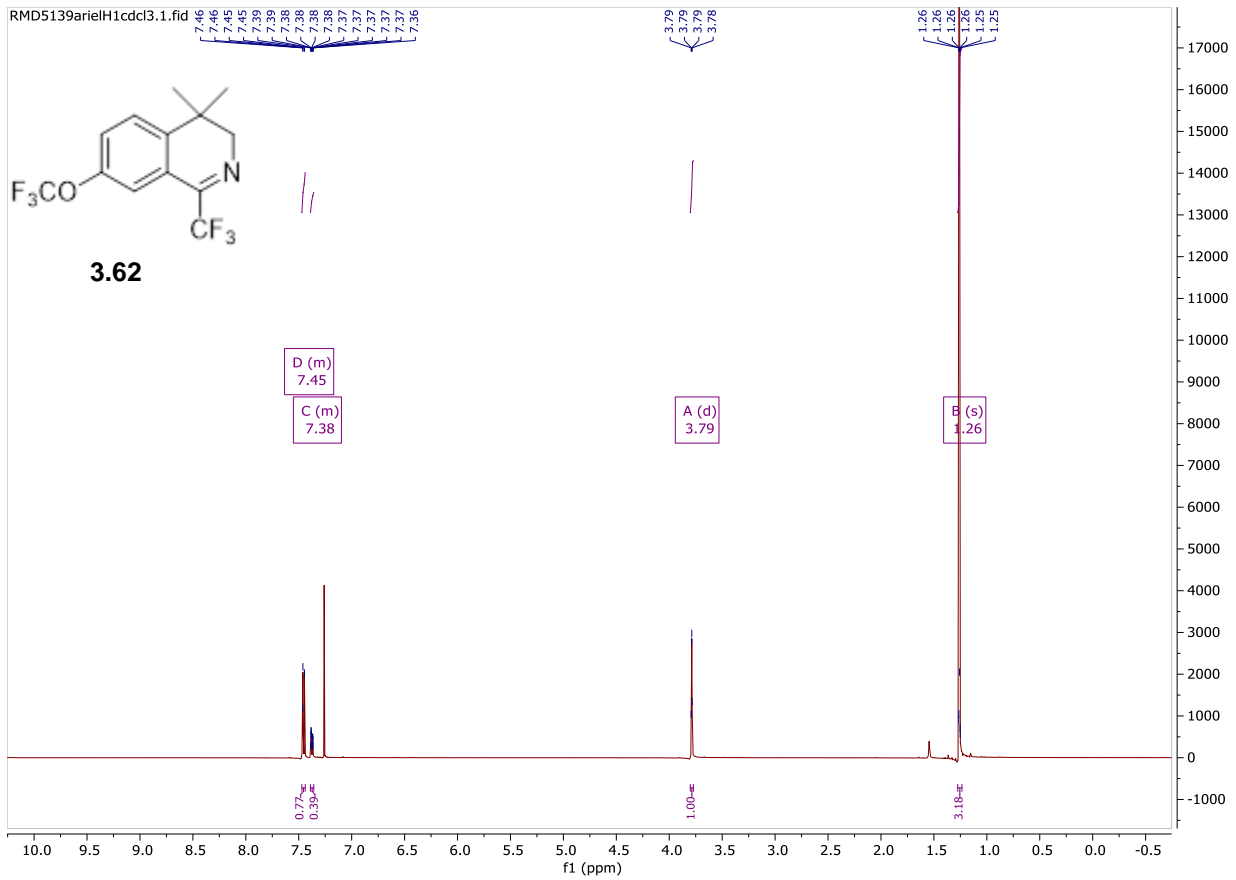
4,4-dimethyl-7-(trifluoromethoxy)-1-(trifluoromethyl)-3,4-dihydroisoquinoline was synthesized following general procedure B for the Bischler Naperialski reaction on a 4.49 mmol scale using 2,2,2-trifluoro-N-(2-methyl-2-(4-(trifluoromethoxy)phenyl)propyl)acetamide, as the respective acetamide. The compound was purified using silica gel chromatography with 10% ethyl acetate/hexane to give 0.27 g of a yellow oil (0.86 mmol, 23% yield).

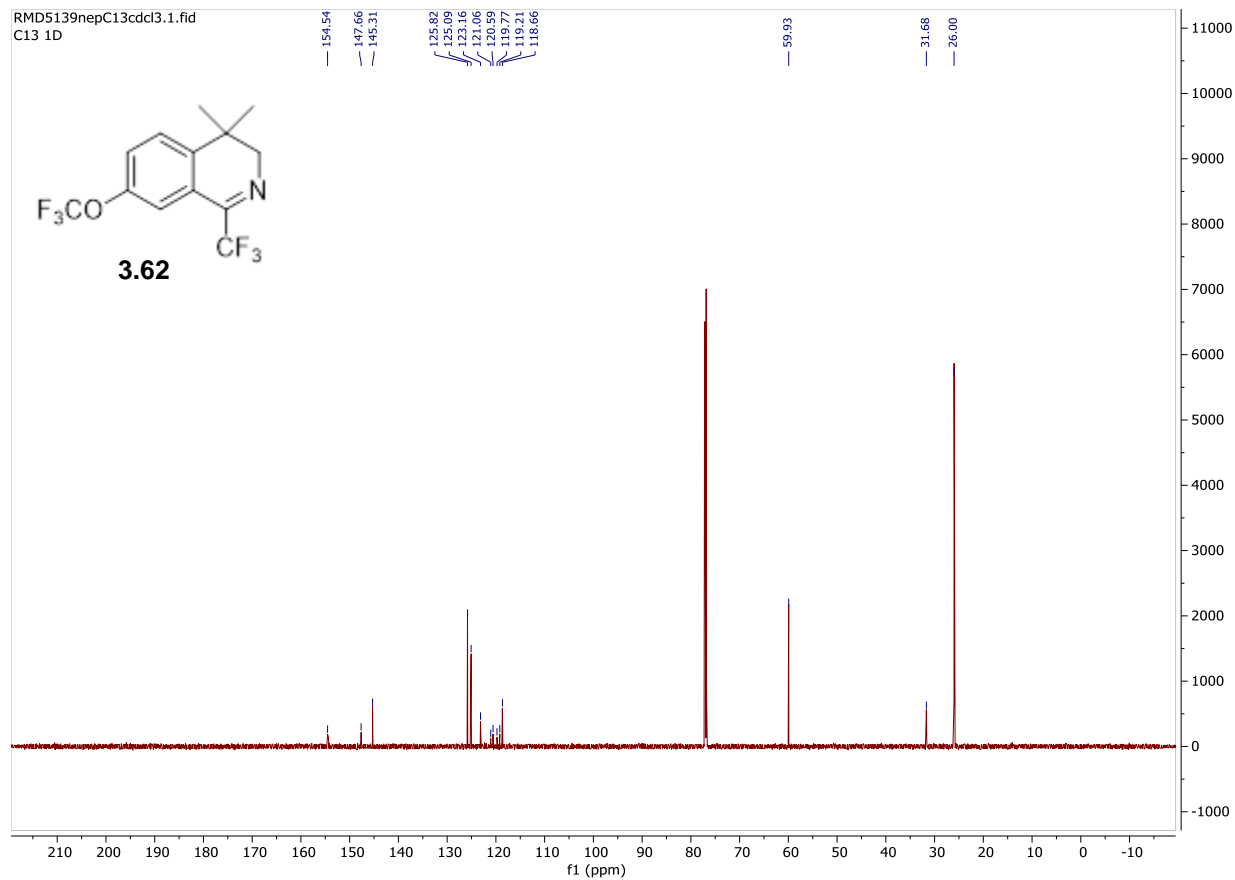
¹H NMR (600 MHz, CDCl₃) δ 7.47 – 7.44 (m, 2H), 7.39 – 7.36 (m, 1H), 3.79 (H_b, d, *J* = 2.9 Hz, 2H), 1.26 (H_a, s, 6H) ppm.

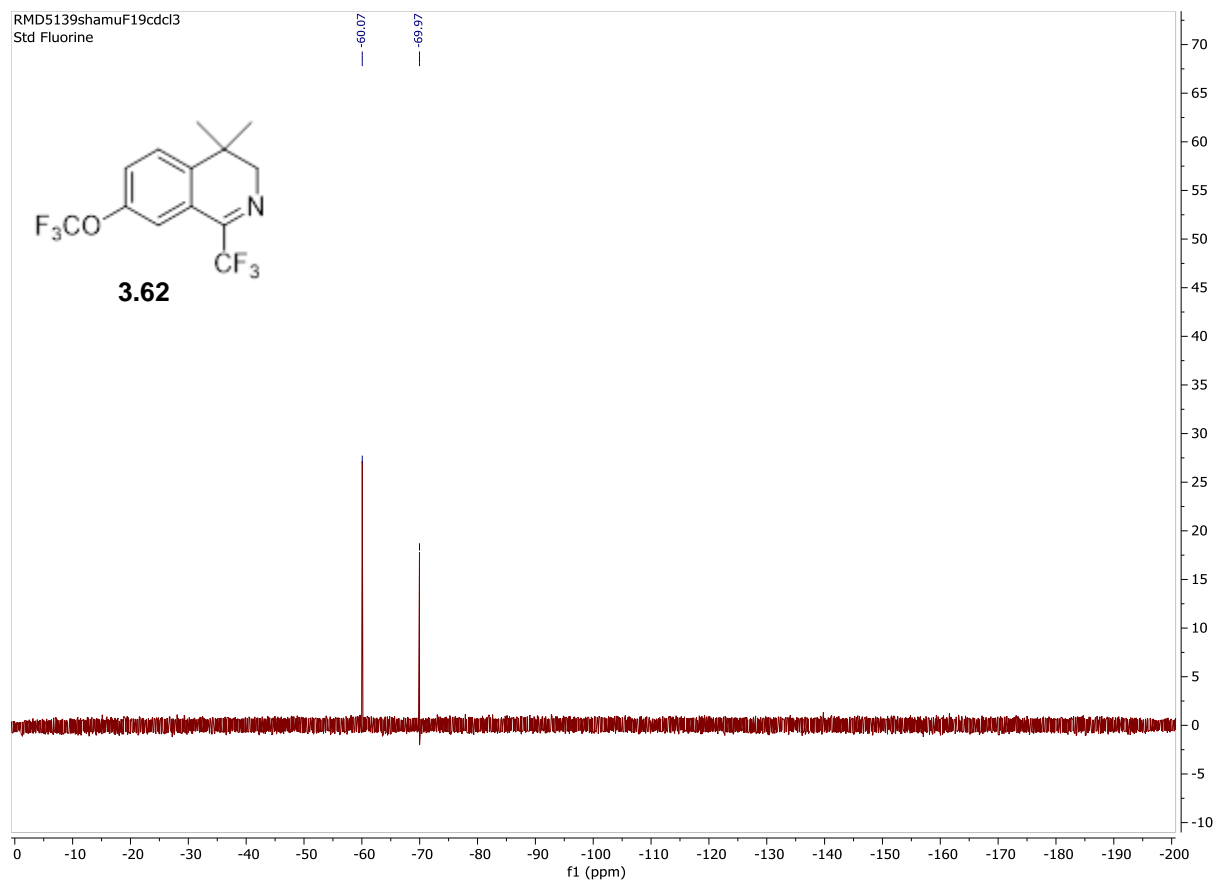
¹³C NMR (201 MHz, CDCl₃) δ 154.5, 147.6, 145.3, 125.82, 125.09, 123.1, 121.0, 120.5, 119.77, 119.21, 118.66, 59.9, 31.6, 26.0 ppm.

¹⁹F NMR (564 MHz, CDCl₃) δ -60.07, -69.97 ppm.

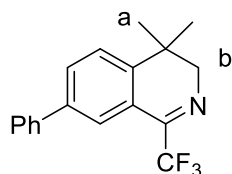
HRMS Calc'd for C₁₃H₁₁F₆NO (M+H): 312.0824 Found: 312.0840







4,4-dimethyl-7-phenyl-1-(trifluoromethyl)-3,4-dihydroisoquinoline (3.63)



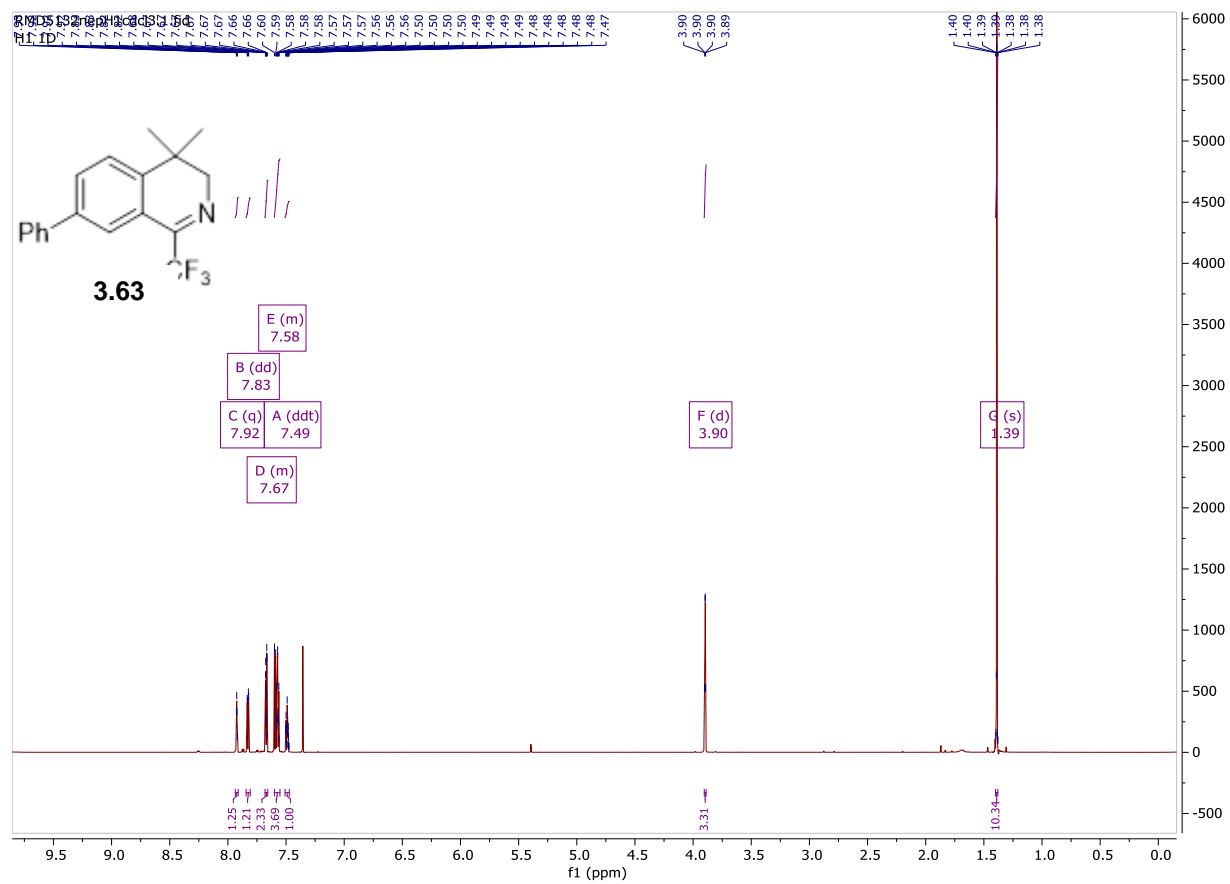
4,4-dimethyl-7-phenyl-1-(trifluoromethyl)-3,4-dihydroisoquinoline was synthesized following general procedure B for the Bischler Naperialski reaction on an 8.56 mmol scale using N-(2-([1,1'-biphenyl]-4-yl)-2-methylpropyl)-2,2,2-trifluoroacetamide, as the respective acetamide. The compound was purified using silica gel chromatography with 10% ethyl acetate/hexane to give 1.10 g of an off yellow solid (3.63 mmol, 42% yield).

¹H NMR (800 MHz, CDCl₃) δ 7.92 (q, *J* = 1.9 Hz, 1H), 7.83 (dd, *J* = 8.0, 1.9 Hz, 1H), 7.68 – 7.66 (m, 2H), 7.60 – 7.55 (m, 4H), 7.49 (ddt, *J* = 7.8, 6.9, 1.2 Hz, 1H), 3.90 (H_b, d, *J* = 2.0 Hz, 2H), 1.39 (H_a, s, 6H) ppm.

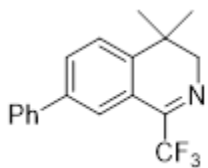
¹³C NMR (201 MHz, CDCl₃) δ 155.61, 155.45, 145.5, 140.02, 140.00, 131.4, 129.15, 129.00, 127.81, 127.67, 127.39, 127.12, 124.55, 124.53, 124.52, 124.50, 122.4, 120.9, 119.5, 60.1, 31.7, 26.0 ppm.

¹⁹F NMR (564 MHz, CDCl₃) δ -67.69 ppm.

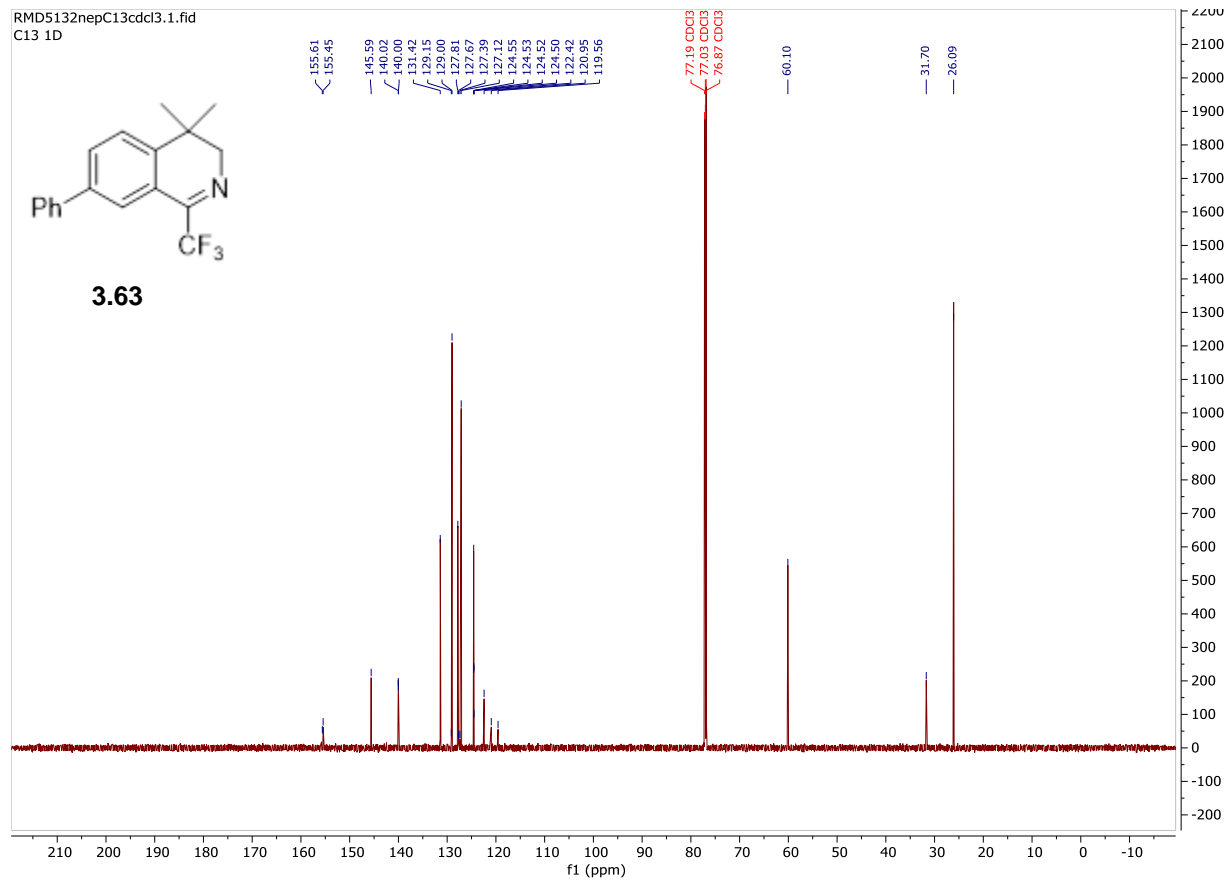
HRMS Calc'd for C₁₈H₁₆F₃N (M+H): 304.1314 Found: 304.1311

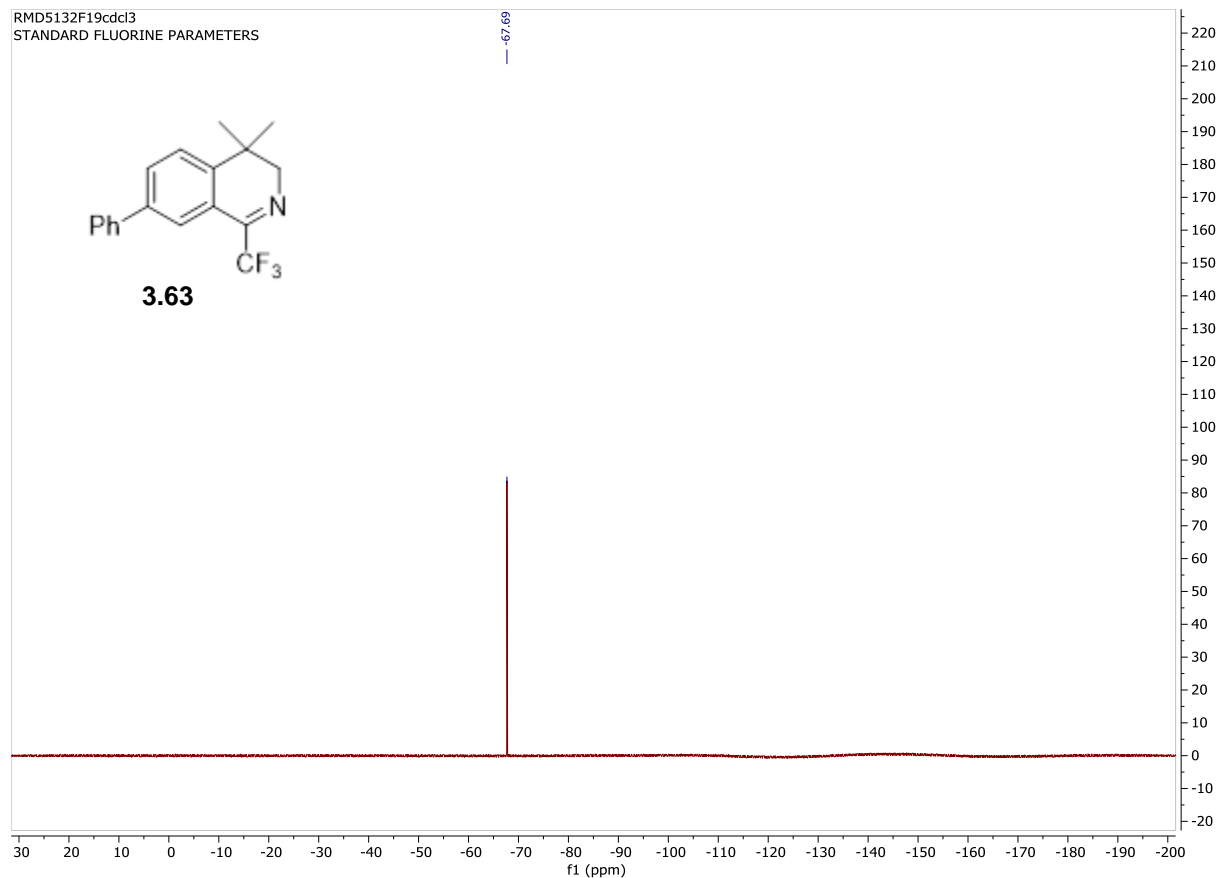


RMD5132nepC13cdcl3.1.fid
C13 1D

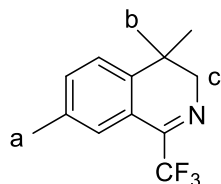


3.63





4,4,7-trimethyl-1-(trifluoromethyl)-3,4-dihydroisoquinoline (3.64)



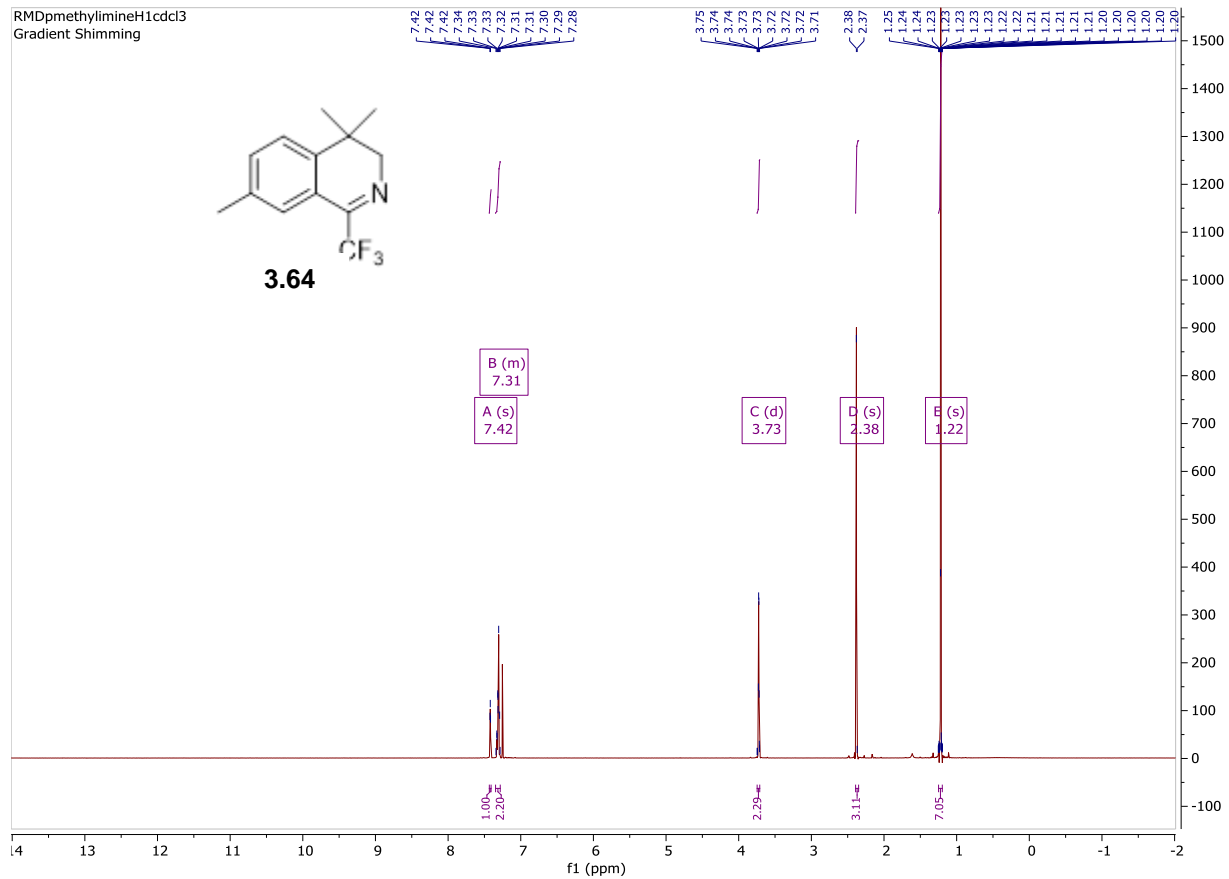
4,4,7-trimethyl-1-(trifluoromethyl)-3,4-dihydroisoquinoline was synthesized following general procedure B for the Bischler Napieralski reaction on an 8.06 mmol scale using 2,2,2-trifluoro-N-(2-methyl-2-(p-tolyl)propyl)acetamide, as the respective acetamide. The compound was purified using silica gel chromatography with 10% ethyl acetate/hexane to give 1.31 g of a yellow oil (5.43 mmol, 67% yield).

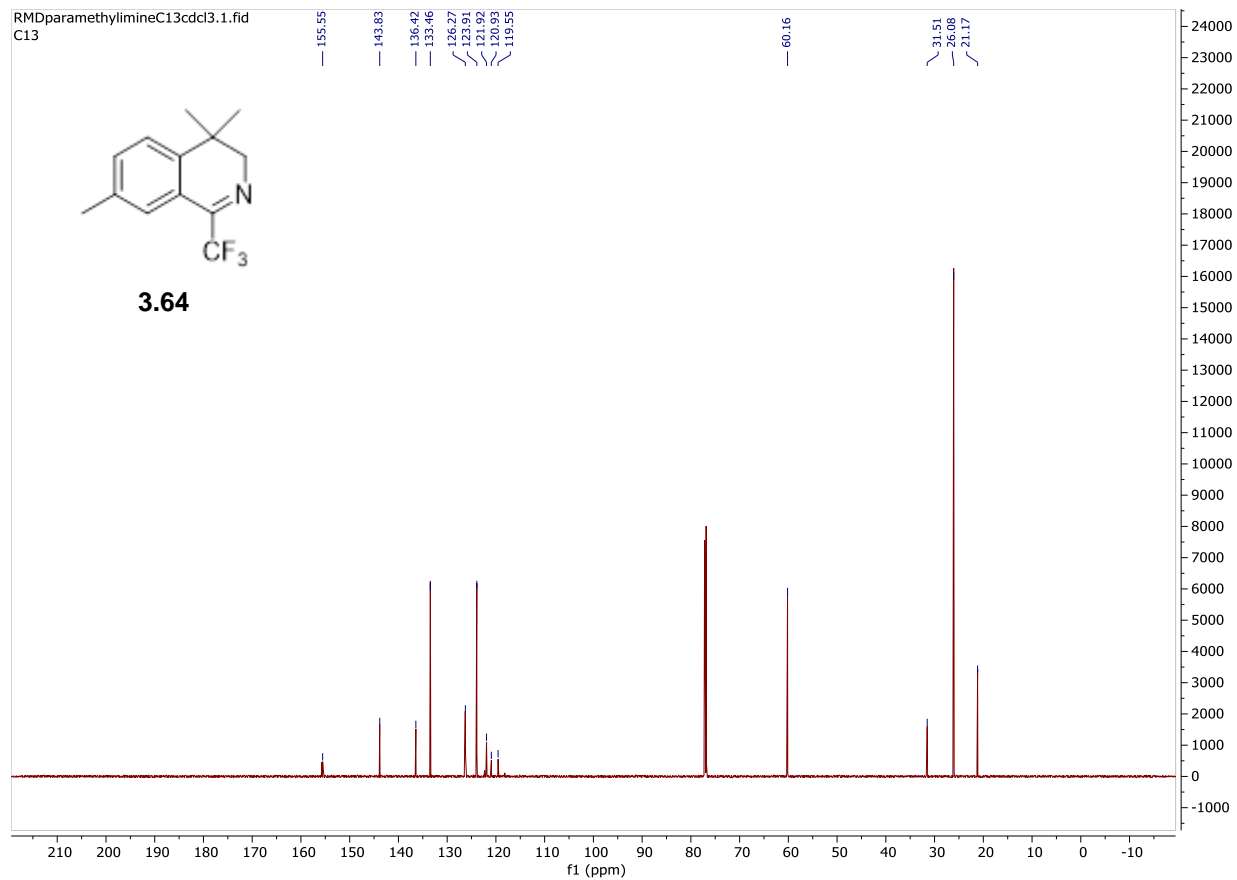
¹H NMR (600 MHz, CDCl₃) δ 7.42 (s, 1H), 7.35 – 7.28 (m, 2H), 3.73 (H_c, d, *J* = 1.8 Hz, 2H), 2.38 (H_a, s, 3H), 1.22 (H_b, s, 6H).

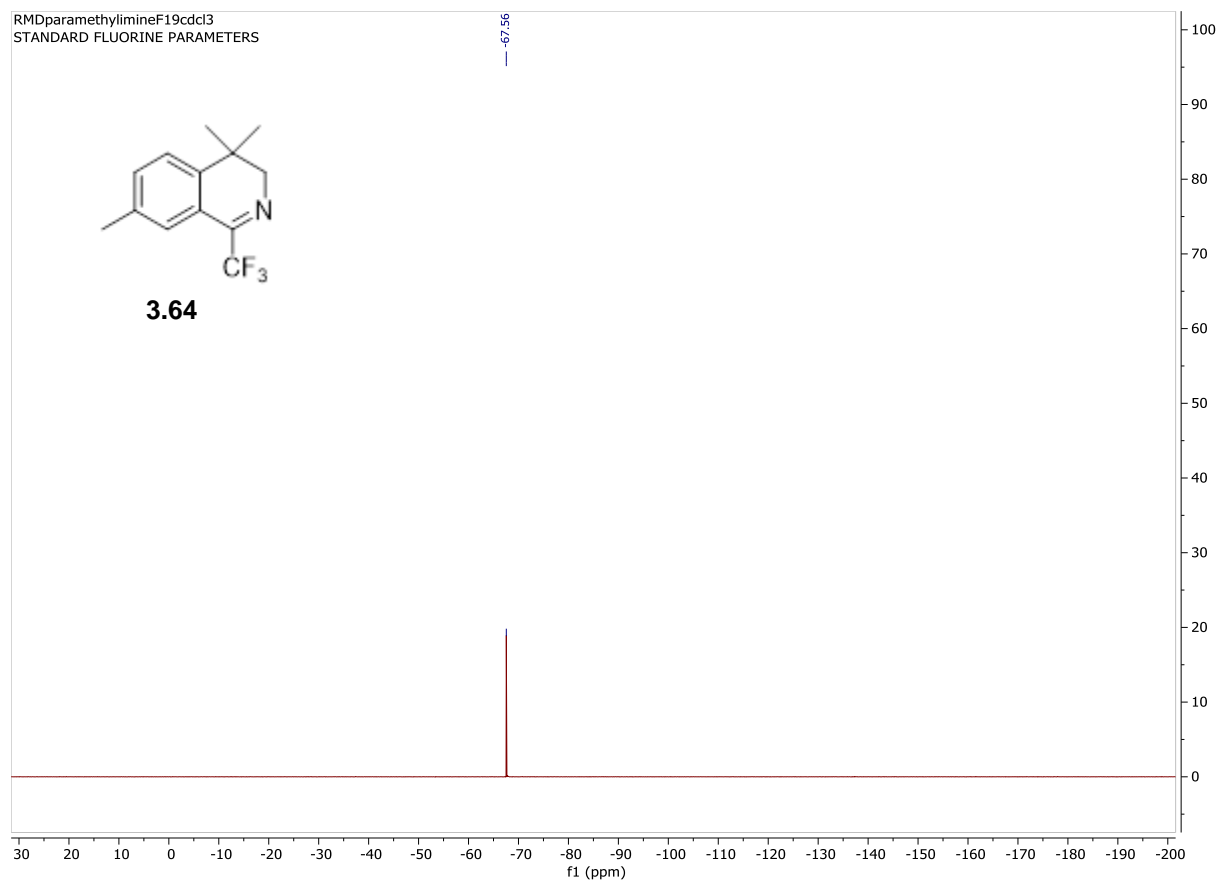
¹³C NMR (201 MHz, CDCl₃) δ 155.5, 143.8, 136.4, 133.4, 126.2, 123.9, 121.9, 120.9, 119.5, 60.1, 31.5, 26.0, 21.1 ppm.

¹⁹F NMR (564 MHz, CDCl₃) δ -67.56 ppm.

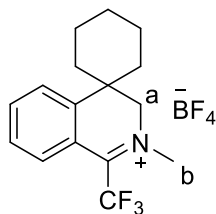
HRMS Calc'd for C₁₃H₁₄F₃N (M+H): 242.1157 Found: 242.1155







2'-methyl-1'-(trifluoromethyl)-3'H-spiro[cyclohexane-1,4'-isoquinolin]-2'-ium tetrafluoroborate (3.67)



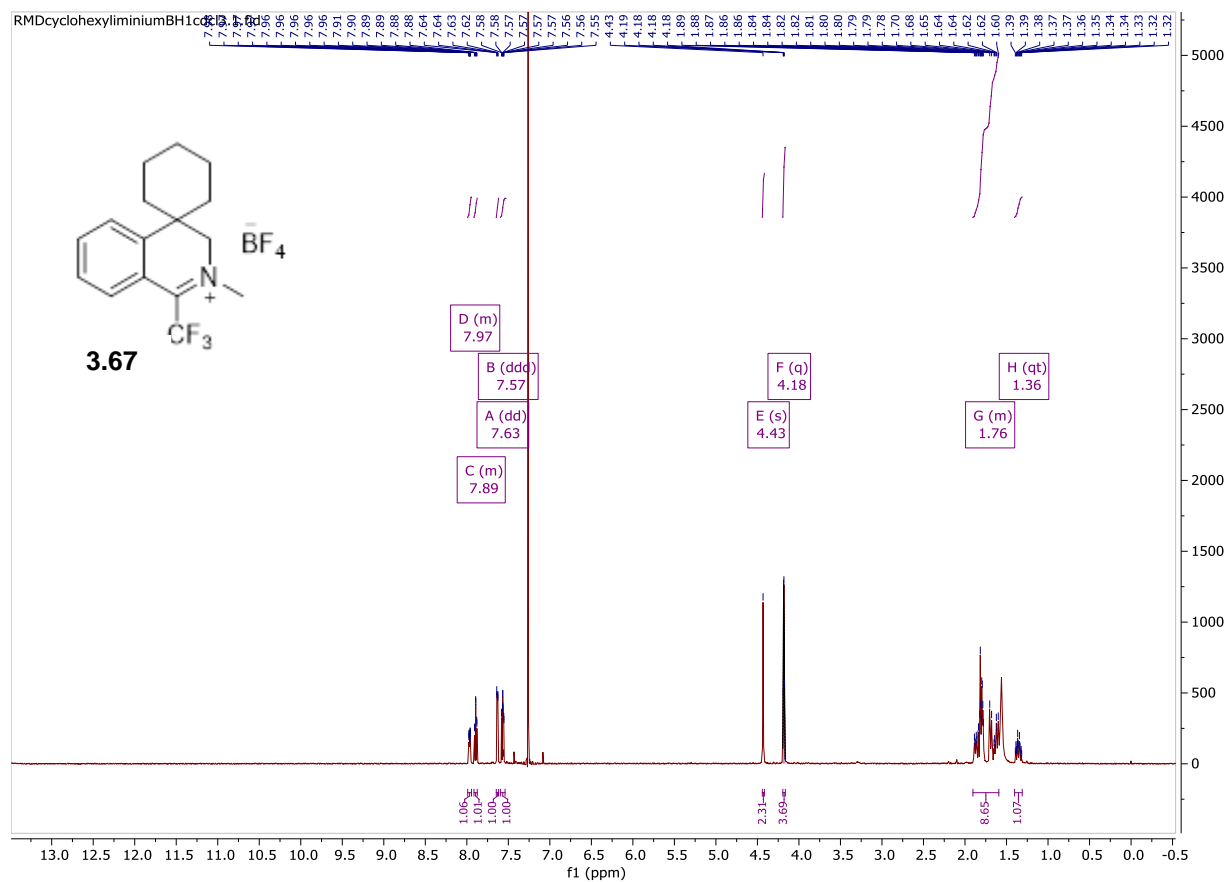
2'-methyl-1'-(trifluoromethyl)-3'H-spiro[cyclohexane-1,4'-isoquinolin]-2'-ium tetrafluoroborate was synthesized following general procedure for imine methylation on a 2.1 mmol scale using 1'-(trifluoromethyl)-3'H-spiro[cyclohexane-1,4'-isoquinoline, as the respective imine, to give 0.660 g of an off white solid (1.79 mmol, 85% yield).

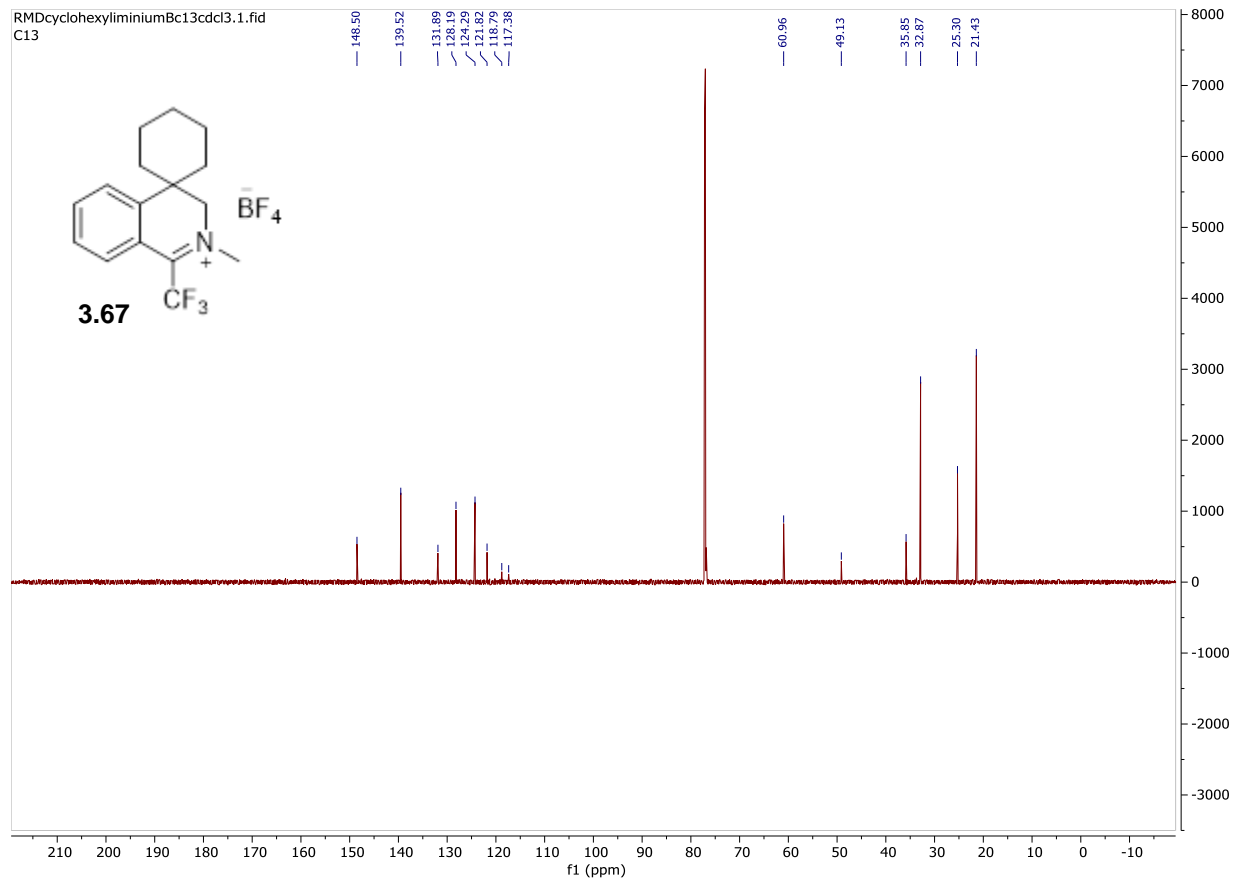
¹H NMR (600 MHz, CDCl₃) δ 7.99 – 7.94 (m, 1H), 7.91 – 7.87 (m, 1H), 7.63 (dd, *J* = 7.7, 1.2 Hz, 1H), 7.57 (ddd, *J* = 8.2, 7.5, 1.1 Hz, 1H), 4.43 (H_a, s, 2H), 4.18 (H_b, q, *J* = 2.5 Hz, 3H), 1.90 – 1.59 (m, 9H), 1.36 (qt, *J* = 12.2, 3.9 Hz, 1H) ppm.

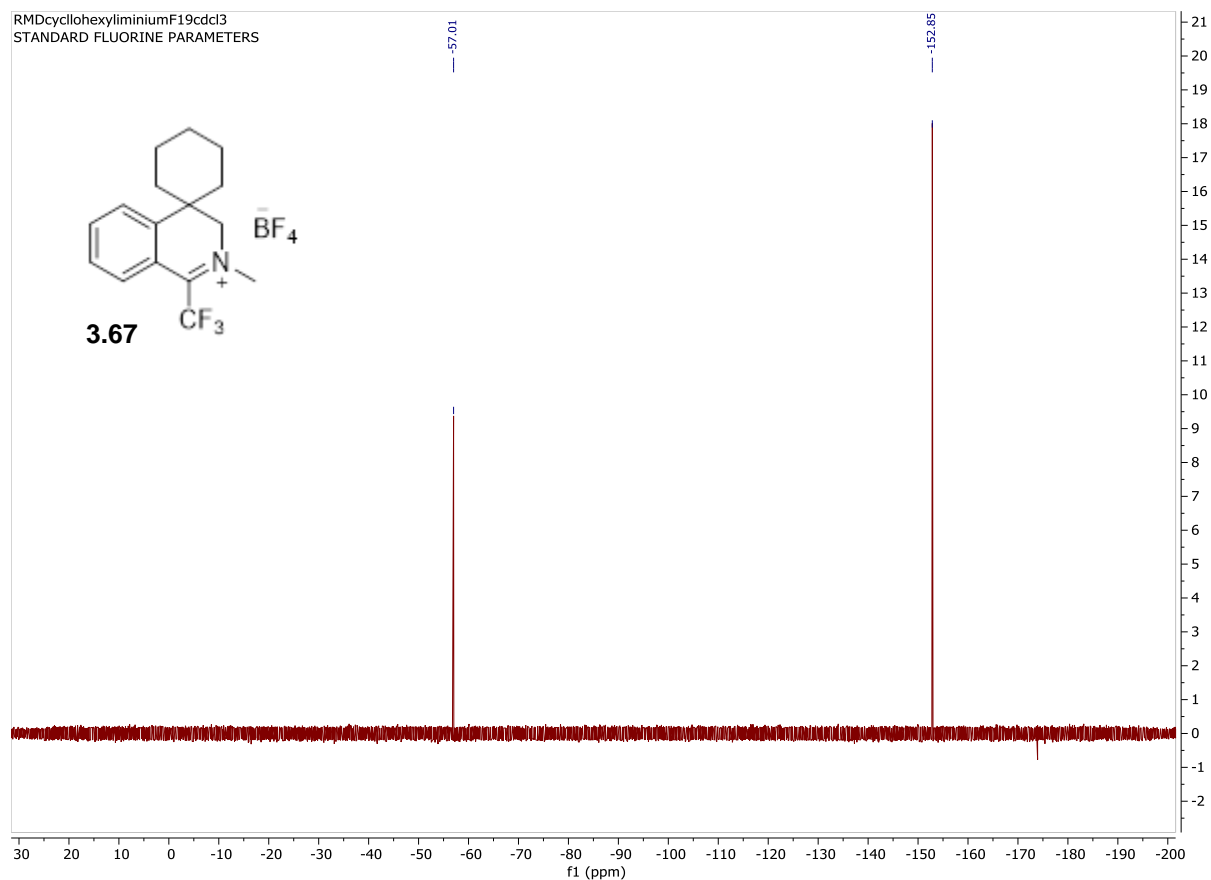
¹³C NMR (201 MHz, CDCl₃) δ 148.5, 139.5, 131.8, 128.1, 124.2, 121.2, 118.7, 117.3, 60.9, 49.1, 35.8, 32.8, 25.3, 21.4 ppm.

¹⁹F NMR (564 MHz, CDCl₃) δ -57.01, -152.85 ppm.

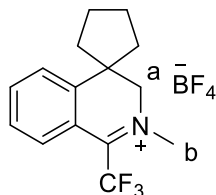
HRMS Calc'd for C₁₆H₁₉F₃N (M+H): 283.1549 Found: 283.1491







2'-methyl-1'-(trifluoromethyl)-3'H-spiro[cyclopentane-1,4'-isoquinolin]-2'-ium tetrafluoroborate (3.68)



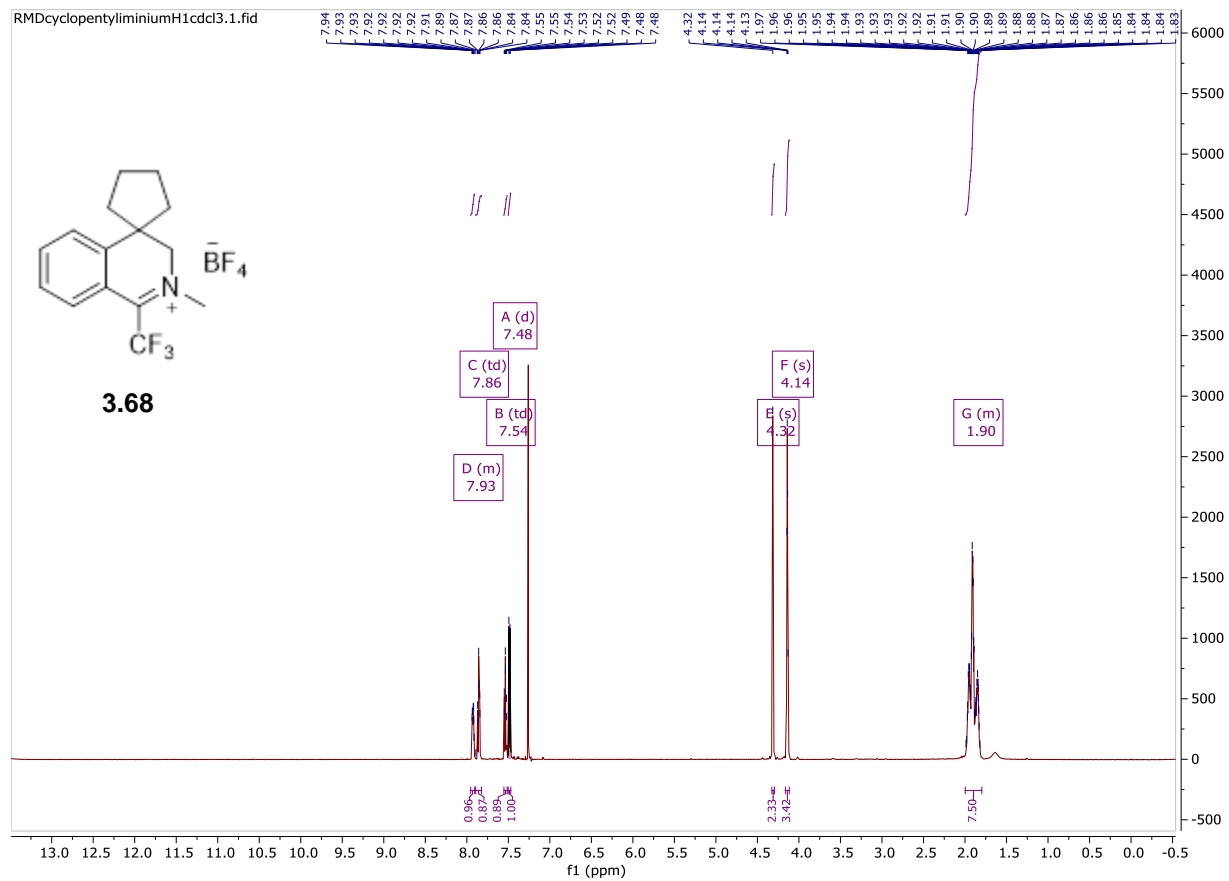
2'-methyl-1'-(trifluoromethyl)-3'H-spiro[cyclopentane-1,4'-isoquinolin]-2'-ium tetrafluoroborate was synthesized following general procedure for imine methylation a 3.22 mmol scale using 1'-(trifluoromethyl)-3'H-spiro[cyclopentane-1,4'-isoquinoline, as the respective imine, to give 0.438 g of an off white solid (1.22 mmol, 38% yield).

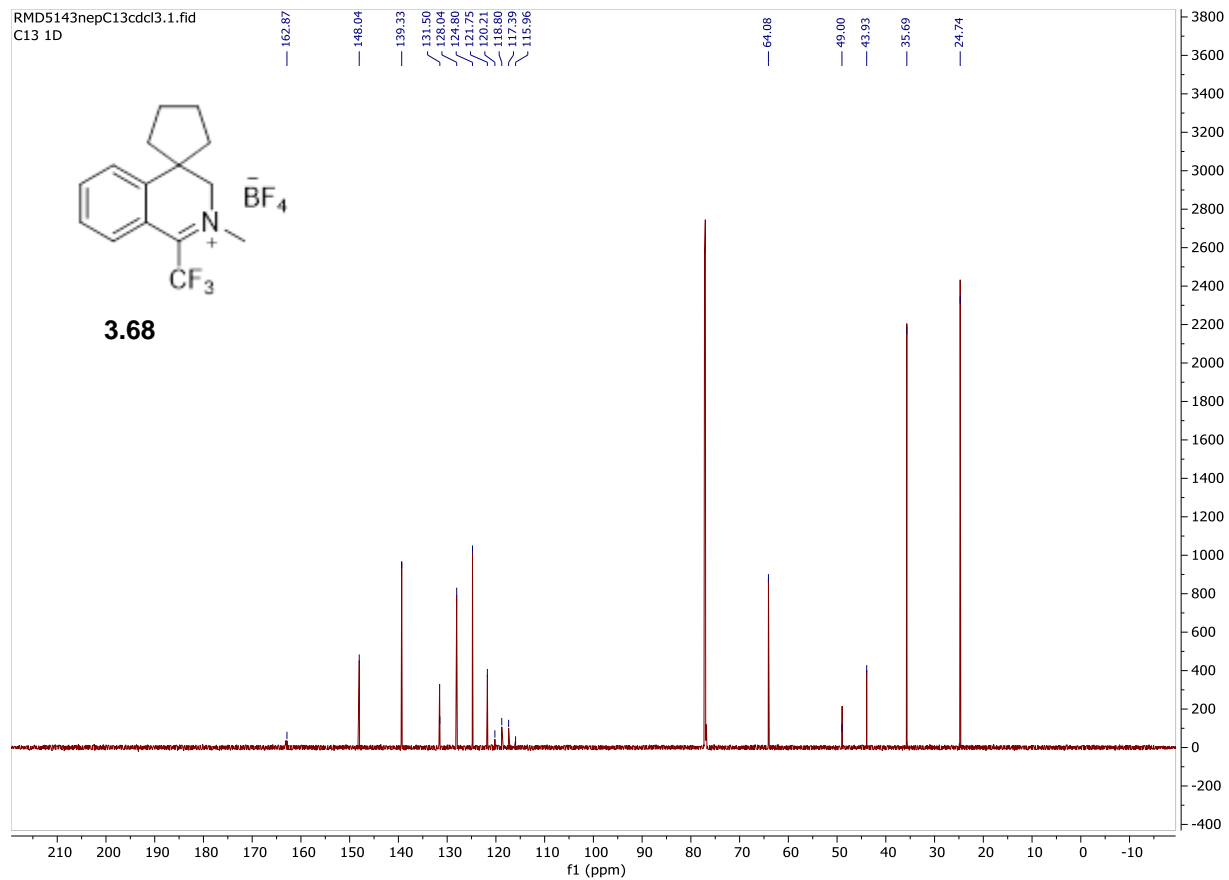
¹H NMR (600 MHz, CDCl₃) δ 7.95 – 7.91 (m, 1H), 7.86 (td, *J* = 7.7, 1.3 Hz, 1H), 7.54 (td, *J* = 7.9, 1.3 Hz, 1H), 7.48 (d, *J* = 7.7 Hz, 1H), 4.32 (H_a, s, 2H), 4.14 (H_b, s, 3H), 2.00 – 1.80 (m, 8H) ppm.

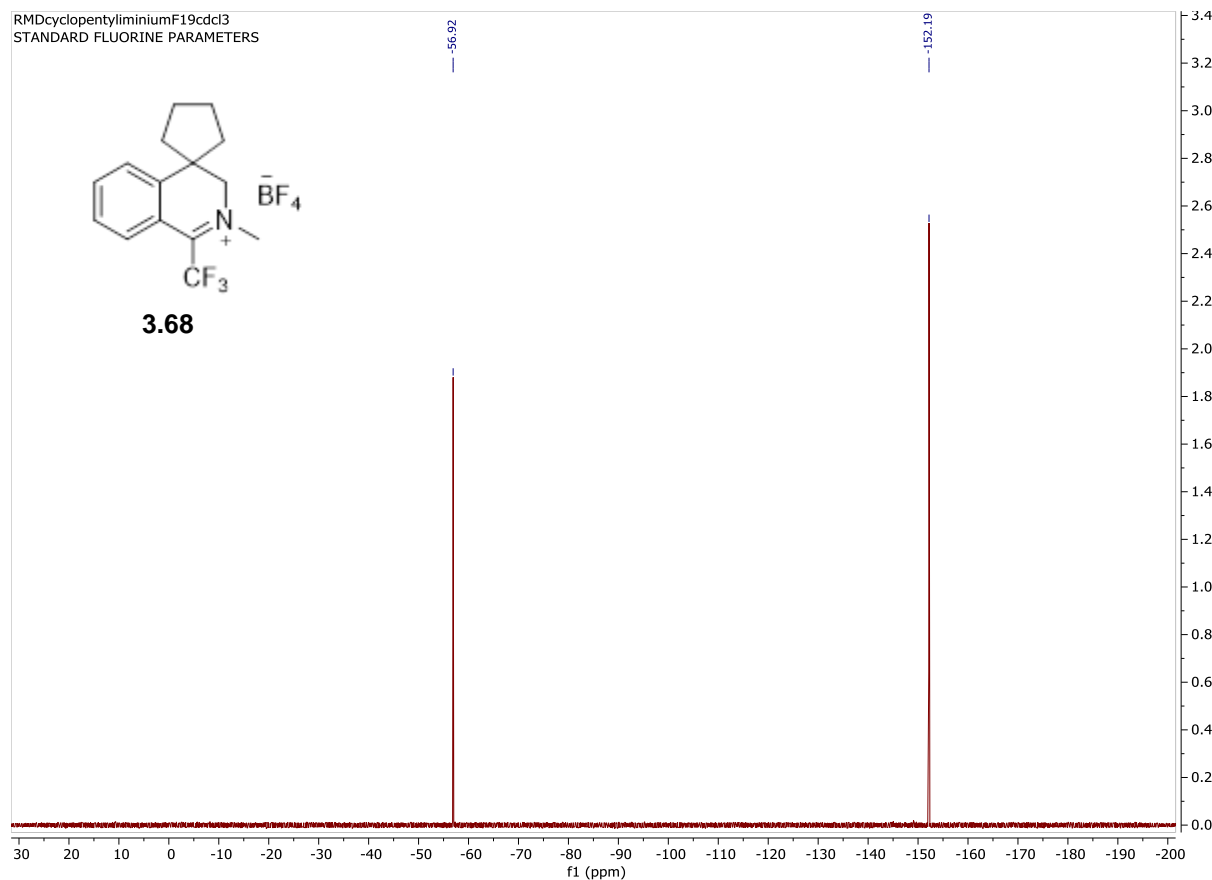
¹³C NMR (201 MHz, CDCl₃) δ 162.8, 148.0, 139.3, 131.5, 128.0, 124.8, 121.7, 120.2, 118.8, 117.3, 115.9, 64.0, 49.0, 43.9, 35.6, 24.7 ppm.

¹⁹F NMR (564 MHz, CDCl₃) δ -56.92, -152.19 ppm.

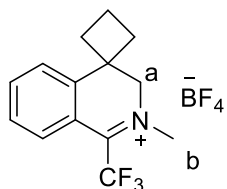
HRMS Calc'd for C₁₅H₁₇F₃N (M): 268.1308 Found: 268.1307







2'-methyl-1'-(trifluoromethyl)-3'H-spiro[cyclobutane-1,4'-isoquinolin]-2'-ium tetrafluoroborate (3.69)



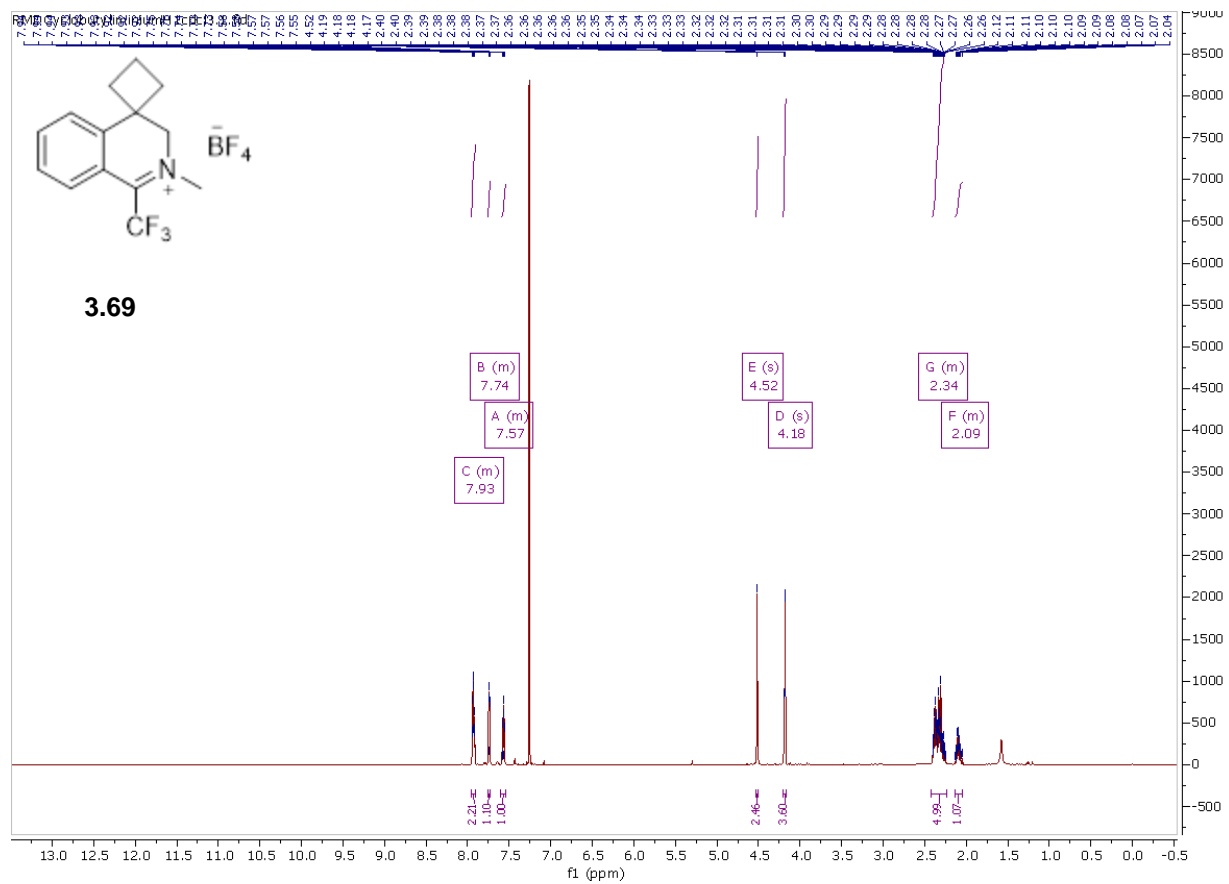
2'-methyl-1'-(trifluoromethyl)-3'H-spiro[cyclobutane-1,4'-isoquinolin]-2'-ium tetrafluoroborate was synthesized following general procedure for imine methylation a 2.93 mmol scale using 1'-(trifluoromethyl)-3'H-spiro[cyclobutane-1,4'-isoquinoline, as the respective imine, to give 0.420 g of an off white solid (1.23 mmol, 42% yield).

¹H NMR (600 MHz, CDCl₃) δ 7.95 – 7.91 (m, 2H), 7.76 – 7.73 (m, 1H), 7.60 – 7.54 (m, 1H), 4.52 (H_a, s, 2H), 4.18 (H_b, s, 3H), 2.42 – 2.24 (m, 5H), 2.14 – 2.04 (m, 1H) ppm.

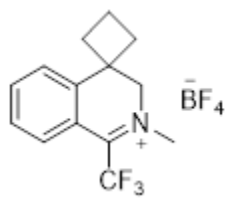
¹³C NMR (201 MHz, CDCl₃) δ 145.7, 139.6, 131.5, 128.3, 124.3, 121.1, 118.7, 117.3, 63.6, 49.1, 38.6, 28.9, 14.5 ppm.

¹⁹F NMR (564 MHz, CDCl₃) δ -57.07, -152.21 ppm.

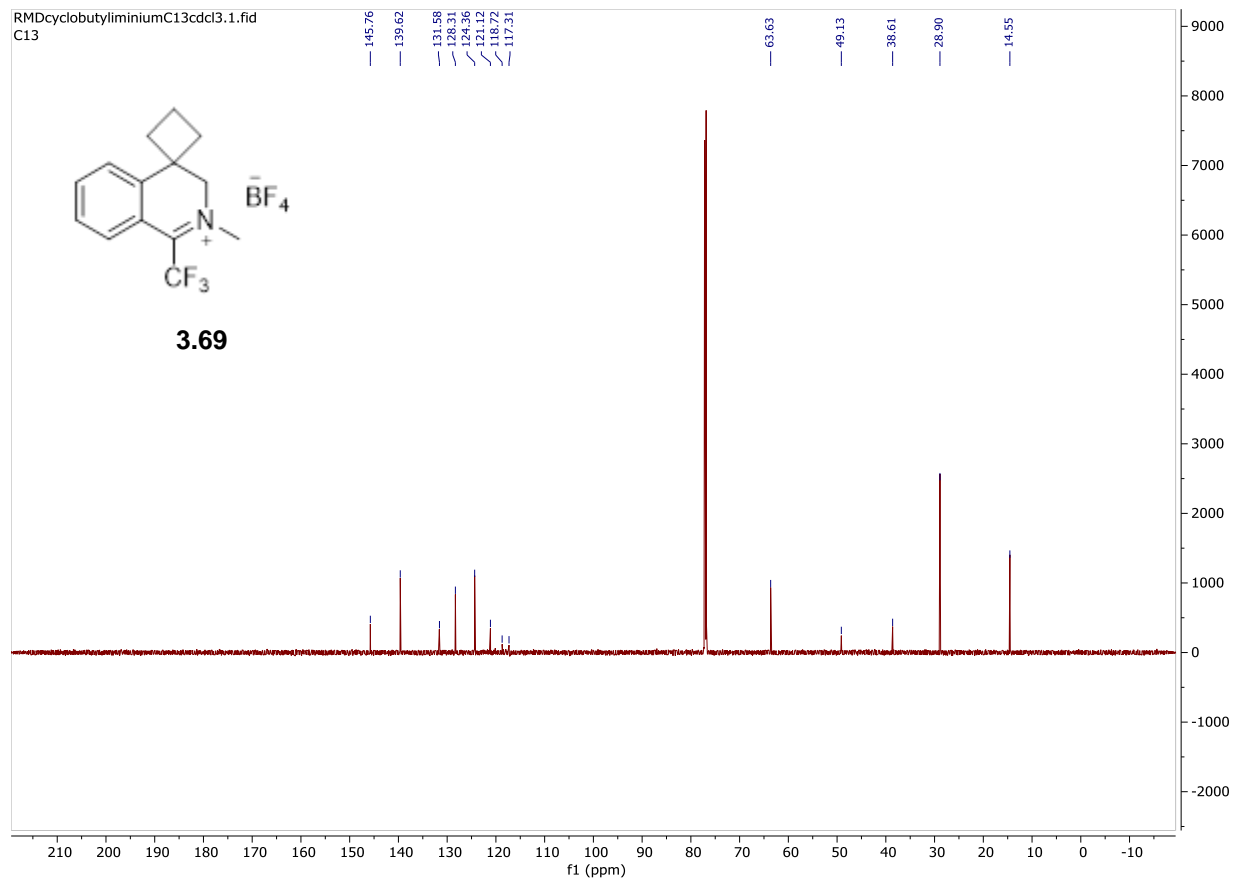
HRMS Calc'd for C₁₄H₁₅F₃N (M): 254.1151 Found: 254.1152

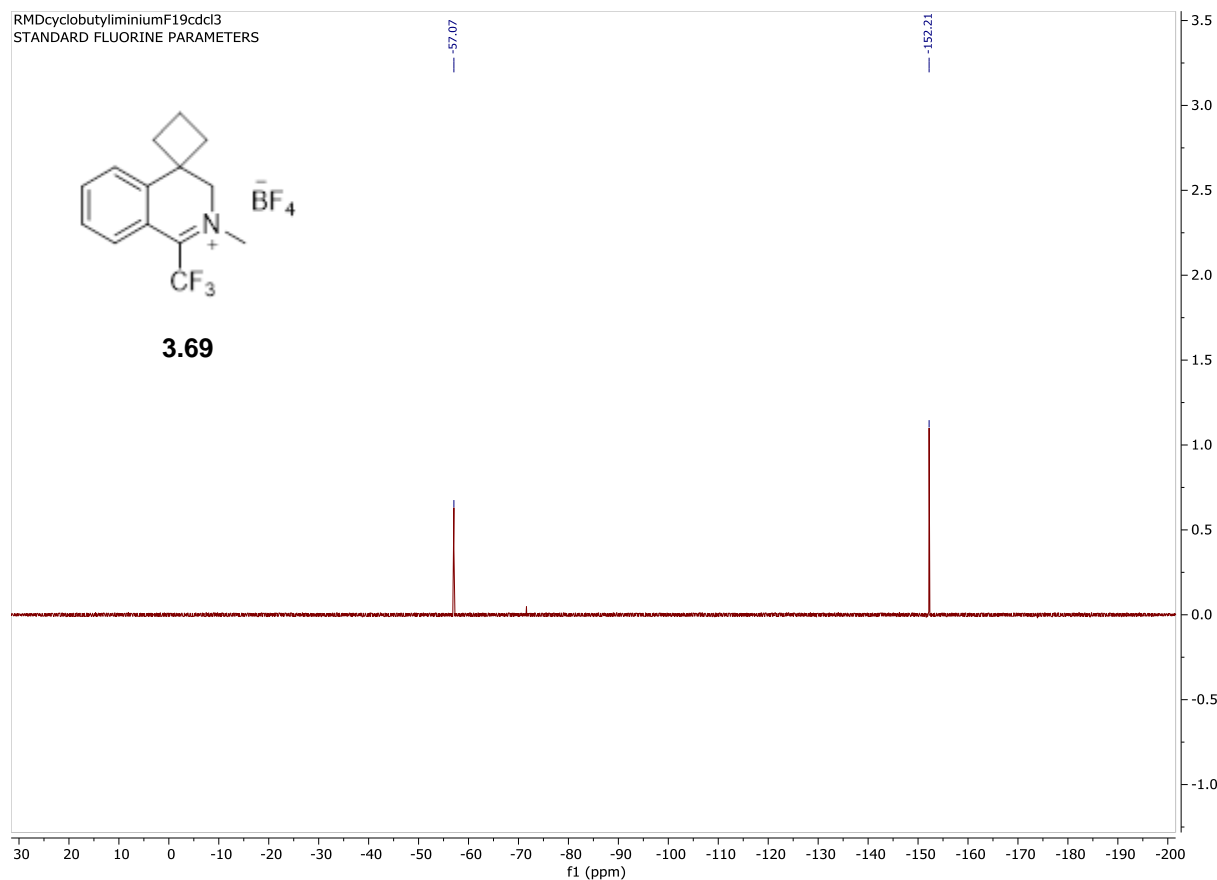


RMDcyclobutyliminiumC13cdcl3.1.fid
C13

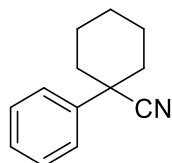


3.69





1-phenylcyclohexane-1-carbonitrile (3.70)

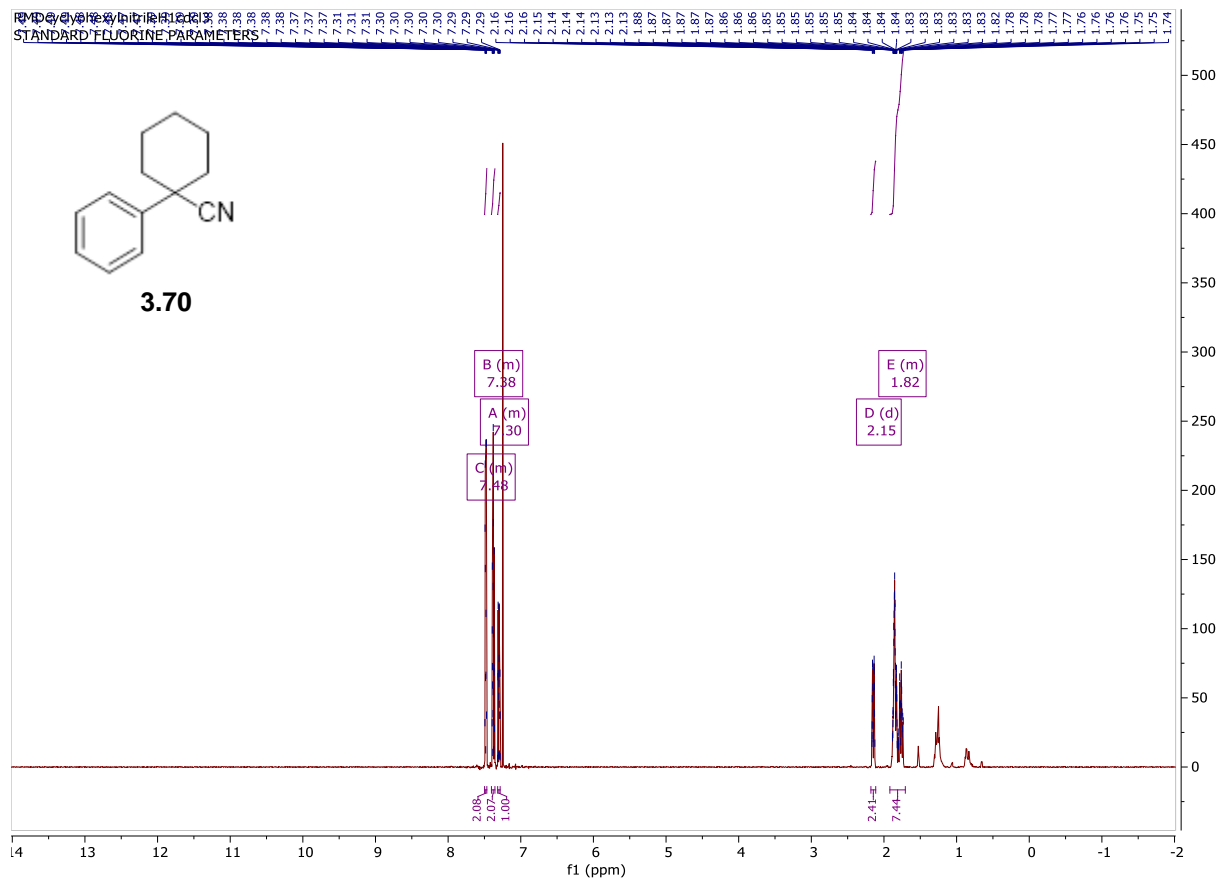


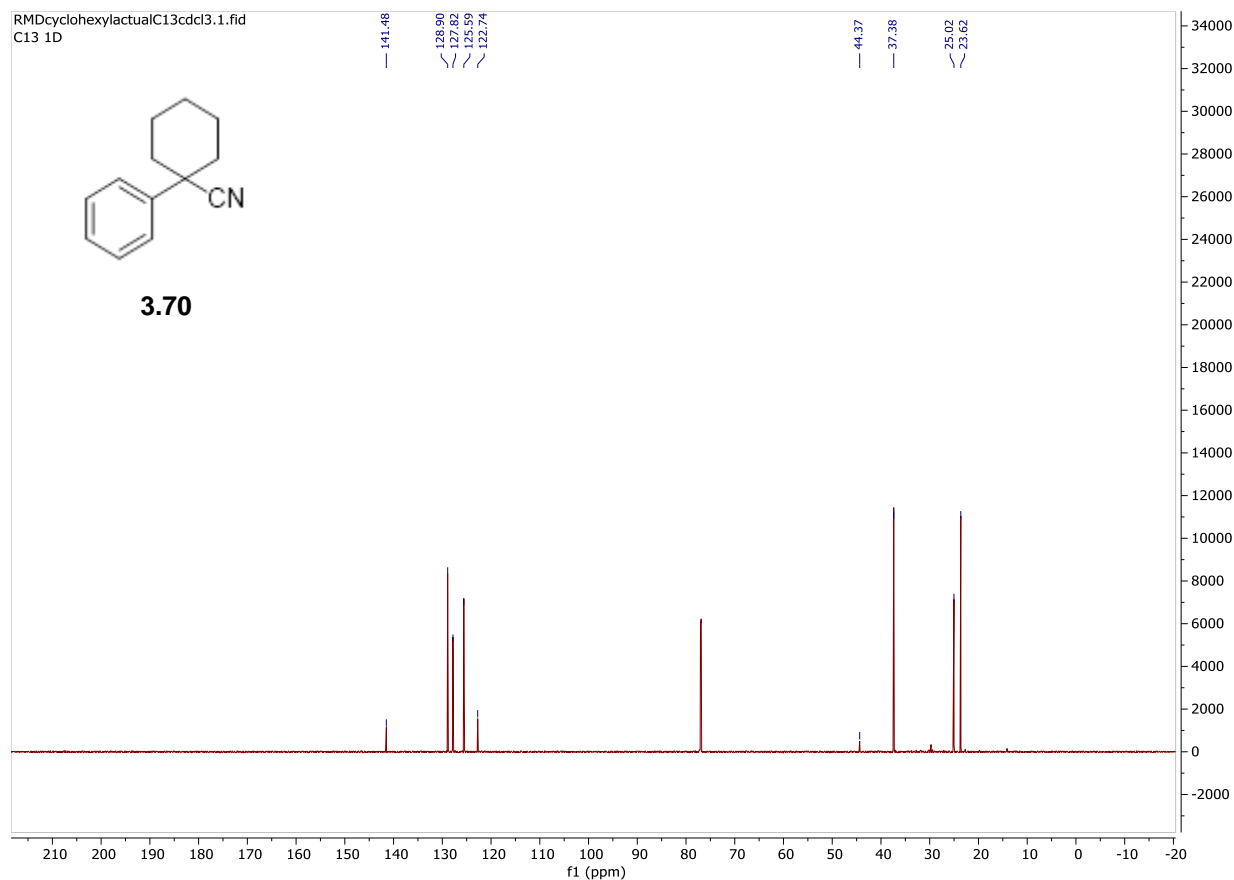
1-phenylcyclohexane-1-carbonitrile was synthesized following the general procedure for benzylic alkylation using 1,5 dibromopentane (1.1 equiv) in DMF on a 10 mmol scale using benzyl nitrile as the respective nitrile. The compound was purified using silica gel chromatography with 10% ethyl acetate/hexane to give 1.76g of a yellow oil (9.50 mmol, 95% yield)

¹H NMR (600 MHz, CDCl₃) δ 7.50 – 7.47 (m, 2H), 7.40 – 7.36 (m, 2H), 7.32 – 7.28 (m, 1H), 2.15 (d, *J* = 11.9 Hz, 4H), 1.92 – 1.71 (m, 6H) ppm.

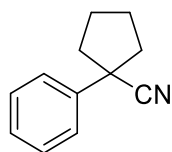
¹³C NMR (201 MHz, CDCl₃) δ 141.4, 128.9, 127.8, 125.6, 122.7, 44.3, 37.3, 25.0, 23.6 ppm.

HRMS Calc'd for C₁₃H₁₅N (M+H): 186.1283 Found: 186.148





1-phenylcyclopentane-1-carbonitrile (3.71)

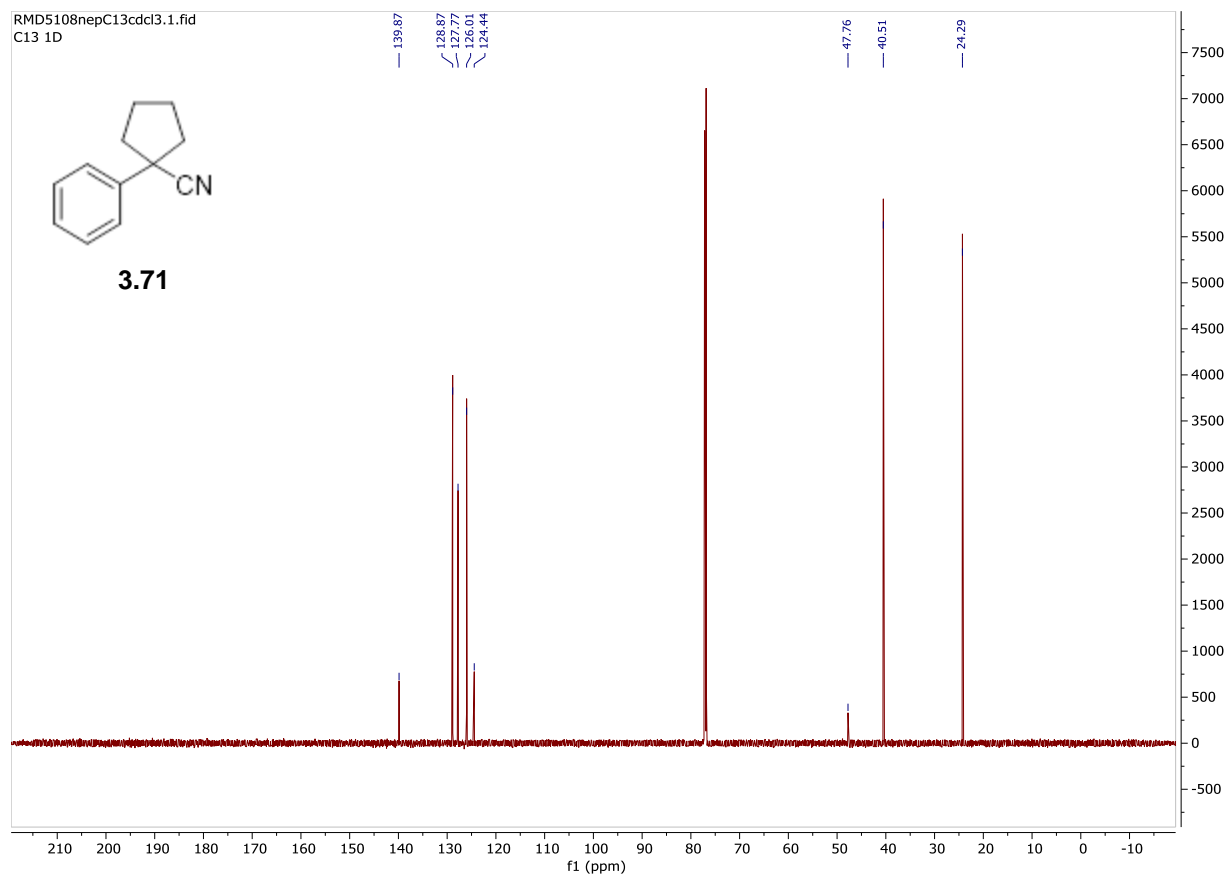


1-phenylcyclopentane-1-carbonitrile was synthesized following the general procedure for benzylic alkylation using 1,4 dibromobutane (1.1 equiv) in DMF on a 10 mmol scale using benzyl nitrile as the respective nitrile. The compound was purified using silica gel chromatography with 10% ethyl acetate/hexane to give 0.80 g of a yellow oil (4.6 mmol, 46% yield)

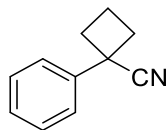
$^1\text{H NMR}$ (600 MHz, CDCl_3) δ 7.48 – 7.44 (m, 2H), 7.40 – 7.35 (m, 2H), 7.33 – 7.29 (m, 1H), 2.52 – 2.45 (m, 2H), 2.12 – 2.00 (m, 4H), 1.98 – 1.90 (m, 2H) ppm.

$^{13}\text{C NMR}$ (201 MHz, CDCl_3) δ 139.8, 128.8, 127.7, 126.0, 124.4, 47.7, 40.5, 24.2 ppm.

HRMS Calc'd for $\text{C}_{12}\text{H}_{13}\text{N}$ (M+Na): 194.0945 Found: 194.0967



1-phenylcyclobutane-1-carbonitrile (3.72)

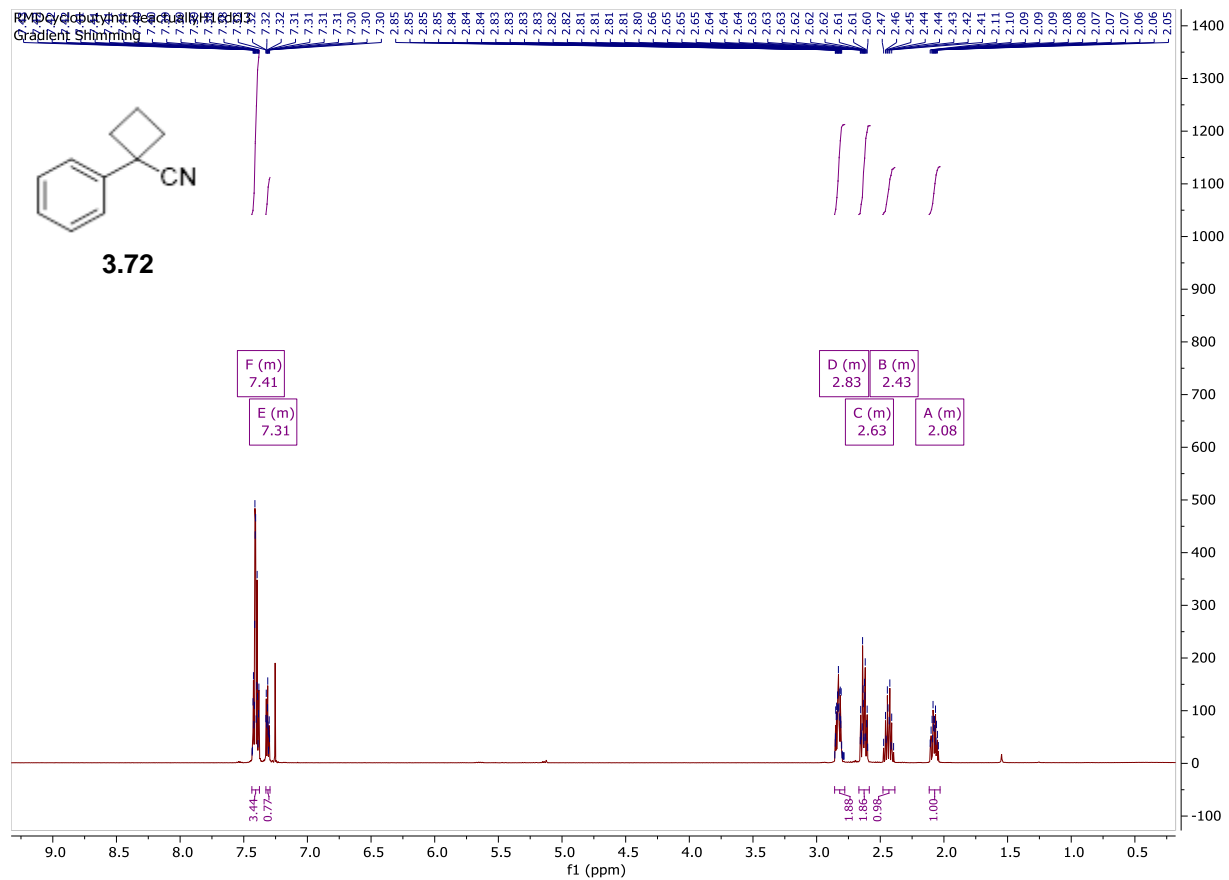


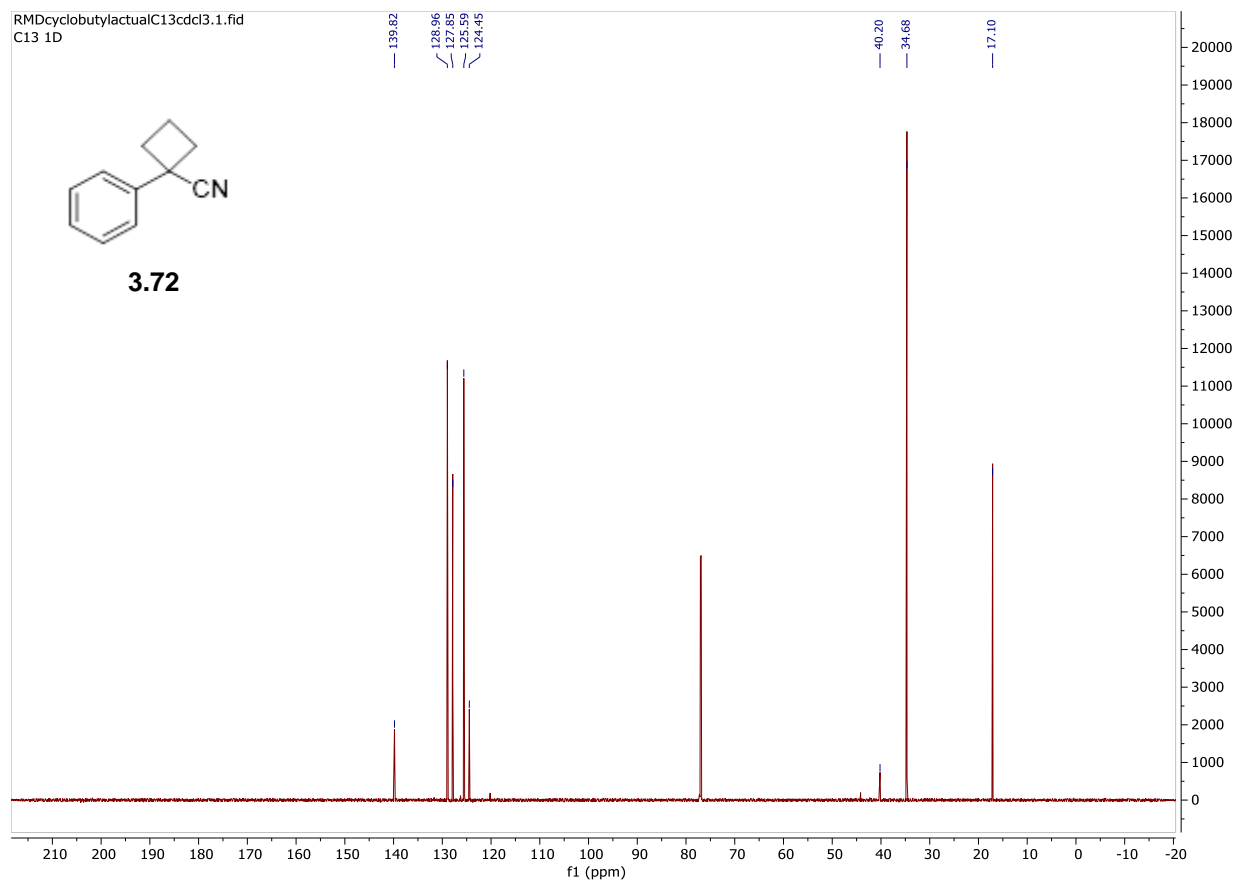
1-phenylcyclobutane-1-carbonitrile was synthesized following the general procedure for benzylic alkylation using 1,3 dibromopropane (1.1 equiv) in DMF on a 10 mmol scale using benzyl nitrile as the respective nitrile. The compound was purified using silica gel chromatography with 5% ethyl acetate/hexane to give 1.39 g of a yellow oil. (8.9 mmol, 89% yield)

¹H NMR (600 MHz, CDCl₃) δ 7.44 – 7.38 (m, 4H), 7.33 – 7.29 (m, 1H), 2.86 – 2.78 (m, 2H), 2.67 – 2.59 (m, 2H), 2.48 – 2.39 (m, 1H), 2.12 – 2.03 (m, 1H) ppm.

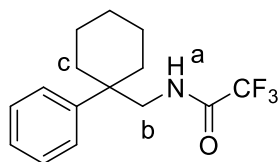
¹³C NMR (201 MHz, CDCl₃) δ 139.8, 128.9, 127.8, 125.6, 124.4, 40.2, 34.7, 17.1 ppm.

HRMS Calc'd for C₁₁H₁₁N (M+Na): 180.0788 Found: 180.0781





2,2,2-trifluoro-N-((1-phenylcyclohexyl) methyl) acetamide (3.73)



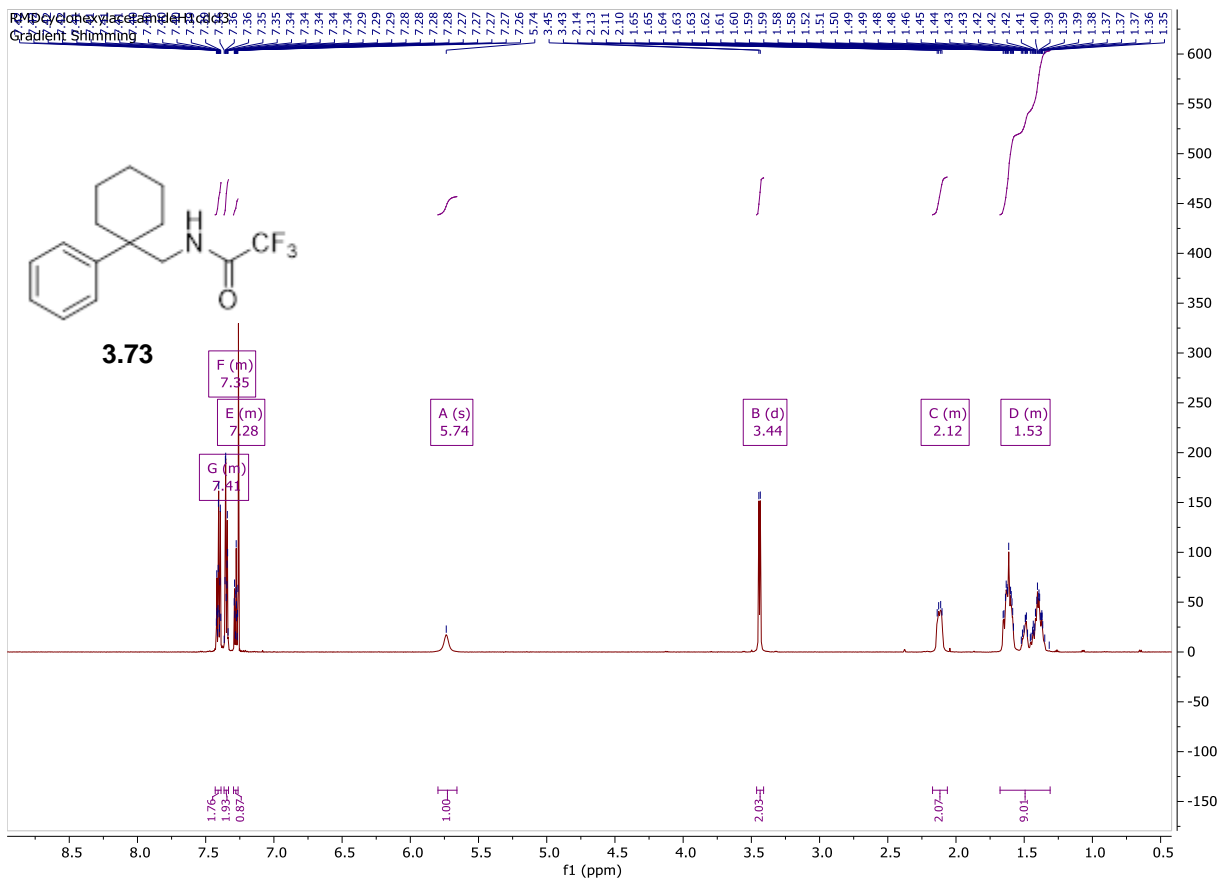
2,2,2-trifluoro-N-((1-phenylcyclohexyl) methyl) acetamide was synthesized following the general procedure for acetamide formation on a 11.41 mmol scale using (1-phenylcyclohexyl)methanamine, as the respective amine. The compound was purified using silica gel chromatography with 10% ethyl acetate/hexane to give a 1.59 g of an off-white solid. (5.57 mmol, 48% yield).

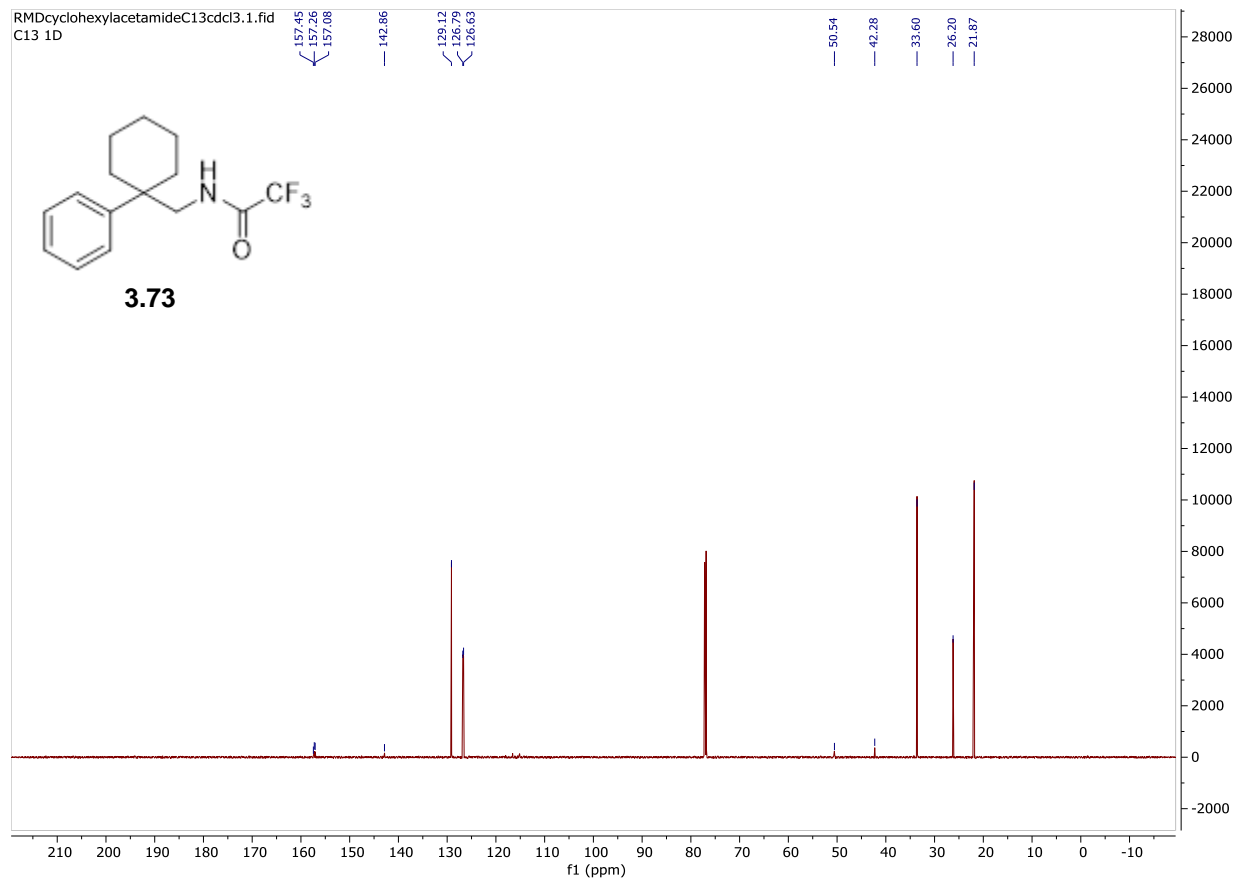
¹H NMR (600 MHz, CDCl₃) δ 7.43 – 7.39 (m, 2H), 7.37 – 7.33 (m, 2H), 7.30 – 7.26 (m, 1H), 5.74 (H_a, s, 1H), 3.44 (H_b, d, *J* = 6.3 Hz, 2H), 2.17 – 2.06 (H_c, m, 2H), 1.68 – 1.31 (m, 8H) ppm.

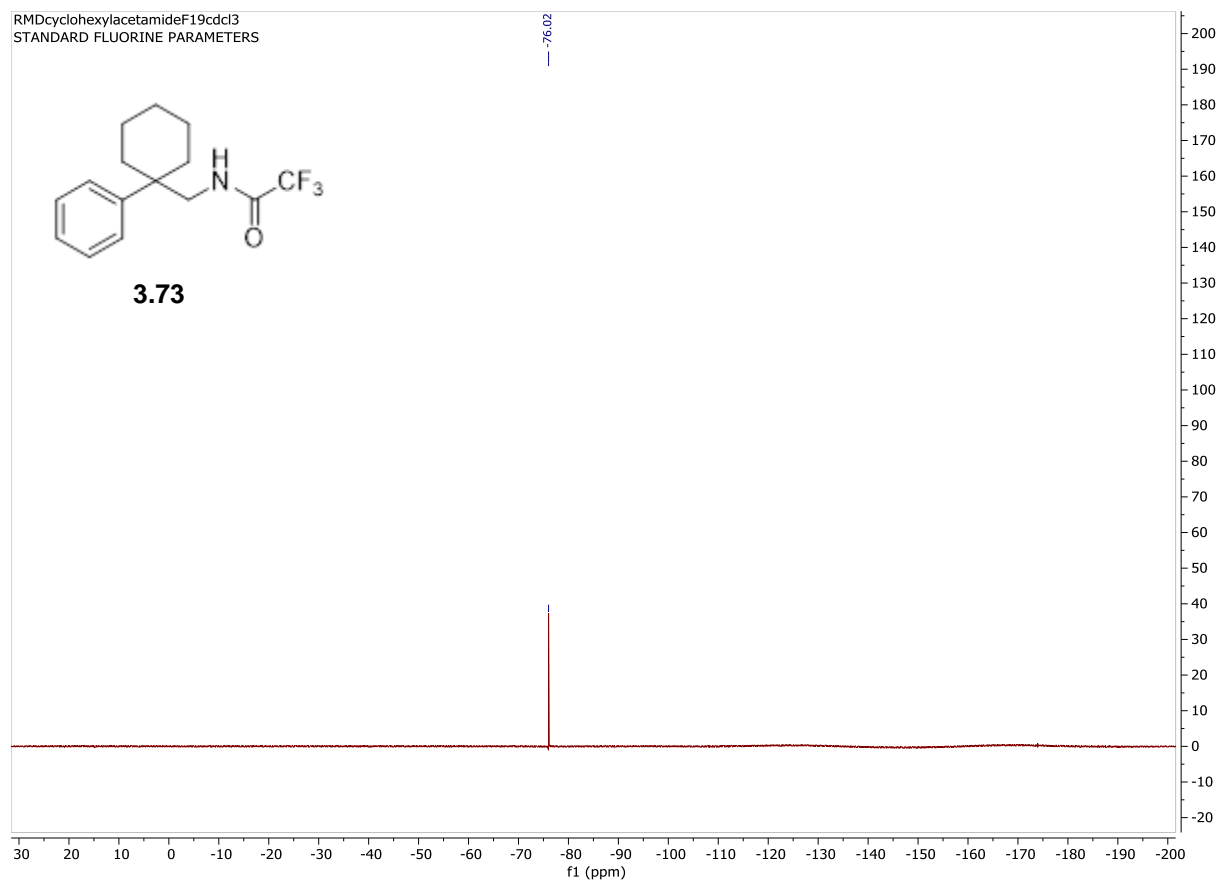
¹³C NMR (201 MHz, CDCl₃) δ 157.4, 157.26, 157.08, 142.8, 129.1, 126.79, 126.63, 50.5, 42.2, 33.6, 26.2, 21.8 ppm.

¹⁹F NMR (564 MHz, CDCl₃) δ -76.02 ppm.

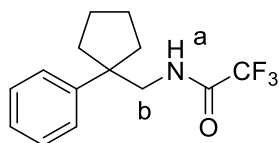
HRMS Calc'd for C₁₅H₁₈F₃NO (M+Na): 308.12377 Found : 308.1238







2,2,2-trifluoro-N-((1-phenylcyclopentyl) methyl) acetamide (3.74)



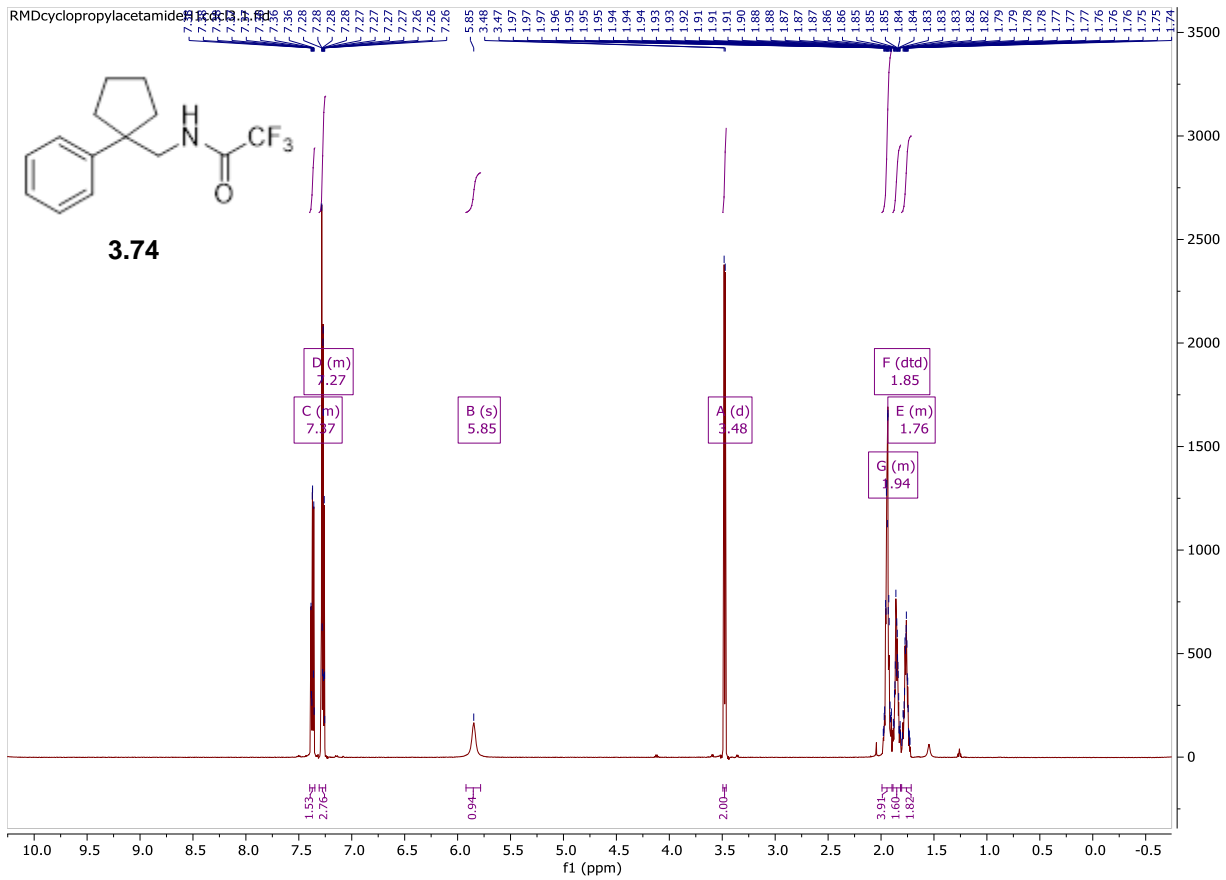
2,2,2-trifluoro-N-((1-phenylcyclopentyl) methyl) acetamide was synthesized following the general procedure for acetamide formation on a 4.33 mmol scale using (1-phenylcyclopentyl)methanamine as the respective amine. The compound was purified using silica gel chromatography with 10% ethyl acetate/hexane to give 1.03 g of a white solid (3.82 mmol, 88% yield).

¹H NMR (600 MHz, CDCl₃) δ 7.40 – 7.35 (m, 2H), 7.31 – 7.25 (m, 3H), 5.85 (H_a, s, 1H), 3.48 (H_b, d, J = 6.2 Hz, 2H), 1.99 – 1.90 (m, 4H), 1.88-1.82 (m, 2H), 1.81 – 1.72 (m, 2H) ppm.

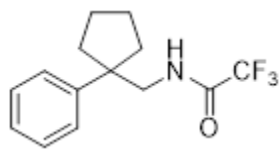
¹³C NMR (201 MHz, CDCl₃) δ 157.1, 145.4, 128.8, 126.8, 126.7, 77.18, 77.02, 76.8, 51.6, 48.2, 35.3, 23.2 ppm.

¹⁹F NMR (564 MHz, CDCl₃) δ -77.95 ppm.

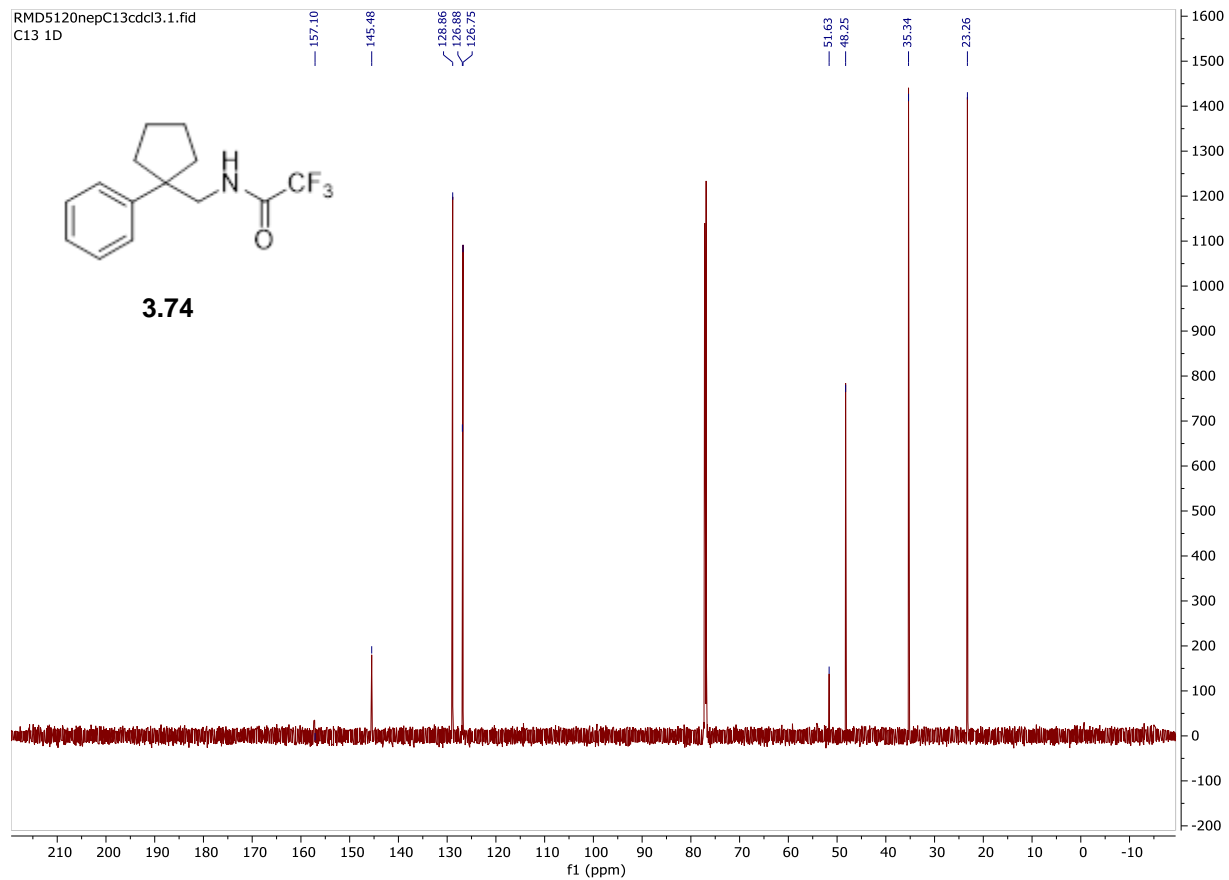
HRMS Calc'd for C₁₄H₁₆F₃NO (M+Na): 294.1081 Found: 294.1092

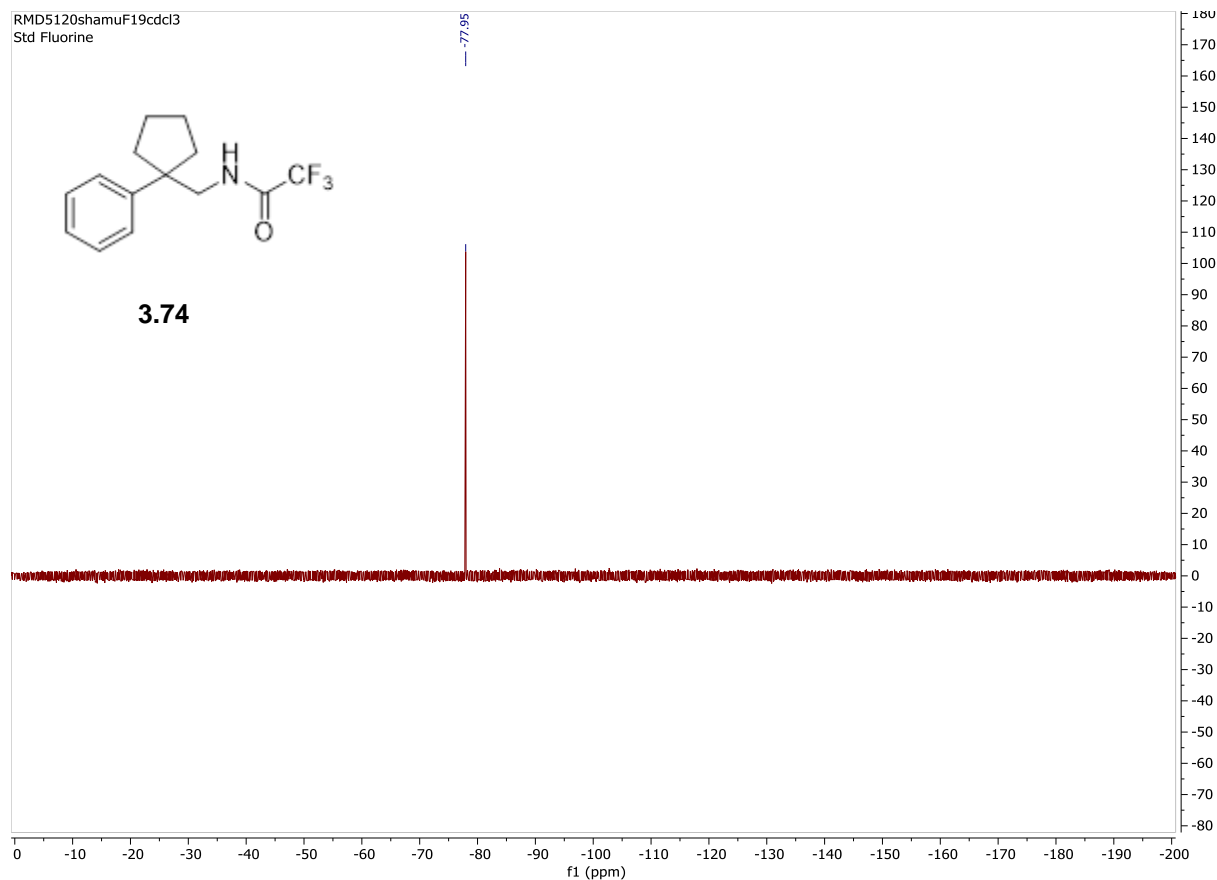


RMD5120nepC13cdcl3.1.fid
C13 1D

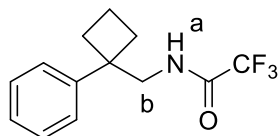


3.74





2,2,2-trifluoro-N-((1-phenylcyclobutyl)methyl) acetamide (3.75)



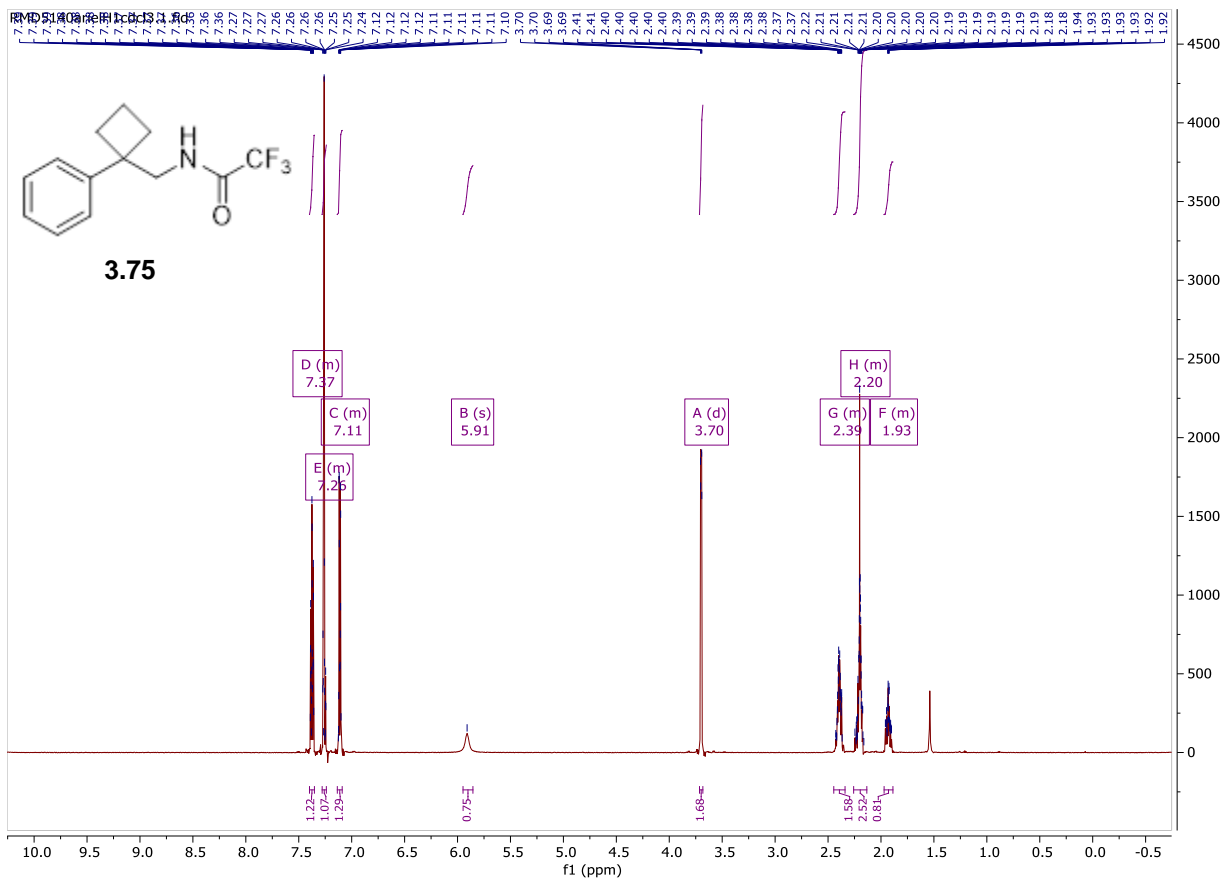
2,2,2-trifluoro-N-((1-phenylcyclobutyl)methyl) acetamide was synthesized following the general procedure for acetamide formation on a 5.9 mmol scale using (1-phenylcyclobutyl)methanamine as the respective amine. The compound was purified using silica gel chromatography with 10% ethyl acetate/hexane to give 1.06 g of an off-white solid (4.12 mmol, 70% yield).

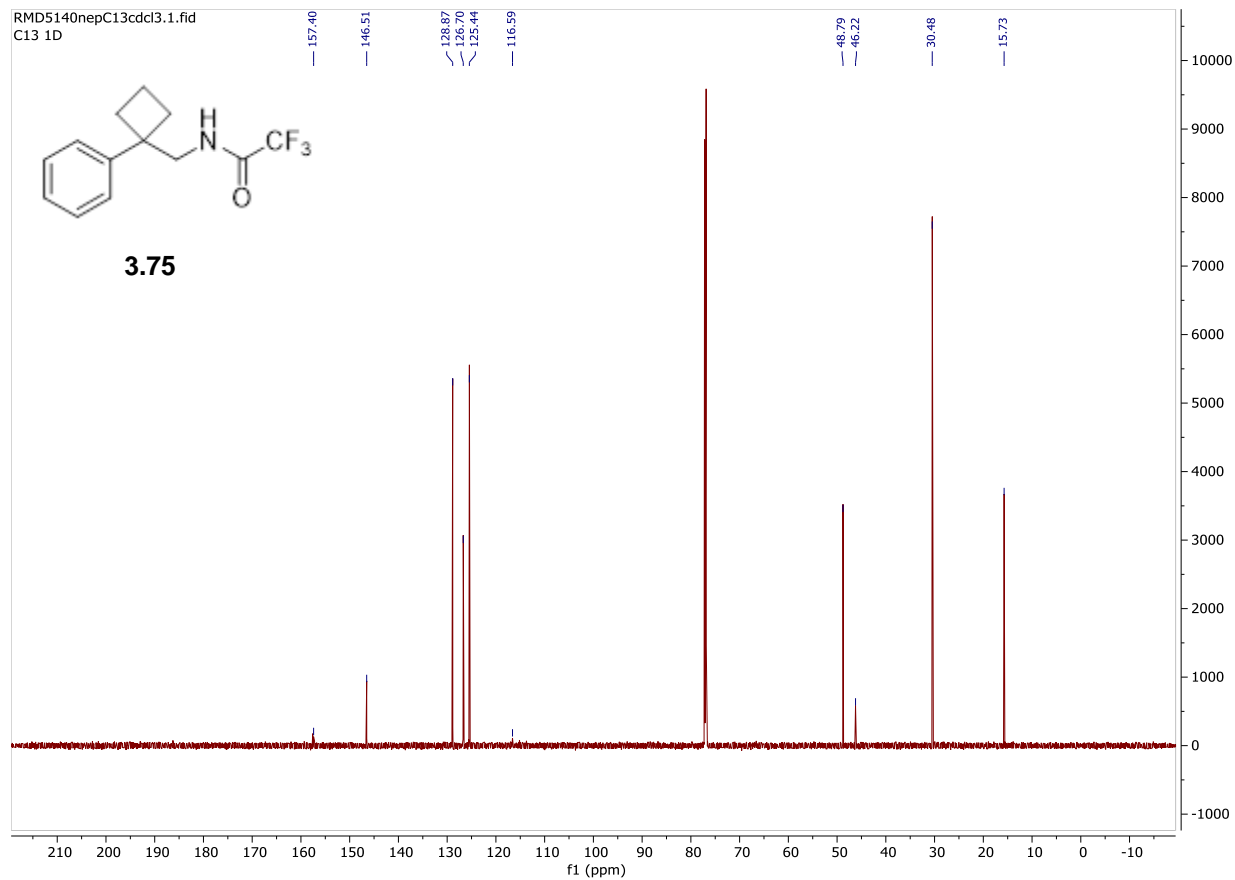
¹H NMR (600 MHz, CDCl₃) δ 7.40 – 7.35 (m, 2H), 7.28 – 7.24 (m, 1H), 7.14 – 7.09 (m, 2H), 5.91 (H_a, s, 1H), 3.70 (H_b, d, *J* = 6.2 Hz, 2H), 2.45 – 2.34 (m, 2H), 2.26 – 2.13 (m, 3H), 1.97 – 1.89 (m, 1H) ppm.

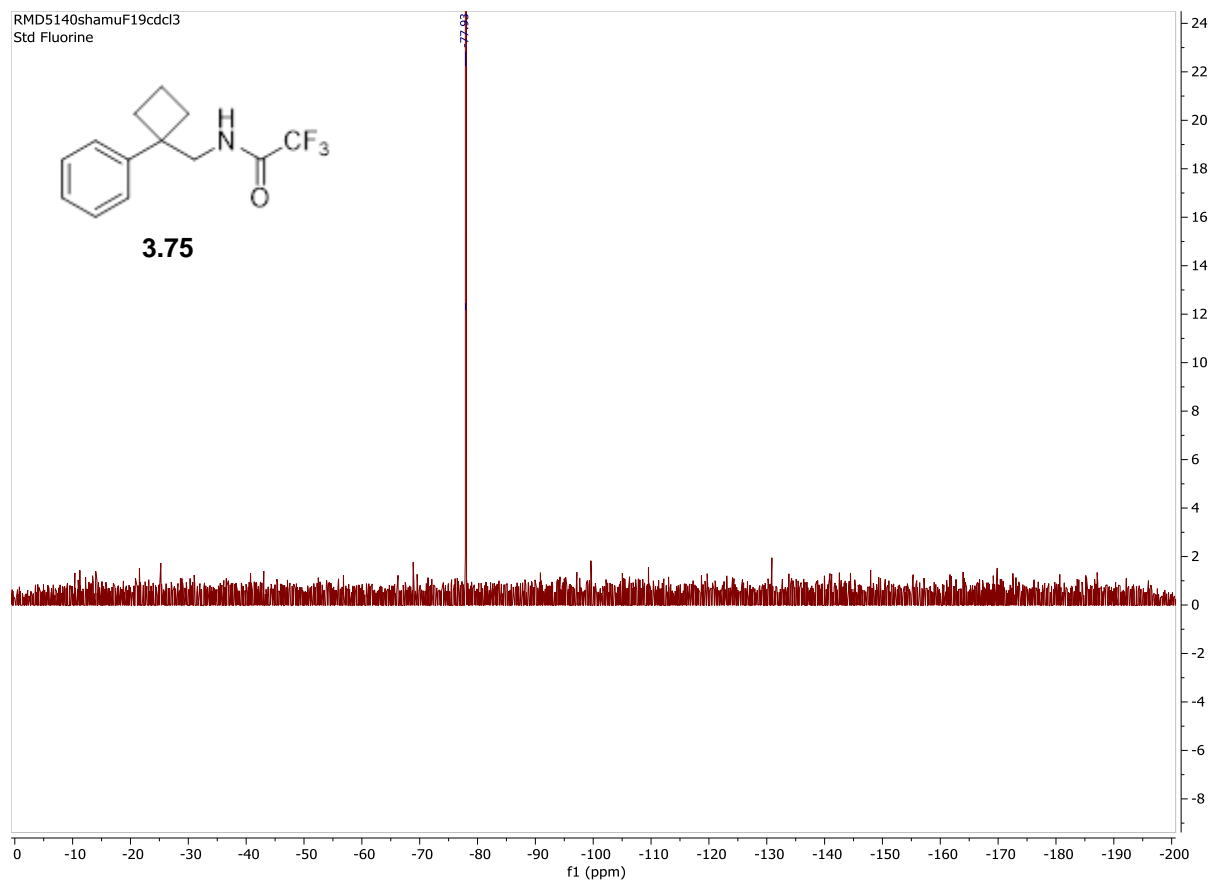
¹³C NMR (201 MHz, CDCl₃) δ 157.4, 146.5, 128.8, 126.7, 125.4, 116.5, 48.7, 46.2, 30.4, 15.7 ppm.

¹⁹F NMR (564 MHz, CDCl₃) δ -77.93 ppm.

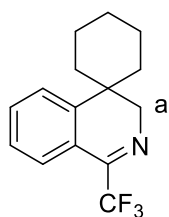
HRMS Calc'd for C₁₃H₁₄F₃NO (M+Na): 280.0924 Found: 280.0928







1'-(trifluoromethyl)-3'H-spiro[cyclohexane-1,4'-isoquinoline] (3.76)



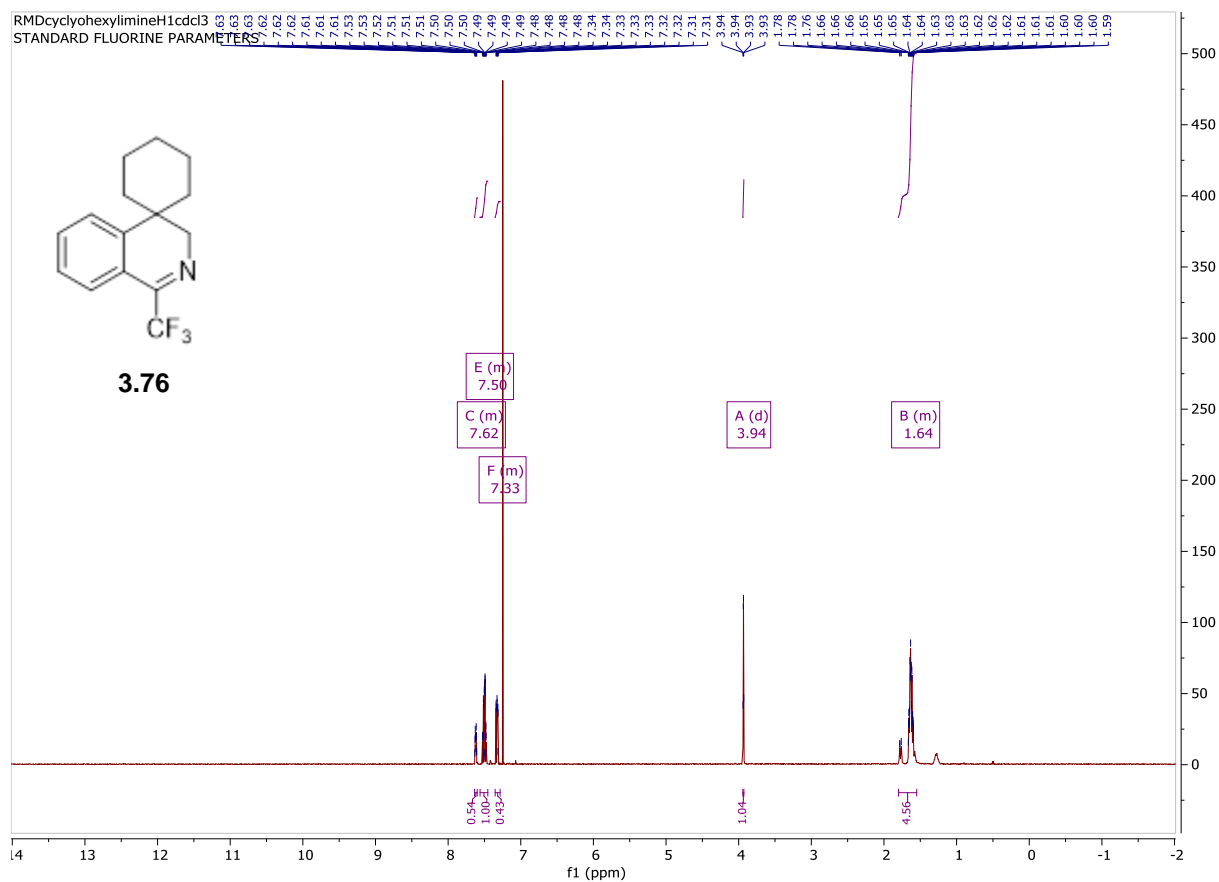
1'-(trifluoromethyl)-3'H-spiro[cyclohexane-1,4'-isoquinoline] was synthesized following general procedure A for the Bischler Napieralski reaction on a 5.57 mmol scale using 2,2,2-trifluoro-N-((1-phenylcyclohexyl)methyl) acetamide as the respective acetamide. The compound was purified using silica gel chromatography with 10% ethyl acetate/hexane to give .561 g of an orange oil (2.10 mmol, 37% yield).

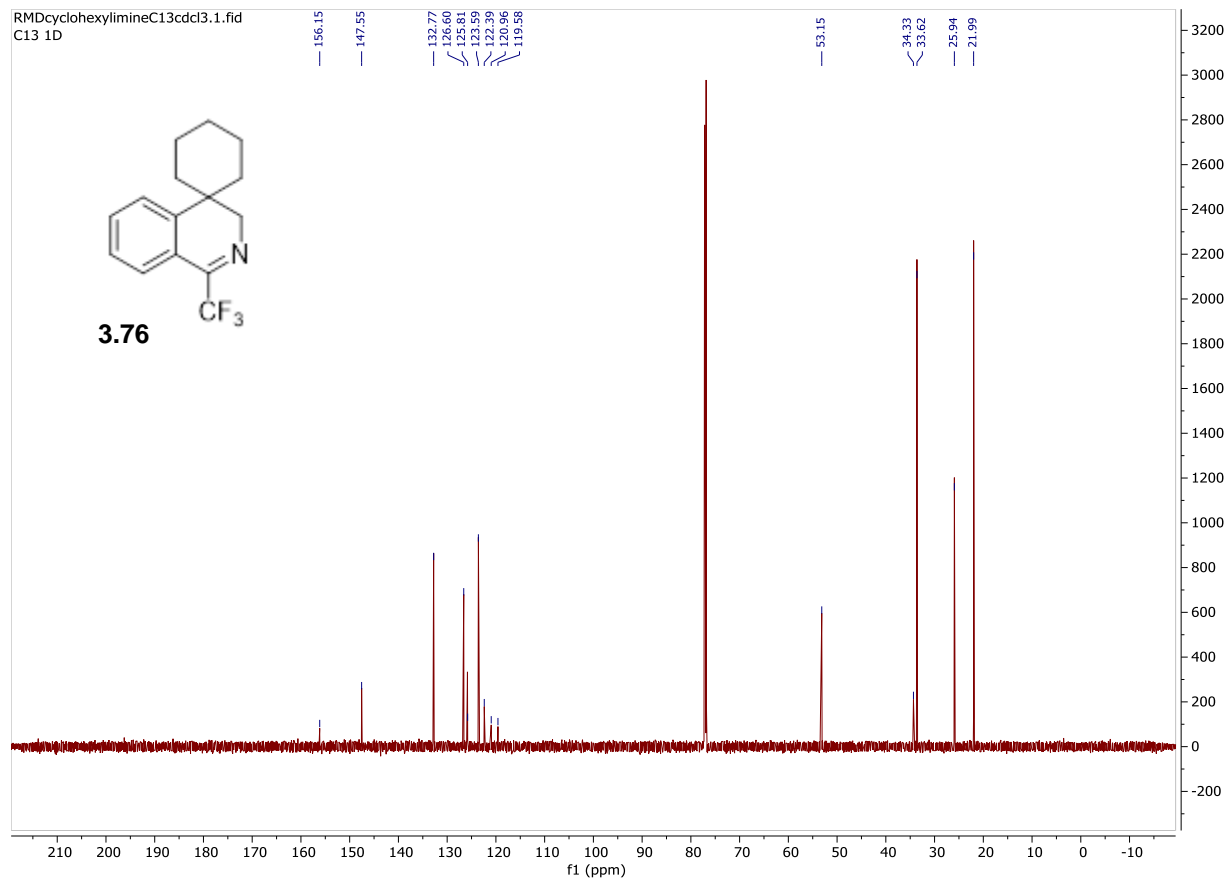
¹H NMR (600 MHz, CDCl₃) δ 7.64 – 7.60 (m, 1H), 7.56 – 7.45 (m, 2H), 7.35 – 7.28 (m, 1H), 3.94 (H_a, d, *J* = 1.8 Hz, 1H), 1.80 – 1.55 (m, 10H) ppm.

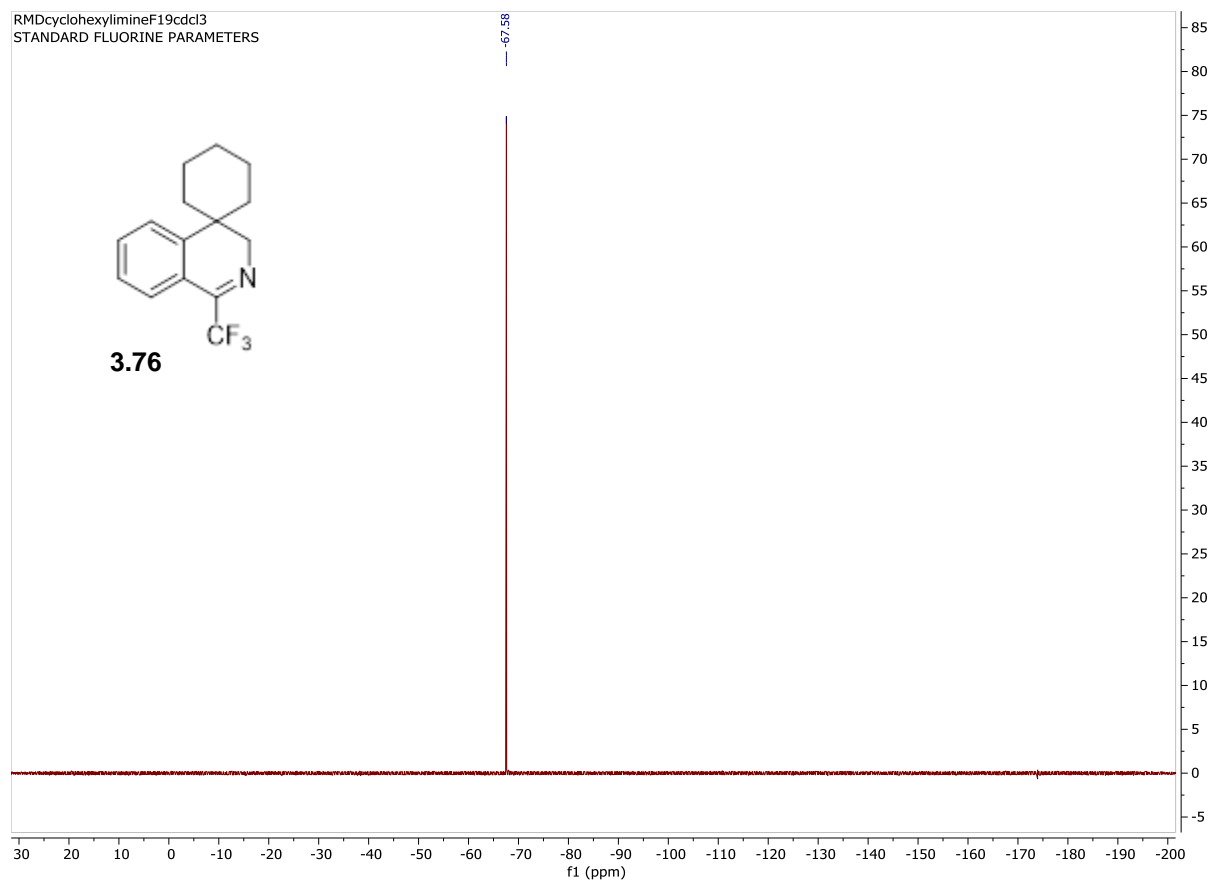
¹³C NMR (201 MHz, CDCl₃) δ 156.1, 147.5, 132.7, 126.6, 125.8, 123.5, 122.3, 120.9, 119.5, 53.1, 34.3, 33.6, 25.9, 21.9 ppm.

¹⁹F NMR (564 MHz, CDCl₃) δ -67.58 ppm.

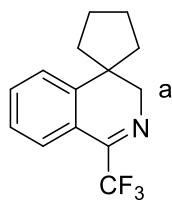
HRMS Calc'd for C₁₅H₁₆F₃N (M+H): 268.1314 Found: 268.1350







1'-(trifluoromethyl)-3'H-spiro[cyclopentane-1,4'-isoquinoline] (3.77)



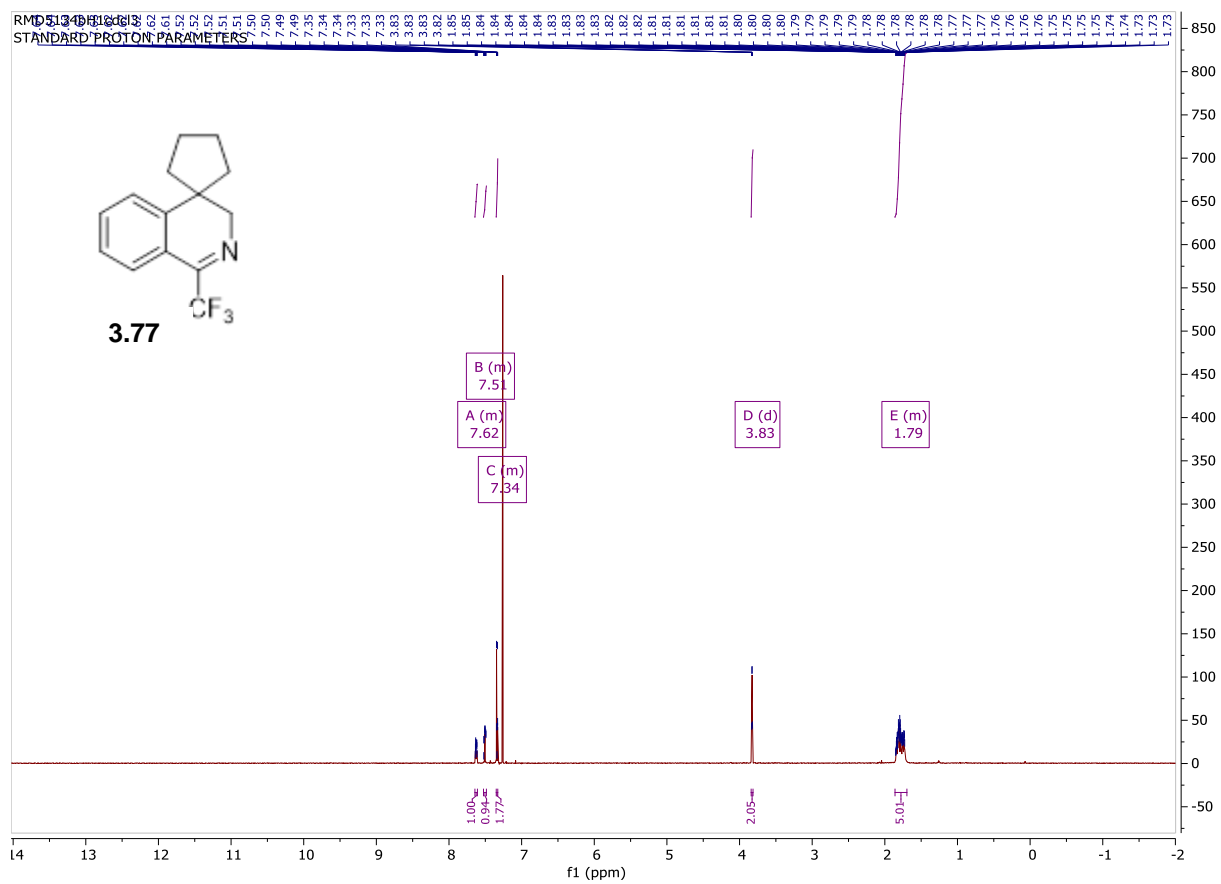
1'-(trifluoromethyl)-3'H-spiro[cyclopentane-1,4'-isoquinoline] was synthesized following general procedure A for the Bischler Napieralski reaction on a 3.68 mmol scale using 2,2,2-trifluoro-N-((1-phenylcyclopentyl)methyl) acetamide, as the respective acetamide. The compound was purified using silica gel chromatography with 10% ethyl acetate/hexane to give 0.820 g of a yellow oil (3.22 mmol, 87% yield).

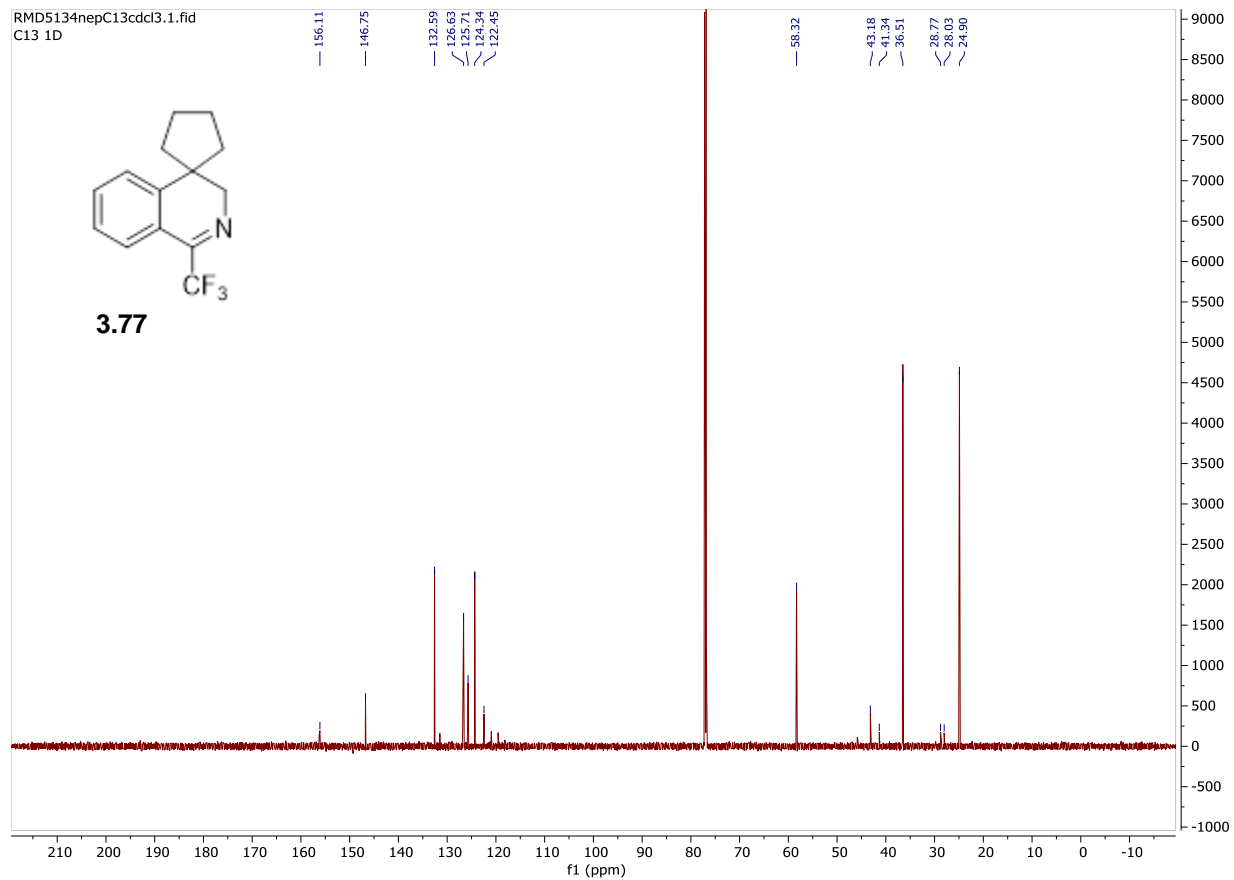
¹H NMR (600 MHz, CDCl₃) δ 7.64 – 7.61 (m, 1H), 7.53 – 7.48 (m, 1H), 7.35 – 7.33 (m, 2H), 3.83 (H_a, d, J = 1.8 Hz, 2H), 1.86 – 1.70 (m, 10H) ppm.

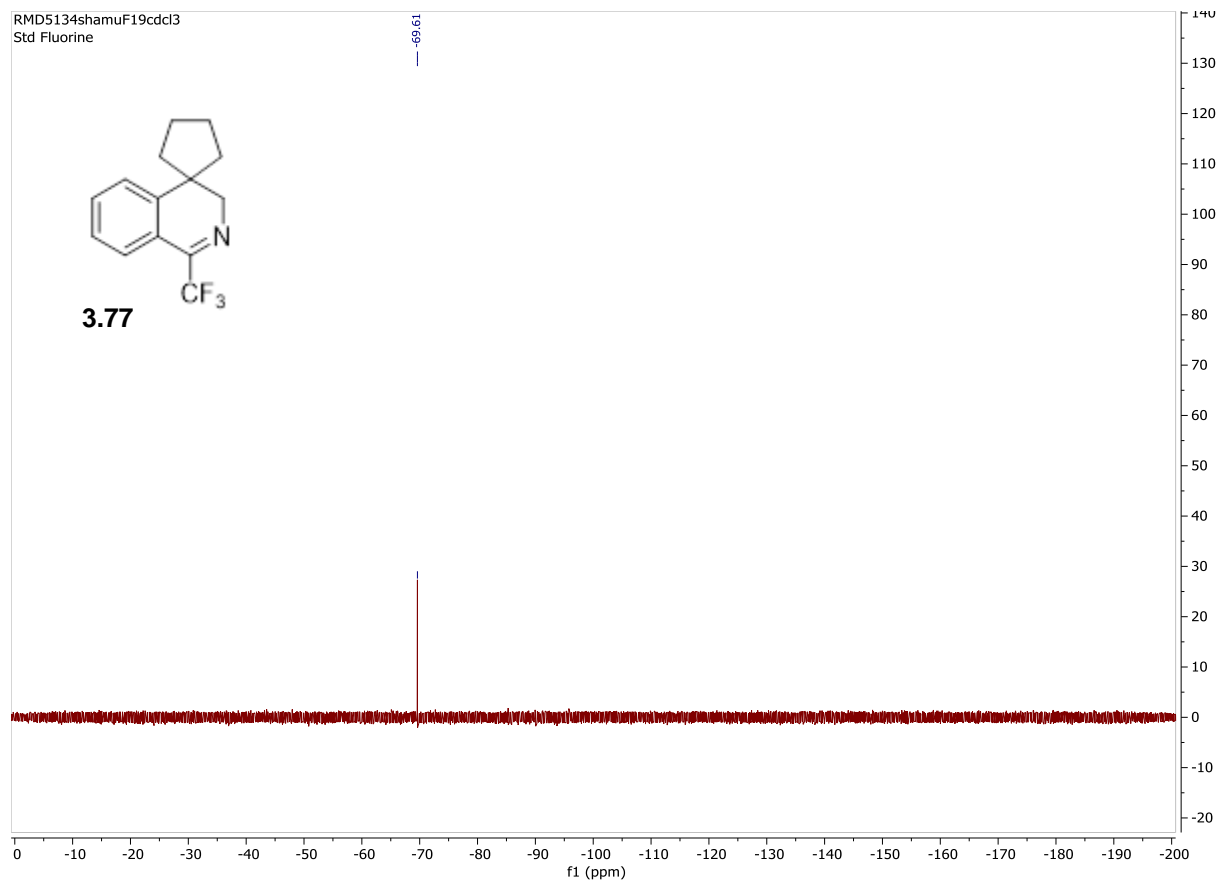
¹³C NMR (201 MHz, CDCl₃) δ 156.1, 146.7, 132.5, 126.6, 125.7, 124.3, 122.4, 58.3, 43.1, 41.3, 36.5, 28.7, 28.0, 24.9 ppm.

¹⁹F NMR (564 MHz, CDCl₃) δ -69.61 ppm.

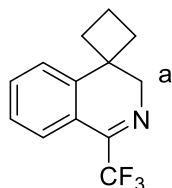
HRMS C₁₄H₁₄F₃N (M+H): 254.1156 Found: 254.1186







1'-(trifluoromethyl)-3'H-spiro[cyclobutane-1,4'-isoquinoline] (3.78)



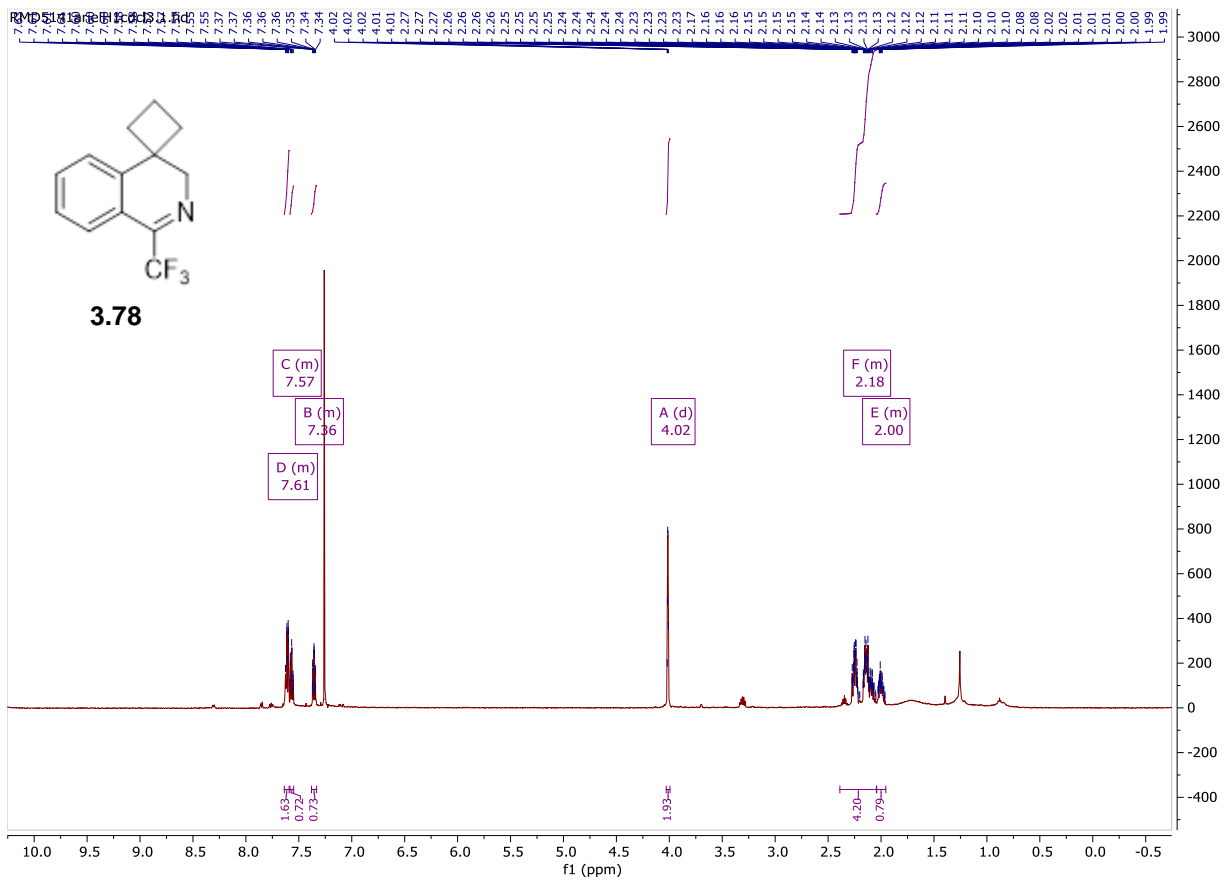
1'-(trifluoromethyl)-3'H-spiro[cyclobutane-1,4'-isoquinoline] was synthesized following general procedure A for the Bischler Napieralski reaction on a 4.12 mmol scale using 2,2,2-trifluoro-N-((1-phenylcyclobutyl)methyl) acetamide as the respective acetamide. The compound was purified using silica gel chromatography with 10% ethyl acetate/hexane to give 0.703 of a yellow oil (2.93 mmol, 71% yield).

¹H NMR (600 MHz, CDCl₃) δ 7.64 – 7.59 (m, 2H), 7.58 – 7.55 (m, 1H), 7.38 – 7.33 (m, 1H), 4.02 (H_a, d, *J* = 1.5 Hz, 2H), 2.39 – 2.04 (m, 5H), 2.04 – 1.96 (m, 1H) ppm.

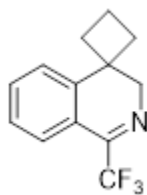
¹³C NMR (201 MHz, CDCl₃) δ 144.6, 132.7, 126.8, 125.7, 121.7, 119.4, 57.7, 38.3, 30.1, 15.1 ppm.

¹⁹F NMR (564 MHz, CDCl₃) δ -69.66 ppm.

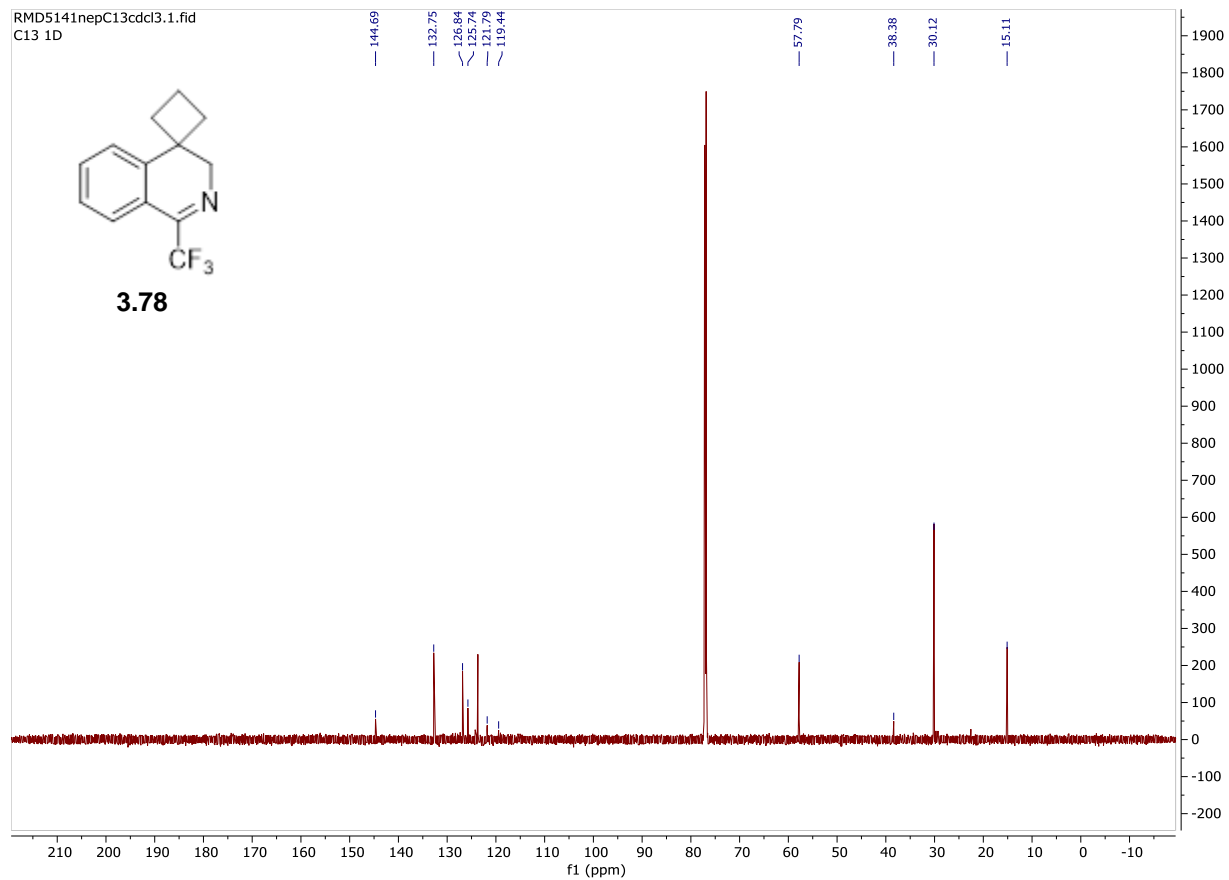
HRMS Calc'd for C₁₃H₁₂F₃N (M+H) 240.1001 Found: 240.1020

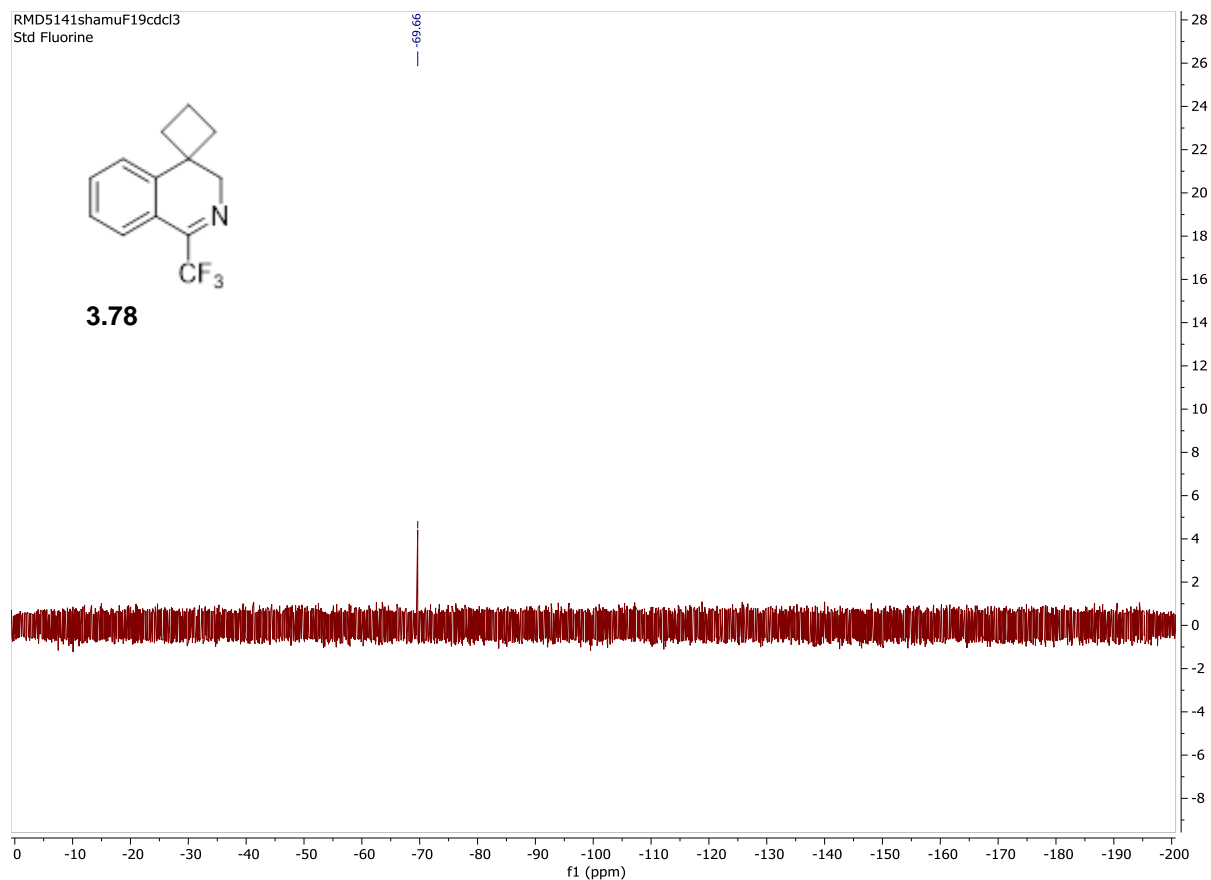


RMD5141nepC13cdcl3.1.fid
C13 1D

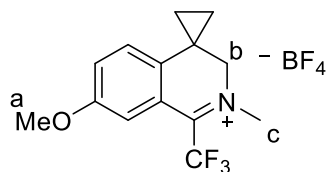


3.78





7'-methoxy-2'-methyl-1'-(trifluoromethyl)-3'H-spiro[cyclopropane-1,4'-isoquinolin]-2'-ium tetrafluoroborate (3.79)



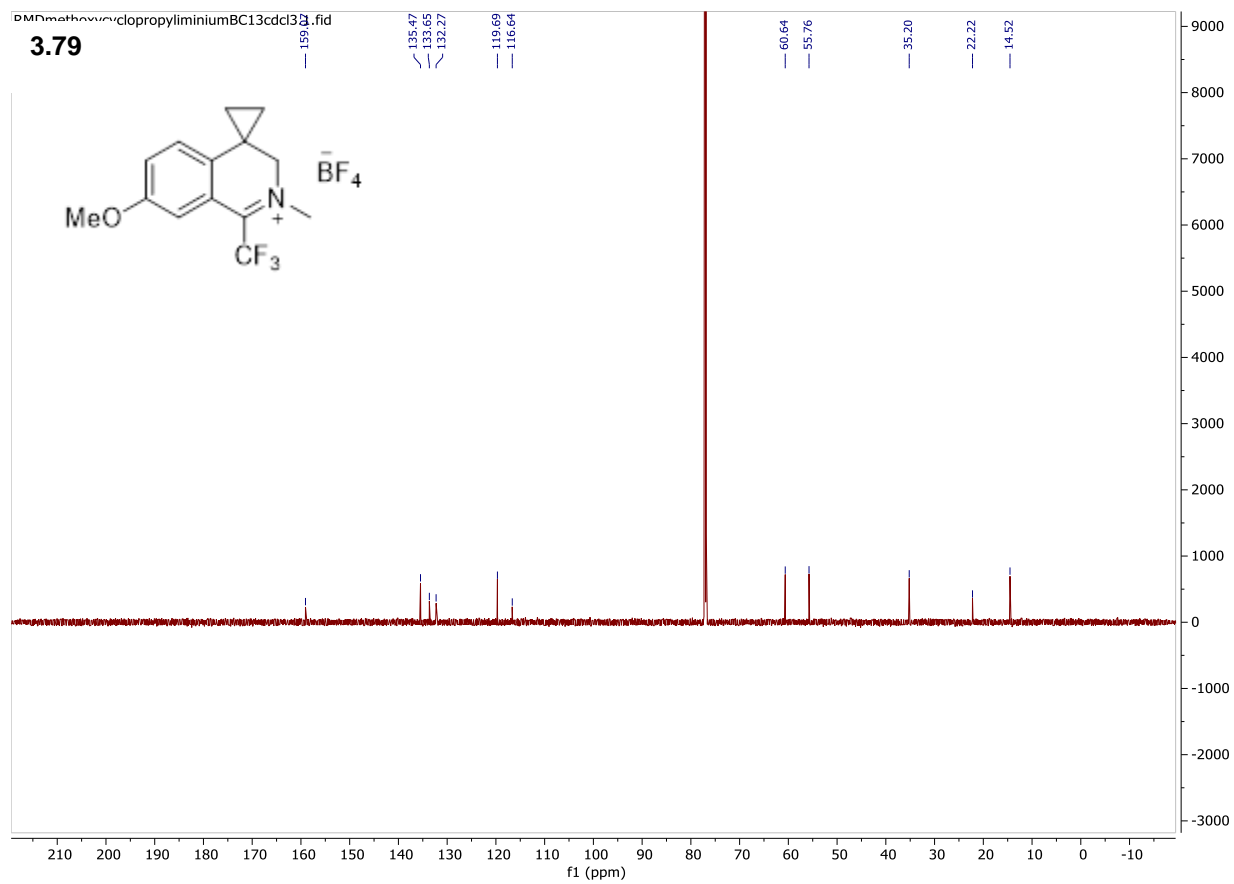
7'-methoxy-2'-methyl-1'-(trifluoromethyl)-3'H-spiro[cyclopropane-1,4'-isoquinolin]-2'-ium tetrafluoroborate was synthesized following general procedure for imine methylation on a 3.15 mmol scale using 7'-methoxy-1'-(trifluoromethyl)-3'H-spiro[cyclopropane-1,4'-isoquinoline], as the respective imine, to give 0.81 g of an off white solid (2.27 mmol, 72% yield).

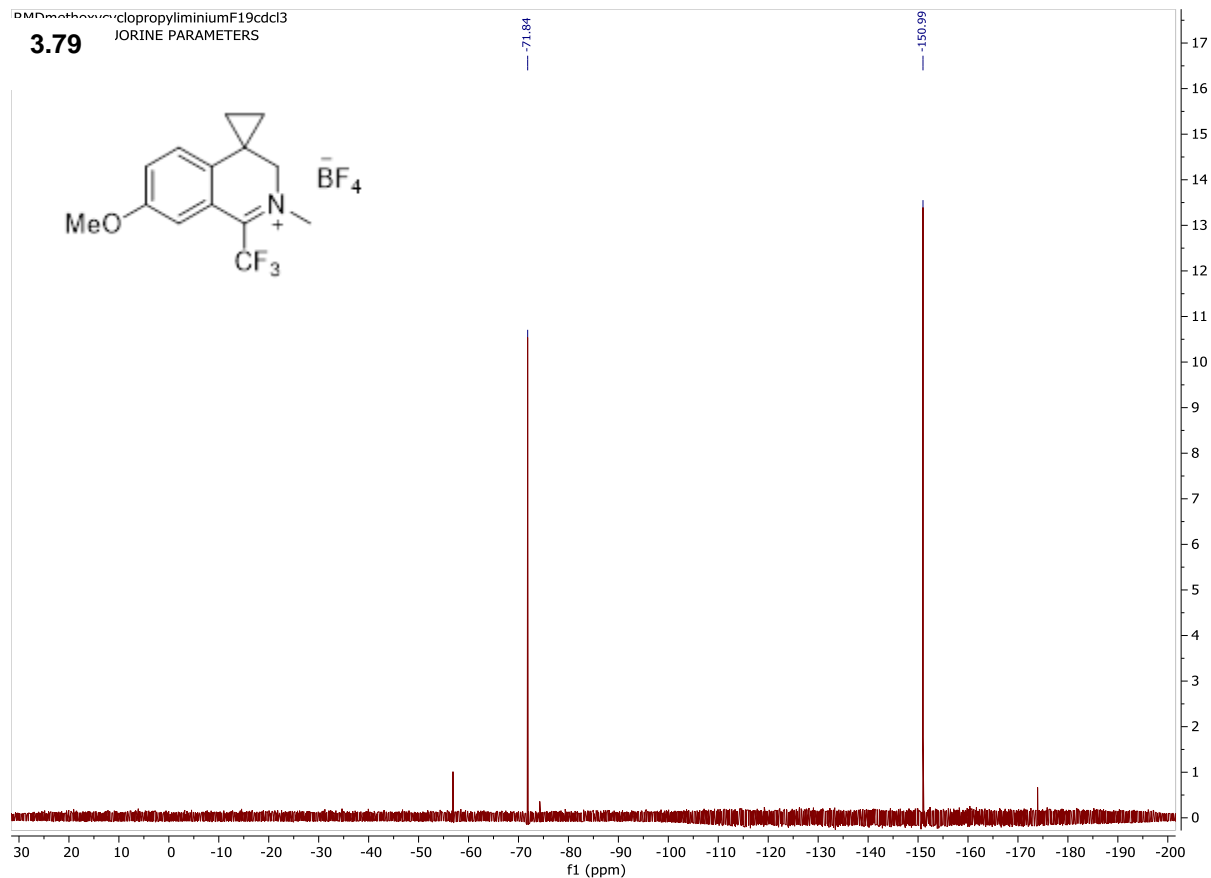
$^1\text{H NMR}$ (600 MHz, CDCl_3) δ 7.36 – 7.32 (m, 2H), 7.07 – 7.03 (m, 1H), 4.27 (H_b , s, 2H), 4.13 (H_c , d, $J = 2.7$ Hz, 3H), 3.86 (H_a , s, 3H), 1.40 – 1.36 (m, 2H), 1.24 – 1.20 (m, 2H) ppm.

$^{13}\text{C NMR}$ (201 MHz, CDCl_3) δ 159.0, 135.4, 133.6, 132.2, 119.6, 116.6, 60.6, 55.7, 35.2, 22.2, 14.5 ppm.

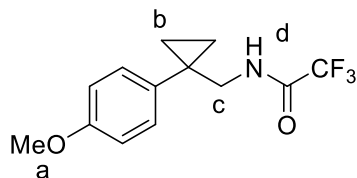
$^{19}\text{F NMR}$ (564 MHz, CDCl_3) δ -71.84, -150.99 ppm.

HRMS Calc'd for $\text{C}_{14}\text{H}_{15}\text{F}_3\text{NO}$ (M) 270.1100 Found: 270.1099





2,2,2-trifluoro-N-((1-(4-methoxyphenyl)cyclopropyl)methyl)acetamide (3.81)



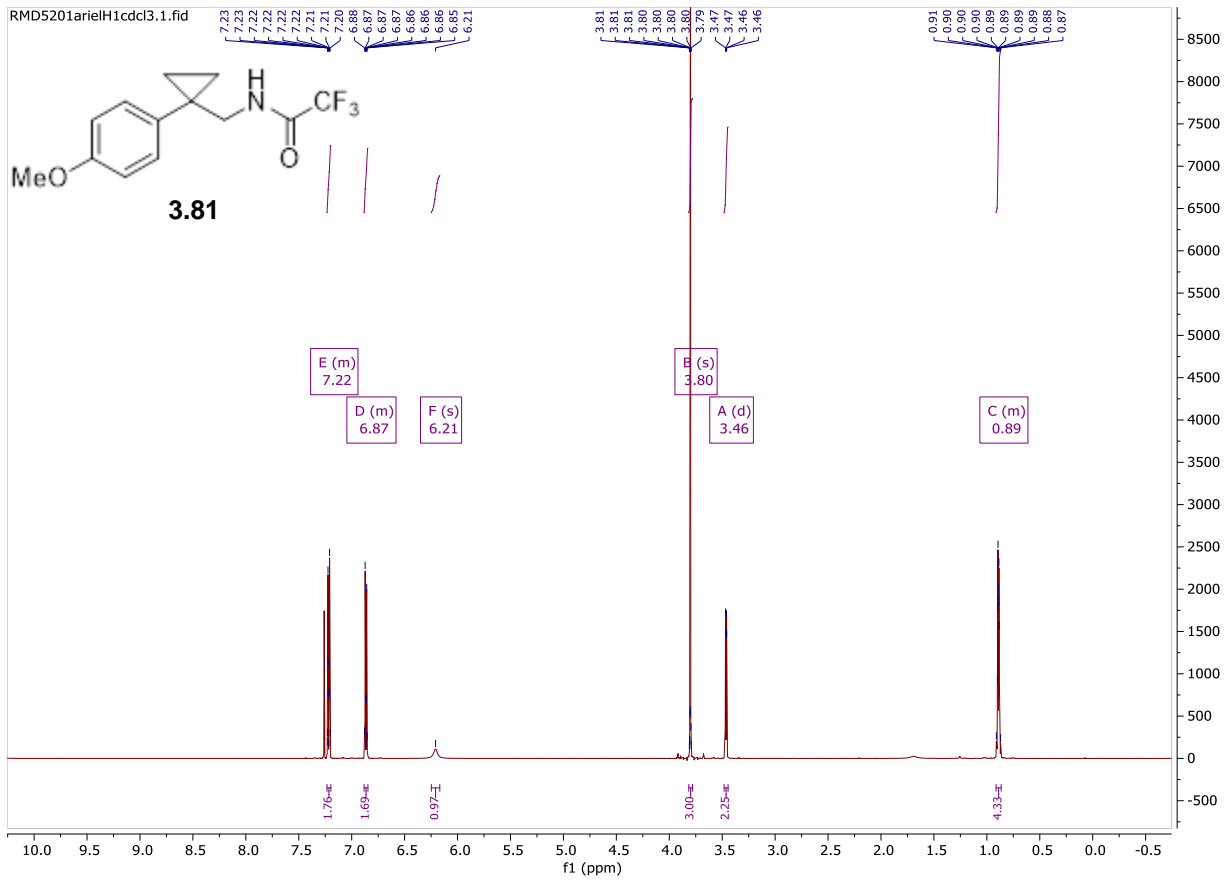
2,2,2-trifluoro-N-((1-(4-methoxyphenyl)cyclopropyl)methyl)acetamide was synthesized following the general procedure for acetamide formation on a 24.82 mmol scale using (1-(4-methoxyphenyl)cyclopropyl)methanamine, as the respective amine. The compound was purified using silica gel chromatography with a gradient column of 5% ethyl acetate/hexanes to 10% ethyl acetate/hexane to give 5.97 g of a white solid (21.8 mmol, 88% yield).

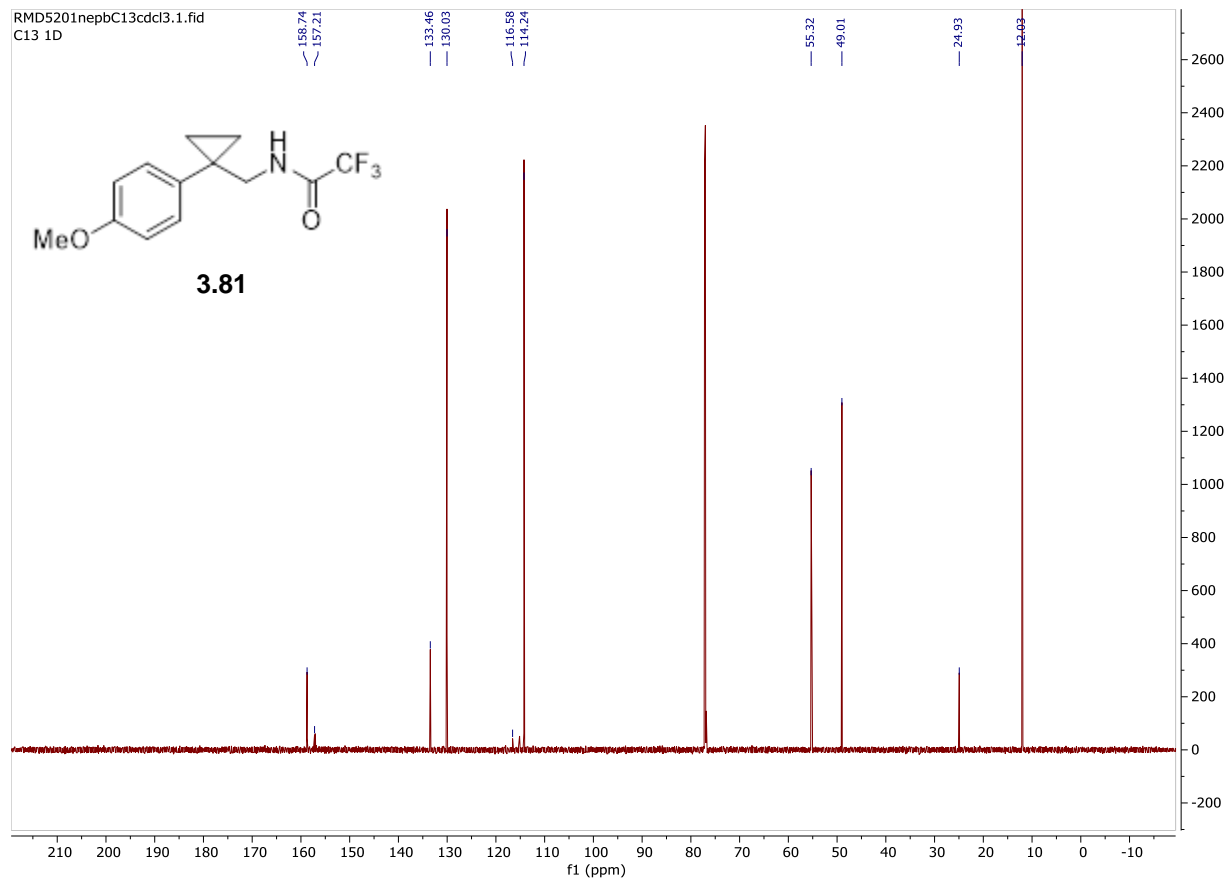
¹H NMR (600 MHz, CDCl₃) δ 7.23 – 7.20 (m, 2H), 6.88 – 6.85 (m, 2H), 6.21 (H_d, s, 1H), 3.80 (H_a, s, 3H), 3.48 – 3.44 (H_c, d, *J* = 6.5 Hz, 2H), 0.91 – 0.86 (H_b, m, 4H) ppm.

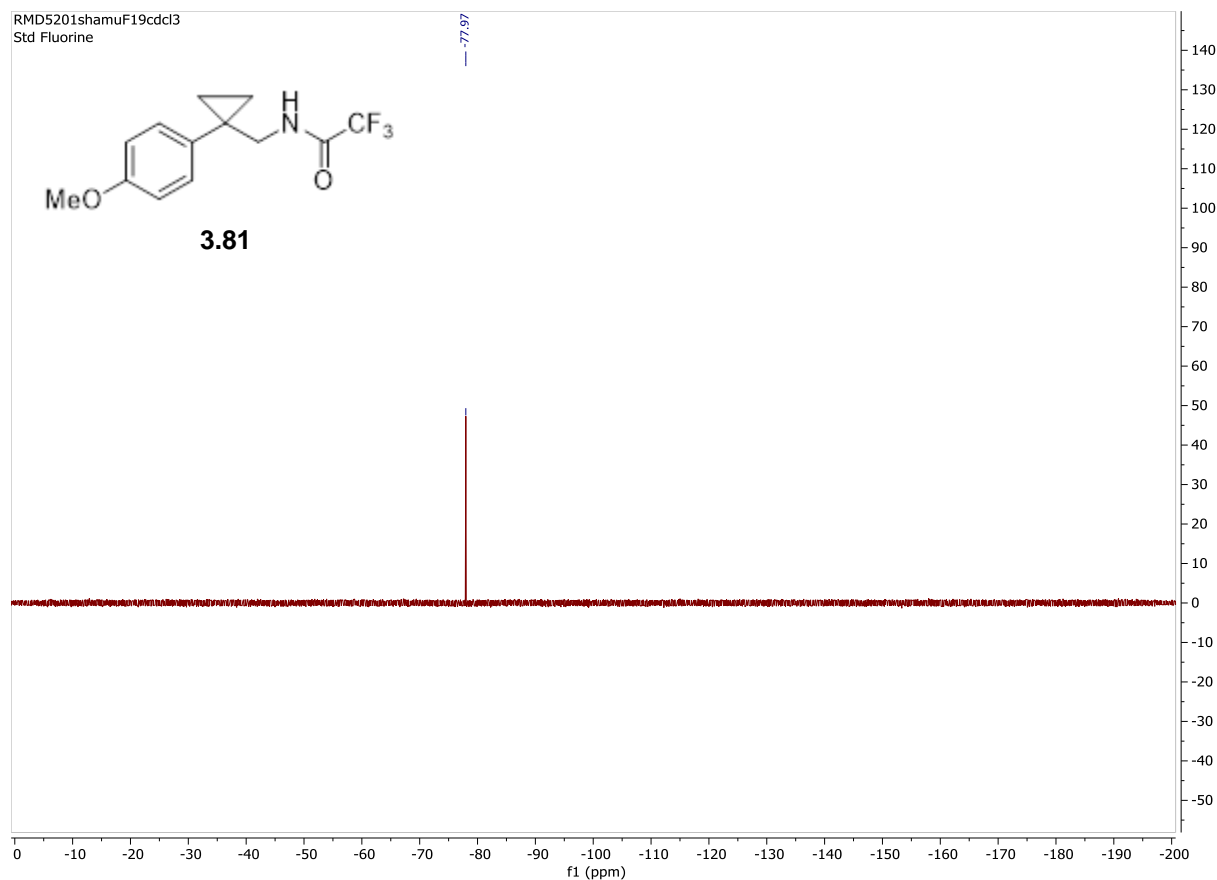
¹³C NMR (201 MHz, CDCl₃) δ 158.7, 157.2, 133.4, 130.0, 116.5, 114.2, 55.3, 49.0, 24.3, 12.0 ppm.

¹⁹F NMR (564 MHz, CDCl₃) δ -77.97 ppm.

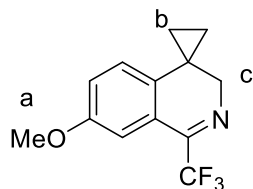
HRMS Calc'd for C₁₃H₁₄F₃NO₂ (M+Na): 296.0874 Found: 296.0907







7'-methoxy-1'-(trifluoromethyl)-3'H-spiro[cyclopropane-1,4'-isoquinoline] (3.82)



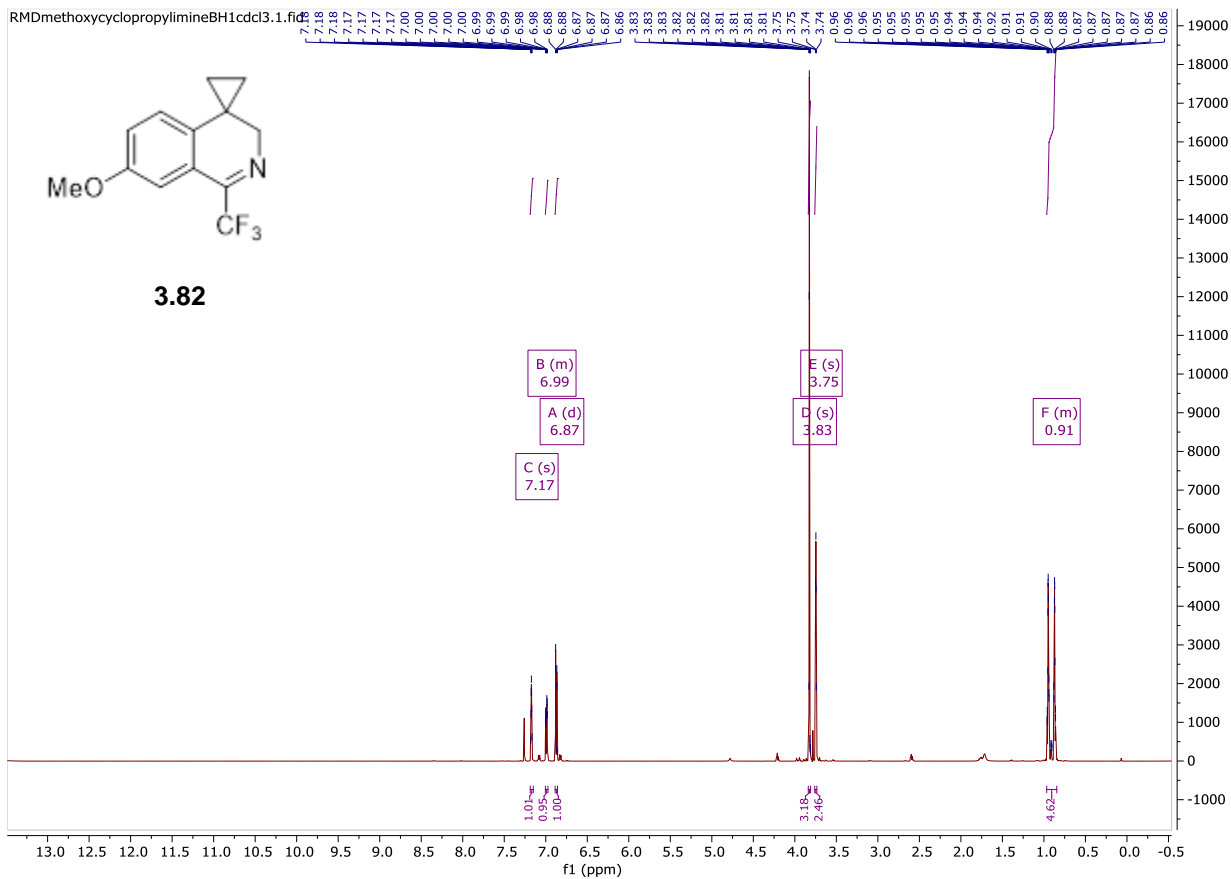
7'-methoxy-1'-(trifluoromethyl)-3'H-spiro[cyclopropane-1,4'-isoquinoline] was synthesized following general procedure A for the Bischler Napieralski reaction on a 21.85 mmol scale using 2,2,2-trifluoro-N-((1-(4-methoxyphenyl)cyclopropyl)methyl)acetamide, as the respective acetamide. The compound was purified using silica gel chromatography with a gradient column from 2% to 10% ethyl acetate/hexane to give 0.806 g of a yellow oil. (3.16 mmol, 14% yield).

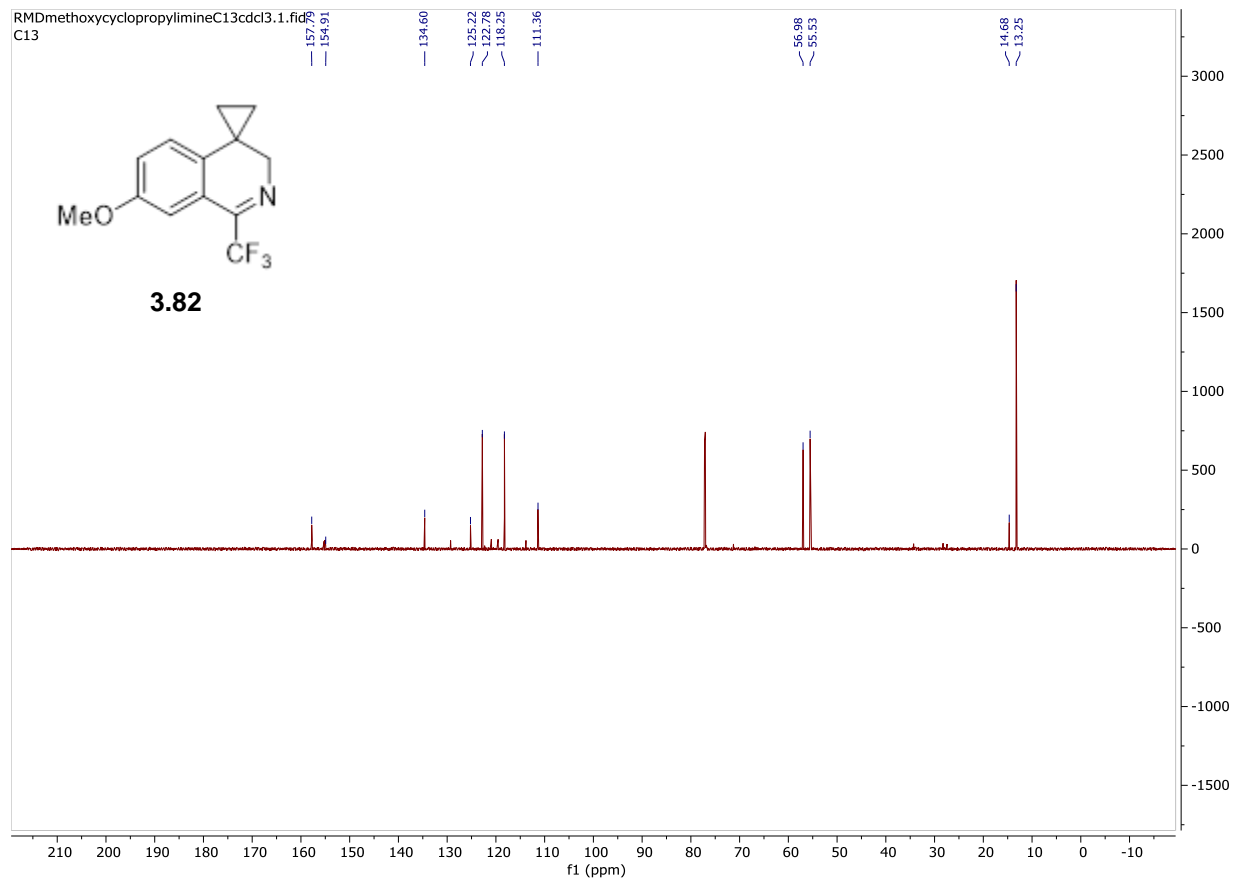
$^1\text{H NMR}$ (600 MHz, CDCl_3) δ 7.17 (s, 1H), 7.00 – 6.97 (m, 1H), 6.87 (d, $J = 8.5$ Hz, 1H), 3.83 (H_a , s, 3H), 3.75 (H_c , s, 2H), 0.97 – 0.85 (H_b , m, 4H) ppm.

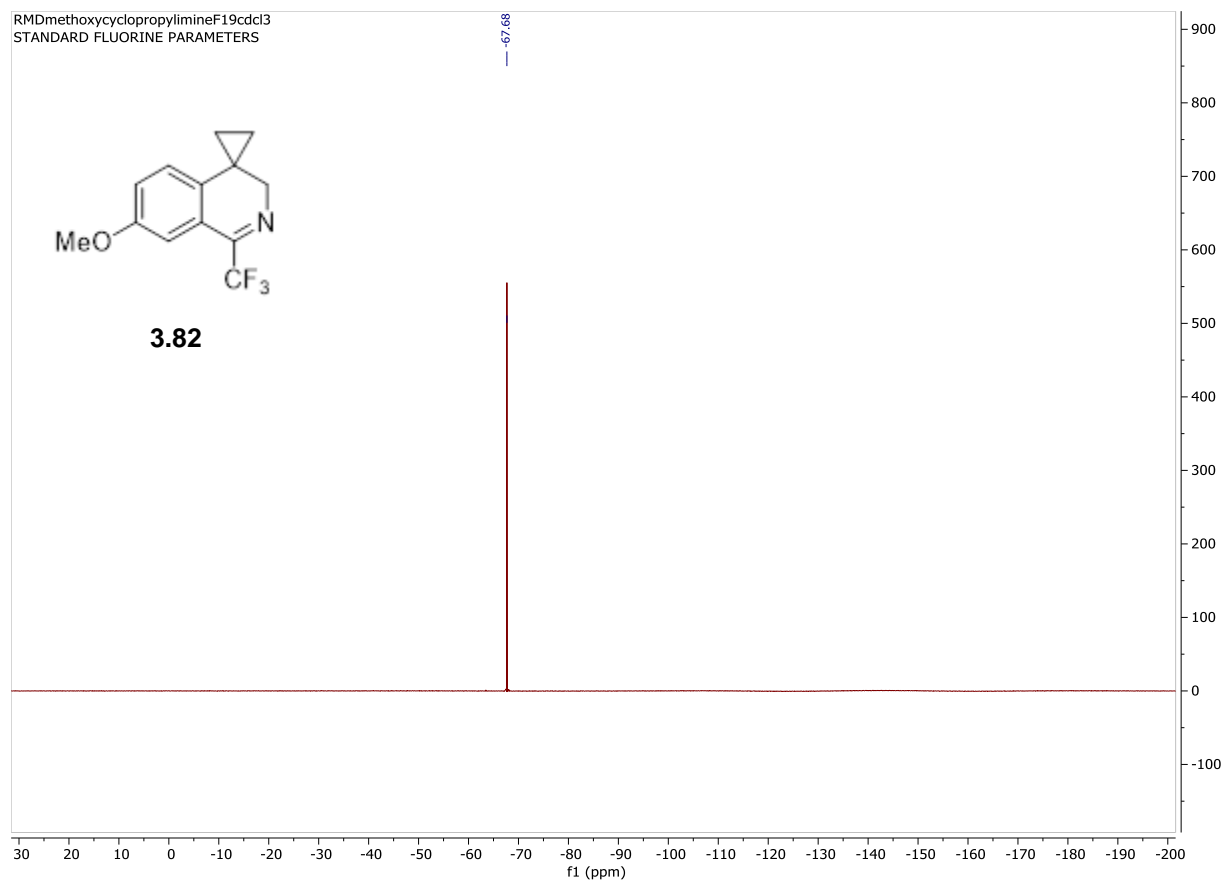
$^{13}\text{C NMR}$ (201 MHz, CDCl_3) δ 157.7, 154.9, 134.6, 125.2, 122.7, 118.2, 111.3, 56.9, 55.5, 14.6, 13.2 ppm.

$^{19}\text{F NMR}$ (564 MHz, CDCl_3) δ -67.68 ppm.

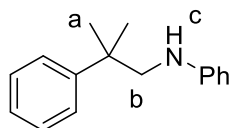
HRMS Calc'd for $\text{C}_{13}\text{H}_{12}\text{F}_3\text{NO}$ (M+H): 256.0950 Found: 256.0953







N-(2-methyl-2-phenylpropyl)aniline (3.87)



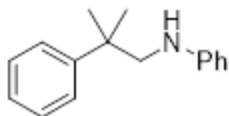
N-(2-methyl-2-phenylpropyl)aniline was synthesized following the general procedure for aniline formation on a 4 mmol scale using 2-methyl-2-phenylpropan-1-amine, as the respective amine. The reaction mixture was purified using silica gel flash chromatography with 10% ethyl acetate/hexanes to give 0.134 g of product (1.20 mmol, 30% yield).

¹H NMR (600 MHz, CDCl₃) δ 7.41 (dq, *J* = 7.3, 1.1 Hz, 2H), 7.38 – 7.34 (m, 2H), 7.24 (ddt, *J* = 7.5, 6.7, 1.2 Hz, 1H), 7.16 – 7.12 (m, 2H), 6.66 (tdt, *J* = 7.3, 2.0, 1.1 Hz, 1H), 6.56 – 6.53 (m, 2H), 3.31 (H_c, s, 1H), 3.29 (H_b, s, 2H), 1.43 (H_a, s, 6H) ppm.

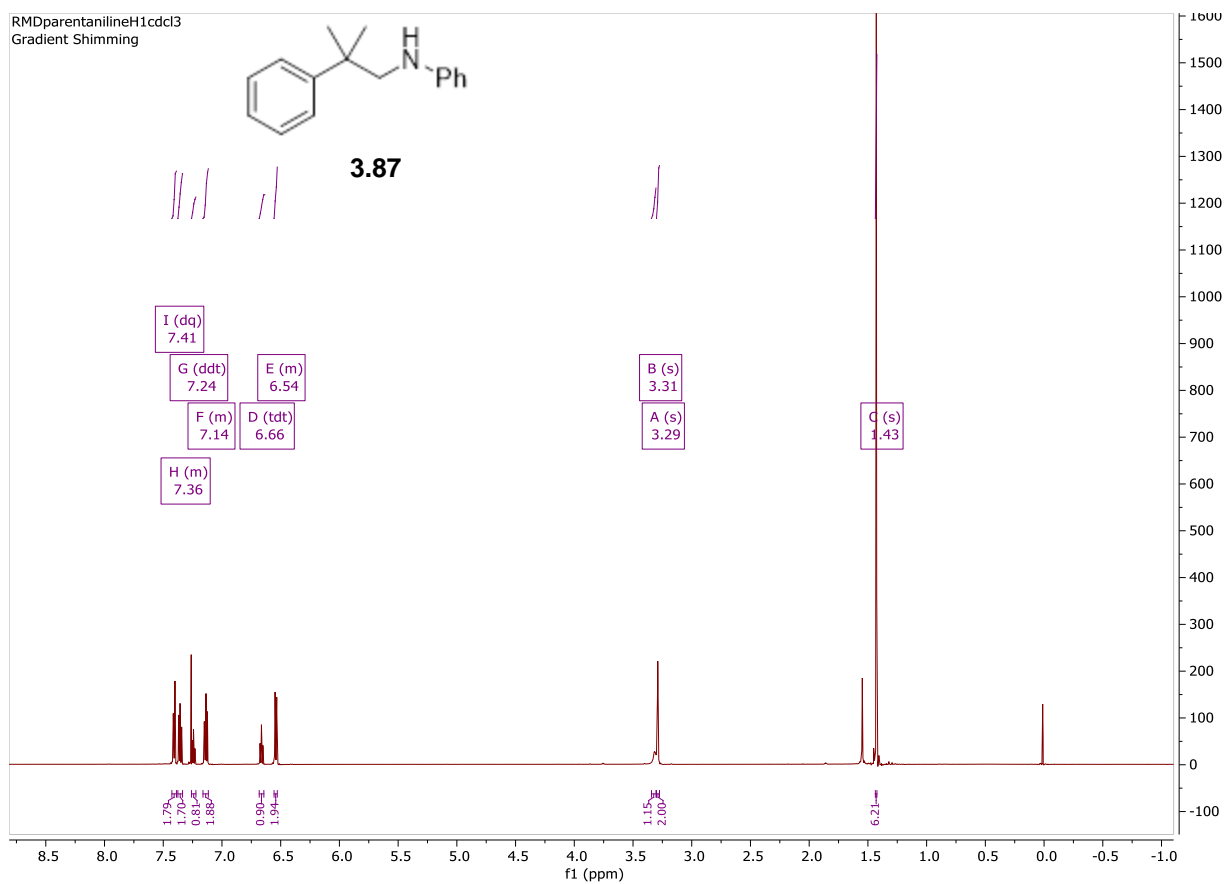
¹³C NMR (201 MHz, CDCl₃) δ 148.80, 146.86, 129.12, 128.47, 126.17, 126.04, 117.14, 112.81, 55.84, 38.96, 27.35 ppm.

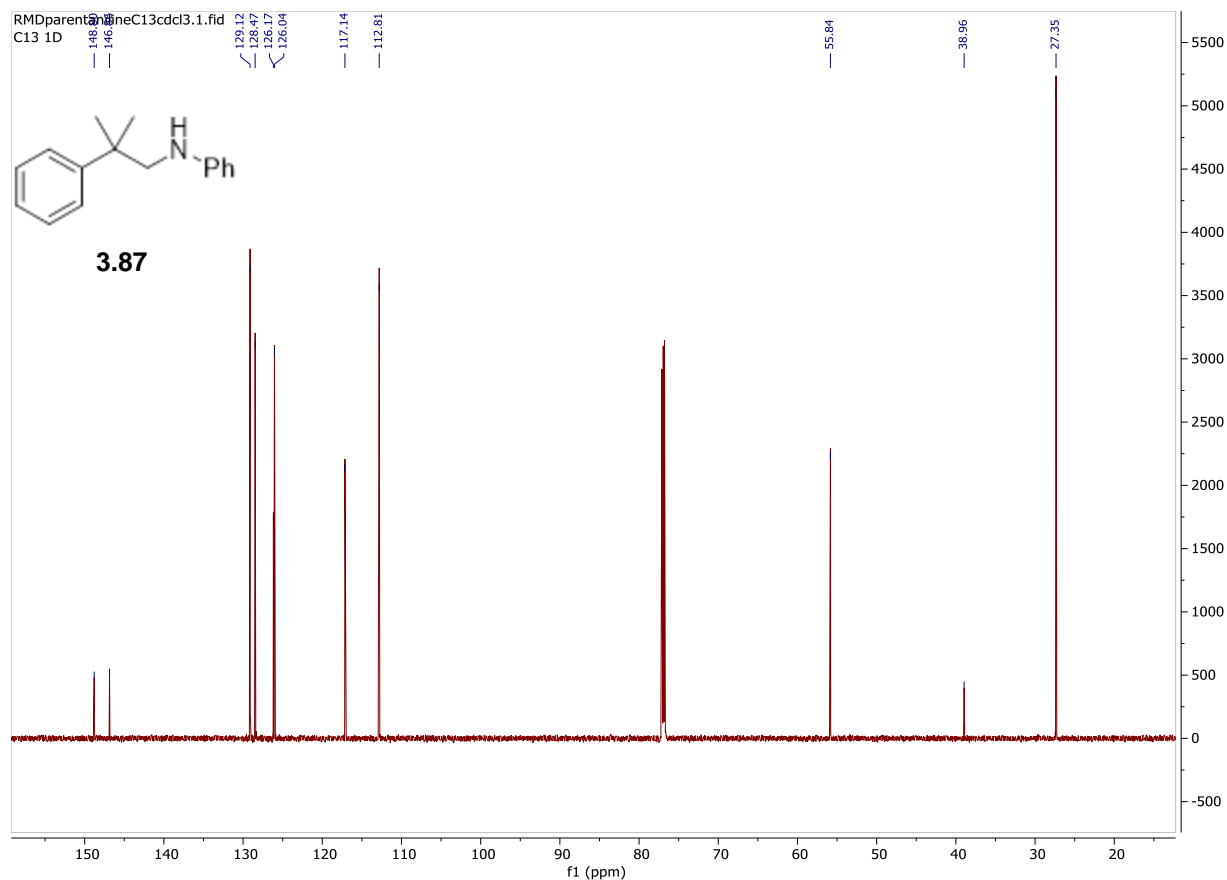
HRMS Calc'd for C₁₆H₁₉N (M+H): 226.1596 Found: 226.1600

RMDparentanilineH1.cdc13
Gradient Shimming

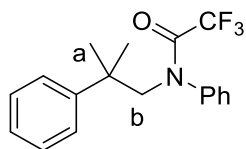


3.87





2,2,2-trifluoro-N-(2-methyl-2-phenylpropyl)-N-phenylacetamide (3.88)



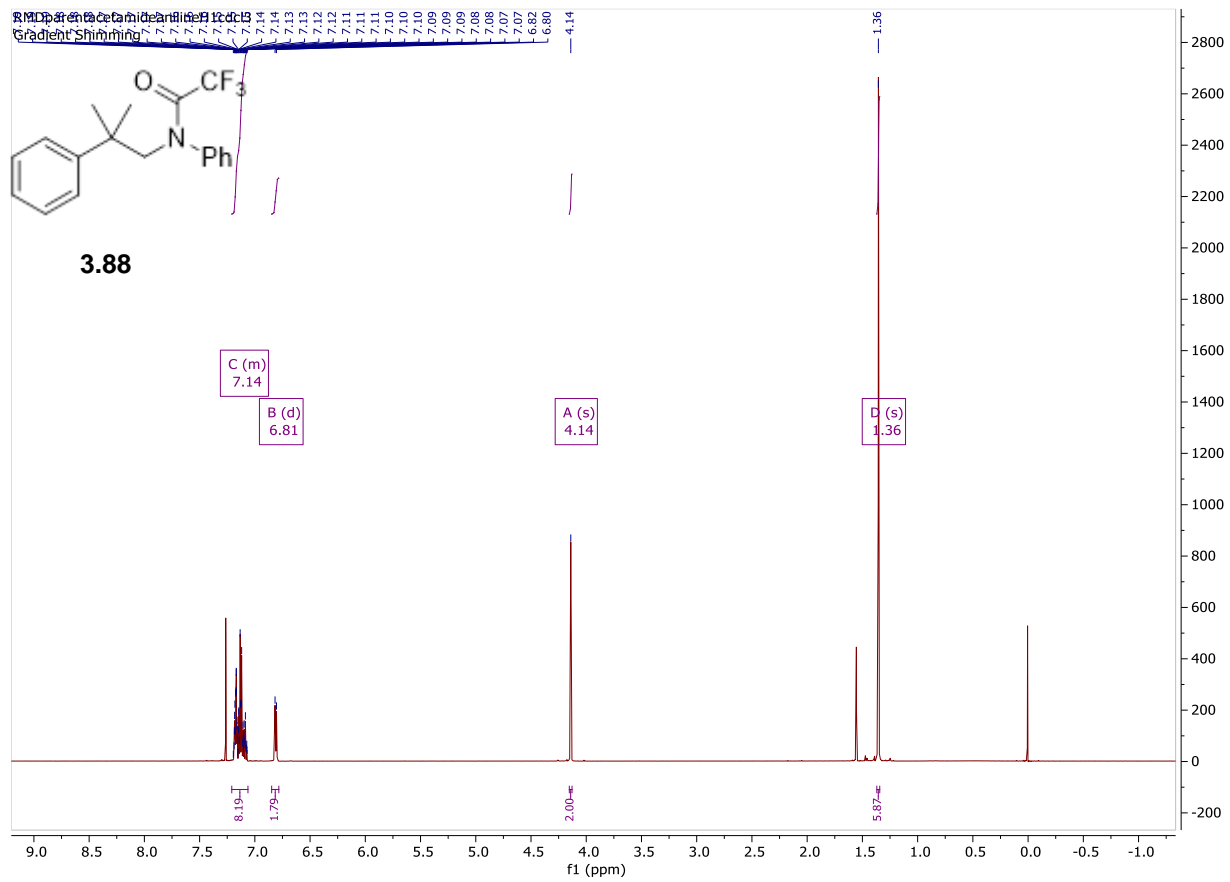
2,2,2-trifluoro-N-(2-methyl-2-phenylpropyl)-N-phenylacetamide was synthesized following the general procedure for acetamide formation on a .6 mmol scale using N-(2-methyl-2-phenylpropyl)aniline, as the respective aniline. The compound was purified using silica gel chromatography with 10% ethyl acetate/hexane to give 0.164 g of an off-white solid (0.510 mmol, 85% yield).

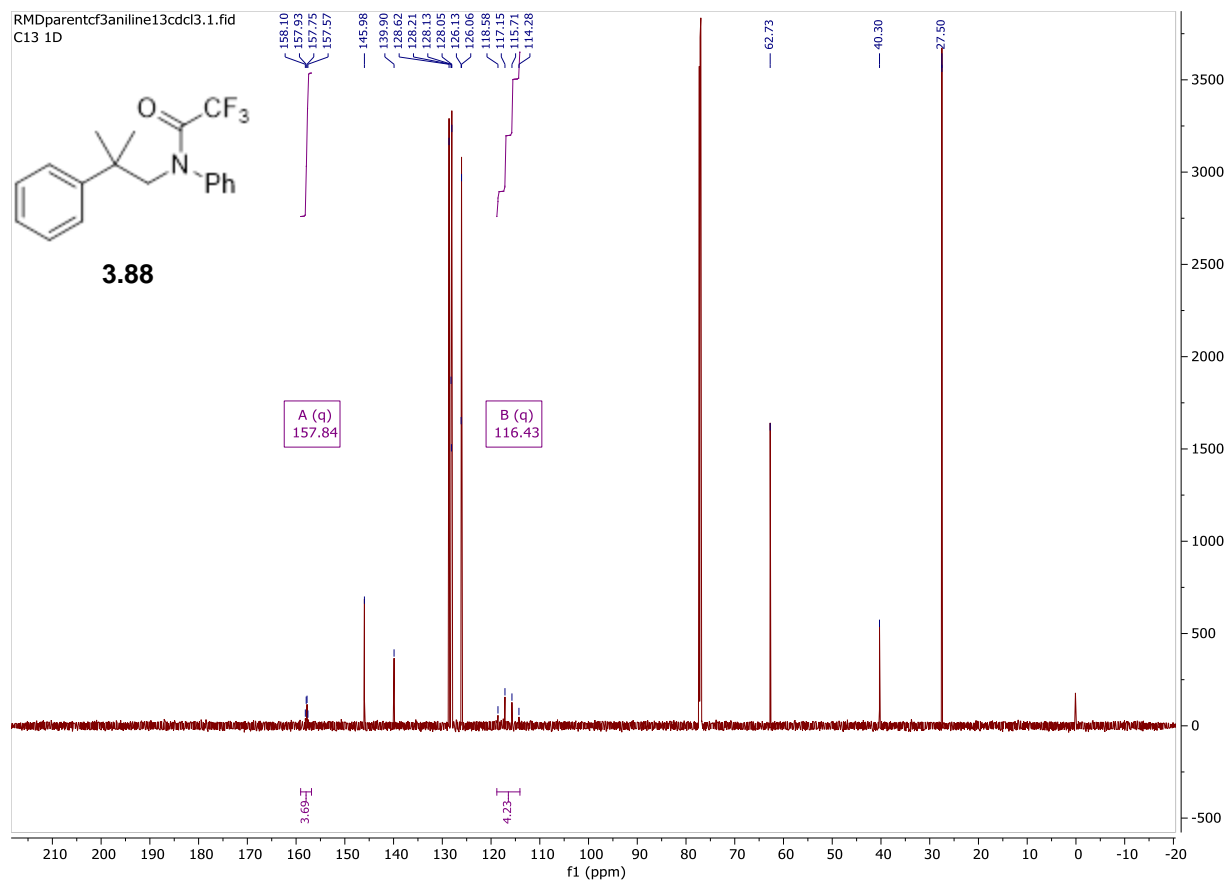
$^1\text{H NMR}$ (600 MHz, CDCl_3) δ 7.21 – 7.06 (m, 8H), 6.81 (d, $J = 7.7$ Hz, 2H), 4.14 (H_b , s, 2H), 1.36 (H_a , s, 6H) ppm.

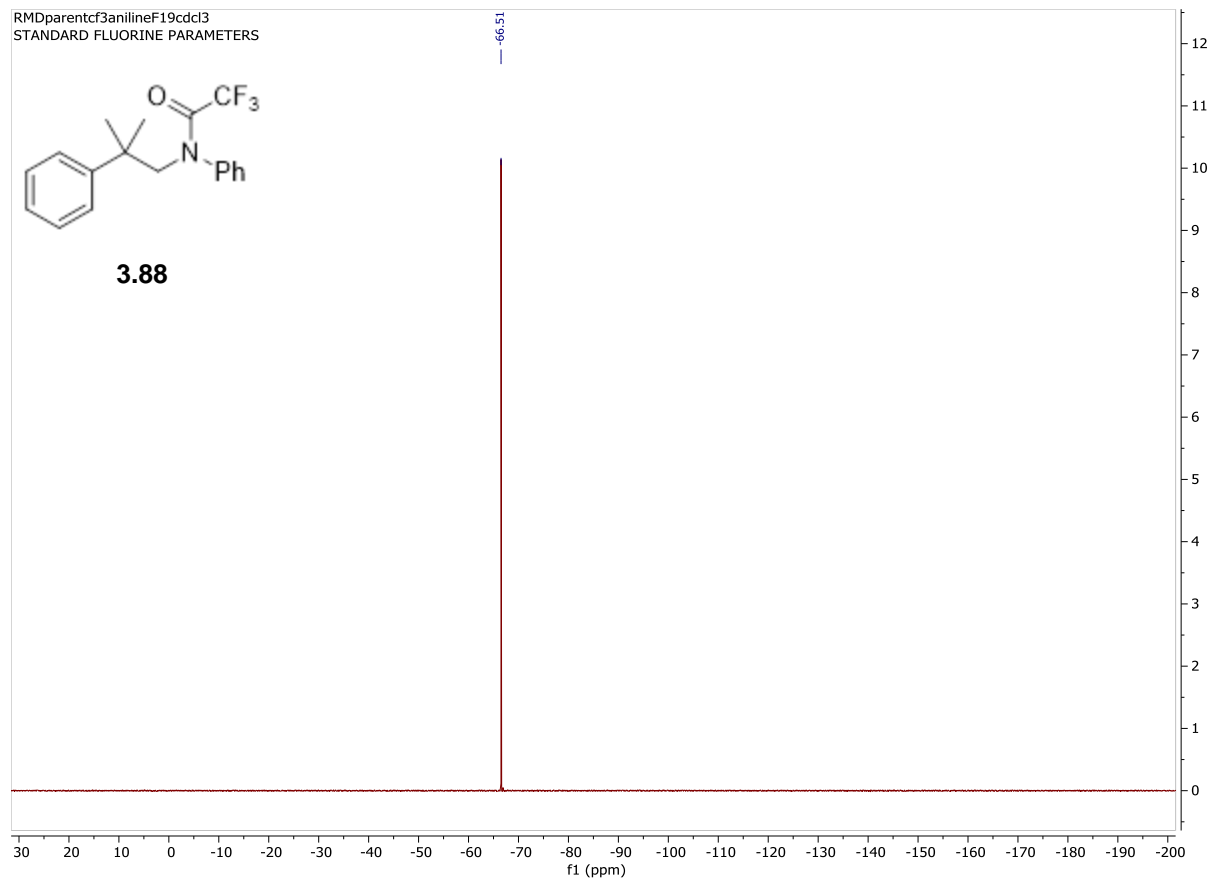
$^{13}\text{C NMR}$ (201 MHz, CDCl_3) δ 157.84 (q, $J = 35.5$ Hz), 146.0, 139.9, 128.6, 128.2, 128.1, 128.0, 126.1, 126.1, 116.4 (q, $J = 288.5$ Hz), 62.7, 40.3, 27.5 ppm.

$^{19}\text{F NMR}$ (564 MHz, CDCl_3) δ -66.51 ppm.

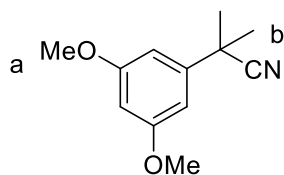
HRMS Calc $\text{C}_{18}\text{H}_{18}\text{F}_3\text{NO}$ for ($\text{M}+\text{Na}$):344.1238 Found: 344.1246







2-(3,5-dimethoxyphenyl)-2-methylpropanenitrile (3.91)



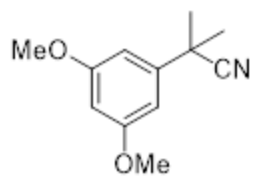
2-(3,5-dimethoxyphenyl)-2-methylpropanenitrile was synthesized following the general procedure for benzylic alkylation on a 30 mmol scale using 2-(3,5-dimethoxyphenyl)acetonitrile as the respective nitrile. The compound was purified using silica gel chromatography with a gradient of 5% to 10% ethyl acetate/hexane to give 6.14 g of a clear oil. (30.0 mmol, 100% yield)

¹H NMR (600 MHz, CDCl₃) δ 6.61 (d, *J* = 2.2 Hz, 2H), 6.40 (t, *J* = 2.2 Hz, 1H), 3.82 (H_a, s, 6H), 1.71 (H_b, s, 6H) ppm.

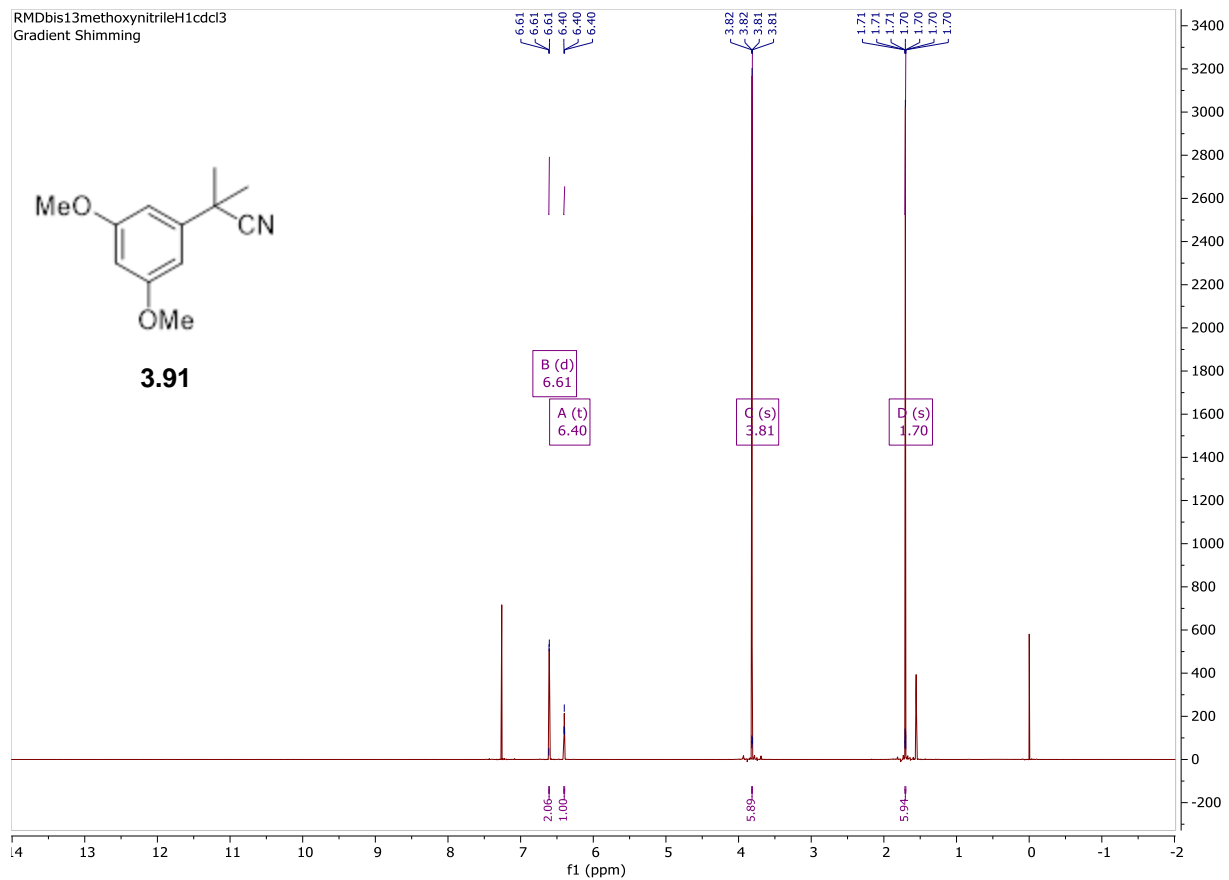
¹³C NMR (201 MHz, CDCl₃) δ 161.26, 143.93, 124.32, 103.79, 99.39, 55.40, 37.33, 29.07 ppm.

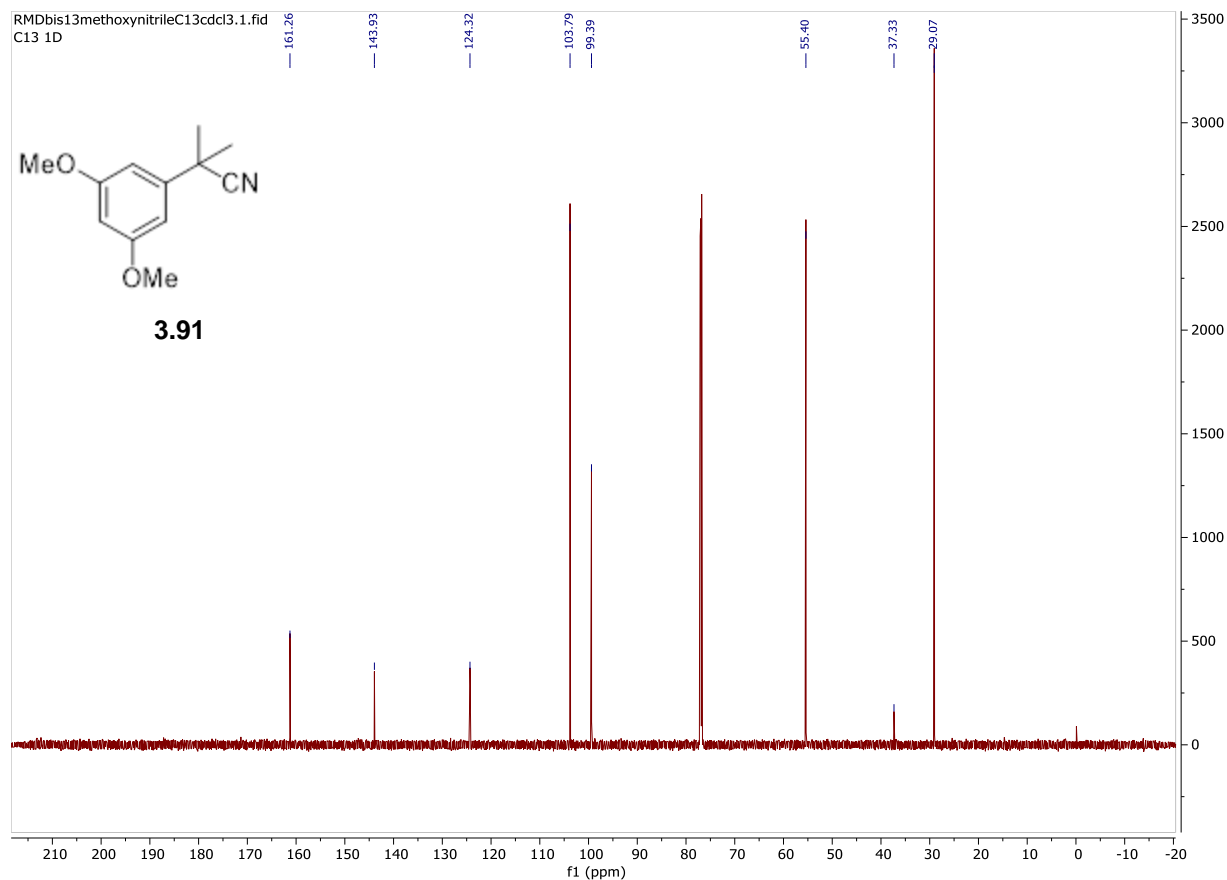
HRMS Calc'd for C₁₂H₁₅NO₂ (M+Na): 252.0612 Found: 252.0689

RMDbis13methoxynitrileH1cdcl3
Gradient Shimming

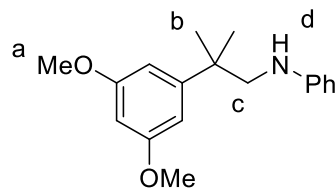


3.91





N-(2-(3,5-dimethoxyphenyl)-2-methylpropyl) aniline (3.93)

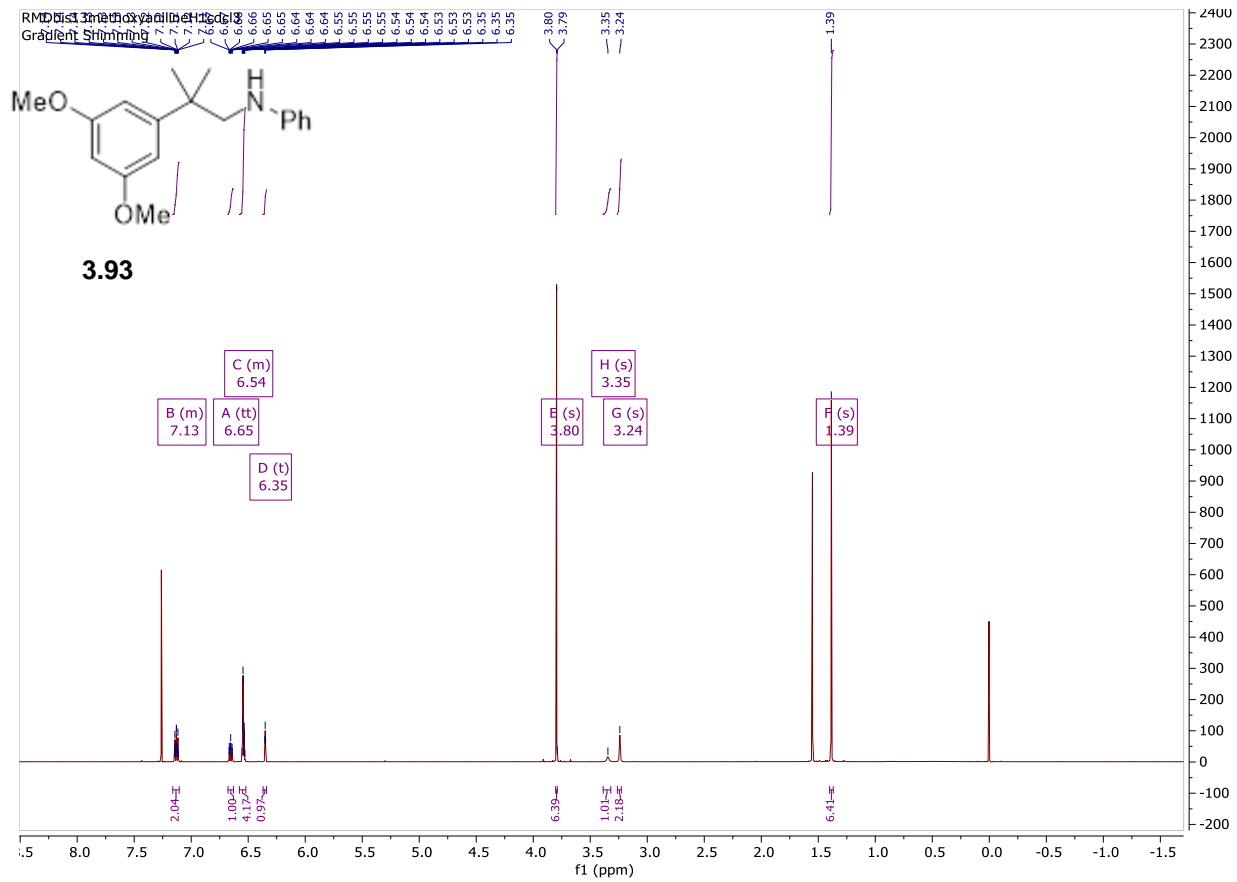


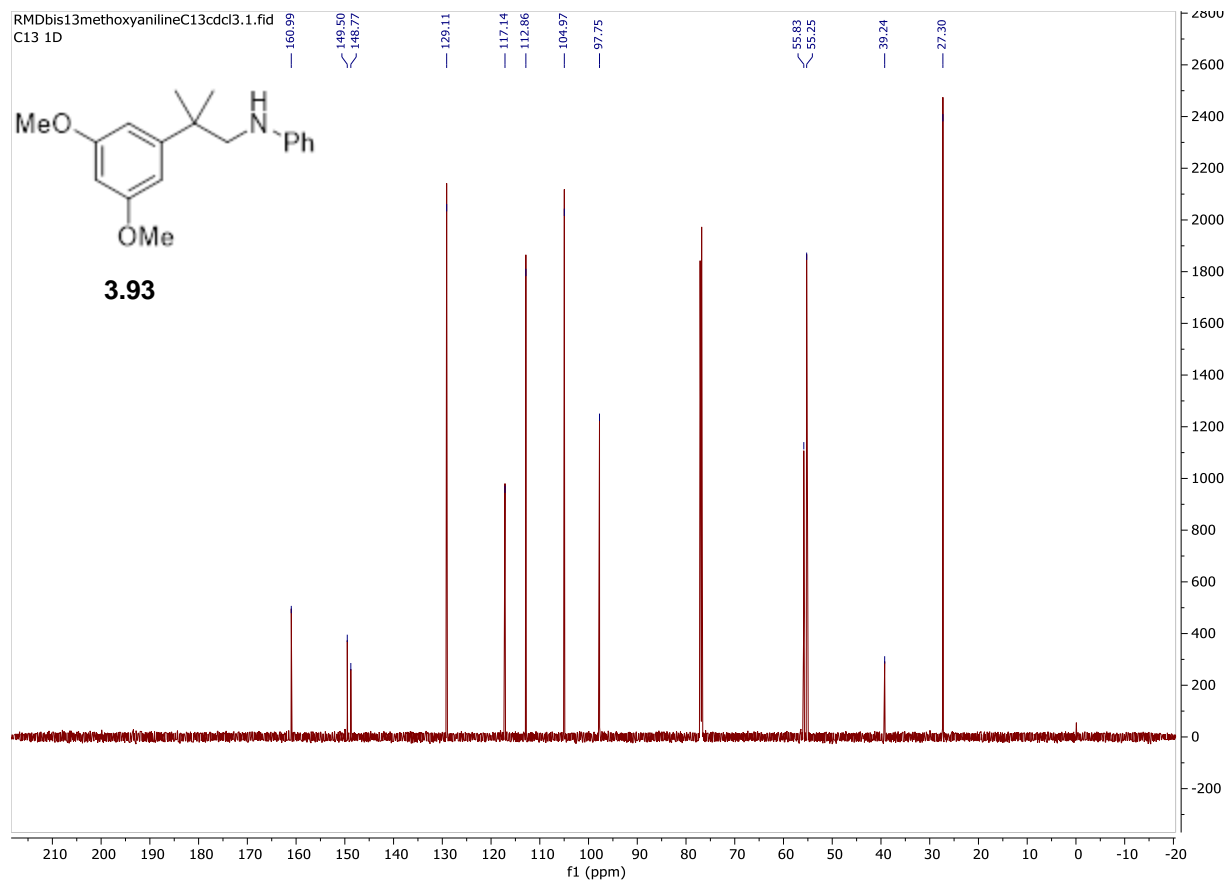
N-(2-(3,5-dimethoxyphenyl)-2-methylpropyl) aniline was synthesized following the general procedure for aniline formation on an 8 mmol scale using 2-(3,5-dimethoxyphenyl)-2-methylpropan-1-amine as the respective amine. The reaction mixture was purified using silica gel flash chromatography with 5% ethyl acetate/hexanes to give 1.17 g of product (5.60 mmol, 70% yield).

¹H NMR (600 MHz, CDCl₃) δ 7.16 – 7.11 (m, 2H), 6.65 (tt, *J* = 7.3, 1.1 Hz, 1H), 6.58 – 6.52 (m, 4H), 6.35 (t, *J* = 2.2 Hz, 1H), 3.80 (H_a, s, 6H), 3.35 (H_d, s, 1H), 3.24 (H_c, s, 2H), 1.39 (H_b, s, 6H) ppm.

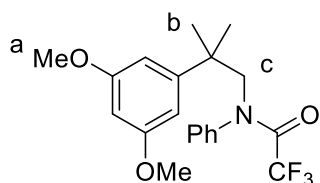
¹³C NMR (201 MHz, CDCl₃) δ 160.99, 149.50, 148.77, 129.11, 117.14, 112.86, 104.97, 97.75, 55.83, 55.25, 39.24, 27.30 ppm.

HRMS Calc'd for C₁₈H₂₃NO₂ (M+Na): 308.1626 Found: 308.1639





N-(2-(3,5-dimethoxyphenyl)-2-methylpropyl)-2,2,2-trifluoro-N-phenylacetamide (3.94)



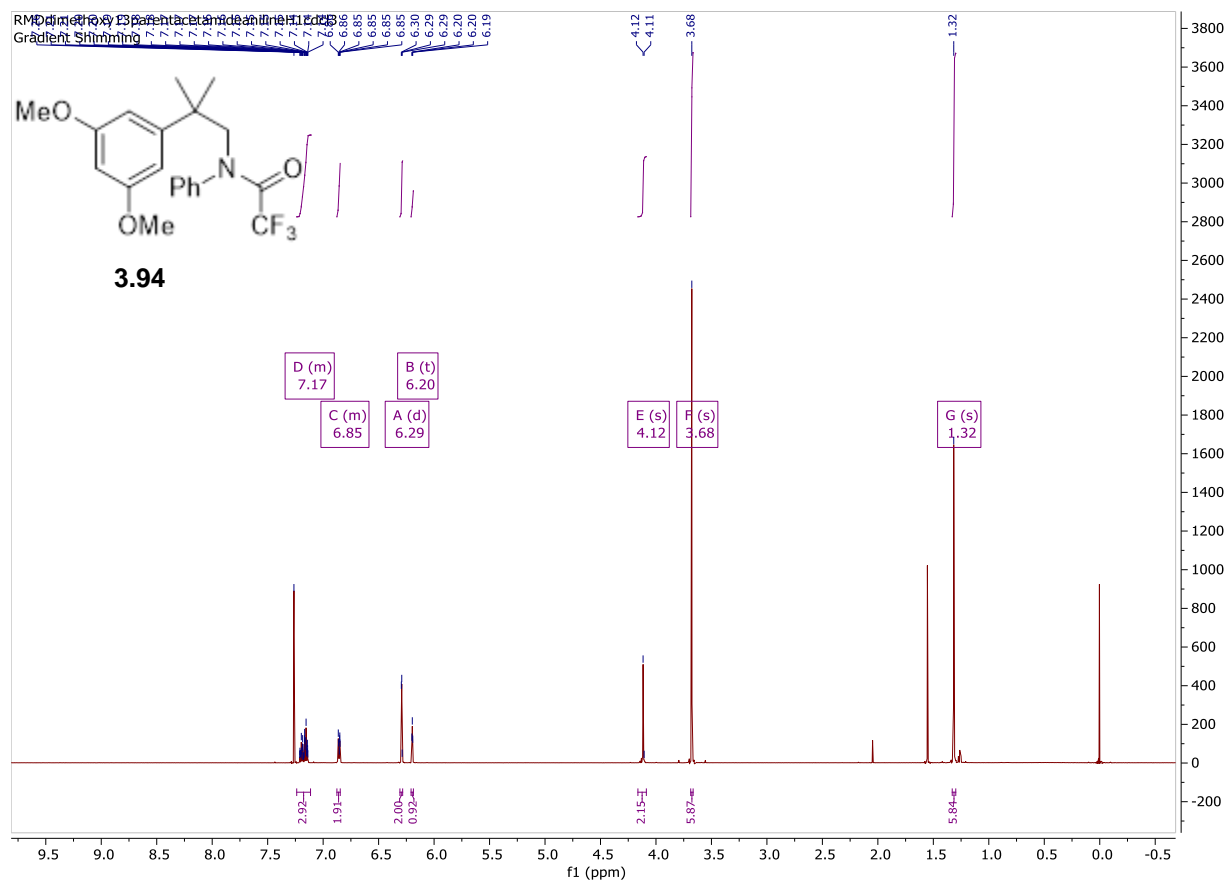
N-(2-(3,5-dimethoxyphenyl)-2-methylpropyl)-2,2,2-trifluoro-N-phenylacetamide was synthesized following the general procedure for acetamide formation on a 1.4 mmol scale using N-(2-(3,5-dimethoxyphenyl)-2-methylpropyl) aniline as the respective amine. The compound was purified using silica gel chromatography with 20% ethyl acetate/hexane to give 0.549 g of an off-white solid (1.37 mmol, 98% yield).

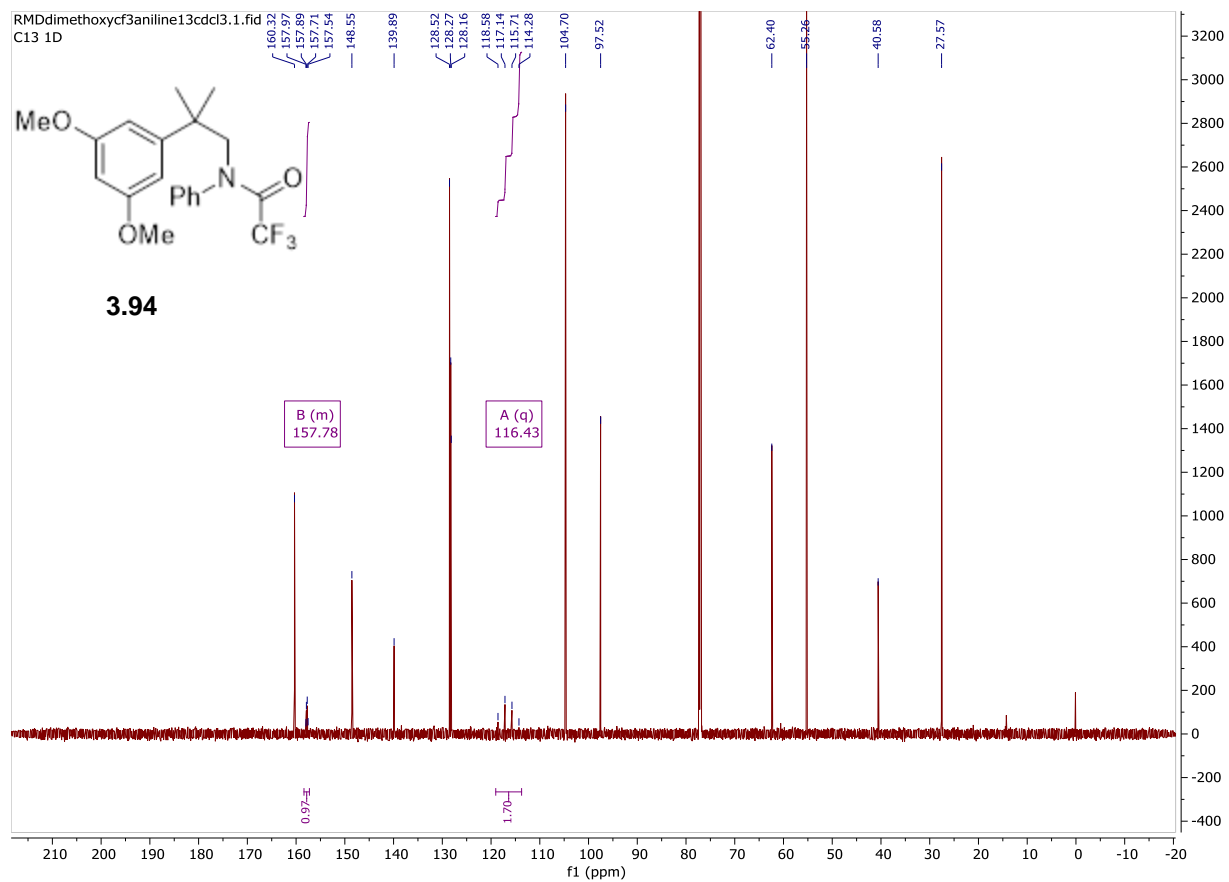
¹H NMR (600 MHz, CDCl₃) δ 7.24 – 7.11 (m, 3H), 6.88 – 6.85 (m, 2H), 6.29 (d, *J* = 2.2 Hz, 2H), 6.20 (t, *J* = 2.2 Hz, 1H), 4.12 (H_c, s, 2H), 3.68 (H_a, s, 6H), 1.32 (H_b, s, 6H) ppm.

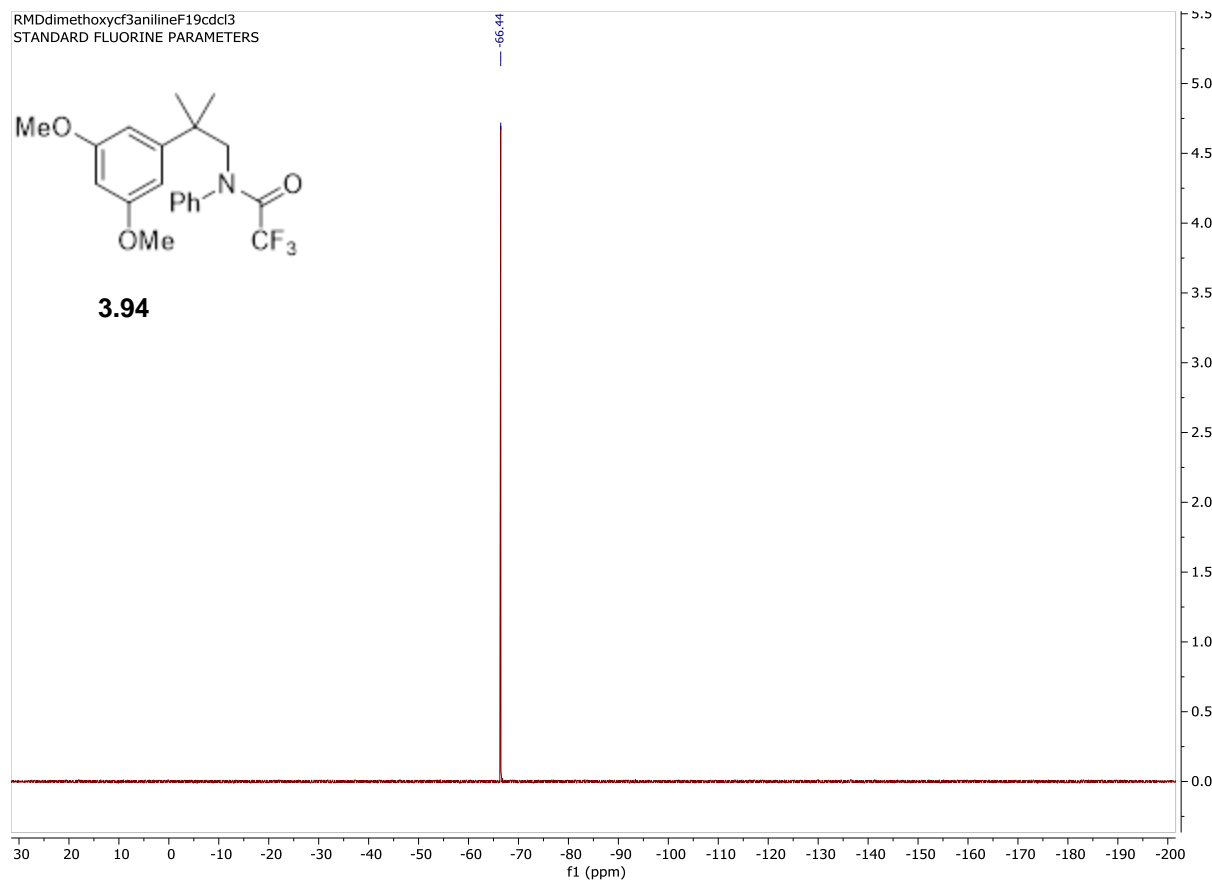
¹³C NMR (201 MHz, CDCl₃) δ 160.32, δ 158.38 – 157.27 (m), 148.55, 139.89, 128.52, 128.27, 128.16, 116.43 (q, *J* = 288.4 Hz), 104.70, 97.52, 62.40, 55.26, 40.58, 27.57 ppm.

¹⁹F NMR (564 MHz, CDCl₃) δ -66.44 ppm.

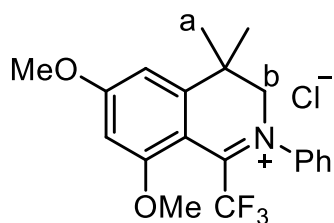
HRMS Calc for C₂₀H₂₂F₃NO₃ (M+Na) 404.1449 Found 404.1466







7'-methoxy-1'-(trifluoromethyl)-3'H-spiro[cyclopropane-1,4'-isoquinoline] (3.95)



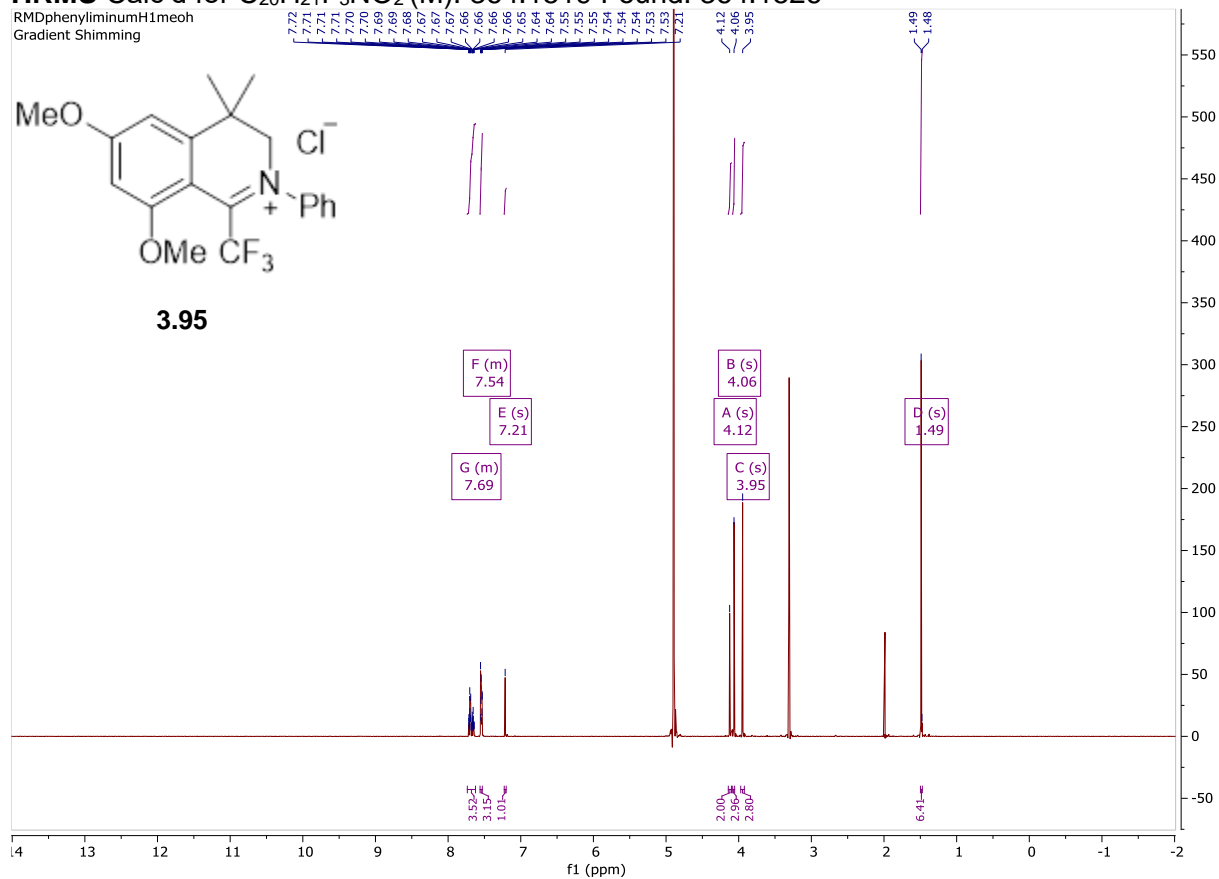
6,8-dimethoxy-4,4-dimethyl-2-phenyl-1-(trifluoromethyl)-3,4-dihydroisoquinolin-2-ium chloride was synthesized following general procedure C for the Bischler Napieralski reaction on a 1.42 mmol scale using N-(2-(3,5-dimethoxyphenyl)-2-methylpropyl)-2,2,2-trifluoro-N-phenylacetamide as the acetamide and a bright yellow oil was collected.

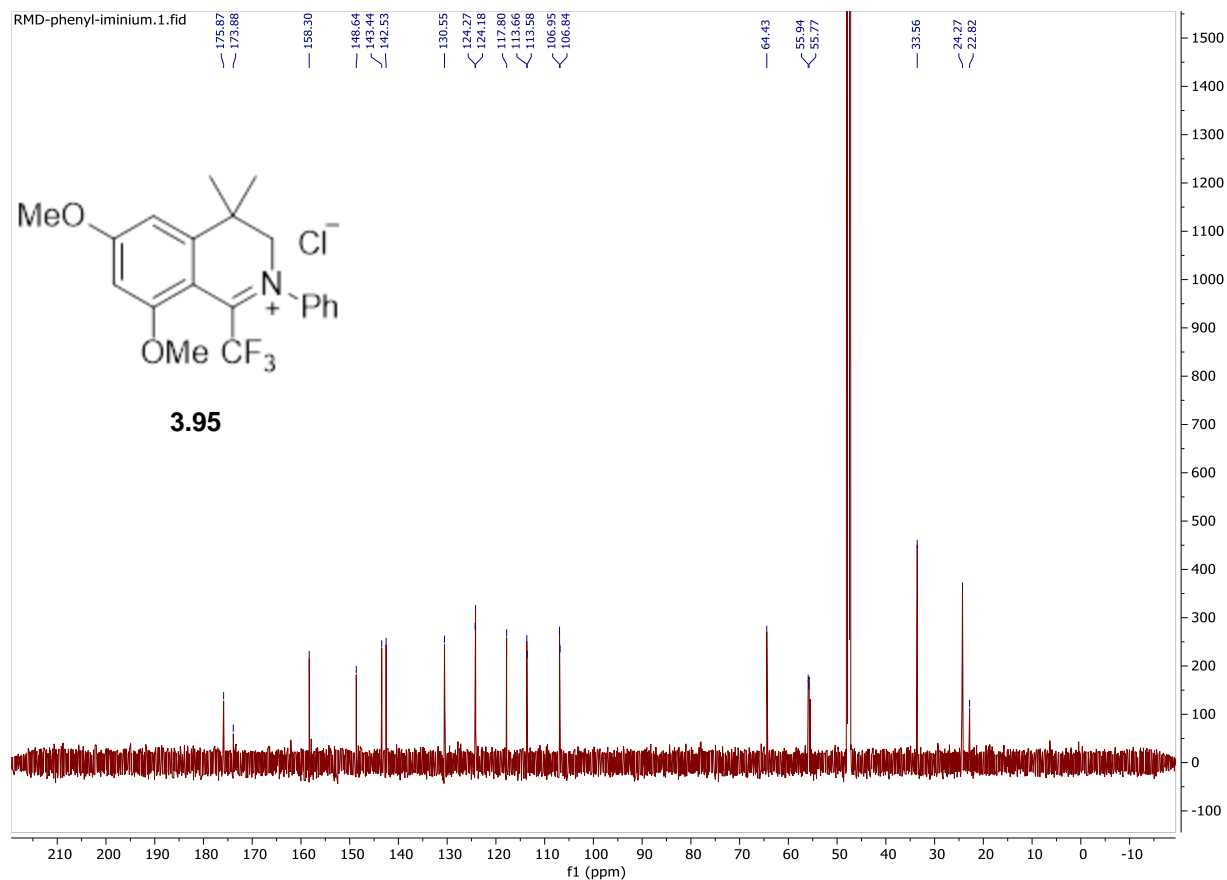
¹H NMR (600 MHz, MeOD) δ 7.74 – 7.62 (m, 3H), 7.56 – 7.53 (m, 3H), 7.21 (s, 1H), 4.12 (H_b, s, 2H), 4.06 (s, 3H), 3.95 (s, 3H), 1.49 (H_a, s, 6H) ppm.

¹³C NMR (201 MHz, MeOD) δ 175.87, 173.88, 158.30, 148.64, 143.44, 142.53, 130.55, 124.27, 124.18, 117.80, 113.66, 113.58, 106.95, 106.84, 64.43, 55.94, 55.77, 33.56, 24.27, 22.82 ppm.

HRMS Calc'd for C₂₀H₂₁F₃NO₂ (M): 364.1519 Found: 364.1526

RMDphenyliminiumH1meoh
Gradient Shimming





2.6 References.

- ¹ Buckley, B. R.; Christie, S. D.; Elsegood, M. R.; Gillings; C. M., Page; P. C. B.; Pardoe, W. J. An aromatic amination approach towards Ancistrocladinium A/B. *Synlett*, **2010**, *6*, 939-943.
- ² Seupel, R.; Hertlein-Amslinger, B.; Gulder, T.; Stawski, P.; Kaiser, M.; Brun, R.; Bringmann, G. Directed synthesis of all four pure stereoisomers of the N, C-coupled naphthylisoquinoline alkaloid ancistrocladinium A. *Org. Lett.*, **2016**, *18* (24), 6508-6522.
- ³ Wang, D.; Shuler, W. G.; Pierce, C. J.; Hilinski, M. K. An iminium salt organocatalyst for selective aliphatic C–H hydroxylation. *Org. Lett.*, **2016**, *18* (15), 3826-3829.

Appendix Three

Chapter Four Supporting Information

3.1 General Information

All reagents were obtained commercially in the highest available purity and used without further purification. Anhydrous solvents were obtained from an aluminum oxide solvent purification system. Flash column chromatography was performed using silica gel or alumina gel (230 - 400 mesh) purchased from Fisher Scientific. Elution of compounds was monitored by UV. ^1H and ^{13}C NMR spectra were measured on a Varian Inova 600 (600 MHz) or Bruker Avance DRX 600 (600 MHz) or Bruker Avance III 800 (800 MHz) spectrometer and acquired at 300 K. Chemical shifts are reported in parts per million (ppm δ) referenced to the residual ^1H or ^{13}C resonance of the solvent. The following abbreviations are used singularly or in combination to indicate the multiplicity of signals: s - singlet, d - doublet, t - triplet, q - quartet, m - multiplet and br - broad. High-resolution mass spectrometry was obtained using an Agilent Q-TOF ESI spectrometer

3.2 General Procedures

Sulfamate Synthesis General Procedure

Formic acid (1.5 equiv) was added dropwise very slowly to neat ClSO_2NCO (1.5 equiv) at 0 °C in a flame dried round bottom flask. Gas evolution was observed and a needle was added to vent excess pressure. Be careful of septum popping off. To the solid mass was then added CH_3CN (1.3M), and the resulting solution was stirred for 1 h at 0 °C and 8 h at 25 °C. The reaction was cooled to 0 °C and a solution of the respective alcohol (1.0 equiv) in DMA (1.3M) was added dropwise via cannula. After stirring for 8 h at 25 °C, the solution was diluted with ethyl acetate and water. The biphasic solution was separated and the aqueous layer was extracted (3x). The combined organic layers were washed 5x with water to remove any excess DMA. The organic layer was dried over MgSO_4 , filtered, and concentrated under reduced pressure. Purification of the oily residue by chromatography on silica gel or crystallization in ethyl acetate afforded the desired product as a white solid.

Iodinane Synthesis General Procedure

In a flame-dried 100 mL round bottom flask under nitrogen was added, the sulfamate (1.0 equiv), (the oxidized iodoarene (1.0 equiv) and anhydrous methanol (0.25M). The contents were stirred to dissolve most of the oxidized iodoarene and then cooled to 0 °C in an ice water bath. Once cooled, potassium hydroxide (2.5 equiv) was added. The reaction was stirred for 30 minutes at 0 °C and then 7.5 hours at room temperature. Upon reaction completion, the contents were transferred to a separatory funnel containing water (1M). Dichloromethane (1M) was added and the contents vigorously shaken to remove all excess potassium hydroxide. The layers were separated and the aqueous layer was further extracted with dichloromethane (2x volume). The combined organic extracts were washed with water (1x volume), shaking vigorously to remove any trace potassium hydroxide, and transferred directly to a round bottom flask and the solvent removed by rotary evaporation at room temperature (do not exceed 30 °C as the iminoiodinane will degrade) to give a solid. The contents were transferred to a smaller round bottom flask using methanol and the solvent was removed by rotary evaporation leaving a solid. The contents were azeotroped once with benzene (.25M) and placed under vacuum for an additional 20 minutes to give a solid. The solid was rinsed with diethyl ether (5 x 10 mL) while

breaking up any solid chunks. The solid was filtered and collected and put on vacuum. After vacuum drying for one hour an off-white powdery solid was obtained and used as is. The contents were capped with a polyethylene cap and stored in the freezer in a nitrogen environment. Adapted from Lit. Conditions.¹⁴

Alkylation of Phenol General Procedure

To a flask was added iodophenol (54.3 mmol, 1.0 eq.) and potassium carbonate (217 mmol, 4 eq.) and 100 mL acetone. To the mixture was added iodomethane (70.6 mmol, 1.3 eq.). The mixture was refluxed overnight (3 h is likely sufficient). The reaction was cooled to room temperature and the acetone was removed by vacuum. The brown paste was dissolved in water (120 mL) and extracted DCM (3 x 60 mL). The organic layer was washed with 1 M HCl (100 mL), dried with MgSO₄, filtered, and concentrated to a dark red oil. The oil was purified by chromatography (100% hexane to 5% to 10% EtOAc:Hexanes).

Iodination General Procedure

To a flask was added the phenol (200 mmol, 1.0 eq.) and p-tolylsulfonic acid (200 mmol, 1.0 eq.) and dissolved in dry acetonitrile (100 mL, 2 M). After stirring for 15 min was added N-iodosuccinimide (204 mmol, 1.02 eq.) and stirred at room temperature for 16 h. The reaction was quenched by addition of saturated Na₂S₂O₃ (20 mL), turning the dark solution into a bright yellow solid, followed by addition of 1 M HCl (20 mL), partially dissolving the solid. The acetonitrile was removed by vacuum, followed by extraction with DCM three times. The organic layer was washed once with 1 M HCl, dried with MgSO₄, filtered and concentrated to form a solid, and used without further purification.

Oxidation of Iodoarenes General Procedure

General Procedure A

To a flask was added aryl iodide (6.9 mmol, 1.0 eq.) to glacial acetic acid (70 mL, 0.11 M). After stirring for 15 min, sodium perborate tetrahydrate (69 mmol, 10 eq.) was slowly added. The mixture was heated at 55 °C overnight (at least 4 hours). The reaction was quenched with 100 mL water, and extracted 3 x 40 mL of DCM. The organic layer was dried with MgSO₄, filtered, and concentrated to produce a viscous yellow oil, and then place on high vacuum to remove remaining acetic acid. The oil was slowly precipitated upon addition of hexane and filtered and washed repeatedly with hexane to remove unreacted starting material to yield a white powder.

General Procedure B

To a flask was added aryl iodide (10 g, 34.4 mmol, 1.0 eq.) and DCM (35 mL, 1 M) and placed in an ice bath. Once stirring, the 70% meta-chloro per benzoic acid (11.9 g, 48.2 mmol, 1.4 eq.) was slowly added. After 3 hours (or, once the starting material is fully consumed based on TLC), the reaction was quenched with 100 mL water, and extracted 3 x 50 mL of DCM. The organic layer was dried with MgSO₄, filtered, and concentrated to produce a viscous yellow oil. The oil was slowly precipitated upon addition of hexane and filtered with a mixture of 10% ether:hexane to produce a light yellow powder.

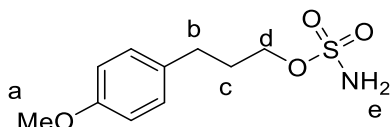
Amination General Procedure

In a nitrogen glovebox at room temperature, the substrate (1.0 equiv), iodine or other oxidant (2.0 equiv) and iminium (20 mol%) and any additional additive were combined in a vial equipped

with a stir bar. Anhydrous dichloromethane (0.1 M) was then added and the reactions mixture was either left in the glovebox and stirred at room temperature for 20 hours or removed from the glovebox, place under positive pressure of nitrogen, and stirred at room temperature for 20 hours. The reaction mixture was then filtered through a silica gel plug, eluting with EtOAc or Diethyl ether. After removal of the solvent under reduced pressure, the crude reaction mixture was then purified by flash chromatography using the conditions noted.

3.3 Compounds

3-(4-methoxyphenyl) propyl sulfamate (4.8)



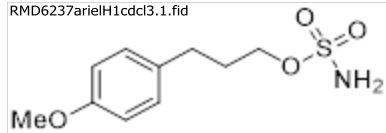
3-(4-methoxyphenyl) propyl sulfamate was synthesized following the general procedure for sulfamate synthesis on a 30 mmol scale of 3-(4-methoxyphenyl)propan-1-ol, as the respective alcohol. The reaction mixture was purified after workup using silica flash chromatography (20% to 40% to 60% EtOAc/hexanes) to give 4.60 g of white solid (18.8 mmol, 63% yield).

¹H NMR (600 MHz, CDCl₃) δ 7.13 – 7.09 (m, 2H), 6.86 – 6.83 (m, 2H), 4.66 – 4.60 (H_e,m, 2H), 4.21 (H_d,t, *J* = 6.3 Hz, 2H), 3.79 (H_a,s, 3H), 2.72 – 2.68 (H_b,m, 3H), 2.08 – 2.02 (H_c,m, 2H) ppm.

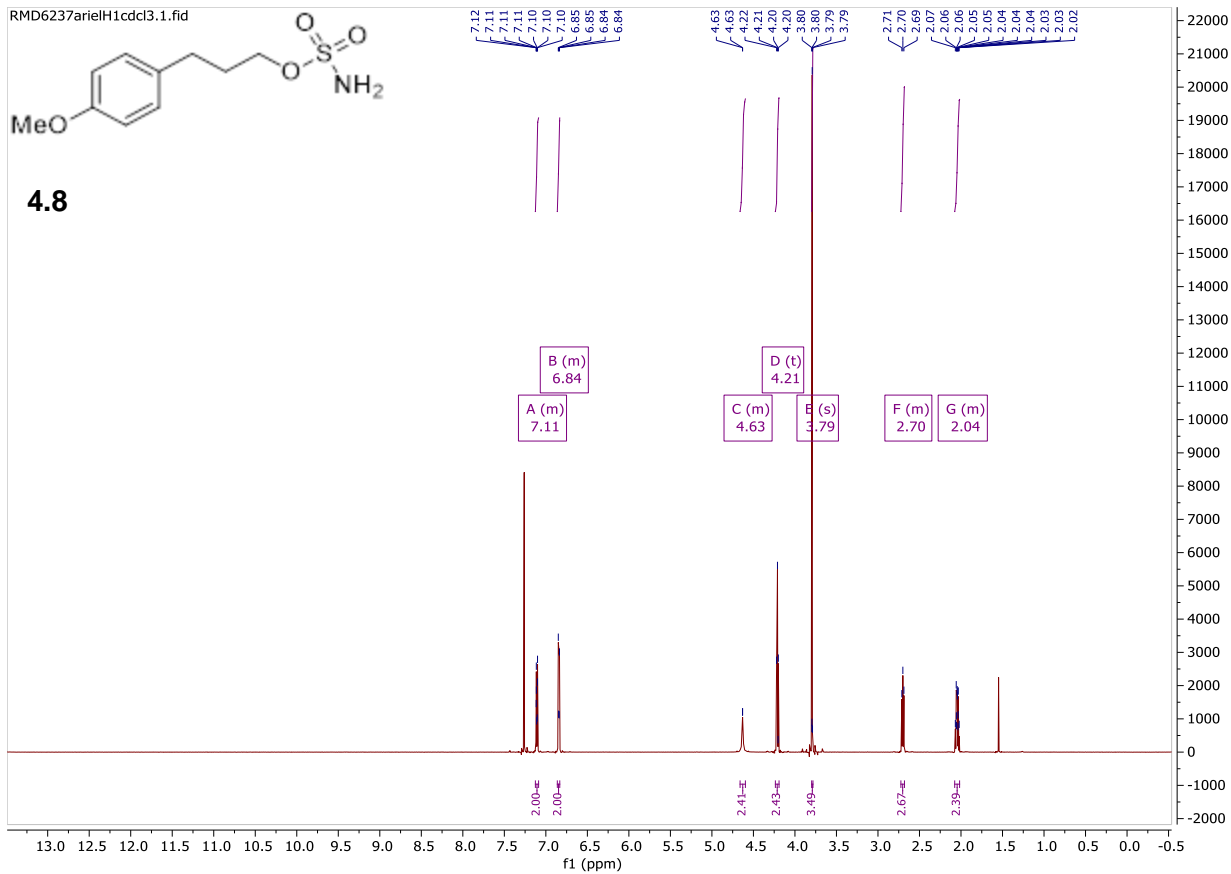
¹³C NMR (201 MHz, CDCl₃) δ 158.2, 132.5, 129.5, 114.1, 70.7, 55.4, 30.7, 30.6 ppm.

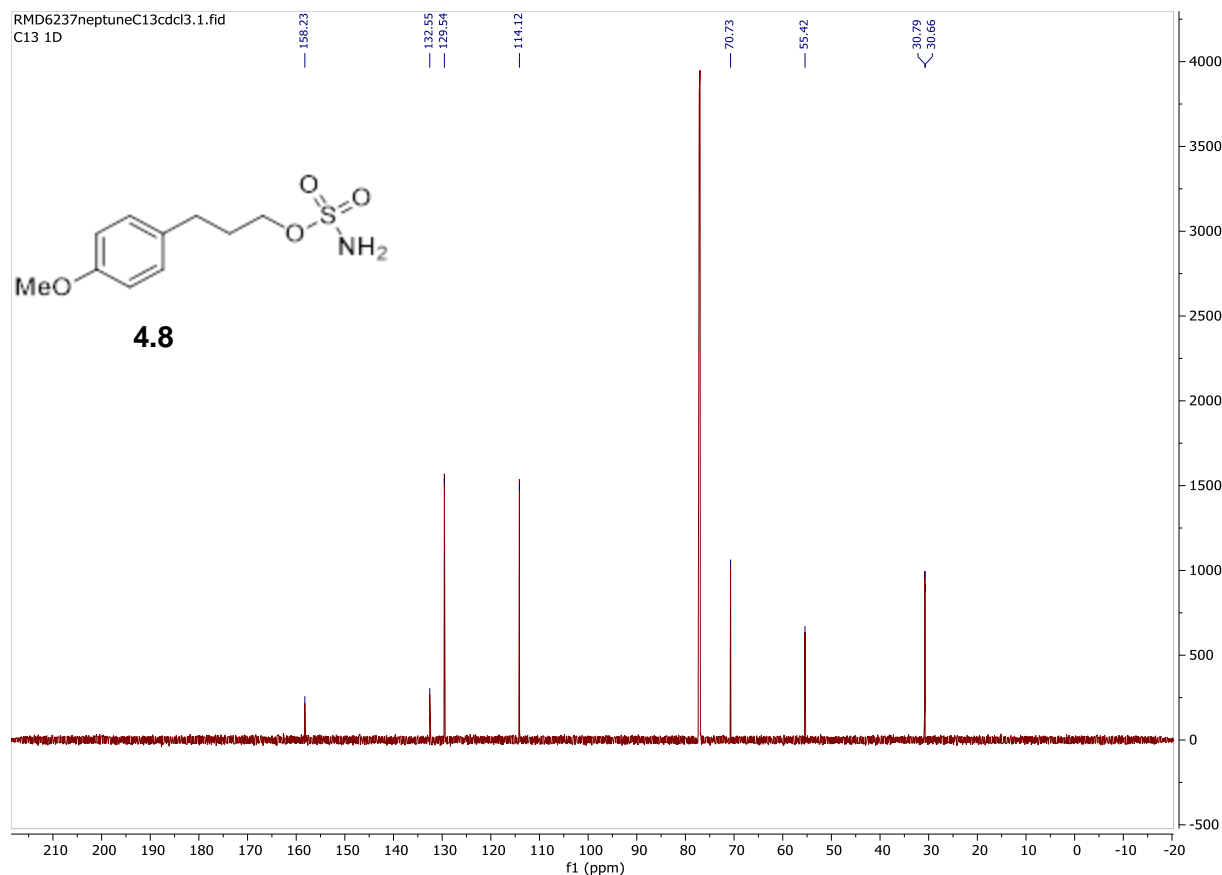
NMR spectra are consistent with literature reports.²

RMD6237arielH1cdcl3.1.fid

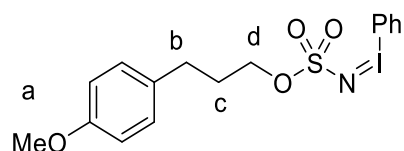


4.8





3-(4-methoxyphenyl)propyl (phenyl-*I*-iodanylidene)sulfamate (4.9)

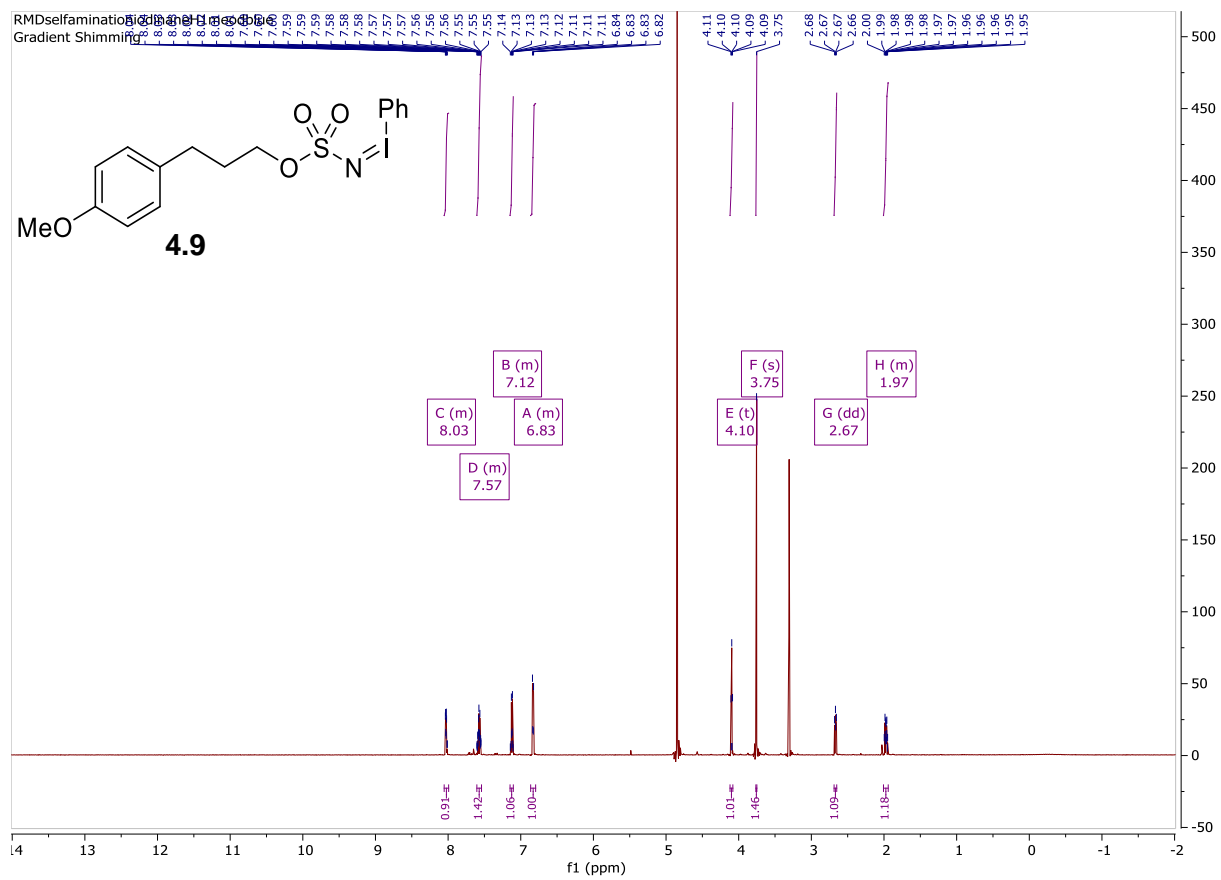


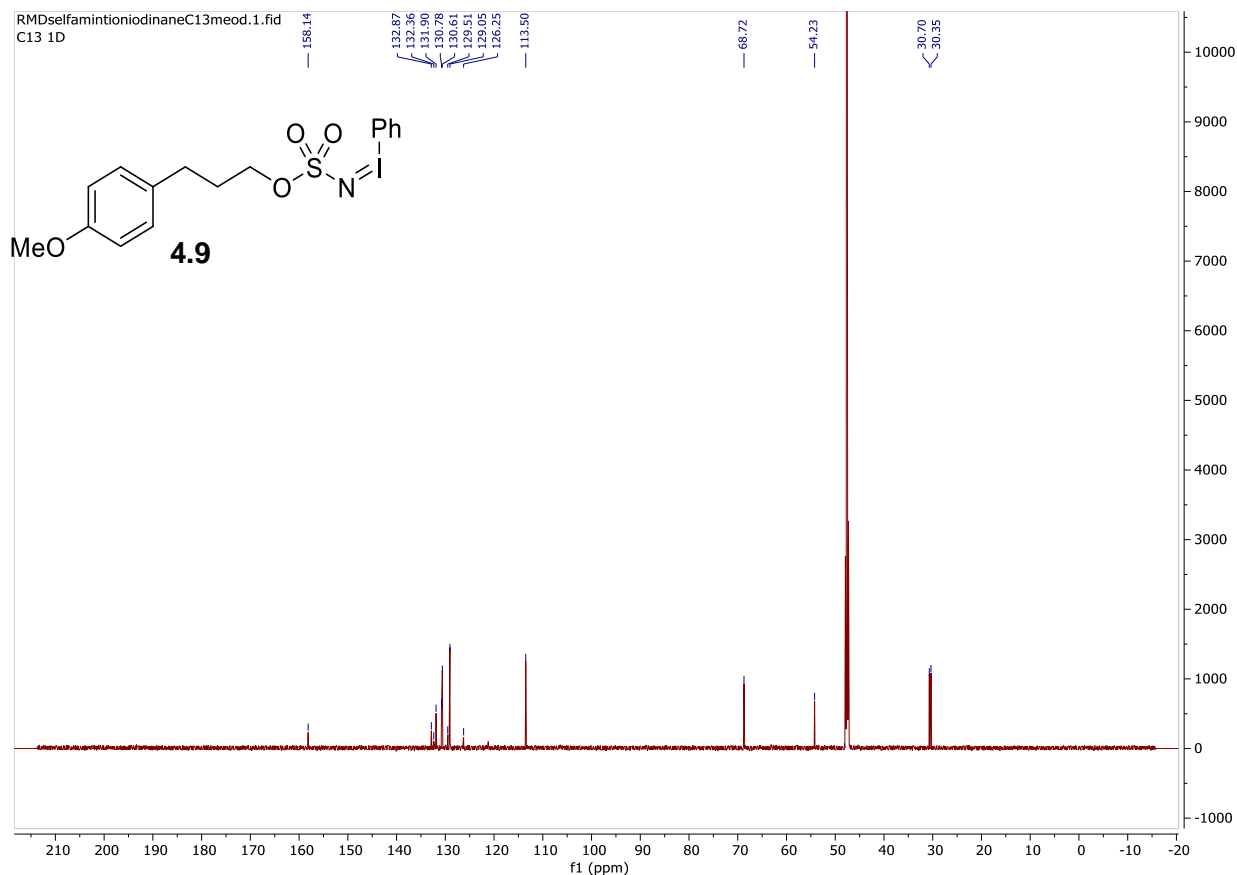
3-(4-methoxyphenyl)propyl (phenyl-*I*-iodanylidene)sulfamate was synthesized following the iodine synthesis general procedure on a 4 mmol scale of 3-(4-methoxyphenyl)propyl sulfamate, as the respective sulfonamide and diacetoxy iodobenzene as the respective oxidized iodoarene to give 0.910 g of a white solid (2.04 mmol, 50% yield).

¹H NMR (600 MHz, MeOD) δ 8.05 – 7.99 (m, 2H), 7.60 – 7.54 (m, 3H), 7.15 – 7.10 (m, 2H), 6.86 – 6.80 (m, 2H), 4.10 (H_d,t, J = 6.3 Hz, 2H), 3.75 (H_a,s, 3H), 2.67 (H_b,t, J = 8.4, 2H), 2.01 – 1.94 (H_c,m, 2H) ppm.

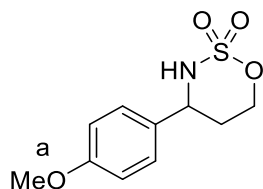
¹³C NMR (201 MHz, MeOD) δ 158.1, 132.8, 132.4, 131.9, 130.8, 130.6, 129.5, 129.0, 126.2, 113.5, 68.7, 54.2, 30.7, 30.3 ppm.

Elemental Analysis Calc'd for C₁₆H₁₈INO₄S : C, 42.96; H, 4.06; N, 3.13. Found: C 41.75 H 3.97 N 3.04





4-(4-methoxyphenyl)-1,2,3-oxathiazinane 2,2-dioxide (4.10)

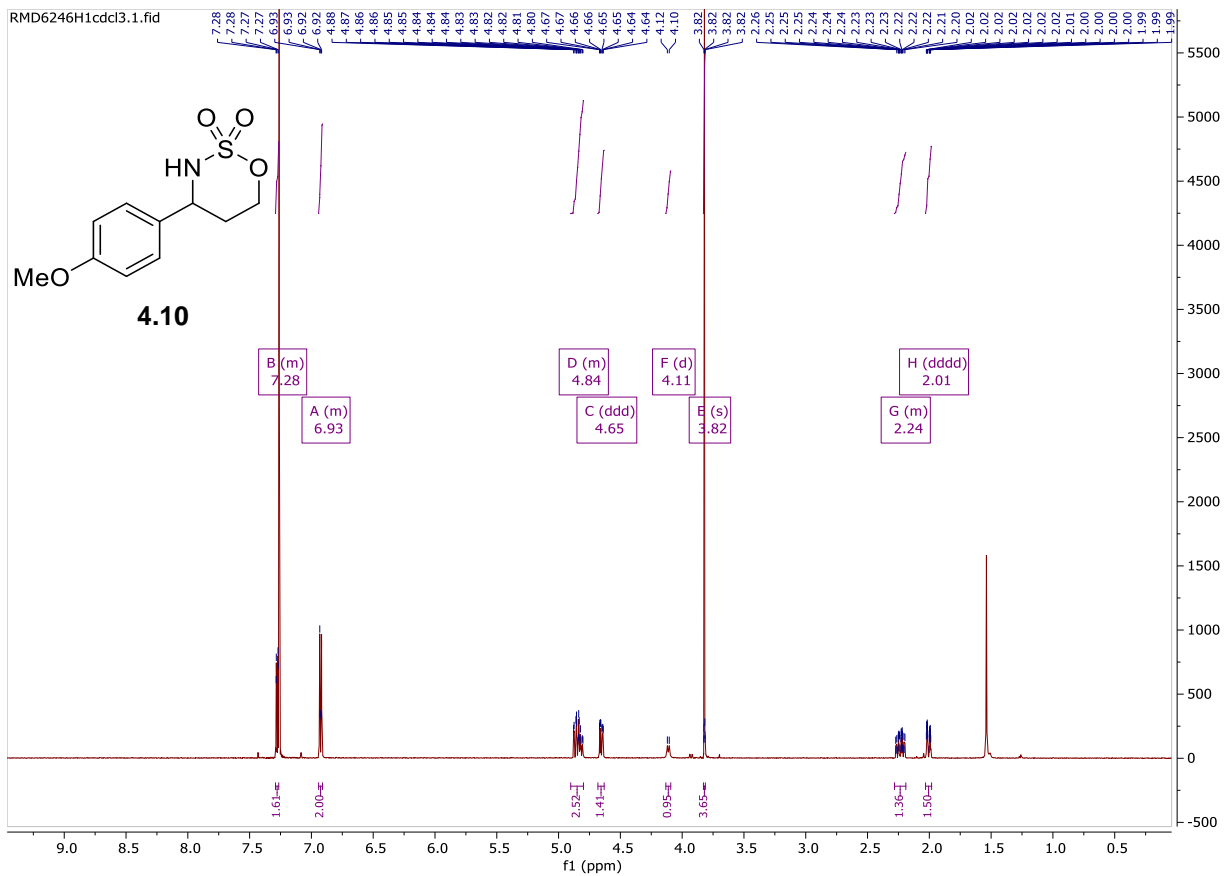


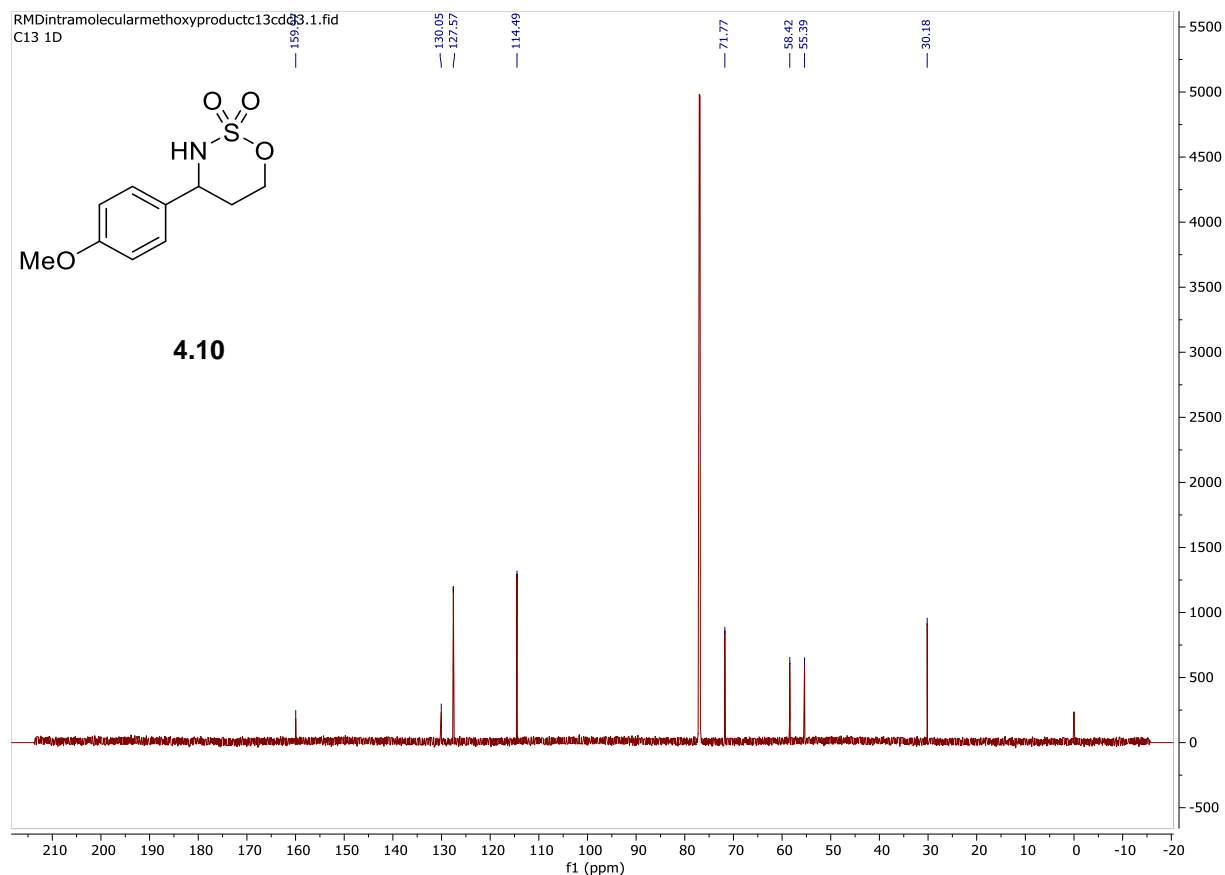
4-(4-methoxyphenyl)-1,2,3-oxathiazinane 2,2-dioxide was synthesized following the general amination procedure on a .2 mmol scale of 3-(4-methoxyphenyl)propyl sulfamate, as the respective sulfamate and 4-bromophenyl ((5-(tert-butyl)-2-methoxyphenyl)-l3-iodaneylidene)sulfamae as the respective iodine. The reaction mixture was purified after workup using silica flash chromatography (20% EtOAC/Hexanes) to give 0.018 g of a yellow solid (0.074 mmol, 37 % yield).

¹H NMR (600 MHz, CDCl₃) δ 7.29 – 7.26 (m, 2H), 6.94 – 6.91 (m, 2H), 4.90 – 4.80 (m, 3H), 4.65 (ddd, *J* = 11.7, 5.0, 1.6 Hz, 1H), 4.11 (d, *J* = 9.3 Hz, 1H), 3.82 (H_a, s, 3H), 2.28 – 2.19 (m, 1H), 2.01 (dddd, *J* = 14.5, 2.9, 2.2, 1.6 Hz, 1H) ppm.

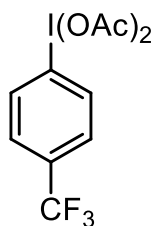
¹³C NMR (201 MHz, CDCl₃) δ 160.0, 130.1, 127.6, 114.6, 71.8, 58.4, 55.4, 30.2 ppm.

NMR spectra are consistent with literature reports.¹





(4-(trifluoromethyl)phenyl)-I3-iodanediyl diacetate (4.21)



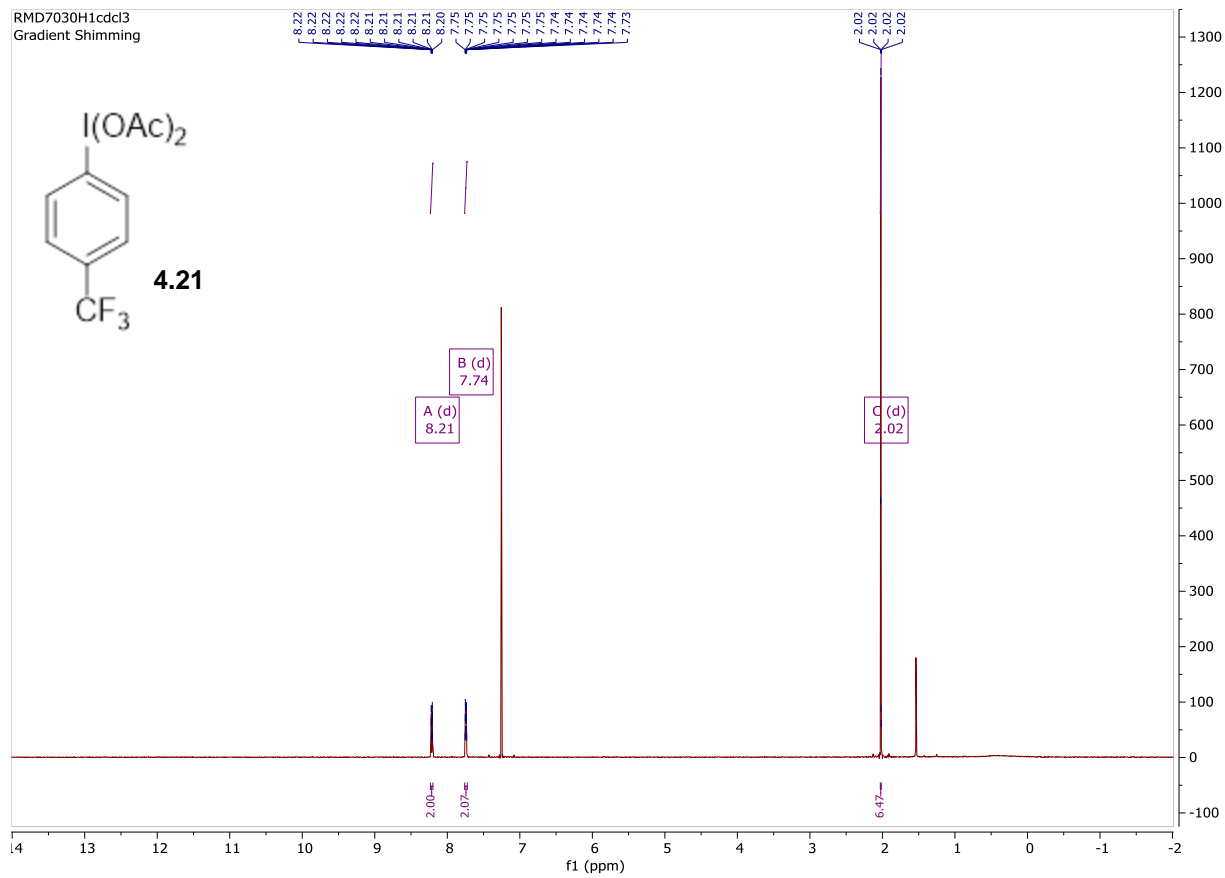
(4-(trifluoromethyl)phenyl)-I3-iodanediyl diacetate was synthesized following general oxidation of iodoarenes procedure A on a 9.2 mmol scale of 1-iodo-4-(trifluoromethyl)benzene, as the respective aryl iodide to give 1.78 g of a white solid (4.51 mmol, 49 % yield).

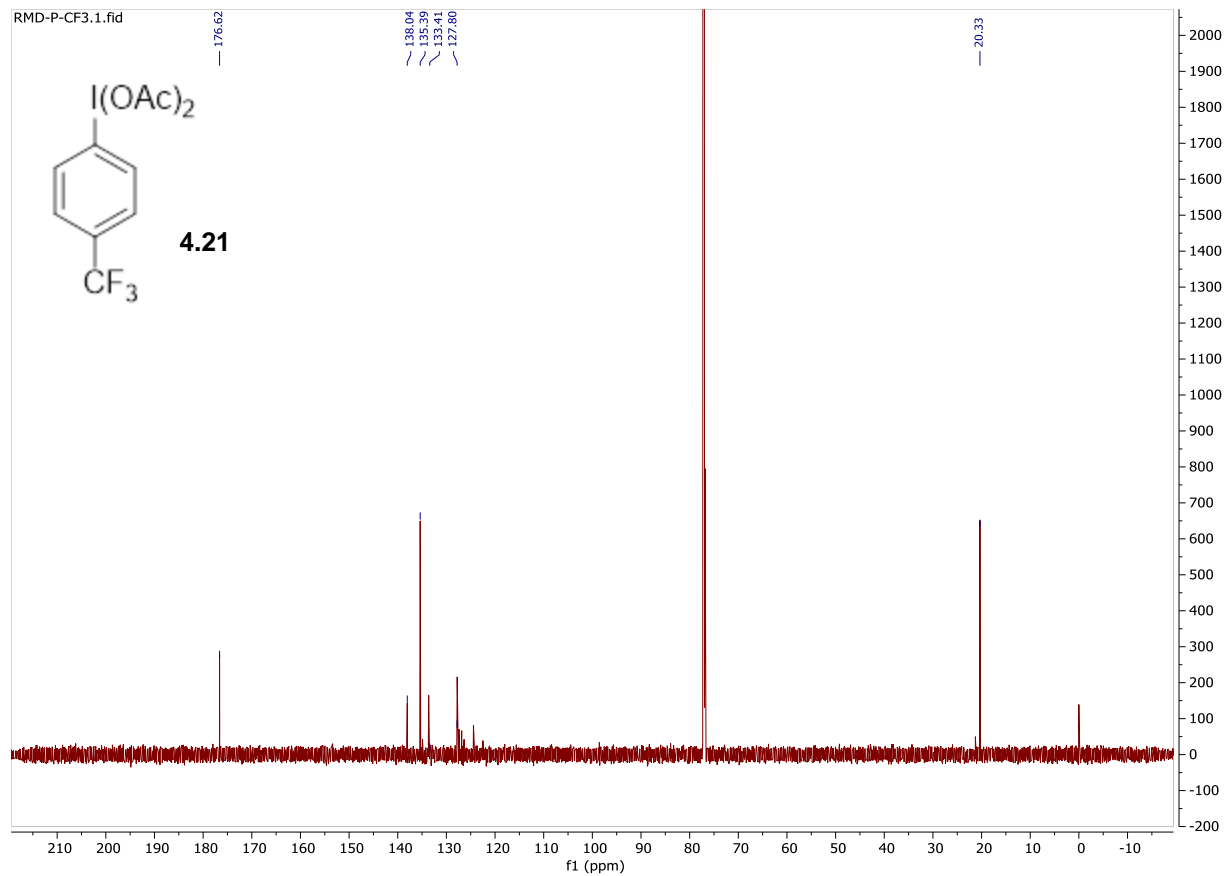
¹H NMR (600 MHz, CDCl₃) δ 8.21 (d, *J* = 8.3 Hz, 2H), 7.74 (d, *J* = 8.4 Hz, 2H), 2.02 (d, *J* = 1.2 Hz, 6H) ppm.

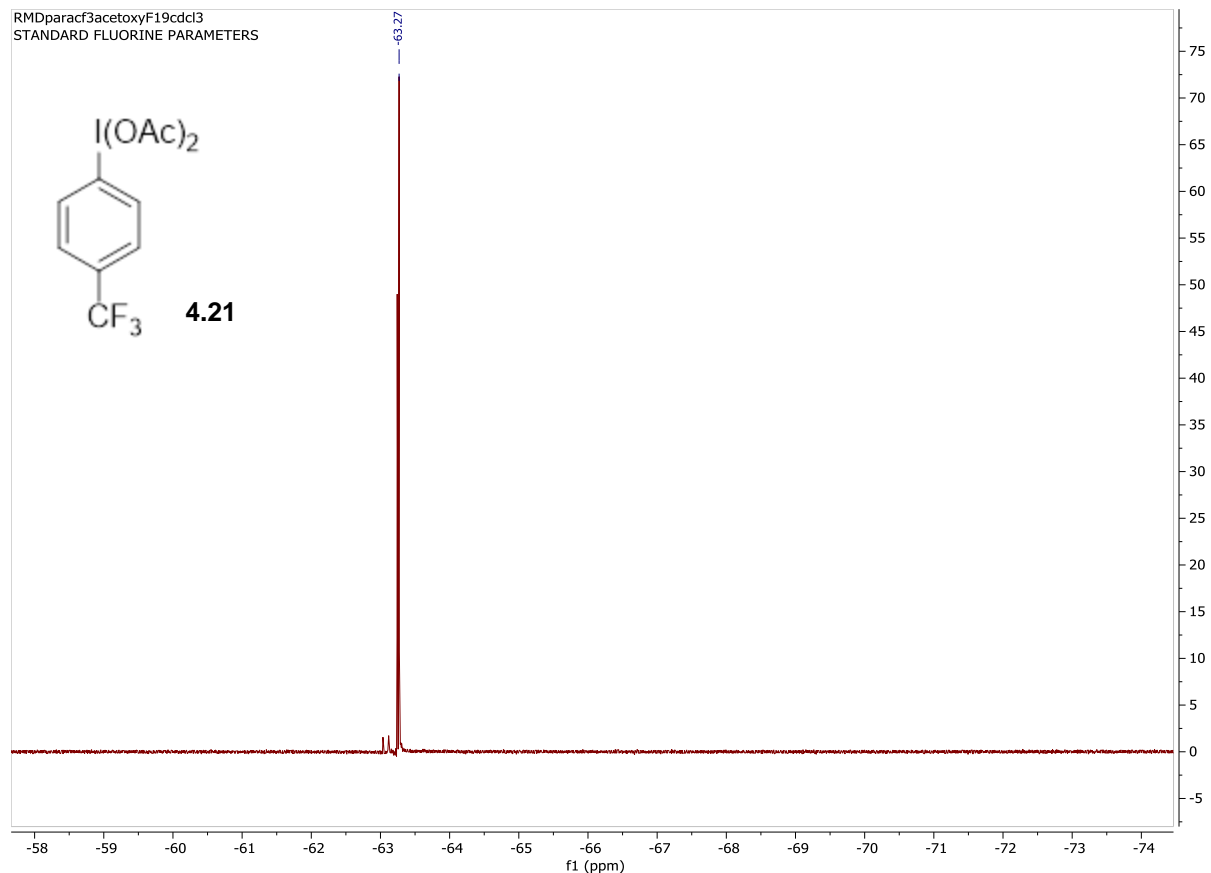
¹³C NMR (201 MHz, CDCl₃) δ 176.6, 138.0, 135.4, 133.4, 127.8, 20.3 ppm.

¹⁹F NMR (564 MHz, CDCl₃) δ -63.27 ppm.

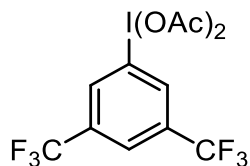
NMR spectra are consistent with literature reports.²







(3,5-bis(trifluoromethyl)phenyl)-I3-iodanediyl diacetate (4.22)



(3,5-bis(trifluoromethyl)phenyl)-I3-iodanediyl diacetate was synthesized following the general oxidation of iodoarenes procedure A on a 7.35 mmol scale of 1-iodo-3,5-bis(trifluoromethyl)benzene, as the respective aryl iodide to give 0.780 g of a white solid (1.69 mmol, 23 % yield).

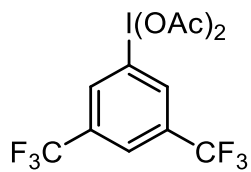
¹H NMR (600 MHz, CDCl₃) δ 8.50 (d, *J* = 1.7 Hz, 2H), 8.07 (s, 1H), 2.05 (s, 6H) ppm.

¹³C NMR (201 MHz, CDCl₃) δ 176.7, 135.0, 133.7, 125.5, 122.8, 121.4, 120.9, 20.2 ppm.

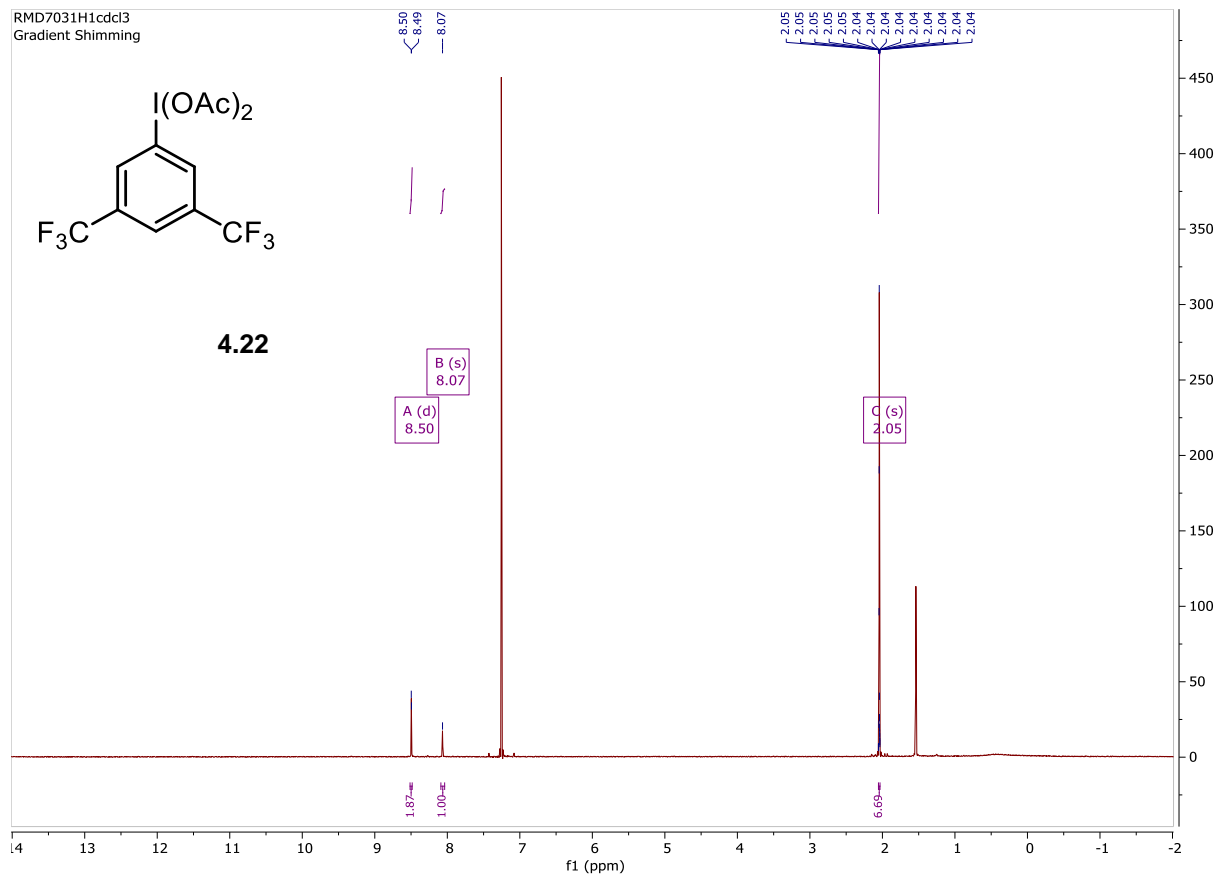
¹⁹F NMR (564 MHz, CDCl₃) δ -62.88 ppm.

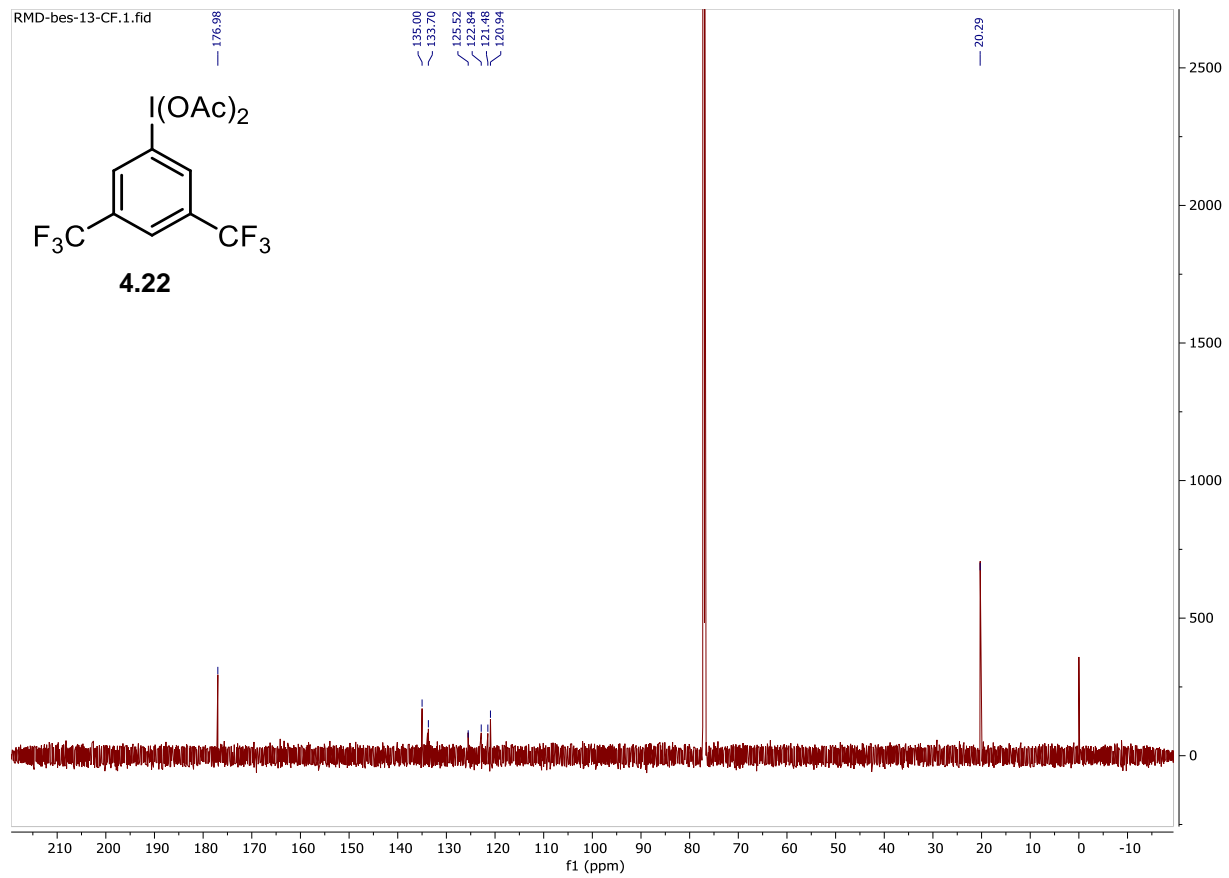
NMR spectra are consistent with literature reports.²

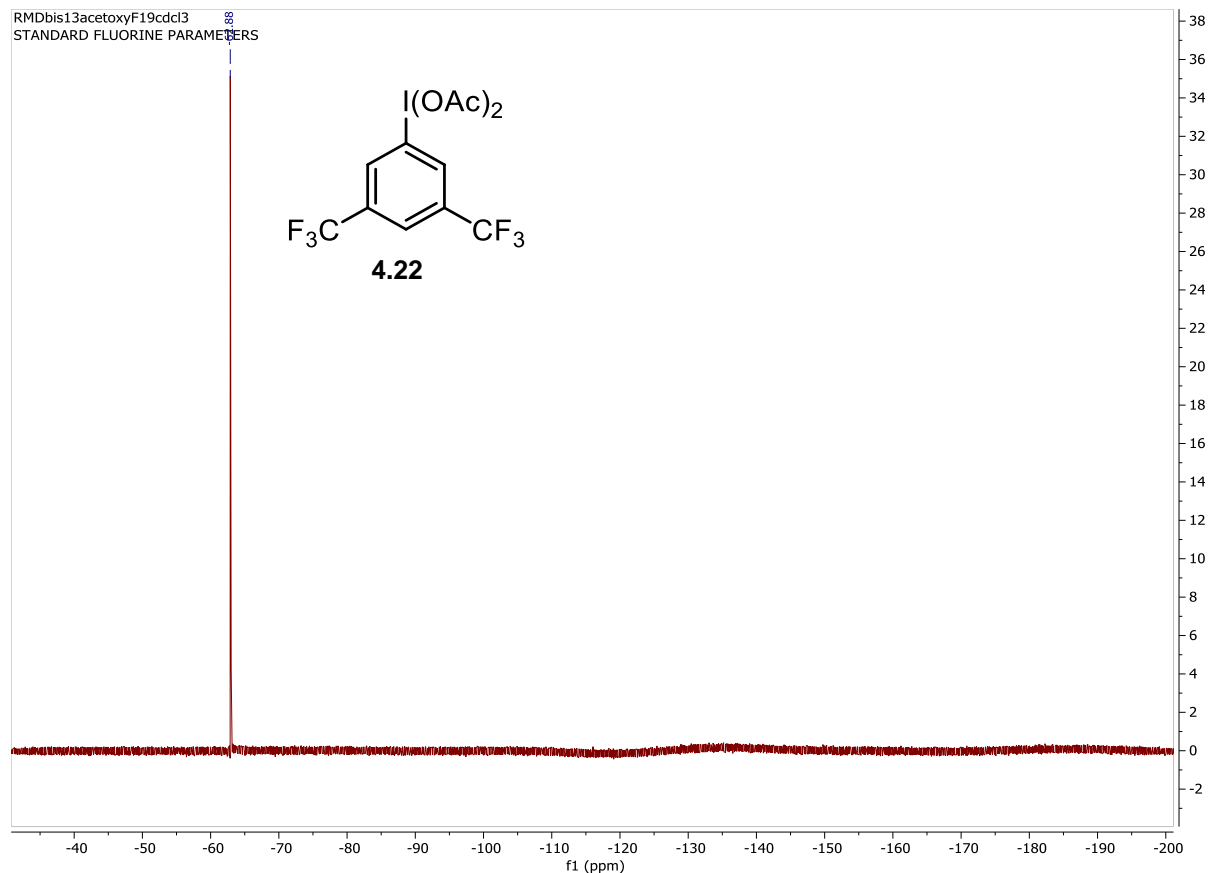
RMD7031H1cdcl3
Gradient Shimming



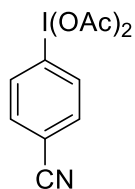
4.22







(4-cyanophenyl)-I3-iodanediyl diacetate (4.24)

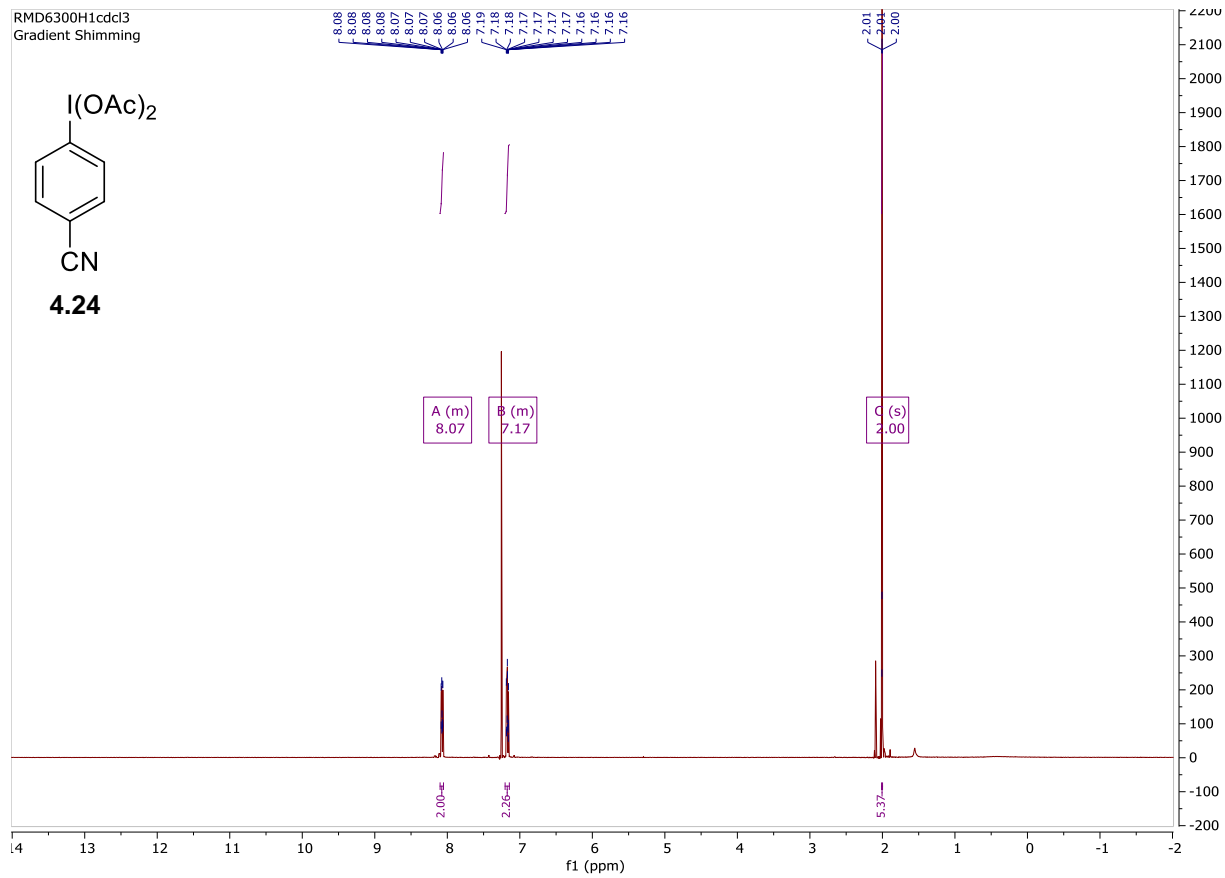


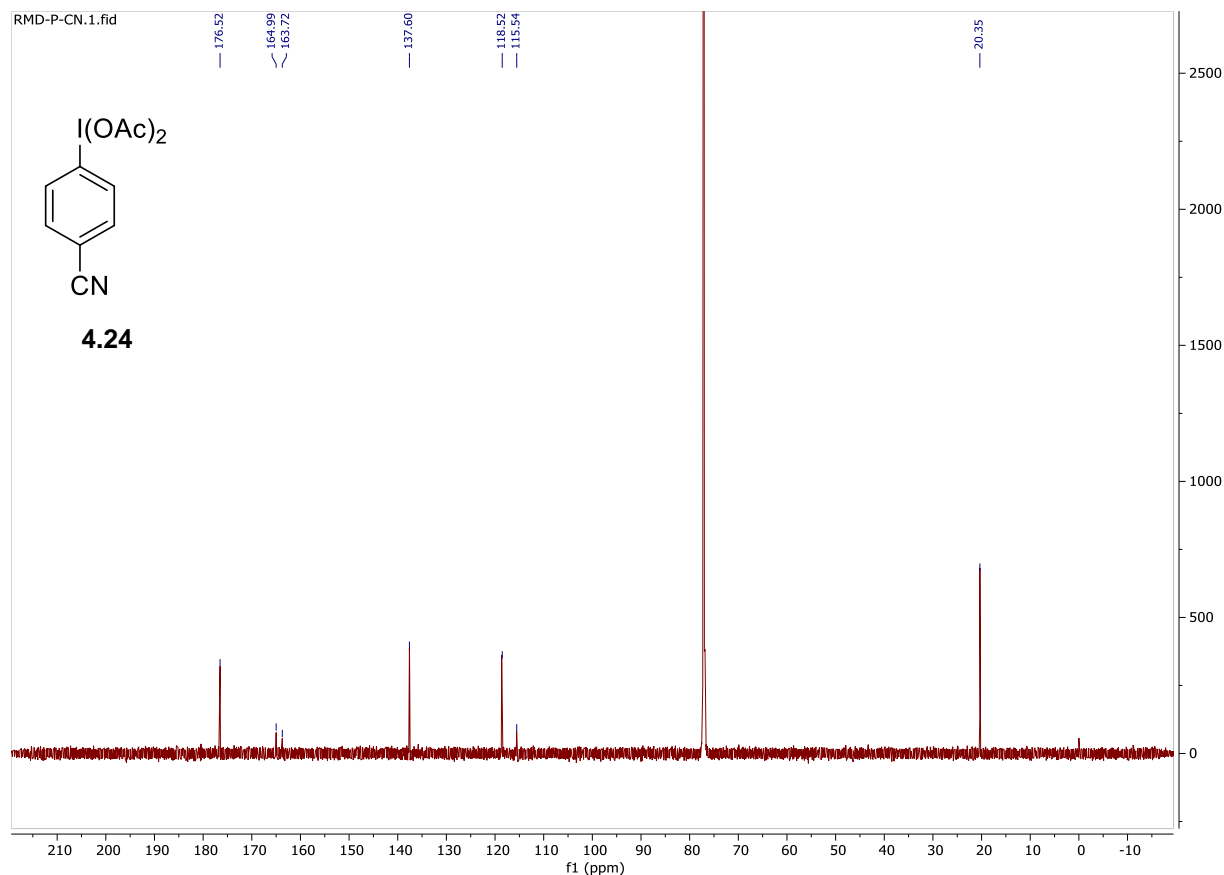
(4-cyanophenyl)-I3-iodanediyl diacetate was synthesized following the general oxidation of iodoarenes procedure A on a 11 mmol scale of 4-iodobenzonitrile, as the respective aryl iodide to give 3.15 g of a white solid (9.07 mmol, 82% yield).

¹H NMR (600 MHz, CDCl₃) δ 8.10 – 8.05 (m, 2H), 7.20 – 7.14 (m, 2H), 2.00 (s, 6H) ppm.

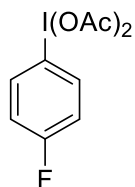
¹³C NMR (201 MHz, CDCl₃) δ 176.5, 165.0, 163.7, 137.6, 118.5, 115.5, 20.3 ppm.

NMR spectra are consistent with literature reports.³





(4-fluorophenyl)-I₃-iodanediyl diacetate (4.26)



(4-fluorophenyl)-I₃-iodanediyl diacetate was synthesized following the general oxidation of iodoarenes procedure A on a 11 mmol scale of 1-fluoro-4-iodobenzene, as the respective aryl iodide to give 1.50 g of a white solid (4.40 mmol, 40% yield).

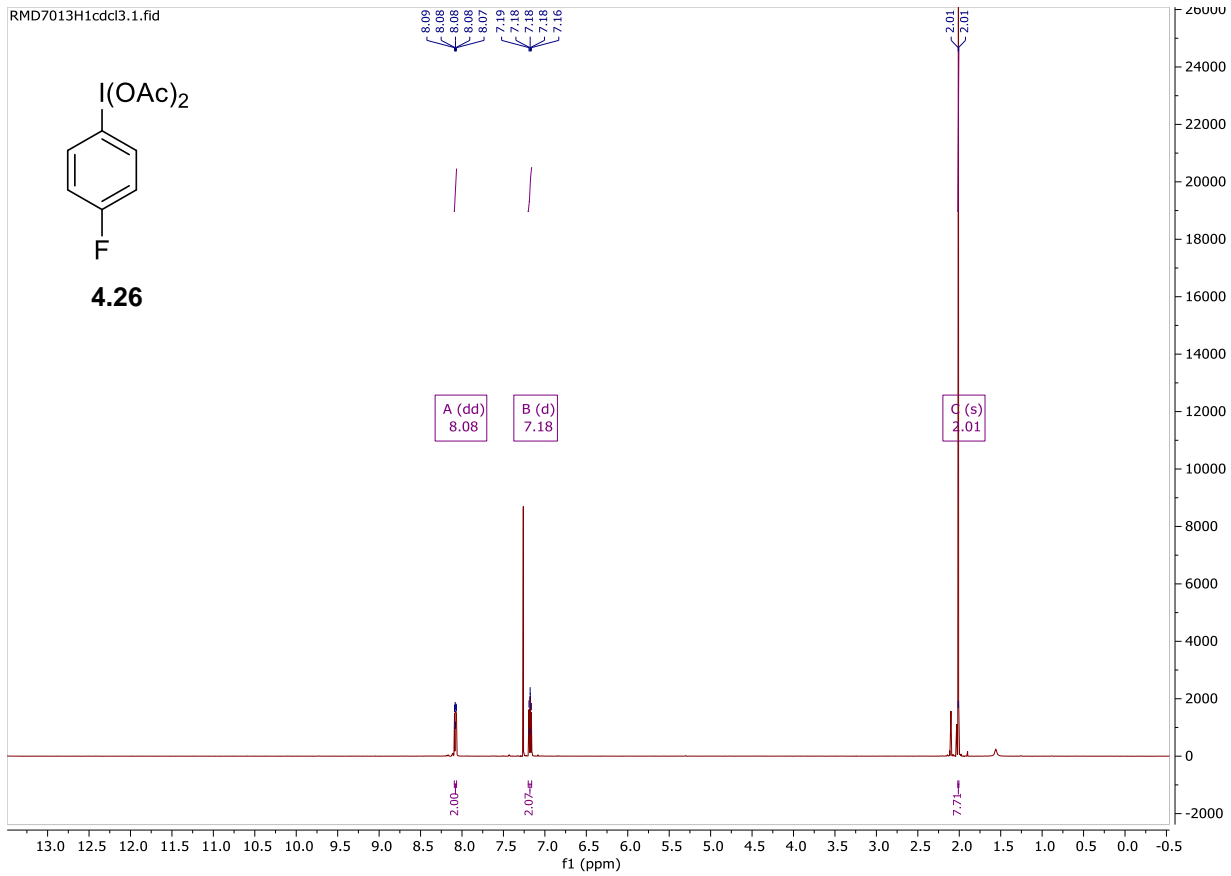
¹H NMR (600 MHz, CDCl₃) δ 8.08 (dd, *J* = 9.8, 4.5 Hz, 2H), 7.18 (d, *J* = 9.0 Hz, 2H), 2.01 (s, 6H) ppm.

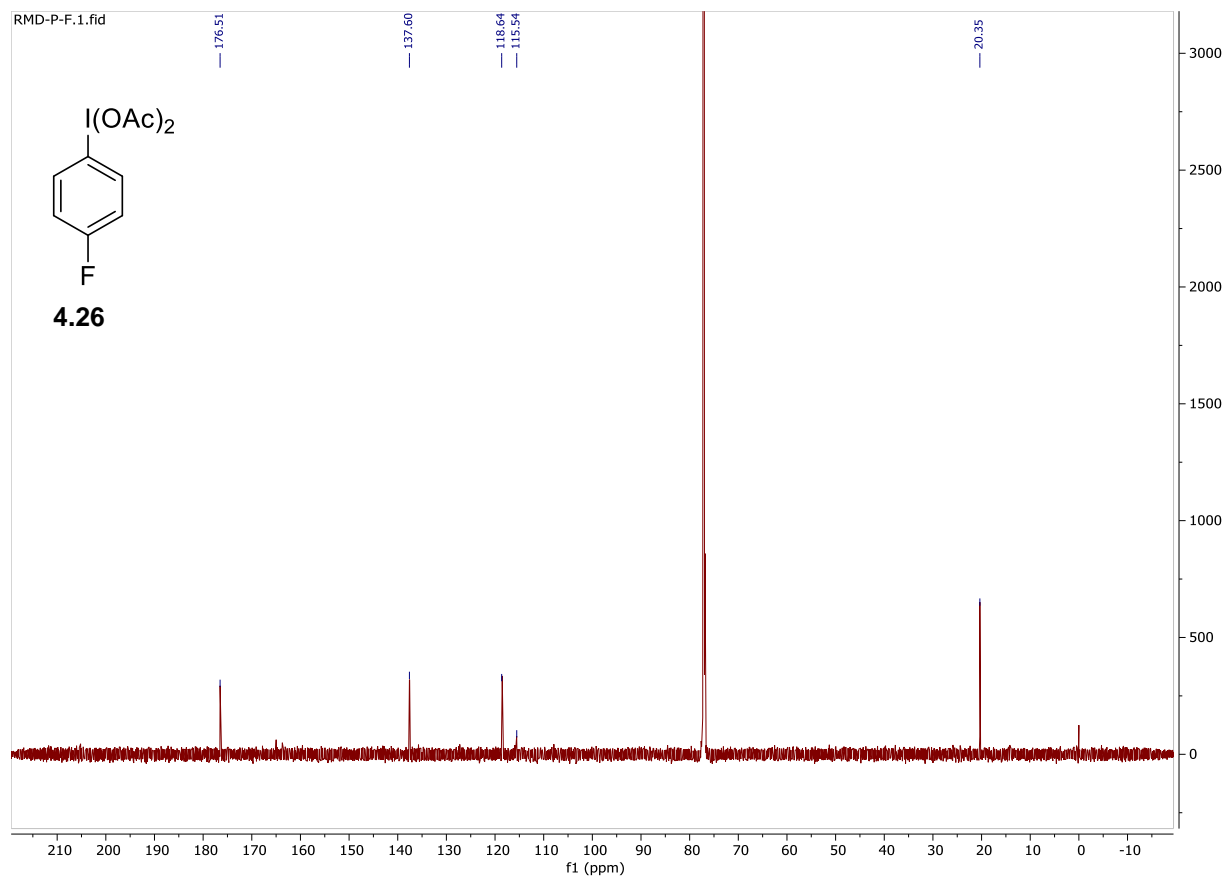
¹³C NMR (201 MHz, CDCl₃) δ 176.5, 137.6, 118.6, 115.5, 20.3 ppm

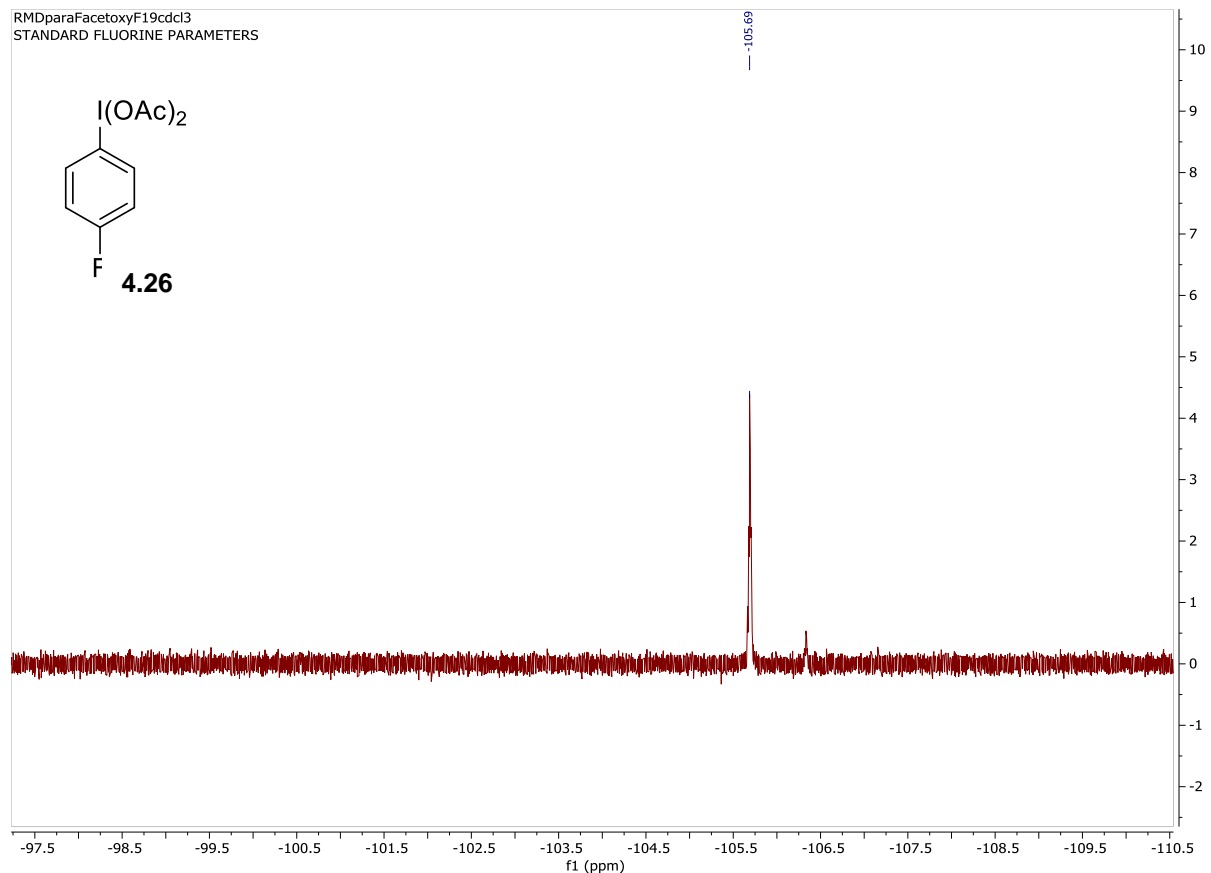
¹⁹F NMR (564 MHz, CDCl₃) δ -105.69 ppm.

NMR spectra are consistent with literature reports.⁴

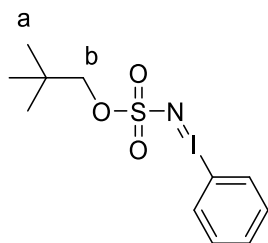
RMD7013H1cdcl3.1.fid







Neopentyl (phenyl-*I*-iodaneylidene)sulfamate (4.31)

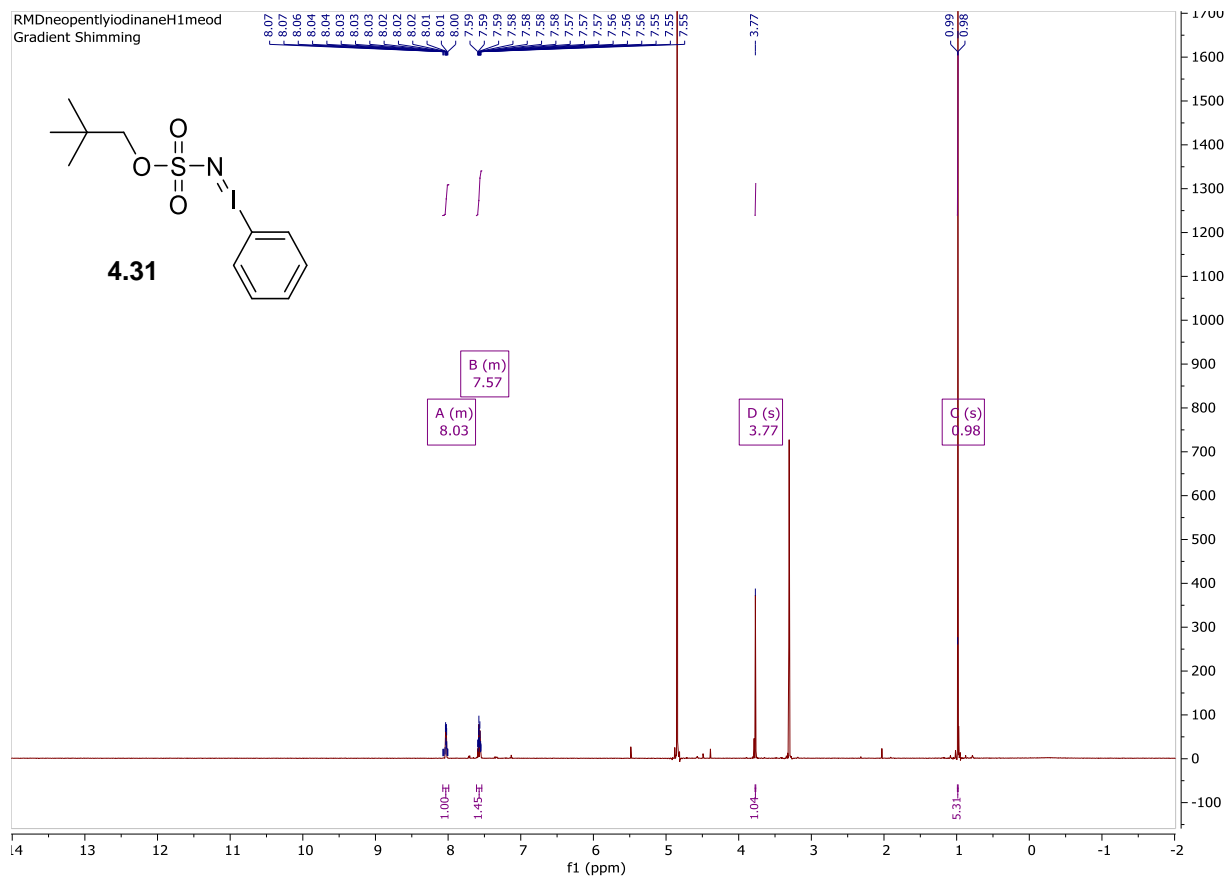


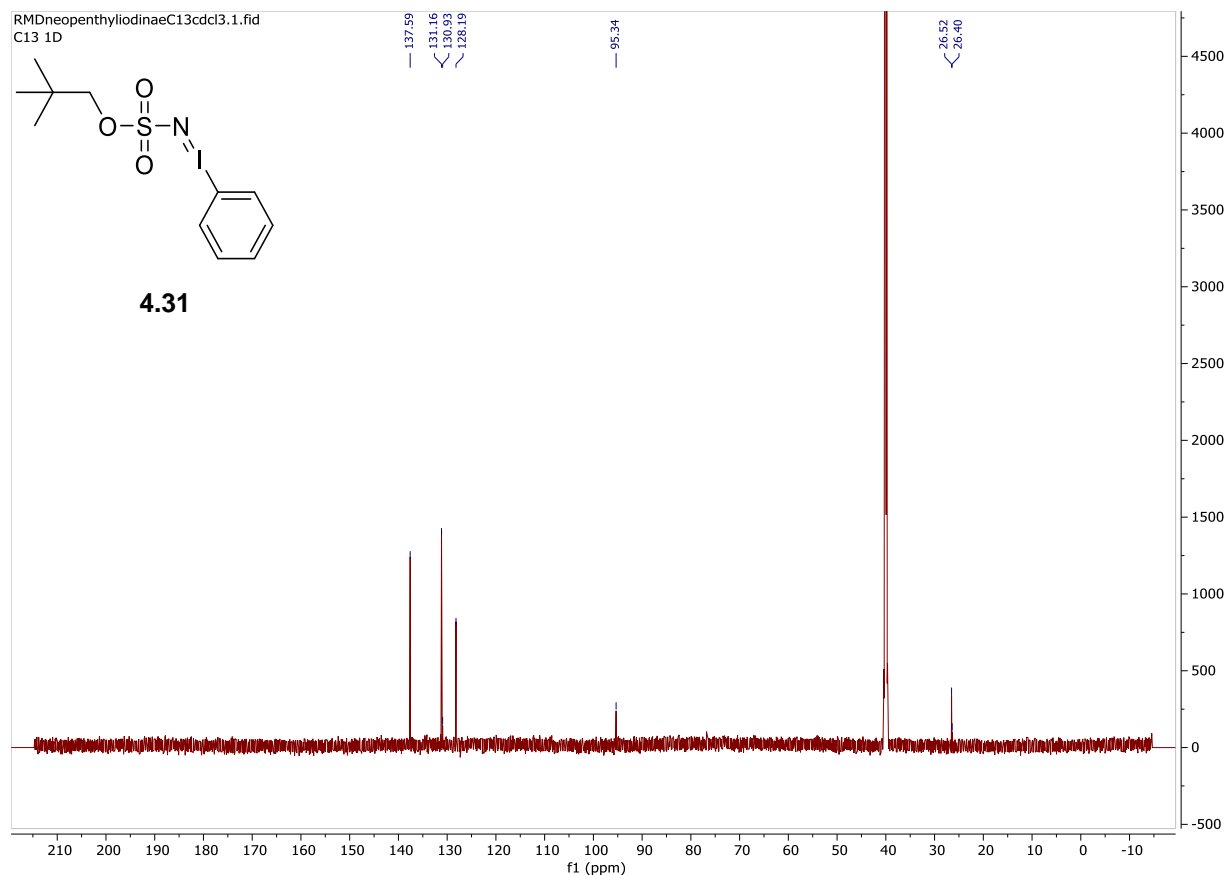
Neopentyl (phenyl-*I*-iodaneylidene)sulfamate was synthesized following the iodine synthesis general procedure on a 21.34 mmol scale of neopentyl sulfamate, as the respective sulfamate and diacetoxy iodobenzene as respect oxidized iodoarene to give 3.22 g of a white solid (8.74 mmol, 41% yield).

¹H NMR (600 MHz, MeOD) δ 8.07 – 7.99 (m, 2H), 7.61 – 7.54 (m, 3H), 3.77 (H_b, s, 2H), 0.98 (H_a, s, 9H) ppm.

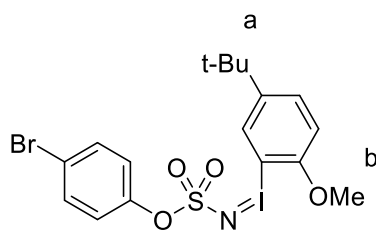
¹³C NMR (201 MHz, DMSO) δ 137.5, 131.1, 130.9, 128.1, 95.3, 26.5, 26.4 ppm.

Elemental Analysis Calc'd for C₁₁H₁₆INO₃S: C, 35.78; H, 4.37; N, 3.79 Found: C: 35.71 H 4.55 N 4.04





4-bromophenyl ((5-(tert-butyl)-2-methoxyphenyl)-I3-iodaneylidene)sulfamate (4.43)

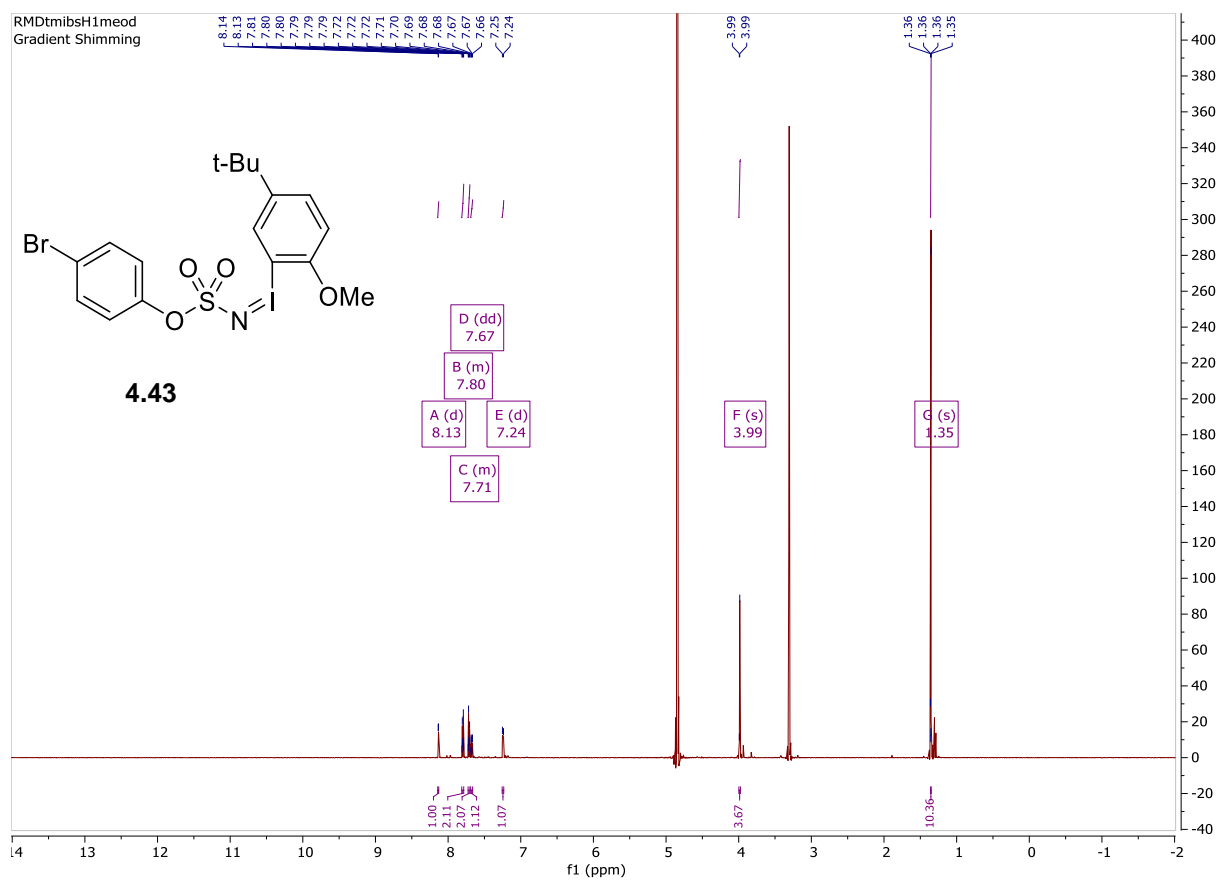


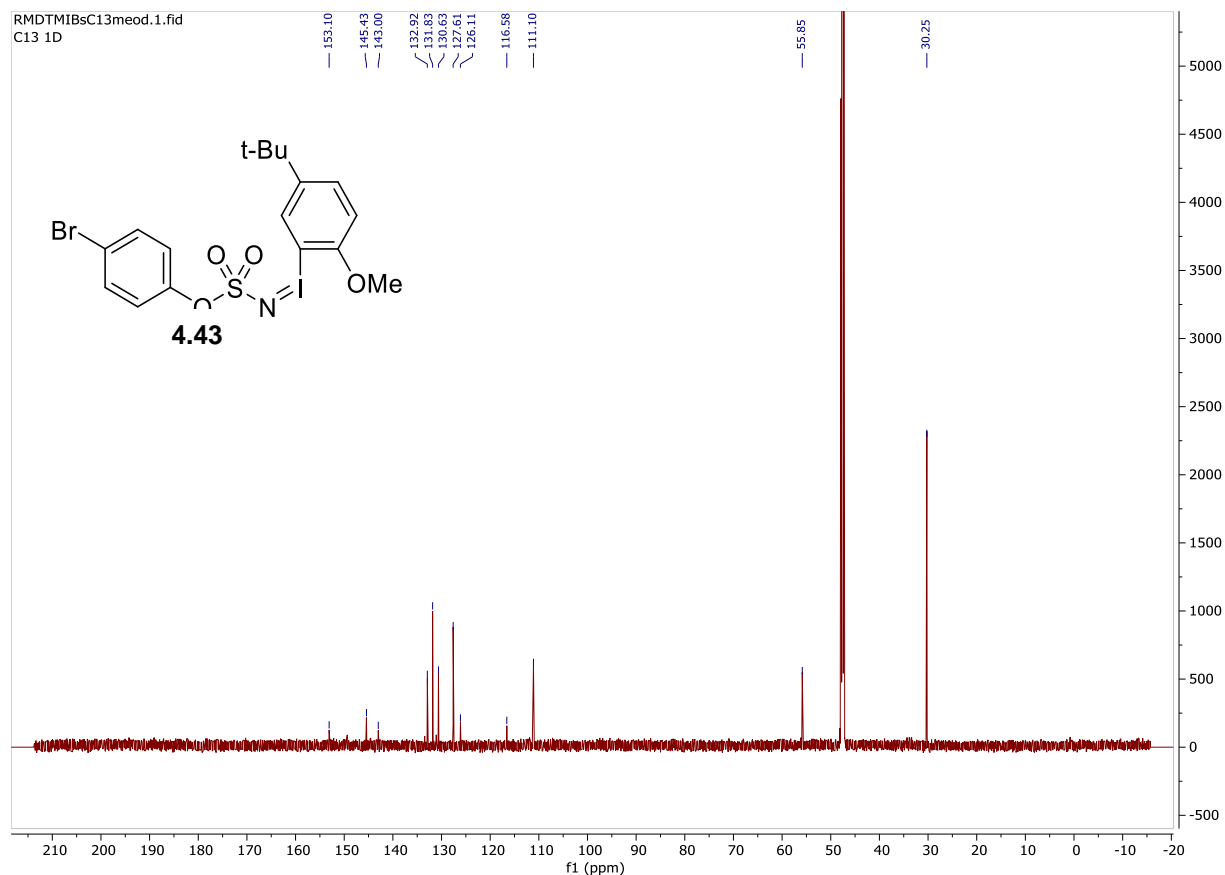
4-bromophenyl ((5-(tert-butyl)-2-methoxyphenyl)-I3-iodaneylidene)sulfamate was synthesized following the iodine synthesis general procedure on a 60 mmol scale of 4-bromobenzenesulfonamide, as the respective sulfamate and (5-(tert-butyl)-2-methoxyphenyl)-I3-iodanediyl bis(3-chlorobenzoate) as the respective oxidized iodoarene to give 6.32 g of a white solid (12.0 mmol, 20% yield).

¹H NMR (600 MHz, MeOD) δ 8.13 (d, J = 2.4 Hz, 1H), 7.81 – 7.78 (m, 2H), 7.72 – 7.70 (m, 2H), 7.67 (dd, J = 8.7, 2.4 Hz, 1H), 7.24 (d, J = 8.8 Hz, 1H), 3.99 (H_b, s, 3H), 1.35 (H_a, s, 9H) ppm.

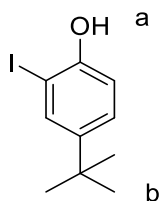
¹³C NMR (201 MHz, MeOD) δ 153.1, 145.4, 143.0, 132.9, 131.8, 130.6, 127.6, 126.1, 116.6, 111.1, 55.8, 30.2 ppm.

Elemental Analysis Calc'd for C₁₇H₁₉BrINO₄S: C, 37.80; H, 3.55; N, 2.59. Found: C 39.19 H 3.57 N 2.49





4-(tert-butyl)-2-iodophenol (4.45)

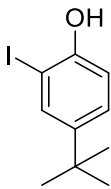


4-(tert-butyl)-2-iodophenol was synthesized following the general iodination procedure on a 60 mmol scale of 4-(tert-butyl)phenol, as the respective phenol, to give 14.2 g of an off white solid (51.6 mmol, 86%).

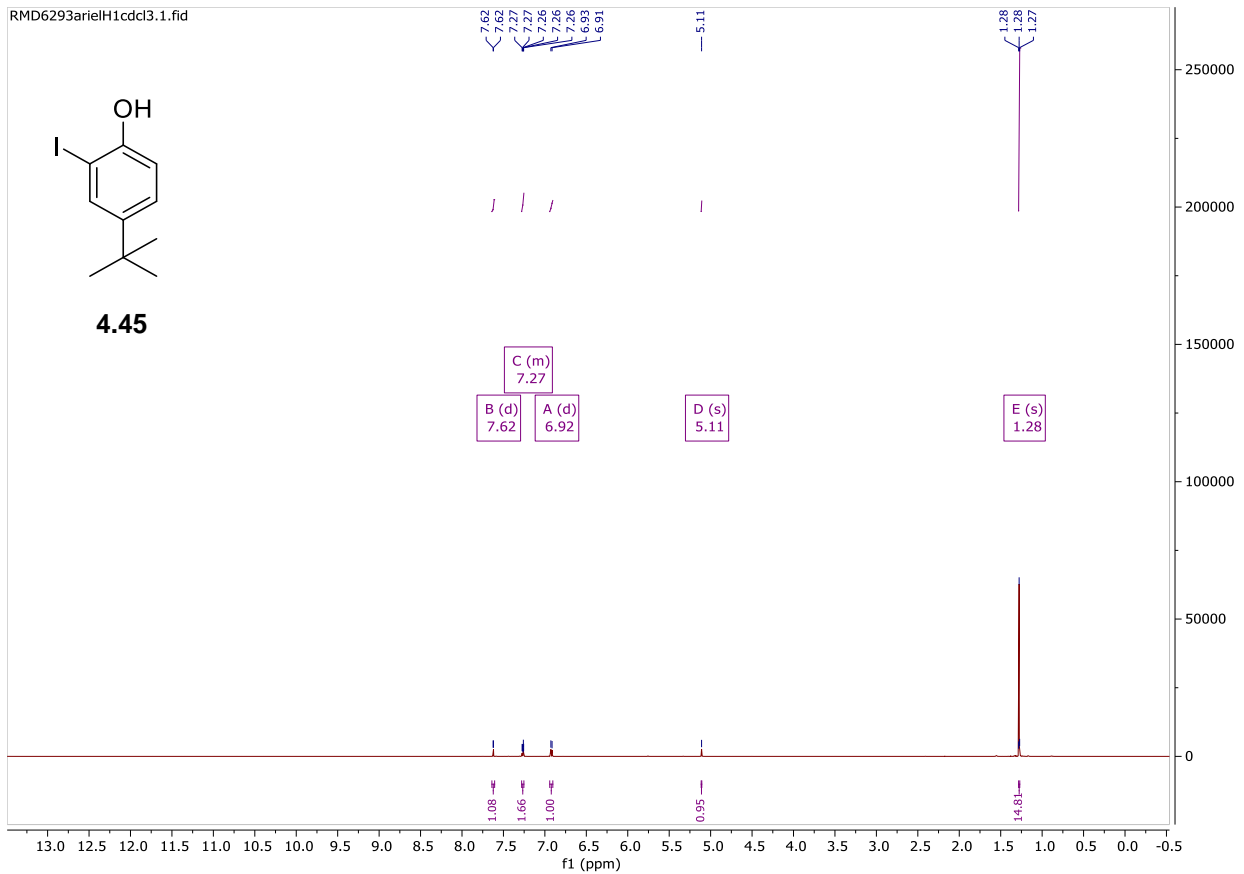
¹H NMR (600 MHz, CDCl₃) δ 7.62 (d, *J* = 2.3 Hz, 1H), 7.28 – 7.25 (m, 1H), 6.92 (d, *J* = 8.5 Hz, 1H), 5.11 (H_a, s, 1H), 1.28 (H_b, s, 9H) ppm.

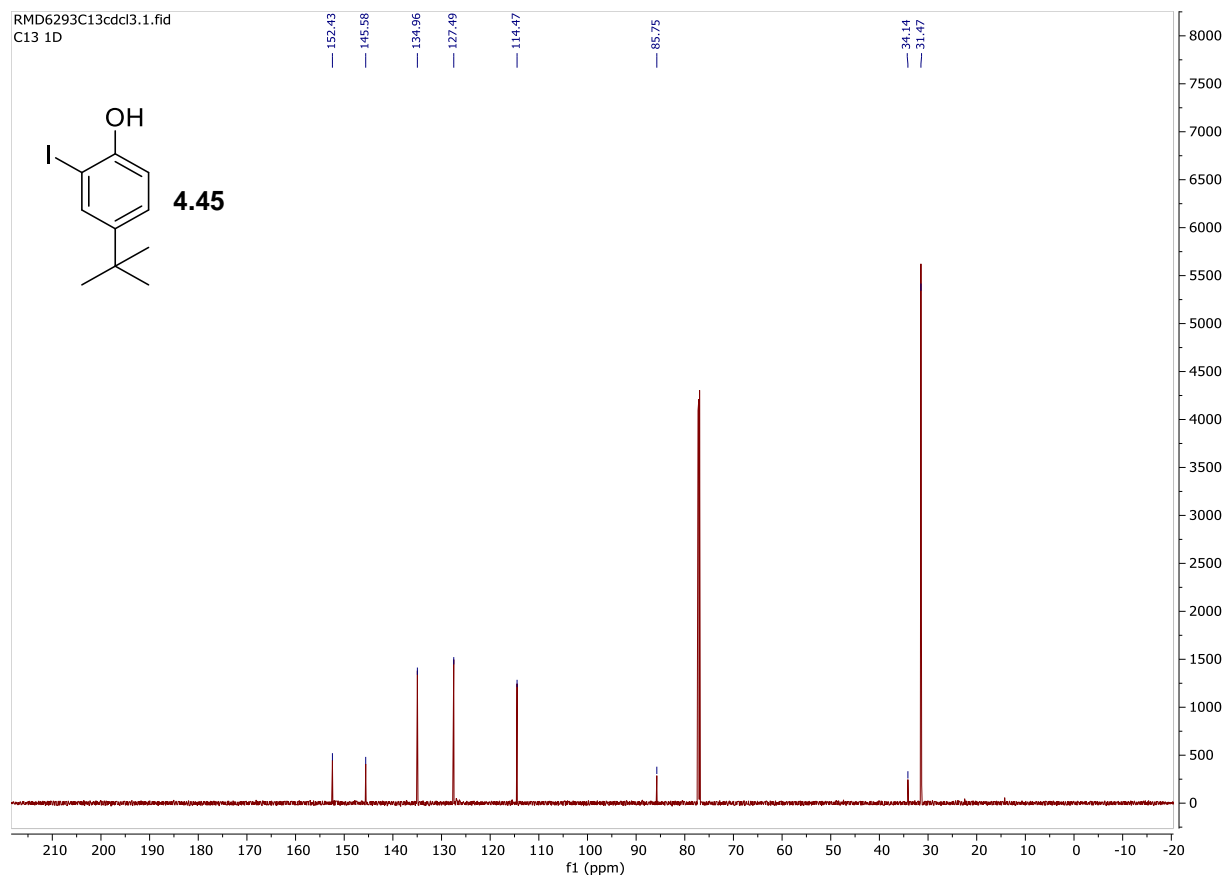
¹³C NMR (201 MHz, CDCl₃) δ 152.4, 145.5, 134.9, 127.4, 114.4, 85.7, 34.1, 31.4 ppm.

RMD6293arielH1cdcl3.1.fid

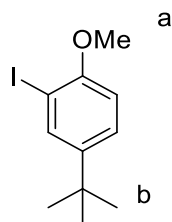


4.45





4-(tert-butyl)-2-iodo-1-methoxybenzene (4.46)

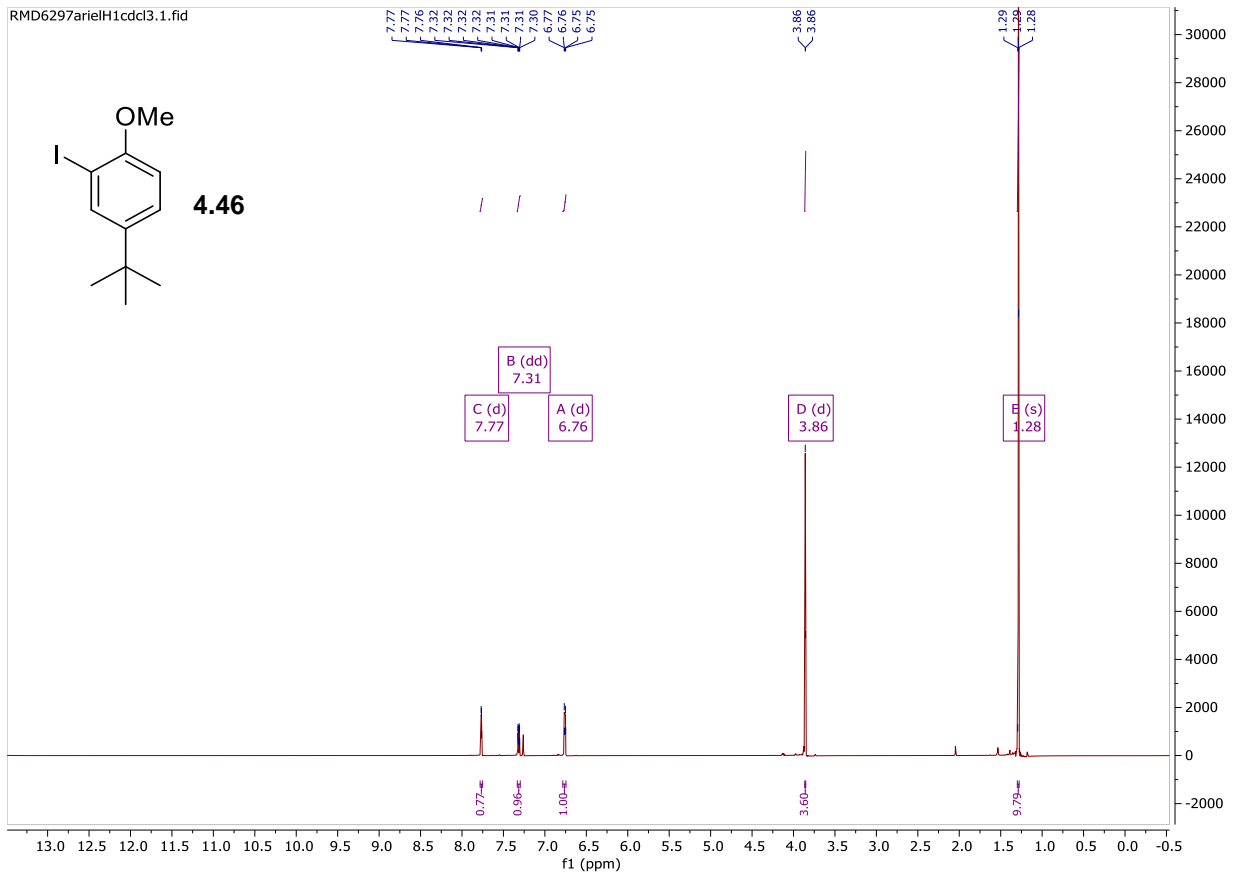
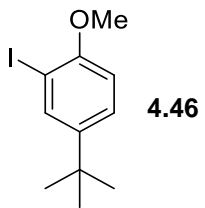


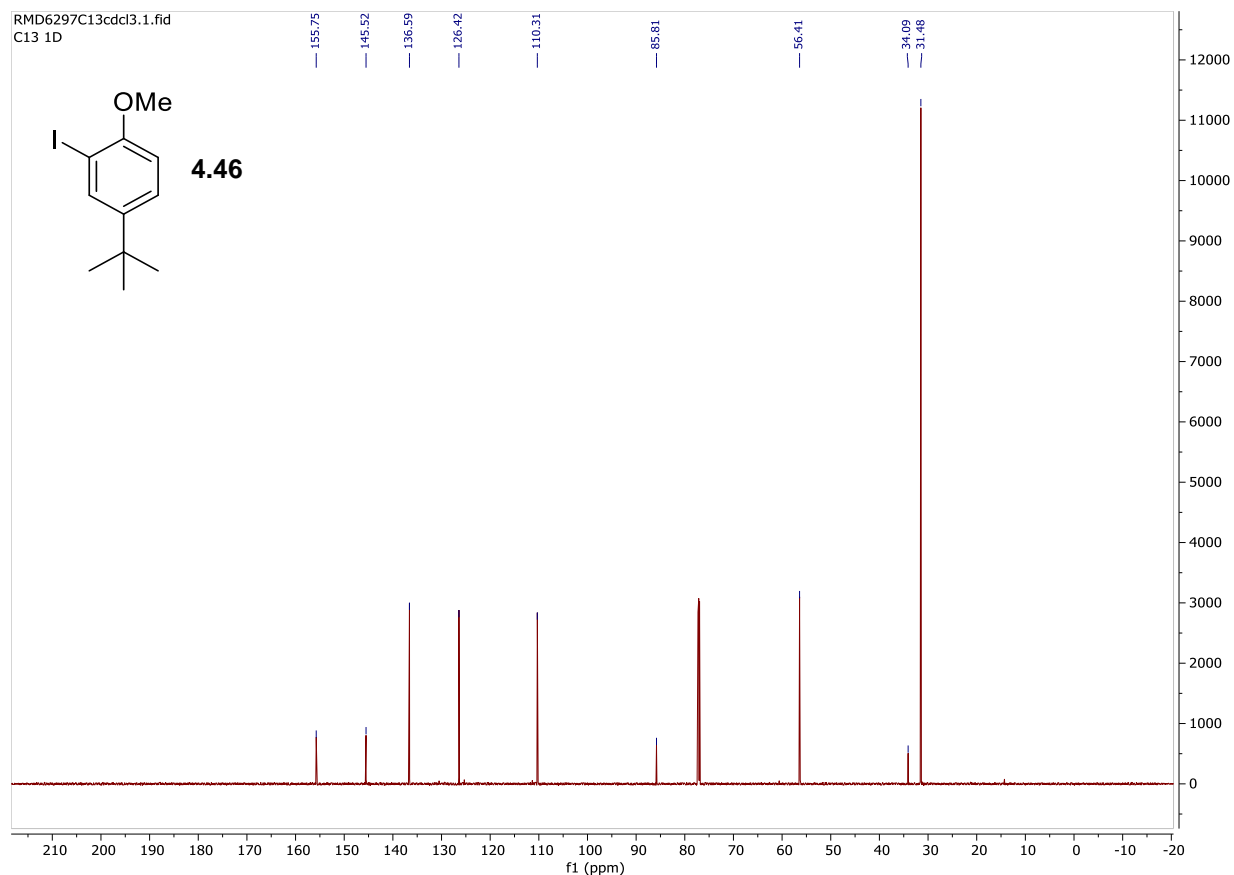
4-(tert-butyl)-2-iodo-1-methoxybenzene was synthesized following the general alkylation procedure on a 54.3 mmol scale of 4-(tert-butyl)-2-iodophenol, as the respective iodophenol, to give 14.2 g of a clear oil (48.9 mmol, 90%).

$^1\text{H NMR}$ (600 MHz, CDCl_3) δ 7.77 (d, $J = 2.3$ Hz, 1H), 7.31 (d, $J = 8.5$ Hz, 1H), 6.76 (d, $J = 8.4$ Hz, 1H), 3.86 (H_a , d, $J = 1.7$ Hz, 3H), 1.28 (H_b , s, 9H) ppm.

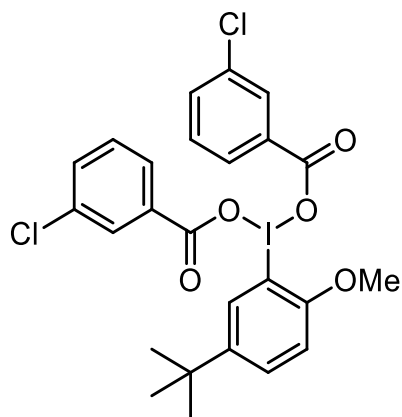
$^{13}\text{C NMR}$ (201 MHz, CDCl_3) δ 155.7, 145.5, 136.5, 126.4, 110.3, 85.8, 56.4, 34.0, 31.4 ppm.

RMD6297arielH1cdcl3.1.fid





(5-(tert-butyl)-2-methoxyphenyl)-1,3-iodanediyl bis(3-chlorobenzoate) (4.47)

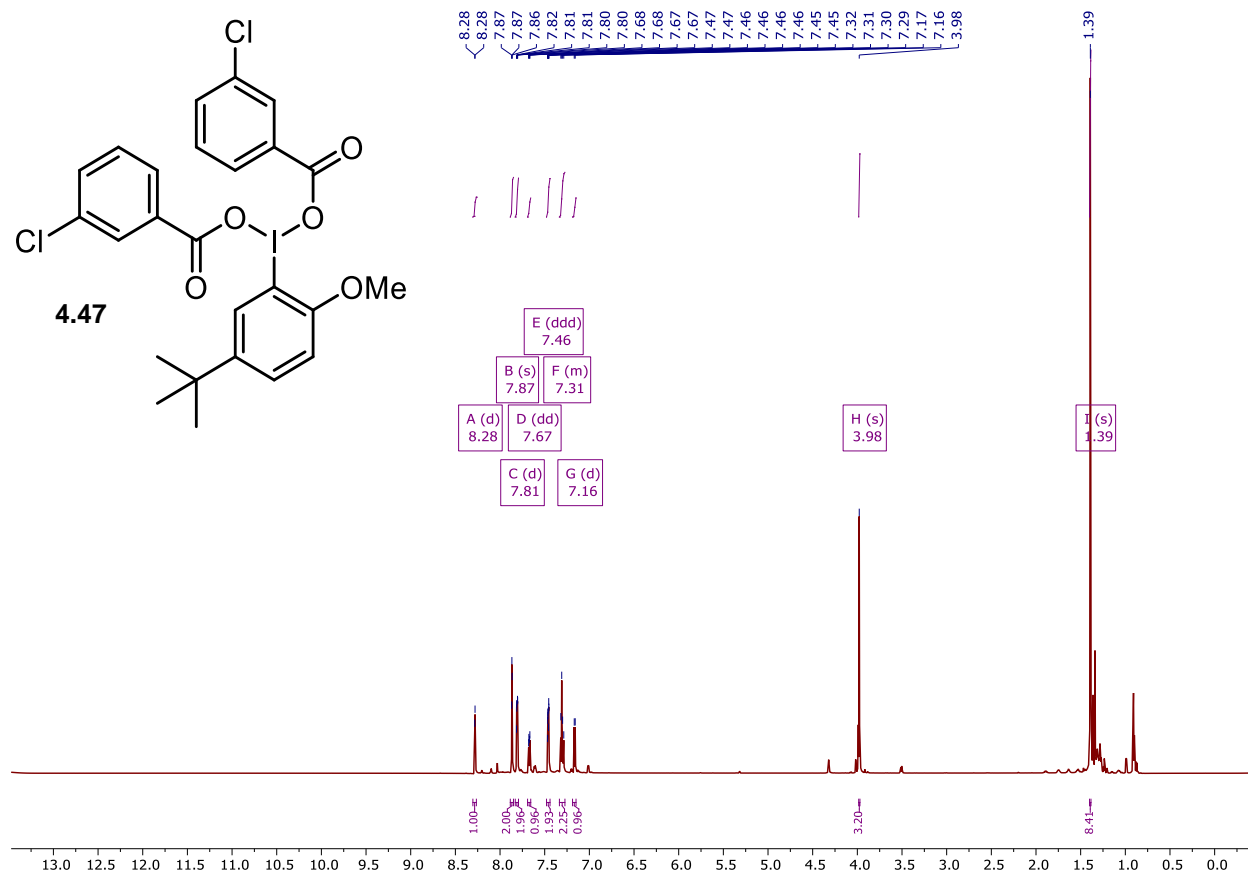


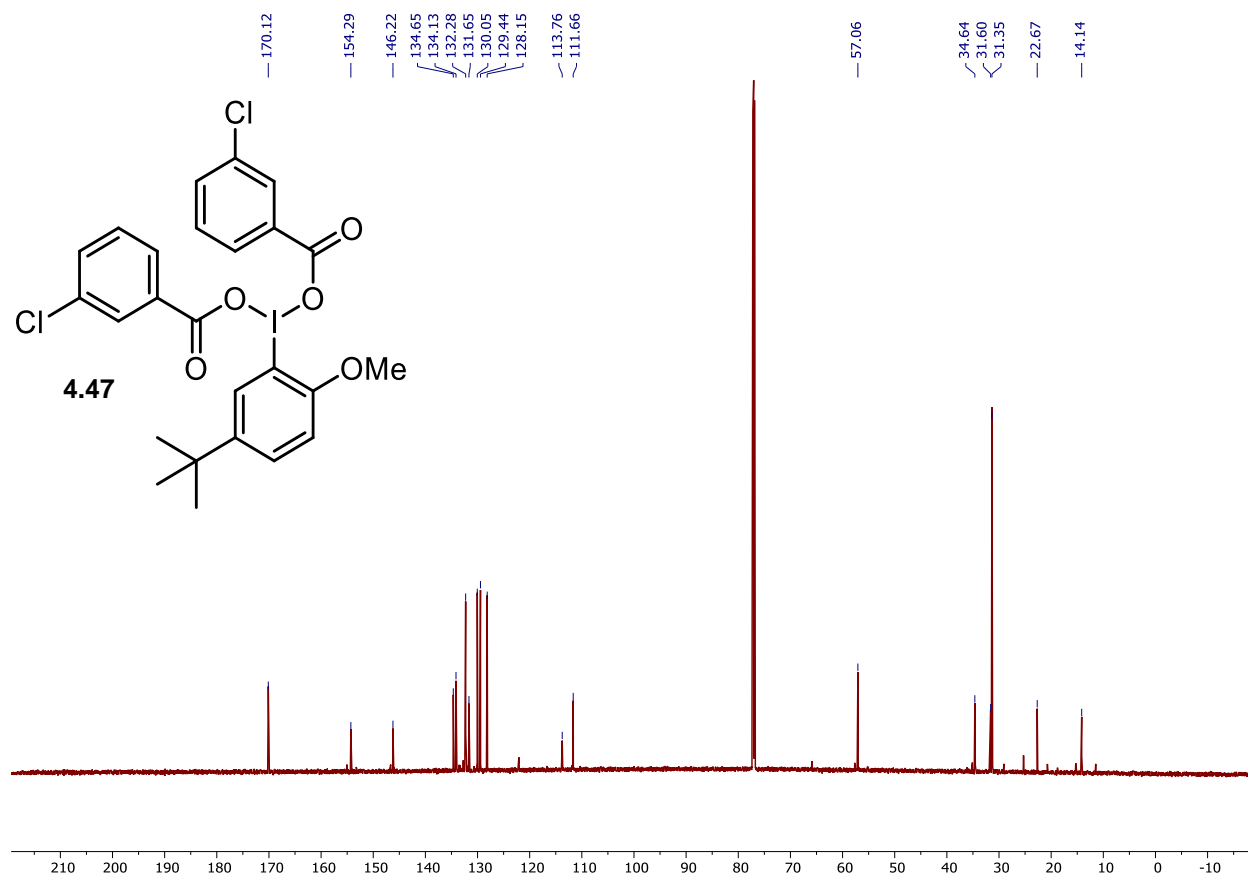
(5-(tert-butyl)-2-methoxyphenyl)-1,3-iodanediyl bis(3-chlorobenzoate) was synthesized following the general oxidation of iodoarenes procedure B on a 34.4 mmol scale of 4-(tert-butyl)-2-iodo-1-methoxybenzene, as the respective aryl iodide, to give 17.9 g of an off yellow solid (29.6 mmol, 86 % yield).

¹H NMR (800 MHz, CDCl₃) δ 8.28 (d, *J* = 2.3 Hz, 1H), 7.87 (s, 2H), 7.81 (d, *J* = 7.7 Hz, 2H), 7.67 (dd, *J* = 8.7, 2.3 Hz, 1H), 7.46 (ddd, *J* = 8.0, 2.4, 1.2 Hz, 2H), 7.34 – 7.27 (m, 2H), 7.16 (d, *J* = 8.6 Hz, 1H), 3.98 (s, 3H), 1.39 (s, 9H) ppm

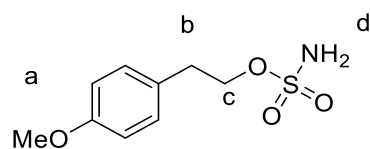
^{13}C NMR (201 MHz, CDCl_3) δ 170.2, 154.4, 146.3, 134.7, 134.2, 132.3, 131.7, 130.1, 129.5, 128.2, 113.8, 111.7, 57.1, 34.7, 31.4 ppm.

Elemental Analysis Calc'd for $\text{C}_{25}\text{H}_{23}\text{Cl}_2\text{IO}_5$: C, 49.94; H, 3.86; N, 0.0; Found: C, 47.51; H, 3.54; N, 0.03.





4-methoxyphenethyl sulfamate (4.48)



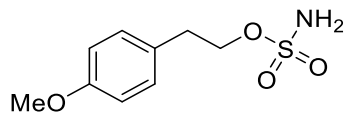
4-methoxyphenethyl sulfamate was synthesized following the general sulfamate synthesis procedure on a 45 mmol scale of 2-(4-methoxyphenyl)ethan-1-ol, as the respective alcohol. The reaction mixture was purified after workup using silica flash chromatography (20% to 40% to 60% EtOAc/hexanes) to give 7.26 g of white solid (32.0 mmol, 70% yield).

¹H NMR (600 MHz, CDCl₃) δ 7.17 – 7.14 (m, 2H), 6.88 – 6.85 (m, 2H), 4.53 (H_d, s, 2H), 4.37 (H_c, t, *J* = 7.0 Hz, 2H), 3.80 (H_a, s, 3H), 3.00 (H_b, t, *J* = 6.9 Hz, 2H) ppm.

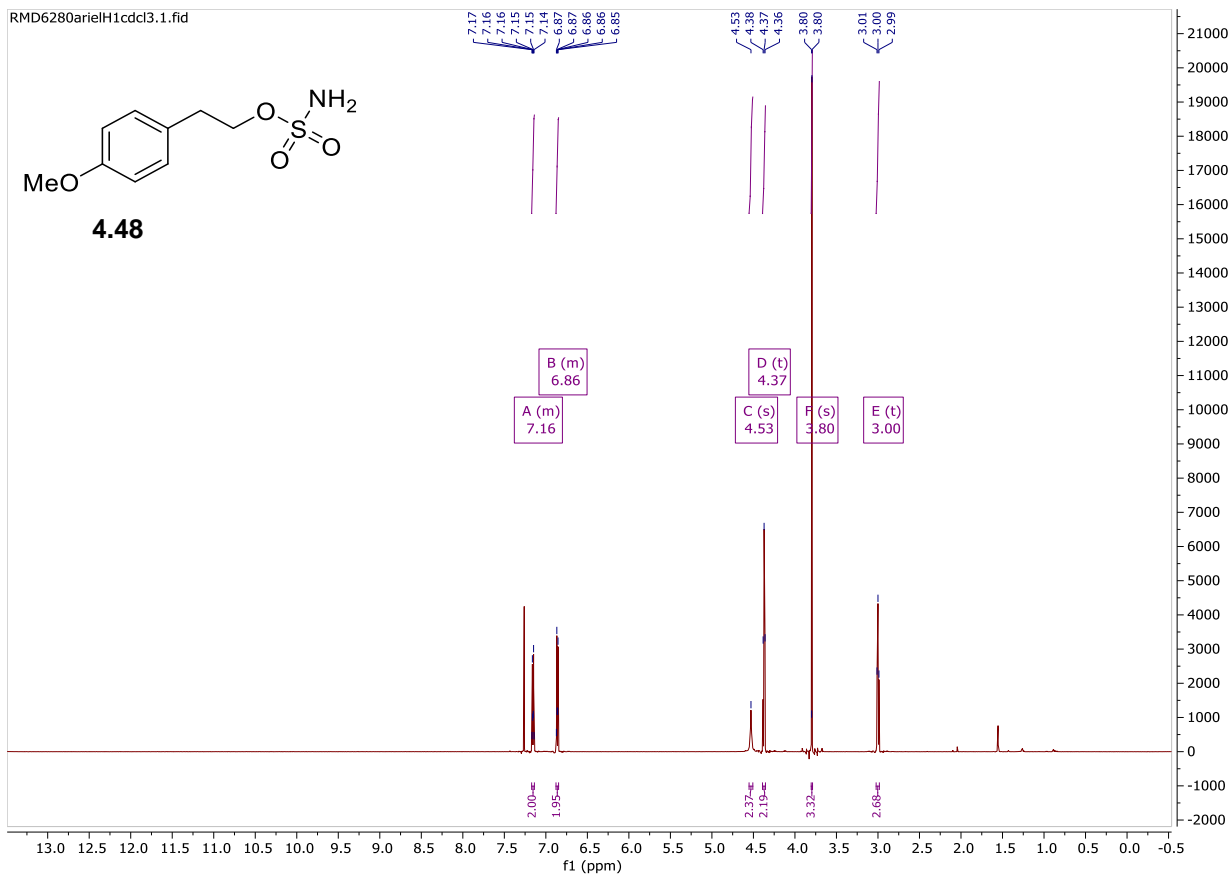
¹³C NMR (201 MHz, CDCl₃) δ 158.6, 130.0, 128.4, 114.1, 71.8, 55.3, 34.4 ppm.

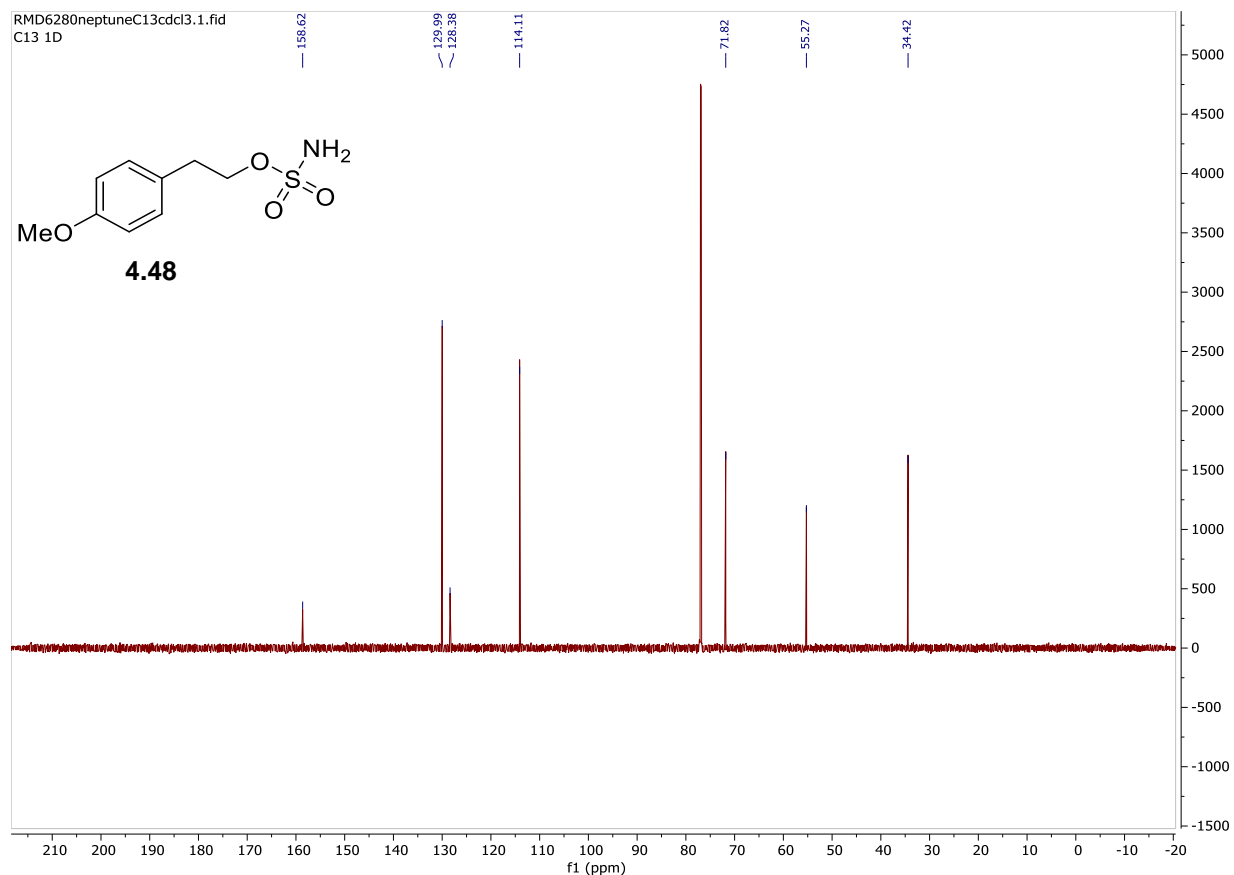
NMR spectra are consistent with literature reports.⁵

RMD6280arielH1cdcl3.1.fid

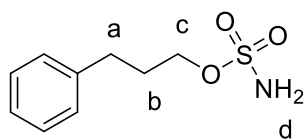


4.48





3-phenylpropyl sulfamate (4.49)

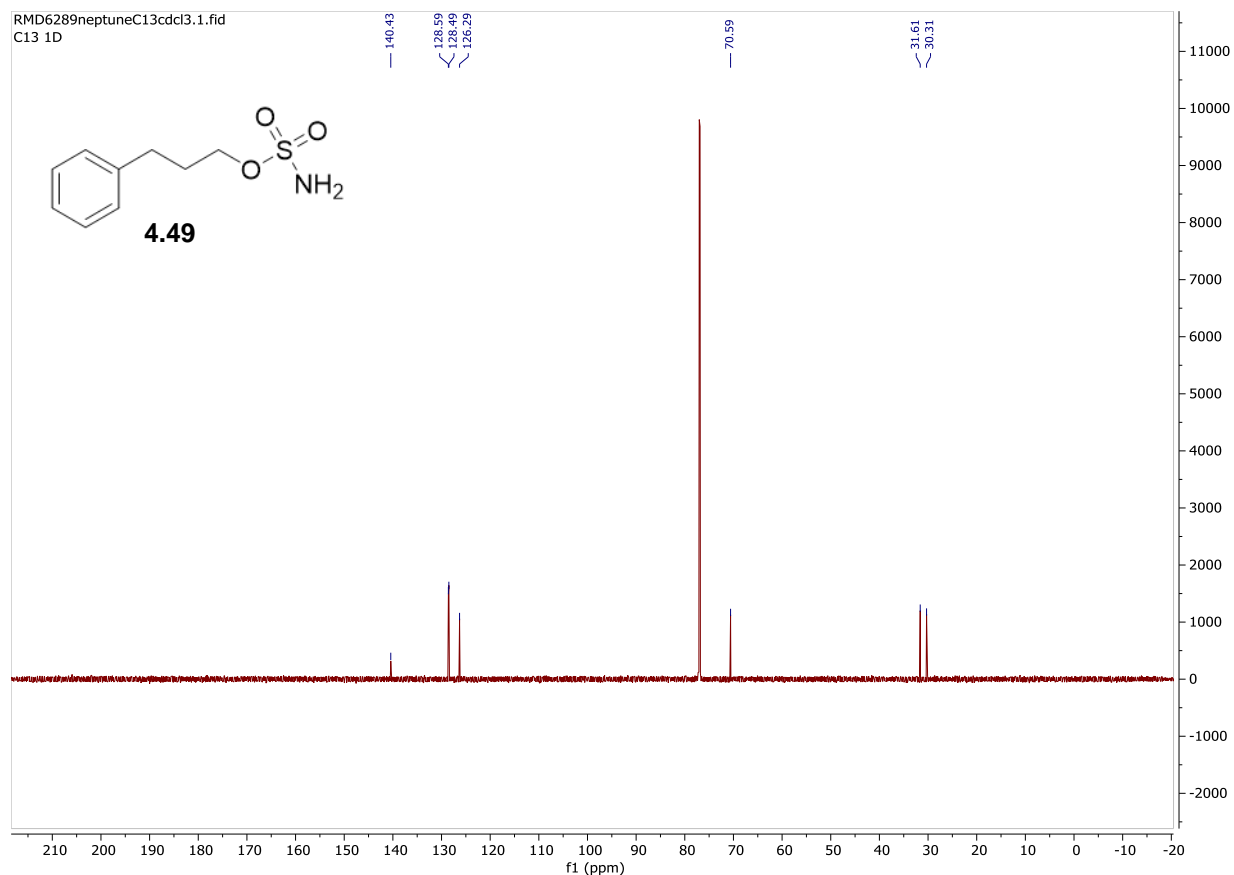


3-phenylpropyl sulfamate was synthesized following the general sulfamate synthesis procedure on a 45 mmol scale of 3-phenylpropan-1-ol, as the respective alcohol. The reaction mixture was purified after workup using silica flash chromatography (20% to 40% to 60% EtOAc/hexanes) to give 6.74 g of white solid (31.5 mmol, 70% yield).

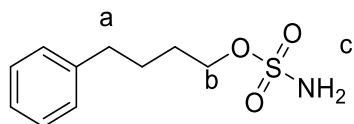
¹H NMR (600 MHz, CDCl₃) δ 7.30 (d, *J* = 7.4 Hz, 2H), 7.23 – 7.18 (m, 3H), 4.60 (H_d, s, 2H), 4.23 (H_c, t, *J* = 6.3 Hz, 2H), 2.76 (H_a, t, *J* = 7.7 Hz, 2H), 2.12 – 2.05 (H_b, m, 2H) ppm.

¹³C NMR (201 MHz, CDCl₃) δ 140.4, 128.5, 128.4, 126.2, 70.5, 31.6, 30.3 ppm.

NMR spectra are consistent with literature reports.⁶



4-phenylbutyl sulfamate (4.50)

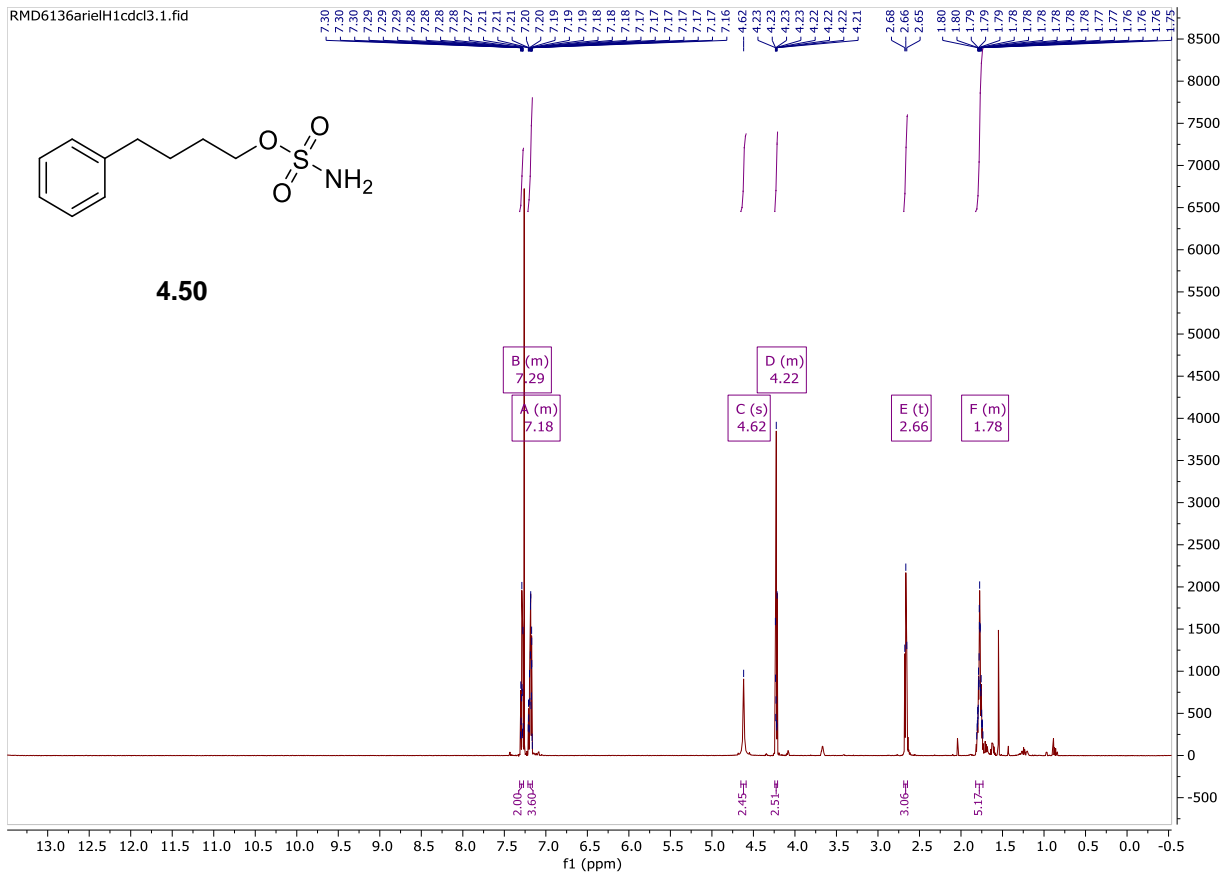


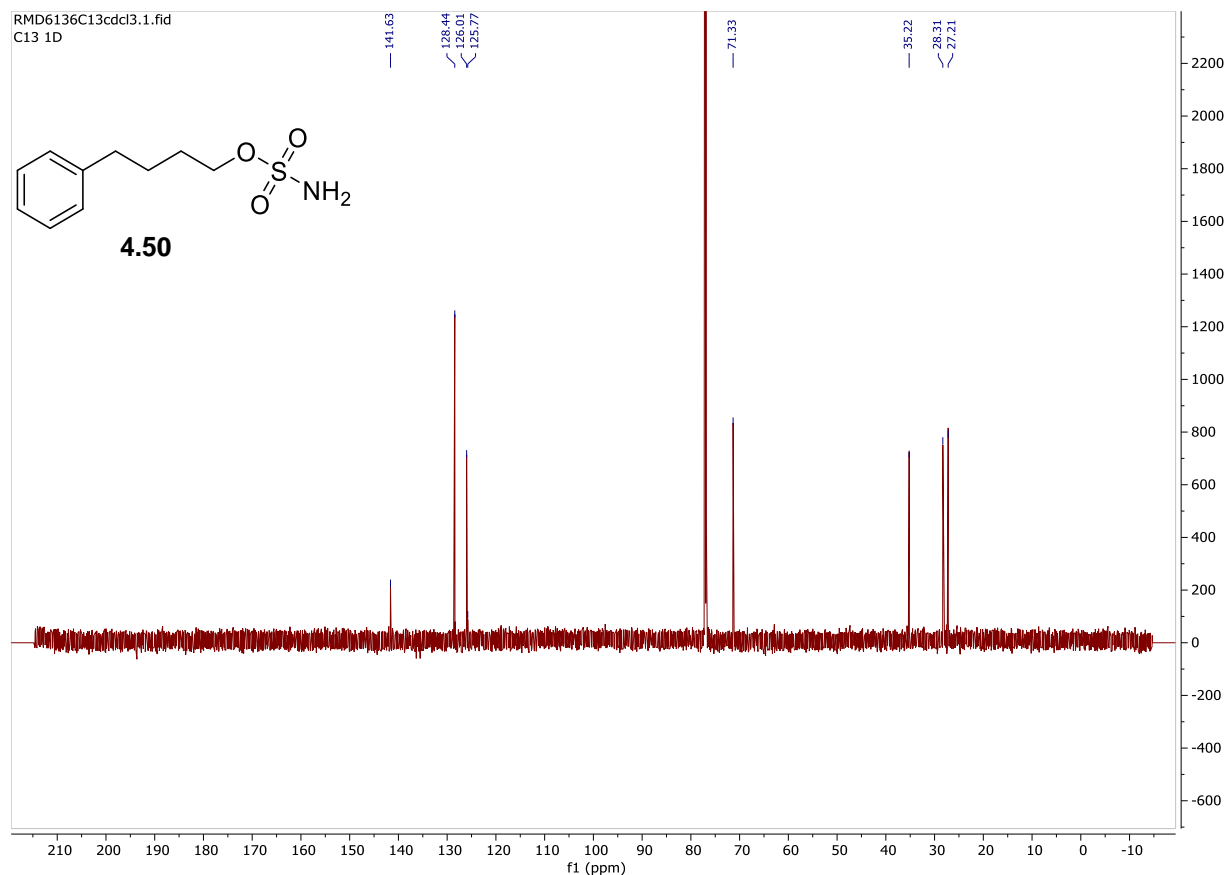
4-phenylbutyl sulfamate was synthesized following the general sulfamate synthesis procedure on a 20 mmol scale of 4-phenylbutan-1-ol, as the respective alcohol. The reaction mixture was purified after workup using silica flash chromatography (20% to 40% to 60% EtOAc/hexanes) to give 6.74 g of white solid (15.4 mmol, 77% yield).

¹H NMR (600 MHz CDCl₃) δ 7.32 – 7.27 (m, 2H), 7.22 – 7.16 (m, 3H), 4.62 (Hc, s, 2H), 4.24 – 4.21 (Hb, m, 2H), 2.66 (Ha, t, *J* = 7.2 Hz, 2H), 1.82 – 1.74 (m, 4H) ppm.

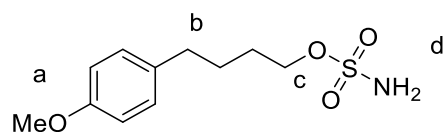
¹³C NMR (201 MHz, CDCl₃) δ 141.6, 128.4, 126.0, 125.8, 71.3, 35.2, 28.3, 27.2 ppm.

HRMS Calc'd for C₁₀H₁₅N₃S for (M+H): 230.0851 Found: 230.0835





4-(4-methoxyphenyl)butyl sulfamate (4.51)

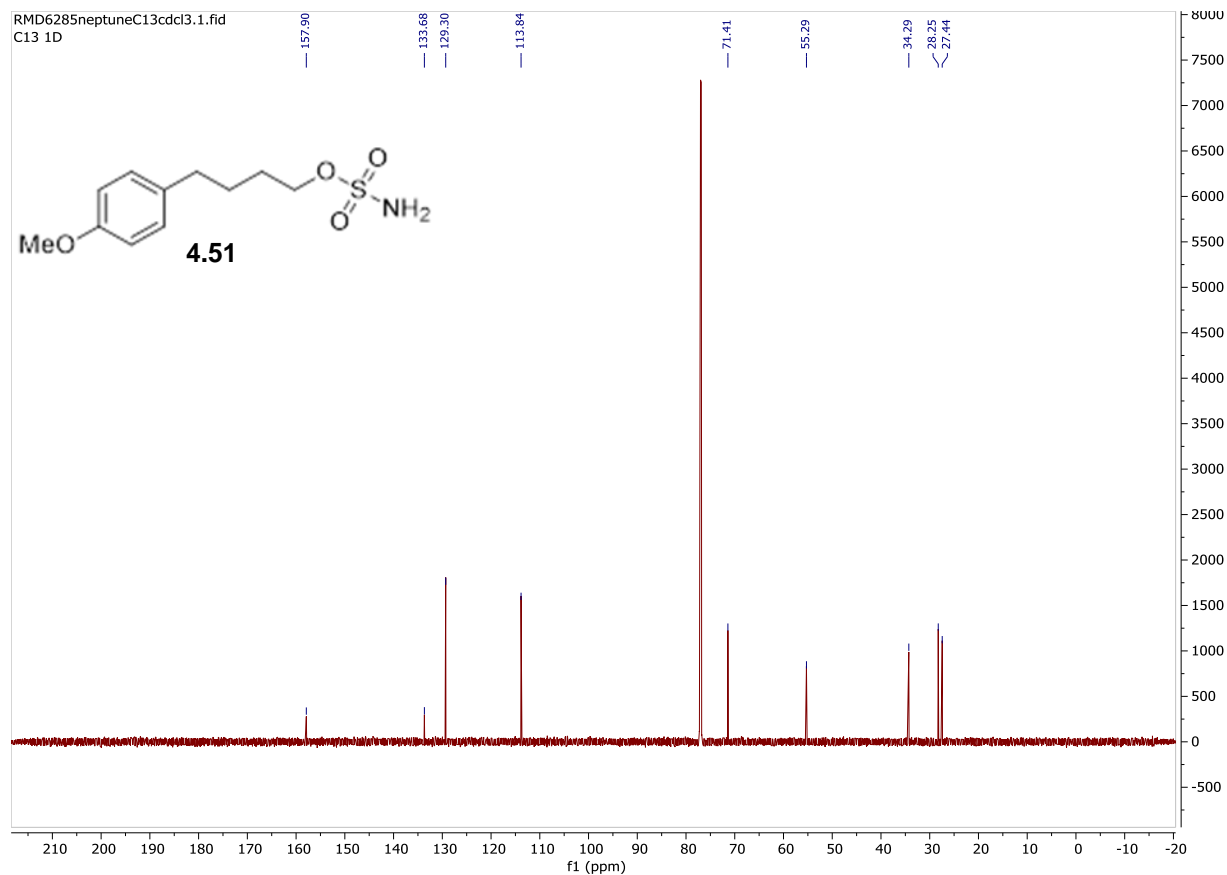


4-(4-methoxyphenyl)butyl sulfamate was synthesized following the general sulfamate synthesis procedure on a 45 mmol scale of 4-(4-methoxyphenyl)butan-1-ol, as the respective alcohol . The reaction mixture was purified after workup using silica flash chromatography (20% to 40% to 60% EtOAc/hexanes) to give 7.56 g of white solid (29.2 mmol, 64% yield).

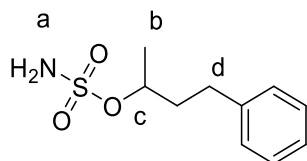
¹H NMR (600 MHz, CDCl₃) δ 7.11 – 7.07 (m, 2H), 6.85 – 6.81 (m, 2H), 4.60 (H_d, s, 2H), 4.22 (H_c, td, *J* = 6.4, 1.7 Hz, 2H), 3.79 (H_a, s, 3H), 2.60 (H_b, dd, *J* = 8.4, 6.3 Hz, 2H), 1.81 – 1.68 (m, 4H) ppm.

¹³C NMR (201 MHz, CDCl₃) δ 157.9, 133.6, 129.3, 113.8, 71.4, 55.2, 34.2, 28.2, 27.4 ppm.

HRMS Calc'd for C₁₁H₁₇NO₄S (M+Na): 282.0776 Found: 282.0756



4-phenylbutan-2-yl sulfamate (4.52)

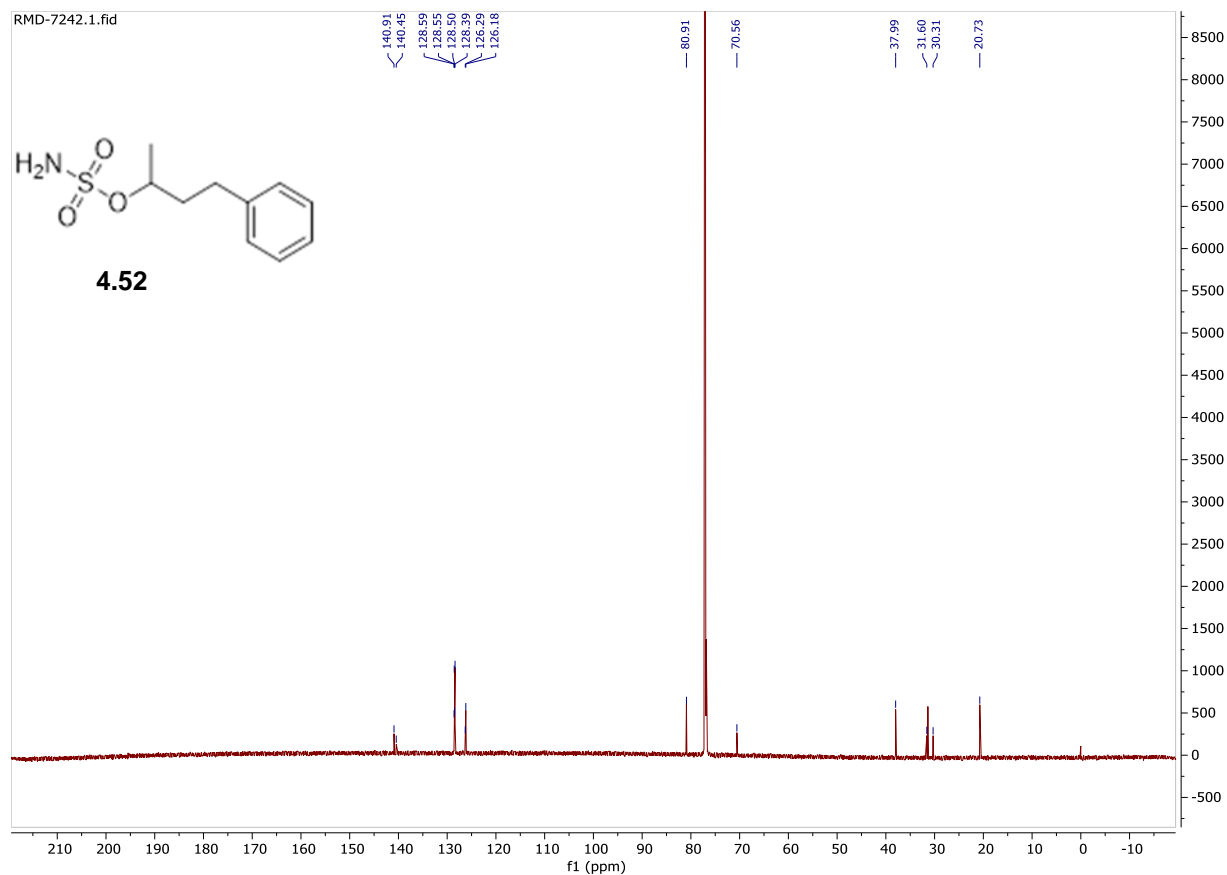


4-phenylbutan-2-yl sulfamate was synthesized following the general sulfamate synthesis procedure on a 10 mmol scale of 4-phenylbutan-2-ol, as the respective alcohol. The reaction mixture was purified after workup using silica flash chromatography (40% to 60% EtOAc/hexanes) to give 1.37 g of a white solid (6.00 mmol, 60% yield).

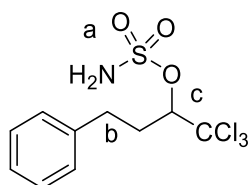
¹H NMR (600 MHz, CDCl₃) δ 7.33 – 7.28 (m, 2H), 7.24 – 7.18 (m, 3H), 4.80 – 4.71 (Hc, m, 1H), 4.64 – 4.56 (Ha, m, 2H), 2.83 – 2.69 (Hd, m, 2H), 2.14 – 2.05 (m, 1H), 2.01 – 1.90 (m, 1H), 1.47 (Hb, d, *J* = 6.3 Hz, 3H) ppm.

¹³C NMR (201 MHz, CDCl₃) δ 140.91, 128.55, 128.39, 126.18, 80.91, 37.99, 31.60, 30.31, 20.73 ppm.

NMR spectra are consistent with literature reports.⁷



1,1,1-trichloro-4-phenylbutan-2-yl sulfamate (4.53)

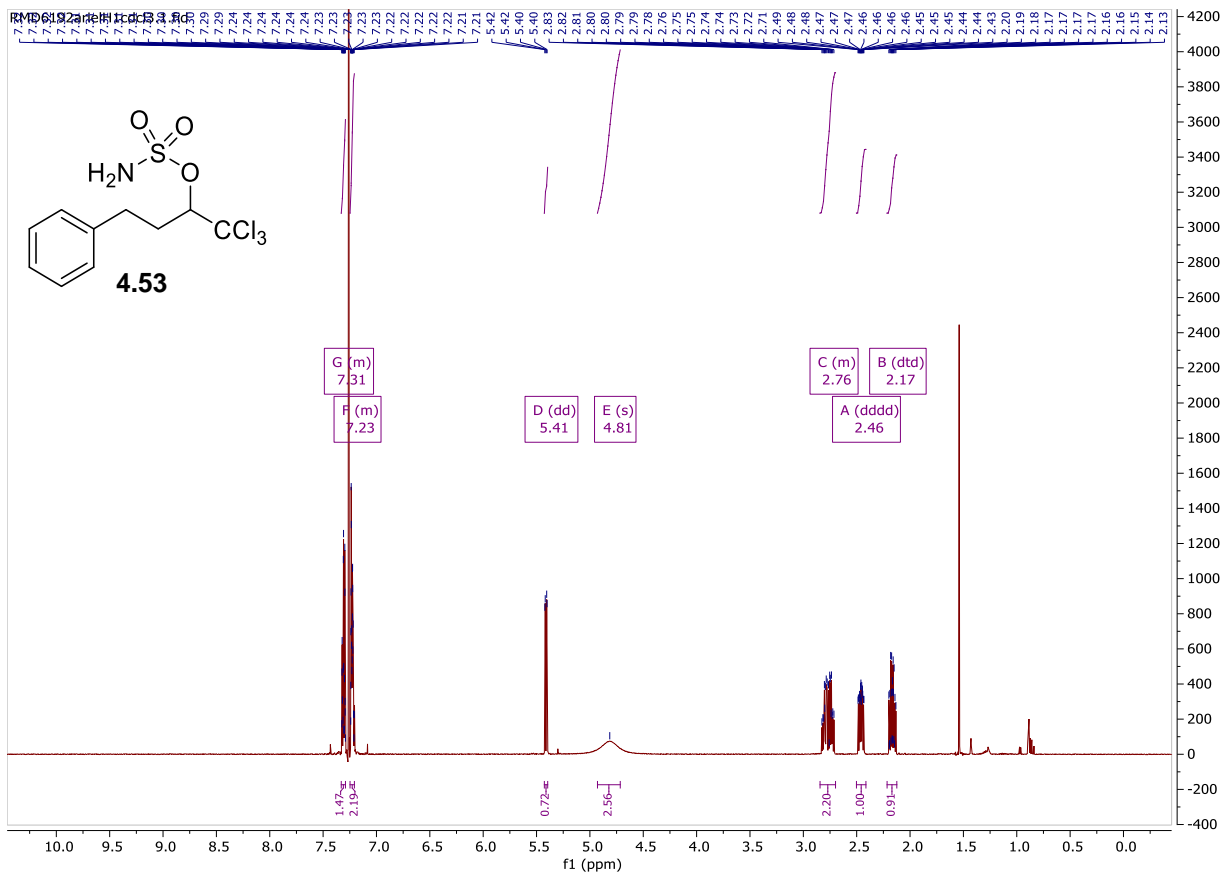


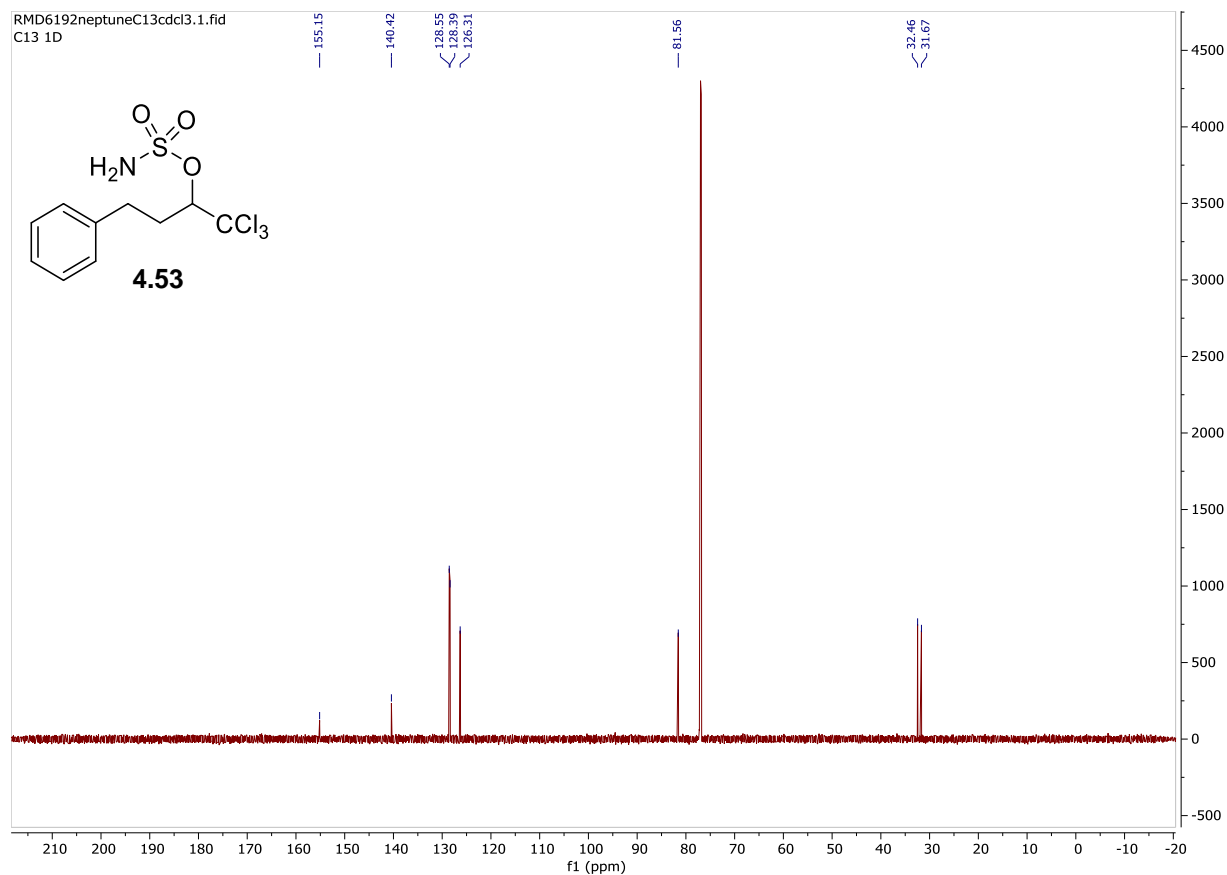
1,1,1-trichloro-4-phenylbutan-2-yl sulfamate was synthesized following the general sulfamate synthesis procedure on a 20 mmol scale of 1,1,1-trichloro-4-phenylbutan-2-ol, as the respective alcohol. The reaction mixture was purified after workup using silica flash chromatography (40% to 60% EtOAc/hexanes) to give 2.26 g of off white thick oil (6.80 mmol, 34% yield).

¹H NMR (600 MHz, CDCl₃) δ 7.33 – 7.29 (m, 2H), 7.25 – 7.21 (m, 3H), 5.41 (H_c, dd, *J* = 10.2, 2.0 Hz, 1H), 4.81 (H_a, s, 2H), 2.84 – 2.70 (H_b, m, 2H), 2.46 (dddd, *J* = 14.1, 10.2, 6.6, 2.0 Hz, 1H), 2.17 (dtd, *J* = 14.1, 10.0, 5.4 Hz, 1H) ppm.

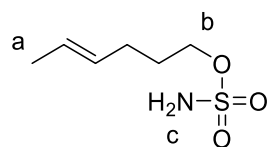
¹³C NMR (201 MHz, CDCl₃) δ 155.1, 140.4, 128.5, 128.3, 126.1, 81.5, 32.4, 31.7 ppm.

HRMS Calc'd for C₁₀H₁₂Cl₃NO₃S (M+Na): 353.9501 Found: 353.9495





(E)-hex-4-en-1-yl sulfamate (4.54)



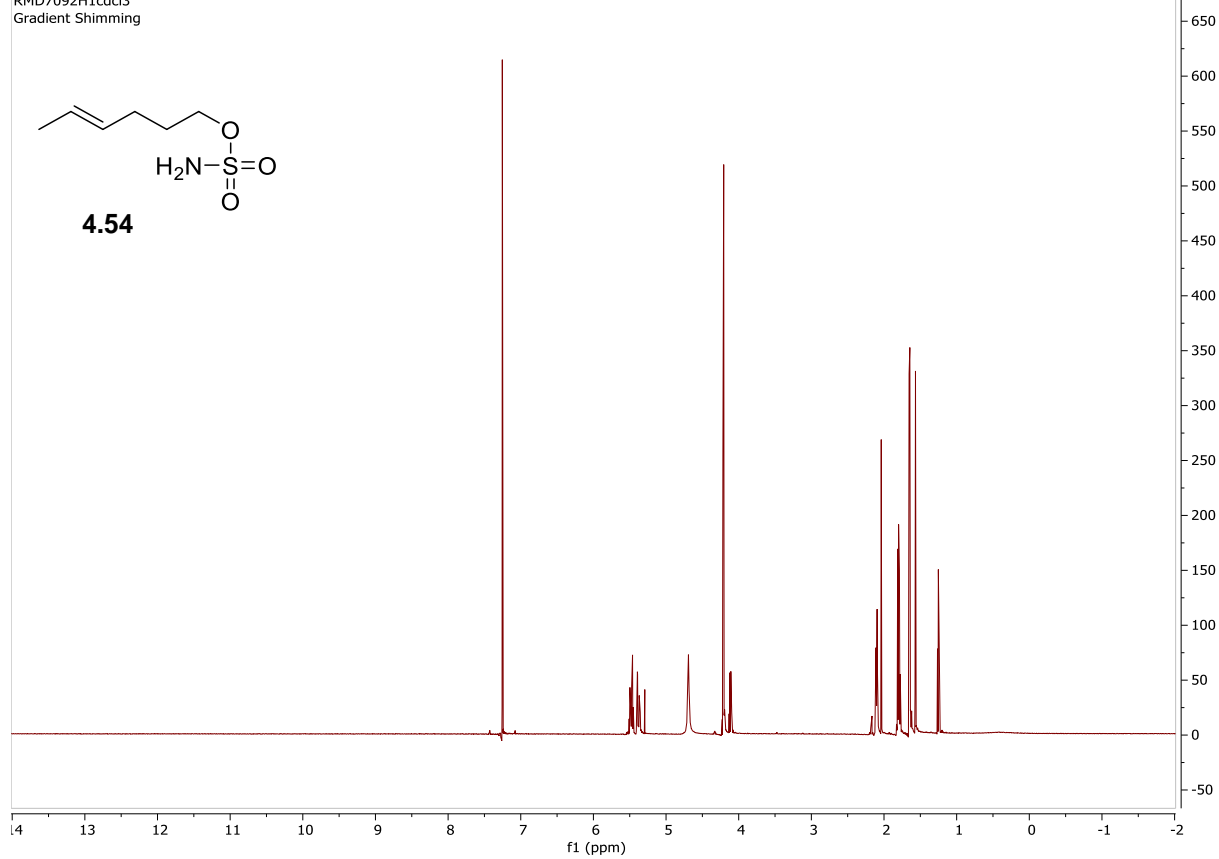
(E)-hex-4-en-1-yl sulfamate was synthesized following the general sulfamate synthesis procedure on a 20 mmol scale of (E)-hex-4-en-1-ol, as the respective alcohol. The reaction mixture was purified after workup using silica flash chromatography (40% EtOAc/hexanes) to give 3.56 g of a white solid (19.8 mmol, 99% yield).

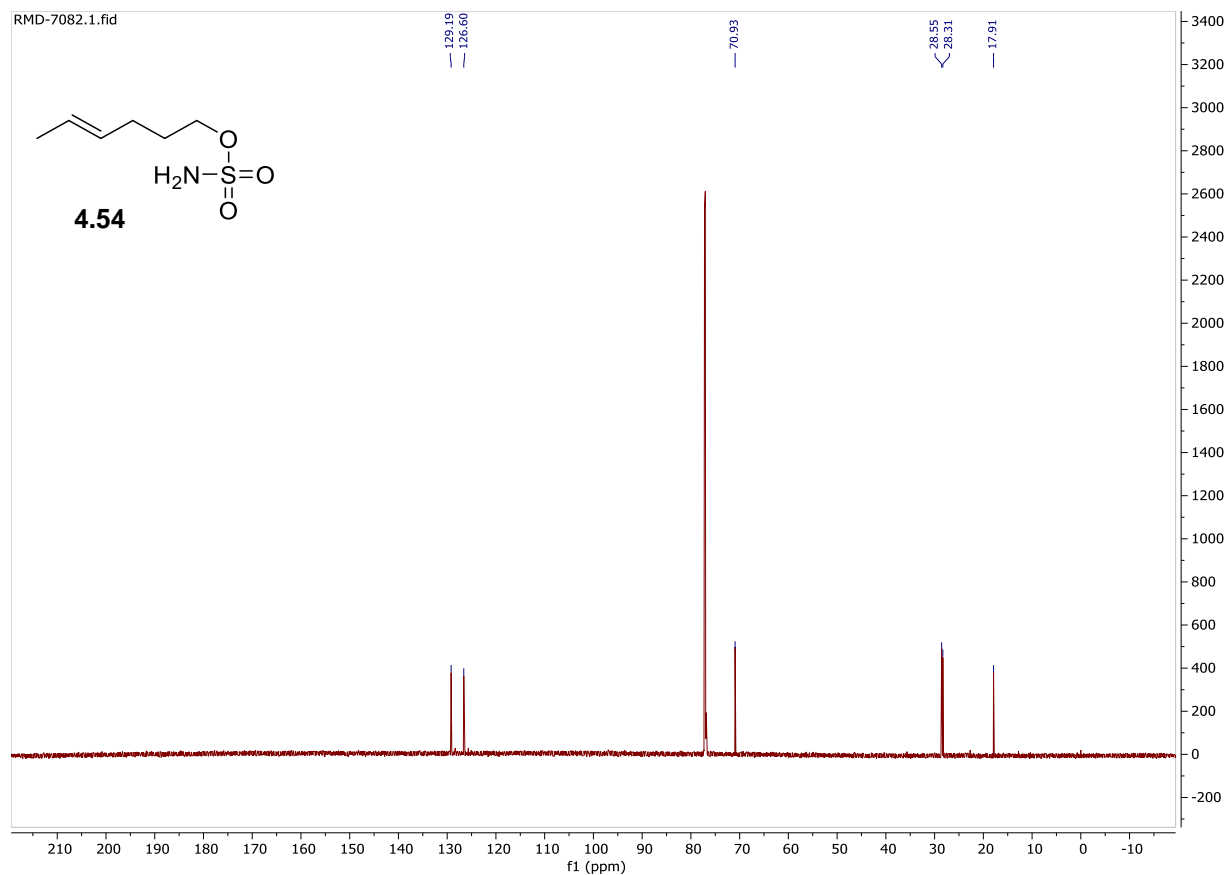
¹H NMR (600 MHz, CDCl₃) δ 5.53 – 5.43 (m, 1H), 5.43 – 5.33 (m, 1H), 4.69 (Hc, s, 2H), 4.21 (Hb, t, *J* = 6.5 Hz, 2H), 2.12 – 2.08 (m, 2H), 1.80 (tt, *J* = 8.1, 6.6 Hz, 2H), 1.65 (Ha, ddd, *J* = 6.3, 1.3 Hz, 3H) ppm.

¹³C NMR (201 MHz, CDCl₃) δ 129.2, 126.6, 70.9, 28.6, 28.3, 17.9 ppm.

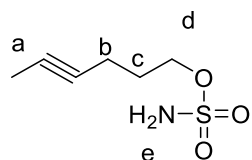
NMR spectra are consistent with literature reports.⁸

RMD7092H1cdcl3
Gradient Shimming





hex-4-yn-1-yl sulfamate (4.55)

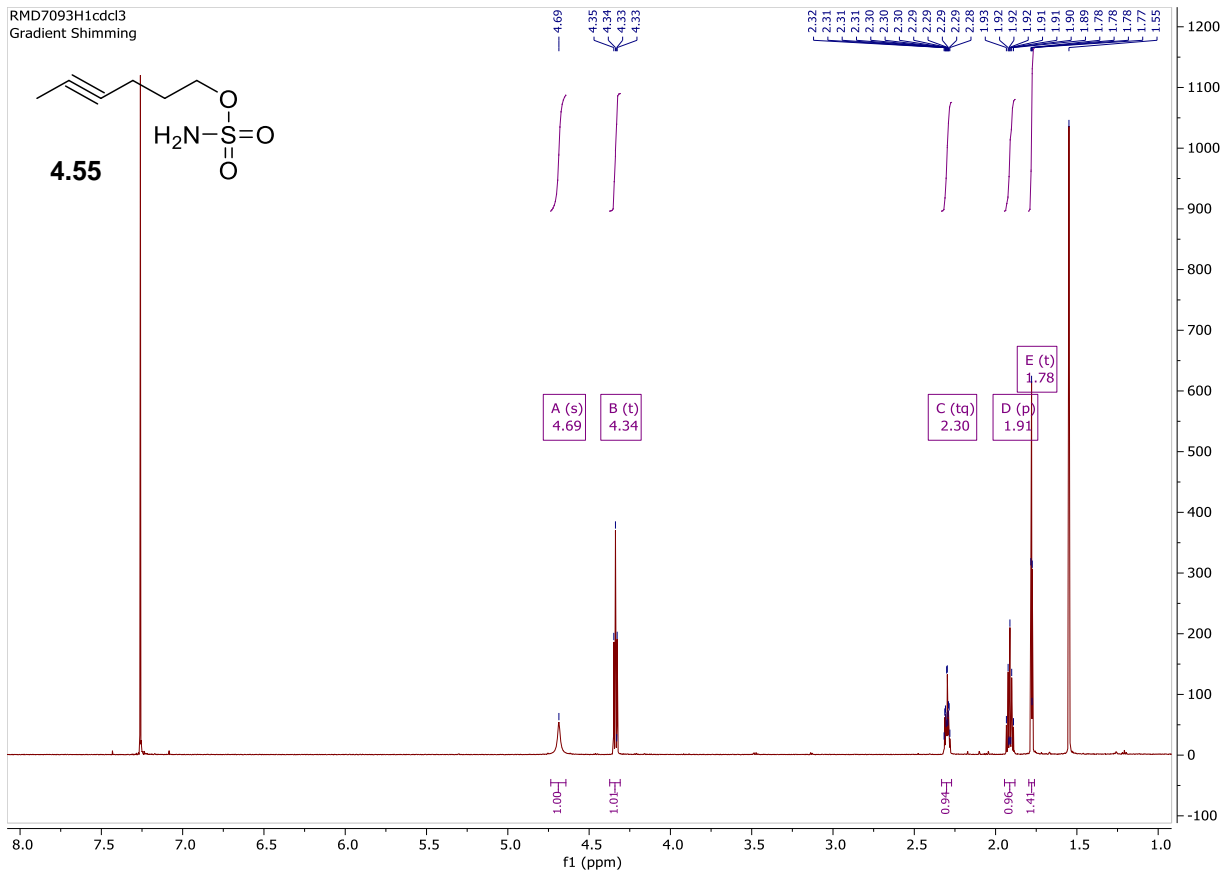


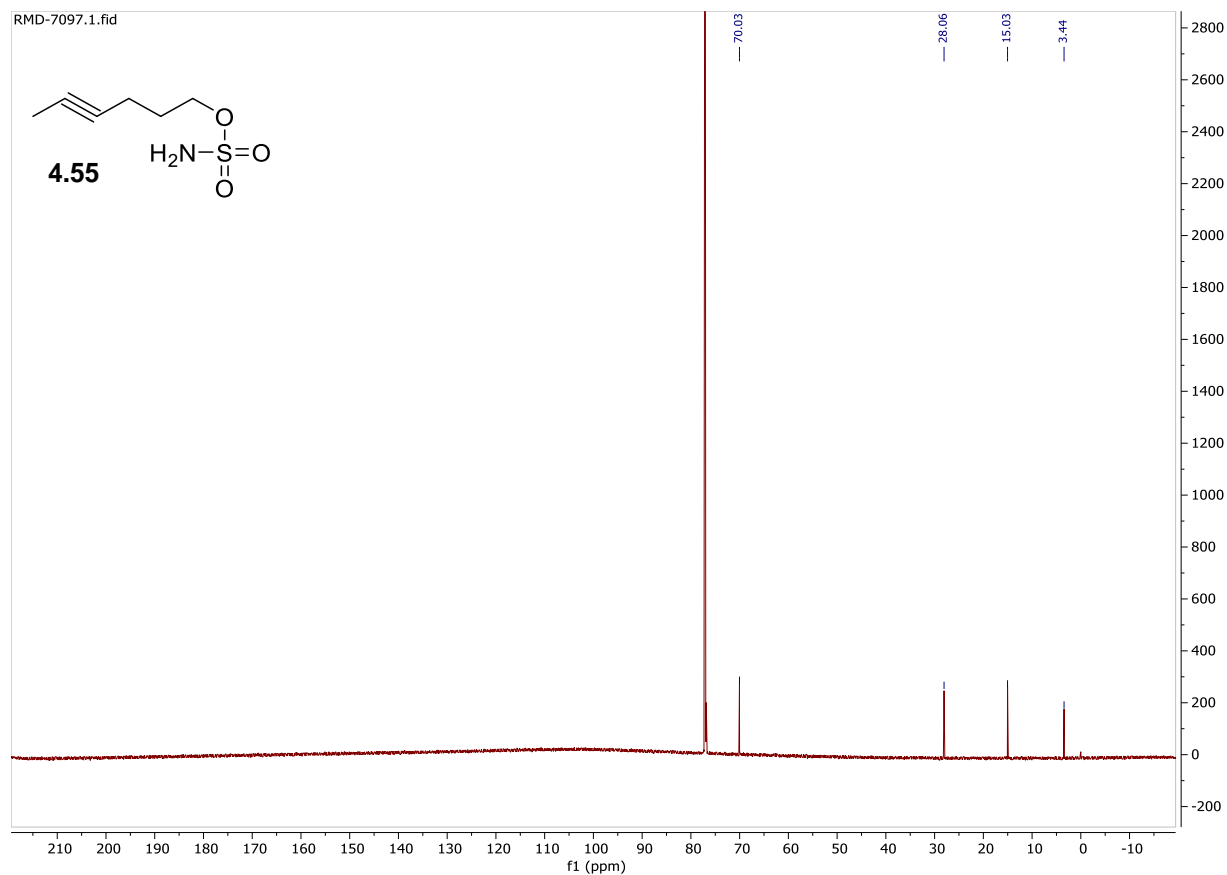
hex-4-yn-1-yl sulfamate was synthesized following the general sulfamate synthesis procedure on a 5.38 mmol scale of hex-4-yn-1-ol, as the respective alcohol. The reaction mixture was purified after workup using silica flash chromatography (40% EtOAc/hexanes) to give 0.640 g of a white solid (3.61 mmol, 67% yield).

¹H NMR (600 MHz, CCl₃) δ 4.69 (He, s, 2H), 4.34 (Hd, t, *J* = 6.2 Hz, 2H), 2.30 (Ha, tq, *J* = 6.8, 2.5 Hz, 2H), 1.91 (Hc, p, *J* = 6.5 Hz, 2H), 1.78 (Hb, t, *J* = 2.6 Hz, 2H) ppm.

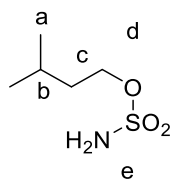
¹³C NMR (201 MHz, CDCl₃) δ 70.0, 28.1, 15.0, 3.4 ppm.

HRMS Calc'd for C₆H₁₁NO₃S (M+Na): 200.0357 Found: 200.0400.





Isopentyl sulfamate (4.56)



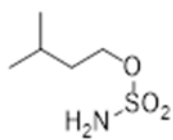
Isopentyl sulfamate was synthesized following the general sulfamate synthesis procedure on a 40 mmol scale of isopentyl alcohol, as the respective alcohol. The reaction mixture was purified after workup using silica flash chromatography (100% DCM) to give 6.10 g of a white solid (36.4 mmol, 91% yield).

¹H NMR (600 MHz, CDCl₃) δ 4.80 (He, s, 2H), 4.24 (Hd, t, *J* = 6.7 Hz, 2H), 1.76 (Hb, dp, *J* = 13.3, 6.7 Hz, 1H), 1.68 – 1.61 (Hc, m, 2H), 0.94 (Ha, d, *J* = 6.7 Hz, 6H) ppm.

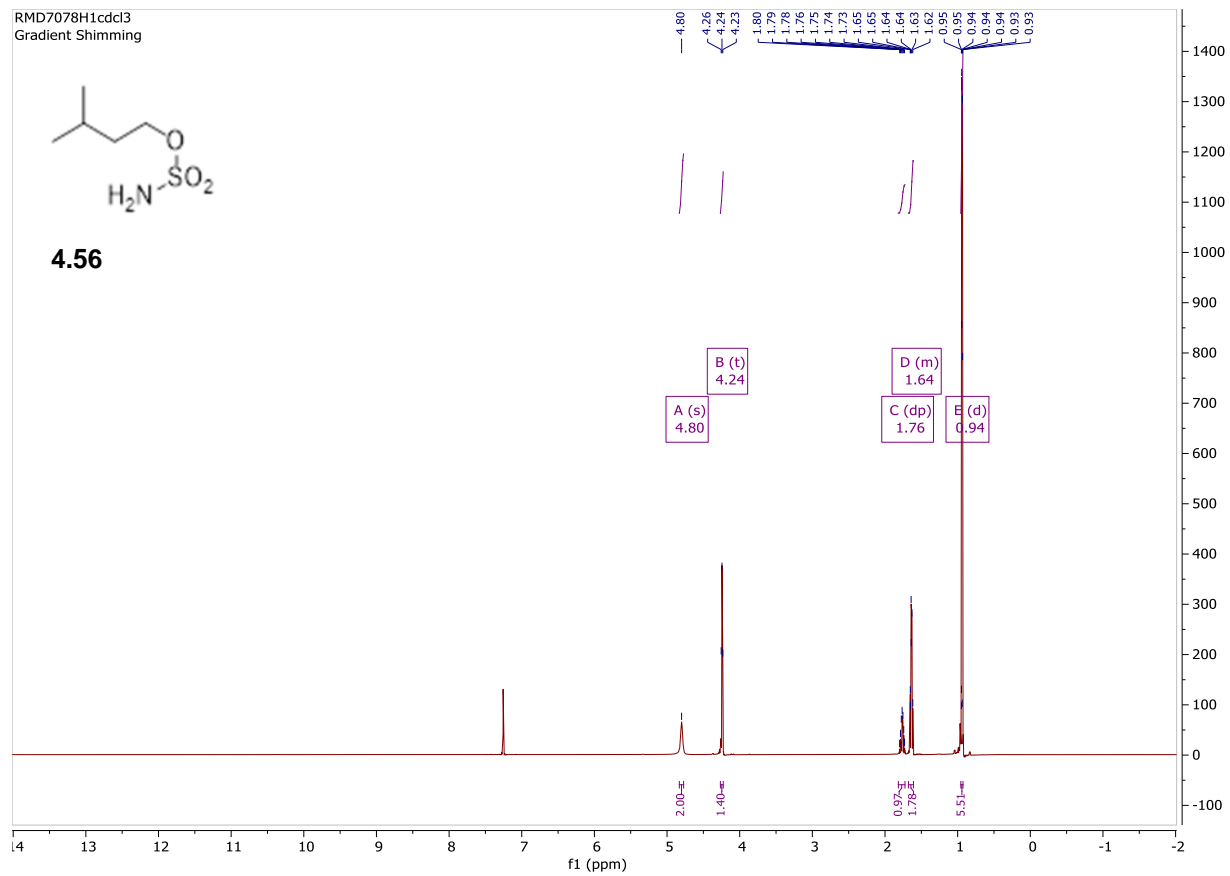
¹³C NMR (201 MHz, CDCl₃) δ 70.1, 37.3, 24.6, 22.3 ppm.

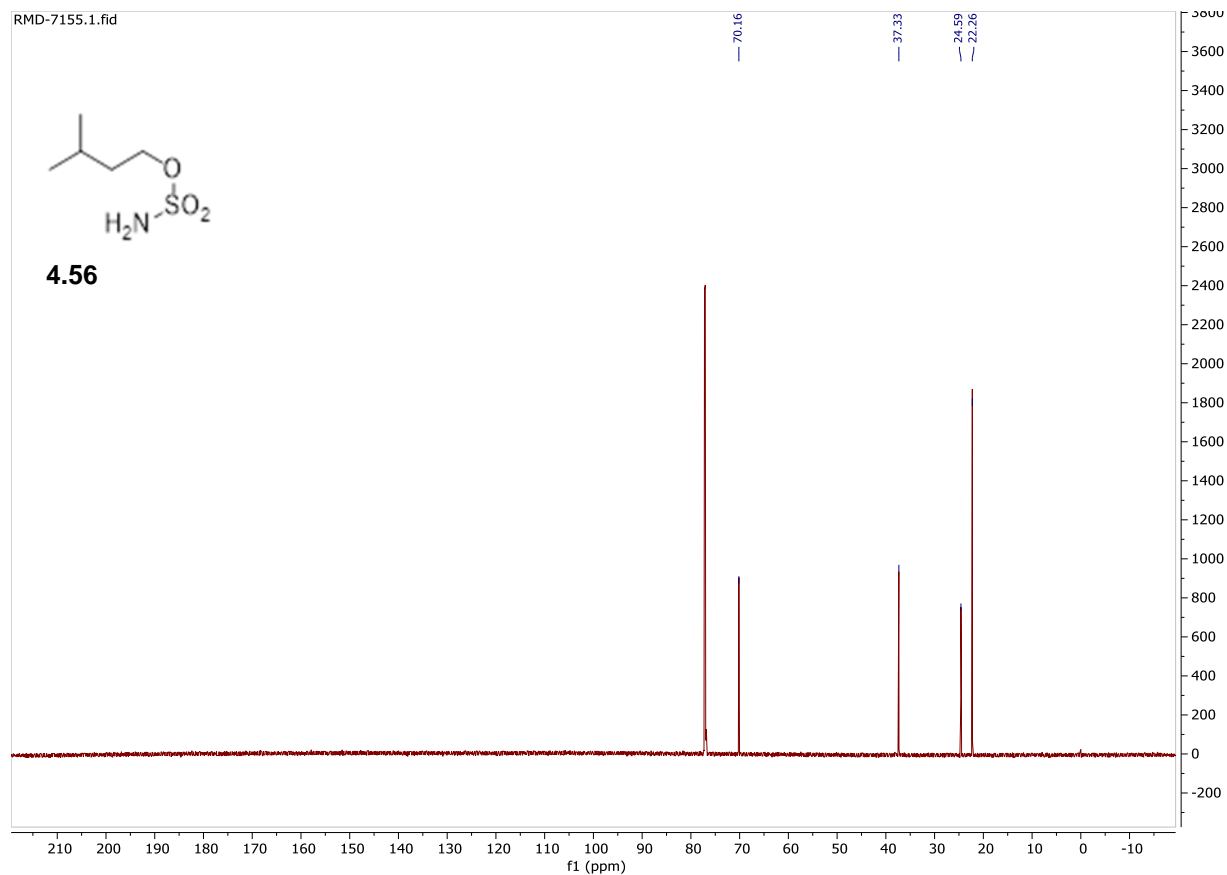
NMR spectra are consistent with literature reports.⁹

RMD7078H1cdcl3
Gradient Shimming

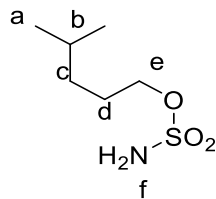


4.56





4-methylpentyl sulfamate (4.57)

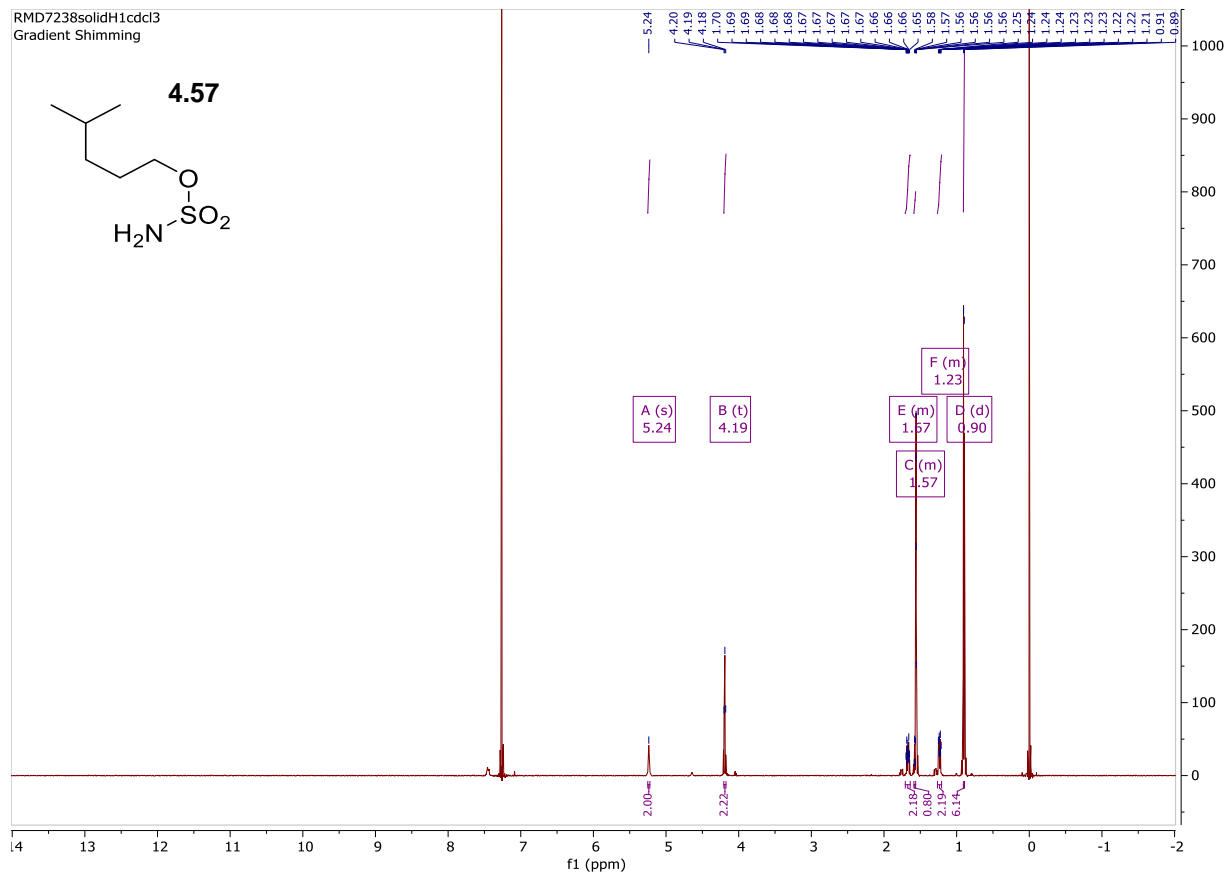
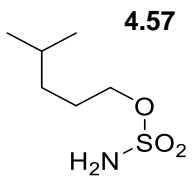


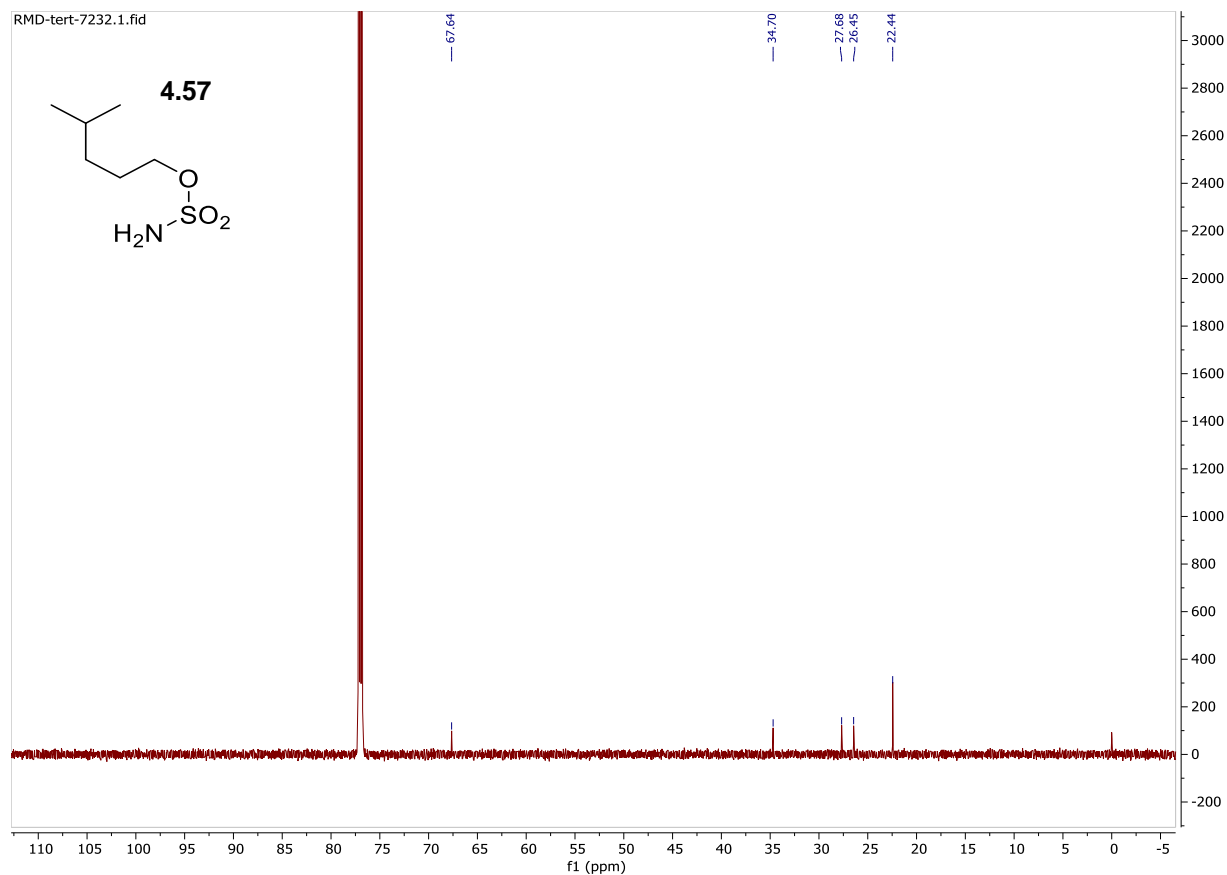
4-methylpentyl sulfamate was synthesized following the general sulfamate synthesis procedure on a 16.1 mmol scale of 4-methylpentyl alcohol, as the respective alcohol. The reaction mixture was purified after workup using silica flash chromatography (90% DCM/EtOAc) to give .380 g of a white solid (2.09 mmol, 13% yield).

¹H NMR (600 MHz CDCl₃) δ 5.24 (Hf, s, 2H), 4.19 (He, t, *J* = 6.8 Hz, 2H), 1.71 – 1.64 (Hd, m, 2H), 1.59 – 1.56 (Hb, m, 1H), 1.26 – 1.21 (Hc, m, 2H), 0.90 (Ha, d, *J* = 6.6 Hz, 6H) ppm.

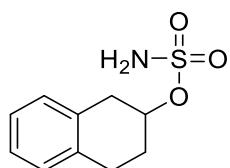
¹³C NMR (201 MHz, CDCl₃) δ 67.6, 34.7, 27.7, 26.4, 22.4 ppm.

RMD7238solidH1cdcl3
Gradient Shimming





1,2,3,4-tetrahydronaphthalen-2-yl sulfamate (4.58)



1,2,3,4-tetrahydronaphthalen-2-yl sulfamate was synthesized following the general sulfamate synthesis procedure on a 6.74 mmol scale of 1,2,3,4-tetrahydronaphthalen-2-ol, as the respective alcohol. The reaction mixture was purified after workup using silica flash chromatography (40% to 60% EtOAc/hexanes) to give 0.880 g of a white solid (3.87 mmol, 57% yield).

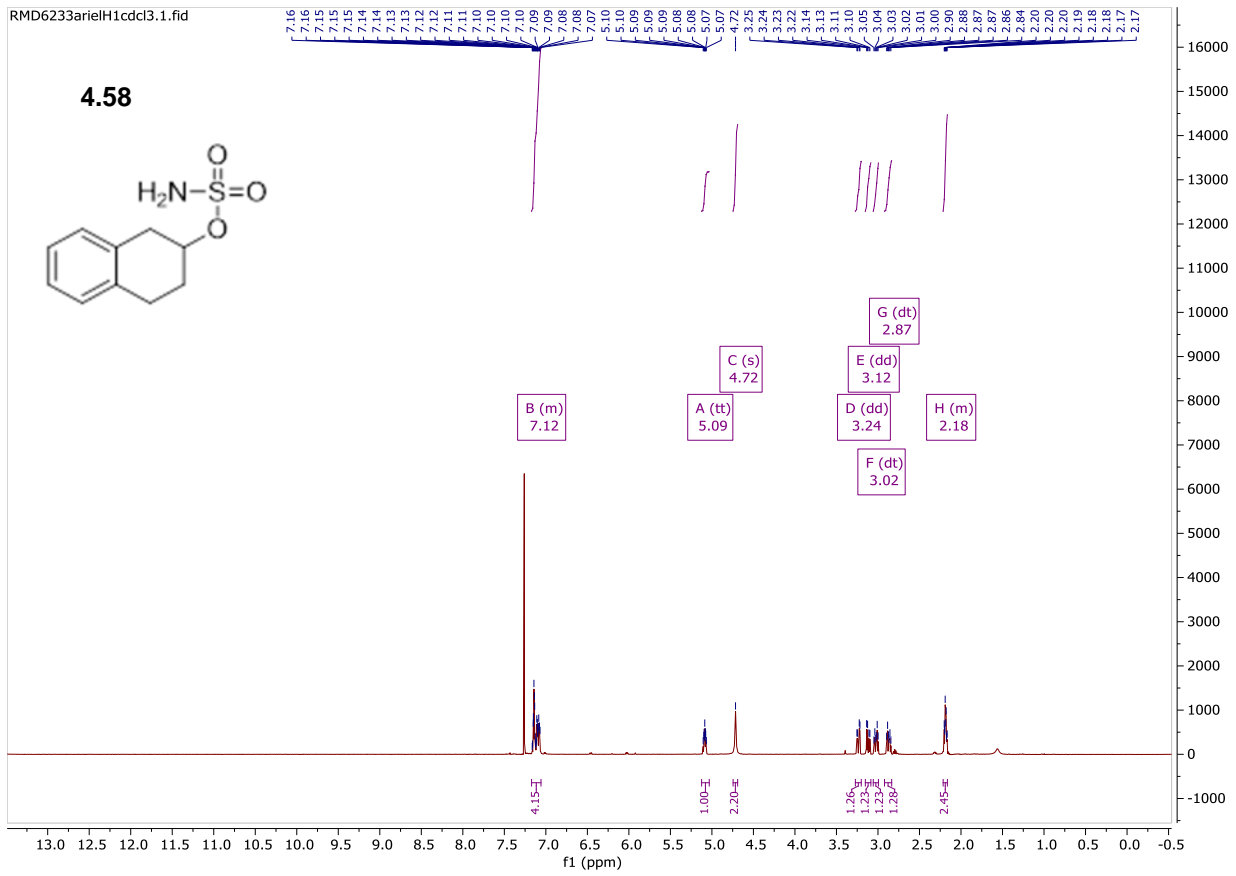
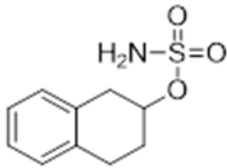
¹H NMR (600 MHz, CDCl₃) δ 7.17 – 7.06 (m, 4H), 5.09 (tt, *J* = 6.9, 4.7 Hz, 1H), 4.72 (s, 2H), 3.24 (dd, *J* = 16.8, 5.0 Hz, 1H), 3.12 (dd, *J* = 16.8, 6.7 Hz, 1H), 3.02 (dt, *J* = 16.9, 6.5 Hz, 1H), 2.87 (dt, *J* = 17.0, 6.9 Hz, 1H), 2.21 – 2.16 (m, 2H) ppm.

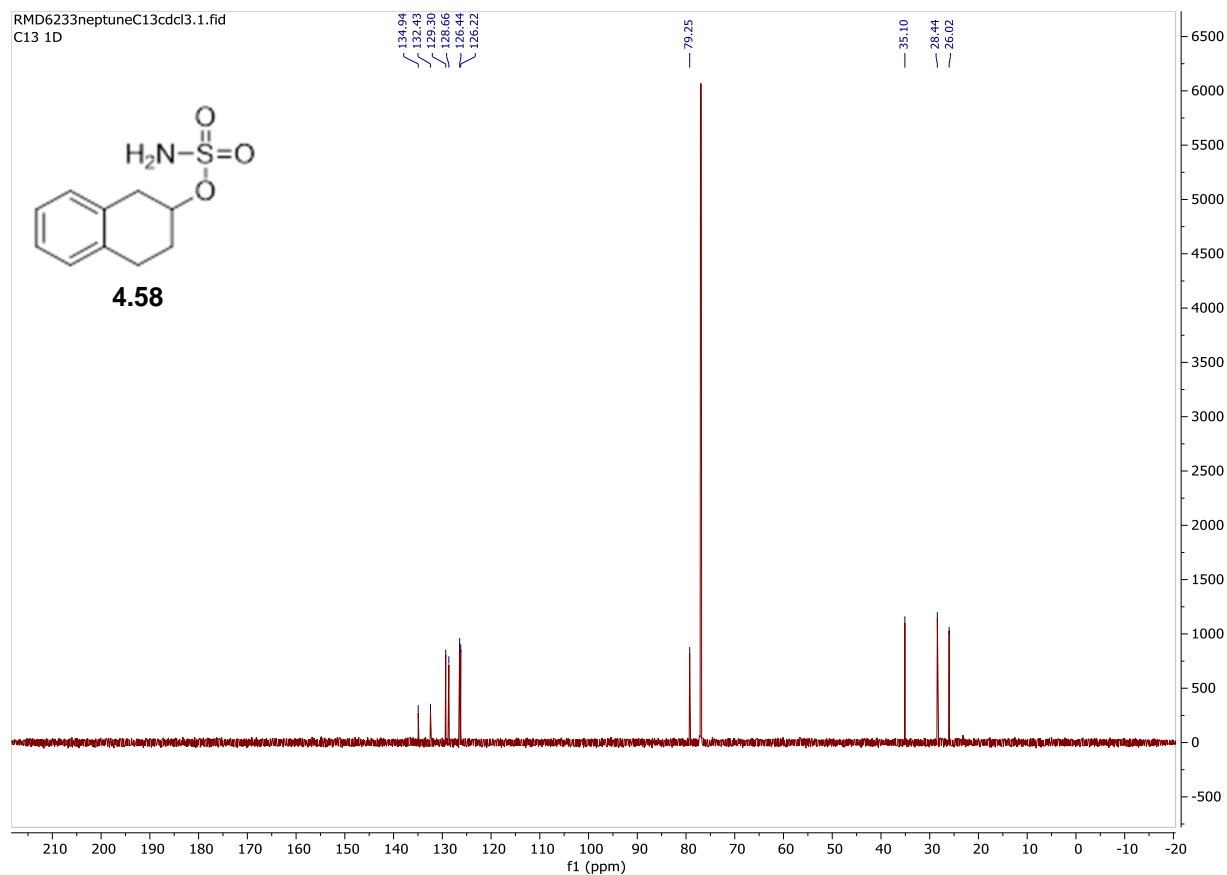
¹³C NMR (201 MHz, CDCl₃) δ 134.9, 132.4, 129.3, 128.6, 126.4, 126.2, 79.2, 35.1, 28.4, 26.0 ppm.

HRMS Calc'd for C₁₀H₁₃NO₃S (M+H): 228.0694 Found: 228.0740

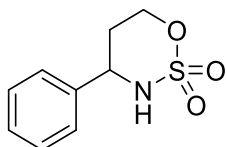
RMD6233arielH1cdcl3.1.fid

4.58





4-phenyl-1,2,3-oxathiazinane 2,2-dioxide (4.59)

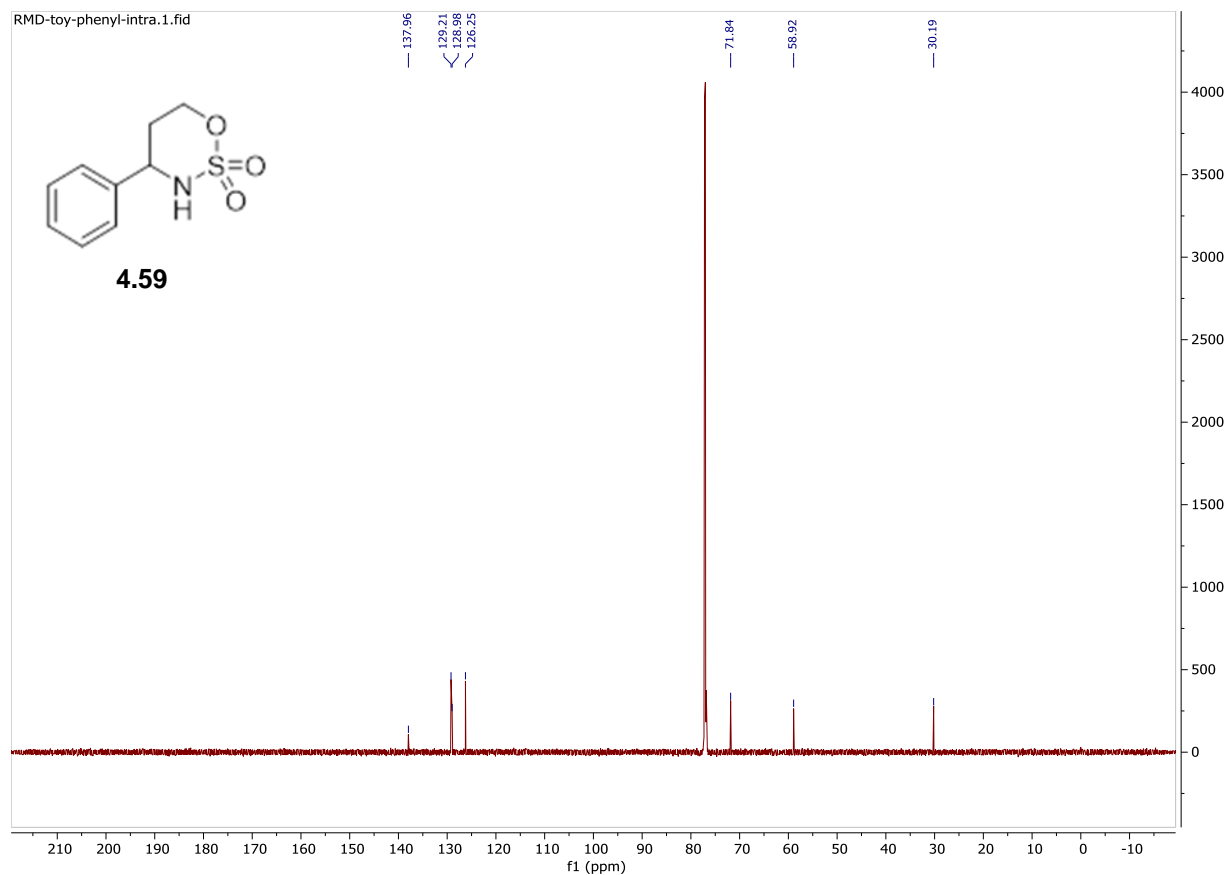


4-phenyl-1,2,3-oxathiazinane 2,2-dioxide was synthesized following the general amination procedure on a .2 mmol scale of 3-phenylpropyl sulfamate, as the respective sulfamate. 4-bromophenyl ((5-(tert-butyl)-2-methoxyphenyl)-I3-iodaneylidene)sulfamate was used as the respective iodine. The reaction mixture was purified after workup using silica flash chromatography (20% EtOAc/Hexanes) to give 0.005 g of a yellow solid (0.022 mmol, 11 % yield).

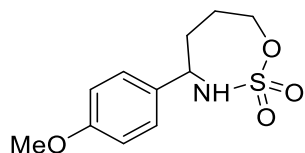
¹H NMR (600 MHz, CDCl₃) δ 7.44 – 7.34 (m, 5H), 4.91 – 4.85 (m, 2H), 4.67 (ddd, *J* = 11.7, 5.0, 1.6 Hz, 1H), 4.27 (d, *J* = 9.5 Hz, 1H), 2.25 (dtd, *J* = 14.4, 12.6, 5.0 Hz, 1H), 2.04 (dq, *J* = 14.5, 2.3 Hz, 1H) ppm.

¹³C NMR (201 MHz, CDCl₃) δ 138.0, 129.2, 129.0, 126.3, 71.8, 58.9, 30.2 ppm.

NMR spectra are consistent with literature reports.¹⁰



4-(4-methoxyphenyl)-1,2,3-oxathiazepane 2,2-dioxide (4.60)

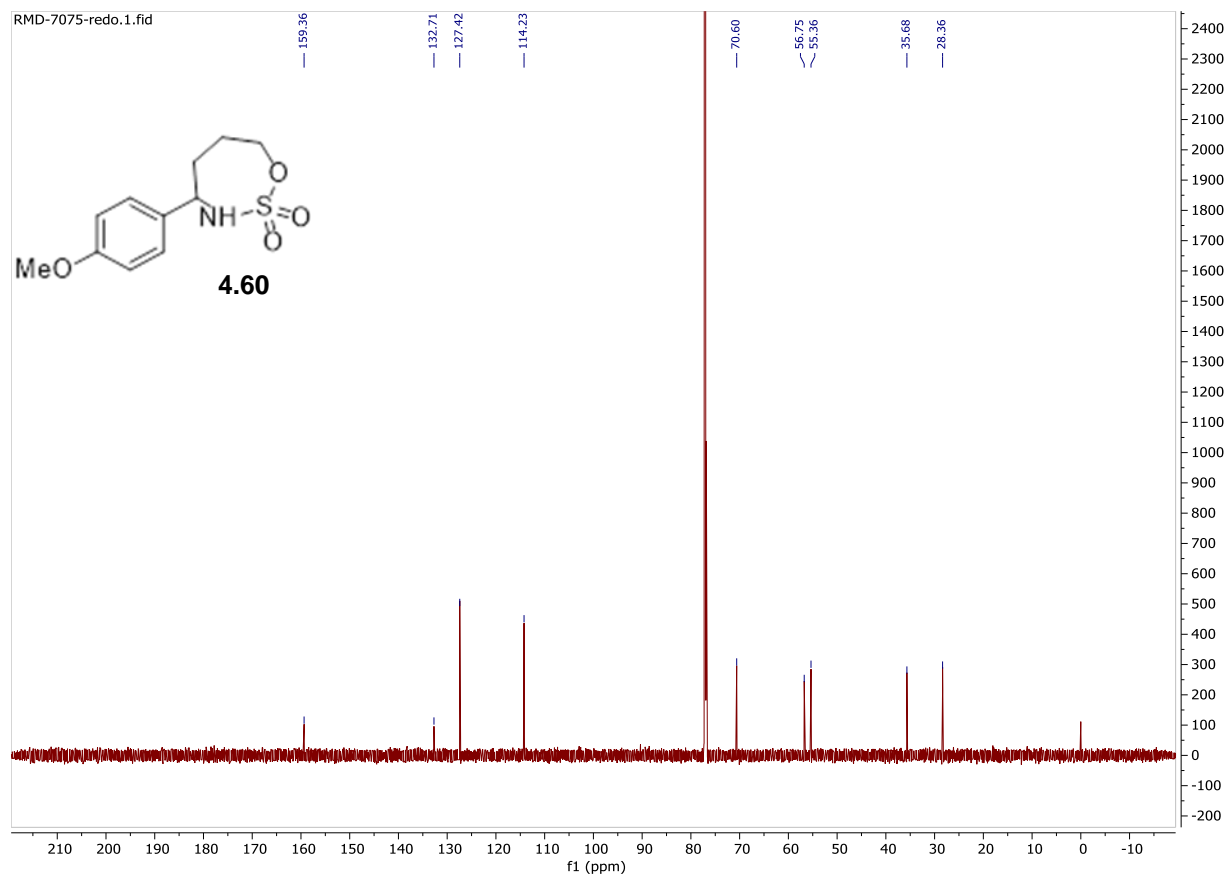


4-(4-methoxyphenyl)-1,2,3-oxathiazepane 2,2-dioxide was synthesized following the general amination procedure on a .2 mmol scale of 4-(4-methoxyphenyl)butyl sulfamate, as the respective sulfamate. 4-Bromophenyl ((5-(tert-butyl)-2-methoxyphenyl)-13-iodaneylidene)sulfamate was used as the respective iodine. The reaction mixture was purified after workup using silica flash chromatography (20% EtOAc/Hexanes) to give 0.010 g of an off yellow solid (0.036 mmol, 18% yield).

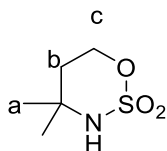
¹H NMR (600 MHz, CDCl₃) δ 7.29 – 7.26 (m, 2H), 6.91 – 6.87 (m, 2H), 4.85 (d, *J* = 8.2 Hz, 1H), 4.49 – 4.34 (m, 3H), 3.81 (s, 3H), 2.32 – 2.27 (m, 1H), 2.25 – 2.18 (m, 1H), 2.16 – 2.05 (m, 2H) ppm.

¹³C NMR (201 MHz, CDCl₃) δ 159.4, 132.7, 127.4, 114.2, 70.6, 56.7, 55.4, 35.7, 28.4 ppm.

HRMS Calc'd for C₁₁H₁₅NO₄S (M+Na): 280.0619 Found: 280.0589



4-(4-methoxyphenyl)-1,2,3-oxathiazinane 2,2-dioxide (4.62)



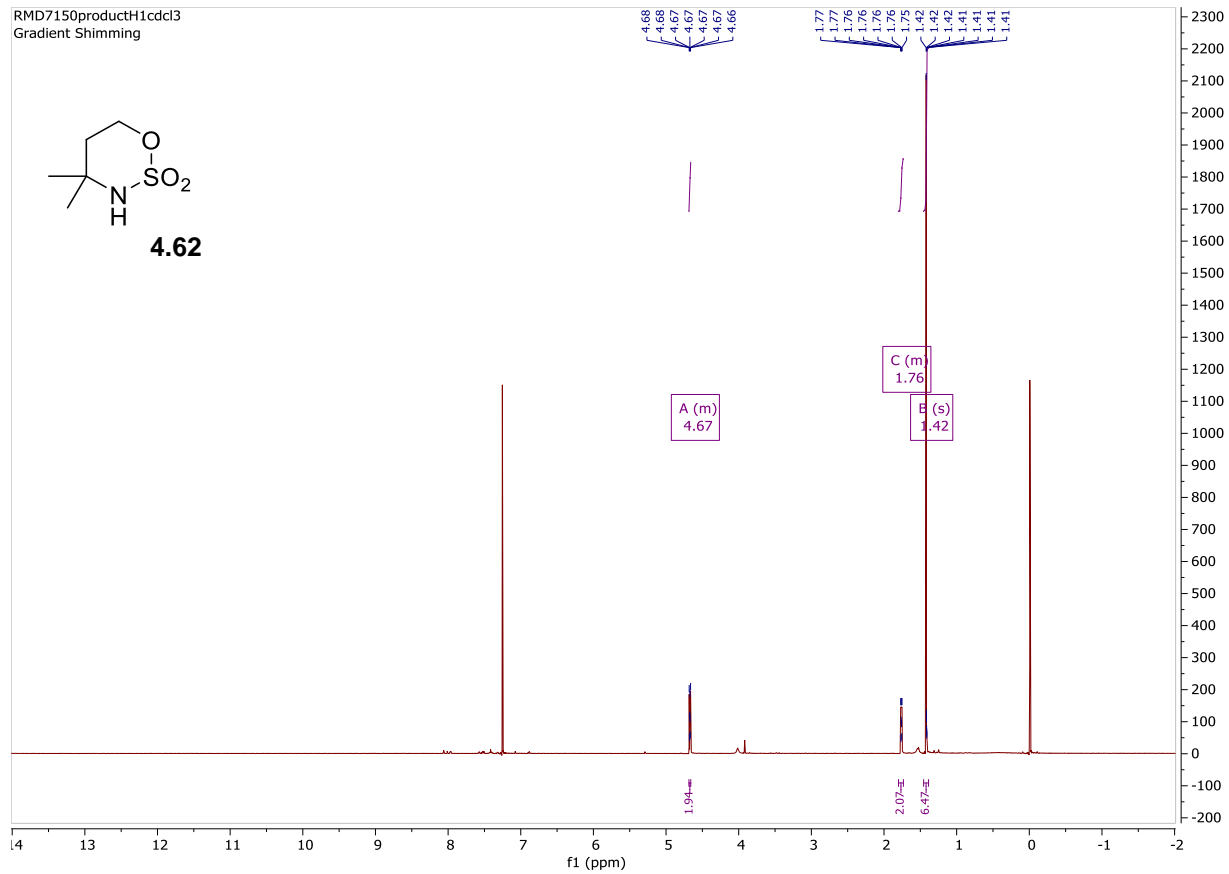
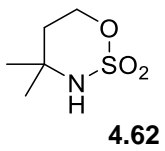
4-(4-methoxyphenyl)-1,2,3-oxathiazinane 2,2-dioxide was synthesized following the general aminaton procedure on a .2 mmol scale of the neopentyl sulfamate, as the respective sulfamate 4-Bromophenyl ((5-(tert-butyl)-2-methoxyphenyl)-I3-iodaneylidene)sulfamate was used as the respective iodine. The reaction mixture was purified after workup using silica flash chromatography (40% EtOAC/Hexanes) to give 0.003 g of a yellow solid (0.016 mmol, 8 % yield).

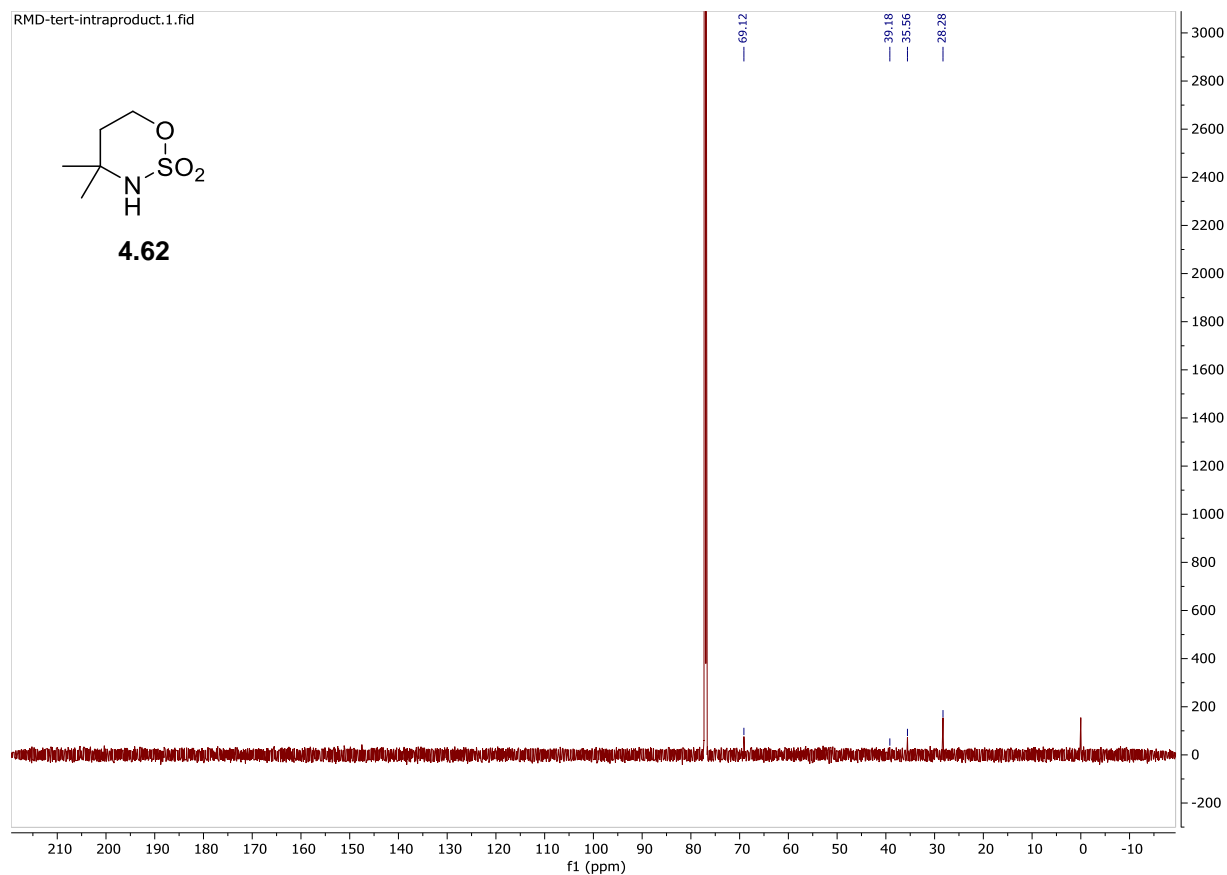
¹H NMR (600 MHz, CDCl₃) δ 4.68 – 4.66 (Hc, m, 2H), 1.80 – 1.73 (Hb, m, 2H), 1.42 (Ha, s, 6H) ppm.

¹³C NMR (201 MHz, CDCl₃) δ 69.1, 39.1, 35.6, 28.3 ppm.

NMR spectra are consistent with literature reports.¹¹

RMD7150productH1cdcl3
Gradient Shimming





3.4 References

- 1 Liang, J.L.; Yuan, S.X.; Huang, J.S.; Che, C.M.; Intramolecular C–N bond formation reactions catalyzed by ruthenium porphyrins: amidation of sulfamate esters and aziridination of unsaturated sulfonamides. *J. Org. Chem.*, **2004**, 69 (11), 3610–3619
- 2 Miralles, N.; Romero, R. M.; Fernández E.; Muñiz, K.; A mild carbon–boron bond formation from diaryliodonium salts. *Chem. Commun.*, **2015**, 51 (74), 14068-14071.
- 3 Chun, J.H.; Telu, S.; Lu, S.; Pike, V. W.; Radiofluorination of diaryliodonium tosylates under aqueous–organic and cryptand-free conditions. *Org. Biomol. Chem.*, **2013**, 11 (31), 5094– 5099.
- 4 Landge, K.P.; Jang, K.S.; Lee, S.Y.; Chi, D.Y.; Approach to the synthesis of indoline derivatives from diaryliodonium salts. *J. Org. Chem.*, **2012**, 77 (13), 5705–5713.
- 5 Pandey, G.; Laha, R.; Mondal, P. K.; Heterocyclization involving benzylic C(sp³)–H functionalization enabled by visible light photoredox catalysis. *Chem. Commun.*, **2019**, 55 (65), 9689-9692.
- 6 Espino, C. G.; Wehn, P. M.; Chow, J.; Du Bois, J. Synthesis of 1,3-difunctionalized amine derivatives through selective C–H bond oxidation. *J. Am. Chem. Soc.*, **2001**, 123 (28), 6935–6936.

⁷ Liu, W.; Zhong, D.; Yu, C.L.; Zhang, Y.; Wu, D.; Feng, Y.L.; Cong, H.; Lu, X.; Liu, W.B.; Iron-catalyzed intramolecular amination of aliphatic C–H bonds of sulfamate esters with high reactivity and chemoselectivity. *Org. Lett.*, **2019**, *21* (8), 2673–2678.

⁸ Harvey, M.E.; Musaev, D.G.; Du Bois, J.; A diruthenium catalyst for selective, intramolecular allylic C–H amination: reaction development and mechanistic insight gained through experiment and theory *J. Am. Chem. Soc.*, **2011**, *133* (43), 17207- 17216.

⁹ Kornecki, K. P.; Berry, J. F.; Introducing a mixed-valent dirhodium (II,III) catalyst with increased stability in C–H amination *Chem. Commun.*, **2012**, *48* (99), 12097–12099.

¹⁰ Espino, C.G.; Du Bois, J.; A Rh-Catalyzed C– H Insertion Reaction for the Oxidative Conversion of Carbamates to Oxazolidinones. *Angew. Chem. Int. Edn. Engl.*, **2001**, *40* (3), 598-600

¹¹ Espino, C.G.; Fiori, K.W.; Kim, M.; Du Bois, J.; Expanding the scope of C–H amination through catalyst design. *J. Am. Chem. Soc.*, **2004**, *126* (47), 15378- 15379.